

WATER IN A CHANGING CLIMATE: MONTANA'S  
FLATHEAD INDIAN RESERVATION, 1961-2100

by

Francesco Zignol, M. S.

A dissertation submitted to the Graduate Council of  
Texas State University in partial fulfillment  
of the requirements for the degree of  
Doctor of Philosophy  
with a Major in Geographic Information Science  
August 2019

Committee Members:

Alberto Giordano, Chair

Jennifer L. R. Jensen

Richard W. Dixon

Thom Hardy

**COPYRIGHT**

by

Francesco Zignol

2019

## **FAIR USE AND AUTHOR'S PERMISSION STATEMENT**

### **Fair Use**

This work is protected by the Copyright Laws of the United States (Public Law 94-553, section 107). Consistent with fair use as defined in the Copyright Laws, brief quotations from this material are allowed with proper acknowledgement. Use of this material for financial gain without the author's express written permission is not allowed.

### **Duplication Permission**

As the copyright holder of this work I, Francesco Zignol, refuse permission to copy in excess of the "Fair Use" exemption without my written permission.

## DEDICATION

To mom and dad

*A mamma e papà*

## **ACKNOWLEDGEMENTS**

First and foremost, I would like to express my gratitude to my advisor and committee chair, Dr. Alberto Giordano, who welcomed me at Texas State University and allowed me to pursue my educational goals. I appreciate all the time and support that he has offered throughout my Ph.D. experience, but also his hard questions, which incited me to widen my research from various perspectives. I also want to thank my committee members, Dr. Jennifer Jensen, Dr. Richard Dixon, and Dr. Thom Hardy, for the insightful comments that have undoubtedly strengthened this work.

Furthermore, I am very grateful to the Confederated Salish and Kootenai Tribes of the Flathead Indian Reservation, whose members and collaborators hosted me during my visits to the reservation, shared with me experience and knowledge that informed this research, and provided datasets that sustained this project. In particular, I would like to thank Francis Auld, Craig Barfoot, John Carter, Michael Durglo Jr., Dan Lozar, Set Makepeace, and Germaine White.

A special thanks goes to the many friends and colleagues of the Department of Geography for the stimulating discussions and the fellowship without which the tough times in the Ph.D. pursuit would have been more difficult to overcome. A heartfelt thanks also goes to the entire Department of Geography staff for their professionalism, assistance, and encouragement. Last but not least, I owe a great deal of gratitude to my family for supporting me unconditionally all these years.

## TABLE OF CONTENTS

	<b>Page</b>
ACKNOWLEDGEMENTS.....	v
LIST OF TABLES .....	vii
LIST OF FIGURES .....	viii
LIST OF ILLUSTRATIONS.....	ix
ABSTRACT.....	xi
CHAPTER	
1. INTRODUCTION.....	1
1.1. Background .....	1
1.2. Study area .....	3
1.3. Research framework and questions.....	7
2. CLIMATE EVOLUTION IN THE FLATHEAD REGION: HISTORICAL OVERVIEW AND POTENTIAL FUTURE SCENARIOS .....	11
2.1. Introduction .....	11
2.2. Literature review .....	14
2.3. Research questions and objectives.....	21
2.4. Data and methods.....	23
2.4.1. Data collection and quality check.....	24
2.4.2. Statistical downscaling of SAT and SWE.....	33
2.4.3. Analysis of SAT 30-year mean and variability and SAT trends .....	47
2.4.4. Analysis of snowpack characteristics and trends.....	57
2.5. Results .....	69
2.5.1. Statistical downscaling .....	69
2.5.2. Air temperature .....	92
2.5.3. Snowpack .....	132
2.6. Conclusions .....	148

3. STREAM AND RIVER TEMPERATURE CHANGES IN THE FLATHEAD RESERVATION: PAST AND FUTURE TRENDS.....	152
3.1. Introduction .....	152
3.2. Literature review .....	154
3.3. Research question and objective .....	163
3.4. Data and methods.....	164
3.4.1. Data collection and quality check .....	165
3.4.2. Design of temporal schemes.....	169
3.4.3. Calibration and validation of the SAT/SWT non-linear models.....	171
3.4.4. Analysis of SWT trends.....	175
3.5. Results .....	177
3.5.1. SAT/SWT non-linear logistic models .....	177
3.5.2. SWT trends.....	190
3.6. Conclusions .....	203
4. CONCLUSIONS .....	206
4.1. Trends in SAT, SWT, and SWE .....	206
4.2. Methodology.....	211
APPENDIX SECTION .....	217
REFERENCES .....	285

## LIST OF TABLES

Table	Page
2-1. Relative skills of dynamical and statistical downscaling .....	17
2-2. General characteristics of all the climate stations used in the analysis .....	27
2-3. Large-scale daily predictor codes and definitions .....	32
2-4. General characteristics and statistics of all the climate time series used for statistical downscaling purposes .....	35
2-5. Model structure and calibration options per climate time series .....	40
2-6. Indices that define annual snowpack characteristics .....	44
2-7. Characteristics of SAT time series before 1961 .....	49
2-8. Additional 30-year periods starting before 1961 per climate station .....	53
2-9. General characteristics and statistics of all the climate time series used for snowpack analysis purposes .....	58
2-10. Large-scale predictors employed for statistically downscaling maximum and minimum SAT .....	71
2-11. Specifications of the calibration processes for statistically downscaling maximum and minimum SAT .....	74
2-12. Large-scale predictors employed for statistically downscaling SA and SM .....	77
2-13. Table 2-13: Specifications of the calibration processes for statistically downscaling SA and SM .....	77
2-14. Specifications and main results of the validation of the downscaled maximum and minimum SAT time series .....	80
2-15. Validation of the mean snowpack characteristics within 2001-2005 .....	89

2-16. Validation statistics of the downscaled SA, SM, $\Delta$ SWE, and SWE time series within 2001-2005 .....	89
2-17. Kendall's correlation coefficient ( $\tau$ ) and magnitude of change ( $\phi$ ) related to Mann-Kendall and regional Kendall tests applied to annual snowpack indices over 1994-2018 .....	133
2-18. Mean SPR and mean corrective factor used to adjust rainfall measurements at each climate station and across the overall Flathead Region.....	134
2-19. Mean values of SA and PRE (both observed and adjusted) monthly totals over the 1994-2018 period, and related SPR values.....	136
2-20. Kendall's correlation coefficient ( $\tau$ ) and magnitude of change ( $\phi$ ) related to Mann-Kendall and regional Kendall tests applied to monthly averages of maximum SAT and SPR over 1994-2018 .....	137
2-21. Monthly average of SWE, SDP, SDN, and CVD over the 2003-2018 period.....	139
2-22. Kendall's correlation coefficient ( $\tau$ ) and magnitude of change ( $\phi$ ) related to Mann-Kendall and regional Kendall tests applied to SDN bimonthly means over 2003-2018 .....	140
2-23. Rate of change ( $\phi$ ) and Kendall's coefficient ( $\tau$ ) of trends in snowpack indices over 1961-2100 according to the three RCP scenarios.....	143
3-1. General characteristics of the water temperature recording stations used in the analysis.....	167
3-2. Basic statistics of the daily maximum and minimum SWT time series used in the analysis.....	168
3-3. Logistic models based on different pairs of independent/dependent variables (the time series created at this stage are highlighted by a gray shade) .....	169
3-4. Best correlation between maximum SAT and maximum SWT for each SWT gaging station and temporal scheme.....	178

3-5. Best correlation between minimum SAT and minimum SWT for each SWT gaging station and temporal scheme .....	180
3-6. Specifications of the optimal SAT/SWT model for each SWT gaging station and SWT variable .....	182
3-7. Distance and elevation difference between SWT gaging stations and SAT recording stations .....	186
4-1. Changes in air temperature, water temperature, and main snowpack characteristics between 1961 and 2100 across the study area according to the three proposed RCP scenarios.....	206
4-2. Projected change by year of maximum SAT, minimum SAT, and mean annual SWE according to different emission scenarios for the Flathead Region (present study) and the South Fork Flathead River Basin (Chase, Hay, and Markstrom 2012) ....	209
4-3. Projected mean annual and summer SWT changes for three 30-year periods within the XXI century across the Pacific Northwest (Wu et al. 2012) and the FIR (present study) according to different emissions scenarios using 1970-1999 as reference period .....	210

## LIST OF FIGURES

Figure	Page
1-1. Flathead Indian Reservation, Montana .....	4
1-2. Dissertation structure .....	8
2-1. Conceptual framework of statistical downscaling .....	16
2-2. Workflow for research questions 1 and 2.....	23
2-3. Location of climate stations used in the analysis .....	25
2-4. Spatial relationship between large-scale and local-scale data .....	31
2-5. Conceptual framework of SDSM 4.2.9 (Wilby and Dawson 2007, 13) .....	33
2-6. Workflow for the analysis and comparison of SAT trends.....	47
2-7. Relationship between daily minimum SAT and daily s850 at Polson Kerr Dam .....	72
2-8. Observed and simulated seasonal averages of daily maximum SAT and estimated prediction error.....	82
2-9. Observed and simulated seasonal averages of daily minimum SAT and estimated prediction errors .....	83
2-10. Annual evolution of the observed and estimated daily SWE means over the period 2001-2005 at Kraft Creek.....	85
2-11. Annual evolution of the observed and estimated daily SWE means over the period 2001-2005 at Moss Peak .....	86
2-12. Annual evolution of the observed and estimated daily SWE means over the period 2001-2005 at North Fork Jocko .....	86
2-13. Historical and future changes in 30-year normals of maximum SAT within 1961-2100 according to the RCP2.6 scenario .....	94

2-14. Historical and future changes in 30-year normals of maximum SAT within 1961-2100 according to the RCP4.5 scenario .....	95
2-15. Historical and future changes in 30-year normals of maximum SAT within 1961-2100 according to the RCP8.5 scenario .....	96
2-16. Historical and future changes in 30-year normals of minimum SAT within 1961-2100 according to the RCP2.6 scenario .....	97
2-17. Historical and future changes in 30-year normals of minimum SAT within 1961-2100 according to the RCP4.5 scenario .....	98
2-18. Historical and future changes in 30-year normals of minimum SAT within 1961-2100 according to the RCP8.5 scenario .....	99
2-19. Difference in maximum temperature normals and variability between the baseline period (1961-1990) and any subsequent 30-year period according to the RCP2.6 scenario.....	102
2-20. Difference in maximum temperature normals and variability between the baseline period (1961-1990) and any subsequent 30-year period according to the RCP4.5 scenario.....	103
2-21. Difference in maximum temperature normals and variability between the baseline period (1961-1990) and any subsequent 30-year period according to the RCP8.5 scenario.....	104
2-22. Difference in minimum temperature normals and variability between the baseline period (1961-1990) and any subsequent 30-year period according to the RCP2.6 scenario.....	105
2-23. Difference in minimum temperature normals and variability between the baseline period (1961-1990) and any subsequent 30-year period according to the RCP4.5 scenario.....	106
2-24. Difference in minimum temperature normals and variability between the baseline period (1961-1990) and any subsequent 30-year period according to the RCP8.5 scenario.....	107

2-25. Daily maximum temperature normals and intraseasonal monthly maximum temperature variability for winter according to historical data and three RCP scenarios .....	110
2-26. Daily maximum temperature normals and intraseasonal monthly maximum temperature variability for spring according to historical data and three RCP scenarios .....	111
2-27. Daily maximum temperature normals and intraseasonal monthly maximum temperature variability for summer according to historical data and three RCP scenarios .....	112
2-28. Daily maximum temperature normals and intraseasonal monthly maximum temperature variability for fall according to historical data and three RCP scenarios ...	113
2-29. Daily minimum temperature normals and intraseasonal monthly minimum temperature variability for winter according to historical data and three RCP scenarios .....	114
2-30. Daily minimum temperature normals and intraseasonal monthly minimum temperature variability for spring according to historical data and three RCP scenarios .....	115
2-31. Daily minimum temperature normals and intraseasonal monthly minimum temperature variability for summer according to historical data and three RCP scenarios .....	116
2-32. Daily minimum temperature normals and intraseasonal monthly minimum temperature variability for fall according to historical data and three RCP scenarios ...	117
2-33. Kendall's correlation coefficient related to the 1961-2100 regional trend in the mean annual and seasonal maximum SAT according to the three proposed RCP scenarios .....	119
2-34. Kendall's correlation coefficient related to the 1961-2100 regional trend in the mean annual and seasonal minimum SAT according to the three proposed RCP scenarios .....	119

2-35. Mean decadal regional trend of the mean annual and seasonal maximum SAT within the 1961-2100 period according to the three proposed RCP scenarios .....	120
2-36. Mean decadal regional trend of the mean annual and seasonal minimum SAT within the 1961-2100 period according to the three proposed RCP scenarios .....	120
2-37. Mean decadal trend of the mean annual/seasonal maximum SAT and related Kendall's correlation coefficient within the 1961-2100 period according to the RCP2.6 scenario.....	123
2-38. Mean decadal trend of the mean annual/seasonal maximum SAT and related Kendall's correlation coefficient within the 1961-2100 period according to the RCP4.5 scenario.....	124
2-39. Mean decadal trend of the mean annual/seasonal maximum SAT and related Kendall's correlation coefficient within the 1961-2100 period according to the RCP8.5 scenario.....	125
2-40. Mean decadal trend of the mean annual/seasonal minimum SAT and related Kendall's correlation coefficient within the 1961-2100 period according to the RCP2.6 scenario.....	126
2-41. Mean decadal trend of the mean annual/seasonal minimum SAT and related Kendall's correlation coefficient within the 1961-2100 period according to the RCP4.5 scenario.....	127
2-42. Mean decadal trend of the mean annual/seasonal minimum SAT and related Kendall's correlation coefficient within the 1961-2100 period according to the RCP8.5 scenario.....	128
3-1. Classification scheme of mathematical models used to predict water temperature .....	159
3-2. Workflow for research question 3 .....	164
3-3. Location of the water temperature recording stations used in the analysis.....	166
3-4. Air-water temperature relationship (adapted from Mohseni, Stefan, and Erickson 1998, 2687).....	171

3-5. Example of hysteresis loop with rising (yellow) and falling (cyan) limbs; the function fitting the annual (i.e., entire) dataset is shown in red .....	173
3-6. Number of SWT gaging stations that exhibit hysteresis (data are shown for both SWT variables together and each variable separately).....	188
3-7. Mean decadal trend of the mean annual maximum SWT and related Kendall's correlation coefficient within the 1961-2100 period according to the three RCP scenarios .....	191
3-8. Mean decadal trend of the mean annual minimum SWT and related Kendall's correlation coefficient within the 1961-2100 period according to the three RCP scenarios .....	192
3-9. Mean decadal trend of the mean annual/seasonal maximum SWT and related Kendall's correlation coefficient by subregion within 1961-2100 based on the RCP2.6 scenario.....	194
3-10. Mean decadal trend of the mean annual/seasonal maximum SWT and related Kendall's correlation coefficient by subregion within 1961-2100 based on the RCP4.5 scenario.....	195
3-11. Mean decadal trend of the mean annual/seasonal maximum SWT and related Kendall's correlation coefficient by subregion within 1961-2100 based on the RCP8.5 scenario.....	196
3-12. Mean decadal trend of the mean annual/seasonal minimum SWT and related Kendall's correlation coefficient by subregion within 1961-2100 based on the RCP2.6 scenario.....	197
3-13. Mean decadal trend of the mean annual/seasonal minimum SWT and related Kendall's correlation coefficient by subregion within 1961-2100 based on the RCP4.5 scenario.....	198
3-14. Mean decadal trend of the mean annual/seasonal minimum SWT and related Kendall's correlation coefficient by subregion within 1961-2100 based on the RCP8.5 scenario.....	199

3-15. Kendall’s correlation coefficient related to the 1961-2100 regional trend in the mean annual and seasonal maximum SWT according to the three proposed RCP scenarios .....	201
3-16. Kendall’s correlation coefficient related to the 1961-2100 regional trend in the mean annual and seasonal minimum SWT according to the three proposed RCP scenarios .....	201
3-17. Mean decadal regional trend of the mean annual and seasonal maximum SWT within the 1961-2100 period according to the three proposed RCP scenarios .....	202
3-18. Mean decadal regional trend of the mean annual and seasonal minimum SWT within the 1961-2100 period according to the three proposed RCP scenarios .....	202
4-1. Potential loss of critical bull trout habitat in response to increasing August stream temperatures in the Flathead River Basin above the Flathead Lake (Jones et al. 2014, 212) .....	216

## LIST OF ABBREVIATIONS

<b>Abbreviation</b>	<b>Description</b>
AOGCM	– Atmosphere-Ocean General Circulation Model
AR5	- Fifth Assessment Report
CanESM2	– second-generation Canadian Earth System Model
CCCma	– Canadian Centre for Climate Modelling and Analysis
CMIP5	– Coordinated Modelling Intercomparison Project Phase 5
CSKT	– Confederated Salish and Kootenai Tribes
DS	– Dual Simplex algorithm
FIR	– Flathead Indian Reservation
GCM	– Global Climate Model
GHCN	– Global Historical Climatology Network
GHG	– Greenhouse Gas
IPCC	– Intergovernmental Panel on Climate Change
MKT	– Mann-Kendall Test
NCAR	– National Center for Atmospheric Research
NCEI	– National Centers for Environmental Information
NCEP	– National Centers for Environmental Prediction
NOAA	– National Oceanic Atmospheric Administration
NRD	– Natural Resource Department

OLS – Ordinary Least Squares algorithm

PBT – Peaks Below Threshold

POT – Peaks Over Threshold

PRE – PREcipitation increment

QA – Quality Assurance

RCM – Regional Climate Model

RCP – Radiative Concentration Pathway

RKT – Regional Kendall Test

SA – Snow Accumulation

SAT – Surface Air Temperature

SDN – Snow DeNsity

SDP – Snow DePth

SDSM – Statistical DownScaling Model

SKT – Seasonal Kendall Test

SM – Snow Melt

SNOTEL – SNOw TELelemetry network

SPR – Snow/Precipitation Ratio

SWE – Snow Water Equivalent

SWT – Surface Water Temperature

WMO – World Meteorological Organization

## **ABSTRACT**

The Confederated Salish and Kootenai Tribes of the Flathead Indian Reservation (MT) have observed drastic changes in the quantity and quality of the water resources of the reservation over the last decades, which is threatening the Tribes' traditional lifestyle and cultural identity. This research evaluates the impacts of climate change, specifically air temperature changes, on the snowpack conditions and stream/river temperatures between 1961 and 2100. Statistical downscaling served as a means to obtain local-scale projections of air temperature and snow water equivalent from coarse-resolution global climate models. A non-linear logistic function was also used to estimate water temperature time series based on air temperature. The observed data indicate an increment in both air and water temperatures and a reduction of the duration and amount of snowpack due to a later snow accumulation in fall and an earlier snowmelt in spring. According to the estimated data, this tendency is expected to continue or intensify in the future. The magnitude of the change and the monotonicity of the trends vary according to the climate scenario, variable, season, spatial scale, and specific location considered. Based on an intermediate scenario, by the end of the XXI century, air and water temperatures will averagely increase by 4.2°C and 1.9°C, respectively, whereas the annual snow water equivalent maximum and the snowpack duration will decrease, on average, by 46% and 66 days, respectively. In general, higher elevation areas are associated with less steep and less consistent trends than those found at lower

elevations. Also, summer is predicted to experience the largest increase in both air and water temperatures. The findings of this research can guide the development of climate change adaptation and water resource strategic plans for the reservation.

# 1. INTRODUCTION

## 1.1. Background

As a consequence of population growth and urban sprawl, the increasing lack of unpolluted fresh water is becoming an issue of major concern worldwide (WWAP 2009). This problem is aggravated by climate change, which might stress water resources even further (IPCC 2013). More specifically, changes in climate alter the water cycle, affecting where, when, and how much water is available for all uses (USGCRP 2009). In addition, climate change may influence the status of certain physical properties of water, such as its temperature. With spatial and temporal changes in water quantity and quality, conflicts around different water uses have arisen that involve a variety of stakeholders, who often have asymmetric power relations. These conflicts have become more serious in the last few decades.

In this context, peoples with fewer financial resources or ethnic minority groups are likely to be most affected by the decrease of water quantity and the degradation of water quality because they potentially have fewer social and economic resources to cope with this problem (IPCC 2007). Native American communities are among the most vulnerable. Historical and contemporary government policies and, sometimes, poor socioeconomic conditions limit their capacity to adapt to water-related challenges (USGCRP 2014). The general purpose of the present dissertation is to investigate the evolving state of water resources in the Flathead Indian Reservation (FIR), Montana, and discuss the implications that potential changes in water quantity and quality might have on native people's traditional lifestyle.

Three major research areas have emerged that address water-related challenges in Native American communities: (1) water quality, (2) water rights, and (3) climate change. Water quality studies analyze the impacts of chemical and/or biological pollutants on surface and/or groundwater resources and, in turn, on native people's health (e.g., McGinnis and Davis 2001; Cummins et al. 2010; Eggers et al. 2015). Water rights studies describe historical and contemporary conflicts between native and non-native populations and/or governments to access water resources and explore the different cultural views behind these conflicts (e.g., Hand 2007; Rogers and Edmiston 2013; Marsh and Smith 2015). The third research area includes studies that analyze various climate change impacts on water resources and native people's traditional lifestyle (e.g., Cozzetto et al. 2013; Dittmer 2013; Gautam, Chief, and Smith Jr. 2013).

Although these three research topics are not mutually exclusive, they are usually treated separately in the literature by different disciplines. The present dissertation lies within the third aforementioned research area as climate change is the primary force driving water resource changes considered in this study. However, the current state of the water resources of the FIR is not only influenced by climate change, but it is also the result of the complex interaction of historical events (e.g., the construction of dams, channels, and reservoirs), social constraints (e.g., the water rights situation), and other water-related stressors (e.g., water pollution due to tourist and recreational activities). Although this research focuses on climate change, it is recognized that the peculiar historical and sociocultural contexts also play crucial roles in determining the overall conditions of the water resources in the FIR.

## **1.2. Study area**

The FIR is the home of the Confederated Salish and Kootenai Tribes (CSKT). This reservation was founded on 16 July 1855 after eighteen leaders of the Bitterroot Salish, Kootenai, and Upper Pend D’Oreilles Tribes were forced to sign the Hell Gate Treaty with the U.S. government (Bigart and Woodcock 1996). This agreement, which is still the legal basis for the relationship between these Tribes and the federal government, stipulated the ceding of what is now known as Western Montana, Northern Idaho, and parts of the southern Canadian provinces (about 81,000 square kilometers of land) to the United States and established the reservation (Figure 1-1), which is approximately 5,330 square kilometers. The FIR is bordered on the northern part by the Flathead Lake, the remnant of a massive glacial lake of the era of the last interglacial, on the eastern part by the Mission Mountains, and on the western part by the Salish Mountains. All the water within the reservation drains into the Flathead River, a tributary of the Columbia River.

According to the U.S. Census Bureau (2011), the total population living within the reservation was 28,359 people in 2010, 7,042 of whom were Native Americans. A Tribal Council, which is composed of ten members, governs the Tribes, offers several services to the community, and regulates the workforce on the reservation. The Salish Kootenai College run by the Tribes is responsible for the education of members of the community. Besides English, two languages are spoken within the reservation: the Salish language, which is spoken by the Bitterroot Salish and Upper Pend D’Oreilles Tribes (today united under the common name of Confederated Salish, because of the shared language), and the Kootenai language, which is spoken by the Kootenai Tribe.

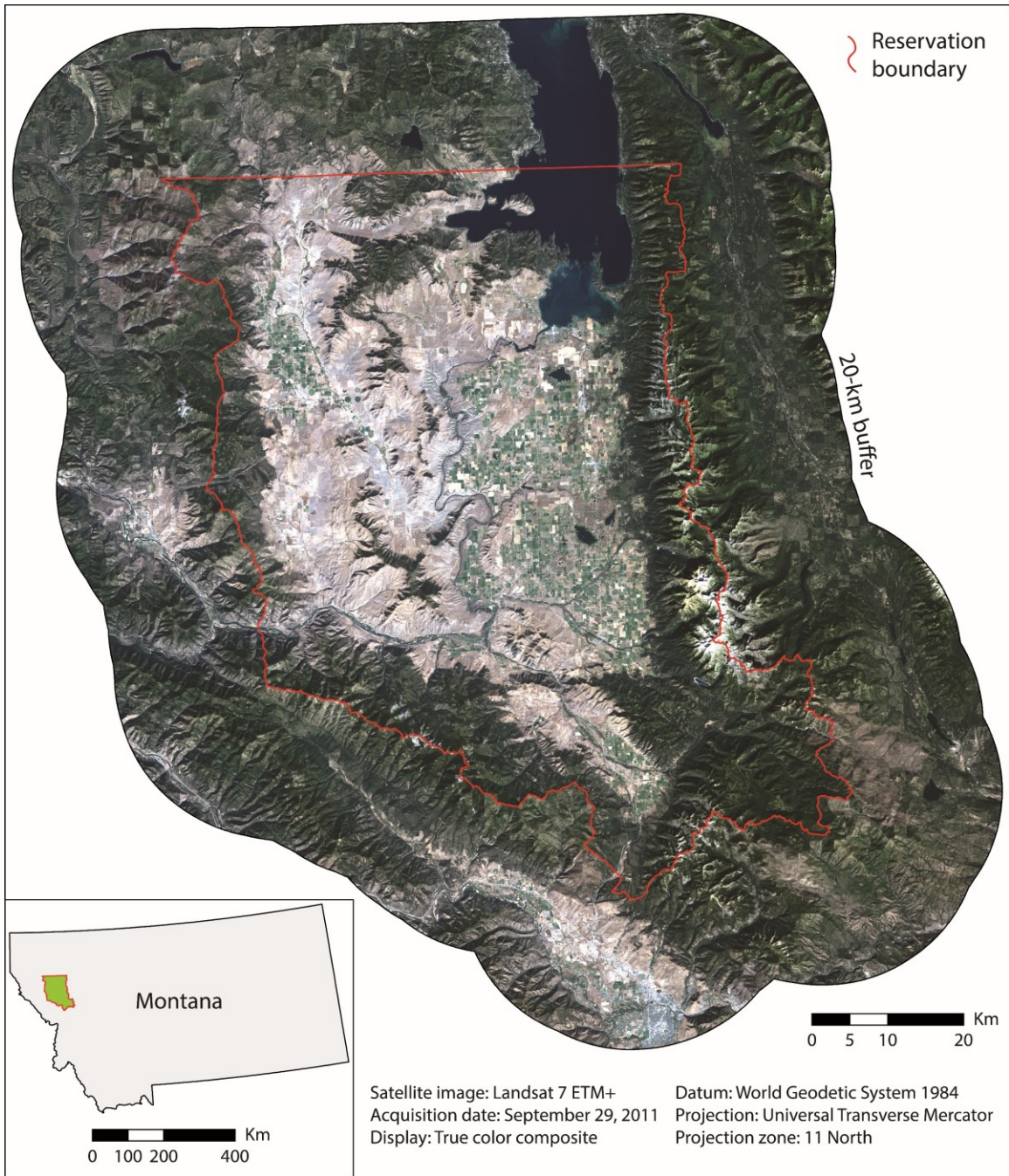


**Figure 1-1: Flathead Indian Reservation, Montana**

The FIR is chosen as the study area for this project for three main reasons. First, in the Northwestern United States the mean annual temperature increased by 0.7°C from 1895 to 2011 and it is expected to increase by 1.8-5.4°C by the end of the 21<sup>st</sup> century, depending on the emission scenario adopted for projections (USGCRP 2014).

Several studies indicate that this warming trend has affected the timing and amount of water availability in the Northwest, especially in basins where snowmelt contributes to streamflow (e.g., Stewart, Cayan, and Dettinger 2005; Elsner et al. 2010; Fritze, Stewart, and Pebesma 2011). Snowmelt-dominated basins usually show earlier spring snowmelt runoff and lower summer base streamflow, reducing the water supply and provoking ecological damages to river ecosystems (e.g., Dittmer 2013; Grah and Beaulieu 2013). According to preliminary interviews with members of the Tribes, the FIR exhibits such characteristics as it is experiencing a general increase in air temperature and a decrease in the spatial and temporal extent of snowpack. Chapter 2 tests this hypothesis by examining trends in air temperature and snowpack conditions over long periods of time.

Second, as a consequence of the increasing air temperature in the Northwestern United States (USGCRP 2014), stream temperatures in this region are also expected to increase, especially in summer (Wu et al. 2012). Warmer summer stream temperature combined with lower summer base streamflow in snowmelt-dominated basins can severely affect cold-water fish habitats, including in Western Montana (Pederson et al. 2010). For example, Jones et al. (2014) affirm that the critical habitat of the threatened bull trout (*Salvelinus confluentus*) is likely to diminish under different climate warming scenarios in the upper portion (above Flathead Lake) of the Flathead River Basin.

Preliminary interviews with members of the Tribes reveal that several fishes, including the bull trout, have already diminished in size and quantity in the water bodies of the reservation. As a first step for assessing fish habitat suitability, Chapter 3 investigates water temperature trends in streams and rivers of the FIR.

Third, the problem of water scarcity and the degradation of water quality assume even greater significance in a place like the FIR. While Western culture tends to view water exclusively as a resource, native cultures perceive water as having both cultural and spiritual values (Cozzetto et al. 2013; Rogers and Edmiston 2013). Francis Auld (personal communication, July 28, 2015, Elmo, Montana), a member of the Kootenai Tribe, describes *napetuk*, which means water in the Kootenai language, as follows: “*Napetuk* is a sacred component to the Kootenai Tribes. (...) It’s a provider. (...) You can see the integration of *napetuk* into everything, it’s all part of our living, it’s all part of what was given here. (...) It’s a big part of our culture. (...) *Napetuk* has a language, has life, is a living being.” It is clear that the decrease in water quantity and the deterioration of water quality not only entail the loss of a vital resource, but also compromise the traditional lifestyle of the Tribes and undermine their cultural identity.

### **1.3. Research framework and questions**

From a methodological point of view, this study largely builds on a rigorous quantitative approach, with statistical analysis being the primary mode of investigation. However, a preliminary exploratory qualitative phase helped develop the research framework. Unofficial interviews with local residents and archival research were conducted during three visits in the FIR in October 2014, summer 2015, and summer 2016 (see Appendix A for the approval of this study by the Institutional Review Board). The qualitative information gathered during this field work served multiple purposes: becoming familiar with the reservation and its history, identifying crucial issues and concerns related to water and climate change, and, eventually, converting them into research questions.

Figure 1-2 illustrates the structure of the overall dissertation. Chapter 1 introduces the research with information regarding the background, the study area, and the research framework and questions. Chapters 2 and 3 constitute the body of the dissertation. Specifically, Chapter 2 examines potential seasonal and annual changes in air temperature and snowpack characteristics. Here the focus is on climate and water quantity, and two main variables are analyzed: surface air temperature (SAT) and snow water equivalent (SWE). Chapter 3 investigates potential seasonal and annual changes in stream and river temperature. Surface water temperature (SWT), an important aspect of water quality, is the key variable treated in this chapter. Finally, Chapter 4 discusses the quantitative results from Chapters 2 and 3 in a comparative fashion, addresses the limitations of this study, and outlines recommendations for future research.

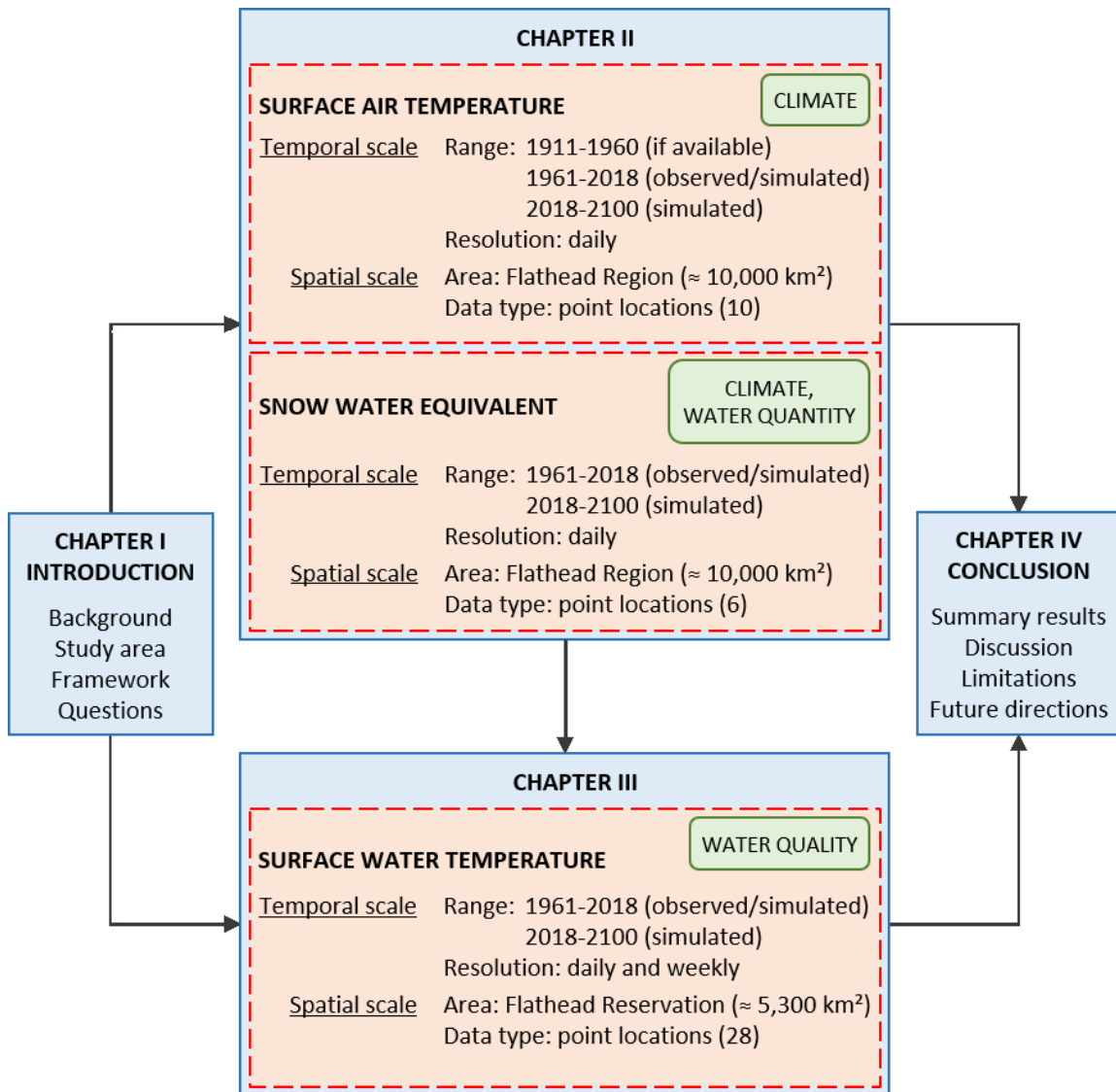


**Figure 1-2: Dissertation structure**

Two remarks should be made regarding the spatial and temporal scales adopted in this research (see the central blocks of Figure 1-2). First, the source data of the three main variables considered in this study are all associated with point locations: ten for SAT, six for SWE, and 28 for SWT. However, the spatial extension within which these sites are distributed varies between about 5,300 and 10,000 square kilometers. Specifically, the stations that record SWT data are located across the Flathead Reservation, whereas those that provide SAT and SWE data lie within the area covered by a 20-kilometer

buffer around the reservation boundaries. This area, hereinafter referred to as Flathead Region, is arbitrarily defined to include an adequate number of stations for the analysis. An overview of the Flathead Region is given in Figure 1-1.

Second, past, present, and future conditions are inquired throughout the dissertation, and the longest timeframe is considered based on data availability. In general, continuous daily time series ranging from 1 January 1961 to 31 December 2100 are generated for each of the three main variables examined in this study. These time series comprise both observed and simulated data. Such a long temporal interval rich in climate information allows us to account for potential impacts of climate change. Indeed, climate is defined as the mean and variability of relevant climate variables (e.g., temperature and precipitation) usually over a period of 30 years (IPCC 2013). Thus, the potential effects of climate change on water resources are only detectable over long periods of time. In the case of SAT, six climate stations provide records older than 1961, as far back as the beginning of the 20<sup>th</sup> century. This information is also included in part of the analysis, which extends the length of some SAT series from 140 years (1961-2100) up to 200 years. However, gaps in the SAT datasets before 1961 could not be filled with simulated data, and these longer time series are, therefore, discontinuous before that year.

In summary, the overall purpose of this research is to examine how water quantity and quality have changed and will possibly evolve across the FIR in response to a changing climate. Understanding the spatial and temporal variability of water is a first essential step for the delineation of effective strategies and practices toward appropriate

management of this resource. The dissertation is divided into three main parts, which are distributed into two core chapters (see Figure 1-2). Each part deals with a research topic (i.e., climate, climate/water quantity, and water quality), focuses on a specific variable (i.e., SAT, SWE, and SWT), and addresses a corresponding research question:

1. What are the historical and potential future changes and trends in air temperature at specific locations and in the whole Flathead Region?
2. What are the spatiotemporal variations and possible trends of snowpack characteristics in the mountain ranges of the Flathead Reservation?
3. What are the historical and potential future trends of water temperature in streams and rivers of the Flathead Reservation?

The reason why the first two parts are combined into a single chapter is because they both build on a common methodological approach, called statistical downscaling, and share the same literature review. Indeed, ample room is reserved for the description of this statistical procedure (Section 2.4.2) and for the presentation of the related results (Section 2.5.1). Each main chapter contains the following six sections: 1) introduction, 2) literature review, 3) research question/s and objective/s, 4) data and methods, 5) results, and 6) conclusions. A conclusive chapter (Chapter 4) summarizes and discusses the major findings, highlights the limitations of this study, and anticipates possible future directions of this research.

## **2. CLIMATE EVOLUTION IN THE FLATHEAD REGION: HISTORICAL OVERVIEW AND POTENTIAL FUTURE SCENARIOS**

### **2.1. Introduction**

The general purpose of the whole research is to investigate how water quantity and quality have evolved over time in the FIR and how they might change in the future. As climate is undoubtedly the most important factor influencing the water cycle, it is essential to understand the climate evolution in the study region to evaluate the impacts of climate change on the water resources of the reservation. Climate can be examined from different perspectives. This research focuses on two fundamental aspects of climate: air temperature and snow precipitation. The first is relevant to this study because its variations considerably influence water quality, with a direct impact on water temperature (see Chapter 3). The second is also important because it determines the amount and duration of snowpack, and, consequently, the quantity of water available throughout the year (see Section 2.5.3).

Thus, the objective of this chapter is to reconstruct the recent climatic history of the Flathead Region and estimate possible future climate scenarios, with a focus on air temperature and snow precipitation. In particular, the evolution of these two components of climate are studied based on daily records of SAT and SWE, respectively. SAT is the temperature of the air near the surface, whereas SWE is the amount of water contained within the snowpack. SWE was chosen over other measurements of snow precipitation (e.g., snow depth) because this climate variable has been recorded in the study area for a longer time and, therefore, longer time series are available for analysis.

Section 2.3 examines in detail the objectives of this chapter and presents the related research questions.

From a methodological point of view, the analysis in this chapter builds on a statistical technique, called statistical downscaling, that allows for synthesizing, with some constraints and limitations, SAT and SWE daily series for both past and future periods based primarily on existing records of these climate variables and other large-scale atmospheric variables. For those stations that provide sufficiently long records, continuous daily series of SAT and SWE from 1961 to 2100 are created using a combination of observed and estimated values. The statistical downscaling approach and the rationale behind it are discussed in Section 2.2, whereas the specific methodology developed in this study is exhaustively described in Section 2.4.2.

The generation of daily time series is only the first stage of the study in this chapter. In order to understand the repercussions on the water resources of the FIR, the second stage deals with identifying long-term changes and trends in air temperature and snowpack characteristics. Given the specific nature of SAT and SWE, two different approaches are employed. In the case of SAT, monthly, seasonal, and annual statistics are directly calculated from the daily time series. Instead, an intermediate process is required for SWE. Several indices that portray the snowpack conditions (e.g., timing and amount of snowpack) are first computed based on the SWE daily series, then annual statistics of these indices are calculated. The methodological steps adopted to investigate long-term changes and trends in air temperature and snowpack characteristics are discussed in Sections 2.4.3 and 2.4.4, respectively.

Section 2.5 is dedicated to the presentation of the results and follows a structure similar to that of the methodology, with a part designated to the statistical downscaling process (Section 2.5.1), another one focusing on air temperature (Section 2.5.1.3), and a third one regarding snowpack conditions (Section 2.5.3). These three parts form the core of this chapter and the first one is a prerequisite for the other two. Indeed, this chapter is developed around two research questions (see Section 2.3), one concerning air temperature, the second one relating to snowpack characteristics. Both questions are included into the same chapter because the implementation of statistical downscaling procedures to obtain future scenarios of SAT and SWE (part 1) is required for evaluating long-term changes and trends in either air temperature (part 2) or snowpack conditions (part 3). Section 2.6 discusses the results of these three parts in a comparative fashion.

In summary, Section 2.2 reviews the rationale behind statistical downscaling, a statistical technique that is at the base of the methodological framework of this chapter. Section 2.2 also highlights the contribution that this study aims to bring to the field of statistical downscaling. Section 2.3 presents the two research questions and related objectives associated with this chapter. Section 2.4 deals with the methodology adopted in this study. After the data preprocessing, three sets of analyses are described in detail: 1) the statistical downscaling procedure that allows us to reconstruct historical values and estimate future scenarios of SAT and SWE; 2) the analysis of SAT 30-year mean and variability and SAT trends; and 3) the analysis of snowpack characteristics and trends. Section 2.5 illustrates the results for these three sets of analyses. Finally, Section 2.6 discusses the results and draws conclusions.

## **2.2. Literature review**

This section discusses the concept of “spatial downscaling” as an approach that allows us to derive past or future local-scale climate information from large-scale (low-resolution) observed or modeled data, respectively (Trzaska and Schnarr 2014). Several climate stations within the Flathead Region have fragmentary historical climate series. Nevertheless, reanalysis data derived by combining observations with a meteorological forecast model provide large-scale information that can be spatially downscaled to reconstruct incomplete historical climate series. Spatial downscaling techniques can also be used for studying future climate trends at the scale of the Flathead Region. This is particularly important because future climate projections are generally available only at coarser spatial resolutions by means of Global Climate Model (GCM) simulations.

GCMs, also known as general circulation models, have been widely used for estimating global future climate. However, these models are restricted in their usefulness for local impacts studies due to their coarse spatial resolution. The horizontal resolution (horizontal grid spacing) of current GCMs typically varies between 100 and 250 kilometers for the atmospheric and land components of the models (IPCC 2013). Thus, GCMs are unable to capture regional-scale phenomena, such as tropical cyclones, sea and land breezes, monsoons, orographic precipitation, and low-level jet streams (Evans, McGregor, and McGuffie 2012). The Flathead Region presents an articulate orography, with vast flat valleys and high, steep mountain ranges, causing a marked spatial variability of climate within the study region. Similarly, Flathead Lake, a large body of water of about 500 square kilometers (Figure 1-1), strongly influences the

climate of the region, acting like a heat reservoir. These local-climate spatial variations are not detectable by GCMs. Therefore, GCM outputs need to be downscaled to a finer spatial resolution.

Several techniques have been employed that successfully accomplish this downscaling process. They are broadly classified into two categories referred to as dynamical and statistical downscaling (Evans, McGregor, and McGuffie 2012). Dynamical downscaling involves driving a Regional Climate Model (RCM) at high resolution (up to 25 kilometers for the most recent models) over a region of interest using global reanalysis or GCM outputs as boundary conditions for past climate or for future climate, respectively (IPCC 2013). Like a GCM, an RCM simulates explicitly the atmospheric dynamics, thermodynamics, and related physical processes through systems of mathematical equations and parametrizations. These models are dynamically- and physically-based.

Conversely, as illustrated in Figure 2-1, statistical downscaling involves deriving an empirical relationship between historical large-scale (low-resolution) climate variables, called predictors, and historical local-scale observations (typically point locations), called predictands (Mearns et al. 2014). Generally, reanalysis data are used as predictors, while climate variables recorded at surface climate stations are used as predictands. This empirical relationship may then be applied to equivalent predictors from GCMs to obtain local-scale future climate estimates (IPCC 2013). The rationale behind statistical downscaling techniques is that climate conditions at a specific location are determined, at least in part, by large-scale climate processes (Mearns et al. 2014).

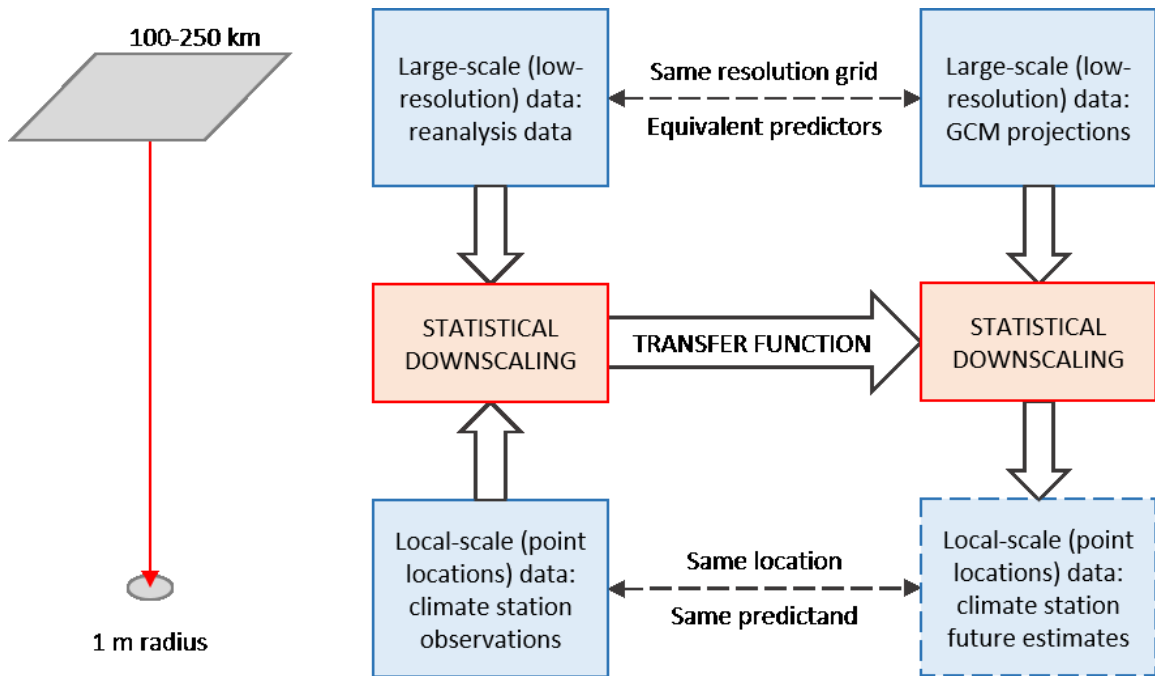


**Figure 2-1: Conceptual framework of statistical downscaling**

Table 2-1 illustrates the main advantages and limitations of dynamical and statistical downscaling. As it can be noticed, most of the weaknesses of one class of downscaling techniques are compensated for by the strengths of the other class, and vice versa. Discussing the details of these two complementary downscaling processes is beyond the scope of this chapter. It is enough to mention that statistical downscaling was preferred as the most appropriate approach for this analysis mainly because of its ability to estimate future values of climate variables at observation points. This facilitates the comparison of these projections with historical records at the same locations. In addition, this method can be easily applied to multiple GCM simulations, which permits, in a certain way, accounting of GCM uncertainty. However, it is also important to remark that the assumption of stationarity in the predictor-predictand relationship over time is the most significant source of uncertainty for statistical downscaling techniques.

**Table 2-1: Relative skills of dynamical and statistical downscaling**

	Dynamical Downscaling	Statistical downscaling
Advantages	<ul style="list-style-type: none"> <li>• Physically consistent processes</li> <li>• Resolves smaller-scale atmospheric processes and climate system feedbacks</li> <li>• Provides information over the entire landscape</li> <li>• Provides output for many climate-relevant variables</li> <li>• Can output variables with high temporal resolution</li> </ul>	<ul style="list-style-type: none"> <li>• Computationally inexpensive</li> <li>• Provides information at observation points</li> <li>• Based on accepted statistical procedures</li> <li>• Optimized for observation locations already used by impacts models</li> <li>• Can be applied to existing GCM ensembles</li> </ul>
Disadvantages	<ul style="list-style-type: none"> <li>• Computationally expensive</li> <li>• Limited ensembles are available</li> <li>• Produces very large datasets that the impacts community is not used to dealing with</li> <li>• Does not provide output at the point locations of current observations sites</li> <li>• Parametrizations are assumed to remain constant for future projections</li> </ul>	<ul style="list-style-type: none"> <li>• Requires long and reliable historical datasets for calibration (only observed variables can be downscaled; cannot be applied to locations without observations)</li> <li>• Dependent on choice of predictors</li> <li>• Assumes stationarity in predictor-predictand relationship</li> <li>• Climate system feedback are not included</li> <li>• Need to account for a tendency to underpredict variance</li> <li>• Lack of physical consistency between climate variables</li> <li>• Assumes a statistical distribution for individual climate variables</li> </ul>

\* Adapted from Evans, McGregor, and McGuffie 2012, 240

The Statistical Downscaling Model (SDSM) is a decision support tool based on robust statistical downscaling procedures that allow for the estimation of multiple, low-cost, single-site scenarios of daily surface climate variables (Wilby, Dawson, and Barrow 2002). In particular, two types of statistical downscaling techniques form the core of SDSM: transfer functions and stochastic weather generators. Transfer-function downscaling methods involve the development and application of empirical relationships between large-scale predictors and local-scale predictands. Examples of these methods include linear and non-linear regression, artificial neural networks, canonical correlation, and principal component analyses (Wilby and Dawson 2007). Stochastic weather generators produce ensembles of synthetic time series of local climate variables with statistical properties (e.g., mean, standard deviation, median, maximum, minimum) that are derived empirically (Mearns et al. 2014). SDSM can be applied to both past and future climate conditions using reanalysis data and GCM outputs as predictors, respectively.

SDSM was chosen as the most appropriate tool for this analysis for several reasons. First, SDSM is a recognized and well-documented software that has been freely available to the public since the summer of 2000 and, since then, has undergone continuous revisions and improvements (see Wilby and Dawson 2013). By the end of 2016, around 390 studies had been published that applied SDSM in a variety of geographic contexts and sectors (e.g., water, agriculture, urban, energy, tourism, transportation). Also, SDSM has been proven to perform well in reproducing observed climate variability, especially extreme temperatures, annual precipitation cycle, seasonal

and annual precipitation totals, extreme areal average precipitation, and inter-site correlation of precipitation amounts.<sup>1</sup>

Second, the weather generator component of SDSM can be used to reconstruct or infill missing records within incomplete historical series of climate variables for which a predictor-predictand relationship can be previously calculated (Wilby et al. 2014). In other words, SDSM allows us to extend back in time relatively short series of climate observations. The weather generator within SDSM synthesizes up to a maximum of 100 individual ensemble sequences, which slightly differ from each another but represent equally plausible outcomes (Wilby and Dawson 2007). This serves the purpose of the present research: rather than reproducing the exact daily sequence of a certain climate variable, the goal of this chapter consists in identifying and evaluating changes in its statistical properties.

Third, differently from other downscaling techniques, SDSM enables the synthesis of exotic predictands, such as evaporation, wave and tidal surge heights, ground-level ozone and particulates, and heat wave indices (Wilby et al. 2014). As one of the objectives of this chapter is to examine trends in snowpack characteristics through the analysis of SWE (see Section 2.4.4), this feature of SDSM is particularly important. SWE is not a typical variable that can be explicitly simulated by RCMs. Wilby et al. (2014) recommend further exploration of direct downscaling of exotic climate variables using SDSM. Within the SDSM literature, there is almost no trace of studies that deal with snow-related variables. As far as I am aware, there has been only one study that aimed

---

<sup>1</sup> For an extensive description of SDSM capabilities and limitations refer to Wilby and Dawson 2013 and Wilby et al. 2014.

to directly downscale snow depth (Tryhorn and DeGaetano 2013), while the direct downscaling of SWE has not been attempted before. Because of the presence in the study region of several climate stations that provide sufficiently long time series of SWE (see Section 2.4.2.1 and Table 2-4), this chapter intends to bridge this gap in the literature by investigating the SDSM potential for directly downscaling an exotic variable such as SWE.

### **2.3. Research questions and objectives**

The general objective of this chapter is to investigate potential long-term climate changes in the Flathead Region. To that end, both observed historical records (as far back as the beginning of the 20<sup>th</sup> century) and estimated future scenarios (up to 2100) are examined in conjunction, providing the possible longest temporal scale for a climatic analysis at this location. This chapter builds on the following research question: how has climate evolved over time and what are the possible future climate trends in the Flathead Region? As stated in the introduction (Section 2.1), this study focuses on two components of climate: air temperature and snow precipitation. Thus, the previous broad question can be split into two and readdressed as follows:

1. What are the historical and potential future changes and trends in air temperature at specific locations and in the whole Flathead Region?
2. What are the spatiotemporal variations and possible trends of snowpack characteristics in the mountain ranges of the Flathead Reservation?

The specific objective behind the first research question is to investigate long-term changes in 30-year mean and variability of maximum and minimum SAT, determine whether consistent upward or downward trends of these variables exist over the entire study period, and, if this is the case, quantify the rate of change. Ten different locations are considered to examine the spatial variability within the Flathead Region and identify the geographic factors that may influence this variability. The potential existence and magnitude of air temperature trends in a consistent direction throughout the whole region is also explored. In addition, monthly, seasonal, and annual temporal scales are

accounted for in order to characterize air temperature variations not only across multiple years, but within years too.

The specific objective behind the second research question is to provide a picture of the snowpack characteristics in the Flathead Region based on observed values of SWE and other snow-related variables recorded at six mountainous locations. Some of the aspects analyzed include timing, amount, and density of snowpack as well as other related factors, such as ratio of snow to precipitation. All this information is reported for each location and the overall region, and examined in a comparative fashion. Temporal variations within the observed period are also studied. Moreover, as part of the objective associated with this research question, direction and magnitude of possible trends in snowpack characteristics over the entire study period are investigated using both observed and estimated SWE values for three different locations.

## 2.4. Data and methods

Figure 2-2 illustrates the methodological workflow for addressing the two research questions and achieving the related objectives described in the previous section. After selecting, collecting, and checking the quality of the data (Section 2.4.1), three sets of analyses are implemented, which correspond to the core of this chapter (in red in Figure 2-2). First (Section 2.4.2), SAT and SWE continuous daily series that include both past and future periods are generated through statistical downscaling techniques. The direct downscaling of SWE using SDSM has not been attempted before; this is the methodological contribution that this chapter aims to bring to the statistical downscaling literature. Second (Section 2.4.3), SAT trends and changes in SAT mean and variability are examined and compared over long periods of time. This part addresses research question 1. Third (Section 2.4.4), spatiotemporal variability and trends in snowpack characteristics are investigated in a comparison fashion. This part addresses research question 2. The four stages outlined in Figure 2-2 are described below.

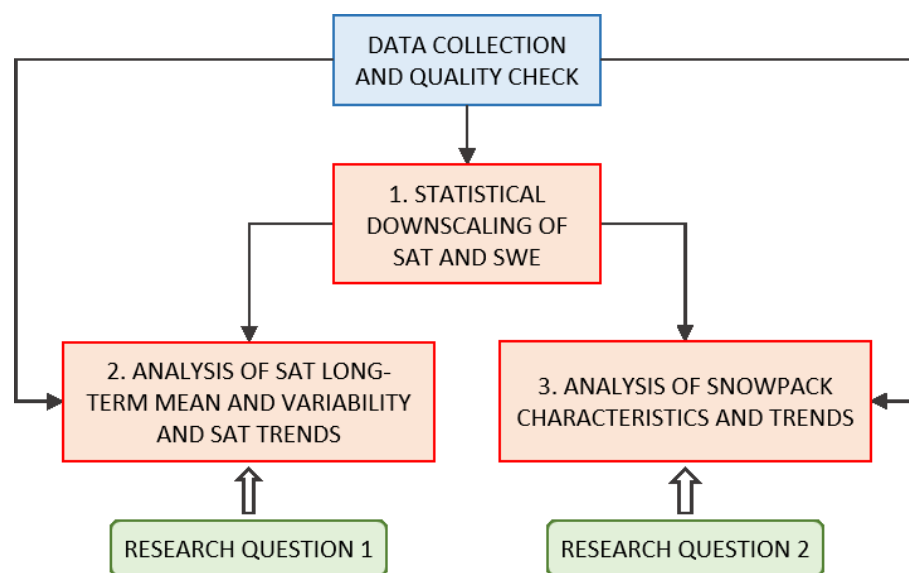


**Figure 2-2: Workflow for research questions 1 and 2**

### **2.4.1. Data collection and quality check**

This section provides information regarding the data collected for all the analyses in this chapter. These data can be divided into two categories based on their spatial scale: local-scale station data and large-scale reanalysis/GCM data. Both are used as input in the statistical downscaling procedure (Section 2.4.2). In addition, as illustrated in Figure 2-2, station data support the analysis of changes in air temperature and snowpack characteristics (Sections 2.4.3 and 2.4.4, respectively).

#### **2.4.1.1. Local scale: station data**

As mentioned in Section 2.1, this chapter focuses on the study of two main local-scale climate variables: SAT (maximum and minimum) and SWE. However, daily SAT (mean, maximum, and minimum), daily PREcipitation increment (PRE), and daily Snow DePth (SDP) are also included in this research as secondary variables to support part of the snowpack-related investigation (Section 2.4.4.1). All the climate station data in this chapter are collected from the Global Historical Climatology Network (GHCN)-Daily dataset provided by the National Oceanic Atmospheric Administration/National Centers for Environmental Information (NOAA/NCEI; Menne, Durre, Korzeniewski et al. 2012). With records gathered from over 80,000 stations all around the world and assembled from numerous sources, the GHCN-Daily of the NOAA/NCEI is the most comprehensive collection of *in situ* land surface weather data at daily temporal resolution. These data undergo an automated multi-tiered Quality Assurance (QA) procedure that looks for inconsistencies within the dataset.<sup>2</sup>

---

<sup>2</sup> for a complete description of GHCN-Daily, including data sources, data integration process, and QA routine, refer to Menne, Durre, Vose et al. (2012).

Figure 2-3 illustrates the thirteen climate stations selected for this research. In addition to stations that are located inside the reservation, the inclusion of stations that are within the 20-kilometer buffer guarantees an adequate amount of climate data for the analysis, a fairly uniform spatial coverage, and the representativeness of different elevations. The selection of these stations was eventually dictated by the length and



**Figure 2-3: Location of climate stations used in the analysis**

quality of the times series associated with each station. In addition to the automated QA procedure, a manual or semiautomatic QA review is recommended because GHCN-Daily has not been homogenized to account for changes in systematic bias (Menne, Durre, Vose et al. 2012). Therefore, each time series was graphed and visually examined to find potential changes in systematic bias (time-series jumps due to changes in station location, its adjacent surrounding environment, recording instrumentation, or time of observation). Stations with time series that show this behavior were discarded.

Figure 2-3 differentiates between stations that provide only SAT information (in red) and stations that are equipped with instruments able to measure SWE as well (in cyan). These six stations are part of the SNOw TELelemetry (SNOTEL) network and are the best source of snow data in the Western United States. Unfortunately, SNOTEL stations were installed quite recently in the study area (1980s and early 1990s), which is part of the reason why other stations with older SAT records are also included in the analysis. PRE data are recorded in all thirteen stations, but only those of SNOTEL stations are used in this research (Section 2.4.4.1). Table 2-2 summarizes the main characteristics of the climate stations displayed in Figure 2-3, such as the geographic location, the source of data, and the period of record. As the data registered in each station are used for different purposes, more details are given at the specific research stage in which they are implemented.

As mentioned at the beginning of this section, the following daily time series are extracted from the GHCN-Daily dataset: SWE, PRE, SDP, and mean SAT for the six SNOTEL stations, whereas maximum and minimum SAT for all the thirteen stations in Table 2-2.

**Table 2-2: General characteristics of all the climate stations used in the analysis**

<b>Id</b>	<b>Name</b>	<b>Latitude (°)</b>	<b>Longitude (°)</b>	<b>Elevation (m)</b>	<b>Source*</b>	<b>Start Date</b>	<b>End Date</b>
USC00240755	Bigfork 13S	47.8751	-114.0331	887.0	C	11/1/1938	6/30/2018
USS0013B25S	Bisson Creek	47.6800	-114.0000	1,499.6	S	9/30/1991	8/31/2018
USR0000MHOT	Hot Springs Montana	47.6156	-114.6694	902.2	R	6/10/1991	8/31/2018
USS0013B22S	Kraft Creek	47.4300	-113.7800	1,447.8	S	9/5/1980	8/31/2018
USW00024153	Missoula International Airport	46.9208	-114.0925	972.9	W	1/1/1948	8/31/2018
USS0013B24S	Moss Peak	47.6800	-113.9600	2,066.5	S	7/11/1985	8/31/2018
USS0013B07S	North Fork Jocko	47.2700	-113.7600	1,929.4	S	8/28/1989	8/31/2018
USC00246640	Polson Kerr Dam	47.6775	-114.2419	832.1	C	3/22/1951	8/31/2018
USC00247286	Saint Ignatius	47.3149	-114.0982	888.5	C	2/6/1896	12/31/2010
USC00247448	Seeley Lake Ranger Station	47.2141	-113.5204	1,249.7	C	10/16/1936	8/31/2018
USS0014B05S	Sleeping Woman	47.1800	-114.3300	1,874.5	S	9/30/1991	8/31/2018
USS0013C01S	Stuart Mountain	47.0000	-113.9300	2,255.5	S	9/13/1994	8/31/2018
USW00024159	Superior	47.1929	-114.8903	826.0	W	1/1/1914	8/31/2018

\*C = U.S. Cooperative Summary of the Day (NCDC DSI-3200); R = Remote Automatic Weather Station (RAWS) data obtained from the Western Regional Climate Center; S = SNOw TElemetry (SNOTEL) data obtained from the Western Regional Climate Center; W = U.S. First-Order Summary of the Day (NCDC DSI-3210)

However, three stations (i.e., Bisson Creek, Sleeping Woman, and Stuart Mountain) do not provide sufficiently long time series to be used for statistical downscaling. Almost all time series were originally discontinuous; if a record was missing, the corresponding date was missing too. For analysis purposes, each time series was converted into a continuous sequence of dates with missing data expressed as -999. Available records that fail any of the automated QA checks (identified by a quality flag) were also marked as missing (i.e., -999). Such daily continuous series of SWE, PRE, SDP, and SAT are ready to be used for analysis. Yet, a further preprocessing step is required for incorporating maximum SAT, minimum SAT, and SWE daily series into SDSM (see Section 2.4.2.1).

#### **2.4.1.2. Large scale: reanalysis and GCM data**

As mentioned in the literature review, reanalysis data are generated by combining historical weather observations from multiple sources around the world (e.g., aerological radiosoundings, surface weather stations, satellites, radar, ships, and buoys) with a meteorological forecast model. This can fill the gaps within the observing system since it acts as a sophisticated interpolator. Thus, reanalysis (or retrospective analysis) is a method that provides information on the past evolution of the state of the atmosphere.<sup>3</sup> Conversely, GCM simulations are mainly used to predict future climate. Due to the complexity of the processes simulated and the computational power needed to run meteorological forecast models and climate models at the global scale, both reanalysis and GCM data have a coarse spatial resolution, which typically varies between 100 and 250 kilometers (see Figure 2-1).

---

<sup>3</sup> For an exhaustive description of climate reanalysis and its role in understanding past climate refer to Chapter 2 in CCSP 2008.

The Coordinated Modelling Intercomparison Project Phase 5 (CMIP5) is a collaborative effort to bring together climate assessment activities undertaken by several climate modeling centers around the world. CMIP5 provides climate change evaluations that form the basis of the Fifth Assessment Report (AR5) promoted by the Intergovernmental Panel on Climate Change (IPCC) of the United Nations. Among all the Atmosphere-Ocean General Circulation Models (AOGCMs) used in the CMIP5, the second-generation Canadian Earth System Model (CanESM2) developed by the Canadian Centre for Climate Modelling and Analysis (CCCma) is selected for this research (Arora et al. 2011). Although statistical downscaling procedures may produce different results when using other AOGCM projections, evaluating the performance and comparing the outputs of the AOGCMs included in the AR5 of the IPCC is beyond the scope of this study.<sup>4</sup>

To account for uncertainty related to the potential impacts of socio-economic factors on climate change, users are advised to consider multiple emissions scenarios, representing different levels of Greenhouse Gas (GHG) emissions. The AR5 delineates four new emissions scenarios, named Radiative Concentration Pathways (RCPs). They are defined according to “their approximate total radiative forcing in year 2100 relative to 1750” (IPCC 2013, 29), measured in watts per square meter ( $W/m^2$ ). Three different emissions scenarios are considered in this research: RCP2.6 ( $2.6 W/m^2$ ), RCP4.5 ( $4.5 W/m^2$ ), and RCP8.5 ( $8.5 W/m^2$ ), representing low, medium, and high GHG emissions levels, respectively. The fourth emissions scenario (RCP6.0) included in IPCC (2013) is not

---

<sup>4</sup> For a comprehensive description of the characteristics of the AOGCMs used in the CMIP5 and their performance refer to Chapter 9 of IPCC 2013.

taken into account here because CanESM2 did not perform simulations for this scenario. It is also important to stress that the RCP2.6 represents a stringent mitigation scenario (i.e., net negative CO<sub>2</sub> emissions after around 2070) that is very unlikely to occur. This has to be kept in mind when discussing the results of the analysis (Section 2.6).

Both reanalysis and GCM predictors used in this research are provided by the CCCma (ECCC n.d.-a). In fact, reanalysis datasets are originally produced by the joint activity of the National Centers for Environmental Prediction (NCEP) and the National Center for Atmospheric Research (NCAR), which is why hereinafter these data are referred to as NCEP/NCAR.<sup>5</sup> However, the CCCma interpolated the NCEP/NCAR variables onto the same grid as the CanESM2 to allow for comparison between past and future climate. The grid has a global domain and is based on a T42 Gaussian grid with 128x64 cells (ECCC n.d.-a). In this grid, the horizontal resolution along the longitude is uniform and equal to 2.8125°, whereas along the latitude is nearly uniform and close to 2.8125°. Figure 2-4 illustrates the grid box that encompasses the Flathead Region. All the ten climate stations used for the statistical downscaling analysis in this research fall within the same grid box, whose area is about 211x310 kilometers.

Both the NCEP/NCAR and CanESM2 predictors provided by the CCCma are available at the daily temporal scale. The NCEP/NCAR dataset ranges from 1 January 1961 to 31 December 2005 for a total of 16,436 records, while the CanESM2 dataset ranges from 1 January 2006 to 31 December 2100 for a total of 34,675 records (for modeling purposes, leap years are also considered as 365 days long). Neither dataset

---

<sup>5</sup> For a detailed description of the NCEP/NCAR reanalysis project and dataset characteristics refer to Kalnay et al. (1996).

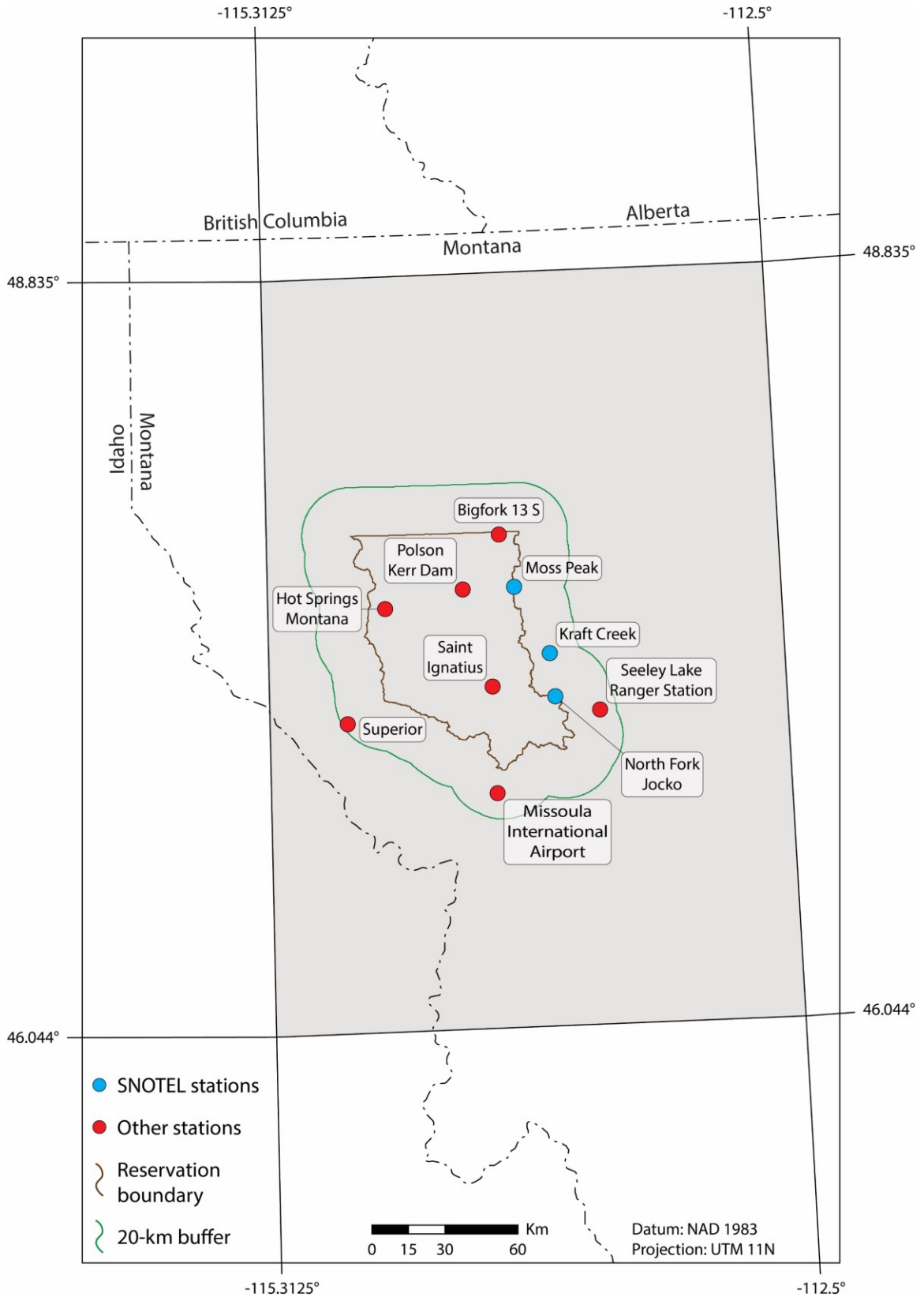


**Figure 2-4: Spatial relationship between large-scale and local-scale data**

Has missing values. Table 2-3 lists the 26 large-scale variables investigated as potential predictors for the statistical downscaling procedure (see Section 2.4.2.2). Obviously, the same set of variables is available for both the NCEP/NCAR and CanESM2 datasets. All the variables in Table 2-3 have been normalized with respect of their means and standard deviations over the 1961-1990 reference period (ECCC n.d.-b). In this way, the distributions of the normalized NCEP/NCAR and CanESM2 predictors are in closer agreement than those of the raw NCEP/NCAR and CanESM2 data.

**Table 2-3: Large-scale daily predictor codes and definitions**

<b>Code</b>	<b>Description</b>
mslp	Mean sea level pressure
p1_f	Geostrophic air flow velocity near the surface
p1_u	Zonal velocity component near the surface
p1_v	Meridional velocity component near the surface
p1_z	Vorticity near the surface
p1th	Wind direction near the surface
p1zh	Divergence near the surface
p5_f	Geostrophic air flow velocity at 500 hPa height
p5_u	Zonal velocity component at 500 hPa height
p5_v	Meridional velocity component at 500 hPa height
p5_z	Vorticity at 500 hPa height
p500	500 hPa geopotential height
p5th	Wind direction at 500 hPa height
p5zh	Divergence at 500 hPa height
p8_f	Geostrophic air flow velocity at 850 hPa height
p8_u	Zonal velocity component at 850 hPa height
p8_v	Meridional velocity component at 850 hPa height
p8_z	Vorticity at 850 hPa height
p850	850 hPa geopotential height
p8th	Wind direction at 850 hPa height
p8zh	Divergence at 850 hPa height
prcp	Precipitation total
s500	Specific humidity at 500 hPa height
s850	Specific humidity at 850 hPa height
shum	Near surface specific humidity
temp	Mean temperature at 2 meters

\* Source: ECCC n.d.-b

**2.4.2. Statistical downscaling of SAT and SWE**

This section examines in detail the procedure to statistically downscale SAT and SWE time series using NCEP/NCAR and GCM data. Figure 2-5 illustrates the main steps of statistical downscaling as conceived by Wilby and Dawson (2007) for the software SDSM 4.2.9 (Wilby and Dawson 2011). The diagram shows the input data (parallelogram shape in green) and the ten main operations that a user can undertake within the software

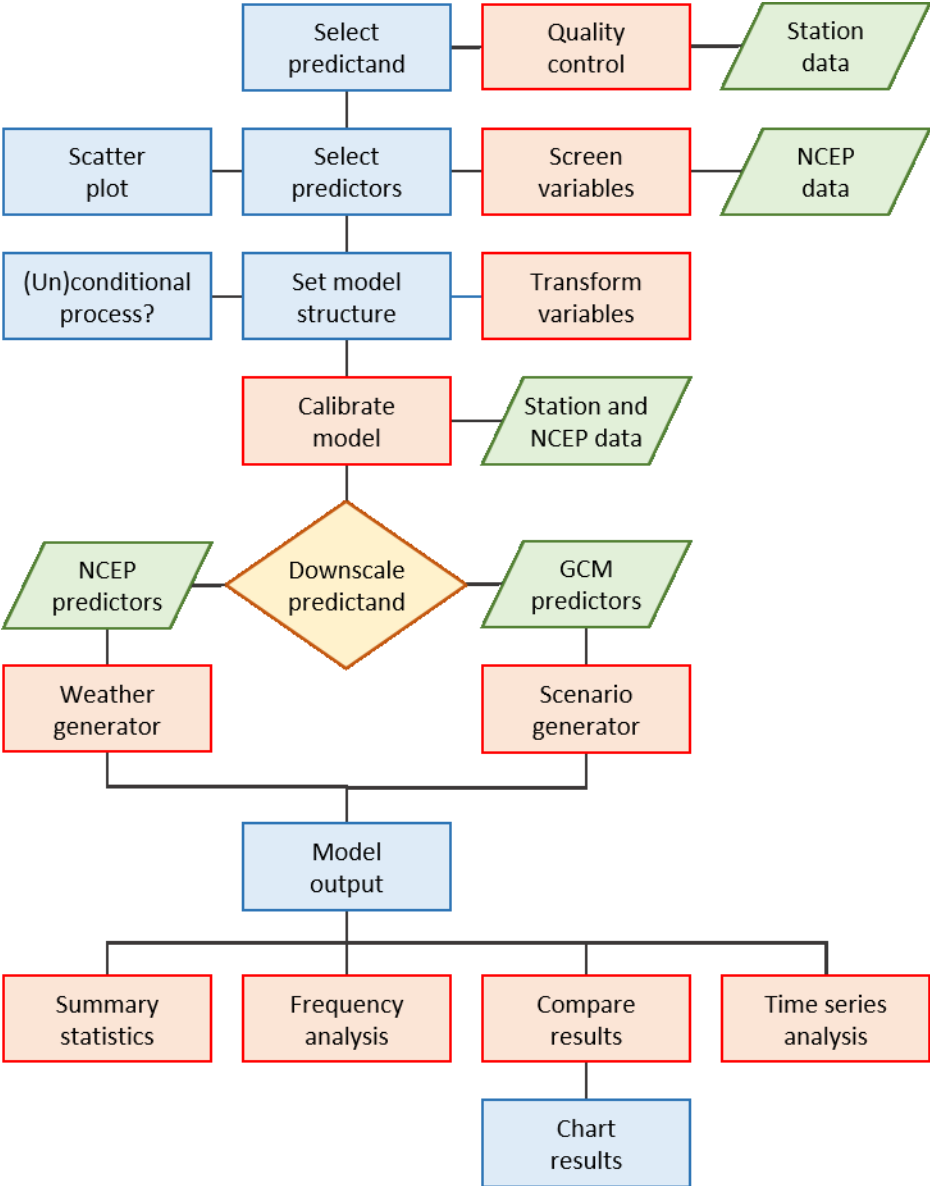


**Figure 2-5: Conceptual framework of SDSM 4.2.9 (Wilby and Dawson 2007, 13)**

interface (rectangular shape in red). The methodology used in this part of research follows a similar workflow. Accordingly, this section is divided into the following five parts: preprocessing of the station data, model calibration, model validation, reconstruction of historical series, and generation of future scenarios. It has to be mentioned that two distinct versions of the software are employed in this research: SDSM 5.2 (Wilby and Dawson 2015b) and SDSM 4.2.9 (Wilby and Dawson 2011). The most recent version of SDSM has additional capabilities (e.g., testing the stability of the models through cross-validation techniques), but does not include the scenario generation functionality (Wilby and Dawson 2015a). Thus, this last step is completed using SDSM 4.2.9. For simplicity, the general term SDSM hereinafter refers to either versions of the software.

#### **2.4.2.1. Preprocessing**

As mentioned in Section 2.4.1.1, thirteen climate stations are selected for this research (see Figure 2-3 and Table 2-2). However, only ten stations provide time series that are sufficiently long to be used for statistical downscaling purposes (data from the remaining three stations are included in the analysis of snowpack characteristics in Section 2.4.4.1). These longer time series, grouped by climate variable (i.e., maximum SAT, minimum SAT, and SWE), are listed in Table 2-4. For each time series, the table shows its length (first day, last day, and total number of days), the number of actual values that passed the QA check, the percentage of missing records, the main statistics (maximum, minimum, range, median, and mean), and the climate station where it was recorded. Maximum and minimum SAT data are available for all the ten stations,

**Table 2-4: General characteristics and statistics of all the climate time series used for statistical downscaling purposes**

Variable	Station	Start	End	Days	Records	% Missing	Max	Min	Range	Median	Mean
Max SAT (°C)	Bigfork 13S	1/1/1961	12/31/2005	16,436	14,552	11.46	38.3	-23.3	61.6	11.7	12.7
	Hot Springs Mt.	6/10/1991	12/31/2005	5,319	5,275	0.83	41.1	-17.8	58.9	14.4	15.1
	Kraft Creek	7/30/1990	12/31/2005	5,634	5,569	1.15	36.5	-25.9	62.4	10.6	11.6
	Missoula Airport	1/1/1961	12/31/2005	16,436	16,436	0.00	40.6	-25.0	65.6	13.3	13.7
	Moss Peak	7/13/1989	12/31/2005	6,016	5,968	0.80	31.6	-30.7	62.3	5.8	6.8
	North Fork Jocko	8/28/1989	12/31/2005	5,970	5,933	0.62	32.4	-25.1	57.5	7.2	8.3
	Polson Kerr Dam	1/1/1961	12/31/2005	16,436	16,058	2.30	38.9	-24.4	63.3	13.3	13.9
	Saint Ignatius	1/1/1961	12/29/2005	16,434	15,643	4.81	38.9	-28.9	67.8	13.9	14.5
	Seeley Lake RS	1/1/1961	12/31/2005	16,436	15,831	3.68	38.3	-25.0	63.3	12.2	12.9
Superior	1/1/1961	12/31/2005	16,436	15,810	3.81	41.1	-20.6	61.7	15.0	15.6	
Min SAT (°C)	Bigfork 13S	1/1/1961	12/31/2005	16,436	14,794	9.99	23.9	-32.8	56.7	2.2	2.4
	Hot Springs Mt.	6/10/1991	12/31/2005	5,319	5,277	0.79	22.2	-29.4	51.6	2.2	2.5
	Kraft Creek	7/29/1990	12/31/2005	5,635	5,505	2.31	17.7	-34.8	52.5	-0.2	-0.7
	Missoula Airport	1/1/1961	12/31/2005	16,436	16,436	0.00	19.4	-34.4	53.8	0.6	0.4
	Moss Peak	7/15/1989	12/31/2005	6,014	5,851	2.71	16.6	-36.3	52.9	-2.2	-2.1
	North Fork Jocko	8/28/1989	12/31/2005	5,970	5,776	3.25	12.7	-38.3	51.0	-2.7	-3.7
	Polson Kerr Dam	1/1/1961	12/31/2005	16,436	16,309	0.77	22.2	-33.3	55.5	1.7	2.1
	Saint Ignatius	1/1/1961	12/29/2005	16,434	15,807	3.82	21.7	-36.1	57.8	1.7	1.1
	Seeley Lake RS	1/1/1961	12/31/2005	16,436	16,180	1.56	17.8	-42.8	60.6	-1.1	-2.2
Superior	1/1/1961	12/31/2005	16,436	15,945	2.99	20.0	-33.3	53.3	1.1	1.2	
SWE (mm)	Kraft Creek	9/5/1980	12/31/2005	9,249	9,249	0.00	770	0	770	8	97
	Moss Peak	7/11/1985	12/31/2005	7,479	7,479	0.00	1,849	0	1,849	290	387
	North Fork Jocko	9/24/1989	12/31/2005	5,943	5,943	0.00	1,801	0	1,801	282	423

whereas only three of them, which belong to the SNOTEL network, also provide SWE data. Figure 2-4 illustrates the location of the ten climate stations listed in Table 2-4, including the three SNOTEL stations (in blue).

While NCEP/NCAR and GCM data are ready to be inserted into SDSM, daily time series of SAT and SWE need to be preprocessed and converted into a format readable by the software. All the preprocessing operations are conducted by means of the open-source software RStudio (RStudio Team 2015). As NCEP/NCAR reanalysis data obtained from the CCCma are available only for the period 1961-2005 (see Section 2.4.1.2), climate station time series are adjusted accordingly to match this time period. Some series are truncated, while others are extended and populated with missing records (i.e., -999). As a result, continuous daily time series of SAT and SWE are created that comprise dates between 1 January 1961 and 31 December 2005 for a total of 16,436 records. Maximum and minimum SAT series are therefore ready to be input into SDSM for calibration (see next section), whereas further preprocessing is required for the SWE variable.

Two daily time series are created from the original SWE time series: one, called Snow Accumulation (SA), including daily increments in snow cover (due to snowfall) and another, called Snow Melt (SM), comprising daily decreases in snow cover (due to snowmelt). These two daily series are populated based on the following equation:

$$\Delta SWE_d = SWE_d - SWE_{d-1}, \quad (1)$$

where  $\Delta SWE_d$  is the alteration in SWE on a given day ( $d$ ), which is equivalent to the difference between the SWE observed on that day ( $SWE_d$ ) and the SWE observed on

the previous day ( $SWE_{d-1}$ ). Based on the resulting  $\Delta SWE_d$  values, three outcomes are possible, as follows:

$$\text{if } \Delta SWE_d > 0 \Rightarrow SA_d = \Delta SWE_d \ \& \ SM_d = 0, \quad (2)$$

$$\text{if } \Delta SWE_d < 0 \Rightarrow SA_d = 0 \ \& \ SM_d = |\Delta SWE_d|, \quad (3)$$

$$\text{if } \Delta SWE_d = 0 \Rightarrow SA_d = 0 \ \& \ SM_d = 0, \quad (4)$$

where  $SA_d$  and  $SM_d$  are the snow accumulation and the snow melting values on a given day ( $d$ ), respectively. Also, if either  $SWE_d$  or  $SWE_{d-1}$  are missing, then  $\Delta SWE_d$  is not calculated and both  $SA_d$  and  $SM_d$  are considered as missing (i.e., -999). Finally, if  $SWE_d$  is null (i.e., no snow on the ground),  $SM_d$  is considered as missing because it is not possible for snowmelt to occur (Tryhorn and DeGaetano 2013). The SWE variable, expressed as SA and SM time series, is now ready to be input into SDSM for calibration.

#### **2.4.2.2. Calibration**

Calibration entails identifying a statistical relationship between a specific subset of large-scale NCEP/NCAR predictors and a local-scale predictand (i.e., the climate station variable). The number and type of predictors and the parameters associated with this relationship vary by location and climate time series (i.e., maximum SAT, minimum SAT, SA, and SM). Therefore, the calibration process has to be repeated each time. In this research, 26 different statistical downscaling models had to be generated. There are three main steps towards the calibration of each statistical model, as shown in the first part of the diagram in Figure 2-5. These include selecting and checking the quality of the predictand time series, screening and selecting the NCEP/NCAR predictors, and setting the model structure (Wilby and Dawson 2007).

Once a predictand time series is loaded into SDSM, the software can first run a basic QA review to identify potential gross data errors, missing data codes, and outliers. For example, to unveil outliers, it is possible to check if the difference between two consecutive days exceeds a certain threshold. The second step, which is the most critical and time-consuming of the entire process, deals with the choice of the NCEP/NCAR predictors. The user's expertise, local knowledge, and judgement are fundamental to identify predictors that, from a physics standpoint, are likely to control the predictand outcomes. This step is assisted by SDSM through the possibility of visually inspecting the data via scatter plots (one predictand vs. one predictor), deriving monthly, seasonal, or annual correlation and partial correlation matrices (one predictand vs. up to a maximum of twelve predictors), and calculating the explained variance by month and predictor with a significance level of 0.05. As third step, the user needs to specify the structure of the model, including its temporal resolution (monthly, seasonal, or annual) and the nature of the downscaling process (conditional or unconditional).

While annual models compute a single set of parameters, monthly and seasonal models account for intra-annual variability by calculating different model parameters for each month or season, respectively. Conditional models work on the assumption that an intermediate process mediates the relationship between large-scale climate forcing and local weather (e.g., like precipitation, where its amounts depend on wet-day occurrence, which, in turn, depends on large-scale predictors such as atmospheric pressure and humidity), whereas unconditional models presuppose that predictors and predictand are directly connected (e.g., like local wind speeds, which may be a function of large-scale

airflow indices such as airflow strength and vorticity). In the case of conditional processes, it is also possible to apply selected transformations (e.g., fourth root and natural log) to predictand variables that present a skewed distribution. For example, a fourth root transformation is employed for downscaling precipitation in Wilby et al. (2014). These authors also acknowledge that the choice of the distribution may affect the robustness of the model as much as the amount of data available for calibration.

Once the model structure is set, the statistical model can be calibrated (Figure 2-5) using either the Dual Simplex (DS; Lemke 1954) or the Ordinary Least Squares (OLS; Gauss 1809) optimization algorithm (Wilby and Dawson 2007). In the case of OLS, SDSM offers the option to build the model via stepwise regression by progressively adding more variables into it and selecting the most parsimonious model according to either the Akaike's Information Criterion (Akaike 1974) or the Bayesian Information Criterion (Schwarz 1978). If necessary, an autoregressive component (i.e., a lagged predictand) can be inserted into the model as an additional predictor. It is also possible to assess the stationarity of the model through the Chow test (Chow 1960), which indicates if there is a break point or a trend in the time series by comparing the first and the second half of the dataset. Finally, a k-fold cross-validation technique (Mosteller and Tukey 1968) can be applied to evaluate model stability within the observed data (Wilby and Dawson 2015a). These data are first divided into k equal-size subsamples, then each subsample is fitted and tested against the remainder.

Table 2-5 shows the model structure and calibration options that are set for each climate time series. Air temperature and snow precipitation follow clear seasonal cycles

in the Flathead Region. Thus, calculating a single set of parameters for the entire year is not recommended in this case. After preliminary analyses on climate series from different stations, monthly and seasonal models are expected to provide the best results for SAT and SWE-related variables, respectively. Also, unconditional models are a better fit for maximum and minimum SAT because a direct link is presumed to exist between large-scale forcing and local air temperature (Wilby and Dawson 2007). Conversely, conditional models, which depend on an intermediate process such as the probability of snow-day occurrence, perform better in the case of SA and SM time series (Tryhorn and DeGaetano 2013). In this instance, snow presence/absence is first modeled as a function of the large-scale predictors. Then, the magnitude of increase (or decrease) is estimated based on a different set of predictor parameters.

**Table 2-5: Model structure and calibration options per climate time series**

	<b>Max SAT</b>	<b>Min SAT</b>	<b>SA</b>	<b>SM</b>
<b>Model type</b>	Monthly	Monthly	Seasonal	Seasonal
<b>Process</b>	Unconditional	Unconditional	Conditional	Conditional
<b>Predictand transformation</b>	No	No	Fourth root	No
<b>Optimization algorithm</b>	DS	DS	DS	DS
<b>Autoregressive component</b>	Yes	Yes	No	No
<b>Chow test</b>	Yes	Yes	Yes	Yes
<b>Cross validation</b>	10 folds	10 folds	2 folds	2 folds

Based on a preliminary assessment of the performance of OLS and DS, the latter is selected as the optimization algorithm for all four time series. Before running the DS

algorithm, the SA variable requires a transformation because the data distribution is skewed. As in the case of rain precipitation (Wilby et al. 2014), the best choice seems to be a fourth root transformation. An autoregressive term is also added to the statistical downscaling models in the case of the SAT variables, while the SA and SM models do not perform better when an autoregressive component is included. Finally, both the Chow and k-fold cross-validation tests are undertaken to evaluate model stationarity and stability, respectively. As temperature time series are generally longer than snow time series, ten folds are considered for cross-validating SAT models whereas two folds for SWE-related models. In the first case, 90% of the data are used to calibrate the models and 10% to validate them; this process is repeated ten times, each one with a different 10% block of data. In the second case, the dataset is equally divided into two halves, one reserved for calibration and the other for validation; on the following run, the 50% blocks of data are reversed.

#### **2.4.2.3. Validation**

Once the 26 statistical downscaling models are calibrated, they can be validated using the stochastic weather generator in SDSM (Figure 2-5). This tool generates up to a maximum of 100 ensemble sequences of synthetic daily climate series given NCEP/NCAR predictor variables and regression model parameters derived from the calibration process. This procedure is applied to independent data that have not been used for calibrating the model. As illustrated in the last part of the diagram in Figure 2-5, observed and downscaled data related to the same validation period can be analyzed and compared in SDSM through summary statistics, frequency analysis, monthly

statistics charts (i.e., compare results screen), and time series analysis. Each model can be accepted or rejected based on its robustness, stability, and ability to reproduce the observed data. To validate the statistical downscaling models, two distinct sets of analyses are conducted by means of the software RStudio (RStudio Team 2015): one for the air temperature variables, the other one for the snow-related variables.

Daily observed and simulated SAT time series are compared over the validation period through a simple linear regression analysis. The ensemble mean of 100 different stochastically-generated sequences is taken as the independent variable, whereas the observed time series as dependent variable. In addition, several monthly, seasonal, and annual statistics are calculated for the ensemble mean and the observed daily series. These basic statistics include mean, median, maximum, minimum, variance, Peaks Over Threshold (POT), Peaks Below Threshold (PBT), and 95<sup>th</sup> percentile. In this research, the POT statistic corresponds to the number of days in a year that show a daily maximum SAT and a daily minimum SAT higher than 25°C and 0°C, respectively. Similarly, the PBT statistic coincides with the number of days in a year when daily maximum SAT is below 0°C and daily minimum SAT is lower than -15°C. The error between the statistics derived from the observed time series and those extracted from the ensemble mean is also computed. Finally, the maximum and minimum mean monthly, seasonal, and annual values among the 100 ensemble members are reported as a way to display the potential prediction error.

An intermediate step is required to validate the statistical downscaling models for the snow-related variables. For each of the 100 daily sequences synthesized by the

weather generator tool, SM is subtracted from SA on a daily fashion to derive SWE increments. Then, the 100 ensemble mean is extracted and the cumulative SWE is calculated from the 1<sup>st</sup> of September of one year to the 31<sup>st</sup> of August of the following year, hereinafter referred to as pseudo water year due to the similarity to the commonly used water year (1 October - 30 September) defined by the United States Geological Survey agency. The pseudo water year allows us to account for snowfall events that occur in September and contribute to the winter snowpack. Finally, the daily mean over the entire validation period, which includes pseudo water years from 2001 to 2005, is computed for both the observed and simulated SWE time series. The two resulting 365-day long SWE series (leap days are excluded from the analysis) are compared for validation purposes in two different ways.

First, ten indices that represent the main characteristics of the annual snowpack are calculated for both observed and synthesized series. Table 2-6 describes these ten indices and specifies the related identification codes that will be used to display the results (see Section 2.5.1.2). Most of the indices are adapted or derived from those mentioned in either Clow (2010) or Tryhorn and DeGaetano (2013). Each pair of SA-SM statistical downscaling models is accepted or rejected based on its ability to reproduce these snowpack characteristics. Second, similarly to the SAT validation procedure, a simple linear regression is conducted between the observed and simulated 1826-day long (i.e., entire dataset) SWE series as well as between the observed and simulated 365-day long (i.e., 5-year mean) SWE series. The same process is applied to pairs of observed/simulated SA, SM, and SWE increment series that are calculated from the

corresponding observed and simulated SWE series. This analysis provides supplementary information regarding the skills of the statistical downscaling models. A graphic reproduction of the observed/simulated 365-day long SWE series at each location (i.e., Kraft Creek, Moss Peak, and North Fork Jocko) is also provided for visual comparison.

**Table 2-6: Indices that define annual snowpack characteristics**

<b>Code</b>	<b>Description</b>
MSWE	Annual maximum value of SWE (mm)
DMSWE	Date of annual maximum SWE
SMO	Onset of snow melt: beginning of the first 5-day period during which SWE has decreased by at least 12.7 mm (half inch)
SM50	Date on which half of the snowpack has melted (based on maximum SWE)
1ASWE	SWE value on the 1 <sup>st</sup> of April (mm)
PSO	Onset of permanent snowpack; permanent is defined as a period during which SWE never falls below 5.08 mm (0.2 inches)
PSE	End of permanent snowpack; permanent is defined as a period during which SWE never falls below 5.08 mm (0.2 inches)
PSD	Duration of permanent snowpack: number of days between PSO and PSE
SMD	Duration of snow melt: number of days between SMO onset and PSE
SWE0	SWE zero: number of days without snow on the ground; absence of snow is defined as any SWE value smaller than 5.08 mm (0.2 inches)

Before moving to the next step, it is necessary to highlight the importance of choosing the best timeframe for calibrating and validating the statistical downscaling models. Wilby et al. (2014) recommend that any period within 1961-2000 should be used to calibrate the model because this timeframe has relatively high data quality/availability and is long enough to capture a wide range of conditions without being influenced by any signals from anthropogenic forcing. Therefore, in this research,

the calibration periods are always selected from within 1961-2000. Whenever possible, the 1961-2000 period is divided into two halves, one for calibrating the model (1961-1980) and the other one for validation (1981-2000).

However, it is not always possible to acquire data from these decades. Hot Springs Montana and the three SNOTEL stations were installed in the 1980s and early 1990s, therefore providing SAT and/or SWE data only for the recent past (see Table 2-4). In these cases, the calibration period is still within the recommended 1961-2000 timeframe, whereas the validation period extends until the year 2005. Extra caution is taken to check for the stationarity of these climate time series (i.e., absence of break points or trends within the datasets) through the Chow test (see Section 2.4.2.1). A description of the specific temporal intervals that are considered for the calibration and validation of each statistical downscaling model is given in Section 2.5.1.

#### **2.4.2.4. Reconstruction of historical series**

The weather generator included in SDSM (see Figure 2-5) can be used not only for validation purposes but also for infilling missing records and reconstructing historical climate series within 1961-2005, timeframe for which NCEP/NCAR predictors are available (see Section 2.4.1.2). As already mentioned, SAT data from Hot Springs Montana and data from the SNOTEL stations have been recorded starting from the 1980s at best. In these situations, if a robust statistical predictand-predictor relationship is identified, the weather generator serves as a means to synthesize continuous daily series of SAT, SA, and SM beginning on 1 January 1961. Sporadic missing records or longer gaps in the observed time series of other climate stations can also be infilled

using the same tool. In all these cases, the ensemble mean of 100 different synthetic daily sequences is eventually considered for replacing missing data. However, all the SAT ensemble members will be used later in this research to estimate potential errors in the predicted SAT time series (Section 2.4.3.3).

#### **2.4.2.5. Scenario generation**

Like the weather generator, the scenario generator synthesizes up to a maximum of 100 daily sequences using the model parameters calibrated and validated in the previous steps (see Figure 2-5). The main difference consists in setting the CanESM2 output variables as predictors, rather than the NCEP/NCAR data. As mentioned in Section 2.4.1.2, CanESM2 generates the same 26 large-scale predictors as NCEP/NCAR (Table 2-3) but for a future period (1 January 2006 to 31 December 2100) and for three distinct emissions scenarios (RCP2.6, RCP4.5, and RCP8.5). If the initial predictand-predictor relationship is now transferred to the CanESM2 outputs, it is possible to synthesize maximum SAT, minimum SAT, SA, or SM daily time series over the period 2006-2100 at the corresponding climate station that provided the data for building the downscaling model. In this case, the ensemble mean represents the final sequence that will be considered for the comparison and analysis of climate trends (Section 2.4.3.4) and the SAT ensemble members will provide a way to display the potential error associated with the SAT future simulations (Section 2.4.3.3).

### 2.4.3. Analysis of SAT 30-year mean and variability and SAT trends

Once maximum SAT and minimum SAT are statistically downscaled for the ten climate stations in the Flathead Region (see Figure 2-4 and Table 2-4), these variables are analyzed to identify long-term changes and potential trends. The structure of this section resembles the workflow presented in Figure 2-6. In the initial step (Section 2.4.3.1), complete daily maximum and minimum SAT time series are assembled using both observed and downscaled values generated within SDSM. To summarize this information, monthly, seasonal, and annual SAT means are computed for all available SAT time series (Section 2.4.3.2). These data form the basis of the following two comparative analyses. On the one hand, SAT normals and intra-annual monthly SAT variability are calculated over different 30-year periods to evaluate long-term changes in air temperature (Section 2.4.3.3). On the other hand, Mann-Kendall and regional Kendall tests are undertaken to identify trends in air temperature (Section 2.4.3.4). All the analyses are conducted by means of the software RStudio (RStudio Team 2015).

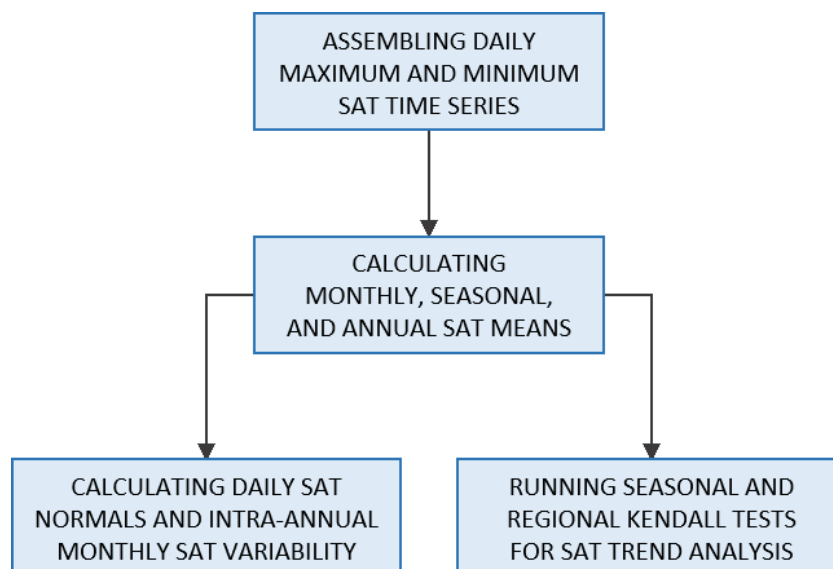


**Figure 2-6: Workflow for the analysis and comparison of SAT trends**

### **2.4.3.1. Complete daily maximum and minimum SAT time series**

As an initial step, new maximum and minimum SAT daily series are assembled that include observed values until 31 August 2018 (Section 2.4.1.1 and Table 2-2), NCEP/NCAR-downscaled values within 1961-2005 (Section 2.4.2.4), and CanESM2-downscaled values within 2006-2100 (Section 2.4.2.5). To combine them into a single time series, the precedence is obviously given to the observed data; if missing, either historical or future downscaled data are considered. Due to the ensemble size set for the weather and scenario generators, each time series actually consists of 100 different sequences, in which observed values are simply duplicated. As already mentioned, this will provide a way to estimate the potential error associate with each simulation (see Section 2.4.3.3). Also, it is noted that three different datasets are created for each location and SAT variable because three distinct scenarios are considered in this research (RCP2.6, RCP4.5, and RCP8.5). The first parts of these three datasets are identical (both observed and downscaled historical values), while the second parts differ from each other as they represent distinct future scenarios.

Each SAT time series comprises 51,114 continuous daily records starting from 1 January 1961 to 31 December 2100 (leap days are not included after 31 August 2018). All the twenty SAT time series (see Table 2-4) are characterized by these equally long blocks of data within 1961-2100. Most of the analyses in this chapter are based on this timeframe because it allows for the comparison between different climate stations. However, six stations provide records older than 1961. This information is also precious and will be used to enrich part of the study (see Section 2.4.3.3). Therefore, records

older than 1961 are added to the corresponding time series. This additional block of data can be discontinuous as missing records cannot be replaced by the weather generator. Table 2-7 presents the main characteristics of the SAT time series before 1961, including the source climate station, the period of record (first day, last day, and total number of days), the number of actual values, and the percentage of missing data. In summary, the twenty daily maximum and minimum SAT time series consist of a block of continuous records within 1961-2100 and, in some instances, a second block of discontinuous records before 1961. Such time series are ready for further processing.

**Table 2-7: Characteristics of SAT time series before 1961**

Variable	Station	Start	End	Days	Records	% Missing
Max SAT	Bigfork 13S	11/1/1938	12/31/1960	8,097	8,051	0.57
	Missoula Airport	1/1/1948	12/31/1960	4,749	4,749	0.00
	Polson Kerr Dam	3/22/1951	12/31/1960	3,573	3,554	0.53
	Saint Ignatius	2/6/1896	12/31/1960	23,705	19,910	16.01
	Seeley Lake RS	10/16/1936	12/31/1960	8,843	8,493	3.96
	Superior	1/1/1914	12/31/1960	17,167	15,807	7.92
Min SAT	Bigfork 13S	11/1/1938	12/31/1960	8,097	8,056	0.51
	Missoula Airport	1/1/1948	12/31/1960	4,749	4,749	0.00
	Polson Kerr Dam	3/22/1951	12/31/1960	3,573	3,551	0.62
	Saint Ignatius	2/6/1896	12/31/1960	23,705	19,938	15.89
	Seeley Lake RS	10/18/1936	12/31/1960	8,841	8,518	3.65
	Superior	1/1/1914	12/31/1960	17,167	15,863	7.60

#### **2.4.3.2. Monthly, seasonal, and annual SAT means**

The second step consists in calculating monthly, seasonal, and annual means over the entire length of each daily SAT time series assembled in the previous step. This process follows the standard procedures as defined by the World Meteorological Organization (WMO; WMO 1989). In particular, either maximum or minimum SAT means are computed as follows:

$$MM_{m,y}^{SAT} = \frac{\sum_{d=1}^n SAT_{d,m,y}}{n}, \quad (5)$$

$$SM_{s,y}^{SAT} = \frac{\sum_{m=1}^3 MM_{m,s,y}^{SAT}}{3}, \quad (6)$$

$$AM_y^{SAT} = \frac{\sum_{m=1}^{12} MM_{m,y}^{SAT}}{12}, \quad (7)$$

where  $MM_{m,y}^{SAT}$  is the monthly mean of SAT for any given month ( $m$ ) and year ( $y$ );  $SAT_{d,m,y}$  is the value of SAT at any given day ( $d$ ), month ( $m$ ), and year ( $y$ );  $n$  is the number of days in a month with actual SAT records;  $SM_{s,y}^{SAT}$  is the seasonal mean of SAT for any given season ( $s$ ) and year ( $y$ );  $MM_{m,s,y}^{SAT}$  is the monthly mean of SAT for any given month ( $m$ ), season ( $s$ ), and year ( $y$ ); and  $AM_y^{SAT}$  is the annual mean of SAT for any given year ( $y$ ).

The so-called “3/5 rule” is applied for Equation 5. According to this rule, “if more than 3 consecutive daily values are missing or more than 5 daily values in total in a given month are missing, the monthly mean [in this case  $MM_{m,y}^{SAT}$ ] should not be computed and the year-month mean should be considered as missing” (WMO 1989, 5). Therefore,  $n$  can vary between 23 to 31 in Equation 5. Regarding Equations 6 and 7, the seasonal and annual means are computed only if the year-month mean exists for all three and twelve months, respectively; otherwise, the seasonal and/or annual mean for that year are considered as missing (WMO 1989). For these data, the 3/5 rule affects only the blocks of data before 1961 because there are no daily missing records beginning in 1961. It is important to remember that monthly, seasonal, and annual means are calculated for the ensemble mean (i.e., the daily mean among 100 ensemble sequences) of each of the

twenty SAT time series. In addition, the monthly mean is computed among the 100 ensemble sequences within each time series. The results obtained so far are used in the next two sets of analyses (Sections 2.4.3.3 and 2.4.3.4).

### 2.4.3.3. SAT normals and intra-annual monthly SAT variability

Climate is defined as the mean and variability of relevant variables (e.g., temperature and precipitation) usually over a period of 30 years (IPCC 2013). Therefore, a way to detect changes in climate is to compare means and variabilities of any climate variable calculated over different 30-year timeframes. In this research, SAT normals and intra-annual monthly SAT variability are computed over a 30-year window moving every ten years. According to the WMO standard procedures (WMO 1989), monthly, seasonal, and annual normals (either maximum or minimum SAT) are calculated as follows:

$$MN_{m,p}^{SAT} = \frac{\sum_{y=1}^k MM_{m,y,p}^{SAT}}{k}, \quad (8)$$

$$SN_{s,p}^{SAT} = \frac{\sum_{m=1}^3 MN_{m,s,p}^{SAT}}{3}, \quad (9)$$

$$AN_p^{SAT} = \frac{\sum_{m=1}^{12} MN_{m,p}^{SAT}}{12}, \quad (10)$$

where  $MN_{m,p}^{SAT}$  is the monthly normal of SAT for any given month ( $m$ ) and 30-year period ( $p$ );  $MM_{m,y,p}^{SAT}$  is the SAT monthly mean derived from Equation 5 for any given 30-year period ( $p$ );  $k$  is the number of years within a 30-year period with available monthly means;  $SN_{s,p}^{SAT}$  is the seasonal normal of SAT for any given season ( $s$ ) and 30-year period ( $p$ );  $MN_{m,s,p}^{SAT}$  is the monthly normal of SAT for any given month ( $m$ ), season ( $s$ ), and 30-year period ( $p$ ); and  $AN_p^{SAT}$  is the annual normal of SAT for any given 30-year period ( $p$ ).

As with the calculation of monthly means (Section 2.4.3.2), the 3/5 rule is applied to data older than 1961 that are input in Equation 8. According to this rule, “if for a given month (e.g. January) 3 consecutive year-month values (e.g. January 1970, 1971, 1972) are missing or more than 5 values in total for the given month are missing, the 30-year standard normal [in this case  $MN_{m,p}^{SAT}$ ] should not be calculated” (WMO 1989, 8). Thus,  $k$  can range between 25 and 30 in Equation 8. In addition, the intra-annual monthly SAT variability, which quantifies the amount of variation of SAT monthly normals within each 30-year period, is computed as follows:

$$AV_p^{SAT} = \sqrt{\frac{\sum_{m=1}^{12} (MN_{m,p}^{SAT} - AN_p^{SAT})^2}{12}}, \quad (11)$$

where  $AV_p^{SAT}$  is the intra-annual monthly variability of SAT for any given 30-year period ( $p$ ), whereas  $MN_{m,p}^{SAT}$  and  $AN_p^{SAT}$  are derived from Equations 8 and 10, respectively. Equations 9, 10, and 11 are executed only if monthly normals are available for all three/twelve months; otherwise,  $SN_{s,p}^{SAT}$ ,  $AN_p^{SAT}$ , and/or  $AV_p^{SAT}$  are considered as missing.

The monthly normals are calculated through Equation 8 for the 100 sequences of monthly means derived in the previous step (Section 2.4.3.2) for each of the twenty original time series. Three new series of monthly normals are generated based on the 100-ensemble mean, maximum, and minimum. In other words, the mean, maximum, and minimum normal values are extracted from the 100 normal values within each 30-year period. Equations 9 and 10 are computed using these three series as inputs. As a result, all monthly, seasonal, and annual normals are associated with upper and lower

limits that define the range of potential prediction error. Obviously, upper and lower limits of any normal derived exclusively from observed data coincide with the normal value itself. Differently, Equation 11 is executed only using monthly and annual normal time series originated from the 100-ensemble mean.

As mentioned at the beginning of this section, normals and variabilities are calculated over a 30-year window moving every ten years. Thus, twelve intervals are defined that are in common among all SAT series: 1961-1990, 1971-2000, 1981-2010, 1991-2020, 2001-2030, 2011-2040, 2021-2050, 2031-2060, 2041-2070, 2051-2080, 2061-2090, 2071-2100. Based on data availability and after applying the 3/5 rule (WMO 1989), additional 30-year periods starting before 1961 can be identified for specific climate stations, as indicated in Table 2-8. If all possible 30-year periods are considered, long-term changes in maximum and minimum SAT can be investigated within each climate station. This information will be displayed through graphics (see Section 2.5.1.3). If only 1961-2100 is considered, then it is possible to undertake a comparative study among all climate stations to understand the spatial variability of air temperature across the Flathead Region. This information will be portrayed through maps and graphics (see Section 2.5.2.1).

**Table 2-8: Additional 30-year periods starting before 1961 per climate station**

Variable	Station	#	30-year periods
Max SAT & Min SAT	Bigfork 13S	2	1941-1970, 1951-1980
	Missoula Airport	1	1951-1980
	Polson Kerr Dam	1	1951-1980
	Saint Ignatius	5	1911-1940, 1921-1950, 1931-1960, 1941-1970, 1951-1980
	Seeley Lake RS	2	1941-1970, 1951-1980
	Superior	4	1921-1950, 1931-1960, 1941-1970, 1951-1980

#### 2.4.3.4. Mann-Kendall and regional Kendall tests for SAT trend analysis

The Mann-Kendall Test (MKT; Mann 1945; Kendall 1975) is a non-parametric test for trend analysis and is very popular in environmental studies. The MKT evaluates whether there is a monotonic upward or downward trend of any variable of interest ( $Y$ ) over time ( $T$ ). A monotonic trend is a single-direction trend that consistently increases (upward) or decreases (downward) through time. The MKT does not assume normal distribution of the data nor linearity of the trend and it is invariant to power transformations such as logarithms and square roots. The null hypothesis ( $H_0$ ) and the alternative hypothesis ( $H_1$ ) are defined as follows:

$$H_0: \text{prob}[Y_j > Y_i] = 0.5, \quad \text{where time } T_j > T_i, \quad (12)$$

$$H_1: \text{prob}[Y_j > Y_i] \neq 0.5 \quad (\text{two-sided test}). \quad (13)$$

After ordering all data pairs by increasing  $T$ , if the  $Y$  values increase and decrease about the same number of times, there is no correlation between  $Y$  and  $T$  ( $H_0$ ). As  $T$  increases, if  $Y$  values increase more often than decrease or, conversely,  $Y$  values decrease more often than increase, a positive or a negative correlation exists, respectively ( $H_1$ ).

The MKT is based on the calculation of the Kendall's tau ( $\tau$ ) correlation coefficient (Kendall 1975). First, all data pairs ( $Y, T$ ) are ordered by increasing  $T$ . Second, the Kendall's statistic ( $S$ ) is computed as follows:

$$S = P - M, \quad (14)$$

where  $P$  is the number of "pluses", which is the number of concordant pairs ( $Y_j > Y_i$  with  $T_j > T_i$ ), while  $M$  is the number of "minuses", which is the number of discordant pairs ( $Y_j < Y_i$  with  $T_j > T_i$ ). If  $P$  is similar to  $M$ , then  $S$  is close to zero, the null hypothesis is

true, and no trend exists in  $Y$ . On the contrary, if  $P$  significantly diverges from  $M$ , then  $S$  is different from zero, the null hypothesis is rejected, and a trend does exist in  $Y$ . At this point, Kendall's tau is calculated by the following equation:

$$\tau = \frac{S}{n(n-1)/2}, \quad (15)$$

where  $n(n-1)/2$  is the number of possible comparisons among  $n$  data pairs. Thus,  $\tau$  ranges between -1 and 1, which represent a strong negative (i.e., downward trend) and positive (i.e., upward trend) correlation, respectively. Values of  $\tau$  close to zero indicate no correlation (i.e., no trend). Finally, the p value is computed to test for significance of  $\tau$ .  $H_0$  is rejected with small p values, as the likelihood that there is no trend is also small.

The Regional Kendall Test (RKT; Helsel and Frans 2006) is a variation of the MKT. The main purpose of the RKT is to determine whether a consistent trend occurs across a region of interest. Kendall's  $S$  is first calculated for each  $m$  location separately. In technical terms, the location ( $m$ ) works as "blocking variable". Then, the regional Kendall statistic ( $S_r$ ) is derived by summing the individual Kendall's statistics ( $S_L$ ) according to the following equation:

$$S_r = \sum_{L=1}^m S_L. \quad (16)$$

It is important to notice that failing to reject the null hypothesis (i.e., no regional trend exists) may be due to two reasons: 1) there are no trends at most locations or 2) there are clear trends, but they have opposite directions at different locations. Therefore, the RKT is not able to detect this heterogeneity of trend. This is the reason why in this research RKT is supported by MKT, which is applied to single locations.

The seasonal and annual SAT means calculated previously (second stage of the research workflow represented in Figure 2-6 and described in Section 2.4.3.2) are now analyzed by running the MKT and the RKT. To allow for comparison, only the 1961-2100 period is considered. Therefore, each maximum/minimum SAT time series is 140-year long as it is composed by only one seasonal or annual value per year. The MKT is first applied to either maximum or minimum SAT time series for each climate station. Then, the ten stations are combined together through the RKT to evaluate whether a consistent air temperature trend is evident across the entire Flathead Region. In addition to the Kendall's statistic and its variance, the Kendall's correlation coefficient, and the p value, the Theil-Sen's slope (Theil 1950; Sen 1968) is also estimated for each test. This statistic is a measure of the magnitude of change. The Theil-Sen's slope is computed by taking the median of slopes of all lines between pairs of points. All the analyses in this section are conducted by means of the software RStudio (RStudio Team 2015) using the rkt package by Marchetto (2017). This R package is also employed in the following section, every time any test from the Mann-Kendall family is required for analysis.

#### **2.4.4. Analysis of snowpack characteristics and trends**

After investigating SAT, this section focuses on the snow-related variables. The objective is to examine the snowpack characteristics in the Flathead Region and understand how they might change in the future. The section is divided into two distinct sets of analyses. In the first one, snowpack conditions are studied using exclusively observed data from six SNOTEL stations in the study area (see Figure 2-3). In addition to calculating indices that describe the snowpack characteristics, the Snow/Precipitation Ratio (SPR) and the Snow DeNsity (SDN) are the key parameters analyzed in this first part. In the second one, the statistically downscaled SA and SM data (see Section 2.4.2) are used to evaluate potential snowpack trends within 1961-2100. All the analyses are conducted within an RStudio environment (RStudio Team 2015).

##### **2.4.4.1. Snowpack characteristics based on observed SNOTEL data**

As mentioned in Section 2.4.1.1, daily SAT (mean, maximum, and minimum), daily PRE, and daily SDP are considered in this study to support the analysis of SWE. These six variables are recorded in the six SNOTEL stations described in Table 2-2 and illustrated in Figure 2-3. The resulting 36 daily series, grouped by climate variable, are listed in Table 2-9. For each time series, the table shows its length (first day, last day, and total number of days), the number of actual records, the percentage of missing data, the basic statistics (maximum, minimum, range, median, and mean), and the SNOTEL station where it was recorded. The objective of this section is to provide a general picture of the snowpack conditions in the study area over the last two or three decades by analyzing SAT, PRE, SDP, and SWE in a comparative fashion at the local and regional scales.

**Table 2-9: General characteristics and statistics of all the climate time series used for snowpack analysis purposes**

Variable	Station	Start	End	Days	Records	% Missing	Max	Min	Range	Median	Mean
PRE (mm)	Bisson Creek	7/26/1992	8/31/2018	9,533	9,532	0.01	76.2	0.0	76.2	0.0	2.3
	Kraft Creek	9/6/1980	8/31/2018	13,874	13,871	0.02	78.7	0.0	78.7	0.0	2.7
	Moss Peak	7/12/1985	8/31/2018	12,104	12,103	0.01	109.2	0.0	109.2	0.0	4.3
	North Fork Jocko	8/29/1989	8/31/2018	10,595	10,588	0.07	132.1	0.0	132.1	0.0	4.8
	Sleeping Woman	7/24/1992	8/31/2018	9,535	9,535	0.00	55.9	0.0	55.9	0.0	2.5
	Stuart Mountain	9/14/1994	8/31/2018	8,753	8,752	0.01	68.6	0.0	68.6	0.0	3.4
SDP (mm)	Bisson Creek	8/9/2002	8/31/2018	5,867	5,865	0.03	1,600	0	1,600	25	264.8
	Kraft Creek	7/8/2003	8/31/2018	5,534	5,532	0.04	1,829	0	1,829	0	287.3
	Moss Peak	8/7/2002	8/31/2018	5,869	5,853	0.27	4,597	0	4,597	1,067	1,192.9
	North Fork Jocko	7/31/2001	8/31/2018	6,241	6,241	0.00	4,293	0	4,293	889	1,112.8
	Sleeping Woman	8/8/2002	8/31/2018	5,868	5,868	0.00	1,956	0	1,956	178	433.9
	Stuart Mountain	8/6/2002	8/31/2018	5,870	5,870	0.00	3,480	0	3,480	838	976.2
SWE (mm)	Bisson Creek	9/30/1991	8/31/2018	9,833	9,833	0.00	535.9	0.0	535.9	7.6	74.2
	Kraft Creek	9/5/1980	8/31/2018	13,875	13,875	0.00	769.6	0.0	769.6	2.5	95.5
	Moss Peak	7/11/1985	8/31/2018	12,105	12,105	0.00	1,849.1	0.0	1,849.1	320.0	417.6
	North Fork Jocko	9/24/1989	8/31/2018	10,569	10,569	0.00	1,800.9	0.0	1,800.9	271.8	427.9
	Sleeping Woman	9/30/1991	8/31/2018	9,833	9,833	0.00	777.2	0.0	777.2	45.7	133.9
	Stuart Mountain	9/30/1994	8/31/2018	8,737	8,737	0.00	1,389.4	0.0	1,389.4	241.3	339.7

Table 2-9. Continued

Variable	Station	Start	End	Days	Records	% Missing	Max	Min	Range	Median	Mean
Mean SAT (°C)	Bisson Creek	7/25/1992	8/31/2018	9,534	9,508	0.27	25.0	-24.8	49.8	3.6	4.6
	Kraft Creek	7/29/1990	8/31/2018	10,261	10,259	0.02	26.4	-32.0	58.4	4.9	5.4
	Moss Peak	7/13/1989	8/31/2018	10,642	10,619	0.22	23.3	-32.2	55.5	1.4	2.3
	North Fork Jocko	8/28/1989	8/31/2018	10,596	10,570	0.25	21.9	-33.7	55.6	2.0	2.4
	Sleeping Woman	7/23/1992	8/31/2018	9,536	9,508	0.29	25.8	-29.4	55.2	3.3	4.2
	Stuart Mountain	9/13/1994	8/31/2018	8,754	8,753	0.01	23.9	-29.9	53.8	1.4	2.5
Max SAT (°C)	Bisson Creek	7/25/1992	8/31/2018	9,534	9,497	0.39	34.1	-22.2	56.3	7.8	9.5
	Kraft Creek	7/30/1990	8/31/2018	10,260	10,194	0.64	36.5	-25.9	62.4	11.0	11.9
	Moss Peak	7/13/1989	8/31/2018	10,642	10,591	0.48	31.6	-30.7	62.3	6.0	7.1
	North Fork Jocko	8/28/1989	8/31/2018	10,596	10,559	0.35	32.5	-25.1	57.6	7.8	8.9
	Sleeping Woman	7/23/1992	8/31/2018	9,536	9,503	0.35	32.6	-26.7	59.3	7.4	8.7
	Stuart Mountain	9/13/1994	8/31/2018	8,754	8,751	0.03	30.2	-27.5	57.7	5.8	7.1
Min SAT (°C)	Bisson Creek	7/25/1992	8/31/2018	9,534	9,466	0.71	17.4	-27.5	44.9	0.8	0.8
	Kraft Creek	7/29/1990	8/31/2018	10,261	10,125	1.33	17.9	-34.8	52.7	0.5	0.2
	Moss Peak	7/15/1989	8/31/2018	10,640	10,474	1.56	17.5	-36.3	53.8	-1.7	-1.6
	North Fork Jocko	8/28/1989	8/31/2018	10,596	10,399	1.86	12.7	-38.5	51.2	-2.1	-3.3
	Sleeping Woman	7/23/1992	8/31/2018	9,536	9,467	0.72	19.5	-31.7	51.2	-0.1	0.2
	Stuart Mountain	9/13/1994	8/31/2018	8,754	8,741	0.15	20.0	-33.4	53.4	-1.8	-1.3

Three analyses are conducted using data from each SNOTEL station separately. The same three analyses are repeated with an extensive dataset that include records from all the six stations to provide an overview of the regional snowpack conditions. In the first analysis, SWE time series are used to calculate thirteen indices that represent snowpack characteristics. In the second analysis, PRE and SWE are processed to estimate SPR. In the third analysis, SDP and SWE are combined to obtain SDN. Each index and snow-related parameter is examined through the MKT or the Seasonal Kendall Test (SKT; Hirsch, Slack, and Smith 1982) to unveil any local trend within the observed period. RKTs are also undertaken to determine whether any consistent trend exists across the overall Flathead Region.<sup>6</sup> According to Clow 2010, the characteristics of RKT, such as its nonparametric nature, its resistance to outliers, its statistical power for detecting trends over short periods of record with substantial interannual variability, make it a perfect candidate for analyzing SNOTEL data. The study period of each analysis is determined based on data availability of the shortest time series among all the stations and variables of interest (Table 2-9). Each of the three analyses are thoroughly described below.

**Analysis 1.** Thirteen indices derived from daily SWE time series are calculated by pseudo water year (i.e., from the 1<sup>st</sup> of September of one year to the 31<sup>st</sup> of August of the following year; see Section 2.4.2.3) over the period 1994-2018. This choice is dictated by the length of the SWE series recorded at Stuart Mountain (see Table 2-9), which covers 24 pseudo water years in total. Ten indices resemble those listed in Table 2-6, with the only difference that some of them are built using different thresholds.

---

<sup>6</sup> MKT and RKT are used throughout this section. For a detailed description of these tests, please refer to Section 2.4.3.4. SKT, which is part of the MKT family, will be briefly illustrated here (see analysis 3).

Based on the remarks by Strasser et al. (2008), the onset of snowmelt (SMO) is defined as the beginning of the first 5-day period during which SWE has decreased by at least 25.4 mm (one inch). Also, the definition of snow presence/absence, which is at the core of five indices (i.e., SWE0, PSO, PSE, and, consequently, PSD and PMD), is not tied to a specific SWE limit. For example, in Section 2.4.2.3, any SWE amount below 5.08 mm (0.2 inches) was labeled as “no snow”. Instead, in this case, any SWE value different from zero represents presence of snow. The reason why two distinct metrics are used is because the indices are now calculated based on actual values, while in the previous case (i.e., Section 2.4.2.3) the indices were computed using daily means over five years.

In addition to the ten modified indices listed in Table 2-6, three more indices are defined as follows. The onset of snow accumulation (SAO) is the beginning of the first 5-day period of continuous snow on the ground during which SWE reaches at least 15 mm. Similarly, the end of snowmelt (SME) is the conclusion of the last 5-day period of continuous snow on the ground during which SWE reaches at least 15 mm. Finally, the duration of the snow season (SSD) is the difference between SME and SAO. Once these thirteen indices are calculated for each pseudo water year, the MKT is executed over the annual time series of each index. The RKT is also applied using the station location as blocking variable. To evaluate if any upward or downward trend related to any snowpack characteristic (i.e., index) exists, several statistics are provided, including the Kendall’s statistic and its variance, the Kendall’s correlation coefficient, the p value, the Theil-Sen’s slope, and the rate of change over the 24-year study period. Results from all the tests are grouped together in a tabular form for comparison purposes.

**Analysis 2.** The SPR is the percentage of precipitation represented by snowfall and is generally expressed as the ratio between SWE increment (i.e., SA) and PRE. SPR can be related to different temporal scales, usually daily or monthly. In this research, monthly SPR is computed as follows:

$$SPR_m = \frac{\sum_{d=1}^n SA_{m,d}}{\sum_{d=1}^n PRE_{m,d}} = \frac{SA_m}{PRE_m}, \quad (17)$$

where  $m$  is any given month and  $n$  is the number of days ( $d$ ) in that month. The numerator of this ratio is derived by summing all daily SA values in a given month  $m$ . Similarly, the denominator corresponds to the sum of all daily PRE values in that month. The first step of this analysis consists in computing monthly SPR values from October through May. These months present a SPR value greater than 0.05 at all SNOTEL stations.

Theoretically, SPR should range between 0 and 1, indicating that all precipitation falls as rain (SPR = 0) or snow (SPR = 1). However, it is not always the case because limitations in the recording instrumentation may introduce measurement errors. Other factors can cause misreading of SWE or PRE levels, such as foreign material being deposited on the snow pillow or drifting, wind scour, sublimation, and blowing snow being recorded as rainfall (Serreze et al. 1999). According to Serreze et al. (1999) rainfall is mostly underestimated, sometimes providing SPR values greater than 1. To account for these errors, observed rainfall values should be adjusted upward. This condition can be expressed in general mathematical terms as follows:

$$PRE^{Adj} = PRE^{Obs} + PRE^{Err}, \quad (18)$$

where  $PRE^{Adj}$  and  $PRE^{Obs}$  are the adjusted and observed precipitation values, respectively; and  $PRE^{Err}$  is the estimated precipitation amount that has not been recorded due to measurement-related errors. Equation 18 can be executed at different temporal scales (e.g., daily or monthly). At this point, a technique proposed by Serreze et al. (1999) is applied to estimate  $PRE^{Err}$  and, consequently,  $PRE^{Adj}$ . Once  $PRE^{Adj}$  is obtained for each month, it can be inserted into Equation 17 to derive monthly SPR.

Serreze et al. (1999) suggest calculating daily SPR values that meet the two following conditions: 1) the daily increment in SWE ( $SA_d$ ) has to be greater than 25 mm, and 2) only data from January and February of all pseudo water years should be included. In this study, March is also incorporated, but only for the stations located at the highest elevation (i.e., Moss Peak, North Fork Jocko, and Stuart Mountain). Being  $PRE_d$  the precipitation increment on a given day ( $d$ ), the daily SPR ( $SPR_d$ ) is computed as follows:

$$SPR_d = \frac{SA_d}{PRE_d}. \quad (19)$$

According to Serreze et al. (1999), considering only large snowfall events (i.e.,  $SA_d$  greater than 25 mm) minimizes the effects of instrument noise. In addition, it is unlikely that mixed snow/rain precipitation events occur during January and February, and March at high elevations. In other words, the assumption is that all precipitation falls as snow in these months. Based on this assumption (i.e.,  $PRE_d^{Adj} = SA_d$ ), it is possible to combine Equations 18 and 19 and solve for  $PRE_d^{Err}$ , as indicated below:

$$PRE_d^{Err} = SA_d * \left(1 - \frac{1}{SPR_d}\right). \quad (20)$$

Serreze et al. (1999) propose calculating the average ( $a$ ) among all the daily SPR values that meet the two aforementioned conditions and using it to adjust the monthly PRE totals so that Equation 17 can be rearranged as follows:

$$SPR_m = \frac{SA_m}{PRE_m^{Obs} + [SA_m * (1 - 1/a)]} \quad (21)$$

Monthly SPR data are computed by means of Equation 21 from October through May within 1994-2018. The choice of this 24-year period is imposed by the length of the SWE and PRE series recorded at Stuart Mountain (see Table 2-9). Once monthly SPR values are obtained, the PRE (both observed and adjusted), SWE, and SPR monthly averages over the 24 pseudo water years are calculated for each SNOTEL station and the overall Flathead Region. PRE and SWE totals as well as SPR averages of the eight snowy months are finally computed. Results are presented in a tabular form for comparison purposes.

To provide a more dynamic picture of precipitation characteristics during the snow season, potential trends in monthly SPR are investigated at the SNOTEL locations and across the Flathead Region using the MKT and RKT, respectively. These tests are not executed if less than 21 out of 24 values exist within each monthly series. For a qualitative comparison, MKTs and RKT are also applied to monthly means of mean, maximum, and daily minimum SAT values for the same snowy months (i.e., October through May). In this case, air temperature monthly means are calculated using only data recorded on wet days (i.e.,  $PRE_d^{Adj} > 0$ ). The SPR trend tests' results are displayed in a table, together with the statistics of the SAT variable (i.e., mean, maximum, or minimum) that presents the best qualitative monthly correlation with SPR.

**Analysis 3.** Density is one of the fundamental physical properties of snowpack (Pomeroy and Brun 2001). It defines the relationship between snow and its water content and is generally expressed as the ratio between SWE and SDP. Being  $\rho_w$  the density of liquid water, SDN is calculated as follows:

$$SDN = \rho_w \frac{SWE}{SDP}. \quad (22)$$

SDN is generally expressed in  $\text{kg}/\text{m}^3$  and  $\rho_w$  is approximately  $1,000 \text{ kg}/\text{m}^3$  at  $0^\circ\text{C}$ . In this research, daily SDN is first computed by means of Equation 22 for every day when both SWE and SDP are available. Following the directions of Mizukami and Perica (2008), a QA is applied to exclude from the analysis daily SDN values outside the range of 30-1,000  $\text{kg}/\text{m}^3$ . However, only two SDN values of the Moss Peak dataset were finally eliminated. Second, the SDN monthly mean and the Coefficient of Variation of snow Density (CVD), which corresponds to the standard deviation normalized by the mean and provides a measure of intra-monthly variability, are calculated for the snowy months (i.e., October through May) within 2003-2018. The selection of this 15-year period is dictated by the SDP data availability for Kraft Creek (see Table 2-9). Third, SWE, SDP, SDN, and CVD monthly means over the fifteen years are calculated for each SNOTEL station and the entire study area. Results are presented in a tabular form for comparison purposes.

In addition to providing a static picture of the SDN-related characteristics across the Flathead Region, the dynamic of SDN within 2003-2018 is also investigated. Due to the short length of SDN monthly series (i.e., fifteen years), the original MKT cannot serve this purpose. Instead, the SKT, which examines potential trends separately for each month or season and then combines the results into an overall test to increase the

statistical power of the analysis (Hirsch, Slack, and Smith 1982), is a better choice. In other words, the SKT works similarly to the RKT, with the difference that the month or season is used as blocking variable rather than the location. In this research, four SKTs are undertaken for pairs of consecutive months from October through May only if at least 20 values exist within each bimonthly dataset (i.e., October-November, December-January, February-March, April-May). Potential trends in bimonthly SPR are therefore examined at the SNOTEL locations and across the Flathead Region through the SKT and RKT, respectively. In the latter case, a code combining both months and locations is used as blocking variable. For a qualitative comparison, SKTs and RKT are also applied to monthly averages of daily mean, maximum, and minimum SAT values for the same four pairs of successive months. The tests' results are displayed through tables.

#### **2.4.4.2. Potential snowpack trends based on statistical downscaling of SWE**

As explained in Section 2.4.2.1 and indicated in Table 2-4, only three SNOTEL stations (i.e., Kraft Creek, Moss Peak, and North Fork Jocko) provide sufficiently long SWE records that can be used to build a robust statistical downscaling model. Therefore, the analysis of trends in snowpack characteristics concern only these three locations. As an initial step, continuous daily SWE time series are generated by combining observed values until 31 August 2018 (Section 2.4.2.1 and Table 2-9) with NCEP/NCAR-downscaled values within 1961-2005 (Section 2.4.2.4) and CanESM2-downscaled values within 2006-2100 (Section 2.4.2.5). Three different datasets are created for each location because three distinct scenarios are considered in this research (i.e., RCP2.6, RCP4.5, and RCP8.5). The first parts of these three datasets are identical (both observed and

downscaled historical values), while the second parts differ from each other as they represent distinct future scenarios.

To combine observed and simulated values into a single SWE series, all the downscaled daily series have to be preprocessed. First, SA series are converted back to their original order of magnitude by applying a fourth power transformation (see Section 2.4.2.2). Second, all downscaled SM series are subtracted from the corresponding downscaled SA series on a daily basis. Then, the ensemble mean is extrapolated from the 100 ensemble sequences of SWE increment for each dataset. Finally, the cumulative SWE is computed by pseudo water year. In the actual process of assembling observed and simulated SWE series, the precedence is obviously given to the observed data; if missing, either historical or future downscaled data are considered. Each of the resulting nine SWE series (i.e., three climate scenarios times three locations) comprises 51,114 continuous daily records starting from 1 January 1961 to 31 December 2100, as leap days are not included after 31 August 2018.

The next step deals with calculating ten indices that represent snowpack characteristics for the three selected locations. These indices are the same as those described in Table 2-6. Similarly to the validation process (see Section 2.4.2.3), they are computed based on the daily SWE mean among five consecutive years. This process is repeated for all the non-overlapping 5-year timeframes within 1961-2100 so that the resulting series of each index include 28 values. At this point, the MKT and RKT are executed to evaluate if any upward or downward trend related to any snowpack characteristic (i.e., index) exists. Several statistics are reported, such as the Kendall's

statistic and its variance, the Kendall's correlation coefficient, the p value, the Theil-Sen's slope, and the rate of change per decade. Results from all the stations and climate scenarios are grouped together in a tabular form for comparison purposes.

## **2.5. Results**

This section presents the results of all the analyses in this chapter and follows a structure similar to that of the methodological section (see Figure 2-2). It is divided into three main parts. The first one is dedicated to the statistical downscaling of SAT and SWE, with a focus on model calibration and validation (Section 2.5.1). The second one examines the outcomes of the study on air temperature (Section 2.5.1.3). The third one displays the results concerning the analysis of snowpack characteristics (Section 2.5.3). As a general note regarding the seasonal results presented in this section, it is important to mention that seasons are defined as follows: winter (December, January, February), spring (March, April, May), summer (June, July, August), and fall (September, October, November).

### **2.5.1. Statistical downscaling**

This section includes the results of the calibration and validation processes related to the statistical downscaling models of SAT and SWE. These two variables are treated separately throughout the section as the corresponding model structures and SDSM calibration options (see Table 2-5), as well as the types of analyses employed to validate these models (see Section 2.4.2.3), are basically different. The validation of the SWE time series is particularly relevant because the direct downscaling of SWE using SDSM has not been attempted before (see Section 2). Testing the ability of SDSM in downscaling SWE, and, more generally, investigating whether it is possible to determine a robust relationship between SWE and large-scale forcings is the core contribution of this chapter.

### 2.5.1.1. Calibration

**SAT.** Table 2-10 illustrates the large-scale predictors used for statistically downscaling maximum and minimum SAT at each station location (for a definition of the predictor codes, refer to Table 2-3). Mean sea level pressure (mslp) and 500 hPa geopotential height (p500), which is the height of the surface where air pressure is equal to 500 hPa, are two key predictors for both maximum and minimum SAT. Mslp is used in all models, whereas p500 is used in all but one (i.e., minimum SAT at Seeley Lake RS). That mslp and p500 are fundamental predictors is not unexpected, because air pressure is strongly related to air temperature. As air temperature increases, the air expands, becomes less dense, and rises up in atmosphere. This upward movement of air tends to create partial vacuum (i.e., lower concentration of molecules) and thus to reduce air pressure at places that are warmer. Therefore, mslp generally decreases with increasing air temperature, and vice versa. In addition, given two columns of air at different temperatures, the same air pressure is measured at a higher altitude in the column of warmer, less dense air. Thus, as air temperature increases, p500 increases too, and vice versa.

Specific humidity at 500 hPa height (s500) is a crucial predictor for maximum SAT, as it is used for downscaling this variable at all locations, with the exception of Superior. Specific humidity is also an important predictor for minimum SAT. However, there is no clear predominance of s500 because in several cases specific humidity at 850 hPa height (s850) is preferred instead. Specific humidity is the ratio of the water vapor mass to the total mass of the moist air parcel. As long as moisture is not added or removed from a

**Table 2-10: Large-scale predictors employed for statistically downscaling maximum and minimum SAT**

Predictand	Station	mslp	p1_u	p1_v	p5_u	p5_v	p500	p8_u	p850	p8zh	s500	s850	Tot.
Max SAT	Bigfork 13S	x				x	x				x		4
	Hot Springs Mt.	x					x				x		3
	Kraft Creek	x					x			x	x		4
	Missoula Int. Airport	x				x	x				x		4
	Moss Peak	x					x			x	x		4
	North Fork Jocko	x			x		x			x	x		5
	Polson Kerr Dam	x		x		x	x				x		5
	Saint Ignatius	x			x		x				x		4
	Seeley Lake RS	x	x			x	x				x		5
	Superior	x				x	x						3
	Partial	10	1	1	2	5	10	0	0	3	9	0	41
Min SAT	Bigfork 13S	x					x		x		x		4
	Hot Springs Mt.	x				x	x					x	4
	Kraft Creek	x				x	x				x		4
	Missoula Int. Airport	x					x	x			x		4
	Moss Peak	x			x		x					x	4
	North Fork Jocko	x	x				x	x		x			5
	Polson Kerr Dam	x					x					x	3
	Saint Ignatius	x			x		x					x	4
	Seeley Lake RS	x							x	x	x	x	5
	Superior	x			x		x					x	4
	Partial	10	1	0	3	2	9	2	2	2	4	6	41
	Total	20	2	1	5	7	19	2	2	5	13	6	82

body of air, this index does not change with temperature or pressure. Thanks to this property, specific humidity is generally employed in meteorology for tracking air masses. Relative humidity, which, on the contrary, is strongly influenced by temperature changes, would be a better predictor for downscaling SAT. In its absence, however, specific humidity is still a useful predictor. If saturated air is cooled, some of the water vapor must condense and, consequently, specific humidity decreases. If saturated air is heated and water vapor is added to it, specific humidity increases. As an example, Figure 2-7 shows the relationship between daily minimum SAT and daily s850 at Polson Kerr Dam.

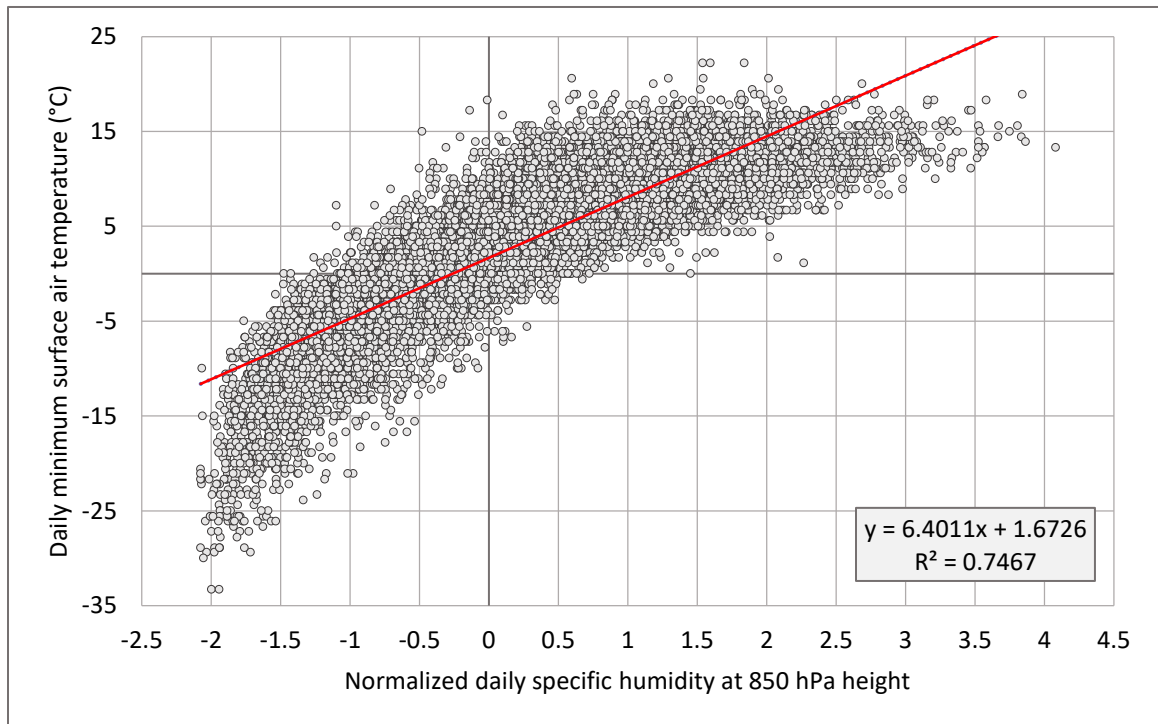


**Figure 2-7: Relationship between daily minimum SAT and daily s850 at Polson Kerr Dam**

Despite these common predictors (i.e., mslp, p500, and s500/s850), each statistical downscaling model usually displays a unique set of predictors, with only a few exceptions (see Table 2-10). This variability is the result of local differences in elevation, aspect, slope, orographic influence, and distance from the Flathead Lake. The number of

predictors in each model varies too. Some models require five predictors to be able to accurately reproduce the observed values. Other models only need three predictors, as the inclusion of a fourth predictor adds superfluous noise and does not improve significantly the accuracy of those models. Finally, it is important to mention that mean temperature at two meters (temp; see Table 2-3) was not considered as a potential candidate for downscaling maximum or minimum SAT, even though this predictor explains the majority of the variance of the two SAT variables. The reason underlying this choice is that temp is derived through the reanalysis process (see Section 2.4.1.2) by combining observations from multiple sources, possibly including the SAT time series recorded at the climate station of interest.

Table 2-11 shows the characteristics of the calibration process for each SAT downscaling model, including: the variable downscaled; the source climate station; the calibration period (first day, last day, and total number of days); the number of actual values; the percentage of missing data; the Chow F-statistic; the standard error (SE; expressed in °C); the percentage of explained variance calculated over the entire dataset ( $R^2$ ) and after applying the cross-validation technique ( $R^2$  C.V.); and, finally, the percentage drop between the two. Table 2-11 reports only the mean statistics, as twelve monthly models are actually generated for each location and SAT variable (see Table 2-5). Each model is accepted only if it passes the Chow test for all twelve months. The null hypothesis stating that there is no break point or trend within the monthly time series (i.e., the time series is stationary) is rejected if the F-statistic is greater than an F-critical value, which delimitates the rejection region of an F-probability distribution. In

**Table 2-11: Specifications of the calibration processes for statistically downscaling maximum and minimum SAT**

Predictand	Station	Start	End	Days	Records	% Mis.	Chow	SE	R <sup>2</sup>	R <sup>2</sup> C.V.	% Drop
Max SAT	Bigfork 13S	01/01/1961	31/12/1976	5,844	5,347	8.50	1.32	2.39	0.76	0.75	0.99
	Hot Springs Mt.	10/06/1991	31/12/2000	3,493	3,461	0.92	1.44	2.86	0.73	0.71	1.30
	Kraft Creek	30/07/1990	31/12/2000	3,808	3,746	1.63	1.95	2.94	0.75	0.73	1.49
	Missoula Int. Airport	01/01/1961	31/12/1980	7,305	7,305	0.00	1.58	2.90	0.72	0.72	0.93
	Moss Peak	13/07/1989	31/12/2000	4,190	4,144	1.10	0.77	2.68	0.75	0.74	1.29
	North Fork Jocko	28/08/1989	31/12/2000	4,144	4,107	0.89	1.88	2.37	0.79	0.77	1.41
	Polson Kerr Dam	01/01/1961	31/12/1980	7,305	7,165	1.92	1.94	2.45	0.75	0.75	0.88
	Saint Ignatius	01/01/1961	31/12/1980	7,305	7,256	0.67	1.45	2.44	0.79	0.79	0.68
	Seeley Lake RS	01/01/1961	31/12/1980	7,305	7,219	1.18	1.45	2.32	0.80	0.79	0.77
	Superior	01/01/1961	30/11/1980	7,274	7,223	0.70	0.82	2.48	0.76	0.76	0.58
Mean				5,797	5,697	1.72	1.46	2.58	0.76	0.75	1.03
Min SAT	Bigfork 13S	01/01/1961	31/12/1976	5,844	5,279	9.67	1.74	2.19	0.65	0.64	1.37
	Hot Springs Mt.	10/06/1991	31/12/2000	3,493	3,463	0.86	1.28	2.28	0.70	0.69	1.39
	Kraft Creek	29/07/1990	30/12/2000	3,808	3,681	3.34	1.88	2.08	0.77	0.75	1.32
	Missoula Int. Airport	01/01/1961	31/12/1980	7,305	7,305	0.00	1.43	2.61	0.62	0.61	1.06
	Moss Peak	15/07/1989	31/12/2000	4,188	4,030	3.77	1.90	2.07	0.78	0.76	1.12
	North Fork Jocko	28/08/1989	31/12/2000	4,144	3,955	4.56	1.96	2.45	0.70	0.68	1.48
	Polson Kerr Dam	01/01/1961	31/12/1980	7,305	7,232	1.00	1.95	2.33	0.64	0.63	1.19
	Saint Ignatius	01/01/1961	31/12/1980	7,305	7,259	0.63	1.84	2.64	0.63	0.61	1.44
	Seeley Lake RS	01/01/1961	31/12/1980	7,305	7,229	1.04	1.07	2.98	0.62	0.61	1.11
	Superior	01/01/1961	30/11/1980	7,274	7,196	1.07	1.71	2.46	0.62	0.61	1.17
Mean				5,797	5,663	2.59	1.68	2.41	0.67	0.66	1.27

addition, each model is accepted only if the percentage drop between the original  $R^2$  and the cross-validated  $R^2$  is less than 10% for all twelve months.

Maximum SAT-related models are generally slightly better than those for minimum SAT. All Chow F-statistics are lower than 2 and the averages are 1.46 and 1.68 for maximum SAT and minimum SAT, respectively.  $R^2$  for maximum SAT ranges between 0.72 and 0.80, with an average of 0.76, whereas  $R^2$  for minimum SAT is usually lower, as it varies between 0.62 and 0.78, with an average of 0.67. Regarding minimum SAT, it can also be noticed that the models with  $R^2$  equal or greater than 0.70 are calibrated over a shorter time period; this may be the reason for having the highest  $R^2$  among all the ten models. On average, the explained variance diminishes by 1.03% and 1.27% after applying the cross validation technique in maximum SAT and minimum SAT models, respectively. In all cases, the drop percentage never exceeds the 1.5% threshold. As with the standard error, minimum SAT is associated with slightly better results (i.e., lower SE) than maximum SAT, but the reason may lie on the fact that daily minimum SAT time series show a smaller variability (see Table 2-4). All standard errors are lower than 3°C, with an average of 2.58°C for maximum SAT and an average of 2.41°C for minimum SAT.

**SWE.** Table 2-12 illustrates the large-scale predictors employed for statistically downscaling SA and SM at each station location (for a definition of the predictor codes, refer to Table 2-3). As in the case of the SAT models (see Table 2-10), each snow-related model is based on a unique set of predictors, whose number ranges between three and five. The types of predictors vary according to local differences in elevation, aspect, slope, orographic influence, heating and cooling characteristics, and air pressure.

Despite these variations, some common traits can be identified. Mean temperature at two meters (temp) is a fundamental predictor in all six downscaling models. Air temperature during a winter storm plays an important role in determining the spatial variability of rain, freezing rain, and snow precipitation. Air temperature is also a key factor in characterizing snowmelt patterns during spring. Besides temp, there are no other predictors in common among all the three SM models. In contrast, zonal velocity component at 500 hPa height (p5\_u) and divergence at 850 hPa height (p8zh) are used as predictors in all the three SA models.

Zonal velocity refers to the air flow velocity component along a line of latitude, from west towards east. In general, scatter plots of SA and p5\_u for the three locations show a slightly positive correlation between the two variables, as SA tends to increase with increasing p5\_u. SA events may be associated with the advent of moist air from the Pacific Ocean into the Flathead Region; depending on temperature conditions, this incoming moist air can condense and fall as snow. The second predictor, divergence, usually refers to the outflow of air from the base of an anticyclone. The divergence of horizontal winds causes downward motion of the air (i.e., subsidence). During winter, cool descending air is subject to adiabatic warming, which can provoke the evaporation of any clouds that might be present. Therefore, anticyclones are usually associated with clear skies and cool, dry air. Snowfall events are mostly uncommon with these atmospheric conditions. The p8zh-SA relationship at the three station locations reflects this scenario. In general, scatter plots of SA and p8zh exhibit a slightly negative correlation between the two variables, as SA tends to decrease with increasing p8zh.

**Table 2-12: Large-scale predictors employed for statistically downscaling SA and SM**

Predictand	Station	p1_z	p5_f	p5_u	p5_z	p500	p850	p8zh	prcp	s500	s850	temp	Tot.
SA	Kraft Creek			x				x				x	3
	Moss Peak			x			x	x		x		x	5
	North Fork Jocko	x		x				x				x	4
	Partial	1	0	3	0	0	1	3	0	1	0	3	12
SM	Kraft Creek				x	x					x	x	4
	Moss Peak		x		x				x			x	4
	North Fork Jocko		x							x		x	3
	Partial	0	2	0	2	1	0	0	1	1	1	3	11
Total		1	2	3	2	1	1	3	1	2	1	6	23

**Table 2-13: Specifications of the calibration processes for statistically downscaling SA and SM**

Predictand	Station	Start	End	Days	Records	% Missing	Chow*	R <sup>2</sup> *	R <sup>2</sup> C.V.*	% Drop*
SA	Kraft Creek	01/09/1980	31/08/2000	7,305	7,300	0.07	0.78	0.10	0.07	2.92
	Moss Peak	01/09/1985	31/08/2000	5,479	5,479	0.00	0.32	0.15	0.13	2.54
	North Fork Jocko	01/09/1989	31/08/2000	4,018	3,994	0.60	1.27	0.15	0.11	4.02
	Mean				5,601	5,591	0.22	0.79	0.13	0.10
SM	Kraft Creek	01/09/1980	31/08/2000	7,305	3,836	47.49	1.48	0.34	0.29	5.10
	Moss Peak	01/09/1985	31/08/2000	5,479	3,966	27.61	1.71	0.38	0.34	4.47
	North Fork Jocko	01/09/1989	31/08/2000	4,018	2,825	29.69	0.63	0.18	0.12	5.57
	Mean				5,601	3,542	34.93	1.27	0.30	0.25

\*The mean statistics among the three seasons (i.e., fall, winter, and spring) are reported for SA, while only the statistics for spring are shown for SM

Table 2-13 illustrates the characteristics of the calibration process for each snow-related downscaling model, including the variable downscaled, the source climate station, the calibration period, the number of actual values, the percentage of missing data, the Chow F-statistic, the percentage of explained variance calculated over the entire dataset ( $R^2$ ) and after applying the cross-validation technique ( $R^2$  C.V.), and finally the percentage drop between the two. Four seasonal models are actually generated for each location and snow variable (see Table 2-5). However, as for the SA predictand, the four main statistics in Table 2-13 (i.e., Chow,  $R^2$ ,  $R^2$  C.V., and % Drop) refer to the average of fall, winter, and spring statistics only. Summer statistics are excluded because snowfall events are extremely rare and almost all daily SA values equal zero in this season. Similarly, only spring statistics are reported for the SM predictand because the vast majority of the SM values in the other three seasons are either null or missing. As a reminder, if any daily SWE value of the original time series was zero, the corresponding SM value was set as missing (see Section 2.4.2.1). Each model is accepted only if it passes the Chow test (i.e., F-statistic smaller than an F-critical value) and the cross-validation test (i.e.,  $R^2$  drop less than 10%) for all the selected seasons.

The Chow F-statistics for the six downscaling models in Table 2-13 varies between 0.32 and 1.71, with an average of 0.79 for the SA predictand and 1.27 for the SM predictand. The mean explained variances of the SA and SM models are approximately 13% and 30%, respectively. As expected, the  $R^2$  of the snow-related models is much lower than that of the SAT models, which is, on average, around 0.72 (see Table 2-11). This is in line with the results encountered within the statistical

downscaling literature. Wilby, Dawson, and Barrow (2002) indicates that a typical explained variance for spatially conservative variables such as temperature is about 70% or greater, while heterogenous variables such as rainfall are associated with explained variances lower than 40%. Tryhorn and DeGaetano (2013) found that the  $R^2$  related to the downscaling of SDP daily series varies between 0.1 and 0.4, which is consistent with the range of  $R^2$  values reported in Table 2-13. The low explained variance, however, does not prevent these models to be used for reconstructing SWE time series. As the next section will show, the validation process undertaken over 5-year averages of SWE downscaled series provides promising results.

#### **2.5.1.2. Validation**

**SAT.** Table 2-14 displays the basic characteristics of the validation process for each SAT downscaling model, including the variable downscaled, the source climate station, the validation period (first day, last day, and total number of days), the number of actual values, and the percentage of missing data. In addition, the table reports the coefficient of determination ( $R^2$ ) of a simple linear regression between daily observed and simulated SAT values over the validation period. The independent variable is the ensemble mean of the 100 sequences stochastically generated by SDSM (see Section 2.4.2.3), whereas the depend variable is the observed time series. In agreement with the calibration results, maximum SAT-related models are generally slightly better than those for minimum SAT.  $R^2$  for maximum SAT ranges between 0.91 and 0.94, with an average of 0.92, whereas  $R^2$  for minimum SAT is usually lower, as it varies between 0.80 and 0.90, with an average of 0.85.

Table 2-14: Specifications and main results of the validation of the downscaled maximum and minimum SAT time series

Predictand	Station	Start	End	Days	Records	% Mis.	R <sup>2</sup>	Annual Average (°C)		
								Obs.	Sim.	Error*
Max SAT	Bigfork 13S	01/01/1981	31/12/2000	7,305	6,699	8.30	0.92	12.72	13.46	0.74
	Hot Springs Mt.	01/01/2001	31/12/2005	1,826	1,814	0.66	0.91	15.40	14.84	-0.57
	Kraft Creek	01/01/2001	31/12/2005	1,826	1,823	0.16	0.91	11.46	11.82	0.36
	Missoula Int. Airport	01/01/1981	31/12/2000	7,305	7,305	0.00	0.92	13.86	13.78	-0.08
	Moss Peak	01/01/2001	31/12/2005	1,826	1,824	0.11	0.91	7.17	6.74	-0.43
	North Fork Jocko	01/01/2001	31/12/2005	1,826	1,826	0.00	0.93	9.09	8.23	-0.86
	Polson Kerr Dam	01/01/1981	31/12/2000	7,305	7,121	2.52	0.94	14.25	13.50	-0.75
	Saint Ignatius	01/01/1981	31/12/2000	7,305	6,998	4.20	0.92	14.64	14.83	0.19
	Seeley Lake RS	01/01/1981	31/12/2000	7,305	6,842	6.34	0.93	13.07	13.47	0.40
	Superior	01/01/1981	31/12/2000	7,305	6,844	6.31	0.93	15.56	15.70	0.14
	Mean			5,113	4,910	2.86	0.92	12.72	12.64	-0.09 (0.45)
Min SAT	Bigfork 13S	01/01/1981	31/12/2000	7,305	6,862	6.06	0.88	3.13	1.95	-1.18
	Hot Springs Mt.	01/01/2001	31/12/2005	1,826	1,814	0.66	0.86	2.34	2.62	0.28
	Kraft Creek	01/01/2001	31/12/2005	1,826	1,824	0.11	0.86	0.33	-0.84	-1.17
	Missoula Int. Airport	01/01/1981	31/12/2000	7,305	7,305	0.00	0.84	0.58	0.05	-0.53
	Moss Peak	01/01/2001	31/12/2005	1,826	1,821	0.27	0.90	-1.18	-2.13	-0.95
	North Fork Jocko	01/01/2001	31/12/2005	1,826	1,821	0.27	0.80	-2.99	-3.87	-0.89
	Polson Kerr Dam	01/01/1981	31/12/2000	7,305	7,254	0.70	0.87	2.36	1.85	-0.52
	Saint Ignatius	01/01/1981	31/12/2000	7,305	7,132	2.37	0.82	1.37	0.86	-0.51
	Seeley Lake RS	01/01/1981	31/12/2000	7,305	7,021	3.89	0.82	-2.24	-2.28	-0.04
	Superior	01/01/1981	31/12/2000	7,305	7,000	4.18	0.82	1.03	1.22	0.19
	Mean			5,113	4,985	1.85	0.85	0.47	-0.06	-0.53 (0.63)

\*The absolute mean error is indicated in parentheses

Finally, Table 2-14 shows the maximum and minimum SAT annual averages calculated for both observed and simulated time series over the validation period, as well as the error between the two. In all locations but three (i.e., Hot Springs Montana, Polson Kerr Dam, and Seeley Lake Ranger Station), the absolute error between observed and simulated annual averages of maximum SAT is smaller than the error between those of minimum SAT. Similarly, the absolute mean error across all ten locations is smaller for maximum SAT (0.45) than for minimum SAT (0.63). In general, both types of models underestimate the mean annual SAT, as indicated by the negative sign of the mean error (i.e., observed value greater than simulated value). However, this tendency is more evident in the case of minimum SAT models, as all locations but two (i.e., Hot Springs Montana and Superior) present a negative error. Differently, only half of the maximum SAT models underestimate the annual average, while the other half overestimate it.

Figure 2-8 and Figure 2-9 illustrate the observed and simulated seasonal averages of maximum and minimum SAT, respectively. For each simulated value (orange bar), the potential prediction error is portrayed through a dark-grey bar, in which the extremes represent the minimum and maximum mean seasonal values among the 100 ensemble members generated by SDSM (see Section 2.4.2.3). Regarding maximum SAT (Figure 2-8), the absolute mean error across all ten locations is 0.46°C for winter, 0.62°C for spring, 0.63°C for summer, and 0.39°C for fall. The maximum SAT seasonal average is generally underestimated in winter and fall (eight and ten locations, respectively), while the situation is more balanced in spring and summer, when the underestimation involves only four locations out of ten. In each season, the mean error falls within the

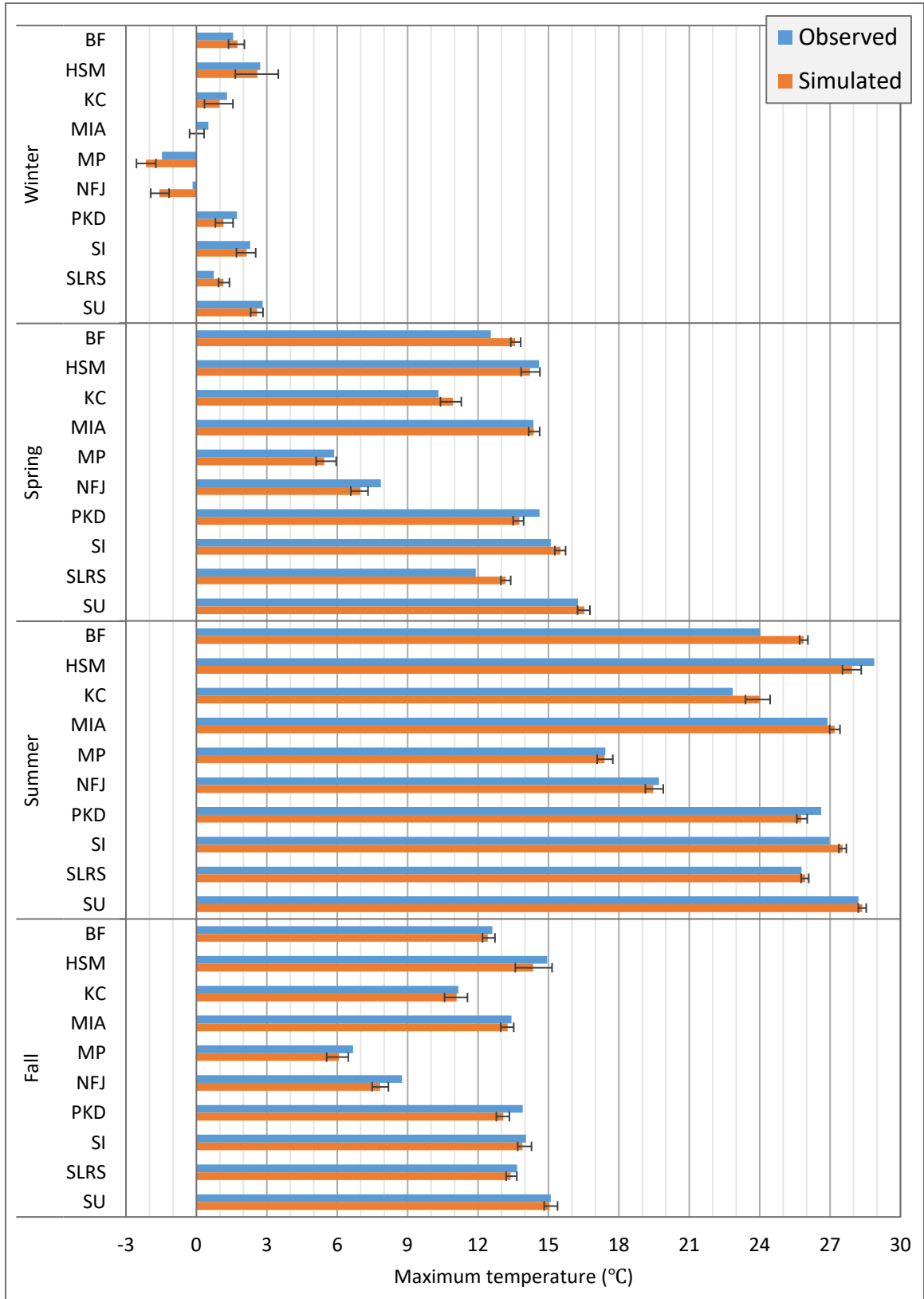


**Figure 2-8: Observed and simulated seasonal averages of daily maximum SAT and estimated prediction error**

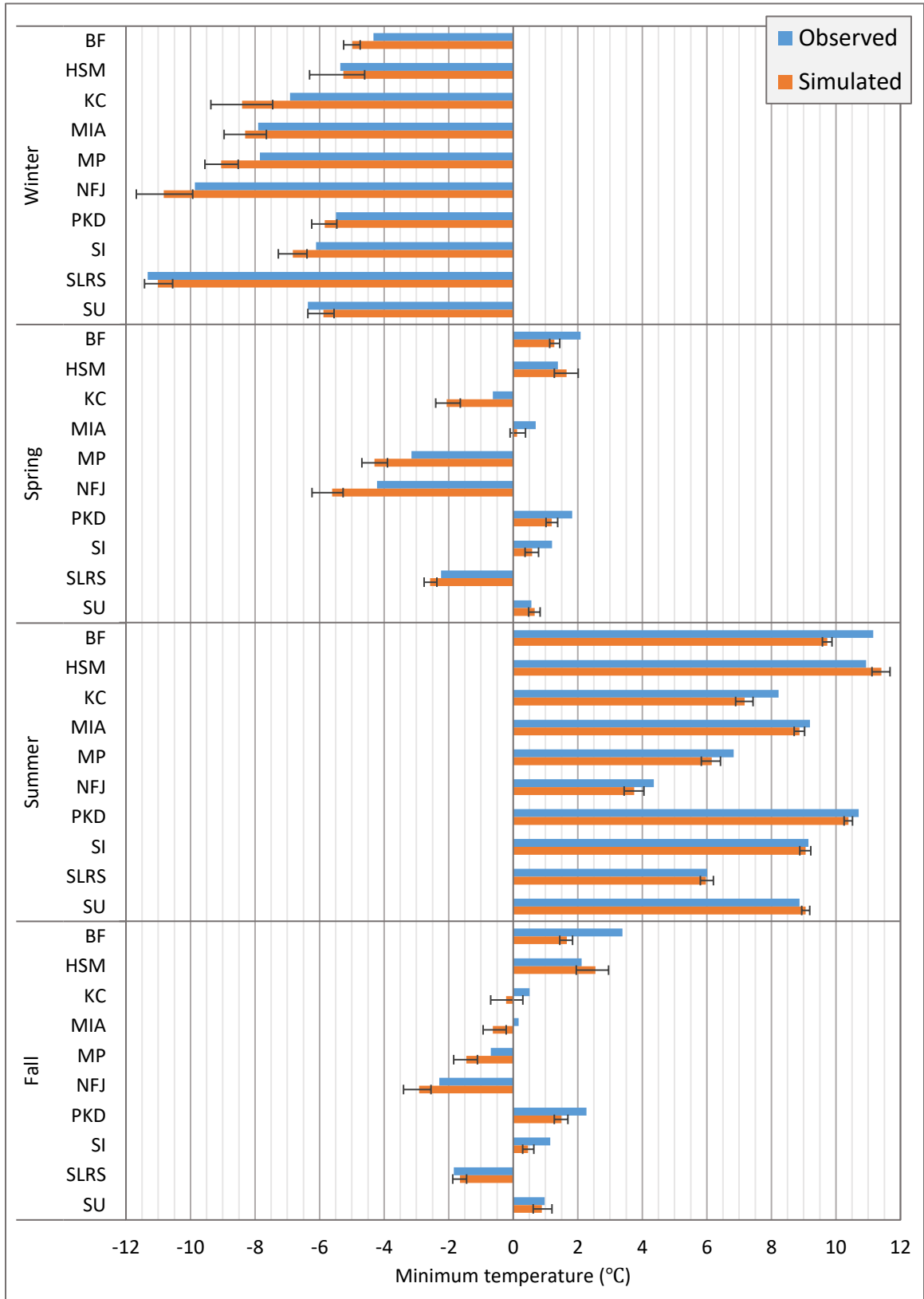


**Figure 2-9: Observed and simulated seasonal averages of daily minimum SAT and estimated prediction errors**

predicted error range in four to six stations. As for minimum SAT (Figure 2-9), the absolute mean error across all ten locations is 0.67°C for winter, 0.73°C for spring, 0.52°C for summer, and 0.68°C for fall. The mean error is negative in seven or eight locations in each season. Hot Springs Montana, Seeley Lake Ranger Station, and Superior are the only stations that overestimate the minimum SAT average in all or some seasons. In each season, the mean error falls within the predicted error range in two to four stations.

Appendix B provides additional material that has been used to further evaluate the skills of the twenty SAT downscaling models. Observed and simulated monthly averages are compared separately for each location and temperature variable. The twenty graphics (Figures B-1 to B-20) illustrate the annual evolution of monthly averages calculated for both observed and downscaled SAT time series over the validation period. The prediction error associated with the simulated series is indicated with vertical bars, in which the extremes represent the minimum and maximum mean monthly values among the 100 ensemble members. Besides monthly, seasonal, and annual averages, other basic statistics are investigated to assess the performance of the SAT downscaling models, including median, maximum, minimum, variance, POT, PBT, and 95<sup>th</sup> percentile (see Section 2.4.2.3). These statistics are calculated for both observed and simulated time series of maximum and minimum SAT at the monthly, seasonal, and annual temporal scales. The error between statistics derived from observed and downscaled values is also computed. Results across the ten locations are grouped together for comparison purposes and the mean error is reported. The resulting fourteen tables, one per statistic and temperature variable, are presented in Appendix B (Tables B-1 to B-14).

**SWE.** Figures 10, 11, and 12 show the annual evolution of the observed and estimated daily SWE means over the period 2001-2005 at Kraft Creek, Moss Peak, and North Fork Jocko, respectively. As pseudo water years are considered (see Section 2.4.2.3), the validation period for the three SWE models actually starts on the 1<sup>st</sup> of September of 2000 and ends on the 31<sup>st</sup> of August of 2005. Within this timeframe, there are no missing data in any of the original or downscaled SWE time series. The information displayed in Figures 10, 11, and 12 is summarized in Table 2-15, which shows the values of the ten indices (see Table 2-6) that define the general conditions of the mean annual snowpack over 2001-2005. These indices are calculated for both the observed and simulated 365-day long SWE series. The error between each pair of indices and the absolute mean error across the three locations are also indicated.

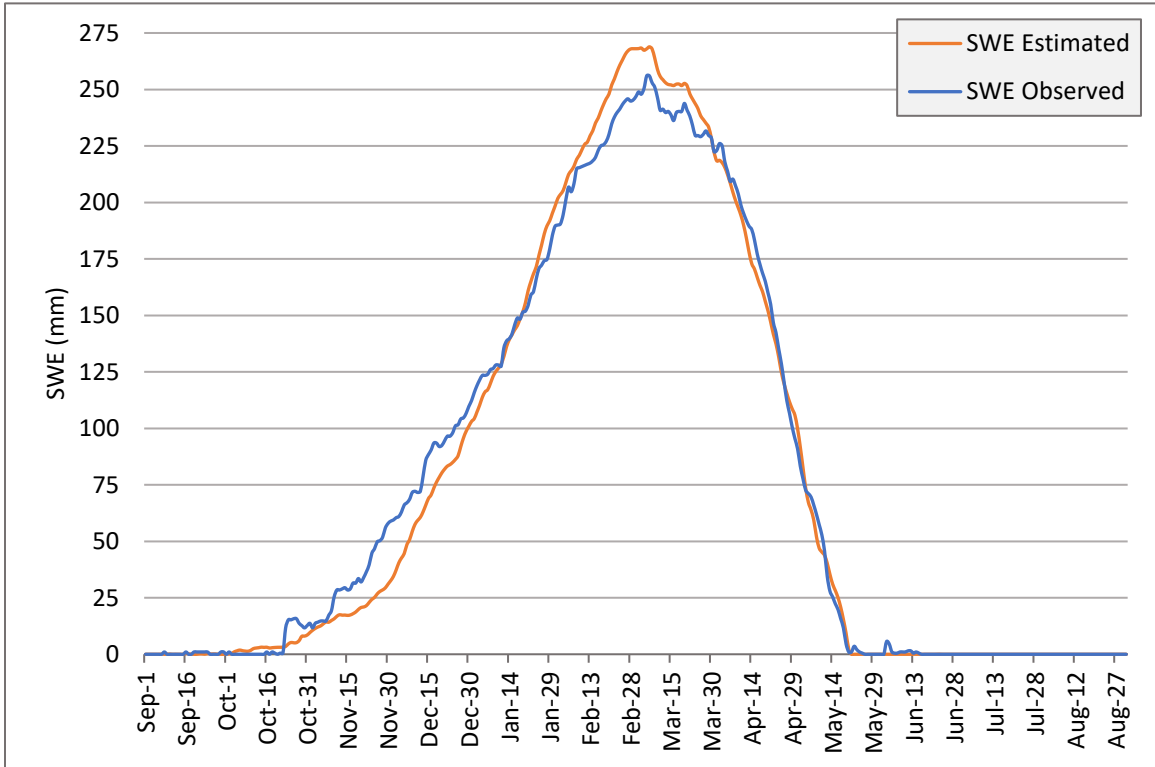


**Figure 2-10: Annual evolution of the observed and estimated daily SWE means over the period 2001-2005 at Kraft Creek**

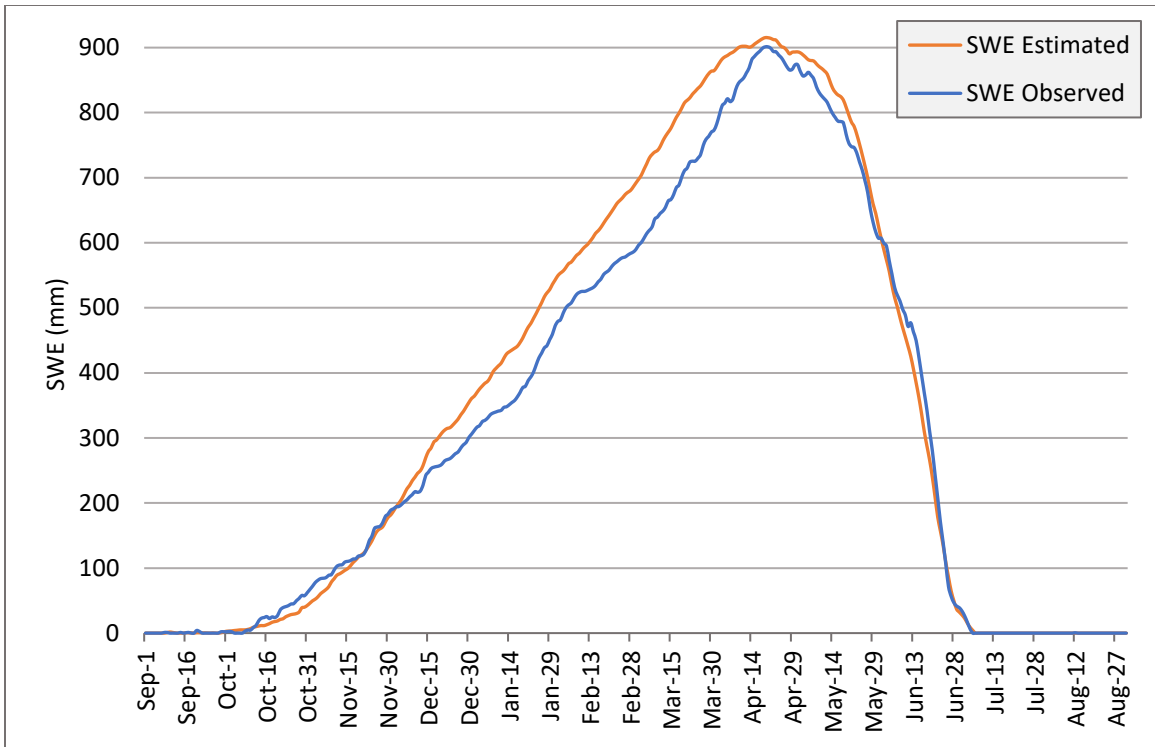


**Figure 2-11: Annual evolution of the observed and estimated daily SWE means over the period 2001-2005 at Moss Peak**

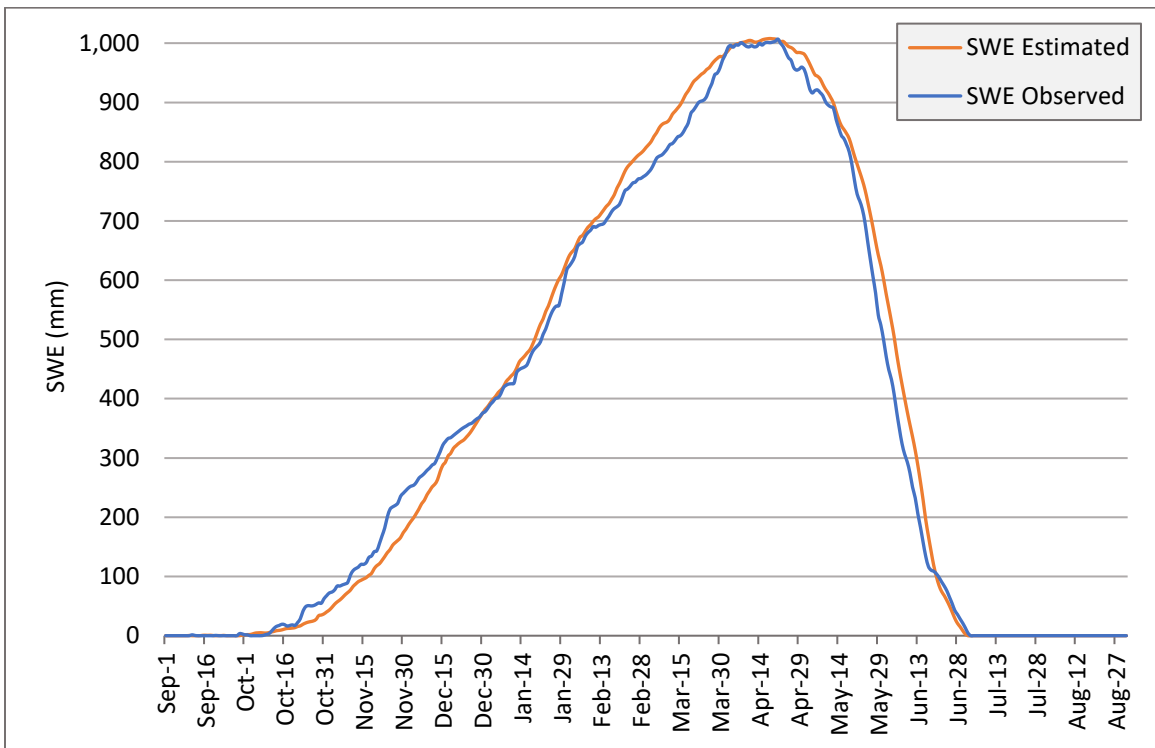


**Figure 2-12: Annual evolution of the observed and estimated daily SWE means over the period 2001-2005 at North Fork Joeko**

In general, the SWE downscaling models perform well in detecting the major characteristics of the annual snowpack at the three locations of interest. SMO is the most accurate index, as the observed date of snowmelt onset is reproduced correctly in all cases. The date of permanent snowpack end (PSE) and, consequently, the duration of snow melt (SMD) are also replicated very accurately. In these instances, the error related to the two indices is not greater than a day. The date of annual maximum SWE (DMSWE), the date of permanent snowpack onset (PSO), the duration of permanent snowpack (PSD), and the number of days without snow on the ground (SWE0) present an intermediate level of accuracy, as the absolute mean error across the three locations is lower than two days. DMSWE is well re-created at Kraft Creek (1-day error) and Moss Peak (no error), but the accuracy drops for North Fork Jocko (3-day error). The observed PSO and the simulated PSO are two days apart at worst; however, the PSO absolute mean error across the three stations (1.67) is slightly higher than that of DMSWE (1.33). A maximum error of two days at any location is also found for PSD and SWE0, with the first index having a better overall absolute mean error (1.00) than the second (1.33).

Among the proposed indices, the date on which half of the snowpack has melted (SM50) generally presents the largest error. The simulated SM50 at each station diverges from the observed SM50 by two/four days, with a mean absolute error of 3.33 days. The annual maximum value of SWE (MSWE) and the SWE value on the 1<sup>st</sup> of April (1ASWE) cannot be directly compared with the remaining indices because their error is expressed in millimeters rather than days. A few considerations can be drawn, nonetheless. All the SWE downscaling models overestimate the observed MSWE. However, the error never

exceeds 1.5 centimeters at any location and the mean error among them is lower than 1 centimeter. The percentage error relative to the observed MSWE is about 5.0% for Kraft Creek, 1.6% for Moss Peak, and 0.1% for North Fork Jocko. A more diverse situation emerges from the analysis of 1ASWE. Two models perform quite well in reproducing the observed value, while the third is not able to accurately replicate it. The simulation error is almost null for Craft Creek and around half centimeter for North Fork Jocko, but is above 9 centimeters for Moss Peak. The percentage errors relative to the observed 1ASWE are 0.1%, 0.6%, and 11.8%, respectively.

Table 2-16 displays the results of 24 simple linear regression analyses that were undertaken to further evaluate the skills of the SWE downscaling models within the 2001-2005 validation period (see Section 2.4.2.3). Four pairs of observed/downscaled series (SA, SM,  $\Delta$ SWE, and SWE) are examined using the entire dataset (1826 days) and the 5-year daily mean (365 days) for each of the three climate stations. Three main statistics are reported for each regression analysis: the percentage of explained variance ( $R^2$ ), the residual standard error (Sigma, expressed in millimeters of SWE), and the F-statistic. Since the p values are always considerably much smaller than 0.05, the null hypothesis stating that there is no relationship between observed and downscaled values is rejected in all cases. In general, results show that the SM series are better simulated than the corresponding SA series, with larger  $R^2$  and smaller Sigma. This is in line with the calibration results presented in Table 13. In addition, Moss Peak and North Fork Jocko are associated with considerable better statistics than those related to Kraft Creek, with the first set of models performing slightly better than the second.

**Table 2-15: Validation of the mean snowpack characteristics within 2001-2005**

Station	Values	MSWE*	DMSWE	SMO	SM50	1ASWE*	PSO	PSE	PSD	SMD	SWE0
Kraft Creek	Observed	256.03	mar-06	mar-08	apr-25	222.5	ott-23	mag-18	208	72	156
	Estimated	268.86	mar-07	mar-08	apr-23	222.22	ott-25	mag-19	207	73	158
	Error	+12.83	+1	0	-2	-0.28	+2	+1	-1	+1	+2
Moss Peak	Observed	901.19	apr-19	apr-21	giu-14	773.18	ott-11	lug-04	267	75	98
	Estimated	915.37	apr-19	apr-21	giu-10	864.53	ott-09	lug-04	269	75	96
	Error	+14.18	0	0	-4	+91.35	-2	0	+2	0	-2
North Fork Jocko	Observed	1006.86	apr-21	apr-22	mag-31	971.3	ott-11	lug-01	264	71	101
	Estimated	1007.78	apr-18	apr-22	giu-04	977.03	ott-10	giu-30	264	70	101
	Error	+0.92	-3	0	+4	+5.73	-1	-1	0	-1	0
Absolute Mean Error		9.31	1.33	0	3.33	32.45	1.67	0.67	1.00	0.67	1.33

\*These indices are expressed in millimeters

68

**Table 2-16: Validation statistics of the downscaled SA, SM, ΔSWE, and SWE time series within 2001-2005**

Dataset	Variable	Kraft Creek			Moss Peak			North Fork Jocko		
		R <sup>2</sup>	Sigma	F-statistic	R <sup>2</sup>	Sigma	F-statistic	R <sup>2</sup>	Sigma	F-statistic
1826-day time series (5 years)	SA	0.17	3.08	380	0.22	5.93	509	0.25	6.39	615
	SM	0.49	2.73	1,751	0.77	4.38	5,969	0.62	5.70	3,016
	ΔSWE	0.37	4.27	1,061	0.58	7.81	2,523	0.52	8.88	1,944
	SWE	0.82	45.95	8,397	0.97	54.67	62,117	0.93	107.36	23,573
365-day time series (5-year mean)	SA	0.32	1.43	174	0.39	2.75	232	0.49	2.95	349
	SM	0.71	1.13	881	0.91	2.15	3,569	0.83	2.94	1,756
	ΔSWE	0.56	1.79	467	0.80	3.74	1,472	0.79	4.19	1,329
	SWE	0.99	8.09	44,934	0.99	30.75	37,319	0.99	27.86	62,143

### **2.5.1.3. Final considerations**

This section aims to summarize the main results related to the statistical downscaling process of SAT and SWE as well as to highlight the relevance of this work. Mean sea level pressure, 500 hPa geopotential height, and specific humidity (either at 500 or 850 hPa height) are key predictors for downscaling air temperature, whereas mean temperature at two meters is an essential predictor of snow-related variables. Also, zonal velocity at 500 hPa height and divergence at 850 hPa height are fundamental when downscaling snowfall. However, the specific set of large-scale predictors varies in number and type across the downscaling models depending on the predictand analyzed as well as the location and geographic features associated with the climate station of interest, such as elevation, aspect, slope, orographic influence, and distance from the Flathead Lake.

The SAT downscaling models perform well in reproducing the observed time series. However, the explained variance is higher for maximum SAT (mean  $R^2 = 0.92$ ) than for minimum SAT (mean  $R^2 = 0.85$ ). In general, both types of models underestimate SAT, as the downscaled seasonal and annual means are usually lower than the corresponding observed means. This pattern is more evident for minimum SAT than for maximum SAT and for the colder seasons (i.e., winter and fall) than for the warmer seasons (i.e., spring and summer). The largest exceptions are represented by Hot Springs Montana and Superior. These two stations are located in the western portion of the study area (see Figure 2-3), where temperatures, especially daily maximums, are generally higher than in the eastern part (see Table 2-2). Looking at these results as a

whole, it can be inferred that the proposed models tend to overestimate SAT values when air temperatures are warmer (due to the geographic location, the time of the year, or both) and underestimate SAT values when temperatures are colder.

While air temperature models are common and thoroughly described within the statistical downscaling literature, the snow-related models presented in this study represent the first tentative of statistically downscaling SWE by means of SDSM. Individually, SA and SM models exhibit low explained variance, with the first type of models performing worse than the latter. However, when outcomes from pairs of SA/SM models are aggregated together, the results are very promising. The major 5-year averaged characteristics of the annual snowpack at the three locations of interest are well replicated. The dates of specific events (e.g., snowmelt onset) and the number of days between certain events (e.g., snowpack duration) are identified with a mean absolute error of 1.25 days at each location (see Table 2-15). In terms of explained variance, the simulated cumulative SWE values are in close agreement with those observed. The mean  $R^2$  across the three locations is about 0.91 (see Table 2-16), which resembles the performance levels obtained using maximum SAT models. It is also evident that the SWE models work better when larger snow quantities are involved (e.g., larger snowfall events), as it is for areas located at higher elevations (i.e., Moss Peak and North Fork Jocko).

### **2.5.2. Air temperature**

This section presents the findings related to the analysis of air temperature. The historical and potential future evolution of this climate variable is investigated by looking at changes in SAT 30-year mean and variability (Section 2.5.2.1) as well as SAT trends (Section 2.5.2.2) over the entire study period (i.e., 1961-2100 or longer, depending on data availability before 1961). Results are reported for several types of analyses (see Section 2.4.3), each of which is usually repeated six times because two different variables (i.e., maximum SAT and minimum SAT) and three distinct scenarios (i.e., RCP2.6, RCP4.5, and RCP8.5) are considered. In addition, results are shown for multiple spatial (i.e., single climate station and overall study area) and temporal (i.e., monthly, seasonal, and annual) scales in order to highlight the geographic variability of air temperature within the Flathead Region as well as its variability within and across years. On the whole, the findings described in this section respond to the first research question associated with this chapter (see Section 2.3).

#### **2.5.2.1. SAT 30-year mean and variability**

Figures 2-13, 2-14, and 2-15 illustrate the evolution of 30-year daily normals of maximum SAT at the ten station locations within 1961-2100 according to the three RCP scenarios. For visualization purposes, the normal value of a given 30-year period is placed at the middle point of that specific 30-year interval. For example, the 1961-1990 normal is marked at the beginning of 1976. Normals obtained exclusively from observed values are represented by solid squares, while normals derived partially or completely from downscaled values are symbolized by an asterisk. Similarly, solid and dashed lines

are used to connect two consecutive observed normals and two subsequent estimated normals, respectively. Each colored curve represents a specific climate station. Figures 2-16, 2-17, and 2-18 include the equivalent graphics for minimum SAT.

Regardless of the variable downscaled, the general trend is unequivocal, as all locations will experience higher air temperatures in the future. The RCP2.6 scenario predicts that, after an increase in the next few decades, SAT will approach a certain value and the trajectory will stabilize along that horizontal asymptote. The RCP4.5 scenario prognosticates that air temperature will continue to increase until 2100, but the rate of increase is expected to diminish with time. Finally, the RCP8.5 scenario manifests constantly increasing temperatures over the entire future study period. Although these positive increments concern both maximum and minimum SAT, the magnitude of change in any given climate scenario is slightly larger for the first variable than for the latter.

A widespread increasing trend in air temperature can also be observed within the historical period (i.e., 1961-1990, 1971-2000, and 1981-2010). All ten locations exhibit an increase in both maximum and minimum SAT normals during this 50-year timeframe. The only exception concerns Big Fork 13S and Seeley Lake Ranger Station, where the maximum SAT normal remains constant or slightly decreases within this period. Appendix C (Figures C-1 to C-20) presents an extended version of these six graphics, as the data are displayed separately for each station and SAT variable. This allows the inclusion of data older than 1961 for those stations that provide this additional information (see Table 2-8). The potential prediction error is also portrayed by means of a vertical dark-grey bar for all estimated normal values (see Section 2.4.3.3).

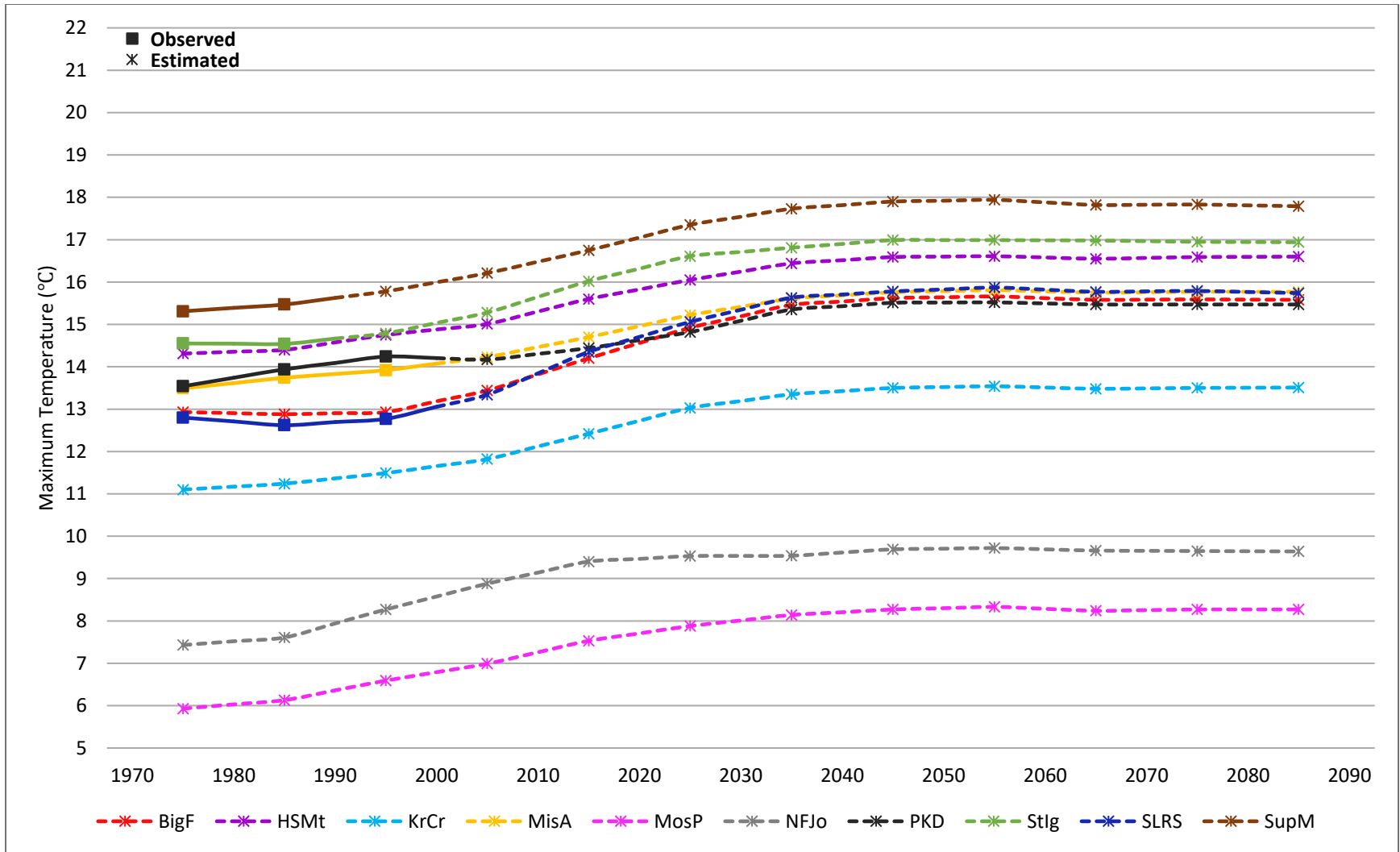


Figure 2-13: Historical and future changes in 30-year normals of maximum SAT within 1961-2100 according to the RCP2.6 scenario

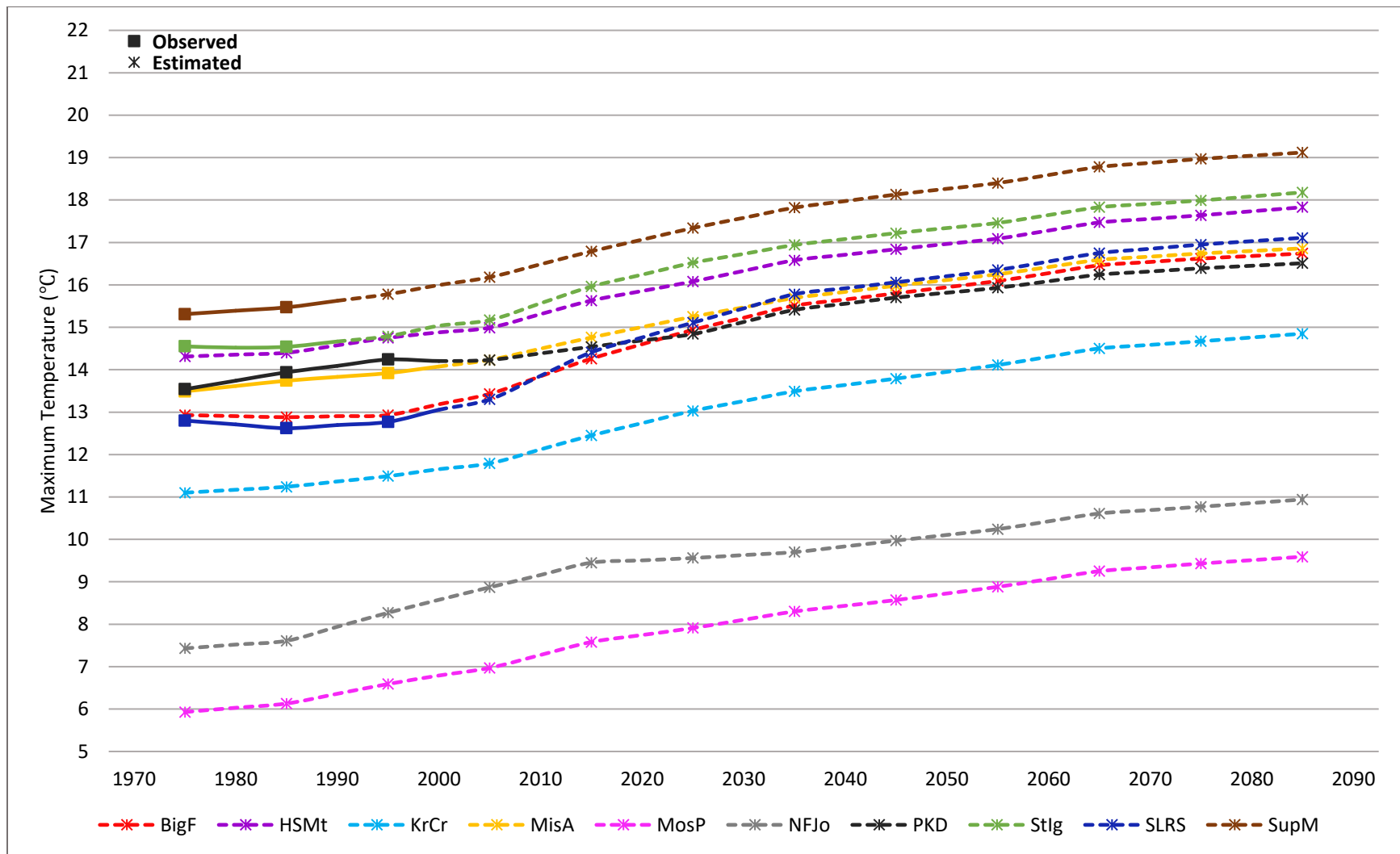


Figure 2-14: Historical and future changes in 30-year normals of maximum SAT within 1961-2100 according to the RCP4.5 scenario

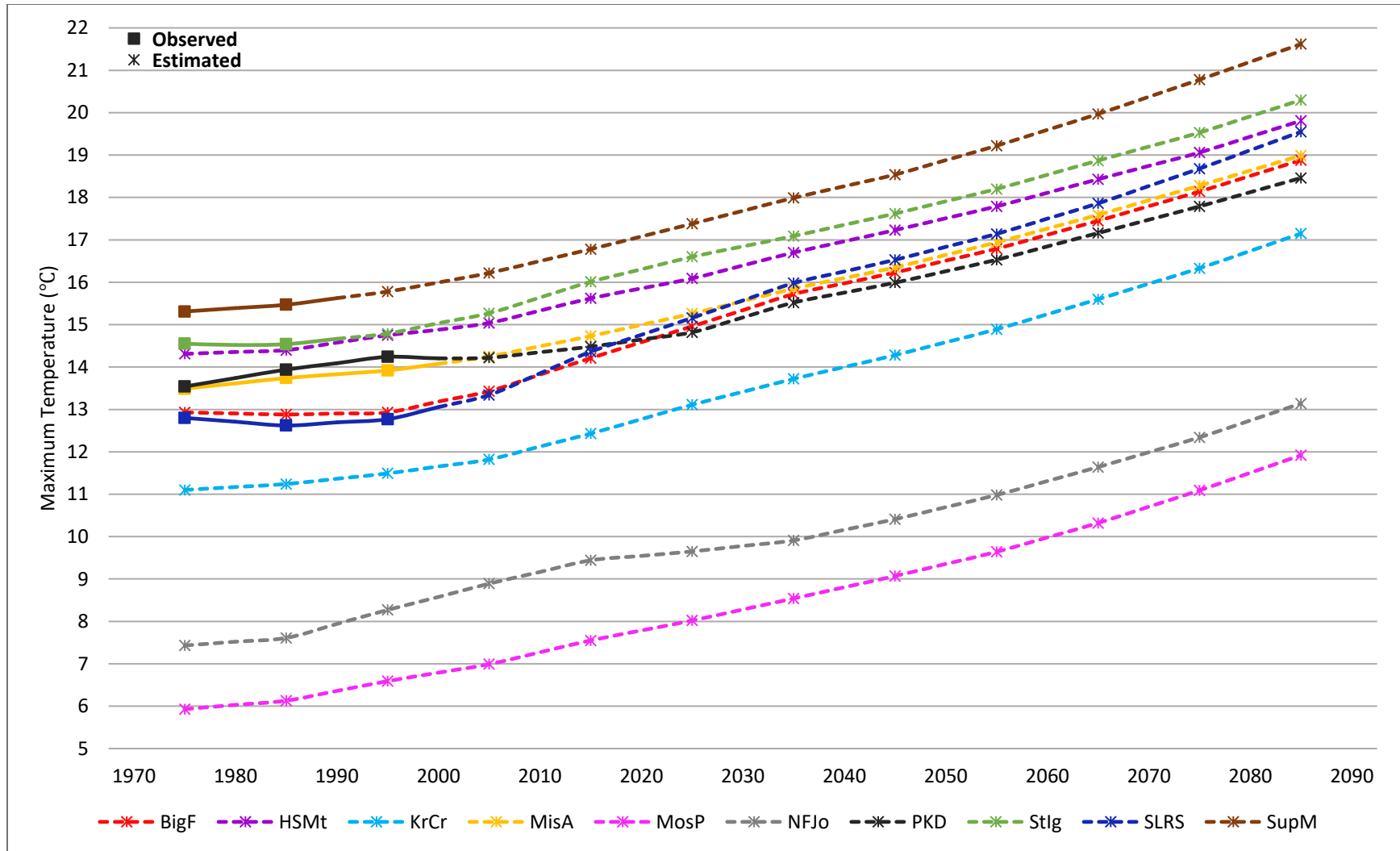


Figure 2-15: Historical and future changes in 30-year normals of maximum SAT within 1961-2100 according to the RCP8.5 scenario

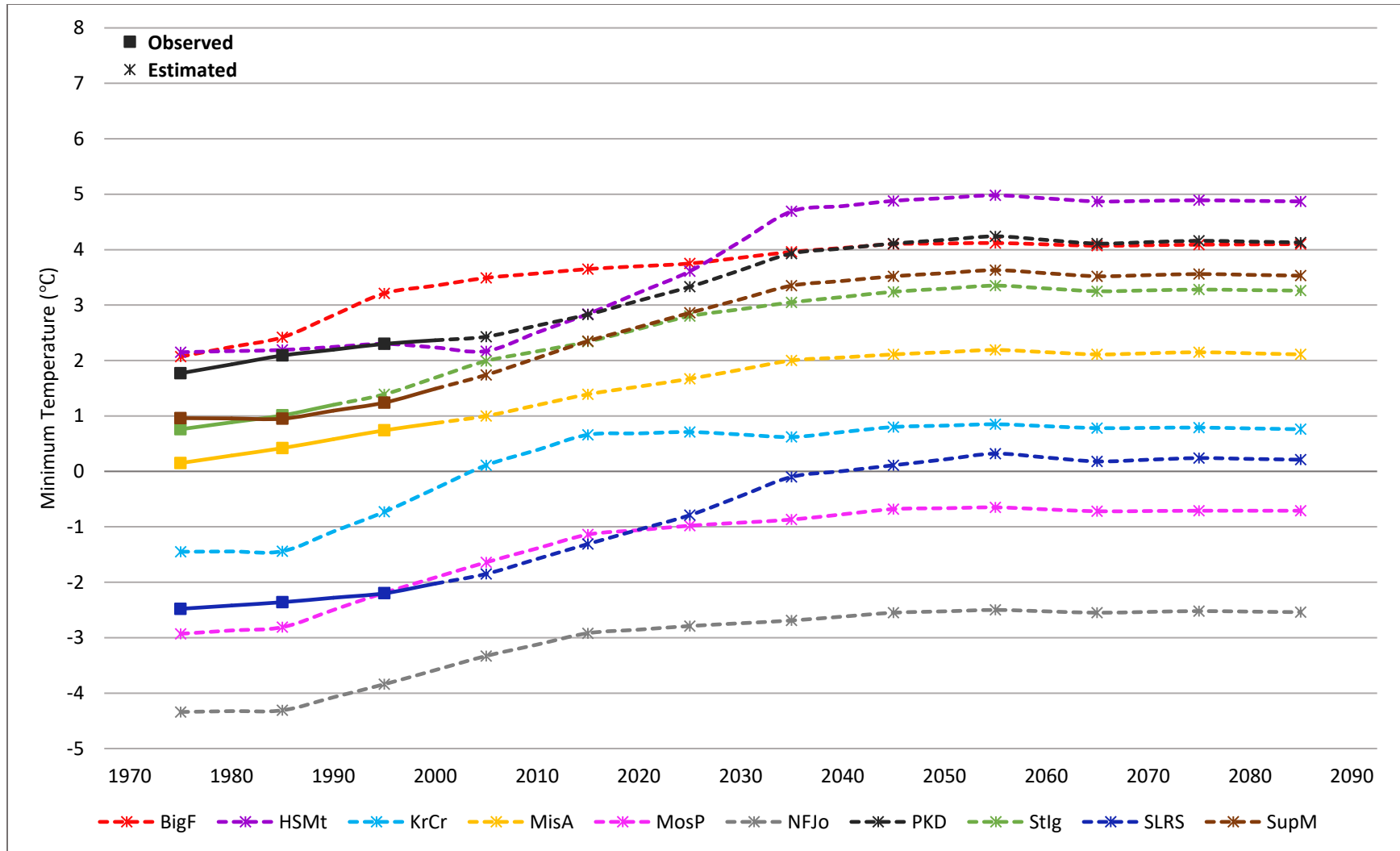


Figure 2-16: Historical and future changes in 30-year normals of minimum SAT within 1961-2100 according to the RCP2.6 scenario

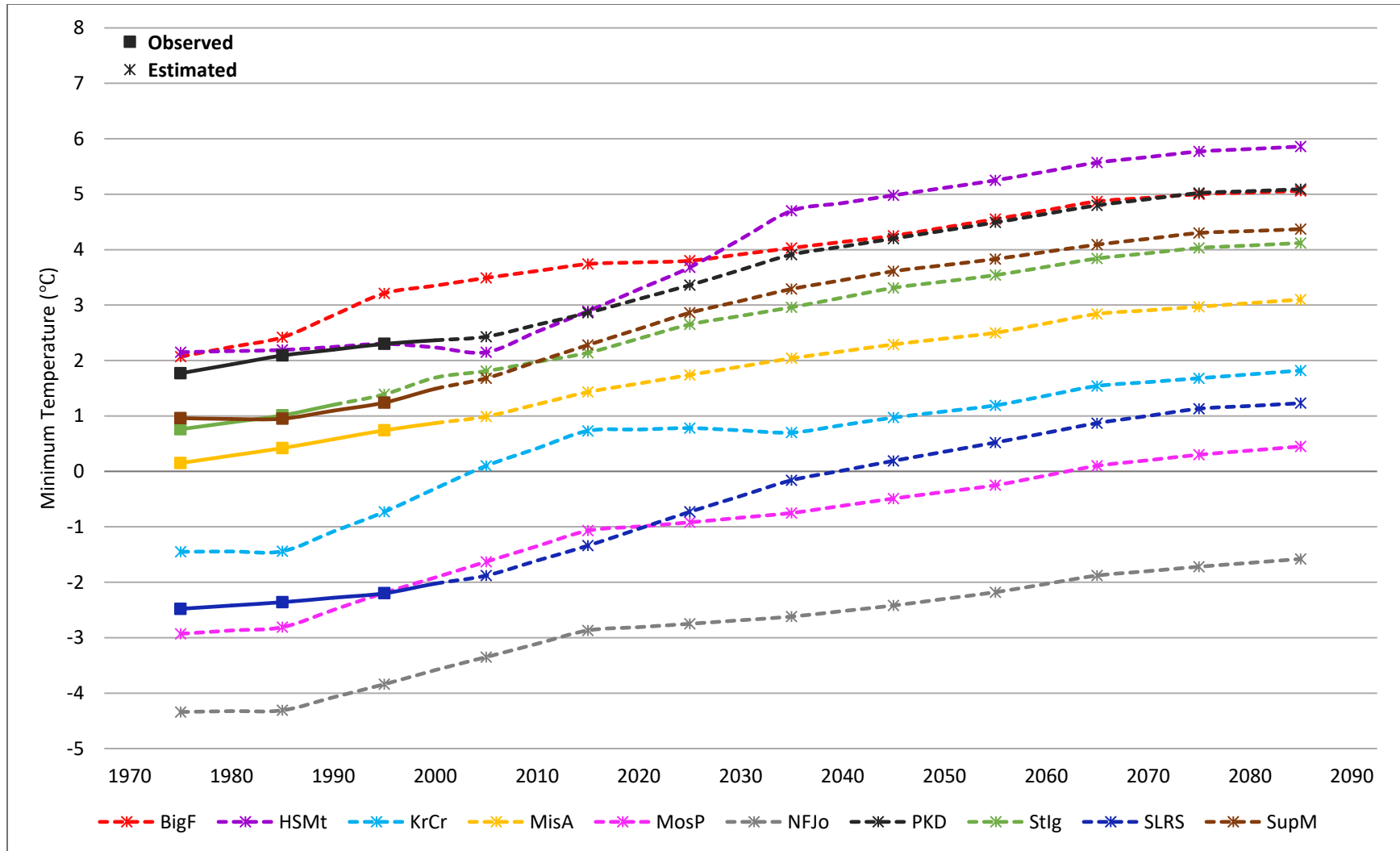


Figure 2-17: Historical and future changes in 30-year normals of minimum SAT within 1961-2100 according to the RCP4.5 scenario

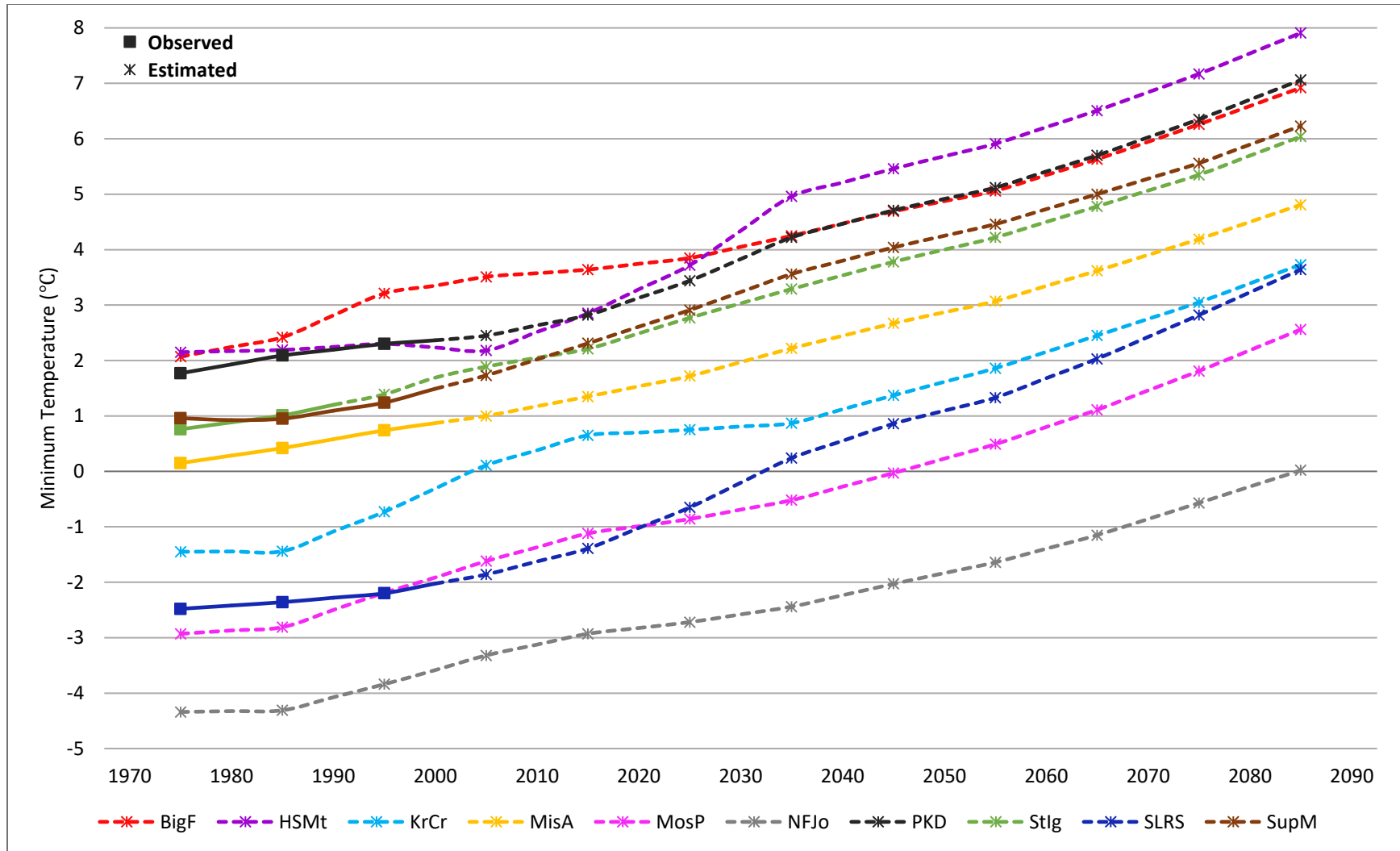


Figure 2-18: Historical and future changes in 30-year normals of minimum SAT within 1961-2100 according to the RCP8.5 scenario

The information contained in the above six graphics is displayed through as many sets of maps (Figures 2-19 to 2-24) to visualize the spatial distribution of air temperature changes within the Flathead Region. Due to design constraints, only five equally spaced 30-year periods (1981-2010, 2001-2030, 2021-2050, 2041-2070, 2061-2090) are included in each figure. Rather than the absolute normal value, the difference in temperature normal between any given 30-year period and the 1961-1990 baseline period is shown through a color scale. In addition to the SAT normal, the difference between the intra-annual monthly SAT variability of any 30-year period and the one calculated over 1961-1990 is illustrated by means of circles, whose size is proportional to the magnitude of change.

In general, air temperature is expected to increase quite uniformly at all locations, but the increment varies depending on the RCP scenario. Maximum SAT will increase up to a maximum of 3.5°C, 4.5°C, and 6°C according to the RCP2.6, RCP4.5, and RCP8.5 scenarios, respectively. On average, minimum SAT presents a rate of increase smaller than that of maximum SAT by 0.5°C in each corresponding scenario. There is no clear spatial distribution pattern of air temperature change within the Flathead Region. However, Polson Kerr Dam shows distinctly the smallest maximum SAT increment within the study period, while Seeley Lake Ranger Station presents the largest one. The increment difference between the two climate stations at the end of the XXI century is about 1.5°C in all the three scenarios. Similarly, North Fork Jocko, followed by Missoula International Airport and Big Fork 13S, exhibit the smallest increase in minimum SAT, while Seeley Lake Ranger Station and Hot Springs Montana the largest one.

Regarding the intra-annual monthly variability of air temperature, Figures 2-19, 2-20, and 2-21 show a constant and spatially uniform increment of maximum SAT variability within the study period. The rate of increase generally increases from the RCP2.6 to the RCP8.5 scenarios. The same trend applies to minimum SAT variability, as illustrated in Figures 2-22, 2-23, and 2-24. However, in this case, it is possible to recognize an evident spatial pattern across the study area. The largest increment of minimum SAT variability takes place along the Mission Mountains range (i.e., Big Fork 13S, Moss Peak, Kraft Creek, and North Fork Jocko), with the addition of Missoula Airport. The analysis of monthly normals of daily minimum SAT reveals that the relatively larger variability observed at these locations is caused by a smaller temperature increase during the coldest months and a larger temperature increase in the warmest months.

Appendix C provides information that complements Figures 2-19 to 2-24. In fact, Figures C-21 to C-26 include data from all the twelve 30-year periods within 1960-2100. Both the air temperature normals and the intra-annual monthly variability related to any given 30-year period are displayed as absolute values. It can be noticed that the spatial distribution of air temperature within the Flathead Region is generally maintained in the future, independently of the scenario considered. Air temperature tends to decrease from west to east (especially maximum SAT) and from lower to higher altitudes. The greatest exception is represented by Seeley Lake Ranger Station, where maximum SAT is expected to increase at higher rates than those of surrounding areas. Also, temperature estimates at Big Fork 13S and Polson Kerr Dam tend to converge in all RCP scenarios, probably due to the geographic contiguity and the influence of the Flathead Lake.

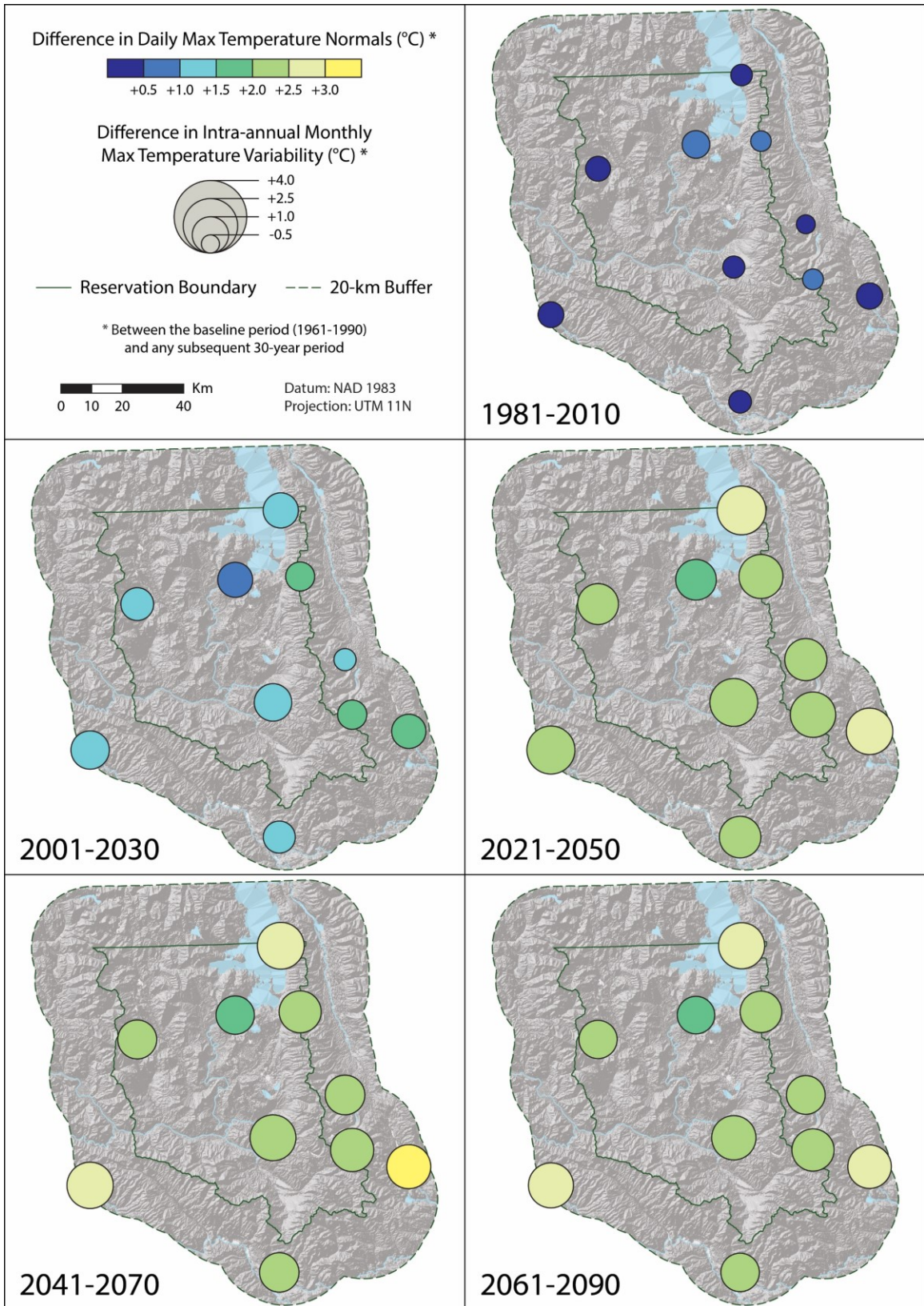


**Figure 2-19: Difference in maximum temperature normals and variability between the baseline period (1961-1990) and any subsequent 30-year period according to the RCP2.6 scenario**

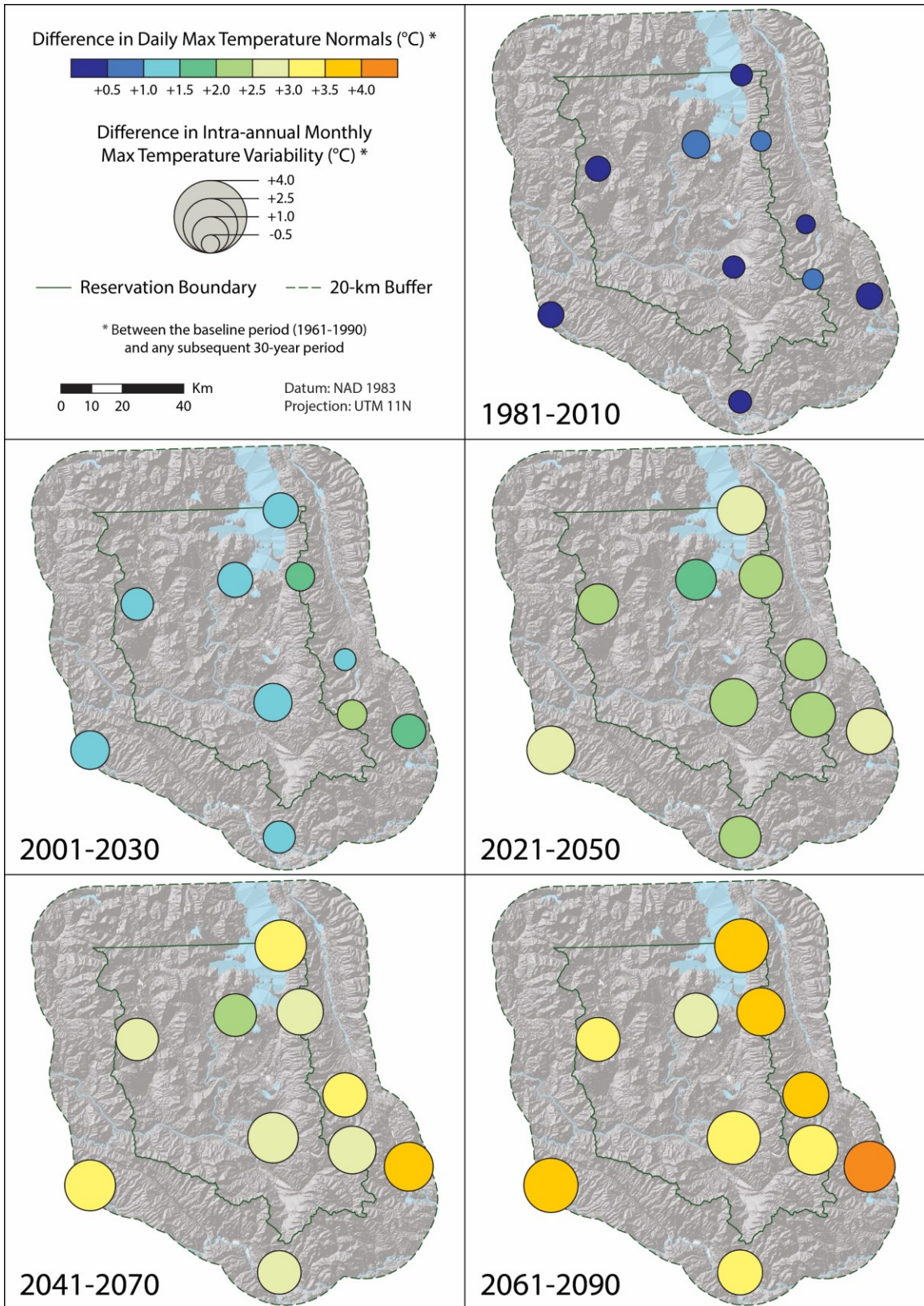


**Figure 2-20: Difference in maximum temperature normals and variability between the baseline period (1961-1990) and any subsequent 30-year period according to the RCP4.5 scenario**

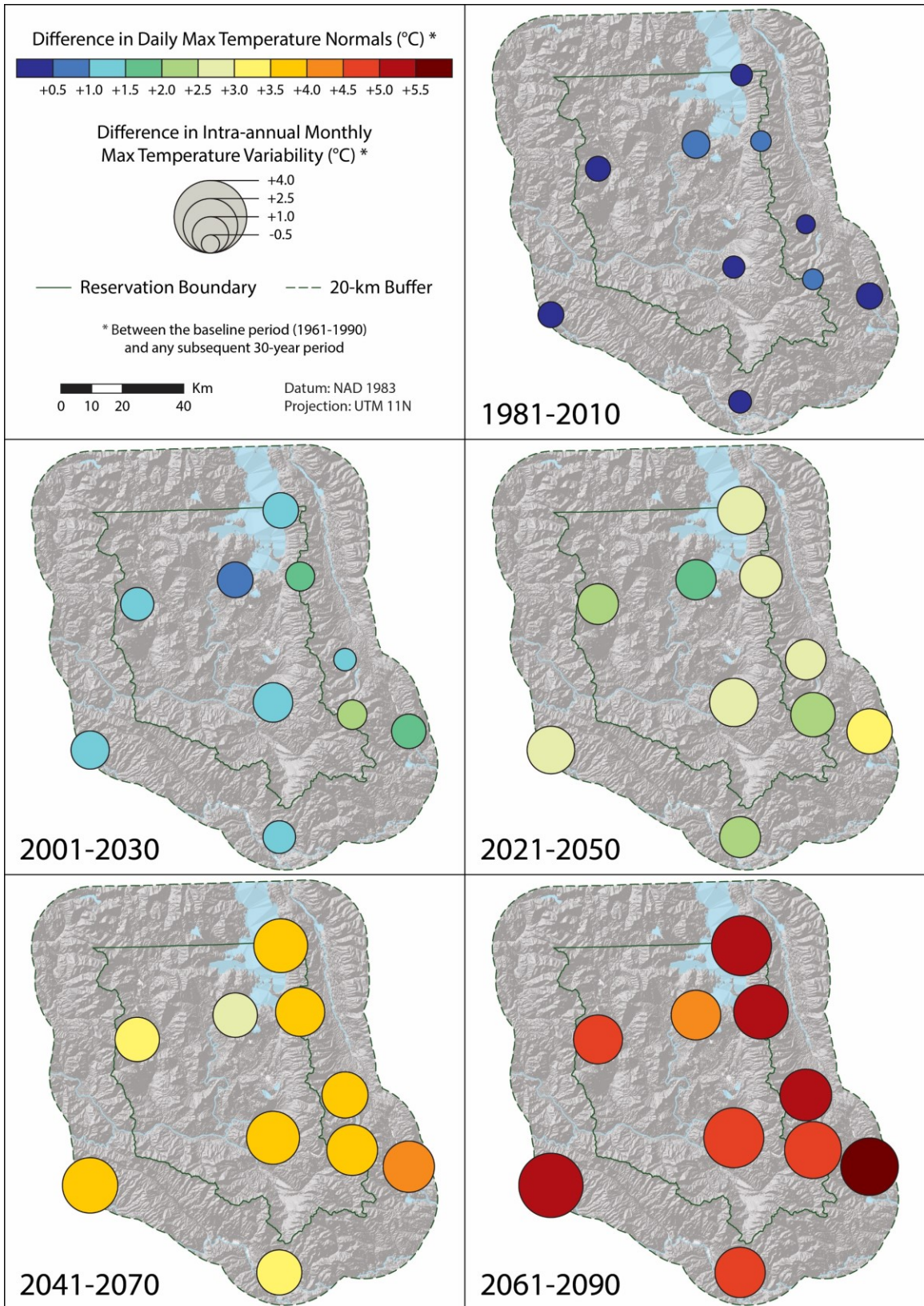


**Figure 2-21: Difference in maximum temperature normals and variability between the baseline period (1961-1990) and any subsequent 30-year period according to the RCP8.5 scenario**

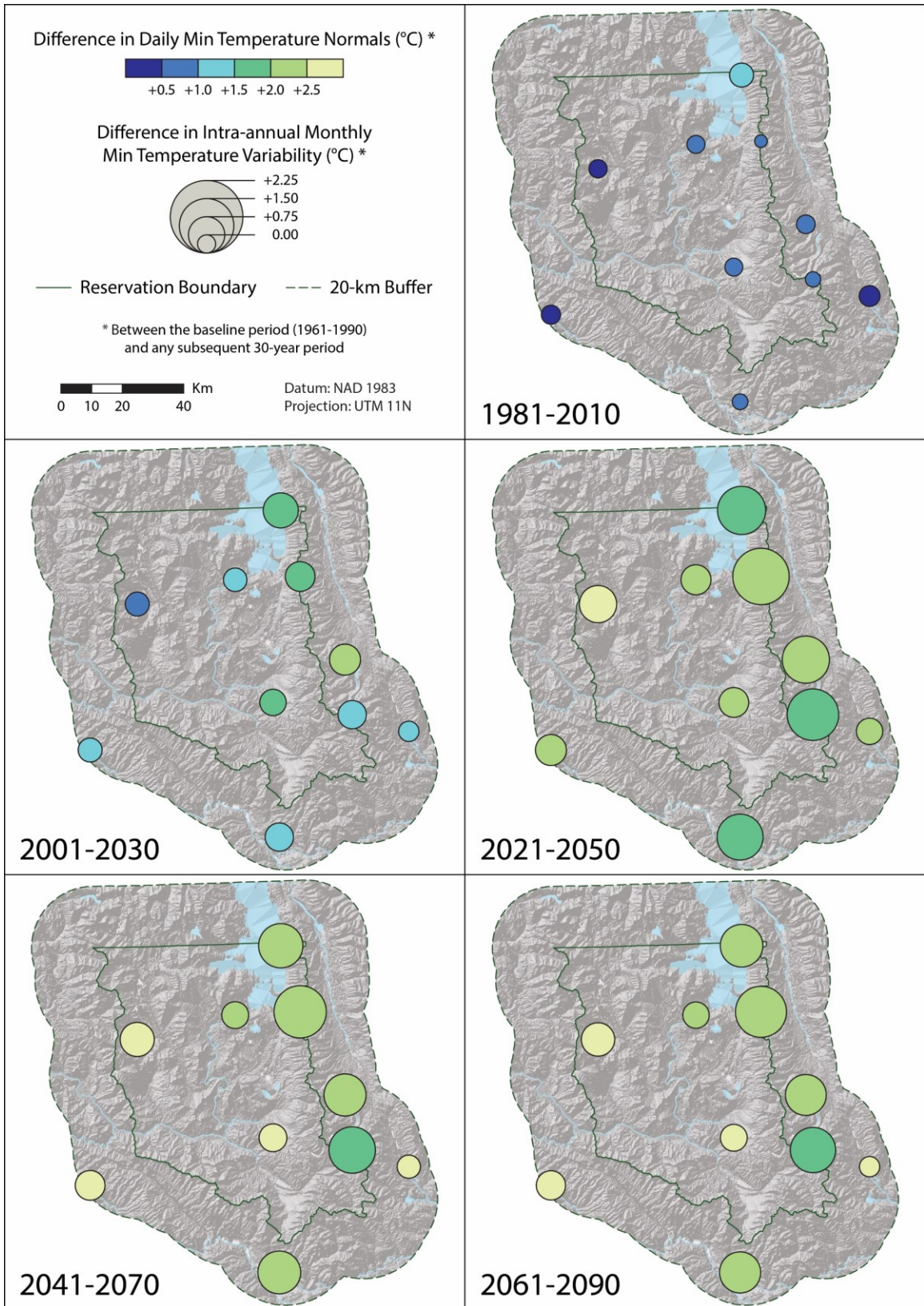


**Figure 2-22: Difference in minimum temperature normals and variability between the baseline period (1961-1990) and any subsequent 30-year period according to the RCP2.6 scenario**

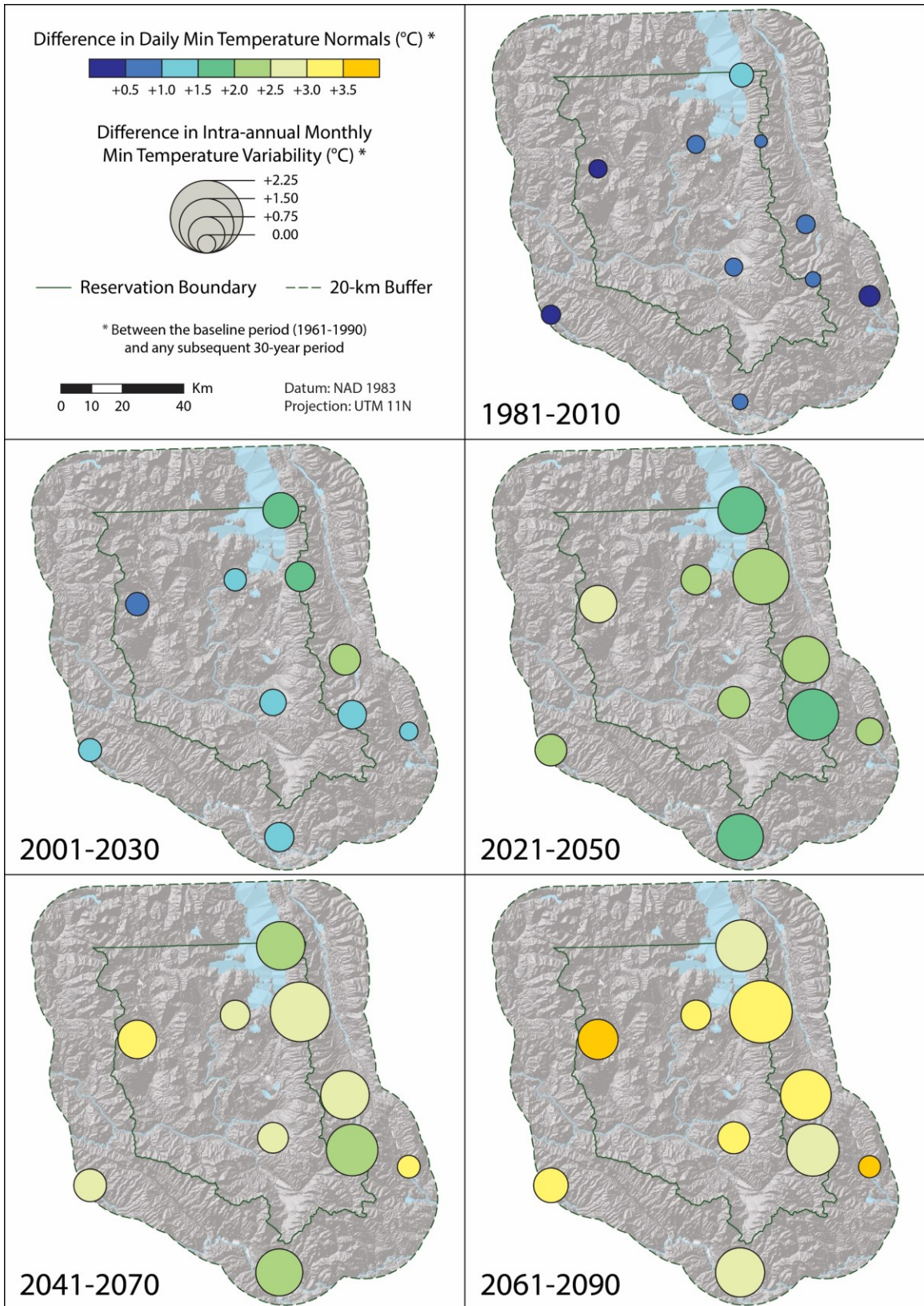


**Figure 2-23: Difference in minimum temperature normals and variability between the baseline period (1961-1990) and any subsequent 30-year period according to the RCP4.5 scenario**

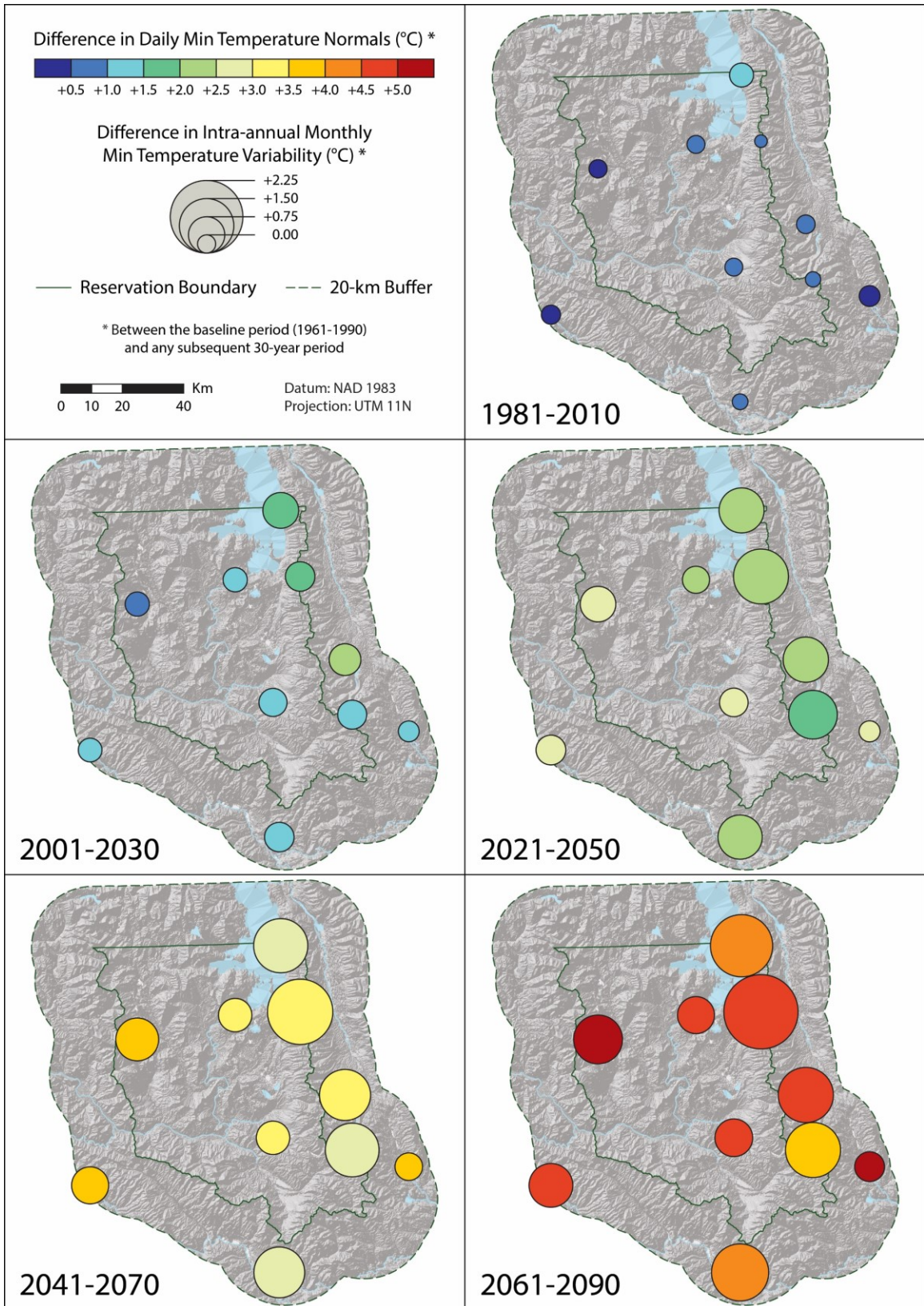


**Figure 2-24: Difference in minimum temperature normals and variability between the baseline period (1961-1990) and any subsequent 30-year period according to the RCP8.5 scenario**

Figures 2-25 to 2-28 and Figures 2-29 to 2-32 illustrate seasonal normals and intraseasonal monthly variability for maximum SAT and minimum SAT, respectively. Each figure includes information of an historical 30-year period (i.e., 1961-1990) and three future 30-year periods (i.e., 2011-2040, 2041-2070, and 2071-2100) for the three RCP scenarios. All temperature data are shown as absolute values. In general, all seasons are expected to manifest higher air temperatures in the future, independently of the scenario considered. However, summer will experience the greatest change in both maximum SAT and minimum SAT, with the first variable showing, according to the RCP8.5 scenario, a mean increment of about 10°C between 1961-1990 and 2071-2100 and the second variable a mean increase of around 8°C between the same two 30-year periods. Although the magnitude of change is proportionally smaller, this tendency is evident for the RCP45 ( $\approx 7^\circ\text{C}$  and  $\approx 5^\circ\text{C}$ ) and RCP26 ( $\approx 5^\circ\text{C}$  and  $\approx 4^\circ\text{C}$ ) scenarios as well.

Similarly to summer, the rate of change in winter, spring, and fall is relatively larger for maximum SAT than for minimum SAT. Also, these three seasons usually present much lower values of air temperature increment in comparison with summer across the three scenarios. The greatest exception is represented by the increase of minimum SAT in winter, which is smaller than that estimated in summer, but generally much larger than those predicted for spring and fall. Regarding the spatial distribution of seasonal normals across the Flathead Region, a pattern similar to that of the annual normals (see Figures C-21 to C-26 in Appendix C) can be identified, as air temperature tends to diminish with altitude and from west to east in all seasons. Big Fork 13S and Seeley Lake Ranger Station sometimes represent an exception to this tendency, as these stations

show unusually high minimum SAT and maximum SAT normals, respectively. In both cases, this anomaly of air temperature is more evident during summer.

The intraseasonal monthly variability of air temperature does not present such a clear regional pattern across the climate scenarios, stations, seasons, and variables considered as it is for the air temperature normals. The most noticeable trend occurs in summer and especially fall, when the monthly variability is expected to constantly increase with increasing time and RCP for both maximum and minimum SAT. On the contrary, the monthly variability of air temperature in winter and spring does not follow an evident path, as it increases, diminishes, or remains constant depending on the climate station and 30-year period analyzed. However, it can be noticed that monthly maximum SAT variability in spring tends to decrease with increasing time and RCP in the most elevated areas (i.e., Moss Peak, North Fork Jocko, and Kraft Creek).

In terms of the set of values taken on by air temperature normals and variability across the region and period of study, there are some seasonal differences. Summer exhibits the most extended range of maximum SAT normals ( $\approx 20^{\circ}\text{C}$ ), followed by spring and fall ( $\approx 15^{\circ}\text{C}$ ), and eventually winter ( $\approx 10^{\circ}\text{C}$ ). Regarding minimum SAT normals, summer is still leading ( $\approx 15^{\circ}\text{C}$ ), but the remaining three seasons present a similar extension of values ( $\approx 10^{\circ}\text{C}$ ). Summer is also showing the largest range of monthly minimum SAT variability ( $\approx 5^{\circ}\text{C}$ ), but this is probably due to the unusually high value estimated at Moss Peak. Fall manifests a considerable large range of this variable as well ( $\approx 3^{\circ}\text{C}$ ). Fall also stands out among all seasons for both the largest magnitude and range ( $\approx 6^{\circ}\text{C}$ ) of monthly maximum SAT variability.

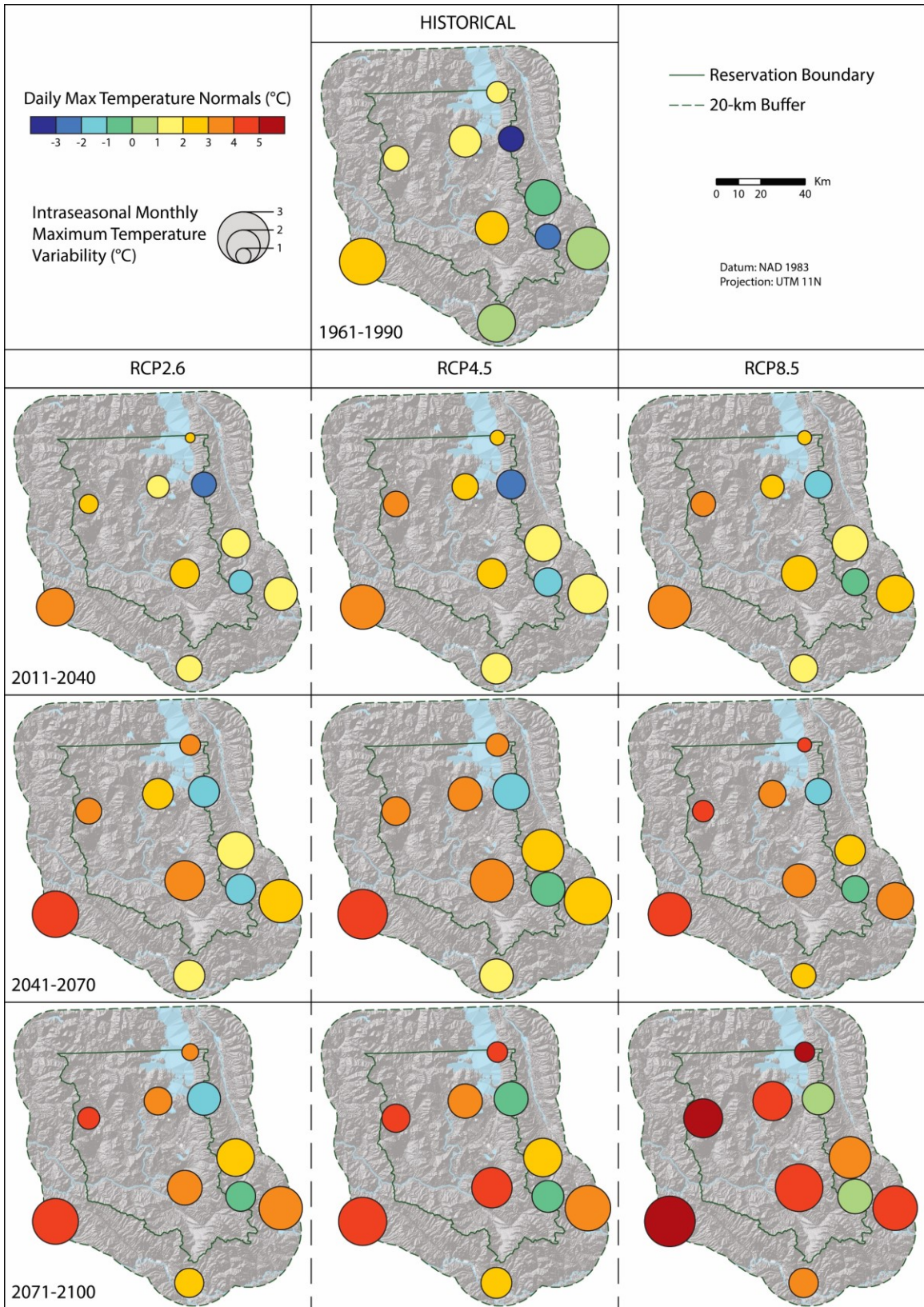


**Figure 2-25: Daily maximum temperature normals and intraseasonal monthly maximum temperature variability for winter according to historical data and three RCP scenarios**

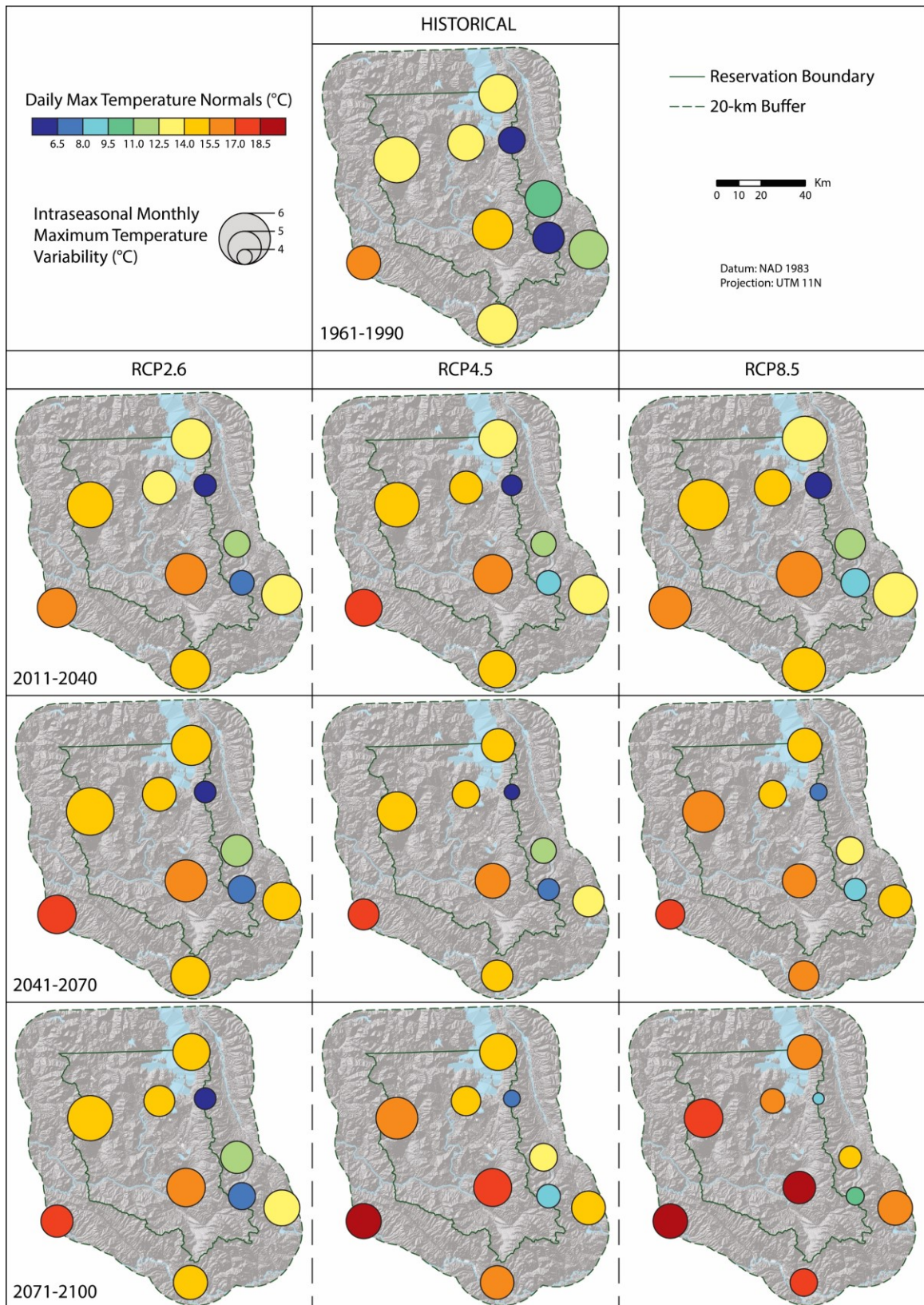


**Figure 2-26: Daily maximum temperature normals and intraseasonal monthly maximum temperature variability for spring according to historical data and three RCP scenarios**

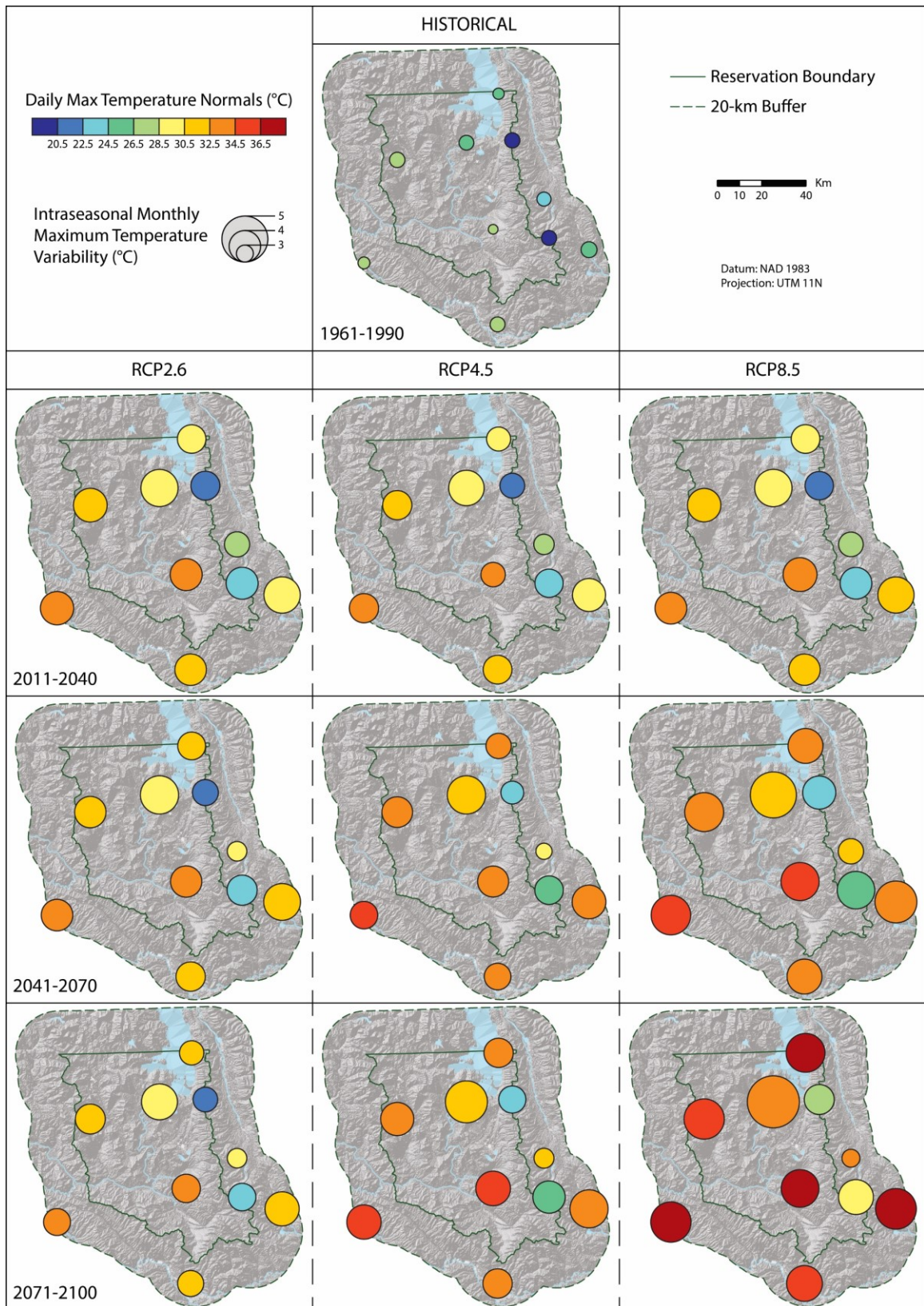


**Figure 2-27: Daily maximum temperature normals and intraseasonal monthly maximum temperature variability for summer according to historical data and three RCP scenarios**

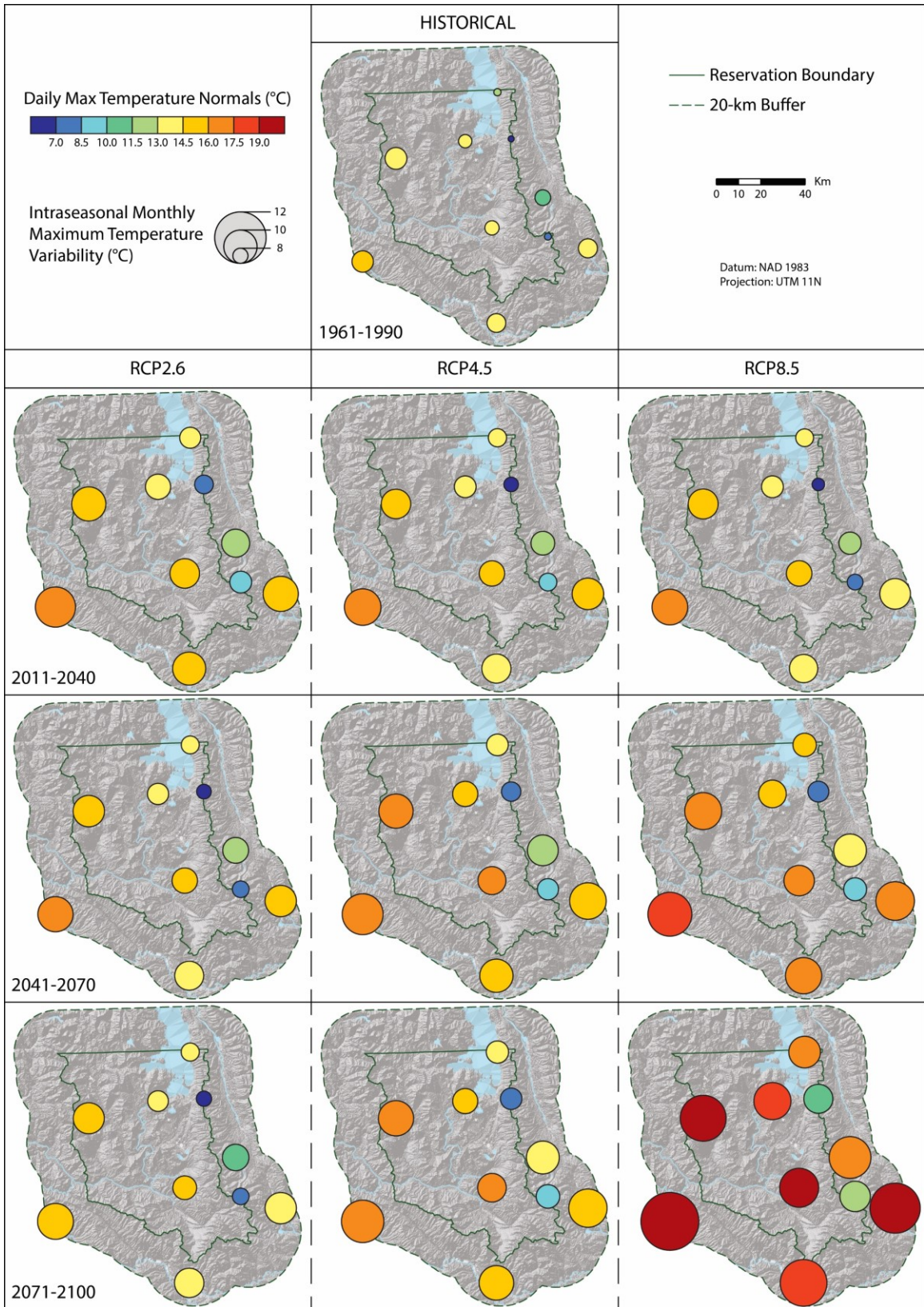


**Figure 2-28: Daily maximum temperature normals and intraseasonal monthly maximum temperature variability for fall according to historical data and three RCP scenarios**

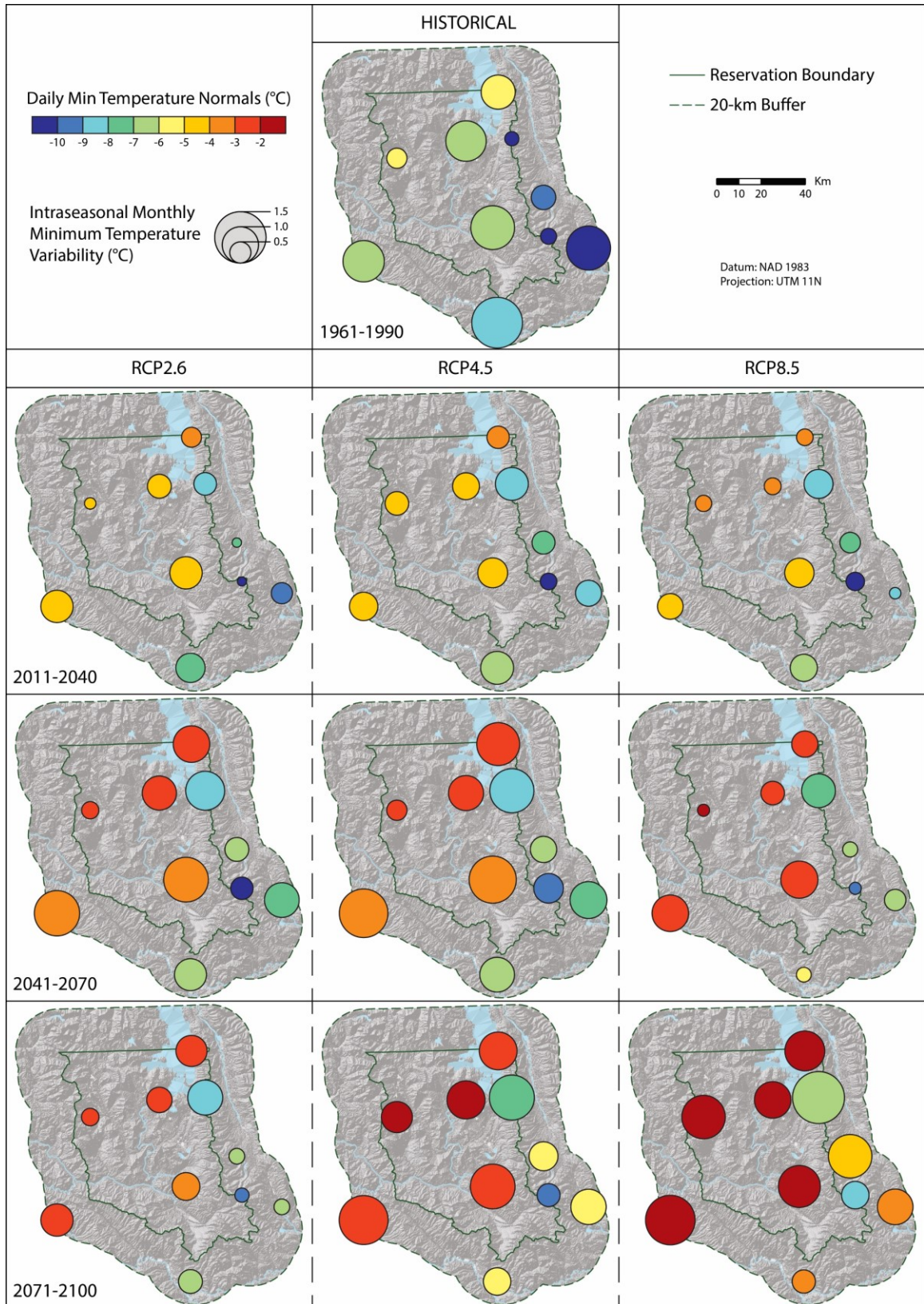


**Figure 2-29: Daily minimum temperature normals and intraseasonal monthly minimum temperature variability for winter according to historical data and three RCP scenarios**

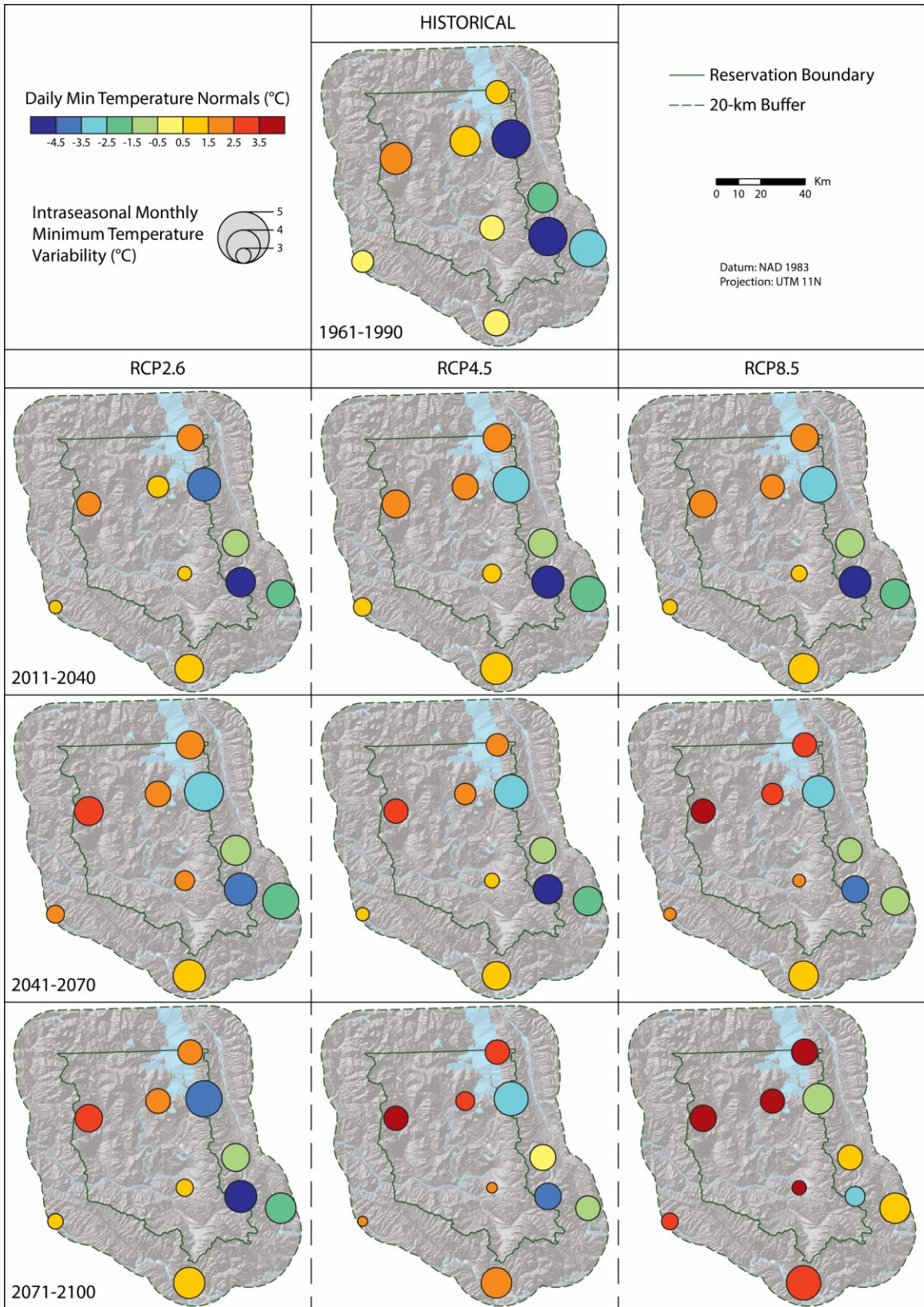


**Figure 2-30: Daily minimum temperature normals and intraseasonal monthly minimum temperature variability for spring according to historical data and three RCP scenarios**

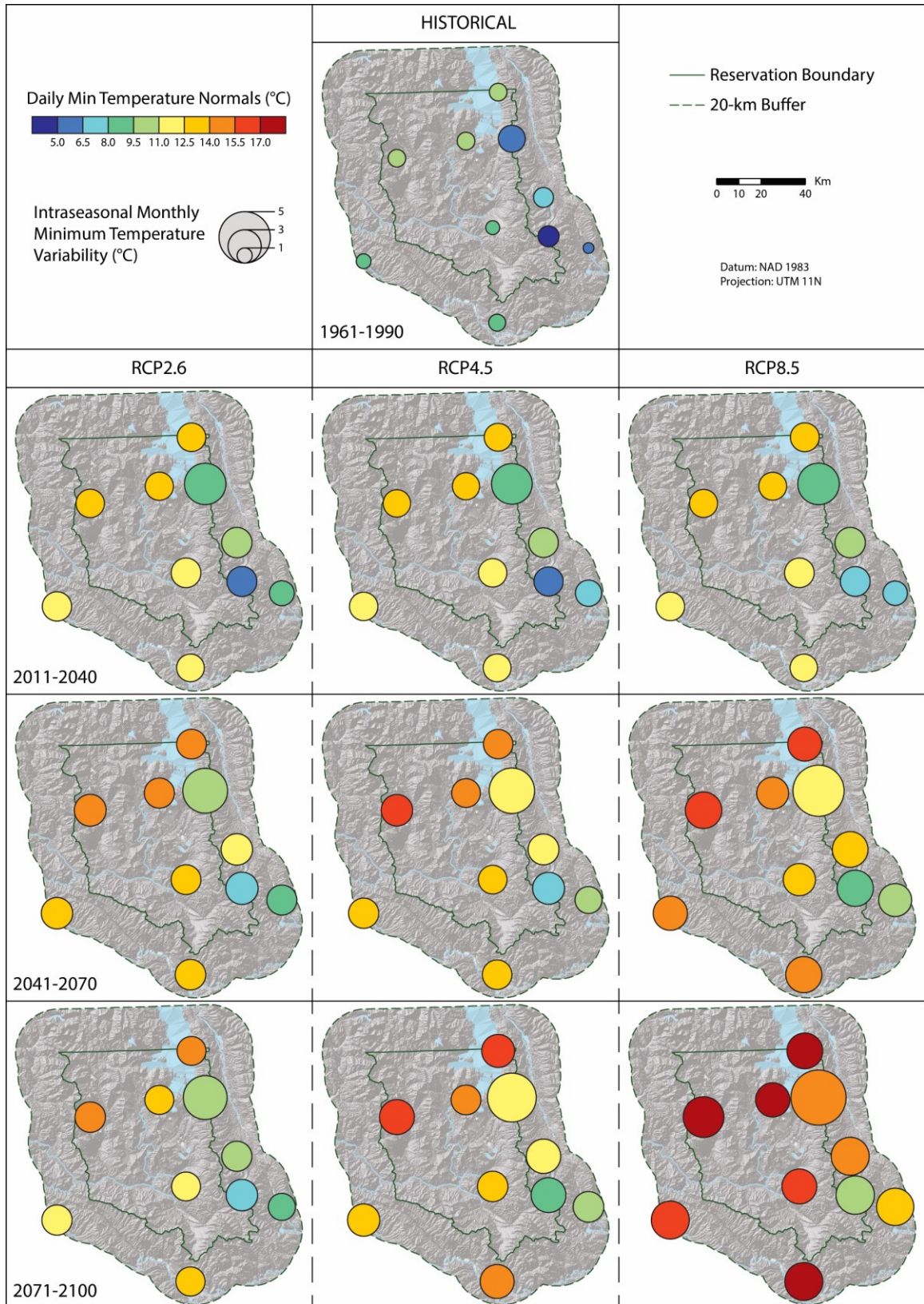


**Figure 2-31: Daily minimum temperature normals and intraseasonal monthly minimum temperature variability for summer according to historical data and three RCP scenarios**

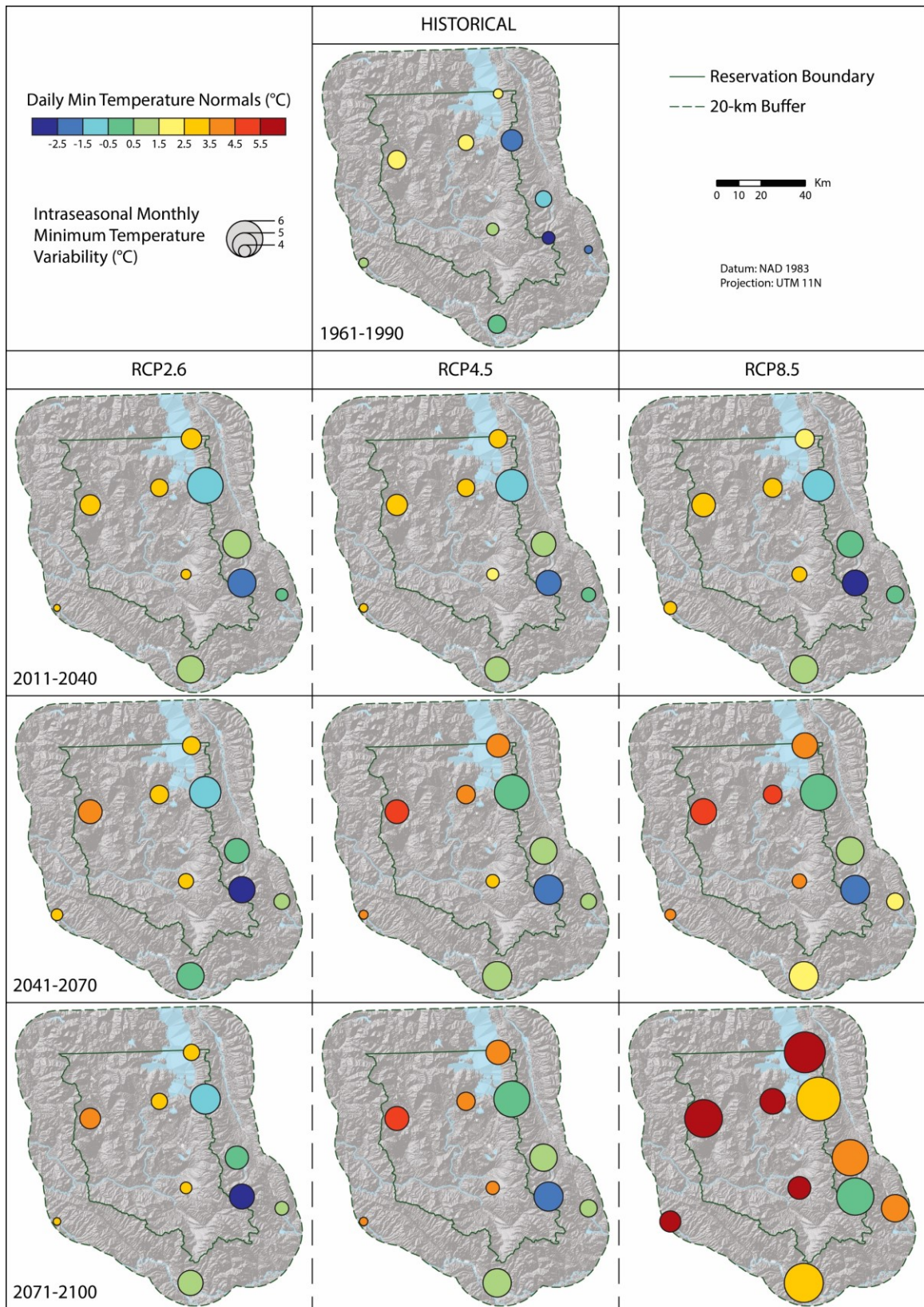


**Figure 2-32: Daily minimum temperature normals and intraseasonal monthly minimum temperature variability for fall according to historical data and three RCP scenarios**

### 2.5.2.2. SAT trends

The graphics in Figures 2-33 to 2-36 illustrate the main results of the RKTs that were applied to the seasonal and annual means of both daily maximum and minimum SAT over the 1961-2100 study period across the entire Flathead Region (see Section 2.4.3.4). In particular, Figures 2-33 and 2-34 present the Kendall's correlation coefficient ( $\tau$ ) derived from the analysis of maximum SAT and minimum SAT, respectively. Similarly, Figures 2-35 and 2-36 show the magnitude of change ( $\phi$ ) related to the trends of maximum SAT and minimum SAT, respectively. This indicator is easily calculated from the Theil-Sen's slope and is measured in °C per decade. Each graphic includes the results associated with the three RCP scenarios. The null hypothesis stating that there is no trend is rejected in all cases because the p values are always smaller than 0.0001. The Kendall's statistic and its variance, the Theil-Sen's slope, and the p value related to each RKT are not reported on these graphics, but they are included in Appendix C (Table C-1).

Figures 2-33 to 2-36 reveal that there is an unequivocal increasing trend in air temperature across the Flathead Region. Both  $\tau$  and  $\phi$  increase with increasing RCP. In general, maximum SAT is associated with smaller  $\tau$  and larger  $\phi$  than minimum SAT. Among the four seasons, summer clearly shows the highest values of either  $\tau$  or  $\phi$ , independently of the variable analyzed. Winter also exhibits large  $\tau$  and  $\phi$  in comparison with spring and fall, but only when minimum SAT is considered. To read correctly the results in Figures 2-33 and 2-34, it is important to highlight that a monotonic association between two variables (air temperature and time in this case) can be defined as "strong" when  $\tau$  values are equal or greater than 0.7. A value of 0.9 or above of the traditional

correlation coefficient  $r$  would result from a linear association of the same strength (Helsel and Hirsch 2002).

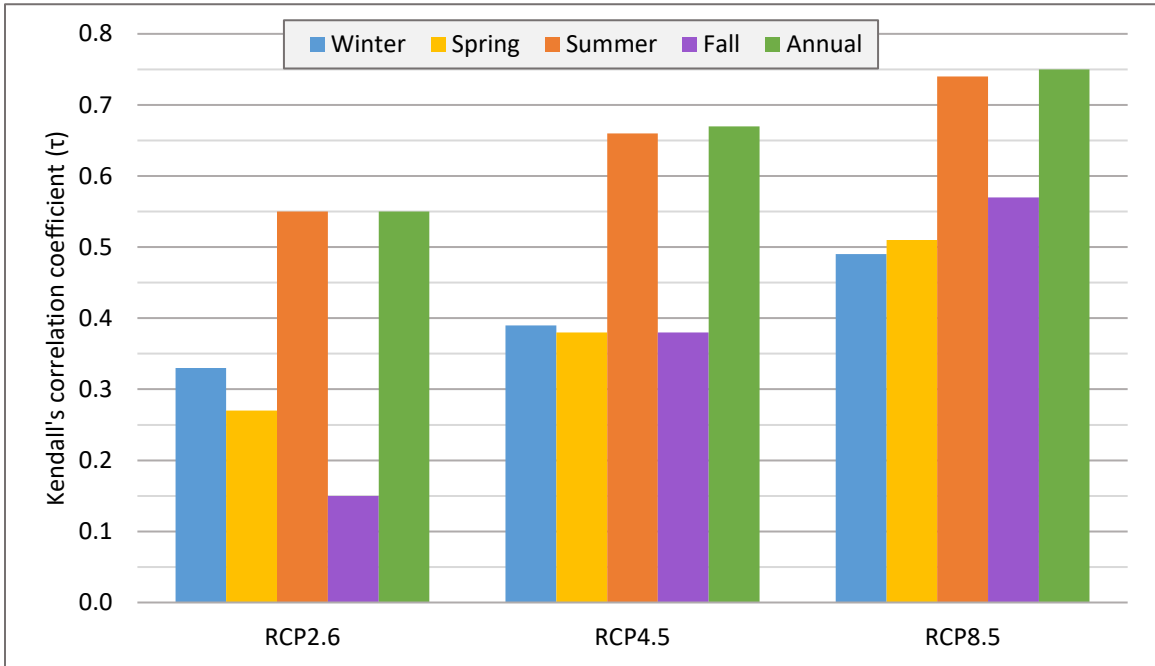


Figure 2-33: Kendall's correlation coefficient related to the 1961-2100 regional trend in the mean annual and seasonal maximum SAT according to the three proposed RCP scenarios

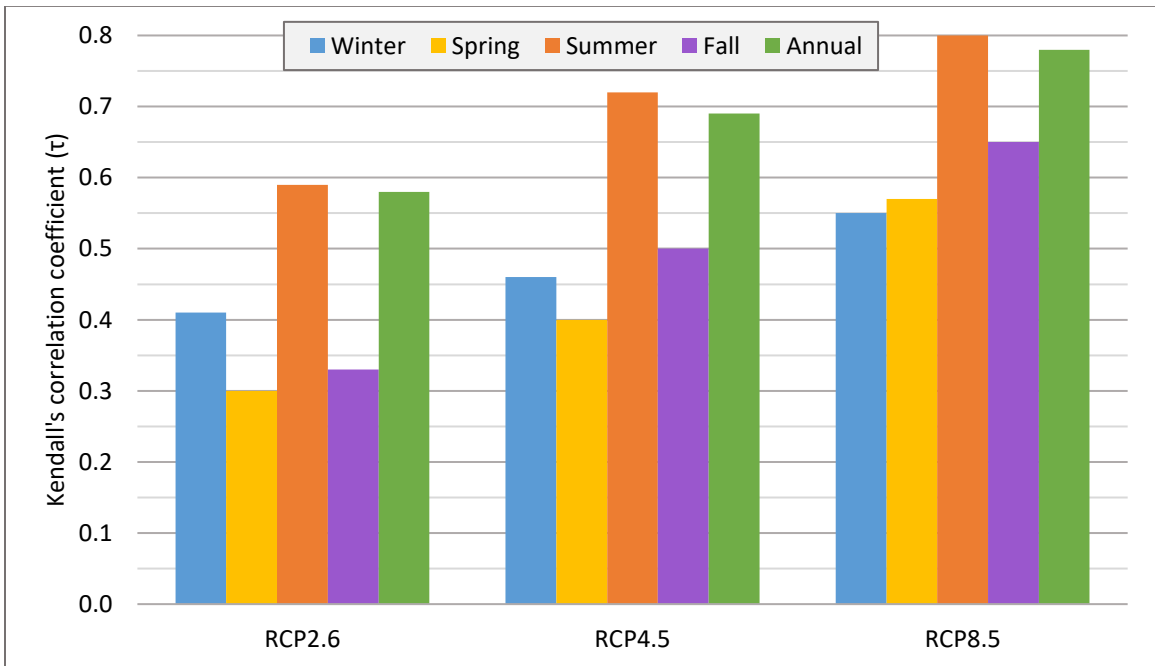
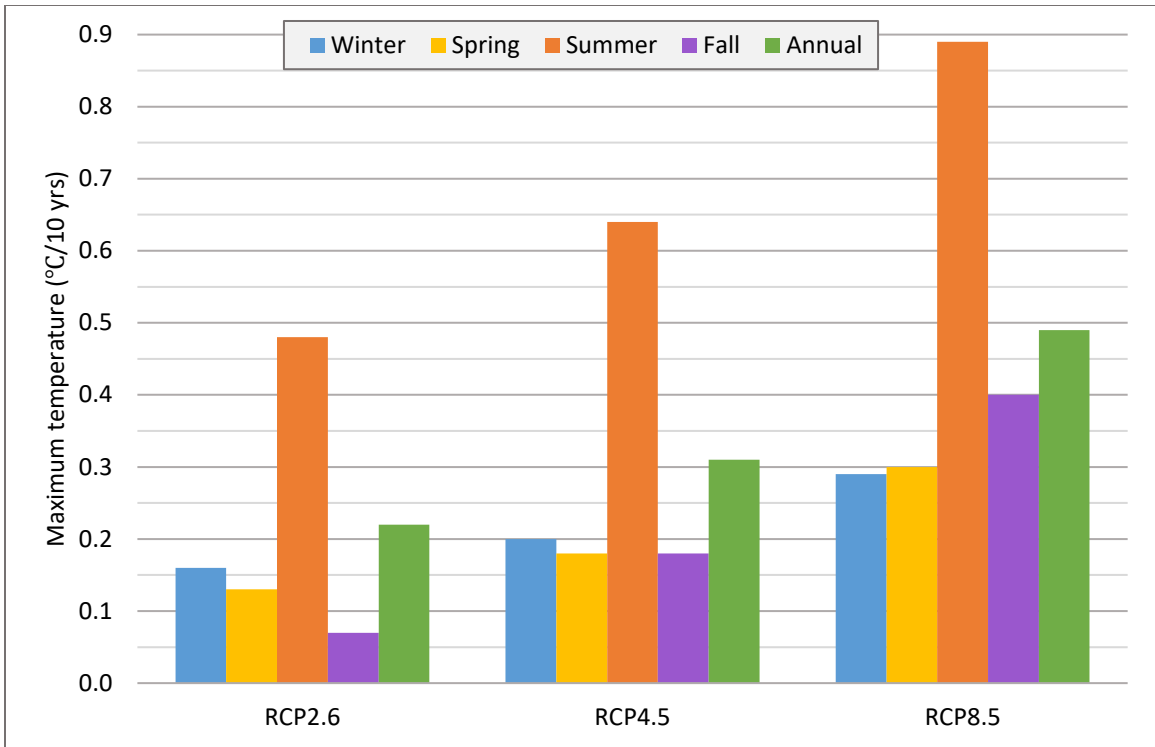
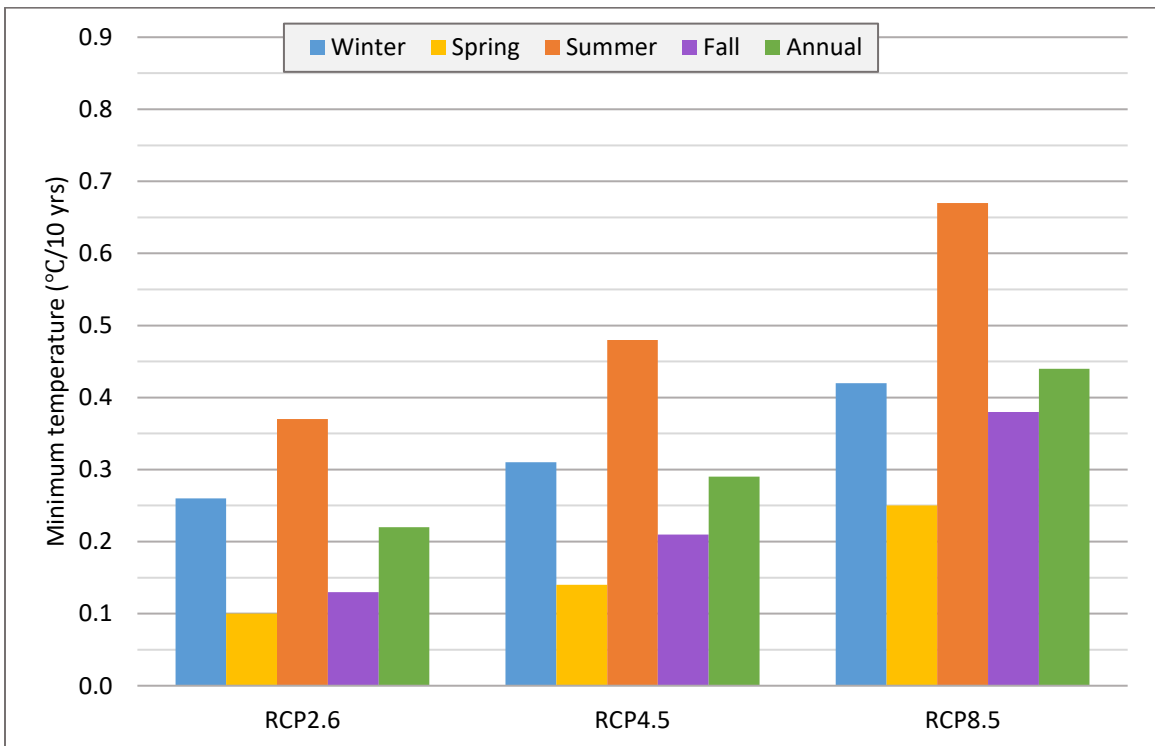


Figure 2-34: Kendall's correlation coefficient related to the 1961-2100 regional trend in the mean annual and seasonal minimum SAT according to the three proposed RCP scenarios



**Figure 2-35: Mean decadal regional trend of the mean annual and seasonal maximum SAT within the 1961-2100 period according to the three proposed RCP scenarios**



**Figure 2-36: Mean decadal regional trend of the mean annual and seasonal minimum SAT within the 1961-2100 period according to the three proposed RCP scenarios**

Figures 2-37 to 2-42 illustrate the main results of the MKTs that were applied to the seasonal and annual means of both daily maximum and minimum SAT over the 1961-2100 study period for the ten climate stations of interest (see Section 2.4.3.4). These sets of maps reveal the spatial distribution of potential air temperature trends within the Flathead Region. As with the previous graphics, these maps display  $\tau$  and  $\phi$ . The first variable is represented by the inclination of an arrow, the second one by graduated colors. The null hypothesis stating that there is no trend is rejected in all cases but three. These exceptions, which are associated with p values greater than the 0.05 significance level, are indicated with a cross hatching pattern inside the arrow shape in the fall maps of Figures 2-37 and 2-40. The Kendall's statistic and its variance, the Theil-Sen's slope, and the p value related to each MKT are not reported on these maps, but they are included in Appendix C (Table C-1).

All MKTs output positive values for both  $\tau$  and  $\phi$ , which reveals that not even one decreasing air temperature trend is detected throughout the entire study area. Rather, the ten locations of interest are mostly characterized by increasing trends. However, the slope of these trends (i.e., the magnitude of the increase) and the strength of the monotonic association between SAT and time vary depending on the location, period, and scenario considered. Finally, in a few cases, no evident air temperature trend can be identified. Some of the general patterns that emerge at the regional scale (especially those that are determined by the choice of a specific period or scenario) are visible in these sets of maps as well. In addition, Figures 2-37 to 2-42 provide unique information about the spatial distribution of  $\tau$  and  $\phi$  within the Flathead Region.

As for maximum SAT trends,  $\phi$  values are usually similar to each other within the Flathead Region at the annual temporal scale, with the exception of Polson Kerr Dam and Seeley Lake Ranger Station. The first location presents a lower rate of change than the average, while the latter a higher one. This tendency is evident for Seeley Lake Ranger Station at the seasonal temporal scales as well, especially in winter and summer, whereas is less clear for Polson Kerr Dam. Big Fork 13S and, to a smaller extent, Superior also exhibit a larger  $\phi$  value than the surrounding areas, but only in summer. The spatial variability of  $\tau$  across the study area is usually very small. Winter and spring show a larger variability according to all the RCP scenarios, but, even in these cases, it is difficult to identify specific spatial patterns of  $\tau$ .

Regarding minimum SAT trends, a clear pattern appears at the annual temporal scale, as the Mission Mountains range (i.e., Big Fork 13S, Moss Peak, Kraft Creek, and North Fork Jocko) and Missoula Airport manifest lower  $\phi$  values than those encountered in other areas. It seems that this pattern changes when the RCP8.5 scenario is adopted, but a closer look at the actual  $\phi$  values reveals that the spatial distribution is maintained with the exception of Moss Peak, where  $\phi$  reaches values similar to those found in the western side of the study area. This is probably due to the unusually high  $\phi$  estimated at Moss Peak in summer. Apart from spring, the spatial variability of  $\tau$  across the Flathead Region is usually higher than that related to maximum SAT. This is especially true for fall, which presents the highest  $\tau$  variability among all seasons. It is also possible to identify a spatial pattern in fall, as the locations along the Mission Mountains and Missoula Airport show lower  $\tau$  values. However, this pattern becomes less evident as the RCP increases.

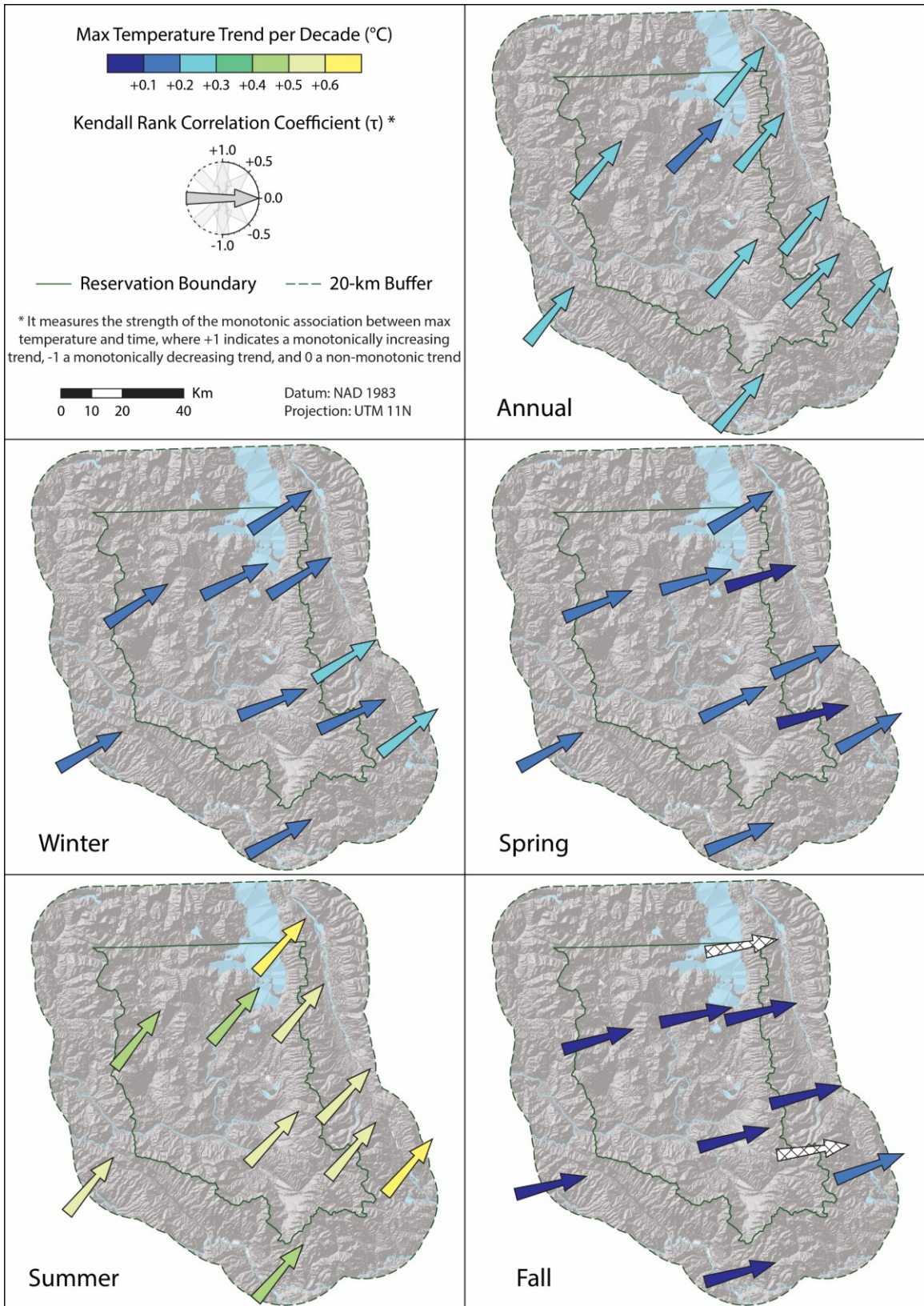


**Figure 2-37: Mean decadal trend of the mean annual/seasonal maximum SAT and related Kendall's correlation coefficient within the 1961-2100 period according to the RCP2.6 scenario**

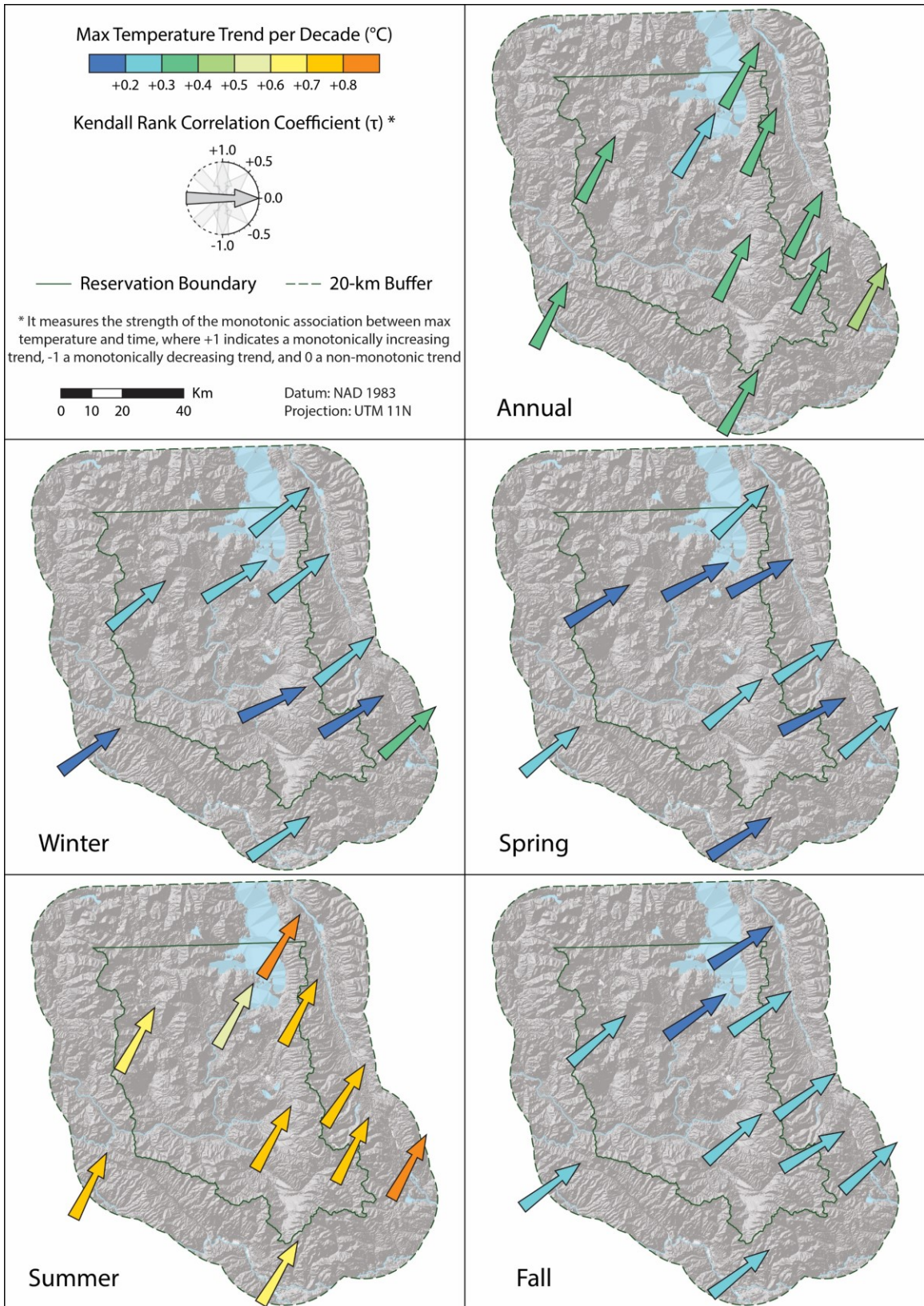


**Figure 2-38: Mean decadal trend of the mean annual/seasonal maximum SAT and related Kendall's correlation coefficient within the 1961-2100 period according to the RCP4.5 scenario**

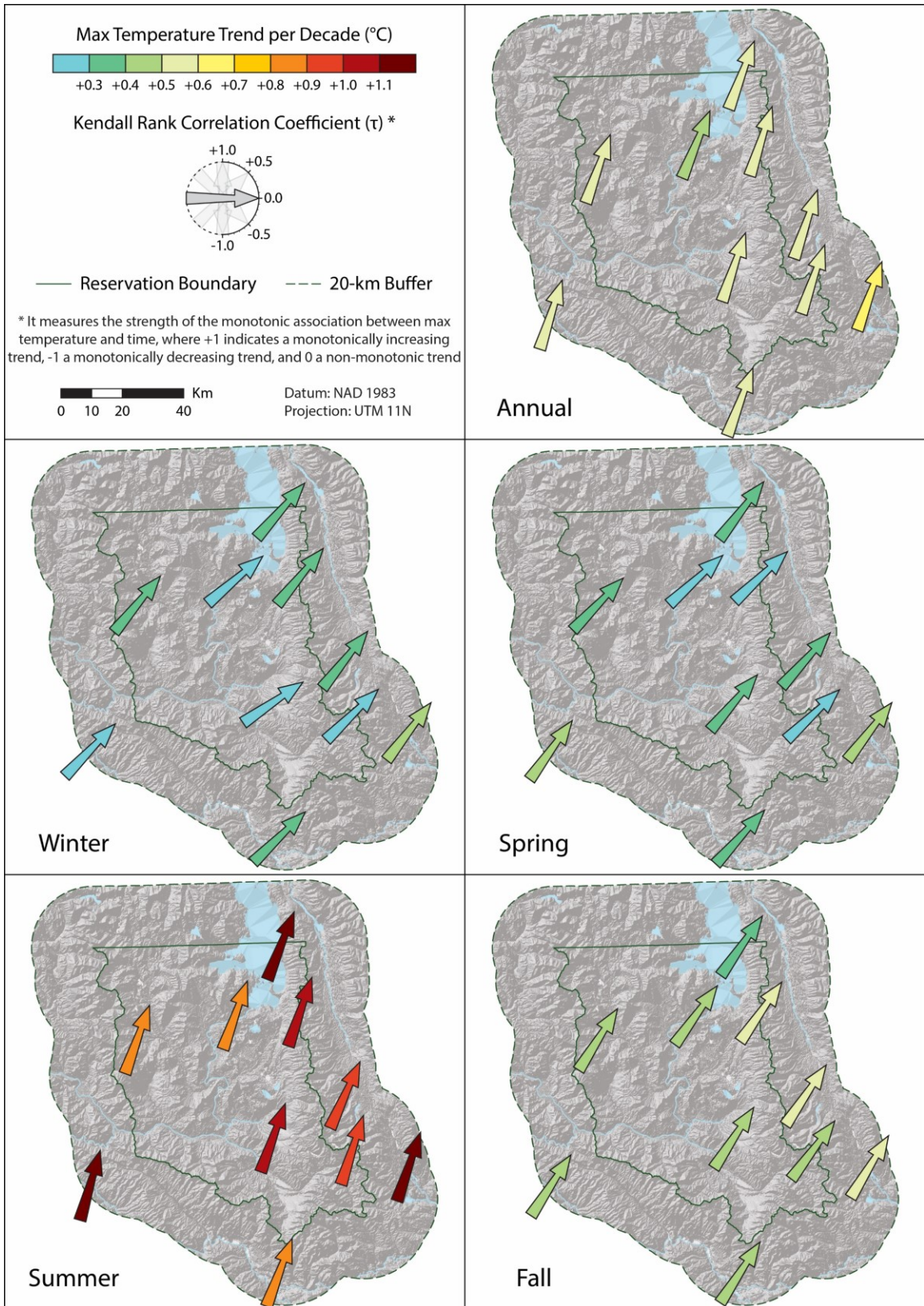


**Figure 2-39: Mean decadal trend of the mean annual/seasonal maximum SAT and related Kendall's correlation coefficient within the 1961-2100 period according to the RCP8.5 scenario**

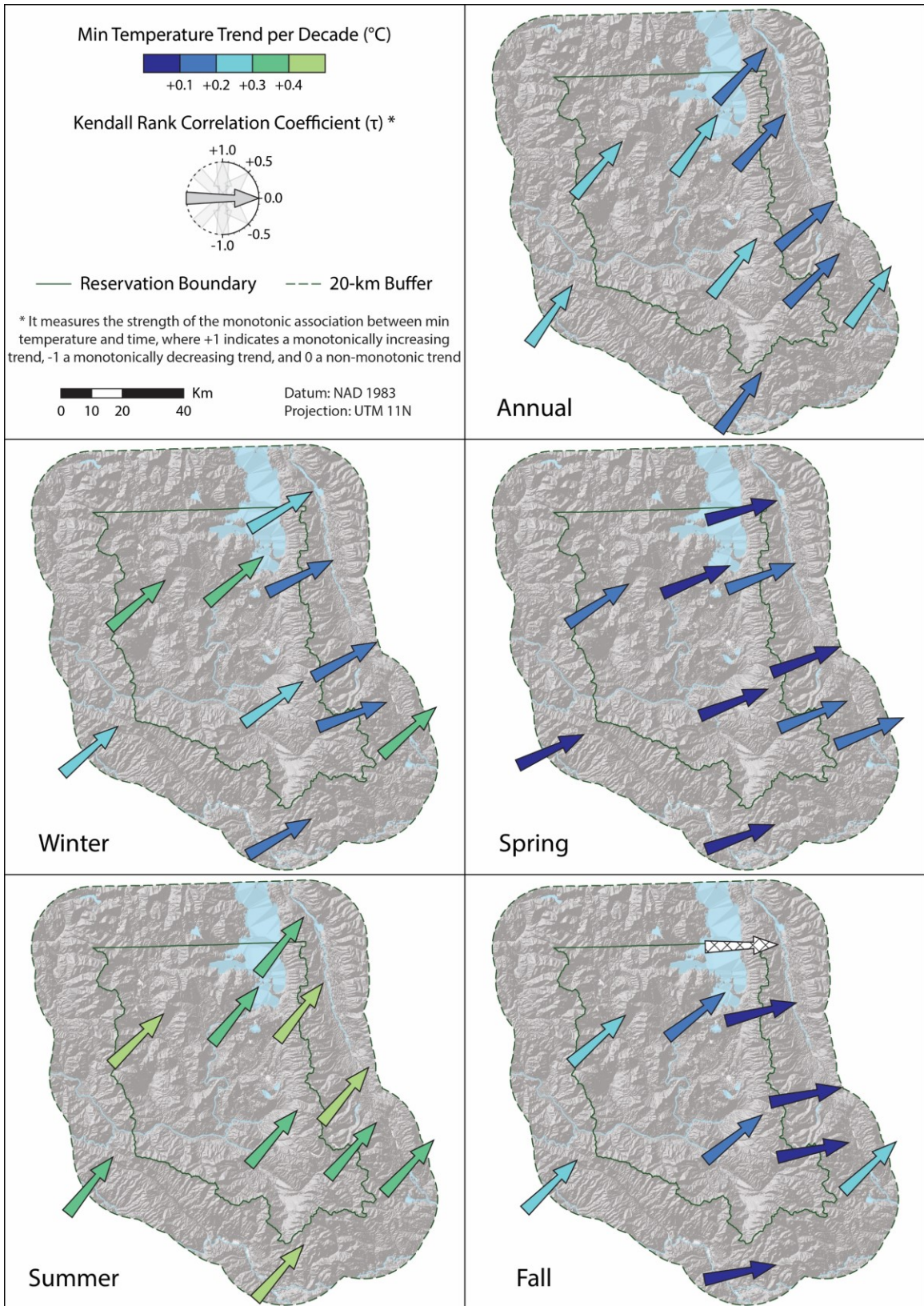


**Figure 2-40: Mean decadal trend of the mean annual/seasonal minimum SAT and related Kendall's correlation coefficient within the 1961-2100 period according to the RCP2.6 scenario**

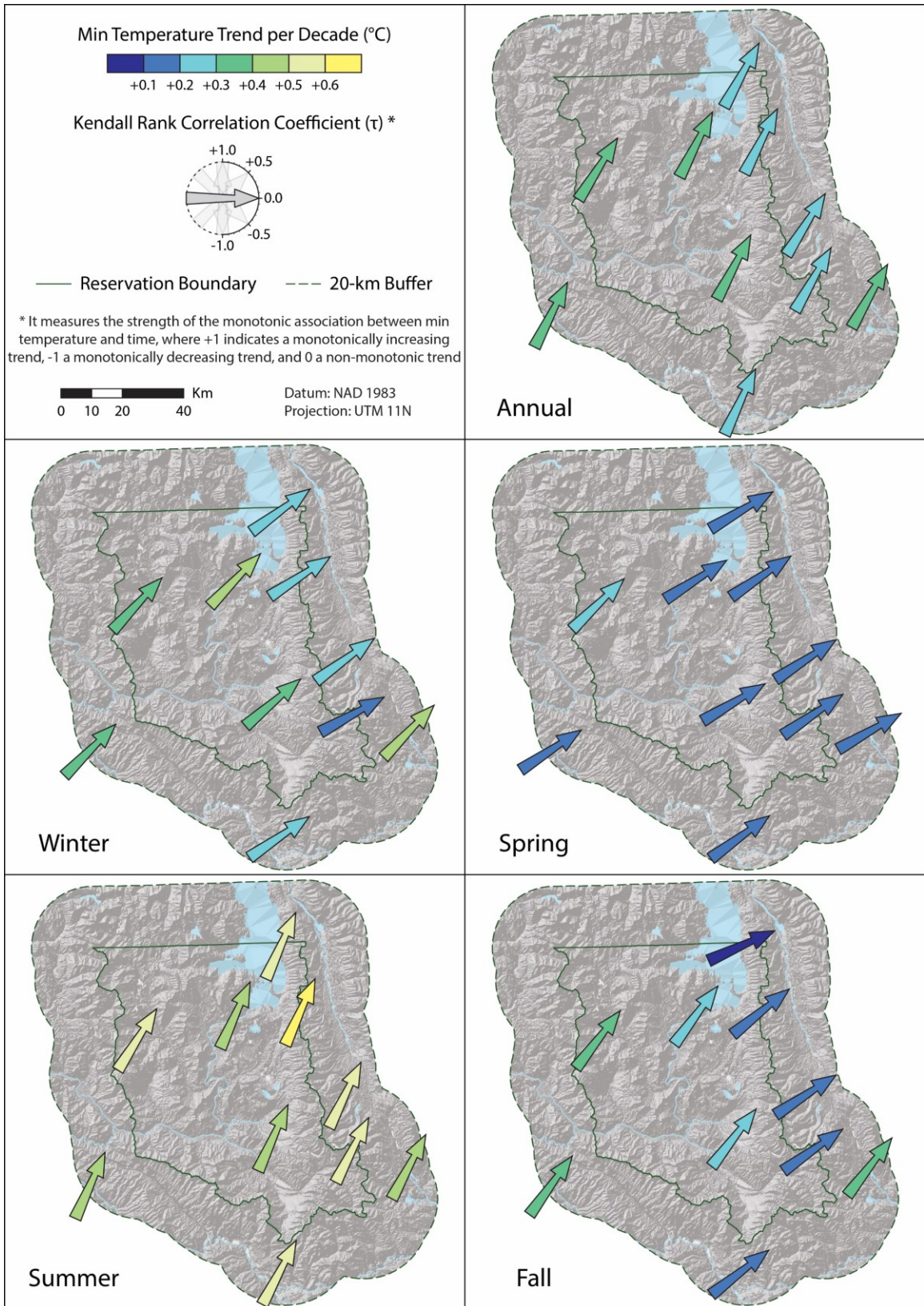


**Figure 2-41: Mean decadal trend of the mean annual/seasonal minimum SAT and related Kendall's correlation coefficient within the 1961-2100 period according to the RCP4.5 scenario**

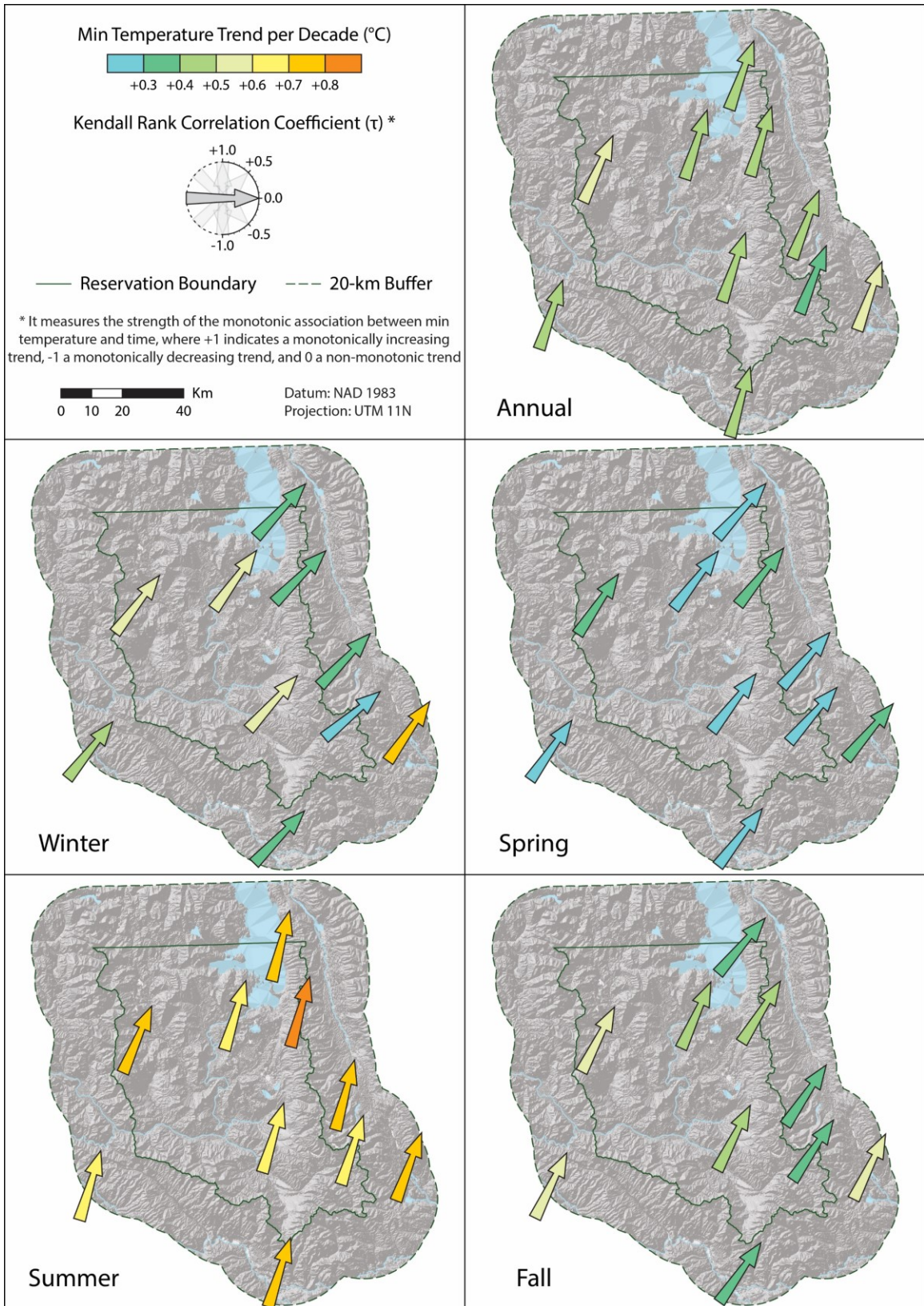


**Figure 2-42: Mean decadal trend of the mean annual/seasonal minimum SAT and related Kendall's correlation coefficient within the 1961-2100 period according to the RCP8.5 scenario**

### **2.5.2.3. Final considerations**

This section intends to summarize the main findings related to the analysis of air temperature, as a way to address the first research question associated with this chapter (see Section 2.3). The two sets of analyses described in the previous two sections corroborate and complement each other, and provide a clear picture of the historical and potential future evolution of maximum and minimum SAT in the Flathead Region. Observed data across the study area indicate that air temperature has been increasing over the last 60 years and this trend is expected to continue in the future, independently of the scenario considered. In general, maximum SAT increases at higher rates than minimum SAT, which causes air temperature variability to increase as well. However, the increase in minimum SAT is usually more constant than that in maximum SAT. Summer is definitely the season that experiences the largest increment in air temperature. The magnitude of the increase is also very pronounced in winter, but only for minimum SAT.

As aforementioned, all the RCP scenarios adopted in this study predict an increment in air temperature, but the rate of change increases with increasing RCP. Also, the trajectory differs based on the specific scenario considered, as it tends to stabilize after 1950 (RCP2.6) or 2100 (RCP4.5), or it continues to constantly increase (RCP8.5). The analysis of changes in 30-year normals (Section 2.5.2.1) reveals that the increments in maximum SAT between 1961-1990 and 2071-2100 at the scale of the Flathead Region are about 2.4°C, 3.6°C, and 5.8°C according to the RCP2.6, RCP4.5, and RCP8.5, respectively. Similarly, the increment values related to minimum SAT are 2.3°C, 3.3°C, and 5.2°C, respectively. The analysis of air temperature trends (Section 2.5.2.2) shows

projections that are consistent with those just described. The mean decadal regional trends of the mean annual maximum SAT from 1961 to 2100 are about 0.22°C, 0.31°C, and 0.49°C based on the RCP2.6, RCP4.5, and RCP8.5, respectively. The correspondent values relative to minimum SAT are 0.22°C, 0.29°C, and 0.44°C, respectively.

The spatial distribution of the air temperature increase within the Flathead Region varies depending on the location, period (i.e., seasonal or annual), and scenario considered. The temperature pattern that consists in decreasing temperatures from west to east and from low to high altitudes is generally maintained in the future. However, there are several exceptions. In comparison with other the other climate stations, Seeley Lake Ranger Station, which is located at a relatively high elevation (i.e., about 1250 meters above mean sea level) on the east side of the Flathead Region (see Section 2.4.1.1), manifest an uniquely high increase in both maximum and minimum SAT, especially in summer and winter. Some locations experience a relatively large increment in either maximum SAT (e.g., Big Fork 13S and Superior, but only in summer) or minimum SAT (e.g., Hot Springs Montana). Similarly, other locations show a lower increase in either maximum SAT (e.g., Polson Kerr Dam) or minimum SAT (e.g., North Fork Jocko, especially in winter) than that encountered in surrounding areas.

Finally, a clear spatial pattern emerges from the analysis of minimum SAT. The areas along the Mission Mountains range (i.e., Big Fork 13S, Moss Peak, Kraft Creek, and North Fork Jocko), with the addition of Missoula Airport, exhibit a relatively small increment in minimum SAT during the coldest months. This tendency is reversed during the warmest months, as minimum SAT generally increases at much higher rates than

those estimated in winter. As a result, the intra-annual monthly variability of minimum SAT in these areas is much larger than that observed elsewhere in the Flathead Region. This is particularly evident at Moss Peak, where the increment in minimum SAT is the second smallest (after North Fork Jocko) in winter, but the largest in summer among all the ten station locations.

### **2.5.3. Snowpack**

This section presents the findings related to the analysis of snowpack in the mountainous areas of the Flathead Region. Snowpack conditions are studied based only on observed data (Section 2.5.3.1) and a combination of both observed and downscaled data (Section 2.5.3.2), which allows us to estimate potential future trends of several snowpack characteristics over the entire study period (i.e., 1961-2100). In this case, three different scenarios are considered (i.e., RCP2.6, RCP4.5, and RCP8.5) to account for uncertainty related to socio-economic factors and political actions. Results are shown for multiple spatial (i.e., single climate station and overall study area) and temporal (i.e., monthly, bimonthly, and annual) scales in order to highlight the geographic variability of certain snow-related variables (e.g., SPR and timing, amount, and density of snowpack) within the Flathead Region as well as their variability within the snow season and across years. On the whole, the findings described in this section respond to the second research question associated with this chapter (see Section 2.3).

#### **2.5.3.1. Snowpack characteristics**

**Analysis 1.** Table 2-17 illustrates the Kendall's correlation coefficient ( $\tau$ ) and the magnitude of change ( $\phi$ ) related to the MKTs and RKTs applied to several indices that represent the snowpack conditions across the Flathead Region within 1994-2018. Results are reported only for those tests in which the null hypothesis stating that no trend exists over the 24-year study period is rejected, namely, when p values are smaller than the 0.05 significance level. This is also the reason why two stations (i.e., Bisson Creek and Stuart Mountain) and five indices (i.e., MSWE, DMSWE, SM50, 1ASWE, and

PSE) are not included in Table 2-17. The complete results of all tests, including the remaining statistics (i.e., p value, Theil-Sen’s slope, Kendall’s statistic S and its variance), can be found in Appendix D (Table D-1).

**Table 2-17: Kendall’s correlation coefficient ( $\tau$ ) and magnitude of change ( $\phi$ ) related to Mann-Kendall and regional Kendall tests applied to annual snowpack indices over 1994-2018**

Location	Statistic*	SMO	PSO	PSD	SMD	SWE0	SAO	SME	SSD
Kraft Creek	$\tau$					0.30	0.33	-0.30	-0.32
	$\phi$					44.6	17.5	-33.4	-49.4
Moss Peak	$\tau$	-0.33							
	$\phi$	-22.1							
North Fork Jocko	$\tau$		0.35						
	$\phi$		18.7						
Sleeping Woman	$\tau$			-0.30	-0.35	0.40			
	$\phi$			-21.3	-18.0	24.0			
Flathead Region	$\tau$		0.16	-0.15		0.21			
	$\phi$		10.7	-14.4		18.0			

\* Test results are reported only if p values are smaller than 0.05;  $\phi$  is measured in days,  $\tau$  is dimensionless

In Table 2-17,  $\phi$  indicates the 24-year mean variation of a given index in terms of number of days. Kraft Creek experiences a decreasing trend of about 50 days in the duration of the snow season (SSD), as the onset of snow accumulation (SAO) presents a delay of about seventeen days in fall and the end of snowmelt (SME) shows an advance of about 33 days in spring. Also, the number of days without snow on the ground (SWE0) increases by around 45 days over the 24-year period. An advance of approximately 22 days in snowmelt onset (SMO) and a delay of almost nineteen days in permanent snowpack onset (PSO) are encountered at Moss Peak and North Fork Jocko, respectively. Finally, Sleeping Woman undergoes a decreasing trend in both the permanent snowpack duration (PSD) and the snowmelt duration (SMD) by about 21 and eighteen days, respectively. Also, SWE0 increases by 24 days over the study period.

The RKT based on all six SNOTEL stations reveals the existence of some trends at the regional scale as well. On average, PSD diminishes by more than fourteen days over the 24-year period in the Flathead mountainous areas. This is mostly due to an evident delay trend in PSO, which tends to occur almost eleven days later in fall. In addition, a mean increasing trend of eighteen days is observed for SWE0. However, these three trends do not consistently increase/decrease through time. The strength of the monotonic association between these indices and time varies, in absolute terms, between 0.15 and 0.21. Single locations manifest absolute  $\tau$  values higher than those observed at the regional scale, as they lie within the 0.3-0.4 range.

**Analysis 2.** Table 2-18 lists the mean corrective factors used to adjust monthly PRE at each SNOTEL station and across the overall Flathead Region (see Section 2.4.4.1). This table also presents the corresponding averages ( $\alpha$ ) among all the daily SPR values greater than 25 mm from January, February, and, in the case of three stations (i.e., Moss Peak, North Fork Jocko, and Stuart Mountain), March. The mathematical relationship between  $\alpha$  and the related corrective factor as well as the rationale behind it are explained in Section 2.4.4.1 (see Equations 20 and 21). Table 2-18 reveals that the

**Table 2-18: Mean SPR and mean corrective factor used to adjust rainfall measurements at each climate station and across the overall Flathead Region**

Location	Elevation (m)	SPR ( $\alpha$ )*	Corrective Factor*
Bisson Creek	1,499.6	1.06	0.06
Kraft Creek	1,447.8	1.06	0.06
Moss Peak	2,066.5	1.29	0.22
North Fork Jocko	1,929.4	1.24	0.20
Sleeping Woman	1,874.5	1.11	0.10
Stuart Mountain	2,255.5	1.17	0.15
Flathead Region	1,845.6	1.16	0.14

\* Both quantities are dimensionless

magnitude of these two quantities is proportional to the elevation of the SNOTEL stations. Understandably, the measurement error of the recording instrumentations is proportional to the amount of precipitation falling as snow. However, Stuart Mountain, which is located at the highest elevation among all stations, represents an exception.

Table 2-19 provides a general picture of the averaged relationship between rain and snow precipitation throughout the snow seasons (i.e., October through May) within 1994-2018 at each location and across the entire Flathead Region. Specifically, the table shows the mean values of PRE (observed and adjusted) and SA monthly totals over the 24-year period, as well as the related SPR values. Elevation is clearly a key geographic feature influencing SPR across the six stations (see Table 2-18 as reference for elevation data). Should the snow season be defined by those months when more than 50% of precipitation falls as snow (gray shade), its length distinctly increases with elevation. Also, the 8-month average of SPR (last column) and the highest SPR value per location (in bold) are proportional to the station elevation. Finally, a temporal trend across the locations is visible as the largest SPR values tend to occur earlier at lower elevations (i.e., December or January) and later at higher elevations (i.e., February or March).

Table 2-20 displays the Kendall's correlation coefficient ( $\tau$ ) and the magnitude of change ( $\phi$ ) related to the MKTs and RKTs applied to monthly SPR values and monthly averages of daily maximum SAT within 1994-2018. The goal is to determine whether any SPR trend exists over the 24-year study period at any location, and, if that is the case, whether this trend is apparently influenced by changes in air temperature. Results are reported only for those tests in which the null hypothesis of no trend is rejected, namely,

**Table 2-19: Mean values of SA and PRE (both observed and adjusted) monthly totals over the 1994-2018 period, and related SPR values**

Location	Var.*	Oct	Nov	Dec	Jan	Feb	Mar	Apr	May	Total
Bisson Creek	PRE (obs)	72.9	74.9	77.8	78.7	65.2	81.2	90.2	91.9	633
	PRE (adj)	73.7	77.8	81.5	82.5	68.2	84.4	92.6	92.4	653
	SA	13.7	50.7	65.9	65.9	53.4	56.7	42.2	9.7	358
	SPR	0.19	0.65	<b>0.81</b>	0.80	0.78	0.67	0.46	0.11	0.56
Kraft Creek	PRE (obs)	90.4	119.8	121.9	133.0	109.3	109.2	79.5	68.4	832
	PRE (adj)	91.5	124.1	127.5	139.1	114.3	113.7	81.3	68.7	860
	SA	18.4	70.8	92.4	100.2	82.2	73.8	29.4	4.8	472
	SPR	0.20	0.57	<b>0.72</b>	0.72	0.72	0.65	0.36	0.07	0.50
Moss Peak	PRE (obs)	136.3	162.3	179.4	186.4	147.0	182.9	169.7	142.2	1,306
	PRE (adj)	157.7	197.1	222.2	232.5	185.2	228.7	210.8	160.2	1,594
	SA	95.8	155.9	191.8	206.8	171.2	205.4	184.4	80.3	1,292
	SPR	0.61	0.79	0.86	0.89	<b>0.92</b>	0.90	0.87	0.50	0.79
North Fork Jocko	PRE (obs)	158.3	221.7	222.9	257.2	193.3	195.1	144.0	111.5	1,504
	PRE (adj)	171.1	255.5	265.1	309.0	233.4	235.9	169.3	122.3	1,762
	SA	65.2	172.8	216.2	265.4	205.5	209.1	129.1	54.8	1,318
	SPR	0.38	0.68	0.82	0.86	0.88	<b>0.89</b>	0.76	0.45	0.71
Sleeping Woman	PRE (obs)	81.6	100.4	99.0	95.7	90.4	96.9	79.9	77.3	721
	PRE (adj)	83.9	107.8	108.0	104.5	98.6	105.6	85.3	78.8	773
	SA	23.9	76.5	93.6	91.2	85.3	90.0	55.8	16.3	533
	SPR	0.29	0.71	0.87	<b>0.87</b>	0.86	0.85	0.65	0.21	0.66
Stuart Mt	PRE (obs)	94.0	134.1	173.0	162.3	127.1	127.1	107.5	100.6	1,026
	PRE (adj)	103.3	154.0	200.9	189.6	148.7	149.1	124.1	109.2	1,179
	SA	62.7	133.8	187.7	183.4	145.2	147.8	111.9	57.4	1,030
	SPR	0.61	0.87	0.93	0.97	0.98	<b>0.99</b>	0.90	0.53	0.85
Flathead Region	PRE (obs)	105.6	135.6	145.7	152.2	122.0	132.1	111.8	98.7	1,004
	PRE (adj)	111.9	150.4	164.7	172.8	138.8	149.7	124.2	103.7	1,116
	SA	46.6	110.1	141.3	152.2	123.8	130.5	92.1	37.2	834
	SPR	0.42	0.73	0.86	0.88	<b>0.89</b>	0.87	0.74	0.36	0.72

\* PRE (observed and adjusted) as well as SWE are measured in mm; SPR is dimensionless; the highest SPR value per location is indicated in bold; SPR values greater than 0.5 are highlighted by a gray shade

when p values are smaller than 0.05. Also, SAT statistics are shown only if at least one SPR monthly trend is identified at a given location. The full results of all tests, including the remaining statistics (i.e., p value, Theil-Sen's slope, Kendall's statistic S and its variance), can be found in Appendix D (Table D-2).

**Table 2-20: Kendall’s correlation coefficient ( $\tau$ ) and magnitude of change ( $\phi$ ) related to Mann-Kendall and regional Kendall tests applied to monthly averages of maximum SAT and SPR over 1994-2018**

Location	Stat.*	Maximum SAT (°C)						SPR			
		Oct	Nov	Jan	Feb	Mar	May	Oct	Nov	Feb	Mar
Moss Peak	$\tau$		0.29		0.30	0.37			-0.31	-0.30	
	$\phi$		2.3		3.0	3.6			-0.08	-0.06	
North Fork Jocko	$\tau$		0.32	0.38		0.56	0.40		-0.30		
	$\phi$		3.1	3.3		4.7	3.4		-0.19		
Sleeping Woman	$\tau$	0.40	0.34	0.38		0.48					-0.27
	$\phi$	3.2	2.0	3.4		3.8					-0.22
Flathead Region	$\tau$	0.32	0.30	0.33		0.46		-0.16	-0.21		
	$\phi$	2.9	2.5	2.9		3.7		-0.15	-0.12		

\* Test results are reported only if p values are smaller than 0.05

Only six clear SPR trends emerge from the analysis, but all of them are negative.

With SPR decreasing over the 24-year study period, more precipitation is converted from snow to rain. November is the month that experiences a decreasing SPR trend in more than one location (i.e., Moss Peak and North Fork Jocko) and at the regional scale as well. These findings, together with the results of the regional trend observed in October, corroborate what Table 2-17 indicates about the permanent snowpack onset (PSO). SA events across the Fathead Region, and, to a greater extent, at North Fork Jocko, occurs later in fall (i.e., October and, especially, November) because less precipitation falls as snow during these months. Two isolated decreasing SPR trends are also found in February and March at Moss Peak and Sleeping Woman, respectively.

In addition, this analysis reveals that, among the three air temperature variables analyzed (i.e., mean, maximum, and minimum SAT), the strongest impact on SPR is exercised by maximum SAT, at least in qualitative terms. Indeed, Table 2-20 shows a direct monthly correspondence between decreasing trends in SPR and increasing trends

in maximum SAT. There is no such clear correlation when mean and minimum SAT are considered, which indicates that maximum daily air temperature is probably the most important factor causing changes in the daily snow/rain relationship in the Flathead Region during the 24-year study period. This is especially true for November, as there is no evidence of increasing trends in mean and minimum SAT on this month. All the tests' results related to the three air temperature variables are presented in Table D-2.

**Analysis 3.** Table 2-21 provides an overview of the averaged conditions of the snowpack density throughout the snow seasons (i.e., October through May) within 2003-2018 at each SNOTEL station and across the overall Flathead Region. In particular, the table illustrates the mean values of monthly SWE, SDP, SDN, and CVD over the 15-year period. For each variable, the last column of the table displays the averages of the eight snowy months. As expected, SDN increases with time at all locations. During the SA months, the snowpack densification is primarily provoked by the continuous compaction resulted from overburden pressure, the sintering process, and snow grain metamorphism (Mizukami and Perica 2008). During the snow melting months, melt metamorphism is the dominant process causing SDN to increase, as snowmelt and meltwater fill the snowpack pore space.

Monthly SDN observed at higher elevations (i.e., Moss Peak, North Fork Jocko, and Stuart Mountain) is typically larger than the related monthly SDN measured at lower elevations (i.e., Bisson Creek, Kraft Creek, and Sleeping Woman). This is probably due to larger overburden pressures acting within thicker snowpacks at higher elevations. CVD varies throughout the snow season approximately according to a U-shaped curve. The

intra-monthly variability of SDN is very large at the beginning of the season, then tends to diminish, and finally slightly increases towards the end of the season. Regardless of the occurrence of the SWE and SDP peaks, this pattern is similar across all locations, with February, usually the coldest month, showing the lowest CVD value (in bold).

**Table 2-21: Monthly average of SWE, SDP, SDN, and CVD over the 2003-2018 period**

Location	Var.*	Oct	Nov	Dec	Jan	Feb	Mar	Apr	May	Mean
Bisson Creek	SWE	2	19	71	141	189	232	216	54	116
	SDP	11	96	317	582	720	770	641	150	411
	SDN	149	201	240	244	268	309	353	353	265
	CVD	0.41	0.29	0.22	0.11	<b>0.06</b>	0.09	0.10	0.16	0.18
Kraft Creek	SWE	1	25	89	183	257	287	182	19	130
	SDP	9	128	409	740	915	820	452	43	440
	SDN	158	205	228	248	281	352	371	405	281
	CVD	0.28	0.35	0.20	0.11	<b>0.08</b>	0.12	0.19	0.33	0.21
Moss Peak	SWE	30	141	310	525	705	887	1,072	1,005	585
	SDP	121	556	1,216	1,830	2,222	2,576	2,745	2,213	1,685
	SDN	261	268	256	286	318	346	393	462	324
	CVD	0.31	0.16	0.08	0.07	<b>0.04</b>	0.05	0.06	0.06	0.10
North Fork Jocko	SWE	12	96	282	536	768	961	1,089	901	581
	SDP	60	442	1,152	1,874	2,370	2,576	2,543	1,776	1,599
	SDN	230	241	246	285	324	375	432	516	331
	CVD	0.38	0.26	0.11	0.08	<b>0.05</b>	0.07	0.06	0.07	0.14
Sleeping Woman	SWE	3	37	113	209	291	375	391	163	198
	SDP	19	199	517	830	1,062	1,193	1,060	401	660
	SDN	162	184	218	251	274	315	373	401	272
	CVD	0.44	0.27	0.11	0.08	<b>0.06</b>	0.07	0.06	0.17	0.16
Stuart Mountain	SWE	18	97	254	447	612	752	867	751	475
	SDP	76	419	1,035	1,594	1,989	2,230	2,263	1,706	1,414
	SDN	252	251	245	280	307	338	385	443	313
	CVD	0.34	0.18	0.08	0.07	<b>0.04</b>	0.05	0.05	0.05	0.11
Flathead Region	SWE	11	69	187	340	470	582	636	482	347
	SDP	49	306	774	1,242	1,546	1,694	1,617	1,048	1,035
	SDN	202	225	239	266	295	339	385	430	298
	CVD	0.36	0.25	0.13	0.09	<b>0.05</b>	0.07	0.09	0.14	0.15

\* SWE and SDP are measures in mm, SDN in kg/m<sup>3</sup>, and CVD is dimensionless; the lowest CVD value per location is indicated in bold

Table 2-22 illustrates the Kendall’s correlation coefficient ( $\tau$ ) and the magnitude of change ( $\phi$ ) related to the SKTs and RKTs applied to SDN bimonthly means within 2003-2018. Results are reported only for those tests in which the null hypothesis stating that no trend exists over the 15-year period is rejected, namely, when p values are smaller than the 0.05 significance level. Mean, maximum, and minimum SAT are also tested for trend based on the same bimonthly intervals and over the same study period. The goal is to determine whether there is an apparent causal relationship between changes in air temperature and SDN at a given location or across the overall study area. However, trend analyses on the three SAT variables do not provide significant results. Thus, these statistics are not included in Table 2-22. For completeness, results of each test (i.e., Kendall’s correlation coefficient, p value, Theil-Sen’s slope, Kendall’s statistic S, variance of the Kendall’s statistic, and magnitude of change) related to either SAT or SDN are reported in Appendix D (Table D-3).

**Table 2-22: Kendall’s correlation coefficient ( $\tau$ ) and magnitude of change ( $\phi$ ) related to Mann-Kendall and regional Kendall tests applied to SDN bimonthly means over 2003-2018**

Location	Statistic*	SDN (kg/m <sup>3</sup> )			
		Oct-Nov	Dec-Jan	Feb-Mar	Apr-May
Bisson Creek	$\tau$				0.33
	$\phi$				64.3
Kraft Creek	$\tau$		-0.26	0.29	0.45
	$\phi$		-30.2	36.6	154.7
Moss Peak	$\tau$	0.30			
	$\phi$	70.3			
North Fork Jocko	$\tau$		-0.29		
	$\phi$		-26.5		
Flathead Region	$\tau$		-0.14		0.17
	$\phi$		-22.1		46.9

\* Test results are reported only if p values are smaller than 0.05

Eight evident SDN trends concerning both the local (four SNOTEL stations) and the regional scales are encountered in this study. Three of them are negative and are concentrated in December/January (Kraft Creek, North Fork Jocko, and Flathead Region). The other five are positive and are distributed among the remaining bimonthly intervals. Although SKTs and RKTs do not reveal clear bimonthly SAT trends during the 15-year study period, air temperature is still probably the main factor determining the bimonthly SDN trends highlighted in Table 2-22. The increase in SDN at the end of winter and especially spring is plausibly due to an increase in air temperature that hastens and accelerates destructive metamorphism and snowmelt processes (Mizukami and Perica 2008). It can be noticed that these SDN increasing trends at the end of the snow season are encountered mainly at lower elevations (i.e., Bisson Creek and Kraft Creek).

An increase in air temperature may also be the cause of the SDN increasing trend detected at Moss Peak in fall. During this time, snow accumulation is the primary process occurring at these elevations. Newly fallen snow has usually low density, but snowpack porosity diminishes at warmer temperatures. Finally, the SDN decreasing trends observed in early winter at the local (i.e., Kraft Creek and North Fork Jocko) and regional scales are possibly caused by either colder temperatures or lesser snowfall accumulations. In the latter case, a thinner snowpack would experience a smaller degree of compaction (i.e., lower density) due to a reduced overburden pressure. All the conjectures regarding the reasons behind the bimonthly SDN trends recognized across the Flathead Region within 2003-2018 should be thoroughly verified through further research.

### 2.5.3.2. Snowpack trends

Table 2-23 shows the Kendall's correlation coefficient ( $\tau$ ) and the mean decadal rate of change ( $\phi$ ) related to the MKTs and RKTs applied to ten indices that represent the snowpack characteristics across the Flathead Region within 1961-2100 according to three different scenarios (i.e., RCP2.6, RCP4.5, and RCP8.5). Regardless of the index, both  $\tau$  and  $\phi$  tend to increase with increasing RCP. The null hypothesis of no trend is mostly rejected, and p values are larger than the 0.05 significance level only in a few cases (empty cells in Table 2-23). The complete results of all tests, including the remaining statistics (i.e., p value, Theil-Sen's slope, Kendall's statistic S and its variance), can be found in Appendix D (Table D-4). As a reminder,  $\phi$  is measured in millimeters per decade or number of days per decade depending on the index (for a description of all indices refer to Table 2-6 in Section 2.4.2.3).

In general, the SWE annual peak is expected to decrease in amount and occur earlier within the snow season, as indicated by the MSWE and DMSWE columns in Table 2-23. As for these two indices, the SNOTEL stations that are located at higher elevations (i.e., Moss Peak and North Fork Jocko) usually manifest smaller  $\tau$  and larger  $\phi$  than those estimated at a lower elevation (i.e., Kraft Creek). This pattern is reversed for the  $\tau$  values relative to the DMSWE of the RCP8.5 scenario. The anticipated decrease in MSWE within the 140-year study period is considerable. If the 1961-1970 mean of the regional annual MSWE (i.e., average among the three SNOTEL stations) is taken as reference, MSWE is predicted to diminish by the end of the XXI century by approximately 34%, 46%, and 52% according to the RCP2.6, RCP4.5, and RCP8.5 scenarios, respectively.

**Table 2-23: Rate of change ( $\phi$ ) and Kendall's coefficient ( $\tau$ ) of trends in snowpack indices over 1961-2100 according to the three RCP scenarios**

Scenario	Station	Variable	MSWE	DMSWE	SMO	SM50	1ASWE	PSO	PSE	PSD	SMD	SWE0
RCP2.6	Kraft Creek	$\tau$	-0.63	-0.53	-0.53	-0.66	-0.65	0.39	-0.62	-0.55		0.54
		$\phi$	-14.5	-1.0	-2.4	-3.9	-22.3	1.8	-1.9	-3.7		3.6
	Moss Peak	$\tau$	-0.49	-0.47	-0.43	-0.52	-0.52		-0.58	-0.51	-0.45	0.49
		$\phi$	-24.8	-1.6	-1.3	-2.2	-19.1		-3.0	-3.7	-1.5	3.8
	North Fork Jocko	$\tau$	-0.46	-0.48	-0.40	-0.53	-0.46		-0.46	-0.46	-0.31	0.47
		$\phi$	-28.6	-2.3	-1.5	-1.9	-27.3		-2.3	-2.8	-1.2	3.1
	Flathead Region	$\tau$	-0.53	-0.49	-0.45	-0.57	-0.54	0.21	-0.56	-0.51	-0.18	0.50
		$\phi$	-19.9	-1.5	-1.7	-2.4	-23.3	0.8	-2.3	-3.3	-0.8	3.5
RCP4.5	Kraft Creek	$\tau$	-0.64	-0.55	-0.60	-0.75	-0.70	0.62	-0.68	-0.68		0.67
		$\phi$	-18.1	-1.0	-2.5	-4.2	-26.6	2.7	-3.2	-6.0		5.9
	Moss Peak	$\tau$	-0.59	-0.52	-0.62	-0.58	-0.63	0.54	-0.56	-0.61		0.58
		$\phi$	-31.8	-2.8	-2.5	-2.8	-26.8	1.8	-3.2	-4.7		4.7
	North Fork Jocko	$\tau$	-0.63	-0.56	-0.63	-0.64	-0.68	0.34	-0.48	-0.66		0.70
		$\phi$	-36.3	-3.1	-3.1	-2.3	-36.9	0.8	-2.5	-3.9		4.1
	Flathead Region	$\tau$	-0.62	-0.54	-0.62	-0.66	-0.67	0.50	-0.57	-0.65		0.65
		$\phi$	-26.6	-2.0	-2.8	-3.0	-29.3	1.8	-3.0	-4.7		4.8
RCP8.5	Kraft Creek	$\tau$	-0.71	-0.54	-0.64	-0.78	-0.75	0.70	-0.72	-0.73		0.74
		$\phi$	-19.4	-1.0	-2.6	-5.0	-27.8	3.2	-4.8	-8.1		8.2
	Moss Peak	$\tau$	-0.70	-0.60	-0.67	-0.67	-0.74	0.69	-0.69	-0.74		0.72
		$\phi$	-38.5	-3.8	-3.5	-3.8	-37.1	2.2	-4.2	-6.4		6.7
	North Fork Jocko	$\tau$	-0.58	-0.71	-0.69	-0.72	-0.72	0.57	-0.60	-0.75		0.78
		$\phi$	-37.9	-4.6	-4.4	-3.0	-43.6	1.7	-3.3	-5.3		5.6
	Flathead Region	$\tau$	-0.66	-0.62	-0.66	-0.72	-0.74	0.65	-0.67	-0.74		0.75
		$\phi$	-29.9	-2.7	-3.4	-3.8	-36.1	2.4	-4.0	-6.4		6.5

\* Test results are reported only if p values are smaller than 0.05;  $\phi$  is measured in mm per decade (MSWE and 1ASWE) or days per decade (all other indices)

Annual SMO and SM50 are likely to occur earlier in the future at rates that vary between 1.3 and 5.0 days per decade depending on location and scenario considered. Both  $\tau$  and  $\phi$  are usually slightly larger for SM50 than for SMO, indicating that, in most cases, the first half of snowpack will probably be melting at a higher pace. The SWE value on the 1<sup>st</sup> of April (1ASWE) is expected to diminish over time, with North Fork Jocko experiencing the most pronounced decreasing trend compared to the other two SNOTEL stations. According to the RCP2.6 scenario, the Flathead Region will undergo a decrease in 1ASWE of about 42% with reference to the 1961-1970 regional mean. The decreasing rates based on the RCP4.5 and RCP8.5 scenarios are 53% and 65%, respectively.

The analysis also estimates that the permanent snowpack duration (PSD) will be reduced by 2.8 to 8.1 days per decade. This is due to a later snow accumulation onset (SAO) in fall and an earlier snowmelt end (SME) in spring. In all cases,  $\tau$  and  $\phi$  related to SME are larger, in absolute terms, than those associated with SAO. However, regarding the snowmelt duration (SMD) index, no trends are found but in three RCP2.6-related instances (i.e., Moss Peak, North Fork Jocko, and Flathead Region). Indeed, both SMO and SME are expected to occur earlier within the snow season, but there is no significant difference between their rates of change. If these indices are analyzed in conjunction with SM50, it can be further anticipated that there will be a slightly attenuation or no change in the snowmelt pace relative to the second half of the snowpack. Finally, the number of days without snow on the ground (SWE0) are likely to increase in the future at rates that range between 3.1 and 8.2 per decade.

### **2.5.3.3. Final considerations**

This section aims to address the second research question associated with this chapter (see Section 2.3) by highlighting the main findings related to the study of snowpack in the mountainous areas of the Flathead Region. The two sets of analyses described in the previous two sections complement each other, as the first one investigates the historical observed conditions of snowpack, whereas the second one focuses on the potential long-term evolution of certain snowpack characteristics derived from both observed and downscaled data. Due to the short period of available SNOTEL records (i.e., 1994-2018 or 2003-2018, according to the snow variable examined), only few evident trends emerge from the analysis of this dataset. When present, these trends vary in magnitude from station to station, mostly depending on elevation attributes. However, there are no discordant trends of a given variable among the six locations.

Results indicate that, on average, the number of days without snow on the ground has increased by eighteen days between 1994 and 2018 in the Flathead Region. This tendency is particularly pronounced at Kraft Creek, where almost 45 days with snow on the ground have been lost during the same period. In addition, the duration of the permanent snowpack has meanly diminished across the study area by more than fourteen days within the 1994-2018 timeframe. This change is primarily ascribable to a mean regional delay of almost eleven days in the start date of snow accumulation over these 24 years. Among all locations, North Fork Jocko manifests the greatest delay in the permanent snowpack onset, which corresponds to almost nineteen days throughout the study period.

These results are corroborated by the trend analysis of SPR, which reveals that, at the regional scale, rainfall in October and November has been increasing since 1994 to the detriment of snowfall. The consistency with the previous analysis is also demonstrated by the fact that the most evident decreasing trend in SPR occurs at North Fork Jocko in November. Based on the trend analysis on the three air temperature variables, it can be inferred that the increase in daily maximum air temperature over the 24-year study period has been the main factor influencing the decrease in snow precipitation and the delay in snow accumulation in fall both at the local and regional scales.

Two regional trends also emerge from the analysis of SDN but, in this case, they have opposite directions. SDN has decreased by approximately 22 kg/m<sup>3</sup> in early winter (i.e., December/January) between 2003 and 2018. At the local scale, only Kraft Creek and North Fork Jocko present an evident decreasing trend in these months. Conversely, SDN has increased by almost 47 kg/m<sup>3</sup> in spring (i.e., April/May) over the same 15-year period across the Flathead Region. Bisson Creek and, even more, Kraft Creek, which are located at the lowest elevations among all SNOTEL stations, show a clear increasing trend in SDN in these months. The trend analysis on the three air temperature variables within 2003-2018 did not provide statistically significant results. However, the local and regional trends in SDN have most probably be driven by changes in air temperature during the 15-year study period, specifically lower temperatures in early winter and higher temperatures in spring. This conjecture needs to be further evaluated through additional research.

Finally, the trend analysis applied to the estimated evolution of several snowpack characteristics within 1961-2100 across the Flathead Region generally reveals a reduction of the annual snowpack in terms of duration and amount both at the local and regional scales. Potential snowpack trends are usually more marked when a higher emissions scenario is considered. In general, the snow season is expected to shorten due to a later snow accumulation in fall and an earlier snowmelt in spring. At the regional scale, the permanent snowpack duration meanly decreases by 3.3, 4.7, and 6.4 days per decade according to the RCP2.6, RCP4.5, and RCP8.5 scenarios, respectively. Among the three SNOTEL stations examined, Kraft Creek, which is located at the lowest elevation, presents the greatest reduction. Correspondingly, the number of days without snow on the ground is likely to increase at a very similar rate.

Three snowpack-related events are expected to occur earlier within the snow season. These include the date of maximum SWE, the snowmelt onset, and the date on which half of the snowpack has melted. On average, the rate of change varies meanly between 1.5 and 3.8 days per decade, depending on the specific index and RCP scenario considered. Regarding the amount of snowpack, the SWE peak and its value on the 1<sup>st</sup> of April are predicted to diminish consistently throughout the 1961-2100 period. According to the RCP2.6 scenario, these two indices are estimated to decrease by 2100 across the Flathead Region by approximately 34% and 42%, respectively. The corresponding decreasing rates related to the RCP4.5 are 46% and 53%, whereas those associated with the RCP8.5 are 52% and 65%. The diminution in snowpack amount is usually less pronounced at lower elevations (i.e., Kraft Creek).

## 2.6. Conclusions

The general purpose of the whole research is to examine the impacts of climate change on water quantity and quality in the FIR. This chapter focused on two crucial components of climate, air temperature and snow precipitation, which influence water resource characteristics. Indeed, changes in air temperature have a direct impact on water temperature, a relevant aspect of water quality. This topic will be treated in the next chapter. Similarly, changes in snow precipitation affect the amount and timing of snowpack, and, in turn, the quantity of water available throughout the year. In particular, air temperature and snow precipitation were studied by looking at the long-term evolution (i.e., 1961-2100) of daily maximum and minimum SAT and daily SWE, respectively. Statistical downscaling served as a means for reconstructing past changes and estimating potential future scenarios of these two variables.

While there are innumerable examples relative to the statistical downscaling of SAT variables, this study represents the first attempt to statistically downscale SWE by means of SDSM. The explained variance of the individual components of SWE (i.e., SA and SM) is very low. However, when the simulated SA and SM are aggregated back as SWE time series, the results are very promising. The selected characteristics of the annual snowpack averaged over the 5-year validation period are replicated quite accurately. In addition, the explained variance of the simulated cumulative SWE is considerably high (i.e., approximately 91% across the three locations examined) and it is comparable to that of the SAT downscaling models (i.e., on average, 92% and 85% for maximum and minimum SAT, respectively). A downside of the SWE downscaling models

is their inability to perform equally well when smaller snow quantities are involved, as it is for areas located at lower elevations. This aspect should be further evaluated by extending this analysis to a larger number of locations.

Both historical observations and future projections indicate a general increment in air temperature across the Flathead Region, with maximum SAT usually increasing at higher rates than those estimated for minimum SAT. As a consequence, daily variability in air temperature is likely to increase as well. Summer is expected to experience the largest increment in both maximum and minimum SAT. In general, minimum SAT is predicted to largely increase in winter, too. Among all locations, Seeley Lake Ranger Station will probably undergo a uniquely high rise in air temperature, especially in summer and winter. In addition, the intra-annual monthly variability of minimum SAT in the areas along the Mission Mountains range is expected to increase due to relatively small and large increases in minimum SAT occurring during the coldest and warmest months, respectively. Future projections of air temperature are strongly scenario dependent. The estimated average increments in mean annual maximum and minimum SAT between 1961 and 2100 across the Flathead Region are about 3.1°C and 3.0°C (RCP2.6), 4.3°C and 4.1°C (RCP4.5), and 6.9°C and 6.2 (RCP8.5), respectively.

The increasing trends in air temperature will certainly affect the snowpack conditions in the mountainous areas of the Flathead Region. The annual snowpack is likely to diminish in terms of duration and amount both at the local and regional scales. The snow season is expected to shorten due to a later snow accumulation in fall and an earlier snowmelt in spring. This general trend is already visible within the observed data.

Indeed, rainfall in October and November has been increasing since 1994 to the detriment of snowfall across the study area and, particularly, at North Fork Jocko (high elevation). As a result, snow accumulation onset has been occurring later in fall during the same 24-year period. Similarly, SDN in April/May has been increasing since 2003 across the Flathead Region and, especially, at Bisson Creek and Kraft Creek (low elevations). This is possibly related to earlier snowmelt processes that have been occurring in spring during the same 15-year period. Future projections of snowpack characteristics are also strongly scenario-dependent. The estimated average reductions in SWE annual maximum and snowpack duration between the first and last decade of the study period (i.e., 1961-2100) across the Flathead Region are about 34% and 18% (RCP2.6), 46% and 26% (RCP4.5), and 52% and 36% (RCP8.5), respectively.

It is important to recall that the RCP2.6 represents a stringent mitigation scenario (i.e., net negative CO<sub>2</sub> emissions after around 2070) that is very unlikely to occur. In this research, the choice of including this scenario was dictated by the lack of an alternative option, as CanESM2 did not perform simulations for the RCP6.0. However, the very low likelihood that the RCP2.6 scenario will occur has to be taken into consideration when planning for adaptation and mitigation strategies. The largest source of uncertainty related to the analyses in this chapter is represented by the choice of the AOGCM. For practical purposes, only CanESM2 was selected in this study. Indeed, evaluating the performance of different AOGCMs was not the focus of this research. However, it is recommended considering simulations from multiple AOGCMs to cover a broad range of projections and, in doing so, reduce the level of uncertainty. The second-largest cause of

uncertainty is associated with the statistical downscaling methodology. The weather generator in SDSM, thanks to its capability of producing ensemble simulations, allows us to statistically determine, to some extent, the error related to the downscaling process. Nevertheless, the uncertainty derived from the assumption of stationarity in the predictand-predictor relationship remains the greatest limitation of this methodology.

### **3. STREAM AND RIVER TEMPERATURE CHANGES IN THE FLATHEAD RESERVATION: PAST AND FUTURE TRENDS**

#### **3.1. Introduction**

The general purpose of the whole research is to investigate past, present, and future changes in water quantity and quality across the FIR in response to a changing climate. After focusing on water quantity by examining air temperature trends in the Flathead Region and their potential impacts on snow accumulation and snowmelt patterns (see Chapter 2), the center of attention is now shifting towards water quality. This chapter focuses on SWT of flowing waters as an indicator of water quality, and investigates historical and potential future trends of this variable in streams and rivers of the FIR.

Water temperature is an important parameter in stream and river ecology because its daily and seasonal variability determines fish habitat suitability and the distribution of aquatic species (Caissie 2006). Freshwater fish is crucially important to the native communities of the FIR, not only because it represents the primary source of their diet, but also because it plays an essential role in their ceremonial traditions and spiritual life. A potential increase in SWT would severely threaten cold water fishes, and especially salmonids, which have a small range of thermal tolerance (Pederson et al. 2010). In turn, a decline of these endangered species would certainly jeopardize the tribes' traditional lifestyle and cultural identity. Thus, identifying trends in SWT is a fundamental step for assessing the health of the aquatic habitat, the distribution of key fishes, and ultimately, the impact on the native peoples.

The analysis in this chapter builds on the assumption that SAT is the most important driving forcing of SWT, as widely documented in the literature (see Section 3.2). Because SWT records in the study area are only available for short periods of time (1998-2011 at best), a statistical model linking SAT to SWT can serve as a means for reconstructing stream/river temperature for days in which SAT data are available and SWT data are missing. Depending on the robustness of the model (i.e., the statistical relationship between SAT and SWT), future projections of SAT that were calculated in Chapter 2 can also be used to predict future estimates of SWT. Similarly to the previous chapter, seasonal and annual trends in SWT are eventually calculated for the 1961-2100 study period at different spatial scales and examined in a comparative fashion.

This chapter resembles the general structure of Chapter 2 and is divided into the following parts. Section 3.2 reviews the methodologies that have been used to investigate temperature of flowing waters, with a focus on the statistical technique selected for this study. Section 3.3 presents the research question and related objective associated with this chapter. Section 3.4 describes the SWT datasets and the methodological steps adopted in this research. Here, ample room is given to the description of the procedure that is undertaken to identify the best air-water temperature relationship among several possible, which are derived by considering multiple SAT locations and different temporal schemes. Section 3.5 illustrates the results obtained by implementing the best statistical model for each SWT station. Finally, Section 3.6 discusses the results and draws some conclusions.

### 3.2. Literature review

This section discusses the importance of studying water temperature and provides a general overview of techniques that have been used to better understand spatial and temporal variability of stream/river temperature. Temperature is a crucial physical property of flowing waters because it regulates most of the chemical and biological processes of lotic systems and determines the overall health of aquatic ecosystems. Indeed, water temperature influences the life cycle of the lotic biota, including growth, reproduction, and migration patterns (Caissie 2006). Thus, changes in the thermal regime of freshwater systems may alter the complex equilibrium among aquatic communities (Basarin et al. 2016). Variations in water temperature provoke a change in the concentration of dissolved oxygen and suspended sediments, both of which are critical to the health of aquatic ecosystems (Webb et al. 2008). For example, lower levels of dissolved oxygen due to warmer temperatures would be highly stressful to fish and other aquatic organisms.

Cold-water fish communities are particularly sensitive to high temperatures and experience physiological collapse at temperature exceeding critical species-specific thermal thresholds (Wehrly, Wang, and Mitro 2007). Salmonids are among the species most threatened by warming temperatures in streams and rivers across the Northwest United States (Isaak et al. 2012). Salmon and trout have not only an important commercial and recreational value, but also a cultural value, especially in places like the FIR. The CSKT, just like other indigenous communities, have relied for centuries on freshwater fishing as the main food source, and salmonids, such as bull trout (*Salvelinus*

*confluentus*), are integral part of their stories that have been handed down from one generation to another. The disappearance of salmonid fishes from the daily life of these tribal communities would undermine their cultural identity as well. For all these reasons, it is important to study historical and future trends of water temperature across streams and rivers of the FIR.

Several types of models are found in the literature that intend to predict thermal behavior of streams/rivers in space and time. These models can be broadly classified into two categories referred to as deterministic and statistical models (Webb et al. 2008). Deterministic models are physically based models that explicitly simulate water temperature dynamics by solving the heat budget equation (e.g., Caissie, Satish, and El-Jabi 2007; Hébert et al. 2011; Beek et al. 2012). These models usually consider energy fluxes at the water-surface interface (e.g., solar radiation, net long-wave radiation, evaporative and sensible heat fluxes) and at the streambed-water interface (e.g., heat conduction and advective heat fluxes). Among the different energy components of the heat budget model, solar radiation is reported as the dominant input that contributes to heat gain (Webb and Zhang 1999; Caissie, Satish, and El-Jabi 2007; Hébert et al. 2011). One of the main advantages of deterministic models lies in their ability to reveal and explain underlying physical processes that relate meteorological parameters to water temperatures (Hébert et al. 2011).

However, some of the meteorological and hydrological data that are required for implementing a deterministic model are often difficult to obtain (Hébert et al. 2015). This drawback can be partially solved by simplifying the heat budget equation. One way

consists in considering only the heat transfer processes across the air-water interface, which are the most relevant (Edinger, Duttweiler, and Geyer 1968). In this case, equilibrium temperature, which is defined as the water temperature at which the sum of all heat fluxes through the water surface is zero, is mostly used to derive water temperature (Mohseni and Stefan 1999; Bogan, Mohseni, and Stefan 2003; Caissie, Satish, and El-Jabi 2005; Hébert et al. 2015). The advantage of using equilibrium temperature is that it can be calculated solely from weather data (Bogan, Mohseni, and Stefan 2003). A further simplification of the heat budget equation involves using air temperature as a surrogate for heat net exchange (Webb et al. 2008). In this case, air temperature is the primary, and often the only parameter, that is used to predict water temperatures.

Statistical models are empirical models that rely on the relationship between air temperature and water temperature. These types of models can be generally classified into two categories: stochastic and regression models. Stochastic modeling techniques involve separating water temperature time series into two components, specifically the long-term annual component and the short-term component (Caissie 2006). The first represents the annual variation of water temperature and can be described by a Fourier series or a sinusoidal function. The latter represents the departure of water temperatures from the annual component and is estimated based on air temperature data. Stochastic models have been applied extensively to predict stream or river temperatures (Caissie, El-Jabi, and St-Hilaire 1998; Ahmadi-Nedushan et al. 2007; Jeong, Daigle, and St-Hilaire 2013). As stochastic modeling techniques account for

autocorrelation within the water temperature series, they are efficient for modeling water temperature at small temporal scales, such as hourly or daily (Caissie 2006).

Regression modeling techniques involve identifying a statistical relationship usually between air temperature (predictor) and water temperature (predictand). Four major types of regression models have been applied to predict temperature of flowing waters: simple linear regression, multiple linear regression, logistic regression, and polynomial regression. Simple linear regression uses only air temperature as predictor variable and it assumes a linear relationship between air temperature and water temperature (e.g., Webb and Nobilis 1997; O'Driscoll and DeWalle 2006; Krider et al. 2013). Multiple linear regression also assumes that the air-water temperature relationship is linear, but other predictors are added in the statistical model, generally through a stepwise (i.e., hierarchical) procedure. Examples of secondary predictors include other climate variables, such as solar radiation, relative humidity, and precipitation (Pedersen and Sand-Jensen 2007), river discharge (Hilderbrand, Kashiwagi, and Prochaska 2014), and accumulated degree-days above mean summer air temperature as an indicator of groundwater temperature (Snyder, Hitt, and Young 2015).

Logistic regression is used when the relationship between air temperature and water temperature is not assumed to be necessarily linear. The non-linear behavior is visible at high air temperature due to evaporative cooling, especially in warm regions (Mohseni and Stefan 1999). Non-linearity also emerges at low air temperature due to groundwater inflow, especially in cold regions (Mohseni and Stefan 1999). Additionally, at low air temperature, water temperature tends to stabilize just above the freezing

point (0°C) due to the high turbulence of the flowing water, even if air temperature continues to decrease (Mohseni and Stefan 1999). Logistic regression has been widely used to predict water temperature from air temperature time series and it generally performs better than linear regression (e.g., Mohseni, Stefan, and Erickson 1998; Morrill, Bales, and Conklin 2005; Basarin et al. 2016). Finally, polynomial regression can be an alternative to logistic regression whenever the relationship between air temperature and water temperature is assumed to be non-linear (e.g., Basarin et al. 2016).

Other more advanced regression techniques have emerged recently that aim to predict water temperature, including a time-varying coefficient regression model (Li et al. 2014), a hierarchical linear autoregressive model (Letcher et al. 2016), and a spatial regression model (Jackson et al. 2017). The time-varying coefficient regression model accounts for the seasonal variability of the air-water temperature relationship through regression coefficients that vary over time. In other words, the model, depending on the specific time of the year, will output different water temperature values, yet are derived from equivalent air temperature values. The hierarchical linear autoregressive model resolves the problem of potential autocorrelation within daily water temperature time series by including an autoregressive coefficient based on the residual error of the day preceding the day under examination. Finally, the spatial regression model predicts water temperatures within a river network composed of nodes (i.e., observations) and lines (i.e., the actual stretches of the river and its tributaries) based on landscape characteristics representative of energy exchange processes (e.g., upstream catchment area, channel width, gradient, orientation, and illumination, percent riparian woodland).

The graphic in Figure 3-1 illustrates what has so far been discussed in this section. This classification scheme summarizes the information derived from the two most recent comprehensive reviews on this topic (i.e., Cassie 2006 and Webb et al. 2008) and the successive literature up to the present day. Two more notes should be added regarding this diagram. First, the concept of equilibrium temperature described above has been derived by simplifying the heat budget equation on which deterministic models rely (Edinger, Duttweiler, and Geyer 1968). However, at a later time, equilibrium temperature has also been used in lieu of air temperature in statistical models to predict

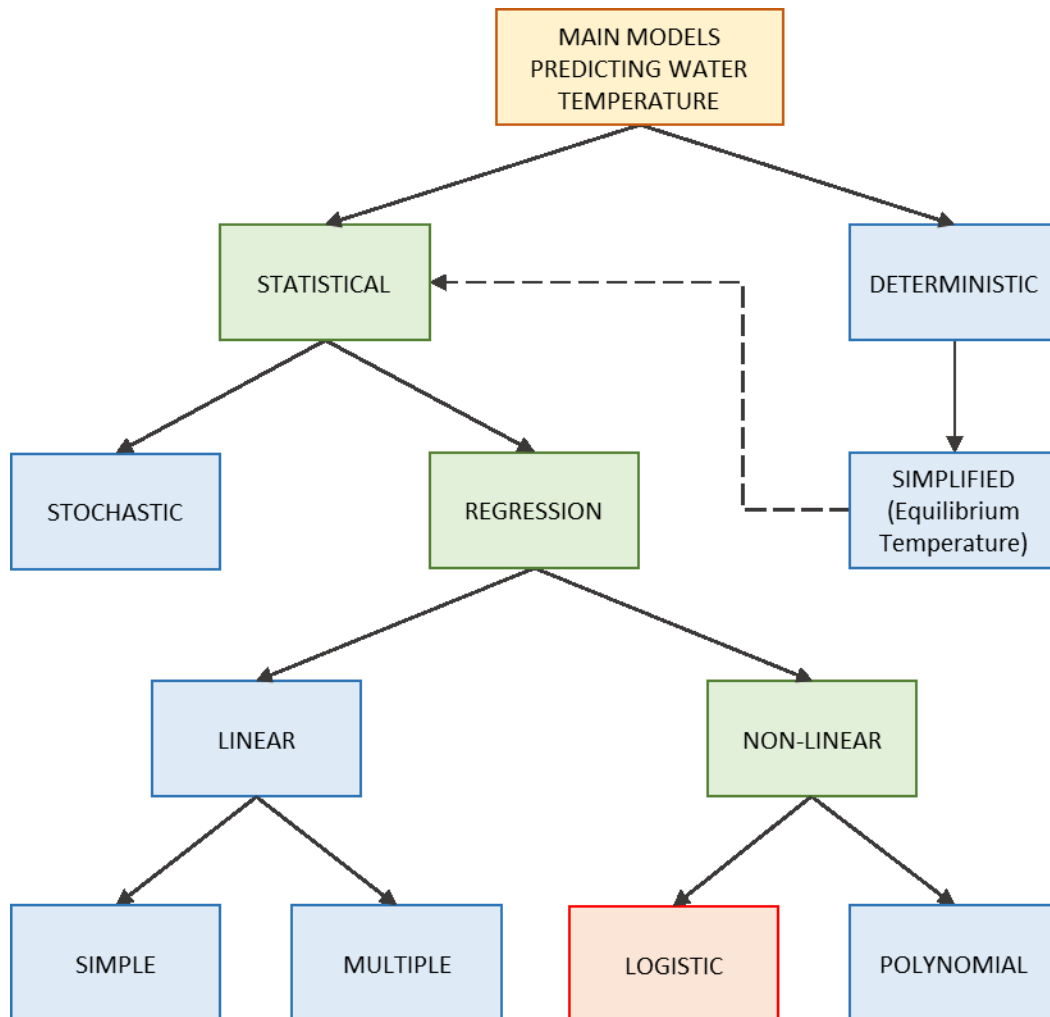


**Figure 3-1: Classification scheme of mathematical models used to predict water temperature**

water temperature (e.g., Bogan, Mohseni, and Stefan 2003; Caissie, Satish, and El-Jabi 2005; Hébert et al. 2015). This is the meaning of the dotted arrow in Figure 3-1. Second, three of the most recent regression techniques presented above (Li et al. 2014; Letcher et al. 2016; Jackson et al. 2017) cannot be categorized within a specific class of regression models (i.e., simple linear, multiple linear, logistic, and polynomial), even if they can be seen as variations of the traditional simple or multiple linear regression models. Therefore, these three techniques are not included in the classification scheme.

Among all the different modeling techniques to predict stream/river water temperature, logistic regression is employed in this research (red box in **Figure 3-1**). The choice of a statistical model that relies on air temperature data to estimate water temperature is due to three main reasons. First, only air temperature is necessary as input variable for these models. Also, this information can be retrieved from weather stations that are located at a distance of several tens of kilometers from the water temperature recording site (Webb, Clack, and Walling 2003). This is the case of the FIR, where water and air temperature data are not recorded at the same location. Second, several stretches of multiple streams and rivers with different catchment characteristics will be analyzed to provide a broad picture of water temperature trends. Statistical models are especially useful when large geographic areas and a variety of landscape characteristics are considered (Webb, Clack, and Walling 2003). Third, the air-water temperature relationship can be used to investigate the future as air temperature projections derived from GCMs (see Chapter 2) can serve as inputs to estimate future water temperature scenarios (Webb, Clack, and Walling 2003).

In addition, logistic regression is selected among other regression techniques because it is easy to implement, but, at the same time, provides better results than the simple linear regression (Morrill, Bales, and Conklin 2005; Johnson, Wilby, and Toone 2014; Basarin et al. 2016) or the polynomial regression (Basarin et al. 2016). Indeed, the logistic function better represents the non-linear nature of the air-water temperature relationship, especially at extreme temperatures. As winter air temperatures usually drop below 0°C in most areas of the FIR while water temperatures remain close to the freezing point (0°C), the air-water temperature relationship becomes non-linear. Similarly, as summer air temperatures sometimes rise above 30°C in the Flathead Valley while water temperatures stabilize around an upper limit due to evaporative cooling, the air-water temperature relationship also departs from linearity. Therefore, the sigmoidal shape of the logistic function better describes this relationship. Finally, the multiple linear regression is excluded because only air temperature is taken into account as an independent variable in this study.

Another consideration has to be made regarding the temporal scale of analysis. Due to the thermal inertia of water, the strength of the correlation between air and water temperatures tends to increase as the temporal scale increases from hourly to monthly (Bogan et al. 2006; Webb et al. 2008; Johnson, Wilby, and Toone 2014). This has been widely documented on the basis of simple linear regression statistics, but only in a few cases (Caissie, El-Jabi, and Satish 2001; Webb, Clack, and Walling 2003; Morrill, Bales, and Conklin 2005) logistic regression has been used to actually test the effect of the temporal scale on the strength of the air-water temperature correlation. Moreover,

these three works some present some important limitations. In two cases (Caissie, El-Jabi, and Satish 2001; Webb, Clack, and Walling 2003), findings are hardly generalizable because are based on a very limited number of recording stations (i.e., one and four, respectively). In another case (Morrill, Bales, and Conklin 2005), three air temperature schemes are examined, but only in relation to daily mean water temperature. Finally, in neither of them, the presence of hysteresis, a phenomenon for which the air-water temperature relationship varies depending on the season (Mohseni, Stefan, and Erickson 1998), was considered.

Therefore, the methodological contribution that this chapter intends to bring to the literature deals with better understanding the role that the choice of a given temporal scale plays in affecting the strength of the air-water temperature logistic correlation. To this end, the performances of different logistic regression models based on multiple temporal schemes (see Section 3.4.2 and Table 3-3) are compared and the best model of each SWT gaging station is selected for further analysis (see Section 3.4.4). In choosing the most robust model, hysteresis is also taken into account (see Section 3.4.3). In order to be able to generalize the results, multiple stretches of several streams and rivers encompassing watersheds of different physiographic characteristics (e.g., size, slope, elevation, land cover, soil, and hydrology) are investigated. Finally, rather than the most-commonly used daily average, maximum and minimum SWT are analyzed separately with the purpose of identifying differences in the strength of the correlation with maximum and minimum SAT, respectively.

### **3.3. Research question and objective**

After examining the trends in air temperature and snowpack characteristics, this chapter addresses the third research question of the whole study:

3. What are the historical and potential future trends of water temperature in streams and rivers of the Flathead Reservation?

The objective behind this question is to determine whether consistent upward or downward trends of maximum and minimum SWT exist over the 1961-2100 study period, and, if this is the case, quantify the rate of change. Five distinct subregions and 28 different locations are considered to investigate the spatial variability within the FIR and identify which physiographic factors may influence this variability. Direction and magnitude of a potential SWT trend across the overall study area are analyzed as well. In addition to the annual temporal scale, all trends are also calculated for each season with the intention of characterizing SWT variations not only across multiple years, but within years too.

### 3.4. Data and methods

Figure 3-2 illustrates the methodological workflow for achieving the research objective and answering the research question associated with this chapter. Water temperature data are first collected, selected, and checked for quality issues (Section 3.4.1). Then, the original SWT time series are processed to generate new series based on four temporal schemes, namely daily, daily lag-1, two-day average, and weekly average (Section 3.4.2). In the third stage, multiple SAT/SWT logistic models are calibrated and validated (Section 3.4.3), with the objective of 1) identifying the presence of hysteresis, 2) understanding how the temporal scale affect the strength of the air-water temperature relationship, and 3) extrapolating the best models. These models are used to reconstruct past and future estimates of water temperature, and, ultimately, evaluate potential SWT trends at the regional, subregional, and local scale (Section 3.4.4). All the analyses are conducted within an RStudio environment (RStudio Team 2015).

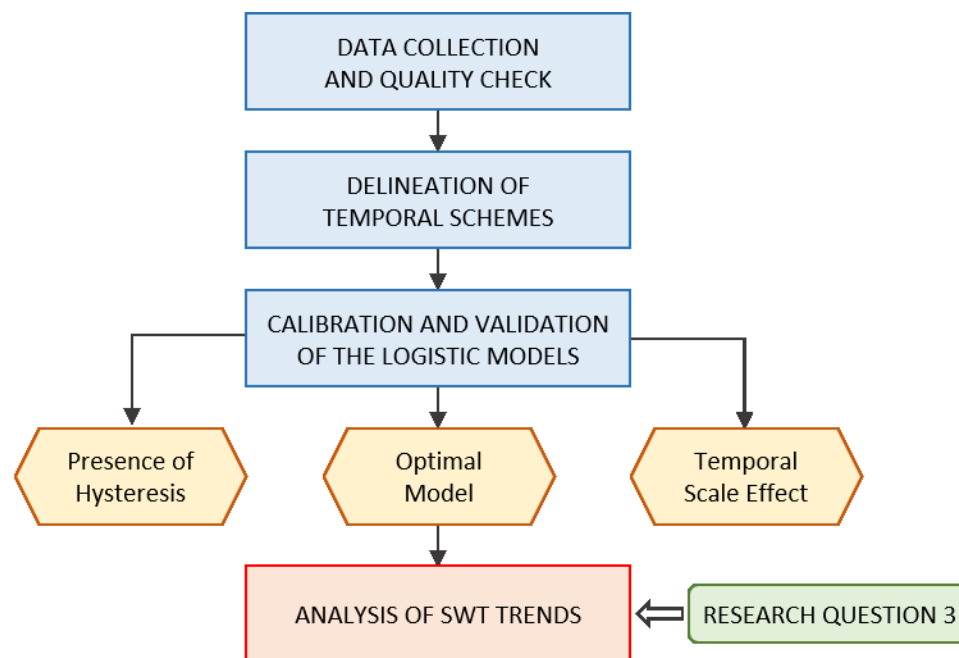


Figure 3-2: Workflow for research question 3

### **3.4.1. Data collection and quality check**

As mentioned in Sections 3.2 and 3.3, this chapter focuses on the study of two water temperature variables: maximum SWT and minimum SWT. All the water temperature data used in this analysis have been collected by the Natural Resource Department (NRD) of the CSKT. The original dataset is composed by hourly SWT measurements that have been automatically recorded between 1998 and 2012 in 50 locations across the FIR. The daily maximum and minimum SWT datasets are therefore assembled by taking the hourly maximum and minimum values of each day, respectively. If more than two hourly observations are missing in a given day (i.e., more than 10% of the data), the two corresponding daily values are not extracted and are marked as missing. An initial screening of the two datasets indicates that many SWT gaging stations have to be excluded from the analysis. Indeed, only 28 sites are selected that provide time series sufficiently long for calibrating and validating the logistic model. These locations are illustrated in Figure 3-3, whereas their general characteristics are presented in Table 3-1.

The original SWT dataset obtained from the NRD of the CSKT has already been checked by means of a primary QA procedure. However, an additional QA review is conducted here to look for inconsistencies within each dataset. The daily maximum and minimum SWT time series are graphed and visually examined to find potential changes in systematic bias (e.g., time-series jumps due to the anomalous exposure of the recording instrumentation above the water surface level). Some basic statistics (i.e., maximum, minimum, range, median, mean) are calculated for each time series with the

purpose of supporting the visual analysis and the identification of outliers (see Table 3-2). Inconsistencies between the two datasets are also examined. For example, the maximum SWT value in any given day is verified to be higher than the corresponding minimum SWT value for that day. Finally, the two datasets are also cleaned and prepared for further elaboration.

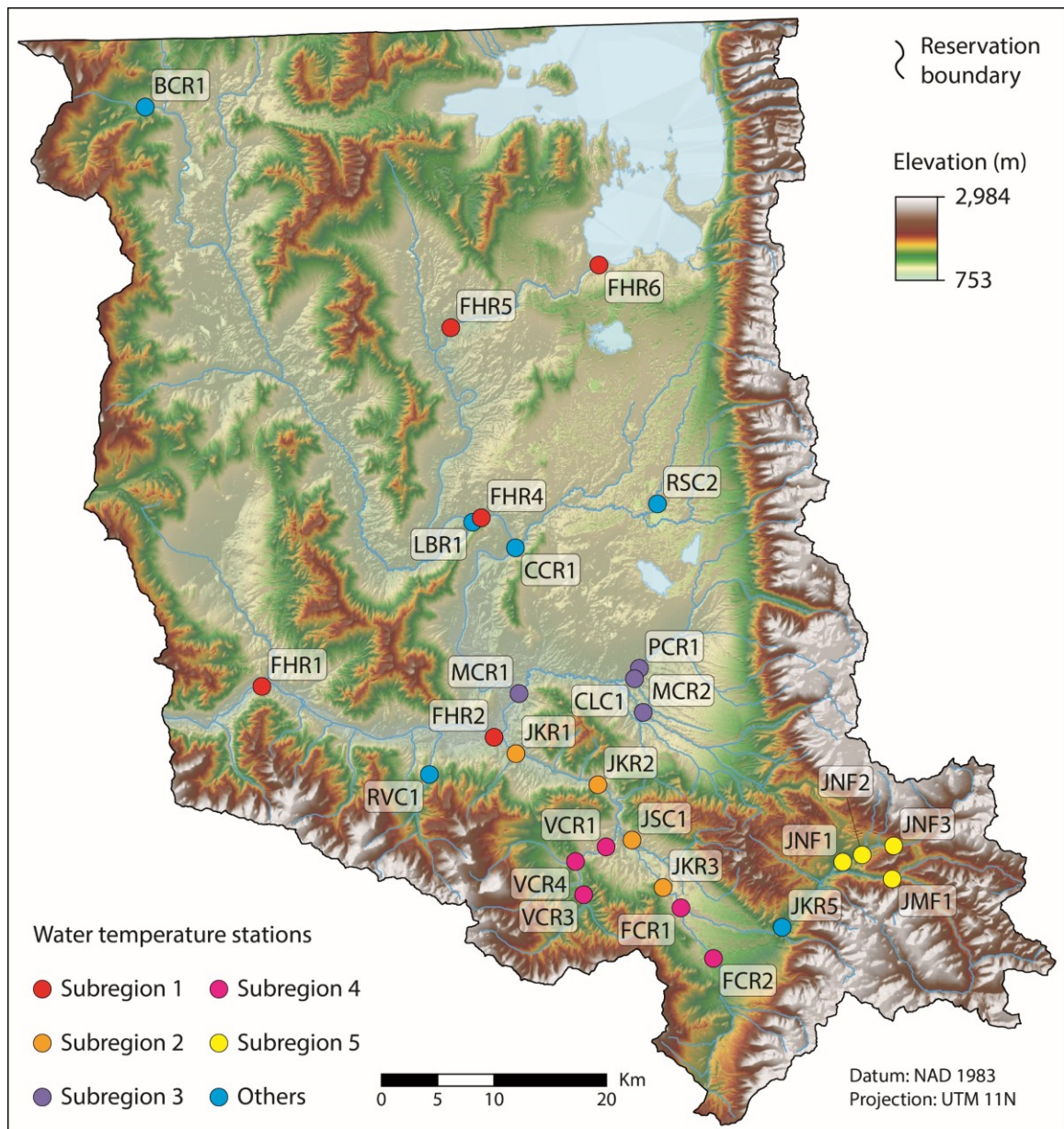


**Figure 3-3: Location of the water temperature recording stations used in the analysis**

**Table 3-1: General characteristics of the water temperature recording stations used in the analysis**

<b>Id</b>	<b>Creek/River Name</b>	<b>Subregion</b>	<b>Latitude (°)</b>	<b>Longitude (°)</b>	<b>Elevation (m)</b>	<b>Start Date</b>	<b>End Date</b>
BCR1	Bassoo Cr.		47.83069	-114.70223	940.3	6/16/2004	1/2/2012
CCR1	Crow Cr.		47.46858	-114.28112	783.2	8/5/1998	12/4/2011
CLC1	Clam Cr.	3	47.36308	-114.14337	816.6	4/30/2004	1/4/2012
FCR1	Finley Cr.	4	47.17825	-114.10177	910.7	8/5/1999	12/4/2011
FCR2	Finley Cr.	4	47.13626	-114.06571	981.6	7/22/1999	12/4/2011
FHR1	Flathead R.	1	47.36471	-114.58508	755.8	8/7/1998	10/6/2010
FHR2	Flathead R.	1	47.32017	-114.31386	763.4	4/23/1998	11/13/2011
FHR4	Flathead R.	1	47.49318	-114.31921	782.1	5/15/1998	1/4/2012
FHR5	Flathead R.	1	47.64634	-114.34580	803.8	5/15/1998	1/4/2012
FHR6	Flathead R.	1	47.69311	-114.16826	880.3	7/24/1998	1/4/2012
JKR1	Jocko R.	2	47.30631	-114.28871	780.7	7/31/1998	8/29/2011
JKR2	Jocko R.	2	47.27820	-114.19547	815.2	8/5/1998	12/4/2011
JKR3	Jocko R.	2	47.19506	-114.12265	890.5	9/3/1998	12/4/2011
JKR5	Jocko R.		47.16000	-113.98401	1,036.4	8/14/1998	12/4/2011
JMF1	Jocko Middle Fork R.	5	47.19286	-113.85311	1,207.5	6/24/1999	12/4/2011
JNF1	Jocko North Fork R.	5	47.20786	-113.90787	1,146.8	6/24/1999	1/2/2012
JNF2	Jocko North Fork R.	5	47.21508	-113.88571	1,180.1	5/12/2004	1/2/2012
JNF3	Jocko North Fork R.	5	47.21994	-113.84943	1,232.7	5/12/2004	8/29/2011
JSC1	Jocko Spring Cr.	2	47.23288	-114.15744	851.2	9/22/1999	12/4/2011
LBR1	Little Bitterroot R.		47.48969	-114.32988	785.1	8/3/1999	7/28/2011
MCR1	Mission Cr.	3	47.35162	-114.28257	766.2	7/24/1998	12/4/2011
MCR2	Mission Cr.	3	47.33654	-114.13950	839.7	7/22/1999	1/4/2012
PCR1	Post Cr.	3	47.36405	-114.14762	815.0	7/1/1999	1/4/2012
RSC2	Ronan Spring Cr.		47.50220	-114.11260	921.6	5/12/2004	12/4/2011
RVC1	Revais Cr.		47.29210	-114.39055	906.2	7/13/2005	11/7/2011
VCR1	Valley Cr.	4	47.22756	-114.18702	877.1	6/24/1999	12/4/2011
VCR3	Valley Cr.	4	47.19223	-114.21618	978.9	7/22/1999	12/4/2011
VCR4	Valley Cr.	4	47.21623	-114.22416	922.1	7/1/1999	12/4/2011

**Table 3-2: Basic statistics of the daily maximum and minimum SWT time series used in the analysis**

Id	Days	Records	% Missing	Daily Maximum SWT					Daily Minimum SWT				
				Max	Min	Range	Median	Mean	Max	Min	Range	Median	Mean
BCR1	2,757	2,512	8.89	22.6	-0.1	22.6	7.3	7.9	18.4	-0.1	18.5	4.1	5.1
CCR1	4,870	4,131	15.17	28.6	0.0	28.6	11.5	12.0	21.3	-0.2	21.4	7.5	8.2
CLC1	2,806	2,409	14.15	24.8	0.0	24.8	12.2	12.6	19.9	-0.1	20.0	7.9	8.1
FCR1	4,505	2,836	37.05	25.4	-0.1	25.5	9.2	9.5	21.7	-0.1	21.8	4.6	5.5
FCR2	4,519	3,653	19.16	23.7	-0.1	23.8	8.9	9.1	16.3	-0.1	16.4	4.8	5.3
FHR1	4,444	3,404	23.40	26.9	-0.1	27.0	11.2	11.6	24.6	-0.1	24.7	9.9	10.4
FHR2	4,953	4,492	9.31	26.2	-0.1	26.4	10.4	11.2	24.7	-0.2	24.9	9.2	10.0
FHR4	4,983	4,365	12.40	26.6	0.0	26.6	10.6	11.4	24.5	-0.1	24.6	9.3	10.2
FHR5	4,983	3,686	26.03	26.0	-0.1	26.1	8.7	10.3	25.0	-0.1	25.1	7.9	9.5
FHR6	4,913	4,454	9.34	25.7	0.1	25.6	9.5	10.6	25.0	-0.1	25.2	8.7	9.9
JKR1	4,778	3,509	26.56	23.9	0.0	24.0	10.6	11.0	16.9	-0.2	17.0	7.4	7.6
JKR2	4,870	4,226	13.22	22.6	-0.1	22.7	10.0	10.4	14.3	-0.1	14.4	6.5	6.8
JKR3	4,841	4,471	7.64	18.5	1.8	16.8	9.4	9.8	12.4	-0.1	12.4	6.3	6.5
JKR5	4,861	3,898	19.81	15.8	0.0	15.8	7.0	7.7	11.3	-0.1	11.4	4.6	5.2
JMF1	4,547	3,997	12.10	17.6	-0.1	17.7	8.8	8.8	13.9	-0.1	14.0	5.6	6.0
JNF1	4,576	4,050	11.49	17.8	-0.1	17.8	6.7	7.3	11.8	-0.1	11.9	3.8	4.3
JNF2	2,792	2,512	10.03	14.7	-0.2	14.9	5.2	6.1	11.1	-0.2	11.3	3.3	4.2
JNF3	2,666	2,456	7.88	15.3	0.0	15.4	4.9	5.9	11.6	-0.1	11.7	3.1	4.1
JSC1	4,457	3,856	13.48	22.0	0.1	21.9	12.6	12.6	13.2	-0.1	13.3	7.5	7.3
LBR1	4,378	3,467	20.81	36.5	-0.1	36.6	12.1	12.8	23.3	-0.3	23.6	7.7	7.9
MCR1	4,882	3,917	19.77	24.6	-0.1	24.7	12.3	11.9	20.4	-0.1	20.5	9.4	9.2
MCR2	4,550	3,872	14.90	21.2	-0.1	21.3	11.1	10.6	16.4	-0.1	16.6	7.6	7.3
PCR1	4,571	3,887	14.96	22.9	0.4	22.6	11.9	11.7	17.9	-0.1	18.0	8.5	8.5
RSC2	2,763	2,475	10.42	22.1	0.3	21.7	11.6	11.7	16.5	0.0	16.5	7.8	8.1
RVC1	2,309	1,895	17.93	18.0	-0.1	18.1	7.0	7.4	15.5	-0.3	15.8	5.3	5.7
VCR1	4,547	4,030	11.37	24.1	-0.2	24.3	9.4	9.3	16.4	-0.4	16.8	4.9	5.1
VCR3	4,519	3,976	12.02	16.3	-0.1	16.4	6.2	6.4	13.6	-0.1	13.7	4.1	4.5
VCR4	4,540	4,050	10.79	25.1	-0.1	25.2	10.4	10.2	19.4	-0.2	19.6	5.2	5.7

### 3.4.2. Design of temporal schemes

After checking the quality of the daily maximum and minimum SWT datasets, two new SWT time series per location are generated based on a 7-day centered moving average. Even if only a value out of seven is missing, the weekly average is reported as missing. In addition, daily maximum and minimum SAT time series related to the ten climate stations included in the statistical downscaling analysis of Chapter 2 (see Table 2-4) are used here to create six new SAT time series per location based on three temporal schemes: daily lag-1 (SAT value of the preceding day), two-day average (average SAT value of the present and the preceding days), and weekly average (7-day centered moving average). If the value of the preceding day is missing, the new value of the lag-1 time series is reported as missing. Regarding the other two schemes, even if only a value is missing, the 2-day or 7-day averages are not computed. Table 3-3 summarizes the eight pairs of independent/dependent variables that are investigated in this research. The eight time series created at this stage (two SWT series and six SAT series) are highlighted in the table by a gray shade.

**Table 3-3: Logistic models based on different pairs of independent/dependent variables (the time series created at this stage are highlighted by a gray shade)**

Pair #	Independent variable (SAT)	Dependent variable (SWT)
1	Daily maximum SAT	Daily maximum SWT
2	Daily lag-1 maximum SAT	Daily maximum SWT
3	Two-day average maximum SAT	Daily maximum SWT
4	Weekly maximum SAT	Weekly maximum SWT
5	Daily minimum SAT	Daily minimum SWT
6	Daily lag-1 minimum SAT	Daily minimum SWT
7	Two-day average minimum SAT	Daily minimum SWT
8	Weekly minimum SAT	Weekly minimum SWT

Each SAT/SWT pair presented in Table 3-3 is examined using the entire datasets and two partial datasets of both variables, for a total of six different runs. Indeed, each original dataset is divided into rising and falling limbs. The rising limb corresponds to the half of the year when air temperatures tends to increase (usually mid-January to mid-July in the FIR), while the falling limb coincides with the complementary half of the year when air temperature tends to decrease (usually mid-July to mid-January in the study area). The first date of the rising limb, which is equivalent to the day after the last date of the falling limb, is calculated by taking the coldest day within the coldest week of each year. Similarly, the first date of the falling limb, which is equivalent to the day after the last date of the rising limb, is computed by considering the warmest day within the warmest week of each year.

The reason why it is recommended splitting each dataset into two parts is because the air-water relationship is not always constant throughout the year. Indeed, this relationship can slightly change depending on the season (warming season vs. cooling season). This phenomenon, called hysteresis (see Section 3.4.3), is especially visible in mountainous areas, such as the FIR, where stream and river temperatures are affected by seasonal snowmelt runoff (Webb et al. 2008). In summary, 6,720 logistic models are assessed in this study as the eight SAT/SWT pairs illustrated in Table 3-3 are evaluated using three datasets (i.e., annual, rising limb, and falling limb) related to ten SAT recording stations and 28 SWT gaging stations. Eventually, only the best model or the best pair of models (if hysteresis is present) is selected for each SWT location/variable. The generic structure of a logistic model is described below.

### 3.4.3. Calibration and validation of the SAT/SWT non-linear models

As mentioned in the literature review of this chapter, a non-linear logistic function usually represents the air-water temperature relationship better than a linear function as this relationship does not remain linear at extreme air temperatures (Mohseni, Stefan, and Erickson 1998). Figure 3-4 displays the sigmoidal shape of a generic logistic function. As air temperature increases, water temperature tends to reach an upper bound imposed by evaporative cooling. As air temperature drops below 0°C, water temperature tends to reach a lower bound that, in cold regions, is usually close to the water freezing point (0°C). The logistic function is mathematically described as follows (adapted from Mohseni, Stefan, and Erickson 1998):

$$SWT = \frac{\alpha}{1 + e^{\gamma(\beta - SAT)}} \quad (23)$$

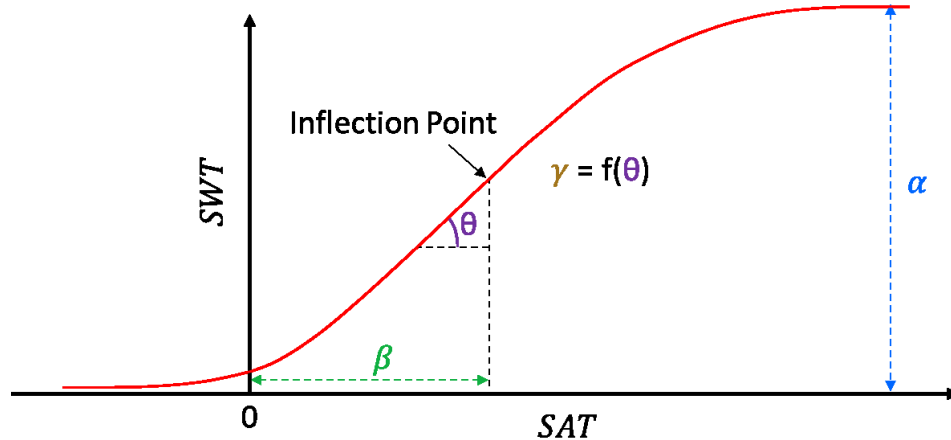


Figure 3-4: Air-water temperature relationship (adapted from Mohseni, Stefan, and Erickson 1998, 2687)

The three regression parameters are physically interpretable and have units as functions of °C (see Figure 3-4):  $\alpha$  is the maximum SWT that the model can predict;  $\gamma$  is a measure of the steepest slope of the function; and  $\beta$  is the SAT at the inflection point. The

minimum SWT is reasonably assumed to be 0°C. The coefficient  $\gamma$  is a function of the slope,  $4 \tan(\theta)$ , and can be estimated as:

$$\gamma = \frac{4 \tan(\theta)}{\alpha}. \quad (24)$$

All 6,720 statistical models are first calibrated and then validated over an independent dataset. The time-series values between 1 January 2008 and 31 December 2009 are used for validating the models (test datasets), while the remaining available data are included in the calibration process (training datasets). The non-linear least squares method is used to estimate the three parameters ( $\alpha$ ,  $\gamma$ , and  $\beta$ ) by implementing the Gauss-Newton algorithm. The accuracy of each model is assessed by comparing simulated (SIM) SWT values with observed (OBS) SWT values of both the training and test datasets. The Nash-Sutcliffe coefficient (NSC) and the root mean squared error (RMSE) are calculated to evaluate the goodness of the fit, and are defined as follows:

$$NSC = 1 - \frac{\sum_{i=1}^n (SIM_i - OBS_i)^2}{\sum_{i=1}^n (OBS_i - \overline{OBS})^2}, \quad (25)$$

$$RMSE = \sqrt{\frac{\sum_{i=1}^n (SIM_i - OBS_i)^2}{n}}, \quad (26)$$

where  $n$  is the number of pairs of SIM/OBS values of SWT. NSC ranges between  $-\infty$  and 1, whereas RMSE, which is measured in °C, varies between 0 and  $+\infty$ , with NSC values close to 1 and RMSE values close to 0 indicating the best fit, respectively. As briefly mentioned, NCS and RMSE are computed for both the training and test datasets. In the first case, the two accuracy measures are used to identify the presence of hysteresis whereas, in the second case, to select the optimal model.

As introduced in Section 3.4.2, each model is calibrated and validated using separately the entire time series (i.e., annual), the warming season time series (i.e., the rising limb), and the cooling season time series (i.e., the falling limb). Indeed, climate, environmental, or human factors can influence the air-water temperature relationship at different times of the year. For example, stream inflow due to snowmelt processes in spring and early summer maintains water temperature relatively low, even if air temperature increases. In the cooling season, this constant contribution of snowmelt-derived cold water is absent. Thus, given similar SAT values in spring and fall, the air-water temperature curve tends to move towards higher SWT values during the cooling season, as illustrated in Figure 3-5. To identify the presence of hysteresis, the NCS of the three training datasets (i.e., annual, rising limb, and falling limb) is observed. If the combined NCS of the rising and falling limbs is more than 0.01 larger than the NCS associated with the annual dataset (e.g., Figure 3-5), it is assumed that the stream exhibits hysteresis at that particular location (Mohseni, Stefan, and Erickson 1998).

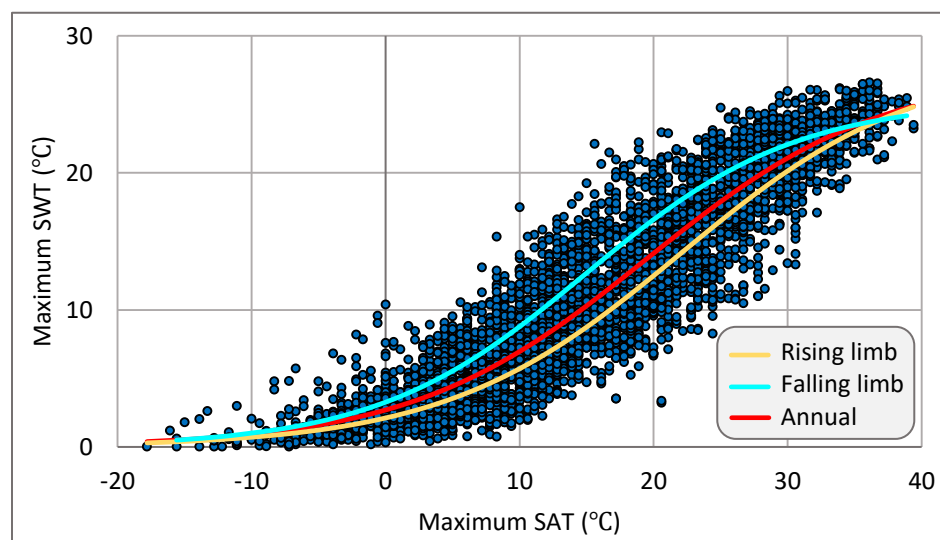


**Figure 3-5: Example of hysteresis loop with rising (yellow) and falling (cyan) limbs; the function fitting the annual (i.e., entire) dataset is shown in red**

The NSC and RMSE related to the validation period (2008-2009) serve as a means to select the optimal air-water temperature model for each SWT location and water temperature variable (i.e., maximum SWT and minimum SWT). Four temporal schemes (i.e., daily, daily lag-1, two-day average, and weekly average) and ten SAT recording stations are analyzed in a comparative fashion. To allow for comparison, the same number of days within the 2008-2009 period is considered for each SWT location and variable. Moreover, the combined NSC and RMSE of the rising and falling limbs are compared to the NSC and RMSE of the annual dataset, respectively. As the length of the warming and cooling seasons slightly varies by location, the number of values used in the validation process of the rising and falling limbs may differ from SAT station to SAT station. However, this is not expected to affect the results because the variation is minimal (7 days at worse). The model with the highest NSC and/or the lowest RMSE is eventually selected. In summary, this analysis contributes to 1) identifying the SWT stations that manifest hysteresis, 2) understanding the effect of the choice of the temporal scale on the strength of the air-water temperature relationship, and 3) extrapolating the optimal model that will be employed in the next research stage.

#### 3.4.4. Analysis of SWT trends

To identify potential trends in water temperature, three steps are necessary. First, the three logistic parameters ( $\alpha$ ,  $\gamma$ , and  $\beta$ ) related to the best statistical air-water temperature relationships derived in the previous stage are applied to a generic logistic function (see Equation 23) to estimate daily SWT time series using the daily SAT time series generated in the previous chapter as inputs (see Section 2.4.3.1). This process is undertaken for all 28 SWT gaging stations, for both maximum and minimum SWT, and for the three climate scenarios (RCP2.6, RCP4.5, and RCP8.5). If a given combination of location and variable manifests hysteresis, two sets of logistic parameters are retained from the previous analysis. In this case, the original SAT time series is divided into rising and falling limbs, and the two sets of logistic parameters are applied accordingly. The two resulting SWT time series are eventually assembled back together and, whenever possible, the modeled values are replaced by the original observed SWT data.

In the end, each of the 56 SWT time series comprises 51,114 continuous daily records starting from 1 January 1961 to 31 December 2100 (leap days are not included after 31 August 2018). If a weekly scheme is considered, then the resulting time series range between 4 January 1961 and 28 December 2100, for a total of 51,108 records. The second step consists in computing monthly, seasonal, and annual means based on equations 5, 6, and 7, respectively (see Section 2.4.3.2). This process follows the WMO standard procedures (WMO 1989). As the averages are calculated over the entire length of the daily SWT time series previously created, the resulting time series are composed by 140 values (i.e., one monthly, seasonal, or annual value per year).

In the third step, monthly, seasonal, and annual trends in water temperature are investigated by running the MKT and the RKT (see Section 2.4.3.4) with the support of the rkt package by Marchetto (2017). The MKT is first applied to either maximum or minimum SWT time series for each of the 28 SWT gaging stations. Then, multiple locations are combined together through the RKT to evaluate whether a consistent water temperature trend is evident within five subregions and across the entire FIR. These subregions, which are illustrated in Figure 3-3 and described in Table 3-1, are delineated based on the spatial contiguity of the SWT gaging stations, the catchment characteristics, and, most importantly, the flow regime of the stream/river where these stations are placed. To guarantee a balanced statistic power when performing the RKT (Helsel and Frans 2006) and, therefore, to allow for comparisons, a similar number of sites is selected for each subregion (four or five in this study). Several statistics are reported for each trend test, including the Kendall's correlation coefficient, the Kendall's statistic and its variance, the Theil-Sen's slope and the related magnitude of change, and the p value.

### **3.5. Results**

This section presents the main findings of the analyses in this chapter and it is divided into two parts. The first one shows the results related to the calibration and validation of the non-linear logistic models (Section 3.5.1). Here, the role of the temporal scale in affecting the goodness of air-water temperature relationship is documented. This part also examines the most correlated climate stations, the presence/absence of hysteresis loops, and the accuracy of the models, with a focus on the difference between accuracies of the rising and falling limbs. These themes are discussed in the light of the physiographic characteristics of the stream/river catchment within which a given SWT gaging station is placed. The second part deals with the outcomes of the trend analysis in water temperature (Section 3.5.2). Results are illustrated for two variables (i.e., maximum SWT and minimum SWT), three climate scenarios (i.e., RCP2.6, RCP4.5, and RCP8.5), three spatial scales (i.e., single locations, small subregions, and entire study area), and two temporal scales (i.e., seasonal and annual). The findings described in this part respond to the third research question associated with this research (see Section 3.3).

#### **3.5.1. SAT/SWT non-linear logistic models**

Table 3-4 shows the best NSC and RMSE (°C) values calculated over the training and test datasets for each temporal scheme and maximum SWT gaging station. Given a certain location and temporal scheme, the highest NSC and the lowest RMSE presented in Table 3-4 are not necessarily associated with the same statistical model. As it is not of interest to the discussion at this stage, the reference climate station and the model type

**Table 3-4: Best correlation between maximum SAT and maximum SWT for each SWT gaging station and temporal scheme**

Station	Calibration (Training Dataset)								Validation (Test Dataset)							
	NSC				RMSE (°C)				NSC				RMSE (°C)			
	Daily	Lag-1	2-day	7-day	Daily	Lag-1	2-day	7-day	Daily	Lag-1	2-day	7-day	Daily	Lag-1	2-day	7-day
BCR1	0.92	0.90	0.92	0.96	1.90	2.13	1.85	1.38	0.93	0.89	0.93	0.97	1.73	2.07	1.63	1.10
CCR1	0.91	0.88	0.91	0.96	2.23	2.54	2.19	1.55	0.89	0.86	0.89	0.94	2.65	2.94	2.57	1.87
CLC1	0.92	0.88	0.92	0.97	1.66	2.01	1.64	1.08	0.90	0.85	0.89	0.94	1.84	2.27	2.01	1.36
FCR1	0.92	0.88	0.92	0.96	1.93	2.35	1.98	1.35	0.92	0.88	0.93	0.96	1.85	2.17	1.70	1.22
FCR2	0.93	0.88	0.92	0.96	1.69	2.14	1.71	1.19	0.84	0.80	0.83	0.90	2.05	2.27	2.06	1.47
FHR1	0.92	0.92	0.93	0.96	2.18	2.20	1.96	1.42	0.91	0.91	0.92	0.96	2.18	2.28	1.96	1.46
FHR2	0.87	0.88	0.90	0.95	2.56	2.55	2.33	1.71	0.89	0.89	0.91	0.95	2.25	2.26	2.07	1.50
FHR4	0.90	0.91	0.92	0.96	2.28	2.25	2.05	1.49	0.88	0.89	0.91	0.94	2.36	2.32	2.11	1.58
FHR5	0.90	0.91	0.92	0.96	2.31	2.20	2.05	1.47	0.86	0.87	0.89	0.94	2.59	2.44	2.33	1.68
FHR6	0.90	0.90	0.92	0.96	2.21	2.12	1.98	1.42	0.87	0.88	0.89	0.94	2.31	2.17	2.08	1.50
JKR1	0.93	0.89	0.92	0.96	1.49	1.85	1.53	1.13	0.89	0.84	0.87	0.94	1.52	1.85	1.61	0.97
JKR2	0.94	0.89	0.93	0.97	1.24	1.65	1.30	0.79	0.92	0.85	0.91	0.96	1.33	1.78	1.37	0.89
JKR3	0.92	0.85	0.91	0.96	1.12	1.49	1.17	0.77	0.91	0.82	0.89	0.95	1.11	1.51	1.20	0.77
JKR5	0.92	0.86	0.92	0.97	0.90	1.22	0.94	0.60	0.92	0.83	0.91	0.95	0.91	1.27	0.96	0.64
JMF1	0.91	0.84	0.90	0.96	1.06	1.43	1.12	0.72	0.87	0.78	0.86	0.92	1.13	1.46	1.16	0.84
JNF1	0.92	0.87	0.91	0.96	1.34	1.68	1.39	0.90	0.88	0.82	0.88	0.94	1.34	1.70	1.43	0.91
JNF2	0.92	0.88	0.92	0.96	0.99	1.29	1.00	0.67	0.89	0.84	0.90	0.95	1.09	1.28	1.05	0.71
JNF3	0.90	0.87	0.90	0.94	1.25	1.40	1.23	0.91	0.89	0.82	0.87	0.93	1.21	1.52	1.28	0.87
JSC1	0.93	0.84	0.90	0.97	1.18	1.79	1.36	0.74	0.93	0.81	0.90	0.97	1.15	1.80	1.36	0.73
LBR1	0.91	0.89	0.91	0.96	3.13	3.50	3.03	2.08	0.91	0.88	0.90	0.95	3.17	3.54	3.08	2.22
MCR1	0.94	0.91	0.94	0.97	1.60	1.87	1.54	1.12	0.92	0.88	0.93	0.97	1.75	2.02	1.63	1.05
MCR2	0.93	0.89	0.93	0.97	1.37	1.71	1.40	0.93	0.89	0.85	0.90	0.94	1.74	2.03	1.67	1.30
PCR1	0.93	0.89	0.93	0.97	1.41	1.68	1.39	1.01	0.92	0.87	0.91	0.95	1.44	1.77	1.45	1.10
RSC2	0.91	0.86	0.90	0.96	1.42	1.76	1.46	0.91	0.91	0.87	0.90	0.96	1.45	1.75	1.49	0.94
RVC1	0.93	0.91	0.94	0.96	1.32	1.44	1.23	0.95	0.90	0.88	0.91	0.95	1.42	1.57	1.32	0.96
VCR1	0.92	0.88	0.91	0.96	1.93	2.34	1.96	1.38	0.88	0.84	0.88	0.92	2.07	2.37	2.09	1.60
VCR3	0.92	0.90	0.93	0.96	1.25	1.38	1.16	0.90	0.90	0.88	0.91	0.93	1.26	1.36	1.20	0.99
VCR4	0.93	0.89	0.92	0.96	2.00	2.47	2.02	1.41	0.91	0.87	0.91	0.94	2.08	2.44	2.03	1.56
<b>MEAN</b>	<b>0.92</b>	<b>0.88</b>	<b>0.92</b>	<b>0.96</b>	<b>1.68</b>	<b>1.94</b>	<b>1.64</b>	<b>1.14</b>	<b>0.90</b>	<b>0.86</b>	<b>0.90</b>	<b>0.95</b>	<b>1.75</b>	<b>2.01</b>	<b>1.71</b>	<b>1.21</b>

(i.e., annual dataset vs. combined rising and falling limbs) related to a specific NSC or RMSE value are not included in the table. Regardless of the dataset (i.e., training vs. test) and accuracy measure (i.e., NSC vs. RMSE) considered, results indicate that the air-water temperature relationship is always much stronger at the weekly time scale. The 2-day average scheme and the daily scheme provide intermediate accuracy values, with about half of the SWT stations performing slightly better using one scheme rather than the other. Finally, the air-water temperature relationship is weaker when considering a 1-day lag between SAT and SWT. However, this hierarchy is not always respected as the daily lag-1 scheme is equally or more accurate than the daily scheme in the case of the SWT stations located along the Flathead River (i.e., subregion 1 in Figure 3-3).

Table 3-5 displays the same type of information included in Table 3-4, with the only difference that minimum SWT is investigated rather than maximum SWT. The role of the temporal scale in affecting the strength of the air-water temperature relationship is quite consistent with that described above. The major difference concerns the accuracy of the 2-day average scheme, which is steadily higher than the accuracy of the daily scheme, with only a few exceptions across subregion 2 (see Figure 3-3). Also, regarding the Flathead River (i.e., subregion 1 in Figure 3-3), applying a 1-day lag between SAT and SWT is a less crucial determinant in improving model accuracy for minimum SWT than it is for maximum SWT. It can be finally noticed that, independently of the temporal scheme used, the maximum SAT/SWT models generally perform better than the minimum SAT/SWT models, as indicated by the higher NSC. However, the RMSE is also higher due to the broader range of values that maximum SWT may assume.

Table 3-5: Best correlation between minimum SAT and minimum SWT for each SWT gaging station and temporal scheme

Station	Calibration (Training Dataset)								Validation (Test Dataset)							
	NSC				RMSE (°C)				NSC				RMSE (°C)			
	Daily	Lag-1	2-day	7-day	Daily	Lag-1	2-day	7-day	Daily	Lag-1	2-day	7-day	Daily	Lag-1	2-day	7-day
BCR1	0.93	0.88	0.94	0.97	1.26	1.62	1.13	0.77	0.93	0.90	0.94	0.97	1.26	1.52	1.14	0.79
CCR1	0.85	0.83	0.88	0.93	2.17	2.33	1.96	1.50	0.87	0.85	0.91	0.94	2.08	2.22	1.78	1.40
CLC1	0.93	0.88	0.94	0.97	1.15	1.54	1.11	0.71	0.94	0.88	0.94	0.98	1.11	1.52	1.06	0.67
FCR1	0.88	0.83	0.89	0.93	1.73	2.04	1.63	1.28	0.90	0.84	0.91	0.94	1.37	1.73	1.32	1.01
FCR2	0.92	0.87	0.92	0.96	1.19	1.57	1.17	0.77	0.88	0.85	0.90	0.93	1.24	1.49	1.16	0.85
FHR1	0.86	0.85	0.89	0.95	2.68	2.77	2.31	1.62	0.86	0.86	0.90	0.93	2.59	2.59	2.16	1.74
FHR2	0.82	0.82	0.86	0.91	2.91	2.95	2.61	1.98	0.84	0.84	0.88	0.93	2.55	2.54	2.17	1.68
FHR4	0.84	0.84	0.88	0.94	2.80	2.80	2.42	1.70	0.84	0.83	0.88	0.92	2.58	2.67	2.24	1.75
FHR5	0.85	0.85	0.89	0.94	2.80	2.75	2.41	1.69	0.85	0.85	0.88	0.91	2.63	2.60	2.34	1.98
FHR6	0.83	0.83	0.87	0.94	2.89	2.90	2.54	1.76	0.81	0.81	0.86	0.92	2.80	2.71	2.35	1.79
JKR1	0.89	0.84	0.89	0.93	1.38	1.59	1.32	1.07	0.87	0.77	0.88	0.92	1.19	1.53	1.16	0.85
JKR2	0.94	0.87	0.93	0.97	0.83	1.21	0.88	0.53	0.93	0.86	0.92	0.96	0.81	1.22	0.88	0.56
JKR3	0.91	0.84	0.91	0.96	0.75	1.04	0.78	0.52	0.92	0.84	0.91	0.95	0.73	1.03	0.77	0.54
JKR5	0.90	0.85	0.90	0.95	0.72	0.92	0.73	0.47	0.91	0.87	0.91	0.95	0.66	0.87	0.67	0.50
JMF1	0.88	0.83	0.88	0.94	1.00	1.19	0.99	0.69	0.83	0.77	0.84	0.88	1.04	1.19	1.03	0.83
JNF1	0.89	0.85	0.91	0.96	0.97	1.17	0.91	0.60	0.89	0.85	0.91	0.95	0.91	1.06	0.84	0.60
JNF2	0.89	0.86	0.91	0.96	0.89	0.99	0.82	0.53	0.87	0.83	0.89	0.93	0.86	1.00	0.83	0.64
JNF3	0.87	0.84	0.90	0.95	1.13	1.23	1.02	0.72	0.83	0.80	0.86	0.91	1.13	1.19	1.00	0.78
JSC1	0.93	0.83	0.90	0.96	0.65	1.00	0.75	0.42	0.92	0.84	0.89	0.96	0.64	0.98	0.81	0.40
LBR1	0.85	0.81	0.87	0.92	2.46	2.69	2.25	1.74	0.88	0.85	0.91	0.94	2.23	2.50	1.96	1.48
MCR1	0.91	0.86	0.93	0.97	1.60	1.94	1.44	0.94	0.91	0.87	0.92	0.96	1.60	1.94	1.43	0.99
MCR2	0.91	0.86	0.92	0.96	1.19	1.48	1.11	0.76	0.89	0.82	0.90	0.93	1.37	1.72	1.33	1.08
PCR1	0.92	0.86	0.94	0.97	1.13	1.52	1.02	0.65	0.93	0.88	0.93	0.97	1.14	1.44	1.08	0.75
RSC2	0.92	0.84	0.92	0.96	0.98	1.38	0.98	0.65	0.93	0.86	0.93	0.96	0.93	1.27	0.92	0.62
RVC1	0.90	0.87	0.92	0.96	1.36	1.47	1.16	0.78	0.89	0.86	0.92	0.95	1.34	1.47	1.12	0.87
VCR1	0.91	0.87	0.93	0.96	1.30	1.57	1.16	0.85	0.91	0.86	0.92	0.95	1.22	1.52	1.18	0.86
VCR3	0.91	0.85	0.93	0.97	1.06	1.42	0.97	0.59	0.92	0.89	0.93	0.96	0.92	1.14	0.84	0.64
VCR4	0.90	0.85	0.92	0.95	1.58	1.93	1.45	1.05	0.90	0.86	0.91	0.95	1.57	1.84	1.48	1.07
<b>MEAN</b>	<b>0.89</b>	<b>0.85</b>	<b>0.91</b>	<b>0.95</b>	<b>1.52</b>	<b>1.75</b>	<b>1.39</b>	<b>0.98</b>	<b>0.89</b>	<b>0.85</b>	<b>0.90</b>	<b>0.94</b>	<b>1.45</b>	<b>1.66</b>	<b>1.32</b>	<b>0.99</b>

Table 3-6 presents the specifications of the optimal SAT/SWT model (or pair of models, if hysteresis is present) for each SWT gaging station and SWT variable, including the most correlated SAT recording station, the type of dataset (i.e., annual, rising limb, and falling limb), the values of the three logistic parameters ( $\alpha$ ,  $\gamma$ , and  $\beta$ ), the NSC and RMSE ( $^{\circ}\text{C}$ ) related to the model calibration and validation, the size of the training and test datasets, and the percentage of records used for the validation process with respect to the total data available. Only models or pairs of models associated with an NSC value equal or greater than 0.90 and a RSME value smaller than  $2.0^{\circ}\text{C}$  over the validation period are accepted and employed in the successive research stage (see Section 3.5.2).

Table 3-6 shows that Polson Kerr Dam and Bigfork 13S are the most commonly correlated climate stations, as the SAT time series recorded at these locations are used as independent variables in 18 and 17 models (or pair of models), respectively. These are followed by Missoula International Airport and Superior (both 8 models), Hot Springs Montana (4 models), and finally Saint Ignatius (1 model). Four climate stations (i.e., Kraft Kreek, Moss Peak, North Fork Jocko, and Seeley Lake Ranger Station) have not been included in any of the models. The distance between SWT gaging stations and SAT recording stations is not a key factor influencing the goodness of the air-water relationship, as demonstrated in Table 3-7. Indeed, the time series of the closest climate station is selected as independent variable only in five cases out of 56 (gray shade), four of which associated with minimum daily temperatures. In the remaining 51 cases, other distances rather than the shortest one separate the SAT/SWT stations of the best model, including the largest possible distance (seven cases, highlighted by a gray shade).

**Table 3-6: Specifications of the optimal SAT/SWT model for each SWT gaging station and SWT variable**

SWT Station	Variable	SAT Station	Dataset	a	y	b	NSC Cal.	RMSE Cal. (°C)	NSC Val.	RMSE Val. (°C)	Training Set Size	Test Set Size	Perc. Test Set
BCR1	Max SWT	Bigfork 13S	Annual	19.3	0.20	16.9	0.96	1.38	0.97	1.10	1,485	488	24.73
	Min SWT	Bigfork 13S	Annual	14.0	0.32	7.4	0.97	0.77	0.97	0.79	1,558	533	25.49
CCR1	Max SWT	Saint Ignatius	Annual	28.6	0.13	19.0	0.96	1.63	0.94	1.87	1,532	463	23.21
	Min SWT	Bigfork 13S	Annual	18.9	0.25	5.9	0.93	1.51	0.94	1.40	2,492	510	16.99
CLC1	Max SWT	Hot Springs Mt.	Rising Limb	23.3	0.12	12.9	0.96	1.15	0.96	1.29	921	318	25.67
			Falling Limb	33.5	0.07	27.8	0.93	1.40	0.89	1.72	732	170	18.85
	Min SWT	Bigfork 13S	Annual	20.9	0.15	8.4	0.97	0.77	0.98	0.67	1,446	533	26.93
FCR1	Max SWT	Superior	Annual	22.3	0.13	18.8	0.94	1.64	0.96	1.22	1,870	329	14.96
	Min SWT	Polson Kerr Dam	Rising Limb	15.1	0.24	6.1	0.94	1.03	0.96	0.91	1,229	205	14.30
Falling Limb			15.7	0.30	4.5	0.92	1.54	0.93	1.11	881	141	13.80	
FCR2	Max SWT	Superior	Annual	21.6	0.12	19.9	0.94	1.42	0.90	1.47	2,462	388	13.61
	Min SWT	Hot Springs Mt.	Rising Limb	13.2	0.23	5.9	0.94	0.88	0.93	1.01	1,583	296	15.75
Falling Limb			12.9	0.28	3.6	0.96	0.88	0.93	0.70	1,445	115	7.37	
FHR1	Max SWT	Superior	Rising Limb	27.3	0.12	22.5	0.93	1.86	0.96	1.45	1,300	225	14.75
			Falling Limb	27.2	0.11	18.4	0.96	1.62	0.95	1.48	972	174	15.18
FHR2	Max SWT	Polson Kerr Dam	Rising Limb	25.8	0.19	6.9	0.94	1.57	0.94	1.74	1,362	278	16.95
			Falling Limb	23.5	0.25	3.6	0.95	1.67	0.92	1.73	1,216	166	12.01
FHR2	Max SWT	Polson Kerr Dam	Rising Limb	27.6	0.13	21.1	0.96	1.40	0.95	1.54	1,907	321	14.41
			Falling Limb	25.2	0.13	15.1	0.90	2.49	0.95	1.47	1,216	174	12.52
FHR2	Min SWT	Polson Kerr Dam	Rising Limb	26.3	0.19	7.8	0.93	1.64	0.93	1.73	2,013	374	15.67
			Falling Limb	23.5	0.23	3.5	0.90	2.32	0.93	1.62	1,565	166	9.59
FHR4	Max SWT	Bigfork 13S	Rising Limb	28.9	0.13	20.6	0.95	1.50	0.96	1.40	1,215	327	21.21
			Falling Limb	26.3	0.15	15.2	0.96	1.48	0.93	1.75	892	168	15.85

Table 3-6. Continued

SWT Station	Variable	SAT Station	Dataset	a	y	b	NSC Cal.	RMSE Cal. (°C)	NSC Val.	RMSE Val. (°C)	Training Set Size	Test Set Size	Perc. Test Set
FHR4	Min SWT	Polson Kerr Dam	Rising Limb	26.8	0.18	8.2	0.93	1.59	0.93	1.67	1,815	374	17.09
			Falling Limb	23.6	0.23	3.3	0.93	1.90	0.91	1.83	1,545	166	9.70
FHR5	Max SWT	Superior	Rising Limb	29.1	0.11	25.3	0.92	1.87	0.92	1.74	1,673	174	9.42
			Falling Limb	26.8	0.11	18.1	0.95	1.71	0.95	1.62	933	86	8.44
	Min SWT	Polson Kerr Dam	Rising Limb	26.7	0.20	8.1	0.95	1.47	0.94	1.57	1,780	184	9.37
			Falling Limb	24.0	0.24	3.6	0.94	1.92	0.88	2.42	1,233	93	7.01
FHR6	Max SWT	Bigfork 13S	Rising Limb	29.4	0.12	22.2	0.95	1.42	0.96	1.37	1,273	327	20.44
			Falling Limb	25.7	0.14	15.3	0.96	1.43	0.93	1.63	917	168	15.48
	Min SWT	Polson Kerr Dam	Rising Limb	30.8	0.17	10.3	0.92	1.71	0.93	1.73	1,876	374	16.62
			Falling Limb	23.9	0.23	3.4	0.93	1.98	0.91	1.85	1,573	166	9.55
JKR1	Max SWT	Bigfork 13S	Annual	25.3	0.09	17.7	0.95	1.16	0.94	0.97	1,704	320	15.81
			Min SWT	Polson Kerr Dam	Annual	17.8	0.15	5.2	0.92	1.12	0.92	0.85	2,846
JKR2	Max SWT	Superior	Annual	26.2	0.07	23.2	0.95	1.01	0.96	0.89	2,823	488	14.74
			Min SWT	Polson Kerr Dam	Rising Limb	17.0	0.13	7.1	0.97	0.56	0.96	0.64	1,746
			Falling Limb	14.0	0.16	2.4	0.98	0.49	0.97	0.48	1,471	166	10.14
			Max SWT	Superior	Annual	28.3	0.05	29.7	0.94	0.92	0.95	0.77	3,027
JKR3	Min SWT	Polson Kerr Dam	Rising Limb	24.5	0.08	16.9	0.94	0.58	0.94	0.62	1,991	374	15.81
			Falling Limb	12.9	0.13	1.3	0.97	0.45	0.96	0.46	1,480	166	10.09
JKR5	Max SWT	Missoula Airport	Annual	28.9	0.05	35.2	0.96	0.66	0.95	0.68	3,163	495	13.53
			Min SWT	Hot Springs Mt.	Rising Limb	31.6	0.08	25.9	0.91	0.59	0.93	0.57	1,784
			Falling Limb	12.3	0.12	4.2	0.96	0.45	0.96	0.46	1,344	165	10.93
			Max SWT	Missoula Airport	Rising Limb	15.8	0.08	13.3	0.94	0.79	0.90	0.94	1,743
JMF1			Falling Limb	16.5	0.09	11.9	0.96	0.80	0.94	0.73	1,531	170	9.99

Table 3-6. Continued

SWT Station	Variable	SAT Station	Dataset	a	y	b	NSC Cal.	RMSE Cal. (°C)	NSC Val.	RMSE Val. (°C)	Training Set Size	Test Set Size	Perc. Test Set
JMF1	Min SWT	Polson Kerr Dam	Rising Limb	14.6	0.11	8.6	0.94	0.55	0.90	0.79	1,611	374	18.84
			Falling Limb	11.9	0.19	1.5	0.93	0.85	0.90	0.90	1,401	166	10.59
JNF1	Max SWT	Superior	Rising Limb	22.1	0.09	28.0	0.91	1.21	0.93	0.96	1,552	319	17.05
			Falling Limb	20.6	0.09	23.6	0.97	0.87	0.95	0.86	1,136	174	13.28
	Min SWT	Bigfork 13S	Rising Limb	16.0	0.16	12.5	0.94	0.69	0.94	0.69	1,189	371	23.78
			Falling Limb	10.2	0.26	5.6	0.98	0.50	0.96	0.57	1,322	168	11.28
JNF2	Max SWT	Bigfork 13S	Rising Limb	27.5	0.08	32.1	0.94	0.82	0.94	0.77	822	327	28.46
			Falling Limb	18.0	0.10	20.8	0.98	0.59	0.95	0.68	673	168	19.98
	Min SWT	Bigfork 13S	Rising Limb	21.2	0.13	16.9	0.94	0.61	0.91	0.71	786	372	32.12
			Falling Limb	10.4	0.21	5.6	0.98	0.46	0.95	0.57	791	168	17.52
JNF3	Max SWT	Polson Kerr Dam	Rising Limb	28.0	0.09	33.8	0.93	0.97	0.90	1.08	882	321	26.68
			Falling Limb	16.5	0.10	20.2	0.96	0.85	0.97	0.66	550	174	24.03
	Min SWT	Polson Kerr Dam	Rising Limb	18.7	0.17	13.5	0.94	0.72	0.86	0.97	833	374	30.99
			Falling Limb	10.0	0.27	3.5	0.93	0.89	0.96	0.59	685	166	19.51
JSC1	Max SWT	Missoula Airport	Rising Limb	20.9	0.10	8.3	0.96	0.85	0.96	0.85	1,709	281	14.12
			Falling Limb	30.4	0.05	25.9	0.97	0.67	0.97	0.61	1,475	170	10.33
	Min SWT	Missoula Airport	Rising Limb	14.2	0.10	1.8	0.97	0.40	0.95	0.50	1,717	301	14.92
			Falling Limb	12.7	0.11	-2.3	0.96	0.44	0.98	0.29	1,467	196	11.79
LBR1	Max SWT	Bigfork 13S	Rising Limb	29.9	0.22	14.6	0.93	2.19	0.96	2.33	993	230	18.81
			Falling Limb	31.9	0.19	18.4	0.97	1.79	0.95	1.66	692	168	19.53
	Min SWT	Polson Kerr Dam	Rising Limb	16.6	0.40	2.1	0.89	2.07	0.95	1.54	1,390	277	16.62
			Falling Limb	17.7	0.29	5.3	0.94	1.47	0.94	1.41	1,254	166	11.69
MCR1	Max SWT	Bigfork 13S	Rising Limb	21.6	0.15	11.8	0.95	1.38	0.97	1.07	1,168	320	21.51
			Falling Limb	28.8	0.10	20.2	0.98	0.95	0.96	1.04	793	168	17.48

Table 3-6. Continued

SWT Station	Variable	SAT Station	Dataset	a	y	b	NSC Cal.	RMSE Cal. (°C)	NSC Val.	RMSE Val. (°C)	Training Set Size	Test Set Size	Perc. Test Set
MCR1	Min SWT	Bigfork 13S	Rising Limb	17.9	0.23	3.3	0.95	1.09	0.96	1.09	1,277	365	22.23
			Falling Limb	20.3	0.20	6.7	0.98	0.79	0.97	0.90	1,222	168	12.09
MCR2	Max SWT	Missoula Airport	Annual	18.5	0.12	11.8	0.95	1.09	0.94	1.30	3,133	495	13.64
	Min SWT	Polson Kerr Dam	Rising Limb	12.4	0.24	1.8	0.96	0.68	0.93	1.07	1,503	374	19.93
Falling Limb			13.5	0.25	1.1	0.96	0.84	0.93	1.10	1,361	166	10.87	
PCR1	Max SWT	Bigfork 13S	Rising Limb	20.1	0.13	10.8	0.94	1.27	0.97	1.00	1,082	327	23.21
			Falling Limb	30.2	0.08	23.4	0.98	0.82	0.94	1.20	826	120	12.68
	Min SWT	Missoula Airport	Annual	19.2	0.14	4.1	0.95	0.85	0.97	0.75	3,220	485	13.09
RSC2	Max SWT	Hot Springs Mt.	Rising Limb	19.6	0.16	7.8	0.92	1.40	0.94	1.28	1,053	316	23.08
			Falling Limb	33.0	0.07	25.8	0.92	1.22	0.90	1.33	719	171	19.21
	Min SWT	Missoula Airport	Annual	22.6	0.10	8.8	0.94	0.80	0.96	0.62	1,772	532	23.09
RVC1	Max SWT	Bigfork 13S	Rising Limb	20.8	0.12	23.2	0.95	1.03	0.91	1.28	626	299	32.32
			Falling Limb	17.3	0.15	16.3	0.97	0.93	0.98	0.65	476	95	16.64
	Min SWT	Bigfork 13S	Rising Limb	16.5	0.21	10.1	0.96	0.87	0.92	1.05	592	337	36.28
			Falling Limb	13.7	0.31	5.6	0.97	0.81	0.98	0.68	505	103	16.94
VCR1	Max SWT	Polson Kerr Dam	Annual	22.6	0.14	19.2	0.96	1.38	0.92	1.65	2,653	494	15.70
	Min SWT	Polson Kerr Dam	Annual	13.4	0.27	6.0	0.96	0.87	0.95	0.86	3,022	536	15.06
VCR3	Max SWT	Bigfork 13S	Annual	14.1	0.15	16.3	0.92	1.22	0.93	0.99	1,858	495	21.04
	Min SWT	Polson Kerr Dam	Rising Limb	12.4	0.23	7.1	0.97	0.59	0.95	0.71	1,570	374	19.24
Falling Limb			11.2	0.27	4.3	0.97	0.59	0.97	0.58	1,396	166	10.63	
VCR4	Max SWT	Superior	Annual	22.3	0.15	19.3	0.95	1.65	0.94	1.56	2,689	495	15.55
	Min SWT	Missoula Airport	Rising Limb	14.0	0.29	5.0	0.92	1.27	0.94	1.08	1,799	344	16.05
Falling Limb			14.7	0.29	3.9	0.97	0.87	0.95	1.05	1,516	196	11.45	

**Table 3-7: Distance and elevation difference between SWT gaging stations and SAT recording stations**

	Distance (km)				Elevation Difference (m)			
	Closest	Furthest	Best Max SWT	Best Min SWT	Smallest	Largest	Best Max SWT	Best Min SWT
BCR1	24.1	112.4	50.3	50.3	32.6	1,126.2	53.3	53.3
CCR1	22.1	64.2	22.1	48.7	42.8	1,283.3	105.3	103.8
CLC1	6.6	59.1	48.2	57.7	9.4	1,249.9	85.6	70.4
FCR1	15.2	77.7	59.8	56.5	8.5	1,155.8	84.7	78.6
FCR2	19.9	82.1	62.8	70.1	8.7	1,084.9	155.6	79.4
FHR1	28.4	82.3	30.1	43.1	70.2	1,310.7	70.2	76.3
FHR2	16.3	65.2	40.1	40.1	62.6	1,303.1	68.7	68.7
FHR4	21.1	68.0	47.4	21.1	43.9	1,284.4	104.9	50.0
FHR5	8.6	83.1	65.0	8.6	22.2	1,262.7	22.2	28.3
FHR6	5.7	86.2	22.6	5.7	6.7	1,186.2	6.7	48.2
JKR1	14.4	66.1	66.1	41.4	45.3	1,285.8	106.3	51.4
JKR2	8.2	67.4	53.6	44.5	10.8	1,251.3	10.8	16.9
JKR3	13.4	75.9	58.3	54.4	2.0	1,176.0	64.5	58.4
JKR5	19.3	79.6	27.9	72.4	63.5	1,030.1	63.5	134.2
JMF1	10.9	78.6	35.5	61.2	42.2	859.0	234.6	375.4
JNF1	13.2	74.5	74.3	74.5	102.9	919.7	320.8	259.8
JNF2	11.4	76.1	74.2	74.2	69.6	886.4	293.1	293.1
JNF3	8.7	78.9	58.7	58.7	17.0	833.8	399.6	399.6
JSC1	10.0	71.9	35.2	35.2	19.1	1,215.3	121.7	121.7
LBR1	21.6	68.5	48.1	21.6	40.9	1,281.4	101.9	47.0
MCR1	14.6	60.9	60.9	60.9	59.8	1,300.3	120.8	120.8
MCR2	3.8	60.5	46.3	38.8	7.6	1,226.8	133.2	7.6
PCR1	6.8	59.3	57.4	49.6	11.0	1,251.5	72.0	157.9
RSC2	20.8	68.1	26.2	64.6	19.4	1,144.9	19.4	51.3
RVC1	22.3	70.2	70.2	70.2	4.0	1,160.3	19.2	19.2
VCR1	11.6	72.7	50.0	50.0	9.9	1,189.4	45.0	45.0
VCR3	16.3	77.2	77.2	54.0	6.0	1,087.6	91.9	146.8
VCR4	14.3	74.4	50.6	34.5	19.9	1,144.4	96.1	50.8

Elevation seems to be slightly more relevant than distance when it comes to selecting the most correlated air-water temperature model (see Table 3-7). In fact, only in seven circumstances (gray shade), six of which associated with maximum daily temperatures, the elevation difference between SAT/SWT stations of the optimal model is the lowest possible. However, almost 61% and about 82% of the climate stations are located within a 100-meter and 150-meter elevation difference from the corresponding SWT gaging station, respectively. Moreover, the elevation difference between a given SWT location and the most correlated SAT site never exceeds 400 meters. In other words, the best air-water temperature model is not necessarily derived from a pair of SAT/SWT stations that are placed at the same or similar elevations, but it is very unlikely that the best fitted model is observed when large elevation differences are at play. This is probably the reason why the four climate stations with the highest elevations (i.e., Kraft Kreek, Moss Peak, North Fork Jocko, and Seeley Lake Ranger Station; see Table 2-2) have not been used in any of the optimal models.

Table 3-6 also indicates the presence/absence of a hysteresis loop for each pair of SWT location/variable. When hysteresis is observed, specifications regarding both the rising limb and falling limb models are included. Otherwise, only the characteristics of the annual model are reported. The hysteresis information is summarized in Figure 3-6. This graphic displays the number of SWT gaging stations that exhibit hysteresis and specifies if the hysteresis loop concerns only maximum SWT, minimum SWT, or both variables together. It appears that hysteresis loops are more likely to occur when minimum SWT is considered (75% of the stations) rather than maximum SWT (about

57% of the stations). In addition, almost half of the SWT gaging sites (thirteen out of 28) manifest hysteresis for both water temperature variables. Finally, if only one variable is associated with hysteresis at a given location (eleven cases out of 28), it usually coincides with minimum SWT (eight times) rather than maximum SWT (three times).

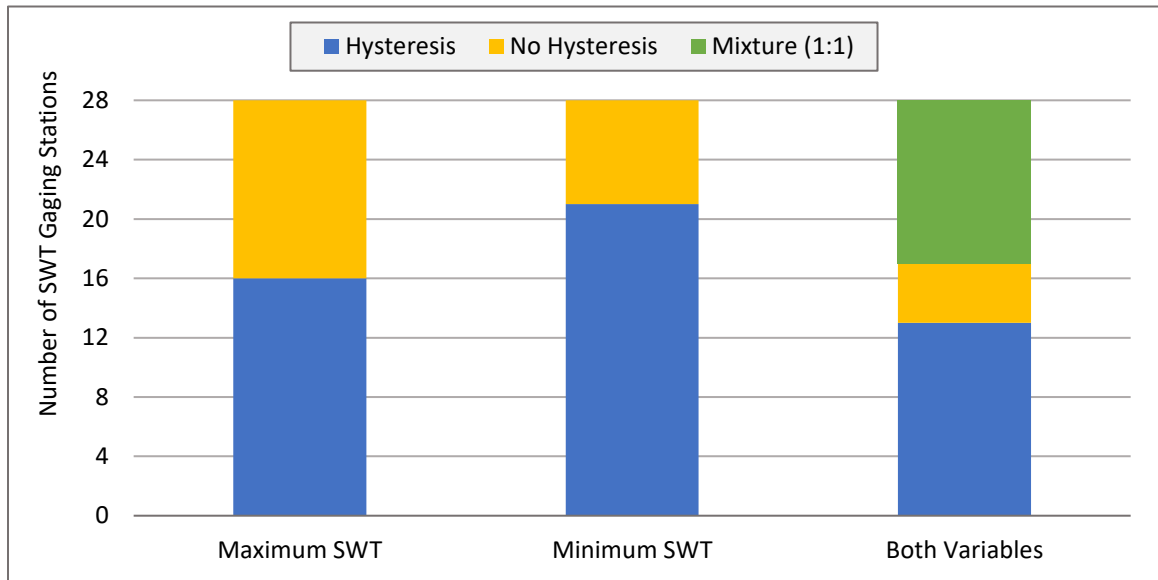


**Figure 3-6: Number of SWT gaging stations that exhibit hysteresis (data are shown for both SWT variables together and each variable separately)**

Nine of the thirteen locations that show hysteresis for both maximum and minimum SWT lie along the Flathead River and the upper portion of the Jocko River (subregions 1 and 5, respectively; see Figure 3-3). In the first case, hysteresis is possibly due to the heat storage effect of the upstream Flathead Lake. Even if the air-water temperature relationship is affected by incoming tributaries, groundwater inflows, thermal pollution, water extraction, and water flow regulation at the Kerr Dam, the seasonal thermal influence of the Flathead Lake is still prominent. In the second case, hysteresis is likely caused by the relevant incoming runoff associated with massive snow- and ice-melt processes occurring in spring and early summer. If compared with the other

SWT gaging stations, these four sites (i.e., subregion 5) are located at the highest elevations (see Table 3-1). Because of the closeness to the stream heads and to the major sources of melting snowpack, the effect of cold-water inflow on the air-water temperature relationship is more pronounced.

Table 3-6 finally reveals that there are differences in the accuracy of the rising limb and falling limb models. On average, models calculated over the cooling season perform better than those computed over the warming season. These findings reflect what has been mentioned above regarding the influence of snowmelt on the air-water temperature relationship during the warming season. In addition, the accuracy difference between the rising and the falling limbs is slightly larger when considering maximum SWT rather than minimum SWT. This is generally due to a stronger correlation between maximum SWT and maximum SAT during the cooling season. There are a few exceptions to this trend. For example, the SWT time series recorded along the Flathead River (i.e., subregion 1) are much better correlated to air temperature during the warming season rather than the cooling season. Indeed, the snowmelt effect is negligible at these locations, but the heat storage effect of the Flathead Lake comes into play, as its waters, during the cooling season, tend to lose heat at lower rates than those associated with much smaller water bodies.

### 3.5.2. SWT trends

Figure 3-7 and Figure 3-8 illustrate the main results of the MKTs that were applied to the 1961-2100 annual means of daily maximum SWT and daily minimum SWT, respectively (see Section 3.4.4). Data are reported for each SWT gaging station and RCP scenario. These two sets of maps disclose the spatial distribution of potential water temperature trends within the FIR. In particular, two variables are displayed here: the Kendall's correlation coefficient ( $\tau$ ) and the magnitude of change ( $\phi$ ), which is expressed as °C per decade. The first variable is represented by the inclination of an arrow, the second one by graduated colors. The null hypothesis stating that there is no trend is rejected in all cases because the p values are always smaller than 0.001. The Kendall's statistic and its variance, the Theil-Sen's slope, and the p value related to each MKT are not reported on these maps, but they are included in Table E-1 of Appendix E. This table also displays the corresponding statistics, with the addition of  $\tau$ , resulted from the seasonal trend analysis of daily maximum and minimum SWT over the 1961-2100 period.

All MKTs output positive values for both  $\tau$  and  $\phi$ , which reveals that the 28 locations of interest are all characterized by increasing water temperature trends. However, the slope of these trends (i.e., the magnitude of the increase) and the strength of the monotonic association between SWT and time vary depending on the scenario, variable, and location considered. In general, both  $\tau$  and  $\phi$  increase with increasing RCP. Also, in comparison with minimum SWT trends, maximum SWT trends have smaller  $\tau$  and larger  $\phi$ . A spatial pattern can be identified within the FIR as the SWT gaging

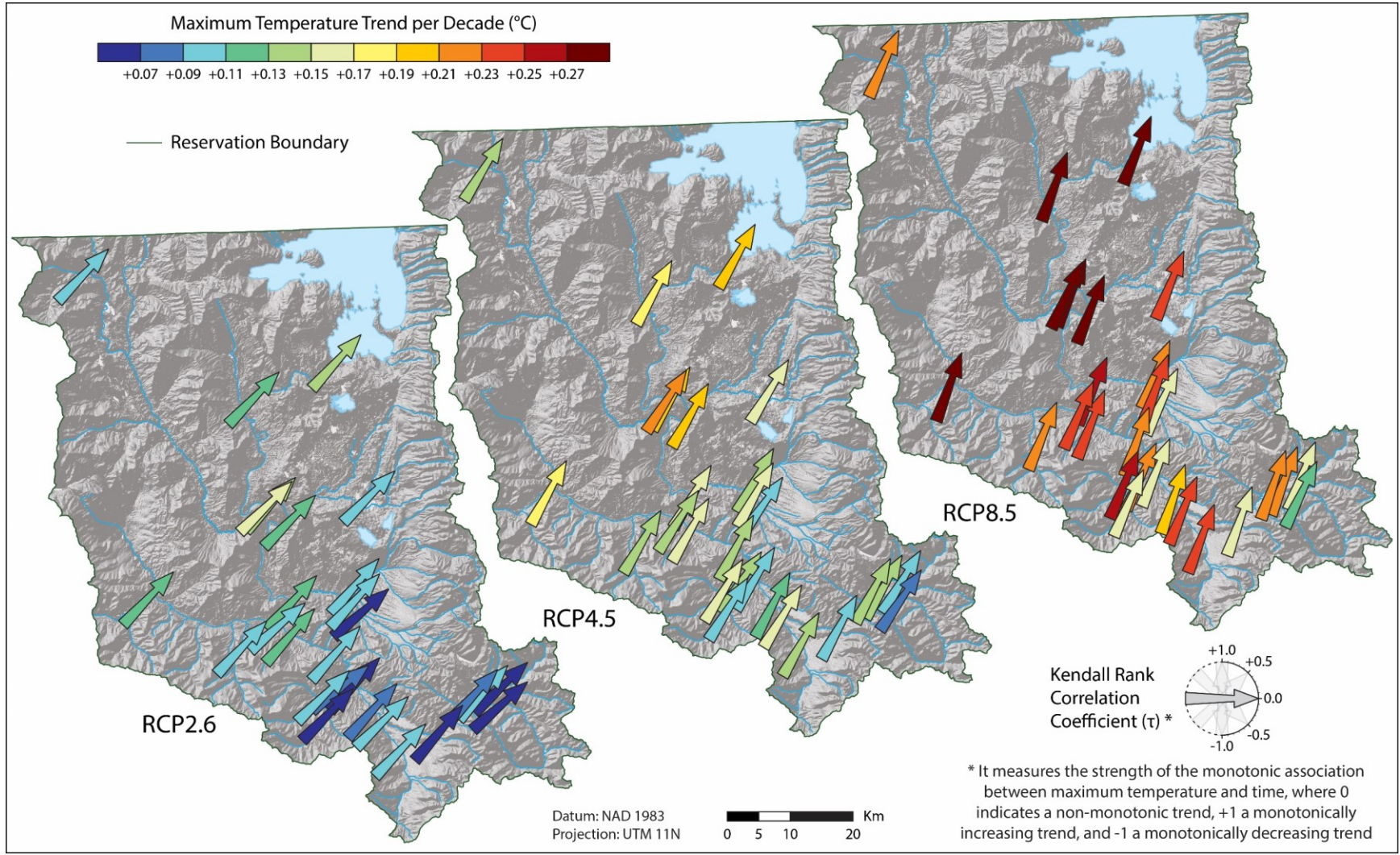
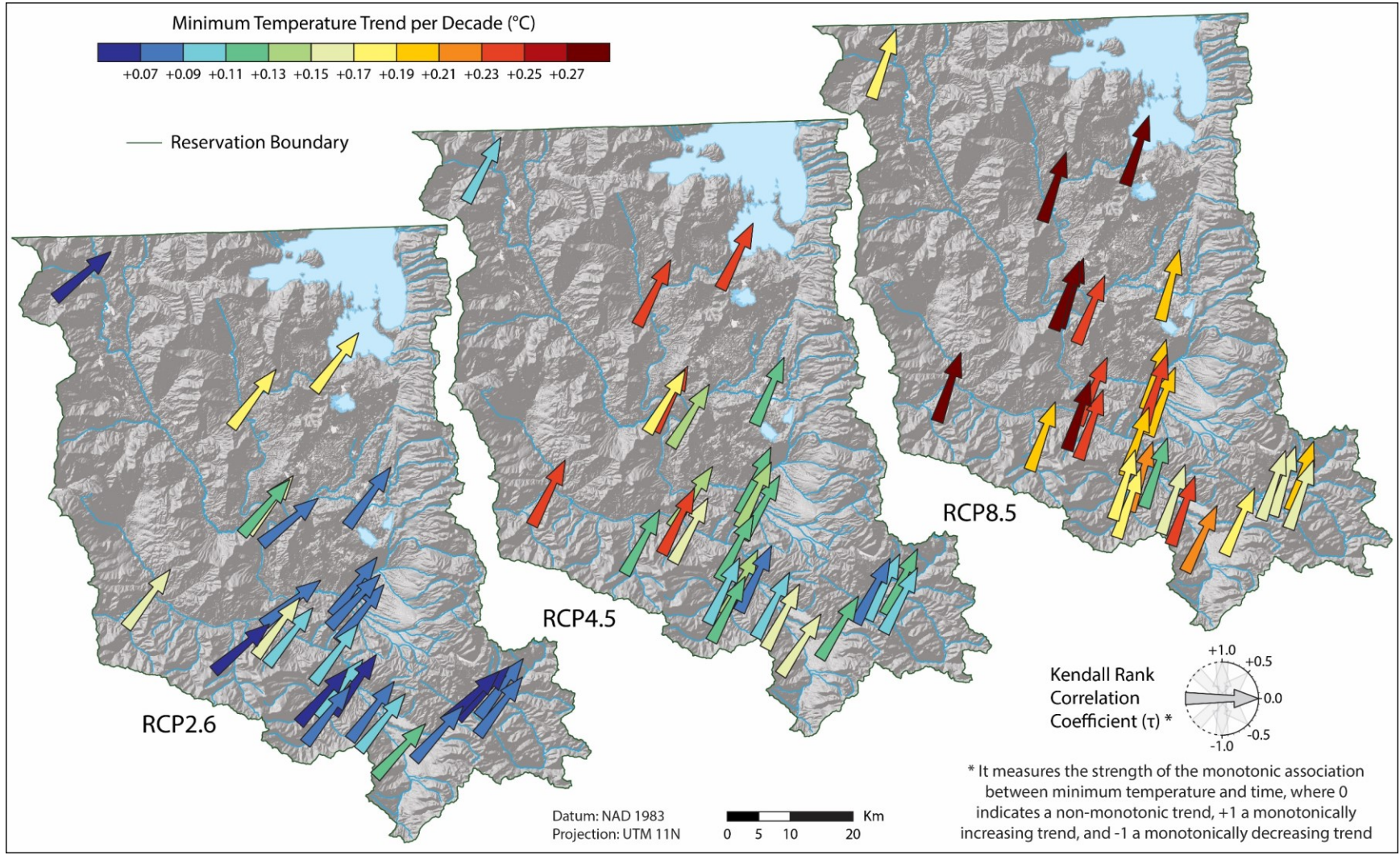


Figure 3-7: Mean decadal trend of the mean annual maximum SWT and related Kendall's correlation coefficient within the 1961-2100 period according to the three RCP scenarios



**Figure 3-8: Mean decadal trend of the mean annual minimum SWT and related Kendall's correlation coefficient within the 1961-2100 period according to the three RCP scenarios**

stations within subregion 1 (see Figure 3-3) generally present the highest  $\phi$  values. Other stations that are close to the Flathead River and are associated with relatively large drainage basins, including CCR1, JKR1, LBR1, and MCR1, show elevated  $\phi$  values as well. On the other hand, the SWT gaging stations within subregion 5 (see Figure 3-3) and other stations located at relatively high elevations and/or related to small drainage basins, such as JKR5, JSC1, MCR2, VCR3, and VCR4, exhibit low  $\phi$  values. The spatial pattern described above is evident both in Figure 3-7 (maximum SWT) and Figure 3-8 (minimum SWT). Conversely, the geographic distribution of  $\tau$  values across the study area does not indicate a clear spatial clustering or pattern of this coefficient.

Figures 3-9 to 3-14 show the same information displayed in Figures 3-7 and 3-8 with the difference that the annual trends are summarized by subregion, as defined in Figure 3-3 and Table 3-1. The seasonal trends in water temperature are represented in these six sets of maps as well. Regardless of the climate scenario, season, and variable considered, subregion 1 has the highest  $\phi$  values, subregions 2, 3, and 4 intermediate  $\phi$  values, and subregion 5 the lowest  $\phi$  values, with two important exceptions. First, maximum SWT trends for subregion 3 are more pronounced (i.e., higher  $\phi$ ) than those for subregion 1 in winter based on all scenarios. Second, summer trends of subregion 5 are relatively steeper (i.e., higher  $\phi$ ) than those related to other subregions for both maximum and minimum SWT according to all scenarios. It has to be finally noted that the null hypothesis of no trend (i.e., p value greater than the 0.05) is accepted in two cases, which are indicated with a cross hatching pattern inside the arrow shape in the fall map of Figure 3-9.

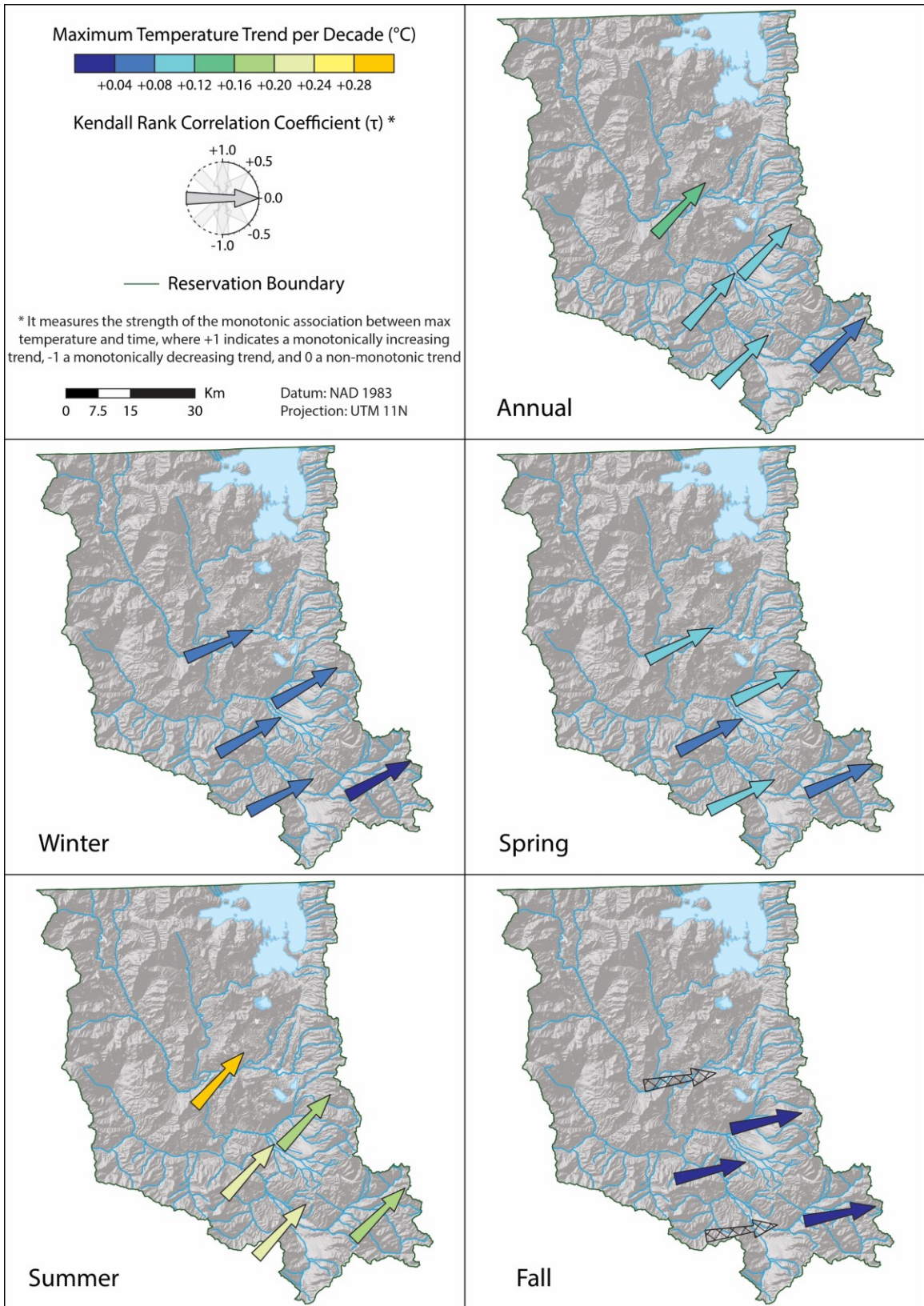


**Figure 3-9: Mean decadal trend of the mean annual/seasonal maximum SWT and related Kendall's correlation coefficient by subregion within 1961-2100 based on the RCP2.6 scenario**

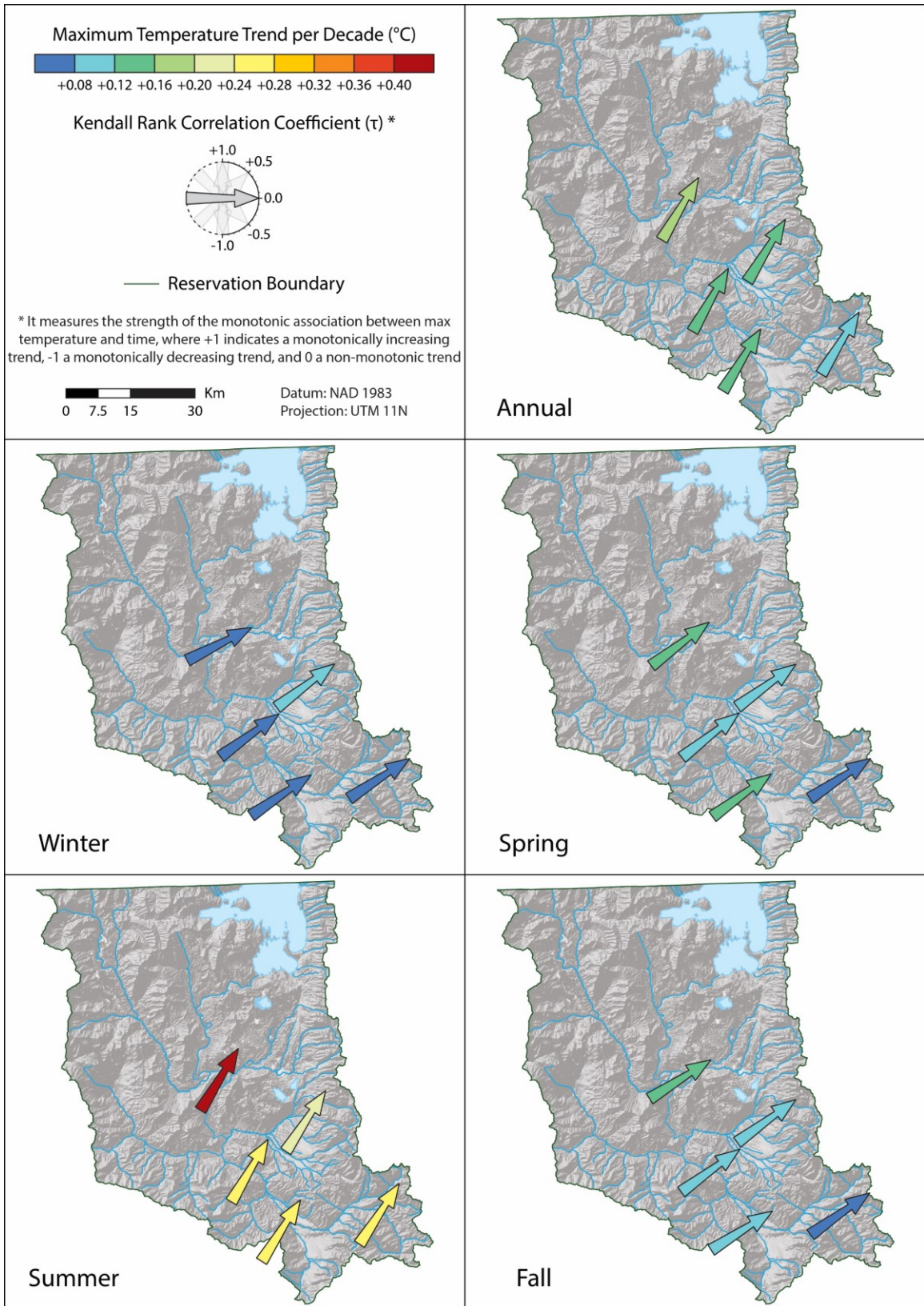


**Figure 3-10: Mean decadal trend of the mean annual/seasonal maximum SWT and related Kendall's correlation coefficient by subregion within 1961-2100 based on the RCP4.5 scenario**

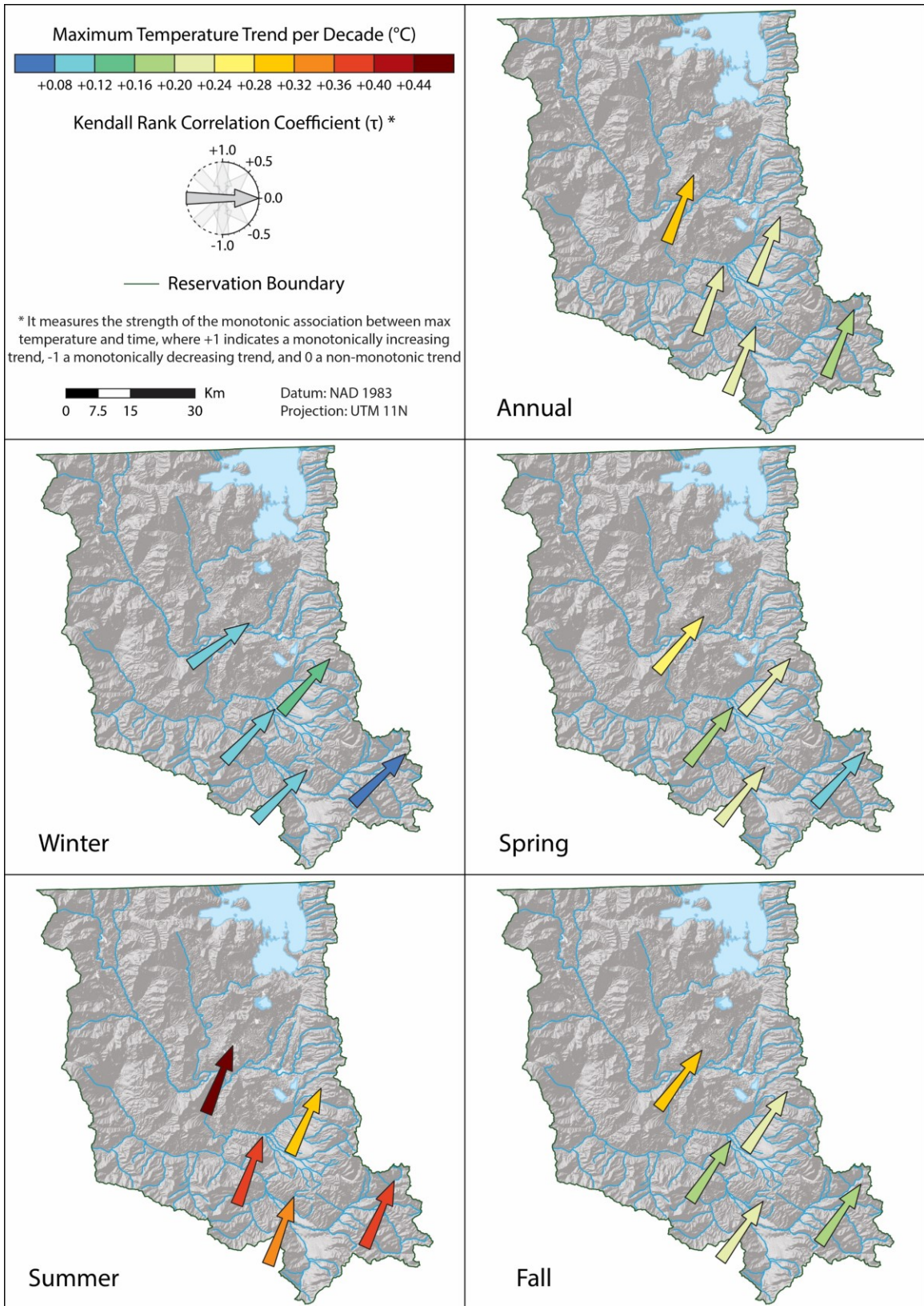


**Figure 3-11: Mean decadal trend of the mean annual/seasonal maximum SWT and related Kendall's correlation coefficient by subregion within 1961-2100 based on the RCP8.5 scenario**

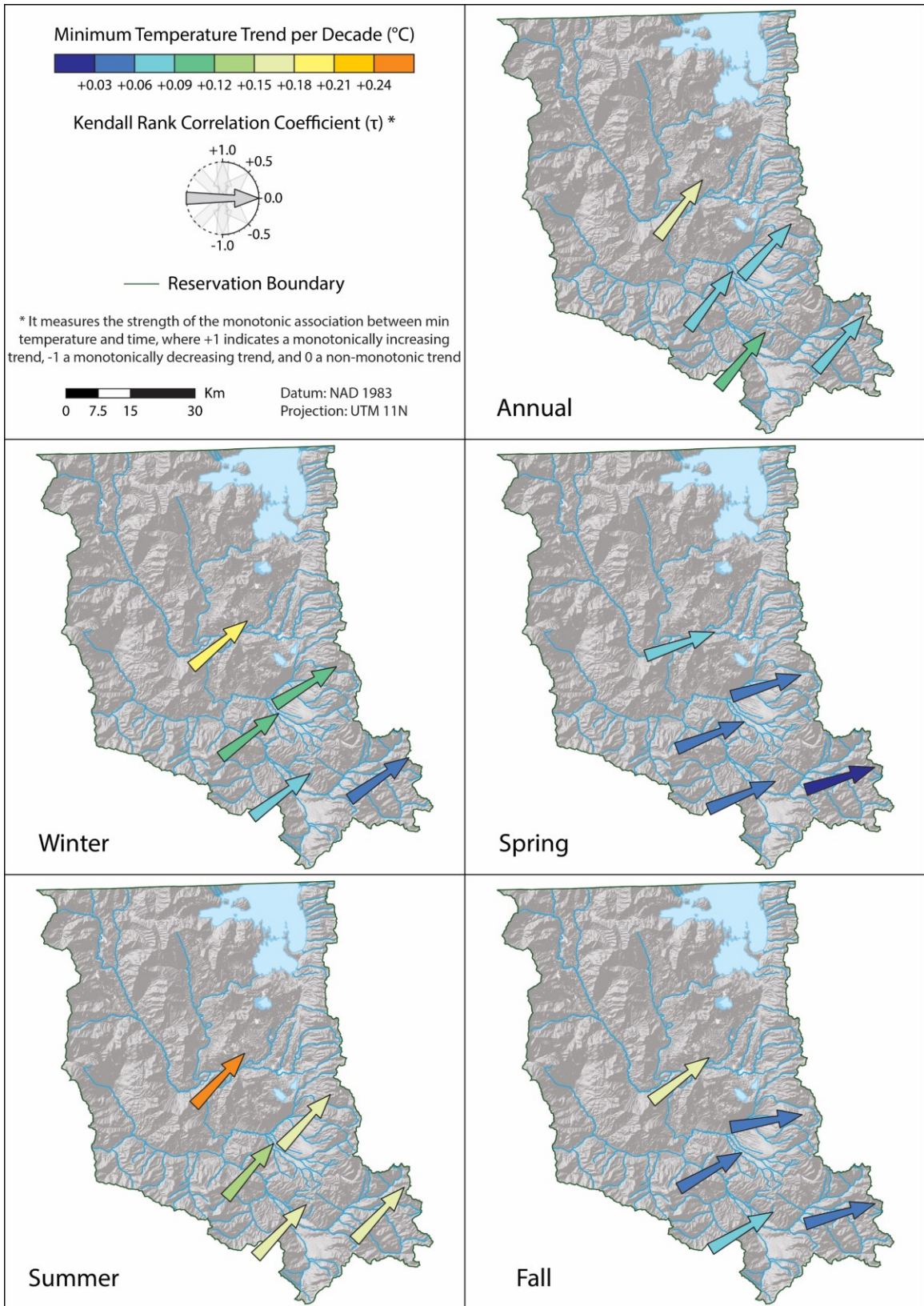


**Figure 3-12: Mean decadal trend of the mean annual/seasonal minimum SWT and related Kendall's correlation coefficient by subregion within 1961-2100 based on the RCP2.6 scenario**

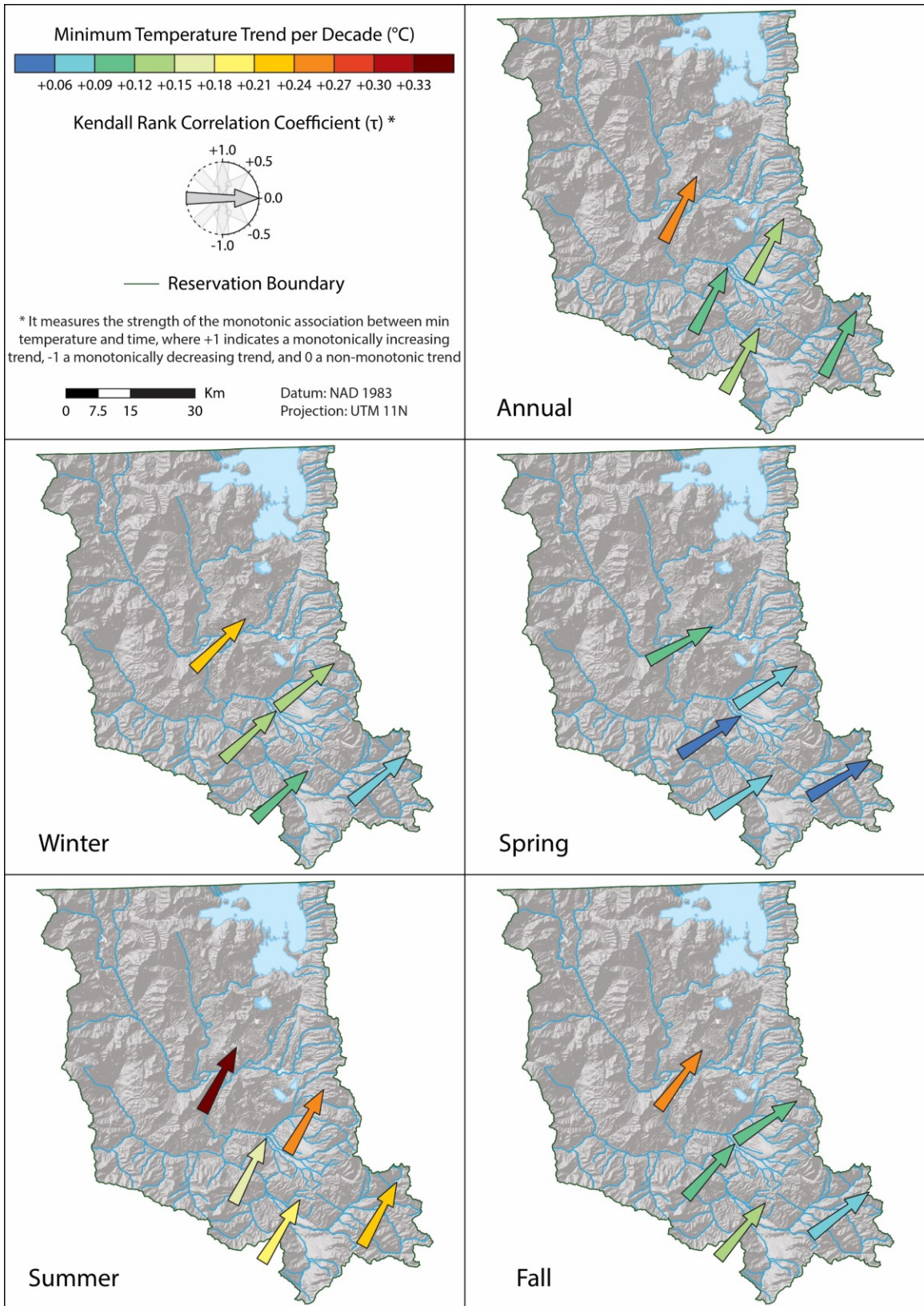


**Figure 3-13: Mean decadal trend of the mean annual/seasonal minimum SWT and related Kendall's correlation coefficient by subregion within 1961-2100 based on the RCP4.5 scenario**

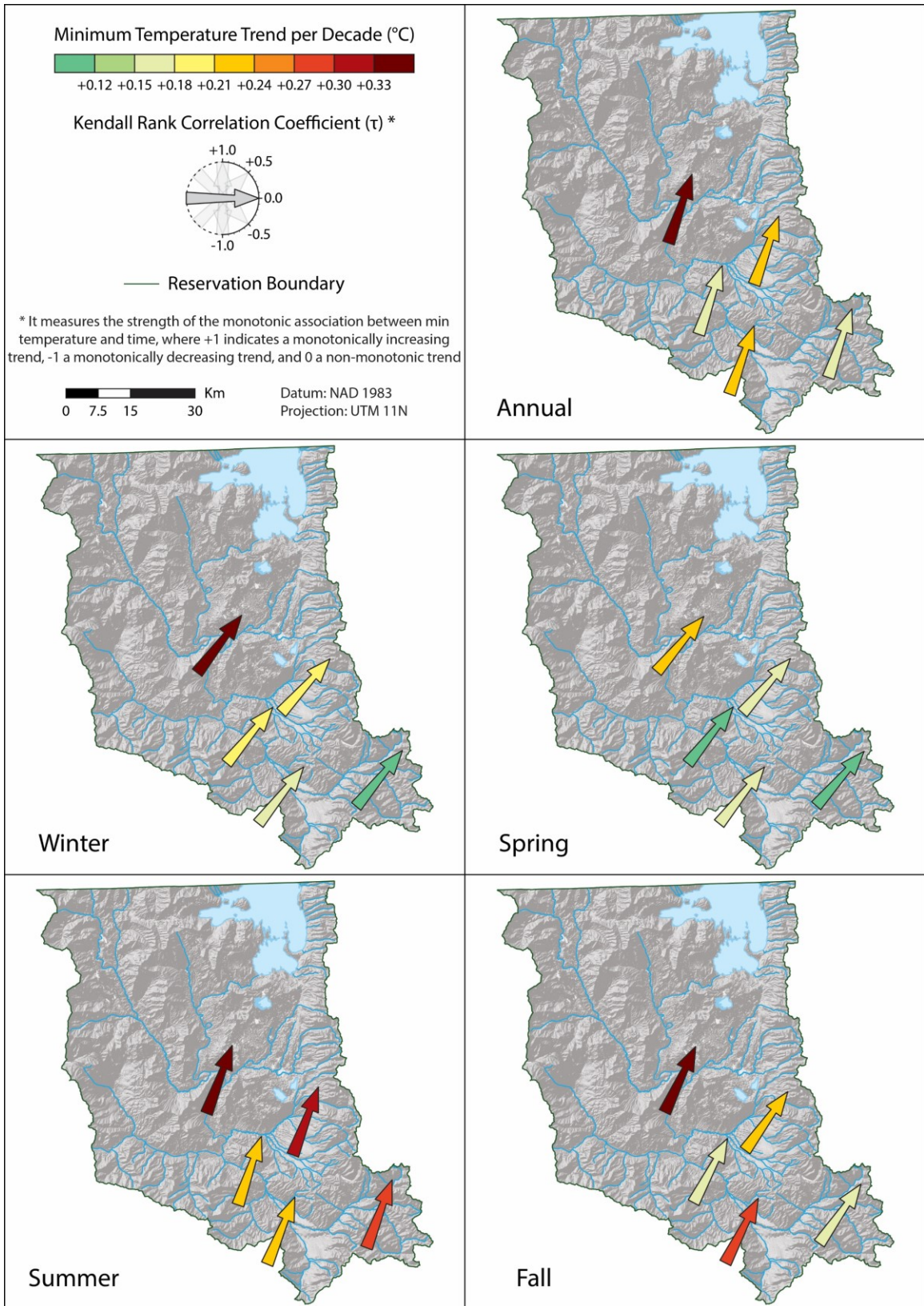


**Figure 3-14: Mean decadal trend of the mean annual/seasonal minimum SWT and related Kendall's correlation coefficient by subregion within 1961-2100 based on the RCP8.5 scenario**

As for  $\tau$ , there is not such a clear spatial pattern that appears consistently across seasons and scenarios and regardless of the SWT variable examined. Nonetheless, some indications concerning the spatial distribution of  $\tau$  emerge as well. Subregion 2 has always the highest  $\tau$  values associated with maximum SWT but in winter. During this season (all three scenarios), subregion 3 outclasses subregion 2 in terms of higher  $\tau$ . Regarding minimum SWT, subregion 1 has the highest  $\tau$  whereas subregion 3 has the lowest  $\tau$  for all three scenarios. However, this hierarchy is visible only in fall and winter and at the annual temporal scale while there is no evident spatial pattern in spring and summer. As a final note related to Figures 3-9 to 3-14, it can be observed that summer exhibits the highest  $\tau$  and  $\phi$  values in comparison with the other seasons (all scenarios).

The graphics in Figures 3-15 to 3-18 illustrate the main outputs ( $\tau$  and  $\phi$ ) of the RKTs that were implemented by aggregating data from all the SWT gaging stations across the FIR. Results are shown for the two SWT variables, the three RCP scenarios, and both the seasonal and annual temporal scales. The null hypothesis of no trend is rejected in all cases. These graphics summarize what has emerged from the trend analysis at the local and subregional level. There is an unequivocal increasing trend in water temperature throughout the FIR. Among the four seasons, summer clearly shows the highest values of both  $\tau$  and  $\phi$ , independently of the variable analyzed. Maximum SWT is associated with smaller  $\tau$  and larger  $\phi$  than minimum SWT. Both  $\tau$  and  $\phi$  increase with increasing RCP and the largest rate of increase occurs in fall. The Kendall's statistic and its variance, the Theil-Sen's slope, and the p value related to each RKT examined in Figures 3-9 to 3-18 are reported in Appendix E (Table E-2).

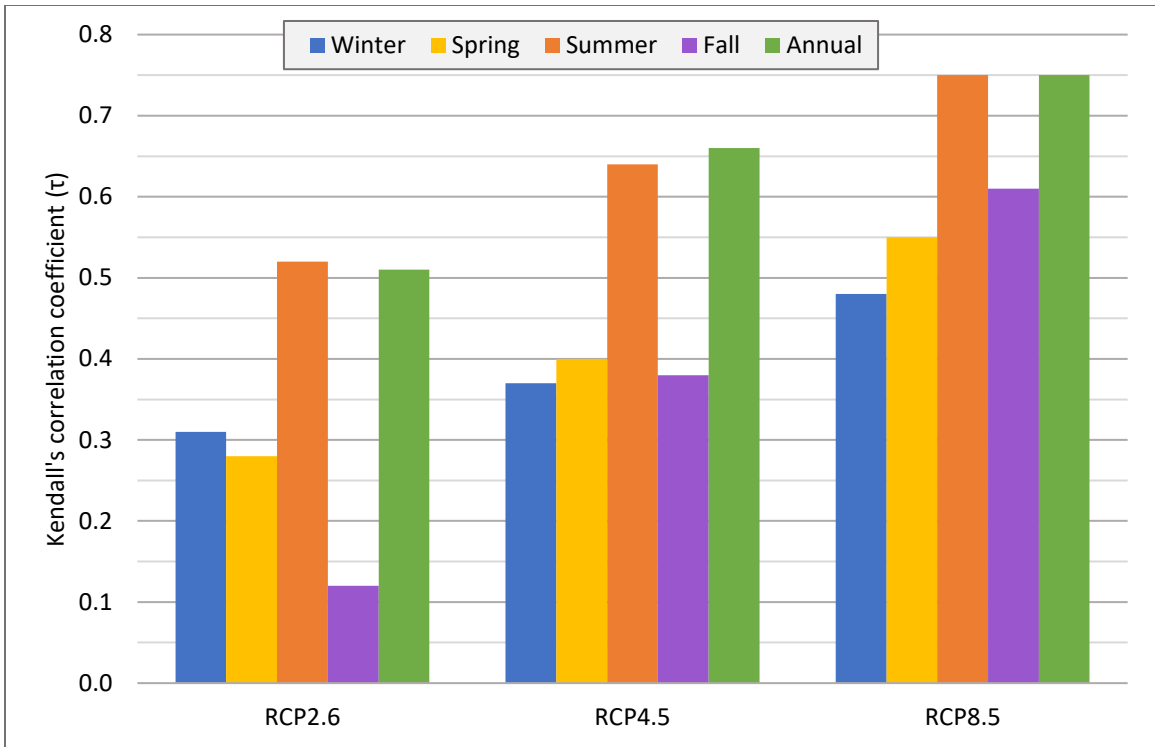


**Figure 3-15: Kendall's correlation coefficient related to the 1961-2100 regional trend in the mean annual and seasonal maximum SWT according to the three proposed RCP scenarios**

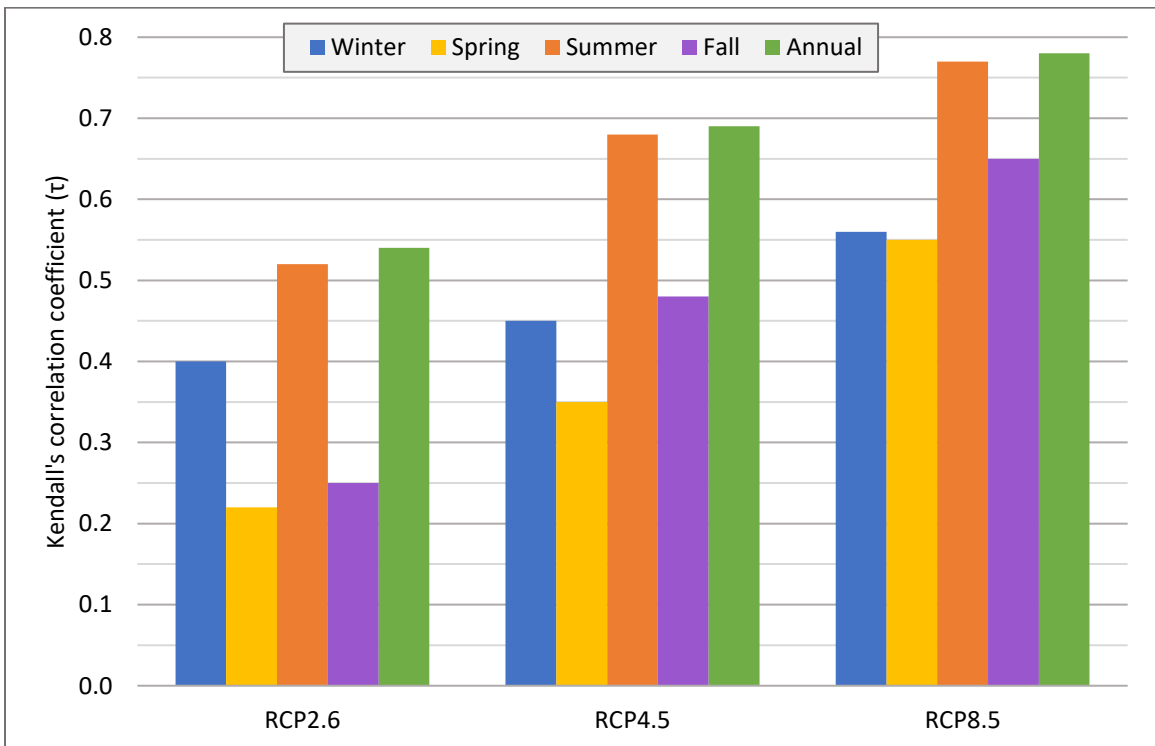


**Figure 3-16: Kendall's correlation coefficient related to the 1961-2100 regional trend in the mean annual and seasonal minimum SWT according to the three proposed RCP scenarios**

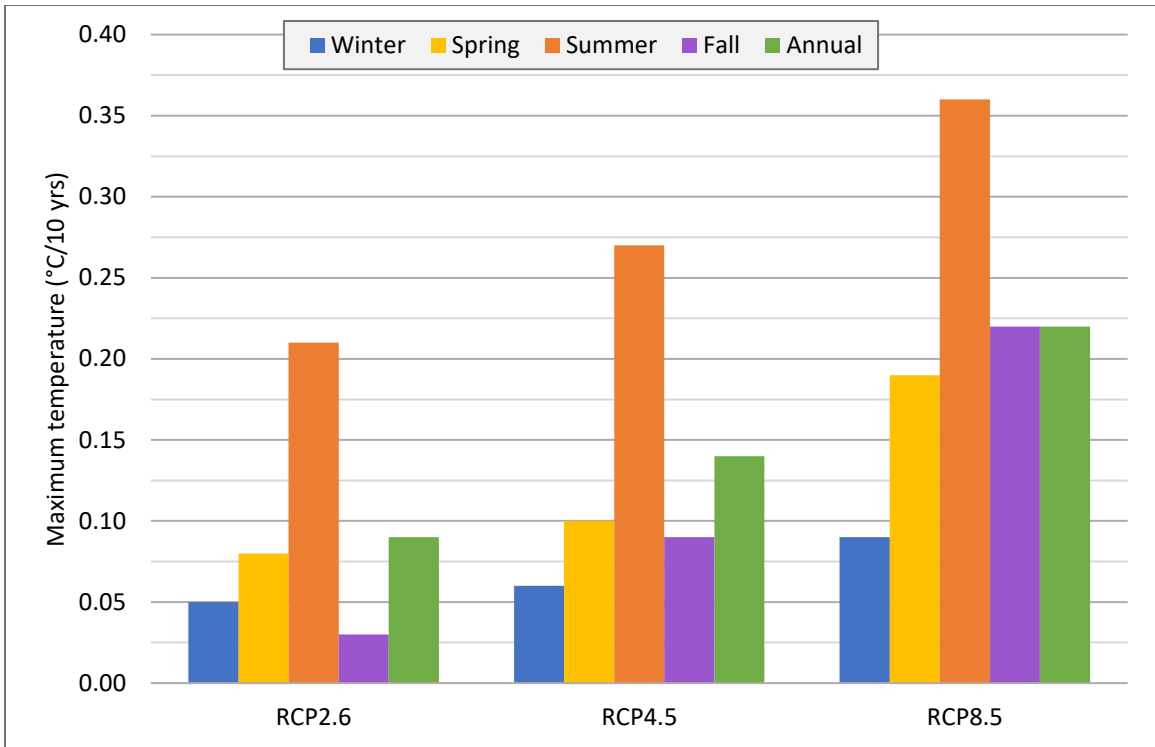


**Figure 3-17: Mean decadal regional trend of the mean annual and seasonal maximum SWT within the 1961-2100 period according to the three proposed RCP scenarios**

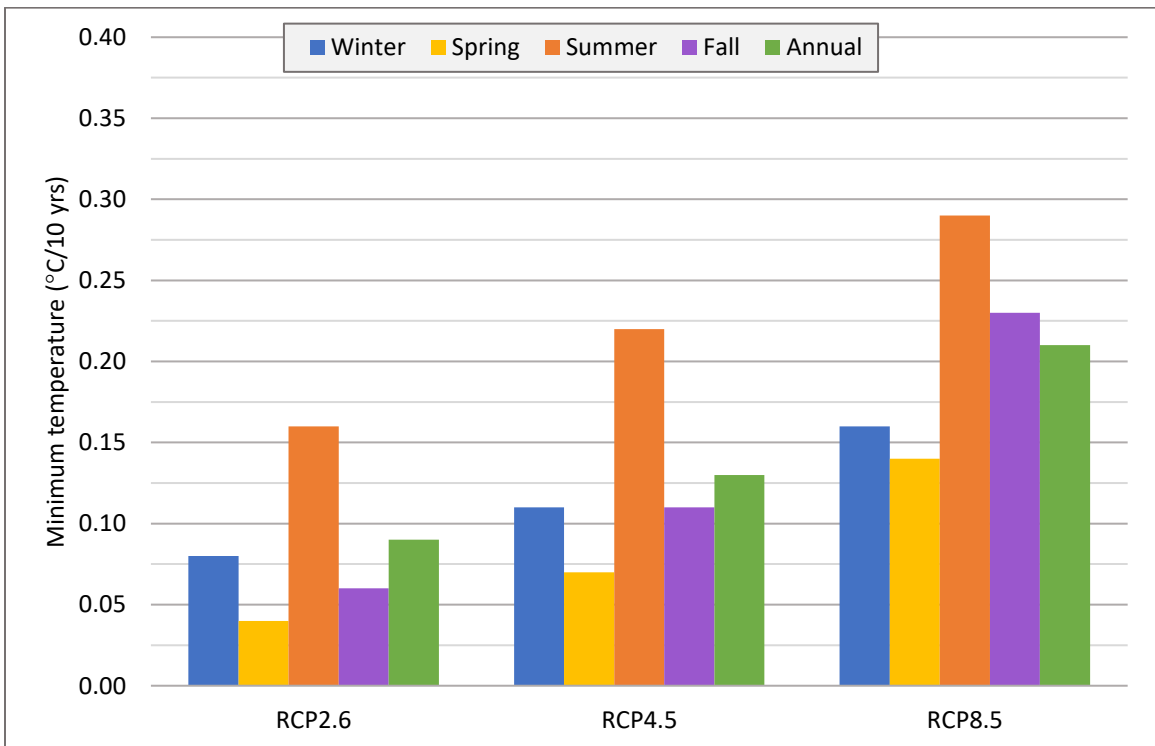


**Figure 3-18: Mean decadal regional trend of the mean annual and seasonal minimum SWT within the 1961-2100 period according to the three proposed RCP scenarios**

### 3.6. Conclusions

The general purpose of the whole research is to examine the impacts of climate change on water quantity and quality in the FIR. This chapter focused on water temperature, a critical aspect of water quality. Warmer water temperatures may pose at great risk the survival of cold-water fish communities, especially salmonids. Therefore, assessing past and future changes in water temperature is a first, essential step in order to predict fish habitat suitability and the distribution of aquatic species in streams and rivers of the FIR. In this research, water temperature was studied by analyzing the potential trends of daily maximum and minimum SWT over 1961-2100. The non-linear logistic statistical relationship established between observed SWT and SAT time series and the SAT time series downscaled in Chapter 2 served as a means for estimating the long-term evolution of water temperature.

This study advocates the use of weekly averages for establishing a strong relationship between air and water temperature. This temporal scale provided by far the best results in comparison with other temporal schemes (i.e., daily, daily lag-1, and two-day average), independently of the pair of SAT/SWT stations considered and the presence or absence of hysteresis loops. The distance between the SWT gaging site and the SAT recording location does not influence the goodness of the air-water temperature correlation. Differently, elevation can be seen as a constraining factor because it does affect the strength of the air-water temperature correlation, but only when the difference in elevation between the pairs of SAT/SWT stations exceed a certain threshold (i.e., 400 meters in this study).

Two third of the best air-water temperature relationships examined in this research exhibit hysteresis, which indicates that caution should be taken in this regard when using air temperature to derive water temperature in mountainous areas. This phenomenon occurs more frequently when minimum SWT is considered rather than maximum SWT. In addition, the air-water temperature correlation is generally worse during the warming season than throughout the cooling season. These two findings together suggest that the cold-water inflow derived from snow- and ice-melt processes occurring in spring and early summer may be a crucial factor influencing the air-water temperature relationship. This study anticipates that incorporating the snowmelt component into the rising limb models would possibly enhance the accuracy of those models and improve the overall prediction of water temperature. It has to be finally noted that the snowmelt contribution is negligible along the Flathead River and at the mouths of its major tributaries. In these cases, hysteresis is mostly caused by the heat storage effect of the Flathead Lake and other reservoirs, and the air-water temperature correlation is usually better in the warming season than in the cooling season.

In response to the third question of the whole research (see Section 3.3), the analysis of water temperature trends in this chapter reveals that streams and rivers of the FIR are expected to become warmer in the future. This tendency emerges unequivocally across the study area, but the magnitude of change and the monotonicity of the trends vary depending on the scenario, variable (i.e., maximum or minimum SWT), period (i.e., seasonal or annual), and location considered. On average, the 1961-2100 mean decadal trends of the mean annual maximum SWT across the FIR are about

0.09°C, 0.14°C, and 0.22°C based on the RCP2.6, RCP4.5, and RCP8.5, respectively. The correspondent values relative to minimum SWT are 0.09°C, 0.13°C, and 0.21°C, respectively. In general, maximum SWT is associated with higher increasing rates and smaller Kendall's correlation coefficients than minimum SWT. Summer is definitely the season that experiences the largest and more consistent increment in water temperature. In addition, SWT increasing trends are usually more pronounced at lower elevations and for relatively larger drainage basins.

## 4. CONCLUSIONS

### 4.1. Trends in SAT, SWT, and SWE

The overall purpose of this research was to identify potential changes and trends in the water resources of the FIR, with a focus on the impacts caused by climate change. Three primary variables were examined in this dissertation: SAT, a crucial component of climate; SWE, another climatic parameter, as it depends on snow precipitation, and an indicator of water quantity, as snowpack is the main source of fresh water in the study area; and SWT, an important characteristic of water quality. In general, observed data indicate an increment in both air and water temperatures and a reduction of the duration and amount of snowpack due to a later snow accumulation in fall and an earlier snowmelt in spring. Based on estimated (i.e., downscaled) data, these trends are expected to continue or intensify in the future. Table 4-1 summarizes the main results related to the trend analysis of air temperature, water temperature, and snowpack conditions. The average data displayed in the table refer to the entire 1961-2100 period and to the overall study area (i.e., the Flathead Region for SAT and SWE, the Flathead Reservation for SWT).

**Table 4-1: Changes in air temperature, water temperature, and main snowpack characteristics between 1961 and 2100 across the study area according to the three proposed RCP scenarios**

Climate scenario	SAT (°C)		SWT (°C)		Snowpack*	
	Max	Min	Max	Min	SWE Annual Max (cm)	Duration (days)
RCP2.6	+3.1	+3.0	+1.3	+1.2	-28 (-34%)	-46 (-18%)
RCP4.5	+4.3	+4.1	+2.0	+1.8	-37 (-46%)	-66 (-26%)
RCP8.5	+6.9	+6.2	+3.1	+2.9	-42 (-52%)	-90 (-36%)

\* The percentages are calculated based on the 1961-1970 average as reference value

The increase of air and water temperatures and the reduction of snowpack are unequivocal. However, the magnitude of the change and the monotonicity of these trends vary according to the climate scenario, variable, period (i.e., month/season), spatial scale, and specific location considered. All trends (either positive or negative) are more pronounced with increasing RCP. Caution should be taken when considering projections associated with the RCP2.6 because this stringent mitigation scenario is very unlikely to occur (i.e., net negative CO<sub>2</sub> emissions after around 2070). Regarding air and water temperatures, trends related to daily maximum time series usually increase at higher rates and less monotonically than those related to daily minimum time series. Summer is predicted to experience the largest and more consistent increment in both air and water temperatures, with a more marked signal emerging from daily maximum time series.

As for the spatial distribution of SAT, SWT, and SWE trends within the study area, this research reveals some important elevation-dependent patterns. In general, daily minimum SAT is expected to considerably increase in winter at low elevations. However, this tendency is not observed at high elevations, where winter minimum SAT increases at much lower rates. Indeed, the areas along the Mission Mountains range show an increasing intra-annual monthly variability of minimum SAT, as this variable presents much larger increasing rates in the warmest months than in the coldest months. These results are corroborated by the analysis of SWE and SWT trends. The duration and relative amount (i.e., percentage of the total) of snowpack are likely to decrease at high elevations not as much drastically as they are predicted to diminish at low elevations.

Also, the SWT increasing trends are generally less steep and less consistent in creeks with small drainage basins and located at high elevations than those identified in streams and rivers with sizable drainage basins and located at low elevations. However, this pattern is not evident in summer, when even the highest elevation locations are expected to experience large increments in water temperature.

On the whole, these findings suggest that climate change, recognizable by warming air temperatures, is affecting and will continue to affect the water resources of the FIR, both in terms of water quantity and quality. Warmer water temperatures combined with lower base streamflows cause the streams and rivers flowing across the Flathead Valley (e.g., the Flathead River and the lower portions of the Little Bitterroot River, Jocko River, Crow Creek, and Mission Creek) to become thermally unsuitable for cold-water fish communities, especially in summer. Therefore, headwater streams, where spawning and rearing mostly occur, are becoming isolated due to thermal fragmentation during summer. With decreasing duration and amount of snowpack, these thermal refuges are also expected to diminish in number and extent.

The climate trends detected and described in this research are in line with those emerged from other studies that focus on Western Montana or, more broadly, on the Pacific Northwest. For example, Chase, Hay, and Markstrom (2012) assessed the impact of climate change on the hydrology of the South Fork Flathead River Basin, a watershed located east of the FIR and with a similar drainage area (i.e., 4,307 square kilometers vs. 5,330 square kilometers of the FIR). Table 4-2 juxtaposes the main results related to three climate variables (i.e., maximum SAT, minimum SAT, and SWE) that were examined

in both the aforementioned study and the present research. However, it should be noted that these results are not directly comparable because different GCMs and emission scenarios were utilized in the two works. In addition, while this research is based on a statistical downscaling approach, Chase, Hay, and Markstrom (2012) did not downscale the GCM outputs in order to further model the overall basin hydrology.

Nevertheless, Table 4-2 reveals at least three important facts. First, the direction of the trends (upward or downward) and the order of magnitude of their slopes coincide, independently of the specific GCM and emission scenario adopted. Second, trends are more pronounced when a higher emission scenario is considered. According to IPCC (2014), the RCP4.5 is broadly comparable to the B1 scenario, which is the reason why they lie on the same row in Table 4-2. Similarly, the RCP8.5 resembles the A2/A1FI scenarios (in this case, only the A2 scenario is available for comparison). Third, the major inconsistency between the two studies concerns the projections of maximum and minimum air temperatures. While this research claims that maximum SAT is expected to change at higher rates than those estimated for minimum SAT, Chase, Hay, and Markstrom (2012) did not find such a marked difference between the projected slopes of these two air temperature variables.

**Table 4-2: Projected change by year of maximum SAT, minimum SAT, and mean annual SWE according to different emission scenarios for the Flathead Region (present study) and the South Fork Flathead River Basin (Chase, Hay, and Markstrom 2012)**

Present study (2001-2100)				Chase, Hay, and Markstrom 2012 (2001-2099)			
Emission scenario	Max SAT (°C)	Min SAT (°C)	Mean annual SWE (mm)	Emission scenario	Max SAT (°C)	Min SAT (°C)	Mean annual SWE (mm)
RCP4.5	0.030	0.025	-0.82	B1	0.024	0.024	-1.04
RCP8.5	0.063	0.053	-1.23	A2	0.040	0.040	-1.45

\* The RCP4.5 is broadly comparable to the B1 scenario and the RCP8.5 to the A2 scenario (IPCC 2014, 57)

A study by Wu et al. (2012) examines the impacts of climate change on the temperature of Pacific Northwest rivers and thus provides another reference work for this research. In this case, the climate projections are based on an A1B scenario, for which an equivalent RCP is not available. This emission scenario lies somehow in between the RCP4.5 and the RCP8.5. Table 4-3 illustrates the projected increment in mean annual and mean summer SWT for rivers across the Pacific Northwest (Wu et al. 2012) and flowing waters of the FIR (present research). Specifically, projected changes are indicated for three different 30-year periods (2010-2039, 2030-2059, and 2070-2099) in comparison with the 1970-1999 reference timeframe. Although this research and the study by Wu et al. (2012) cannot be compared directly, three considerations can be made regarding Table 4-3. Regardless of the specific GCM and emission scenario selected, all changes in SWT are positive, present the same order of magnitude, and are much larger in summer than during the other seasons.

**Table 4-3: Projected mean annual and summer SWT changes for three 30-year periods within the XXI century across the Pacific Northwest (Wu et al. 2012) and the FIR (present study) according to different emissions scenarios using 1970-1999 as reference period**

Study	Emission scenario	Mean annual SWT (°C)			Mean summer SWT (°C)		
		10-39	30-59	70-99	10-39	30-59	70-99
Wu et al. 2012	A1B	0.56	0.91	1.63	1.23	1.82	2.74
Present	RCP4.5	0.65	1.03	1.44	1.55	2.32	2.74
	RCP8.5	0.65	1.19	2.36	1.57	2.48	3.56

## 4.2. Methodology

From a methodological point of view, this research brings two major contributions. First, this study represents the only attempt to statistically downscale SWE by means of SDSM. Although the explained variance of the two downscaled components of SWE, namely SA and SM, is very low, the explained variance of the simulated cumulative SWE is considerably high and is comparable to that of the SAT downscaling models (i.e., on average, 91% for SWE, 92% for maximum SAT, and 85% for minimum SAT). Also, the selected characteristics of annual snowpack, such as duration, maximum SWE, beginning of snowmelt, are replicated quite accurately. However, the SWE downscaling models do not perform equally well when considering low elevation locations. In these cases, mixed snow/rain precipitation events are more common and smaller snow quantities are generally involved, which makes the simulation less reliable. As part of future research, this hypothesis should be tested by extending the analysis to a larger number of SNOTEL stations located at different elevations.

Second, this study examines the effect of the temporal scale, the distance and the elevation difference between pairs of SAT/SWT recordings stations, and the presence of hysteresis loops on the goodness of the non-linear logistic relationship between air and water temperatures. The weekly average is, by far, the most suitable temporal scale for predicting water temperature using air temperature as independent variable. Also, the distance between the SWT gaging site and the SAT recording station does not affect the strength of the air-water temperature correlation, whereas their elevation difference is a constraining factor. If a pair of SAT/SWT stations are located at the same or similar

elevations, it does not necessarily mean that they are well correlated; however, if their elevation difference is very large (i.e., more than 400 meters in this study), is it very unlikely that a good air-water temperature correlation can be found. Finally, this research suggests developing two separate models for the rising and falling limbs (i.e., warming and cooling seasons, respectively) in mountainous areas like the FIR because hysteresis is very likely to occur in snowmelt-dominated basins.

This research also reveals that cold-water inflow derived from snow- and ice-melt processes occurring in spring and early summer may be a crucial factor affecting the accuracy of the rising limb models, particularly in high-elevation and small-size drainage basins. Future works should focus on examining the role of snowmelt in modulating the air-water temperature relationship. If any correlation exists between SWT and SM and once the extent to which SWT variations lag behind SM events is identified, SM should be included into the SAT/SWT models as additional independent variable to test whether the accuracy of these models improves significantly or remains nearly unaltered. This research may be also expanded by exploring the predictability of the three logistic parameters ( $\alpha$ ,  $\gamma$ , and  $\beta$ ) based on catchment properties. In the absence of stream/river management, the relationship between SWT and landscape controls is universal (Johnson, Wilby, and Toone 2014). It would be interesting to investigate if watersheds with similar characteristics (e.g., size, mean elevation, mean slope, mean permeability, percent of vegetation coverage) are associated with analogous values of the three logistic parameters. If that were the case, it would be possible to predict water temperature in equivalent drainage basins that lack actual SWT measurements.

This research has finally some limitations that have to be highlighted. The largest source of uncertainty comes from the AOGCM simulations. As assessing the output of different AOGCMs was not the focus of this dissertation, only CanESM2 was employed here. However, future studies should aim for reducing the level of uncertainty by considering simulations from multiple AOGCMs to cover a broad range of projections and climate scenarios (i.e., RCP2.6 should be replaced by the more realistic RCP6.0). The second-largest source of uncertainty is associated with the statistical downscaling methodology, specifically its intrinsic assumption that the predictand-predictor relationship will remain constant (i.e., stationary) in the future.

Another limitation of this investigation deals with the source data type, as the input data are all tied to point locations. Although multiple sites were considered that are representative of different parts of the study area (e.g., different elevations, geographic surroundings, and physiographic characteristics of drainage basins), the spatial distribution of the three variables examined (i.e., SAT, SWT, and SWE) would be better understood using spatially homogenous data, such as remotely sensed imagery. This approach would be particularly useful for studying changes in snowpack coverage. Indeed, the six SNOTEL stations that were selected for this work provide information concerning the duration and amount of snowpack, but not about its spatial extension. This research might be expanded by including the analysis of remotely sensed snow cover data, such as the daily Moderate Resolution Imaging Spectroradiometer products. Because of the analogous temporal resolution, these datasets might be used in combination with SNOTEL data to enrich the analysis of snowpack changes.

A final consideration regarding the overall research design has to be made. As mentioned in the introduction of this dissertation (see Chapter I), changes in the water resources of the FIR are not exclusively driven by climate change. Rather, a variety of factors, such as historical events (e.g., the construction of dams, channels, and reservoirs), social constraints (e.g., the water rights situation), and other water-related stressors (e.g., water pollution due to tourist and recreational activities), have determined the current state of the water resources in the FIR. Originally, this study was conceived with the purpose of exploring all these aspects in order to reach a more comprehensive understanding of the water-related issues that concern the reservation. In addition, because of the peculiarity of the study area, consulting traditional ecological knowledge about these issues would have certainly enriched this research by bringing into discussion a different perspective on reality. For these reasons, a wider qualitative-based phase was initially planned to support and integrate with the quantitative analysis presented here. If that had been the case, a mixed methods approach, which relies upon multiple types of data, modes of analysis, and ways of knowing (Elwood 2010), would have been the best methodological strategy to conduct this type of research.

Unfortunately, the collection of the qualitative information faced multiple setbacks, mostly related to the reluctance of the native people to share their personal experiences and traditional knowledge within an outside Western-culture framework (i.e., the interview process) and language (i.e., the system of communication). After centuries of exploitation, the tribes' intention of protecting themselves is fully legitimate. At the end of the field work in the FIR, the qualitative data gathered from a

few interviews and archival research served as a means to develop the structure of this study, but were not sufficient to design a full-fledged mixed-methods research. Therefore, the quantitative analysis became the core component of this work and climate change became the only forcing of water resource changes treated in this dissertation.

In spite of these limitations, this research provides information that can be extremely useful to develop climate change adaptation strategies for water resources in the FIR. Ideally, this phase should be carried out in conjunction with the NRD of the CSKT, as to be effective these policies and adaptation plans should be formulated based on specific objectives, subject to the economic and human resources available, consistent with the particular water rights context, and within the framework of existing water management practices. Moreover, elders and tribal practitioners need to be consulted throughout the entire planning process, as traditional ecological knowledge is the result of centuries of observation of the local environment and a long and successful experience in managing natural resources. Local knowledge can also address issues related to vulnerability and adaptability to new scenarios and can identify adaptation measures that are cost-effective, participatory, and sustainable.

Since the very beginning, this dissertation is addressed to the CSKT of the FIR, in the hope that they would benefit from this work. An example of how the findings of this research may be used relates to the management of fishing resources, in that water temperature projections as described in this study may serve to identify potential thermal refuges for target fish species. In this regard, the  $\alpha$  coefficient of the non-linear

logistic function (see Equation 23 and Table 3-6), which represents the maximum SWT estimated by the air-water temperature model, provides some useful indications when compared with the critical thermal threshold of certain fishes being studied. Therefore, the spatial distribution of the  $\alpha$  coefficient across the FIR reveals water bodies that are more or less likely to become thermally unsuitable for the target species. Figure 4-1 shows an example of how increasing August air temperatures might reduce bull trout's habitats in the Flathead River Basin above the Flathead Lake (Jones et al. 2014). Similar curves may be obtained from the water temperature projections presented in this research. Potential thermal refuges should eventually be afforded special protection. This could be achieved, for instance, by preserving and intensifying riparian vegetation that keeps stream temperature lower through its shade.

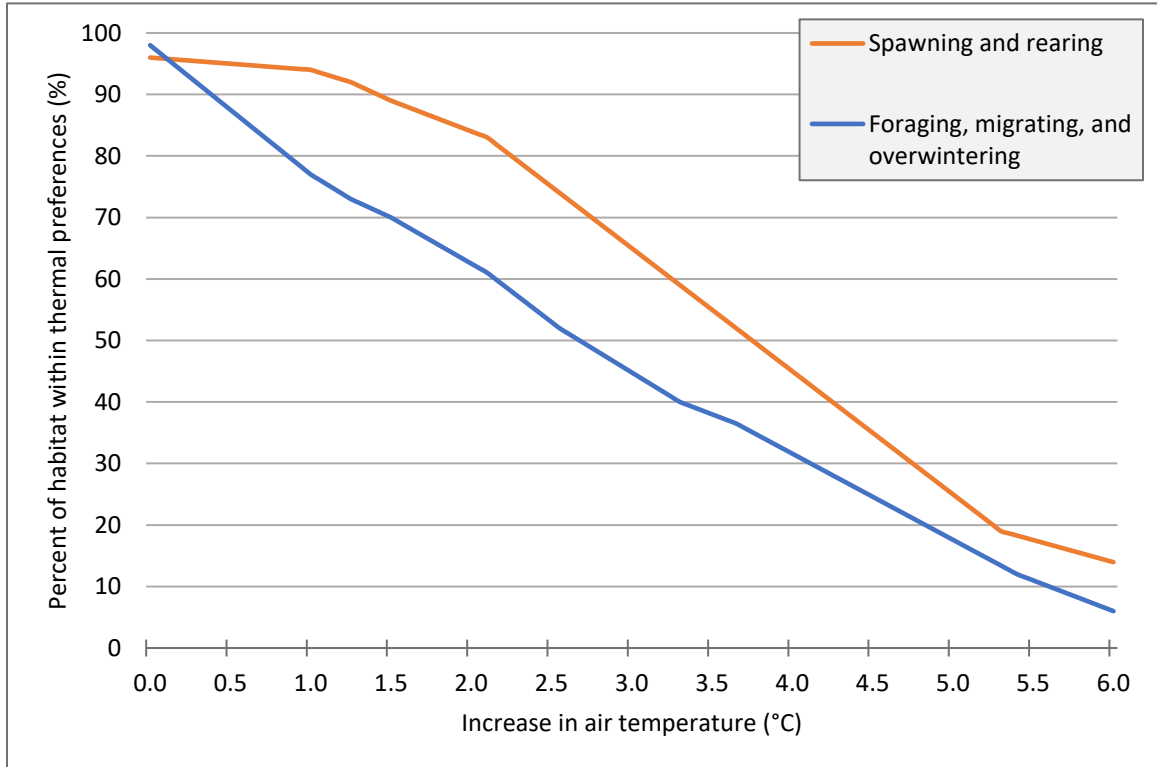


**Figure 4-1: Potential loss of critical bull trout habitat in response to increasing August stream temperatures in the Flathead River Basin above the Flathead Lake (Jones et al. 2014, 212)**

## APPENDIX SECTION

### APPENDIX A: Institutional Review Board approval



July 27, 2017

Francesco Zignol  
Texas State University  
San Marcos, TX 78666

Dear Mr. Zignol:

Your IRB application 2017867 titled, *Past, present, and future changes in water quality and quantity within the Flathead Reservation*, was reviewed by the Texas State University IRB. According to the application, the purpose of your study is to collect historical documents about the Flathead Reservation and integrate this information by interviewing members of the community to obtain their present and past perspective on water resources at the Reservation and the region.

The IRB concluded that the project is categorized as "oral history" and does not meet the criteria and definition of "research" by OHRP, which defines research as a "systematic investigation, including research development, testing and evaluation, designed to develop or contribute to generalizable knowledge." The IRB is under the assumption that the collected information will not contribute to generalizable knowledge, and is solely intended to study historical information about the water quality at Flathead Reservation. Therefore, your project does not require oversight from the Texas State IRB.

If the intent your project changes in the future, please contact Research Integrity and Compliance to initiate an IRB assessment. The changes may have an effect on whether the study meets OHRP's criteria of "research".

Feel free to contact me if you have any questions.

Regards,



Sean Rubino, MPA  
Director, Office of Research Integrity and Compliance  
Texas State University  
(512) 245-2314

OFFICE OF THE ASSOCIATE VICE PRESIDENT FOR RESEARCH  
601 University Drive | Building and Suite | San Marcos, Texas 78666-4616  
Phone: 512.245.2314 | fax: 512.245.3847 | WWW.TXSTATE.EDU

MEMBER THE TEXAS STATE UNIVERSITY SYSTEM™

APPENDIX B: Validation of downscaling models of SAT

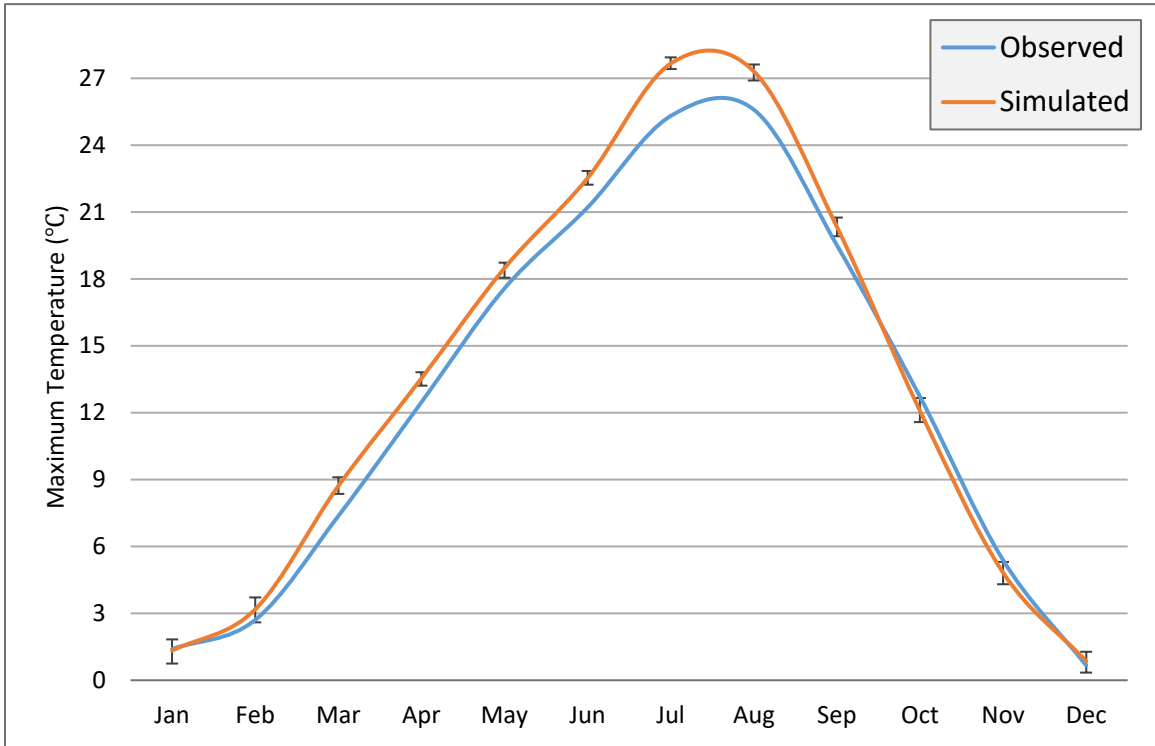


Figure B-1: Monthly averages of daily maximum SAT at Big Fork 13S (1981-2000)

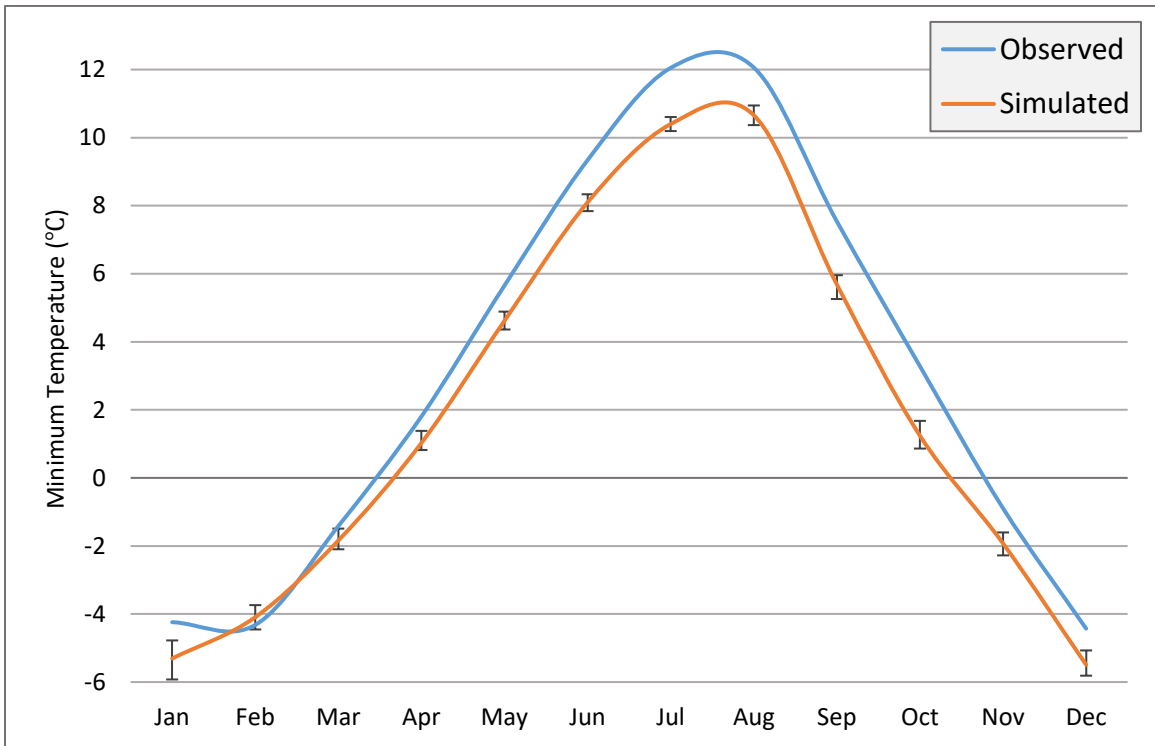
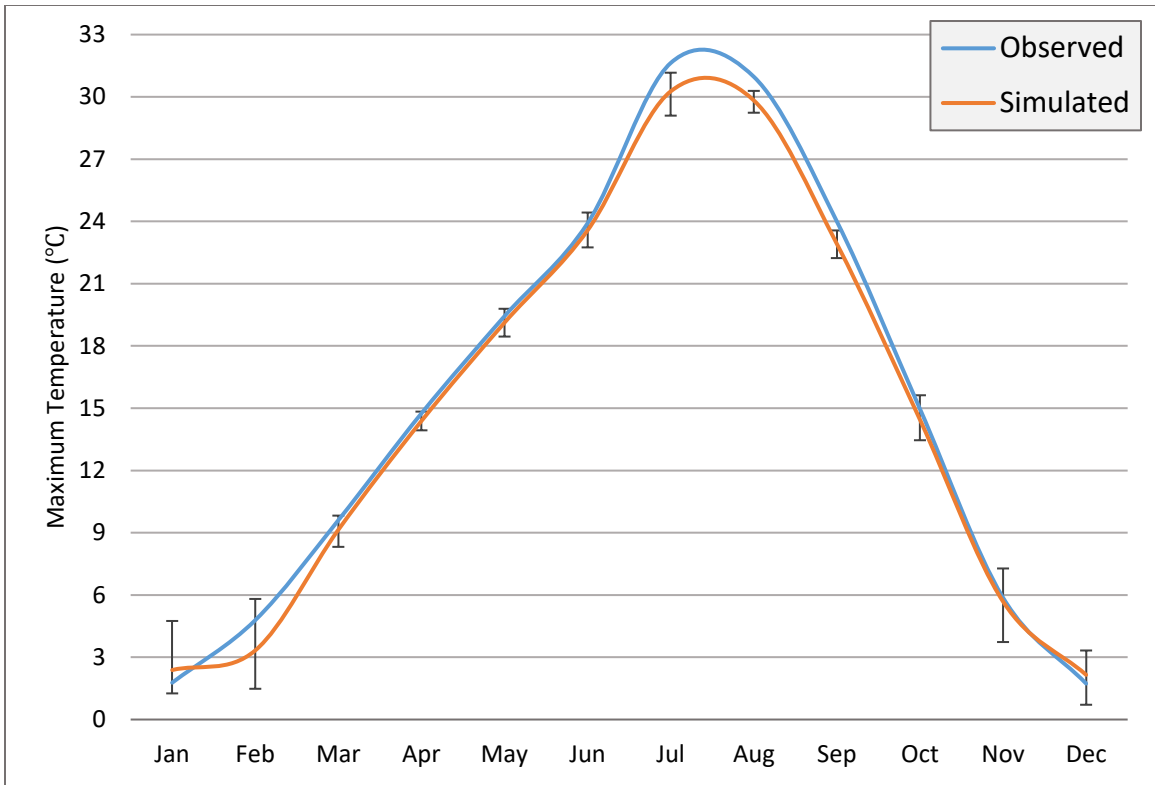
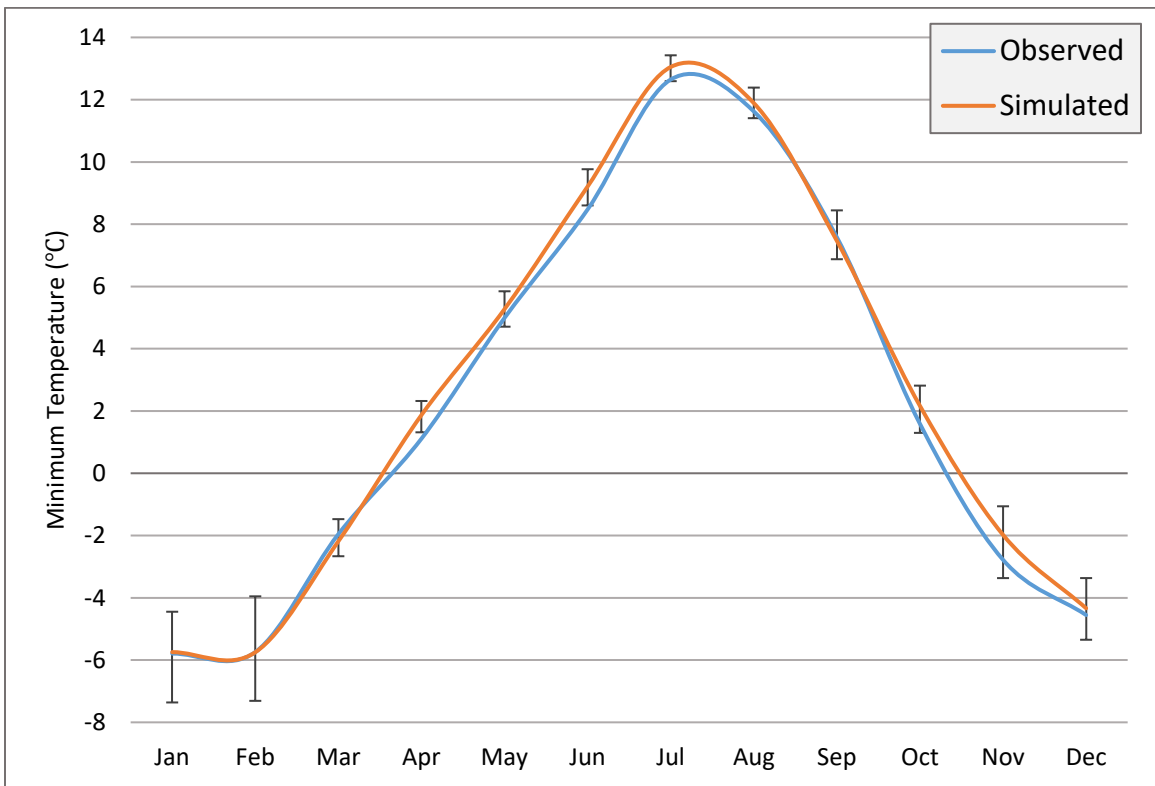


Figure B-2: Monthly averages of daily minimum SAT at Big Fork 13S (1981-2000)



**Figure B-3: Monthly averages of daily maximum SAT at Hot Springs Montana (2001-2005)**



**Figure B-4: Monthly averages of daily minimum SAT at Hot Springs Montana (2001-2005)**

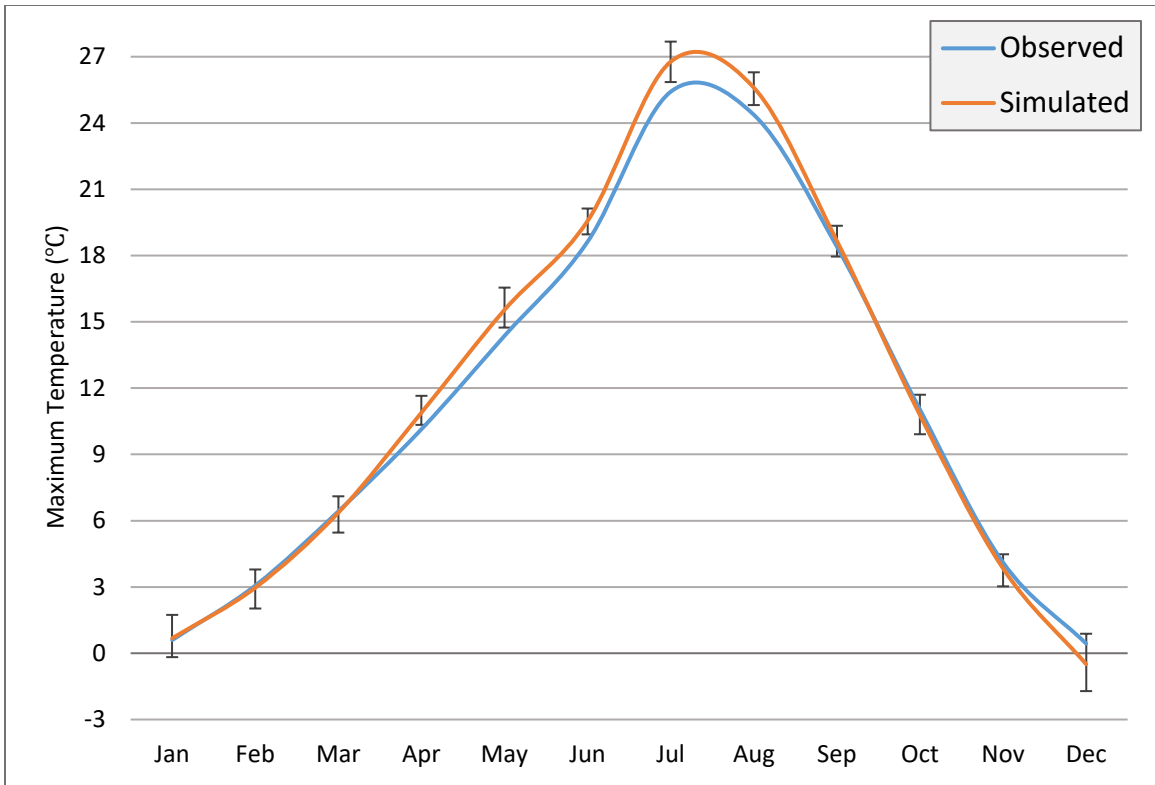


**Figure B-5: Monthly averages of daily maximum SAT at Kraft Creek (2001-2005)**

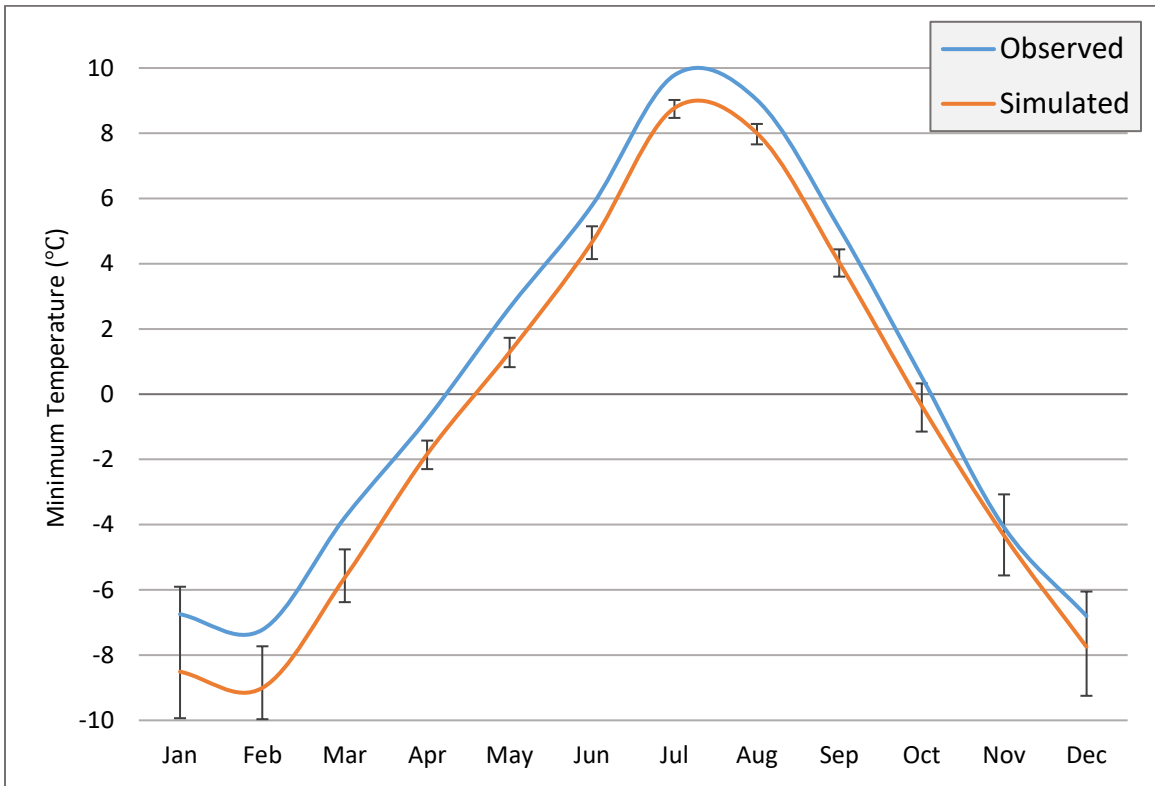


**Figure B-6: Monthly averages of daily minimum SAT at Kraft Creek (2001-2005)**

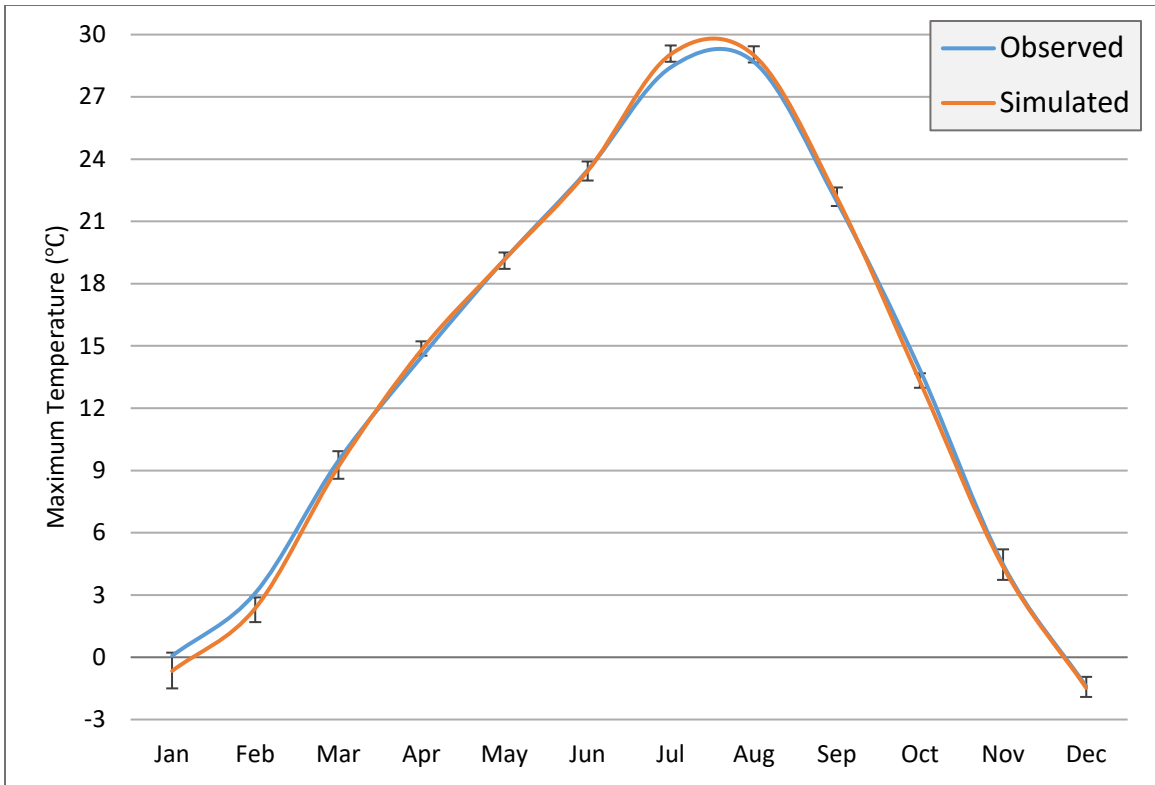


**Figure B-7: Monthly averages of daily maximum SAT at Missoula Int. Airport (1981-2000)**

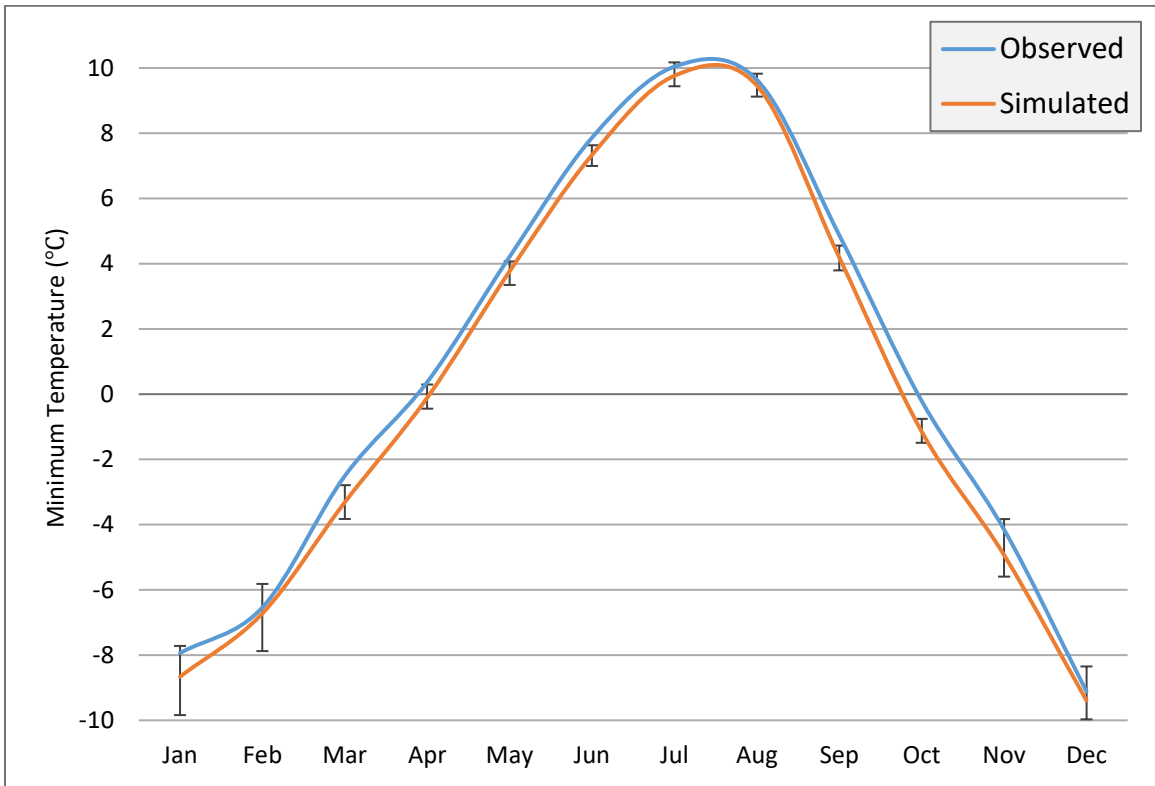


**Figure B-8: Monthly averages of daily minimum SAT at Missoula Int. Airport (1981-2000)**

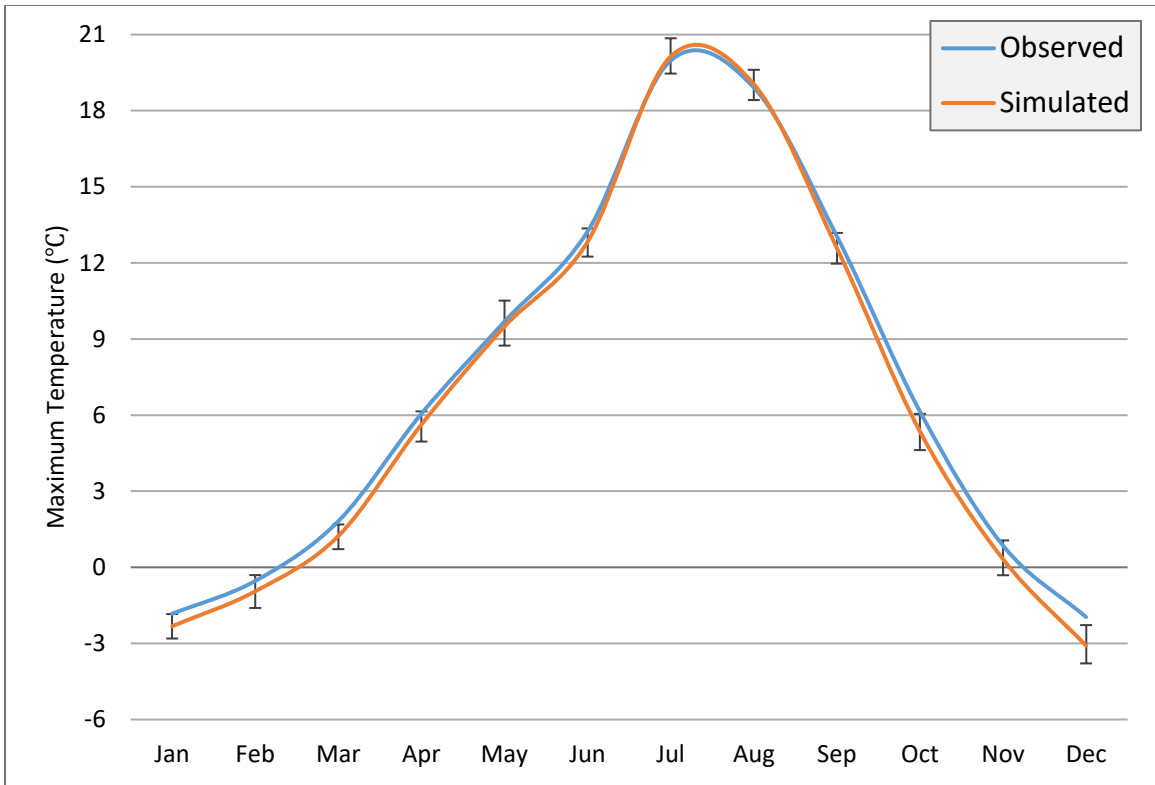


**Figure B-9: Monthly averages of daily maximum SAT at Moss Peak (2001-2005)**

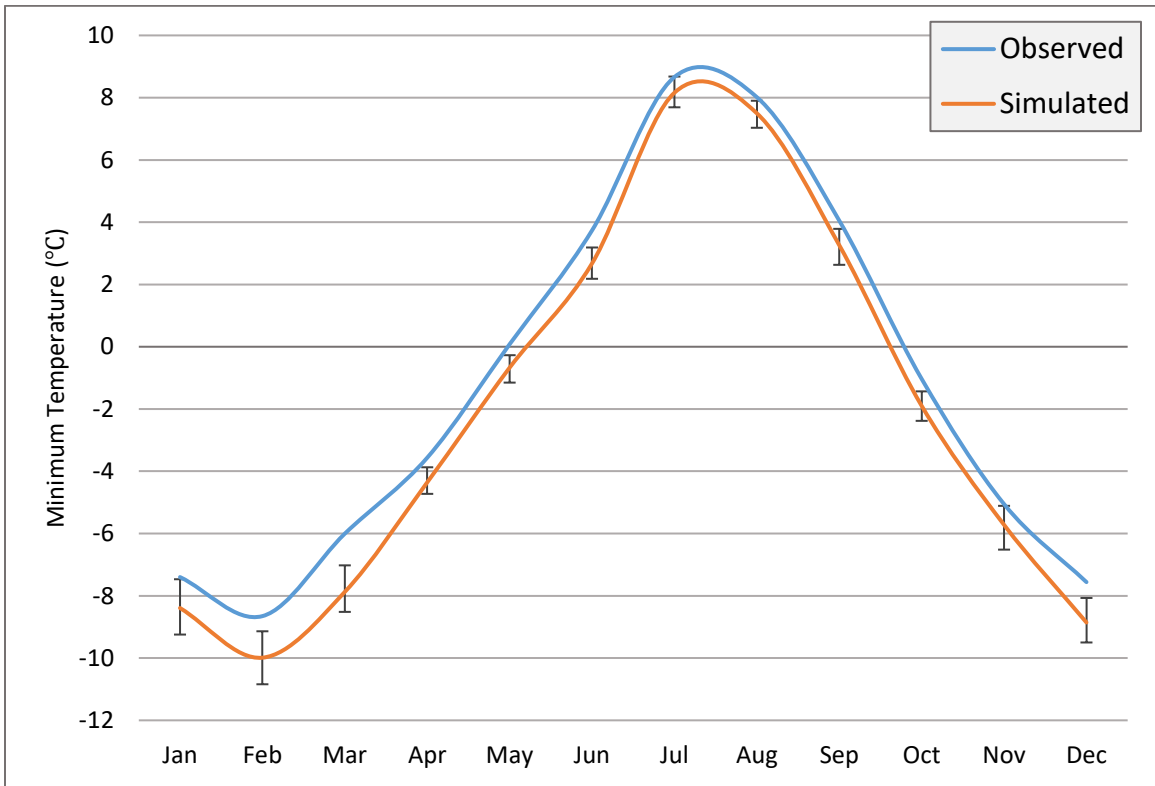


**Figure B-10: Monthly averages of daily minimum SAT at Moss Peak (2001-2005)**

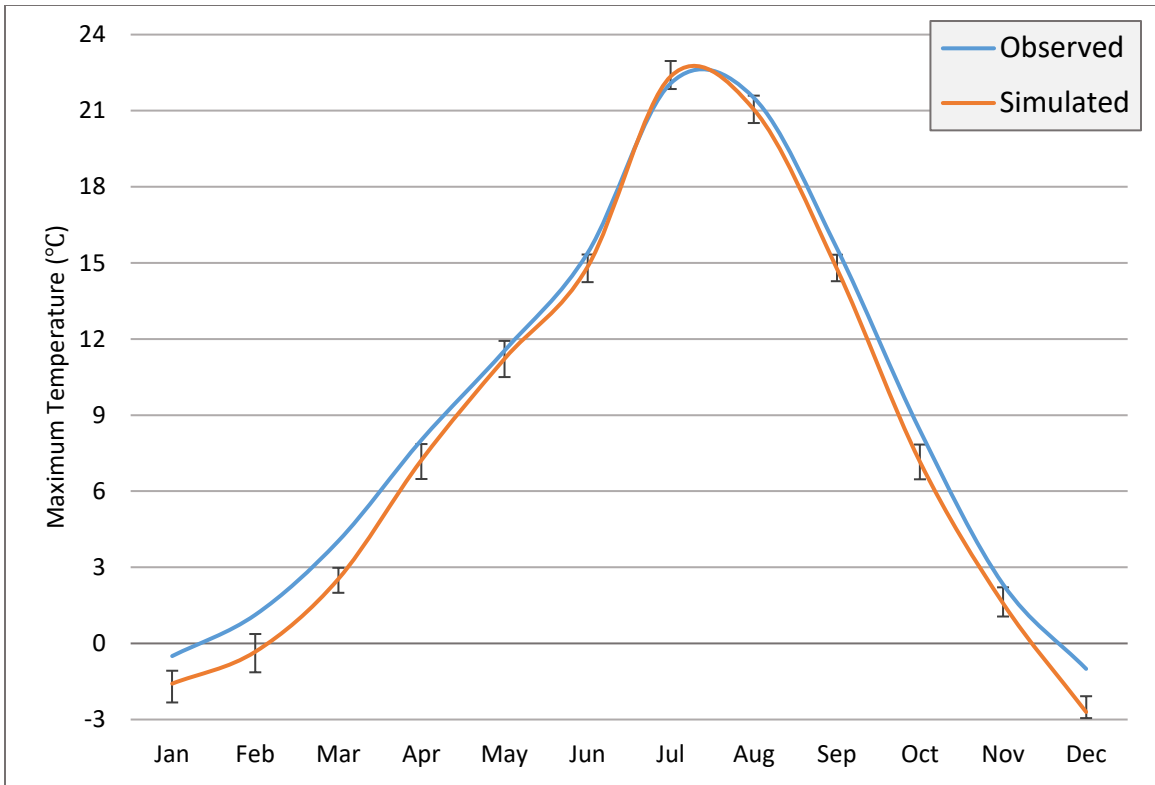


**Figure B-11: Monthly averages of daily maximum SAT at North Fork Jocko (2001-2005)**

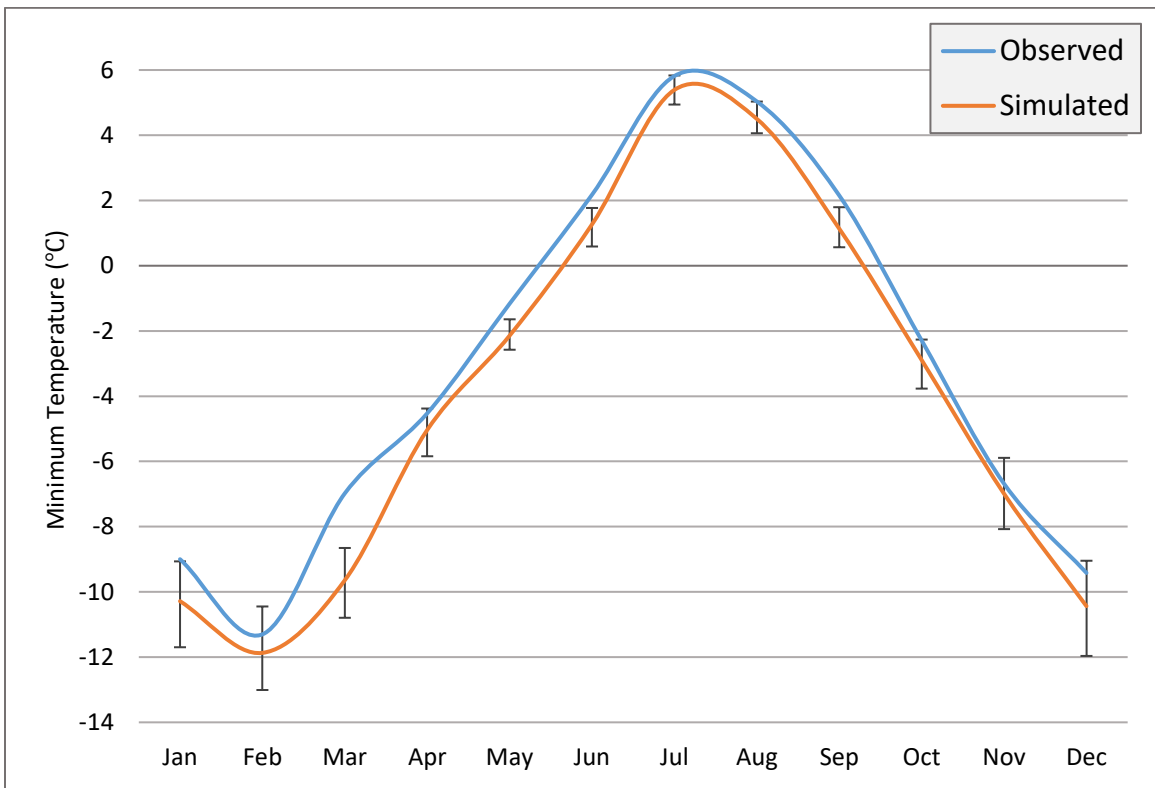


**Figure B-12: Monthly averages of daily minimum SAT at North Fork Jocko (2001-2005)**

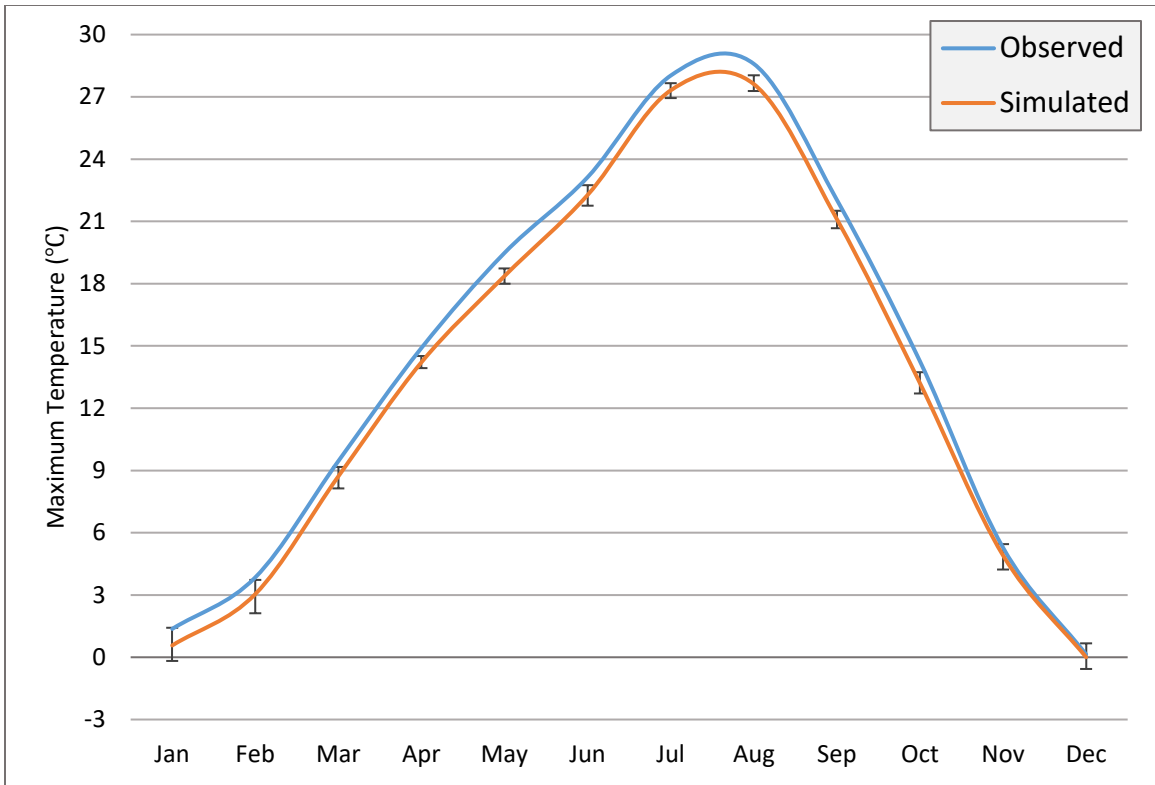


**Figure B-13: Monthly averages of daily maximum SAT at Polson Kerr Dam (1981-2000)**

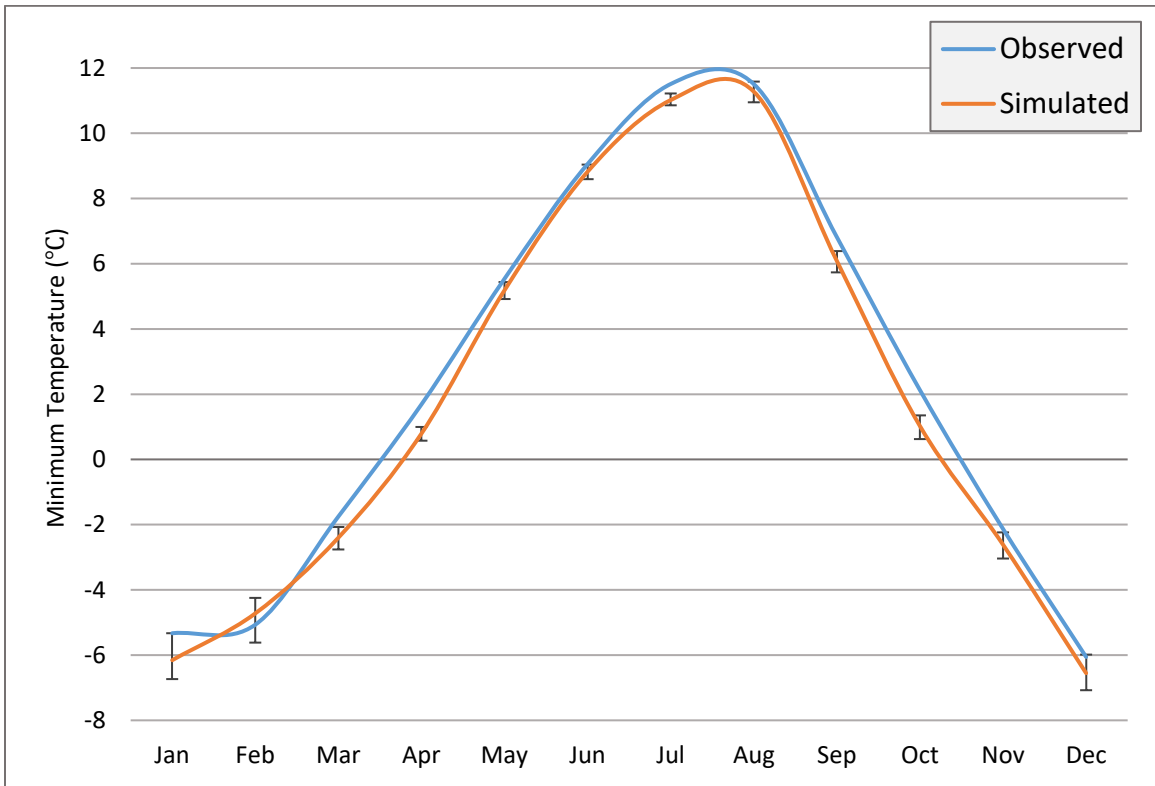


**Figure B-14: Monthly averages of daily minimum SAT at Polson Kerr Dam (1981-2000)**

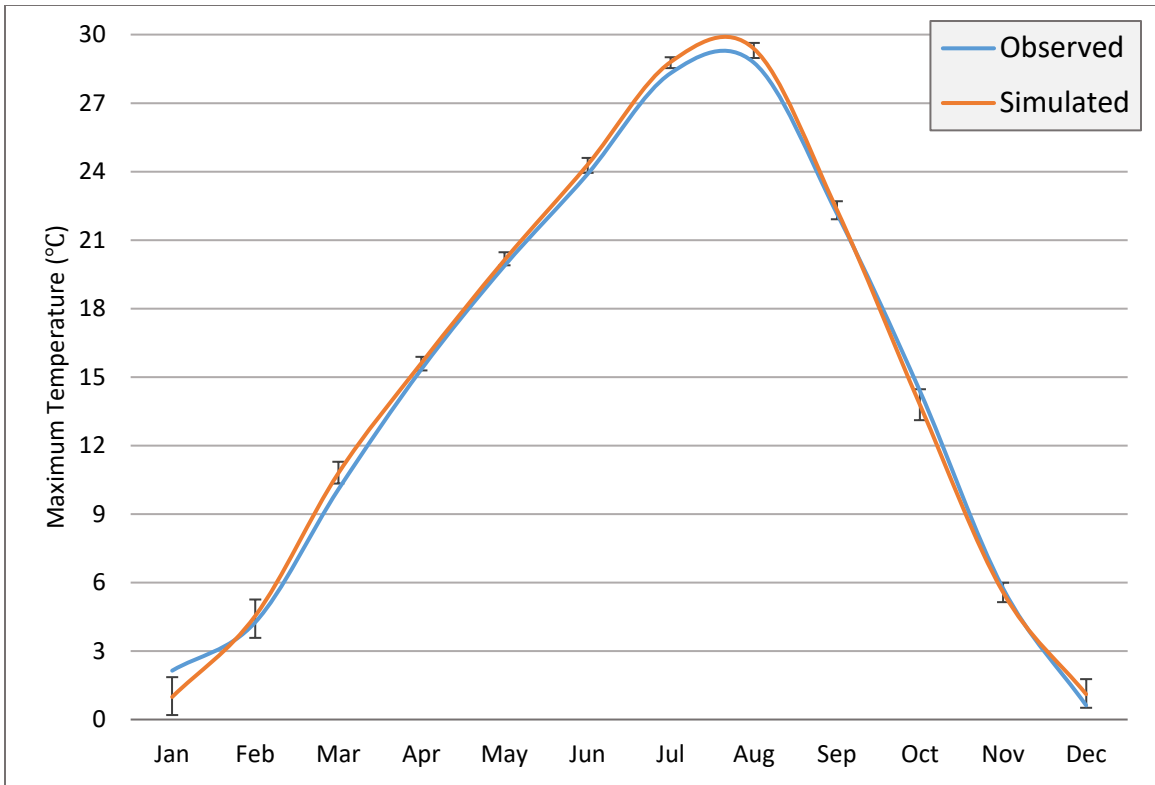


**Figure B-15: Monthly averages of daily maximum SAT at Saint Ignatius (1981-2000)**

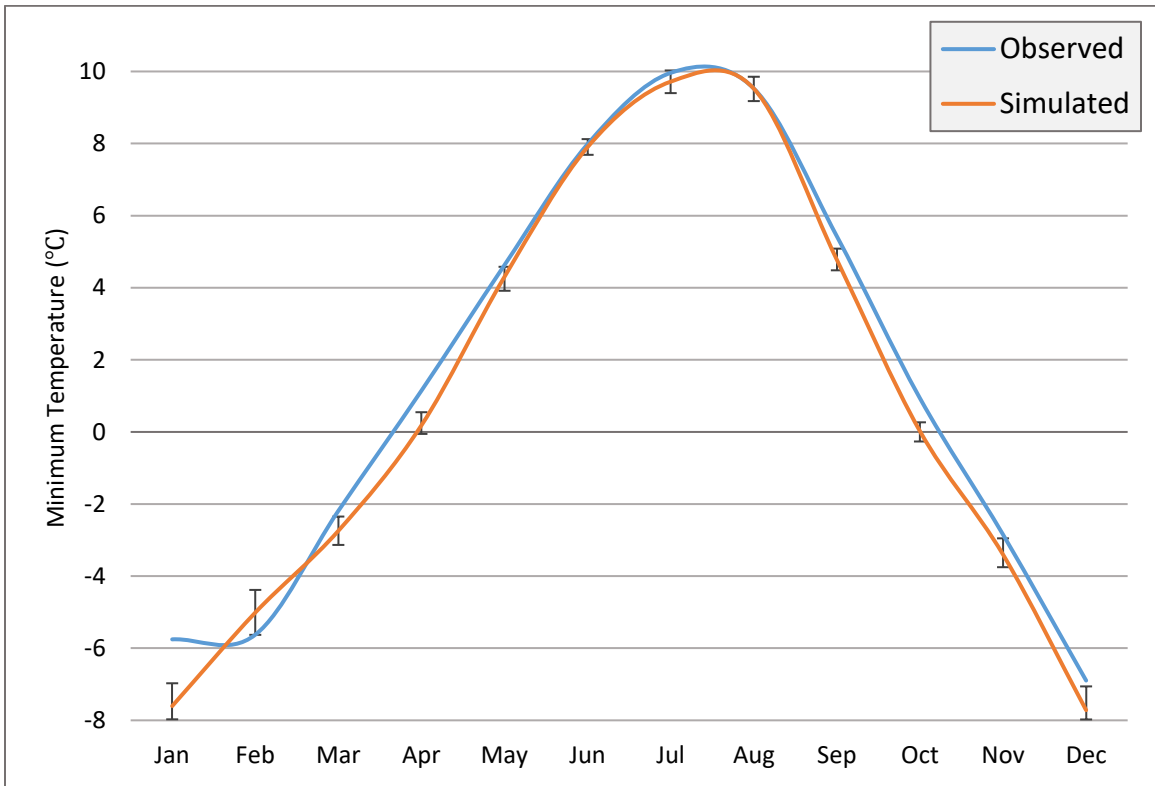


**Figure B-16: Monthly averages of daily minimum SAT at Saint Ignatius (1981-2000)**

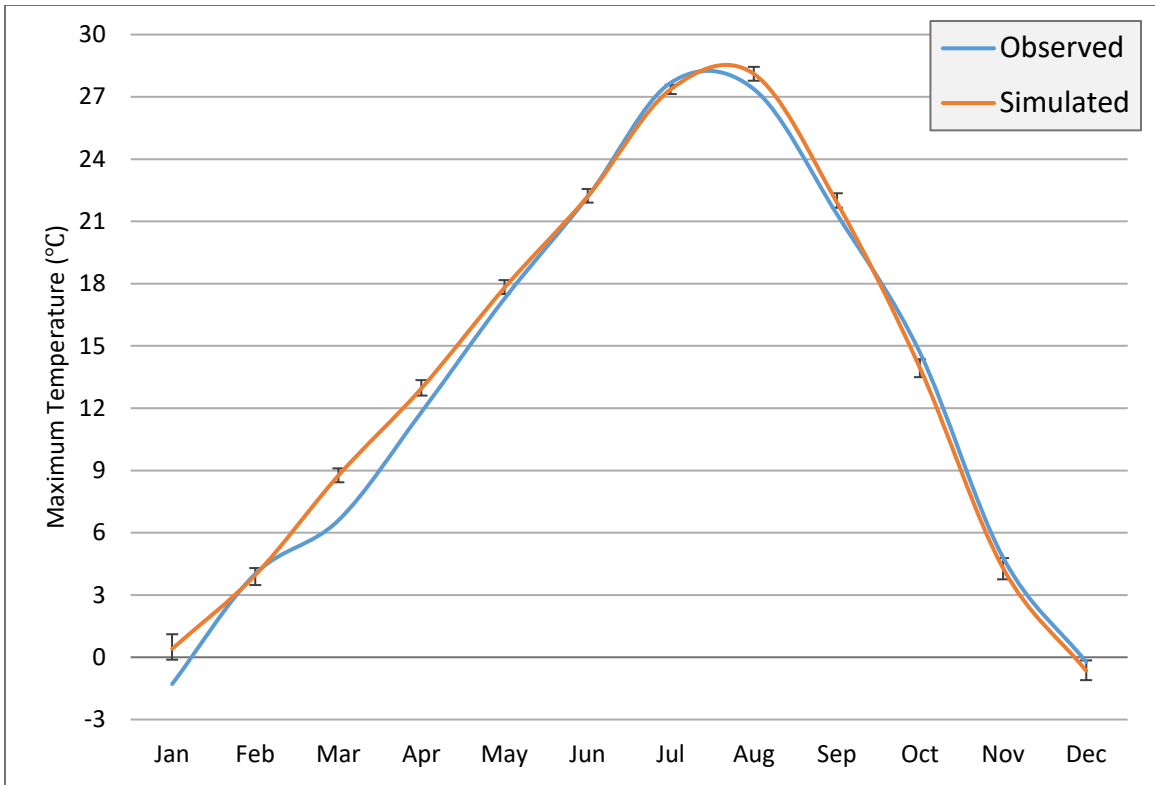


**Figure B-17: Monthly averages of daily maximum SAT at Seeley Lake RS (1981-2000)**

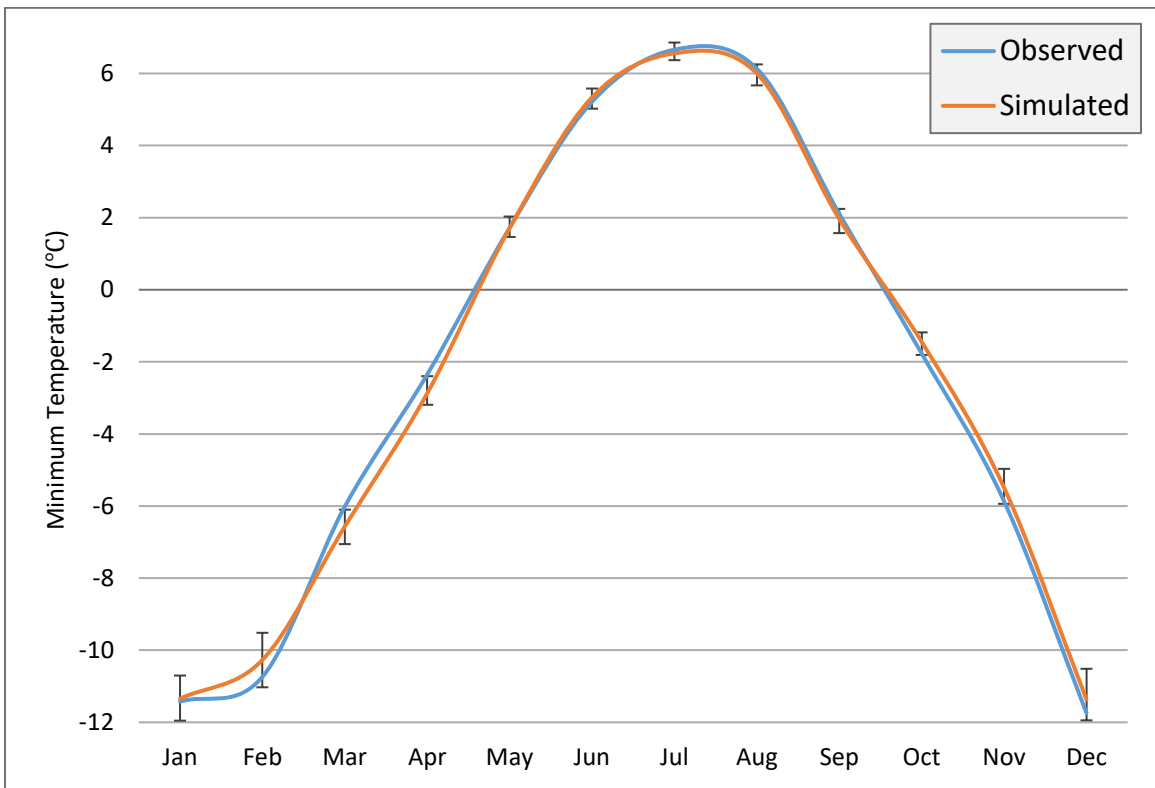


**Figure B-18: Monthly averages of daily minimum SAT at Seeley Lake RS (1981-2000)**

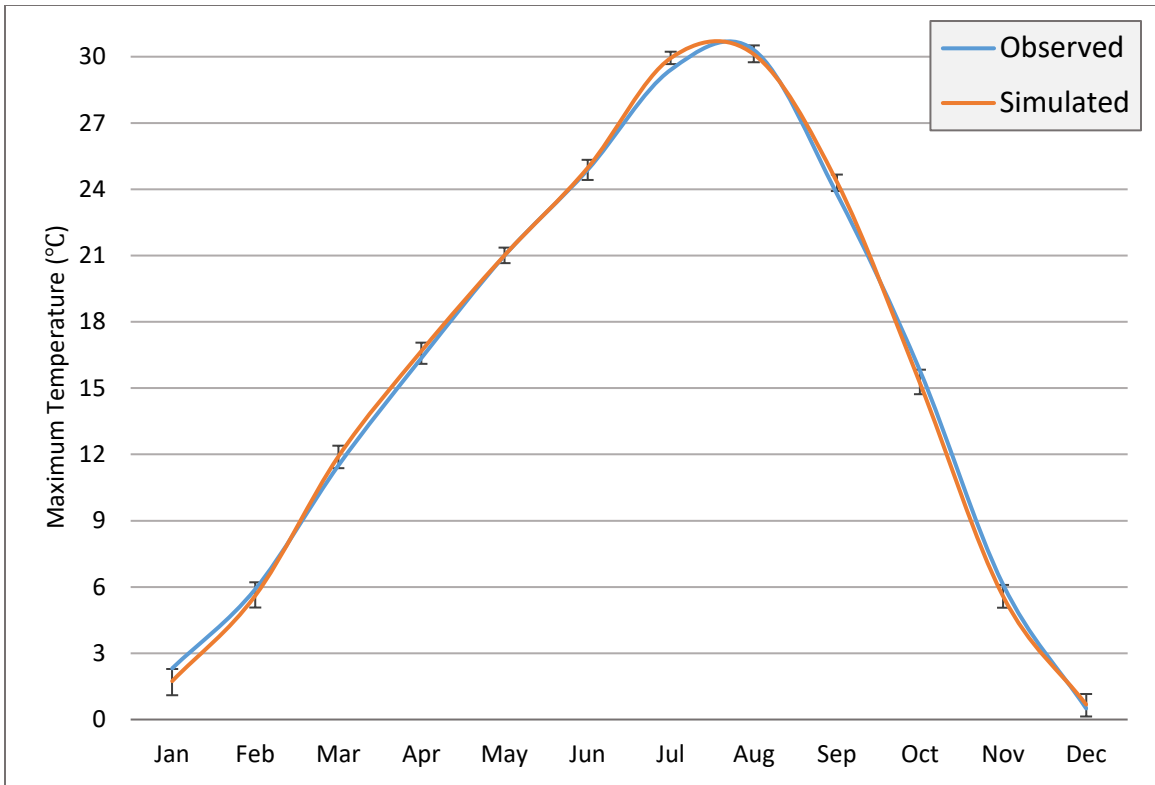


**Figure B-19: Monthly averages of daily maximum SAT at Superior (1981-2000)**

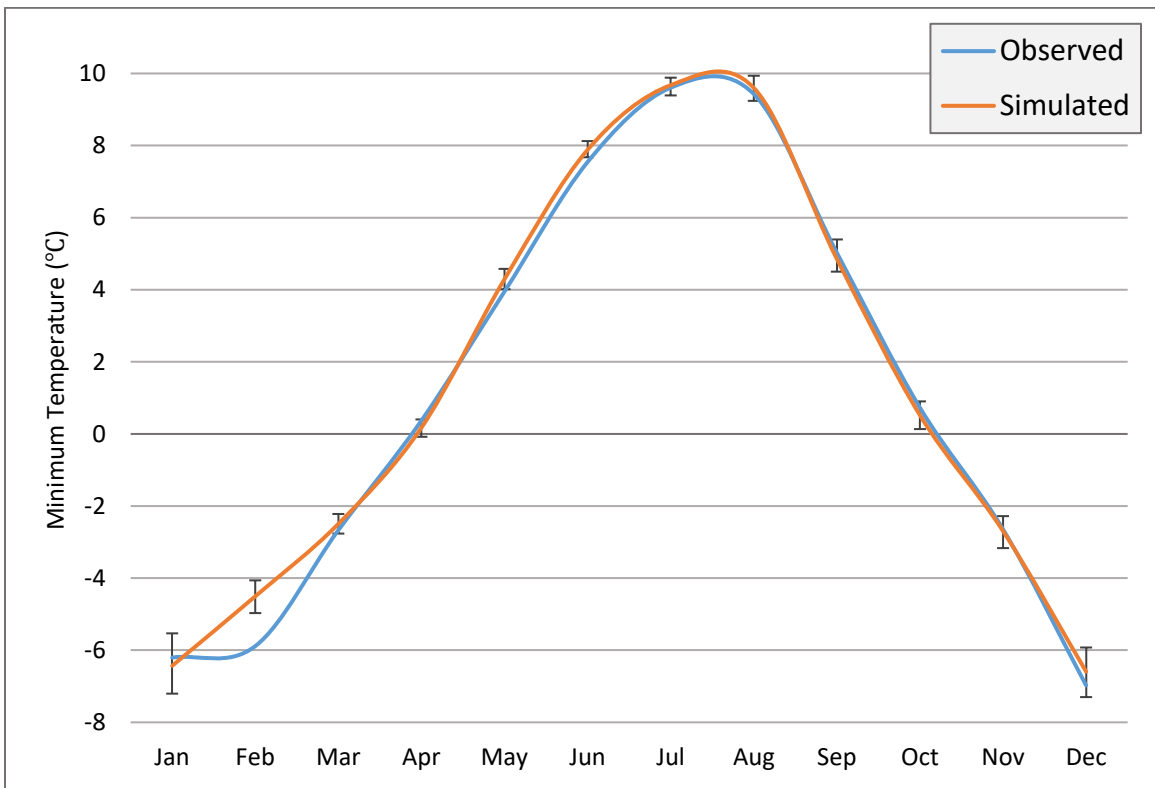


**Figure B-20: Monthly averages of daily minimum SAT at Superior (1981-2000)**

**Table B-1: Median of observed and estimated daily maximum SAT time series and related error over the validation period**

Station	Value	Jan	Feb	Mar	Apr	May	Jun	Jul	Aug	Sep	Oct	Nov	Dec	Win	Spr	Sum	Fal	Ann
Bigfork 13S	Obs	2.2	3.9	7.8	12.2	17.2	21.1	26.1	26.1	19.4	12.2	6.1	1.1	2.2	12.2	24.4	12.2	12.2
	Est	1.8	3.6	8.8	13.4	18.1	22.4	27.8	27.5	20.5	12.0	5.0	1.6	2.3	13.2	26.2	11.8	12.7
	Err	-0.4	-0.3	1.0	1.2	0.9	1.3	1.7	1.4	1.1	-0.2	-1.1	0.5	0.1	1.0	1.8	-0.4	0.5
Hot Springs Montana	Obs	1.7	5.6	9.4	14.2	18.9	23.6	31.7	31.7	24.4	14.4	6.1	1.7	2.8	14.4	30.0	14.4	14.4
	Est	2.4	3.3	9.2	14.1	18.9	23.5	30.1	29.9	22.8	14.3	5.8	2.1	2.7	14.2	28.3	14.2	14.3
	Err	0.7	-2.3	-0.2	0.0	0.0	-0.1	-1.6	-1.8	-1.6	-0.1	-0.3	0.4	-0.1	-0.2	-1.7	-0.2	-0.1
Kraft Creek	Obs	0.8	2.9	6.1	9.2	13.7	18.8	25.4	24.7	18.9	10.5	3.9	0.5	1.6	9.9	23.6	10.6	10.4
	Est	1.2	3.1	6.8	10.7	15.6	19.7	26.6	25.8	18.4	10.7	4.1	-0.6	1.3	11.1	24.6	10.7	10.8
	Err	0.4	0.3	0.7	1.5	1.9	0.9	1.2	1.1	-0.5	0.2	0.2	-1.1	-0.3	1.2	1.0	0.1	0.4
Missoula Int. Airport	Obs	1.1	3.9	9.4	13.3	18.6	23.3	29.4	29.4	22.2	13.3	4.4	-0.6	1.7	13.3	27.8	12.8	13.3
	Est	-0.3	2.9	9.2	14.6	18.7	23.3	29.2	29.1	22.4	13.3	4.5	-0.9	0.5	14.1	27.4	12.8	13.6
	Err	-1.4	-1.0	-0.2	1.3	0.1	0.0	-0.2	-0.3	0.2	0.0	0.1	-0.3	-1.2	0.8	-0.4	0.0	0.3
Moss Peak	Obs	-1.5	-1.2	1.3	5.5	9.0	13.2	20.3	19.5	13.1	5.4	0.2	-2.0	-1.5	5.6	18.4	6.1	6.1
	Est	-1.9	-0.9	1.5	5.5	9.6	12.8	20.0	19.3	12.4	5.3	0.5	-3.0	-2.0	5.6	18.1	6.2	5.8
	Err	-0.4	0.3	0.2	0.0	0.6	-0.4	-0.3	-0.2	-0.7	-0.1	0.4	-1.0	-0.5	0.1	-0.3	0.1	-0.3
North Fork Jocko	Obs	0.0	0.8	3.1	7.0	11.0	15.5	22.2	22.1	16.1	7.8	1.6	-0.5	-0.1	7.5	20.5	8.0	7.9
	Est	-1.2	-0.1	2.9	7.0	11.2	15.1	22.3	21.3	15.0	7.3	1.7	-2.5	-1.3	7.1	20.2	7.9	7.2
	Err	-1.2	-0.9	-0.2	0.0	0.2	-0.4	0.1	-0.8	-1.0	-0.5	0.1	-2.0	-1.2	-0.4	-0.3	-0.1	-0.7
Polson Kerr Dam	Obs	2.2	5.0	9.4	14.4	18.9	22.8	28.3	29.4	22.2	13.9	5.6	0.6	2.8	14.4	26.7	13.9	13.9
	Est	1.0	3.7	8.9	14.1	18.1	22.2	27.4	27.8	21.4	13.2	5.2	0.5	1.6	13.8	25.8	12.9	13.5
	Err	-1.2	-1.3	-0.5	-0.3	-0.8	-0.6	-0.9	-1.6	-0.8	-0.7	-0.4	-0.1	-1.2	-0.6	-0.9	-1.0	-0.4
Saint Ignatius	Obs	2.8	5.6	10.6	14.4	19.4	23.9	28.9	29.4	22.8	13.3	6.1	1.1	2.8	14.4	27.8	13.3	14.4
	Est	1.3	5.2	10.8	15.4	19.9	24.3	29.1	29.7	22.5	13.8	5.7	1.5	2.5	15.4	27.9	13.7	14.9
	Err	-1.5	-0.4	0.2	1.0	0.5	0.4	0.2	0.3	-0.3	0.5	-0.4	0.4	-0.3	1.0	0.1	0.4	0.5
Seeley Lake RS	Obs	0.0	4.4	6.7	11.1	17.2	22.2	28.3	27.8	22.2	14.4	4.7	0.0	1.1	11.1	26.7	13.3	12.2
	Est	0.8	4.5	8.9	12.8	17.5	22.2	27.5	28.4	22.2	13.9	4.5	0.0	1.6	12.8	26.3	13.1	13.0
	Err	0.8	0.1	2.2	1.7	0.3	0.0	-0.8	0.6	0.0	-0.5	-0.2	0.0	0.5	1.7	-0.4	-0.2	0.8
Superior	Obs	2.8	6.7	11.7	15.6	20.6	25.0	30.0	30.6	24.4	15.6	6.1	1.1	3.3	15.6	28.9	14.4	15.0
	Est	2.1	6.0	11.9	16.5	20.7	24.9	30.1	30.2	24.6	15.2	5.8	1.2	2.8	16.2	28.7	14.6	15.6
	Err	-0.7	-0.7	0.2	0.9	0.1	-0.1	0.1	-0.4	0.2	-0.4	-0.3	0.1	-0.5	0.6	-0.2	0.2	0.6
Mean Error		0.9	0.8	0.6	0.8	0.5	0.4	0.7	0.8	0.7	0.3	0.3	0.6	0.6	0.8	0.7	0.3	0.4

**Table B-2: Maximum of observed and estimated daily maximum SAT time series and related error over the validation period**

Station	Value	Jan	Feb	Mar	Apr	May	Jun	Jul	Aug	Sep	Oct	Nov	Dec	Win	Spr	Sum	Fal	Ann
Bigfork 13S	Obs	17.8	16.7	19.4	23.3	29.4	31.7	35.6	33.9	33.3	26.1	20.0	14.4	17.8	29.4	35.6	33.3	35.6
	Est	15.2	15.9	20.1	28.3	35.1	36.8	39.2	41.5	35.2	27.5	16.5	13.9	16.4	35.1	41.6	35.2	41.6
	Err	-2.6	-0.8	0.7	5.0	5.7	5.1	3.6	7.6	1.9	1.4	-3.5	-0.5	-1.4	5.7	6.0	1.9	6.0
Hot Springs Montana	Obs	13.3	17.2	25.6	26.7	33.9	36.7	41.1	38.9	36.1	30.6	17.8	11.7	17.2	33.9	41.1	36.1	41.1
	Est	21.3	15.1	25.0	27.2	34.2	37.8	44.5	40.9	36.5	28.6	17.9	15.9	21.4	34.2	44.5	36.5	44.5
	Err	8.0	-2.1	-0.6	0.5	0.3	1.1	3.4	2.0	0.4	-2.0	0.1	4.2	4.2	0.3	3.4	0.4	3.4
Kraft Creek	Obs	13.9	13.5	20.4	22.9	29.8	31.7	36.5	34.6	31.1	24.6	14.8	12.5	13.9	29.8	36.5	31.1	36.5
	Est	13.8	14.7	23.2	25.4	32.0	38.6	42.3	39.3	33.6	27.3	15.6	13.9	15.8	32.0	42.6	33.6	42.6
	Err	-0.1	1.2	2.8	2.5	2.2	6.9	5.8	4.7	2.5	2.7	0.8	1.4	1.9	2.2	6.1	2.5	6.1
Missoula Int. Airport	Obs	13.3	18.9	22.8	30.6	35.0	36.7	38.3	37.8	36.7	28.9	22.8	13.9	18.9	35.0	38.3	36.7	38.3
	Est	15.6	15.7	24.1	31.5	37.4	38.9	42.5	44.4	39.6	29.5	18.9	14.5	16.7	37.4	44.6	39.6	44.7
	Err	2.3	-3.2	1.3	0.9	2.4	2.2	4.2	6.6	2.9	0.6	-3.9	0.6	-2.2	2.4	6.3	2.9	6.4
Moss Peak	Obs	9.6	11.5	16.7	17.2	24.2	25.5	31.6	27.9	26.3	19.5	14.1	6.9	11.5	24.2	31.6	26.3	31.6
	Est	8.7	11.8	17.5	20.7	23.8	29.9	33.4	31.3	26.9	21.0	12.7	8.3	11.9	24.0	33.7	26.9	33.7
	Err	-0.9	0.3	0.8	3.5	-0.4	4.4	1.8	3.4	0.6	1.5	-1.4	1.4	0.4	-0.2	2.1	0.6	2.1
North Fork Jocko	Obs	10.2	12.5	17.8	19.4	25.4	27.9	32.4	31.7	27.2	22.3	15.8	6.1	12.5	25.4	32.4	27.2	32.4
	Est	9.3	10.4	17.1	20.3	25.4	30.8	34.8	33.3	27.8	23.1	13.4	7.5	10.7	25.5	35.1	27.8	35.1
	Err	-0.9	-2.1	-0.7	0.9	0.0	2.9	2.4	1.6	0.6	0.8	-2.4	1.4	-1.8	0.1	2.7	0.6	2.7
Polson Kerr Dam	Obs	12.8	19.4	23.9	27.2	31.1	35.0	37.2	37.2	35.0	27.2	21.7	15.0	19.4	31.1	37.2	35.0	37.2
	Est	16.0	17.4	21.3	27.7	32.7	34.2	39.1	40.8	36.3	28.4	18.9	15.2	17.9	32.8	41.0	36.3	41.0
	Err	3.2	-2.0	-2.6	0.5	1.6	-0.8	1.9	3.6	1.3	1.2	-2.8	0.2	-1.5	1.7	3.8	1.3	3.8
Saint Ignatius	Obs	19.4	20.0	27.8	28.3	35.0	38.3	37.8	38.9	36.7	28.3	22.8	16.1	20.0	35.0	38.9	36.7	38.9
	Est	18.9	20.0	24.4	30.9	37.1	37.3	40.2	41.5	36.6	29.0	20.3	17.4	20.6	37.1	41.7	36.6	41.8
	Err	-0.5	0.0	-3.4	2.6	2.1	-1.0	2.4	2.6	-0.1	0.7	-2.5	1.3	0.6	2.1	2.8	-0.1	2.9
Seeley Lake RS	Obs	12.8	16.1	19.4	27.8	30.0	34.4	36.1	38.3	34.4	28.9	18.3	13.3	16.1	30.0	38.3	34.4	38.3
	Est	13.3	17.0	21.3	29.6	35.6	36.0	38.3	40.7	38.4	31.8	17.9	12.1	17.0	35.6	40.8	38.4	40.9
	Err	0.5	0.9	1.9	1.8	5.6	1.6	2.2	2.4	4.0	2.9	-0.4	-1.2	0.9	5.6	2.5	4.0	2.6
Superior	Obs	14.4	20.0	22.8	32.2	36.1	35.6	38.9	39.4	37.8	28.9	23.3	11.7	20.0	36.1	39.4	37.8	39.4
	Est	14.4	18.2	25.2	33.6	38.6	39.4	42.0	43.4	40.5	32.6	17.9	12.5	18.3	38.6	43.6	40.5	43.7
	Err	0.0	-1.8	2.4	1.4	2.5	3.8	3.1	4.0	2.7	3.7	-5.4	0.8	-1.7	2.5	4.2	2.7	4.3
Mean Error		1.9	1.5	1.7	2.0	2.3	3.0	3.1	3.9	1.7	1.7	2.3	1.3	1.7	2.3	4.0	1.7	4.0

**Table B-3: Minimum of observed and estimated daily maximum SAT time series and related error over the validation period**

Station	Value	Jan	Feb	Mar	Apr	May	Jun	Jul	Aug	Sep	Oct	Nov	Dec	Win	Spr	Sum	Fal	Ann
Bigfork 13S	Obs	-17.2	-23.3	-9.4	1.1	5.0	8.9	11.1	7.8	7.2	-1.7	-15.0	-20.6	-23.3	-9.4	7.8	-15.0	-23.3
	Est	-16.2	-15.9	-4.6	0.4	5.2	8.1	15.1	9.1	3.9	-4.3	-11.9	-26.2	-26.2	-4.6	7.6	-11.9	-26.2
	Err	1.0	7.4	4.8	-0.7	0.2	-0.8	4.0	1.3	-3.3	-2.6	3.1	-5.6	-2.9	4.8	-0.2	3.1	-2.9
Hot Springs Montana	Obs	-17.8	-8.3	-9.4	2.8	7.2	6.7	18.9	16.1	11.7	-1.7	-5.6	-8.9	-17.8	-9.4	6.7	-5.6	-17.8
	Est	-16.5	-8.6	-7.0	2.5	5.8	9.5	17.1	15.3	10.0	-0.4	-7.3	-11.4	-16.5	-7.0	9.5	-7.4	-16.5
	Err	1.3	-0.3	2.4	-0.3	-1.4	2.8	-1.8	-0.8	-1.7	1.3	-1.7	-2.5	1.3	2.4	2.8	-1.8	1.3
Kraft Creek	Obs	-19.2	-8.6	-10.3	-0.6	0.7	3.1	11.4	11.5	4.5	-5.9	-7.6	-11.9	-19.2	-10.3	3.1	-7.6	-19.2
	Est	-16.4	-9.2	-13.9	-2.5	-1.3	-0.8	12.7	8.4	3.0	-6.0	-10.3	-15.0	-17.2	-13.9	-0.8	-10.4	-17.4
	Err	2.8	-0.6	-3.6	-1.9	-2.0	-3.9	1.3	-3.1	-1.5	-0.1	-2.7	-3.1	2.0	-3.6	-3.9	-2.8	1.8
Missoula Int. Airport	Obs	-16.7	-25.0	-11.7	1.7	3.9	6.7	12.8	9.4	5.0	-3.9	-14.4	-25.0	-25.0	-11.7	6.7	-14.4	-25.0
	Est	-20.0	-19.1	-6.9	-0.1	4.3	7.9	14.8	10.7	3.8	-5.2	-14.9	-27.6	-27.6	-6.9	7.7	-14.9	-27.6
	Err	-3.3	5.9	4.8	-1.8	0.4	1.2	2.0	1.3	-1.2	-1.3	-0.5	-2.6	-2.6	4.8	1.0	-0.5	-2.6
Moss Peak	Obs	-19.6	-12.0	-9.9	-4.1	-0.5	0.5	7.6	6.3	1.2	-12.0	-13.4	-12.5	-19.6	-9.9	0.5	-13.4	-19.6
	Est	-16.0	-14.4	-17.1	-8.1	-4.8	-5.0	7.7	3.2	-2.0	-11.0	-14.6	-15.1	-16.9	-17.1	-5.0	-14.8	-18.1
	Err	3.6	-2.4	-7.2	-4.0	-4.3	-5.5	0.1	-3.1	-3.2	1.0	-1.2	-2.6	2.7	-7.2	-5.5	-1.4	1.5
North Fork Jocko	Obs	-18.3	-11.4	-9.2	-1.3	-0.1	1.3	9.0	7.5	2.5	-8.8	-11.4	-9.7	-18.3	-9.2	1.3	-11.4	-18.3
	Est	-14.4	-12.0	-13.9	-5.1	-3.4	-3.6	10.4	5.4	-0.4	-10.1	-12.4	-13.5	-14.8	-13.9	-3.6	-12.5	-15.5
	Err	3.9	-0.6	-4.7	-3.8	-3.3	-4.9	1.4	-2.1	-2.9	-1.3	-1.0	-3.8	3.5	-4.7	-4.9	-1.1	2.8
Polson Kerr Dam	Obs	-18.9	-21.1	-10.0	2.8	7.8	10.6	16.1	8.3	7.8	-1.7	-14.4	-24.4	-24.4	-10.0	8.3	-14.4	-24.4
	Est	-19.5	-18.6	-6.9	1.8	6.4	10.5	15.1	10.9	4.2	-3.8	-14.4	-24.4	-24.5	-6.9	9.7	-14.4	-24.5
	Err	-0.6	2.5	3.1	-1.0	-1.4	-0.1	-1.0	2.6	-3.6	-2.1	0.0	0.0	-0.1	3.1	1.4	0.0	-0.1
Saint Ignatius	Obs	-20.0	-21.7	-10.6	2.8	6.1	11.1	15.0	15.0	6.7	-1.7	-15.0	-28.9	-28.9	-10.6	11.1	-15.0	-28.9
	Est	-19.4	-18.2	-3.9	2.2	6.5	11.2	15.2	12.5	6.1	-2.9	-12.0	-23.7	-23.9	-3.9	10.9	-12.0	-23.9
	Err	0.6	3.5	6.7	-0.6	0.4	0.1	0.2	-2.5	-0.6	-1.2	3.0	5.2	5.0	6.7	-0.2	3.0	5.0
Seeley Lake RS	Obs	-22.8	-12.2	-10.0	-1.1	4.4	7.8	10.6	11.7	3.3	-3.3	-13.3	-22.2	-22.8	-10.0	7.8	-13.3	-22.8
	Est	-16.5	-16.6	-6.1	-2.1	3.7	8.1	15.6	10.2	3.5	-7.2	-14.9	-23.7	-23.7	-6.2	7.8	-14.9	-23.7
	Err	6.3	-4.4	3.9	-1.0	-0.7	0.3	5.0	-1.5	0.2	-3.9	-1.6	-1.5	-0.9	3.8	0.0	-1.6	-0.9
Superior	Obs	-15.0	-20.6	-6.7	3.3	8.3	10.0	13.9	10.0	8.3	0.0	-11.1	-20.6	-20.6	-6.7	10.0	-11.1	-20.6
	Est	-14.3	-12.9	-2.5	0.3	5.1	9.9	16.1	14.7	7.5	-4.5	-11.9	-20.0	-20.0	-2.7	9.8	-11.9	-20.0
	Err	0.7	7.7	4.2	-3.0	-3.2	-0.1	2.2	4.7	-0.8	-4.5	-0.8	0.6	0.6	4.0	-0.2	-0.8	0.6
Mean Error		2.4	3.5	4.5	1.8	1.7	2.0	1.9	2.3	1.9	1.9	1.6	2.7	2.2	4.5	2.0	1.6	2.0

**Table B-4: Variance of observed and estimated daily maximum SAT time series and related error over the validation period**

Station	Value	Jan	Feb	Mar	Apr	May	Jun	Jul	Aug	Sep	Oct	Nov	Dec	Win	Spr	Sum	Fal	Ann
Bigfork 13S	Obs	29.3	32.9	16.2	18.0	22.9	21.1	20.3	16.4	26.2	18.8	26.9	28.2	30.7	36.5	23.3	56.4	100
	Est	28.6	25.9	15.9	22.2	26.8	26.6	17.8	27.5	30.5	24.2	19.7	34.2	30.7	37.7	29.4	64.5	114
	Err	-0.7	-6.9	-0.3	4.2	3.9	5.6	-2.5	11.1	4.4	5.4	-7.2	6.0	0.0	1.2	6.1	8.1	13.7
Hot Springs Montana	Obs	32.4	23.8	35.8	24.8	34.5	36.2	25.5	24.9	32.3	40.4	24.7	19.3	27.2	48.1	40.9	86.7	136
	Est	50.1	22.6	36.6	26.4	32.3	36.1	29.3	23.5	28.4	32.1	24.6	29.9	35.1	48.7	38.9	77.5	130
	Err	17.7	-1.1	0.8	1.6	-2.2	-0.1	3.8	-1.3	-3.9	-8.3	-0.1	10.6	7.9	0.6	-2.0	-9.2	-5.6
Kraft Creek	Obs	28.9	18.7	26.0	23.0	31.8	36.7	23.2	24.3	34.6	36.9	23.0	18.9	23.7	37.6	36.8	65.2	99.3
	Est	33.3	21.4	50.8	32.2	40.9	63.5	32.6	34.0	37.5	46.1	29.2	33.2	31.7	55.7	53.1	74.0	121
	Err	4.3	2.7	24.8	9.2	9.1	26.8	9.4	9.7	2.9	9.2	6.2	14.4	8.0	18.1	16.3	8.8	21.2
Missoula Int. Airport	Obs	31.4	38.8	24.5	29.7	35.1	32.9	27.4	25.5	41.0	30.3	29.1	34.6	38.2	45.6	34.2	83.9	137
	Est	36.3	29.3	25.9	29.0	33.2	30.1	22.3	29.4	40.9	30.0	27.8	38.2	37.4	46.2	34.1	85.1	143
	Err	4.9	-9.5	1.4	-0.8	-1.9	-2.8	-5.1	3.9	-0.1	-0.2	-1.3	3.6	-0.8	0.6	-0.1	1.1	5.7
Moss Peak	Obs	23.0	20.7	25.1	23.2	26.5	32.1	19.5	22.3	32.5	37.0	27.2	16.7	20.5	35.4	33.2	56.9	82.0
	Est	23.0	25.5	41.5	33.4	30.5	51.9	25.1	28.0	33.7	42.8	34.5	20.8	23.8	46.7	45.1	62.2	93.2
	Err	0.0	4.8	16.4	10.2	3.9	19.8	5.6	5.7	1.2	5.8	7.3	4.0	3.3	11.3	11.9	5.3	11.2
North Fork Jocko	Obs	21.8	18.9	27.3	21.1	25.4	32.1	20.8	23.5	36.3	38.5	27.2	12.7	18.5	34.1	34.5	63.1	87.5
	Est	22.1	18.5	36.0	27.4	30.5	49.6	22.5	25.9	31.1	43.6	32.5	17.4	20.3	44.1	43.1	64.8	99.1
	Err	0.4	-0.4	8.8	6.3	5.1	17.5	1.7	2.4	-5.2	5.1	5.3	4.7	1.8	10.0	8.7	1.7	11.6
Polson Kerr Dam	Obs	27.7	37.0	20.3	21.2	23.0	20.8	20.6	18.9	29.5	23.6	28.3	31.2	34.2	38.8	26.0	73.6	121
	Est	34.8	36.2	20.5	20.3	20.9	16.7	17.0	22.5	31.0	25.4	26.8	34.9	37.0	36.4	24.7	71.0	118
	Err	7.0	-0.8	0.2	-0.8	-2.0	-4.1	-3.6	3.6	1.5	1.8	-1.5	3.7	2.8	-2.4	-1.3	-2.6	-3.0
Saint Ignatius	Obs	35.9	45.7	24.9	25.2	27.6	27.3	22.4	20.0	33.6	28.8	34.0	41.5	43.2	42.4	28.1	76.7	123
	Est	41.6	41.2	23.1	24.9	27.2	23.4	20.2	19.9	29.8	25.8	28.1	38.0	42.9	39.8	26.3	74.2	126
	Err	5.7	-4.6	-1.8	-0.4	-0.3	-3.9	-2.1	0.0	-3.8	-3.0	-5.9	-3.5	-0.4	-2.7	-1.8	-2.5	3.2
Seeley Lake RS	Obs	36.4	20.5	24.8	30.9	27.7	28.5	14.7	23.8	36.2	38.1	24.5	29.0	34.0	47.0	28.5	79.4	126
	Est	24.4	28.5	18.6	30.3	28.9	25.9	16.0	22.7	39.2	39.3	24.3	30.5	31.6	39.7	28.3	85.7	123
	Err	-12.0	8.0	-6.2	-0.6	1.3	-2.7	1.4	-1.1	2.9	1.2	-0.2	1.5	-2.4	-7.3	-0.2	6.3	-3.3
Superior	Obs	22.4	31.1	22.0	30.7	32.7	31.6	25.2	20.1	39.4	29.7	23.0	23.7	30.5	43.8	31.2	81.8	128
	Est	22.5	24.4	21.2	34.4	33.8	27.8	19.6	23.6	35.8	33.3	20.6	23.4	27.8	43.8	29.3	88.0	130
	Err	0.0	-6.7	-0.8	3.7	1.1	-3.7	-5.7	3.5	-3.5	3.5	-2.4	-0.3	-2.7	0.0	-2.0	6.1	2.4
Mean Error		5.3	4.6	6.1	3.8	3.1	8.7	4.1	4.2	2.9	4.4	3.7	5.2	3.0	5.4	5.0	5.2	8.1

**Table B-5: POT (25°C) of observed and estimated daily maximum SAT time series and related error over the validation period**

Station	Value	Jan	Feb	Mar	Apr	May	Jun	Jul	Aug	Sep	Oct	Nov	Dec	Win	Spr	Sum	Fal	Ann
Bigfork 13S	Obs	0.0	0.0	0.0	0.0	2.2	6.9	16.9	18.0	4.6	0.1	0.0	0.0	0.0	2.2	41.7	4.6	48.5
	Est	0.0	0.0	0.0	0.2	3.7	9.7	22.7	20.9	6.3	0.2	0.0	0.0	0.0	3.9	53.3	6.5	63.7
	Err	0.0	0.0	0.0	0.2	1.5	2.8	5.9	2.9	1.8	0.1	0.0	0.0	0.0	1.8	11.6	1.9	15.3
Hot Springs Montana	Obs	0.0	0.0	0.2	0.8	5.8	13.2	27.8	26.6	14.6	2.4	0.0	0.0	0.0	6.8	67.6	17.0	91.4
	Est	0.0	0.0	0.1	0.6	4.8	12.4	25.7	26.2	10.4	1.0	0.0	0.0	0.0	5.5	64.3	11.3	81.1
	Err	0.0	0.0	-0.1	-0.2	-1.0	-0.8	-2.1	-0.4	-4.2	-1.4	0.0	0.0	0.0	-1.3	-3.3	-5.7	-10.3
Kraft Creek	Obs	0.0	0.0	0.0	0.0	1.8	5.2	16.8	14.4	4.2	0.0	0.0	0.0	0.0	1.8	36.4	4.2	42.4
	Est	0.0	0.0	0.0	0.1	2.2	8.0	18.8	17.1	4.9	0.5	0.0	0.0	0.0	2.4	43.9	5.4	51.7
	Err	0.0	0.0	0.0	0.1	0.4	2.8	2.0	2.7	0.7	0.5	0.0	0.0	0.0	0.6	7.5	1.2	9.3
Missoula Int. Airport	Obs	0.0	0.0	0.0	1.5	5.8	12.6	23.7	24.2	11.7	1.1	0.0	0.0	0.0	7.3	60.5	12.8	80.5
	Est	0.0	0.0	0.0	1.0	5.1	11.6	24.8	23.8	10.5	0.5	0.0	0.0	0.0	6.1	60.2	11.0	77.3
	Err	0.0	0.0	0.0	-0.5	-0.6	-1.0	1.1	-0.4	-1.1	-0.6	0.0	0.0	0.0	-1.1	-0.3	-1.7	-3.1
Moss Peak	Obs	0.0	0.0	0.0	0.0	0.0	0.4	3.8	2.0	0.4	0.0	0.0	0.0	0.0	0.0	6.2	0.4	6.6
	Est	0.0	0.0	0.0	0.0	0.1	1.2	5.4	3.9	0.4	0.0	0.0	0.0	0.0	0.1	10.5	0.4	11.0
	Err	0.0	0.0	0.0	0.0	0.1	0.8	1.6	1.9	0.0	0.0	0.0	0.0	0.0	0.1	4.3	0.0	4.4
North Fork Jocko	Obs	0.0	0.0	0.0	0.0	0.2	0.8	9.4	8.4	1.6	0.0	0.0	0.0	0.0	0.2	18.6	1.6	20.4
	Est	0.0	0.0	0.0	0.0	0.2	2.1	9.1	7.0	0.7	0.0	0.0	0.0	0.0	0.2	18.2	0.7	19.1
	Err	0.0	0.0	0.0	0.0	0.0	1.3	-0.3	-1.4	-0.9	0.0	0.0	0.0	0.0	0.0	-0.4	-0.9	-1.3
Polson Kerr Dam	Obs	0.0	0.0	0.0	0.5	4.9	9.9	23.6	24.8	10.3	0.5	0.0	0.0	0.0	5.3	58.3	10.7	74.3
	Est	0.0	0.0	0.0	0.2	2.6	7.7	22.0	22.0	7.7	0.3	0.0	0.0	0.0	2.8	51.8	8.0	62.6
	Err	0.0	0.0	0.0	-0.2	-2.2	-2.2	-1.6	-2.7	-2.6	-0.1	0.0	0.0	0.0	-2.5	-6.5	-2.7	-11.7
Saint Ignatius	Obs	0.0	0.0	0.1	1.1	5.8	12.6	22.7	24.3	10.6	0.6	0.0	0.0	0.0	7.0	59.5	11.2	77.7
	Est	0.0	0.0	0.0	0.9	5.5	13.3	24.9	26.1	9.9	0.4	0.0	0.0	0.0	6.5	64.3	10.4	81.1
	Err	0.0	0.0	0.0	-0.2	-0.3	0.7	2.3	1.8	-0.7	-0.2	0.0	0.0	0.0	-0.4	4.8	-0.8	3.5
Seeley Lake RS	Obs	0.0	0.0	0.0	0.6	2.5	10.2	24.2	22.7	10.2	1.5	0.0	0.0	0.0	3.1	57.1	11.7	71.8
	Est	0.0	0.0	0.0	0.4	3.0	9.1	22.3	23.2	9.9	1.2	0.0	0.0	0.0	3.5	54.6	11.1	69.2
	Err	0.0	0.0	0.0	-0.2	0.5	-1.1	-1.9	0.6	-0.3	-0.2	0.0	0.0	0.0	0.4	-2.4	-0.6	-2.6
Superior	Obs	0.0	0.0	0.0	2.5	7.8	14.9	24.7	24.6	13.1	2.1	0.0	0.0	0.0	10.3	64.1	15.2	89.5
	Est	0.0	0.0	0.0	2.5	7.7	14.8	26.7	26.3	14.3	1.4	0.0	0.0	0.0	10.3	67.8	15.7	93.8
	Err	0.0	0.0	0.0	0.0	0.0	0.0	2.1	1.7	1.2	-0.7	0.0	0.0	0.0	0.0	3.8	0.5	4.3
Mean Error		0.0	0.0	0.0	0.2	0.7	1.4	2.1	1.7	1.3	0.4	0.0	0.0	0.0	0.8	4.5	1.6	6.6

**Table B-6: PBT (0°C) of observed and estimated daily maximum SAT time series and related error over the validation period**

Station	Value	Jan	Feb	Mar	Apr	May	Jun	Jul	Aug	Sep	Oct	Nov	Dec	Win	Spr	Sum	Fal	Ann
Bigfork 13S	Obs	10.7	6.4	1.2	0.0	0.0	0.0	0.0	0.0	0.0	0.3	3.3	11.6	28.6	1.2	0.0	3.6	33.3
	Est	11.5	6.9	0.6	0.0	0.0	0.0	0.0	0.0	0.0	0.3	3.7	11.6	30.0	0.6	0.0	4.0	34.6
	Err	0.8	0.6	-0.6	0.0	0.0	0.0	0.0	0.0	0.0	0.0	0.4	0.1	1.5	-0.6	0.0	0.4	1.3
Hot Springs Montana	Obs	13.0	4.4	2.0	0.0	0.0	0.0	0.0	0.0	0.0	0.8	4.6	12.2	29.6	2.0	0.0	5.4	37.0
	Est	11.2	7.0	2.4	0.0	0.0	0.0	0.0	0.0	0.0	0.2	3.9	11.0	29.1	2.4	0.0	4.1	35.6
	Err	-1.8	2.6	0.4	0.0	0.0	0.0	0.0	0.0	0.0	-0.6	-0.7	-1.2	-0.5	0.4	0.0	-1.3	-1.4
Kraft Creek	Obs	13.6	5.4	3.4	0.2	0.0	0.0	0.0	0.0	0.0	1.0	7.0	13.6	32.6	3.6	0.0	8.0	44.2
	Est	13.0	7.2	5.5	0.6	0.2	0.2	0.0	0.0	0.0	1.8	7.3	16.7	36.9	6.3	0.2	9.2	52.6
	Err	-0.6	1.8	2.1	0.4	0.2	0.2	0.0	0.0	0.0	0.8	0.3	3.1	4.3	2.7	0.2	1.2	8.4
Missoula Int. Airport	Obs	13.6	6.7	0.9	0.0	0.0	0.0	0.0	0.0	0.0	0.2	5.6	18.3	38.5	0.9	0.0	5.8	45.1
	Est	16.1	8.3	1.1	0.0	0.0	0.0	0.0	0.0	0.0	0.3	5.6	17.5	42.0	1.2	0.0	5.9	49.1
	Err	2.5	1.7	0.3	0.0	0.0	0.0	0.0	0.0	0.0	0.1	0.0	-0.7	3.5	0.3	0.0	0.2	4.0
Moss Peak	Obs	20.2	16.8	12.0	2.4	0.4	0.0	0.0	0.0	0.0	4.0	14.8	21.2	58.2	14.8	0.0	18.8	91.8
	Est	20.6	16.0	12.5	5.2	1.5	1.1	0.0	0.0	0.4	6.5	14.1	22.9	59.5	19.2	1.1	21.0	101
	Err	0.4	-0.8	0.5	2.8	1.1	1.1	0.0	0.0	0.4	2.5	-0.7	1.7	1.3	4.4	1.1	2.2	9.1
North Fork Jocko	Obs	15.8	12.8	6.4	0.4	0.2	0.0	0.0	0.0	0.0	1.8	10.6	17.2	45.8	7.0	0.0	12.4	65.2
	Est	18.6	14.5	9.7	2.4	0.7	0.6	0.0	0.0	0.1	4.2	11.9	22.4	55.6	12.8	0.6	16.3	85.3
	Err	2.8	1.7	3.3	2.0	0.5	0.6	0.0	0.0	0.1	2.4	1.3	5.2	9.8	5.8	0.6	3.9	20.1
Polson Kerr Dam	Obs	10.8	6.2	1.0	0.0	0.0	0.0	0.0	0.0	0.0	0.2	3.9	13.6	30.5	1.0	0.0	4.1	35.5
	Est	13.3	7.9	1.0	0.0	0.0	0.0	0.0	0.0	0.0	0.2	4.6	14.4	35.6	1.1	0.0	4.8	41.5
	Err	2.5	1.7	0.1	0.0	0.0	0.0	0.0	0.0	0.0	0.1	0.7	0.9	5.1	0.1	0.0	0.8	6.0
Saint Ignatius	Obs	9.3	6.0	1.1	0.0	0.0	0.0	0.0	0.0	0.0	0.2	4.1	13.1	28.4	1.1	0.0	4.3	33.7
	Est	13.2	6.2	0.4	0.0	0.0	0.0	0.0	0.0	0.0	0.2	4.2	12.4	31.8	0.4	0.0	4.4	36.5
	Err	3.9	0.3	-0.7	0.0	0.0	0.0	0.0	0.0	0.0	0.0	0.1	-0.7	3.4	-0.7	0.0	0.1	2.9
Seeley Lake RS	Obs	16.5	5.0	2.4	0.1	0.0	0.0	0.0	0.0	0.0	0.2	4.6	16.0	37.4	2.4	0.0	4.7	44.5
	Est	13.4	5.9	0.7	0.2	0.0	0.0	0.0	0.0	0.0	0.5	5.0	15.5	34.8	0.9	0.0	5.5	41.2
	Err	-3.0	0.9	-1.6	0.1	0.0	0.0	0.0	0.0	0.0	0.4	0.4	-0.4	-2.5	-1.5	0.0	0.8	-3.2
Superior	Obs	7.8	3.6	0.5	0.0	0.0	0.0	0.0	0.0	0.0	0.1	2.5	12.4	23.7	0.5	0.0	2.6	26.8
	Est	10.4	3.6	0.1	0.0	0.0	0.0	0.0	0.0	0.0	0.2	3.0	12.2	26.3	0.2	0.0	3.2	29.6
	Err	2.7	0.1	-0.3	0.0	0.0	0.0	0.0	0.0	0.0	0.1	0.5	-0.2	2.6	-0.3	0.0	0.6	2.9
Mean Error		2.1	1.2	1.0	0.5	0.2	0.2	0.0	0.0	0.1	0.7	0.5	1.4	3.5	1.7	0.2	1.1	5.9

**Table B-7: 95<sup>th</sup> percentile of observed and estimated daily maximum SAT time series and related error over the validation period**

Station	Value	Jan	Feb	Mar	Apr	May	Jun	Jul	Aug	Sep	Oct	Nov	Dec	Win	Spr	Sum	Fal	Ann
Bigfork 13S	Obs	8.9	10.0	13.9	20.6	25.6	28.9	32.1	31.1	27.2	20.5	12.8	8.3	8.9	23.3	31.1	25.0	28.3
	Est	9.4	10.7	15.1	21.5	27.6	31.0	34.5	35.5	29.1	20.2	11.6	8.8	9.7	24.5	34.3	26.2	30.8
	Err	0.5	0.7	1.2	0.9	2.0	2.1	2.4	4.4	1.9	-0.2	-1.2	0.5	0.8	1.2	3.2	1.2	2.5
Hot Springs Montana	Obs	10.9	11.7	19.1	23.3	30.8	33.1	39.4	37.8	32.8	25.6	14.4	9.0	10.6	26.1	37.8	30.6	35.0
	Est	13.8	11.0	18.9	23.1	28.8	33.3	39.4	37.3	31.8	23.8	13.6	11.1	12.1	25.5	37.5	28.7	33.5
	Err	3.0	-0.7	-0.1	-0.2	-1.9	0.3	0.0	-0.5	-1.0	-1.8	-0.8	2.2	1.5	-0.6	-0.3	-1.9	-1.5
Kraft Creek	Obs	9.2	10.7	14.1	18.9	25.4	27.3	32.3	31.3	27.0	21.7	12.8	7.0	9.0	20.4	31.6	24.7	28.6
	Est	9.3	10.2	17.1	20.3	26.0	32.0	36.4	34.6	28.8	22.0	12.0	8.9	9.6	22.8	34.9	25.6	30.4
	Err	0.1	-0.5	3.1	1.4	0.5	4.7	4.1	3.3	1.9	0.3	-0.8	1.9	0.6	2.4	3.3	0.9	1.8
Missoula Int. Airport	Obs	7.8	11.1	17.8	24.4	28.9	33.3	36.1	35.6	31.7	23.9	12.8	7.2	9.4	26.7	35.0	28.9	32.2
	Est	8.7	10.2	17.5	23.9	29.3	32.5	36.6	37.7	32.2	22.3	12.6	7.5	9.1	26.1	36.4	28.9	32.7
	Err	0.9	-0.9	-0.3	-0.5	0.4	-0.8	0.5	2.1	0.5	-1.7	-0.2	0.3	-0.3	-0.6	1.4	0.0	0.5
Moss Peak	Obs	5.7	7.4	10.7	15.2	19.3	21.4	26.2	25.1	22.2	16.1	8.9	4.8	6.3	15.4	25.4	19.4	23.0
	Est	4.8	7.1	11.2	15.3	18.4	24.3	28.3	27.0	22.2	16.1	9.3	4.1	5.6	16.3	27.2	19.2	23.3
	Err	-0.9	-0.3	0.5	0.1	-0.8	2.9	2.2	1.9	0.0	0.1	0.3	-0.7	-0.6	0.9	1.8	-0.3	0.4
North Fork Jocko	Obs	6.6	9.0	12.9	16.8	20.9	23.3	28.6	27.7	24.8	19.2	10.9	4.3	6.7	17.3	27.8	22.0	25.3
	Est	5.5	6.3	11.7	16.0	20.2	25.7	30.1	28.7	23.4	17.6	10.3	3.7	5.4	17.6	28.8	20.9	25.1
	Err	-1.1	-2.7	-1.2	-0.8	-0.7	2.5	1.5	1.0	-1.4	-1.5	-0.6	-0.6	-1.3	0.3	1.0	-1.1	-0.2
Polson Kerr Dam	Obs	8.9	11.7	16.7	23.3	28.3	31.7	34.4	34.4	29.7	22.2	13.3	7.8	10.0	25.6	34.4	27.8	31.7
	Est	9.5	11.8	15.9	21.7	26.3	29.1	34.0	35.1	29.8	21.5	12.8	8.8	10.3	23.7	33.8	26.9	30.4
	Err	0.6	0.1	-0.8	-1.6	-2.0	-2.6	-0.4	0.7	0.1	-0.7	-0.5	1.0	0.3	-1.9	-0.6	-0.9	-1.3
Saint Ignatius	Obs	10.6	13.3	18.3	24.4	28.9	32.2	35.0	34.4	30.1	23.3	14.4	10.0	11.7	26.7	34.4	28.3	32.2
	Est	11.1	13.9	18.7	24.0	29.1	32.3	35.8	36.1	30.9	22.0	14.0	10.4	12.2	26.1	35.4	28.1	32.2
	Err	0.5	0.6	0.4	-0.4	0.2	0.1	0.8	1.7	0.8	-1.3	-0.4	0.4	0.5	-0.6	1.0	-0.2	0.0
Seeley Lake RS	Obs	6.7	11.1	15.6	22.2	26.1	30.6	33.0	33.9	30.0	24.5	13.3	7.8	9.0	23.9	33.3	27.8	30.6
	Est	7.8	11.7	15.6	22.2	27.0	30.5	33.8	35.4	31.7	24.2	11.9	7.1	9.6	24.1	34.0	28.7	31.0
	Err	1.1	0.6	0.0	0.0	0.9	-0.1	0.8	1.5	1.7	-0.3	-1.4	-0.7	0.6	0.2	0.7	0.9	0.4
Superior	Obs	8.9	13.9	19.4	26.1	30.0	33.3	36.1	36.7	33.3	25.6	14.4	7.2	11.1	28.3	35.6	30.6	33.3
	Est	9.0	13.0	19.4	26.5	31.0	33.6	37.0	37.8	33.7	24.8	12.5	7.6	10.8	28.1	36.8	30.7	33.5
	Err	0.1	-0.9	0.0	0.4	1.0	0.3	0.9	1.1	0.4	-0.8	-1.9	0.4	-0.3	-0.2	1.2	0.1	0.2
Mean Error		0.9	0.8	0.8	0.6	1.0	1.6	1.4	1.8	1.0	0.9	0.8	0.8	0.7	0.9	1.4	0.7	0.9

**Table B-8: Median of observed and estimated daily minimum SAT time series and related error over the validation period**

Station	Value	Jan	Feb	Mar	Apr	May	Jun	Jul	Aug	Sep	Oct	Nov	Dec	Win	Spr	Sum	Fal	Ann
Bigfork 13S	Obs	-2.8	-2.8	-1.1	1.7	5.6	9.4	12.2	12.2	7.8	3.3	0.0	-3.3	-2.8	1.7	11.1	3.3	2.8
	Est	-4.8	-2.9	-1.5	1.0	4.7	8.1	10.4	10.7	5.9	1.3	-1.6	-4.7	-4.2	1.4	9.8	1.7	2.1
	Err	-2.0	-0.1	-0.4	-0.7	-0.9	-1.3	-1.8	-1.5	-1.9	-2.0	-1.6	-1.4	-1.4	-0.3	-1.3	-1.6	-0.7
Hot Springs Montana	Obs	-5.0	-5.0	-1.1	0.6	5.0	8.3	12.8	11.7	7.8	1.7	-2.2	-3.9	-4.4	1.1	11.1	2.8	1.7
	Est	-5.3	-5.7	-2.0	1.8	5.3	9.2	13.1	12.0	7.5	2.5	-1.8	-4.2	-5.0	1.5	11.5	3.0	2.6
	Err	-0.3	-0.7	-0.9	1.2	0.3	0.9	0.3	0.3	-0.3	0.8	0.4	-0.3	-0.6	0.4	0.4	0.2	0.9
Kraft Creek	Obs	-5.9	-6.3	-2.7	-0.3	2.5	5.7	9.9	9.1	4.9	0.7	-3.5	-6.6	-6.3	-0.3	8.1	0.9	0.5
	Est	-8.2	-8.8	-5.3	-1.9	1.3	4.5	8.7	8.2	3.9	-0.2	-4.2	-7.8	-8.3	-1.7	7.3	0.4	-0.2
	Err	-2.3	-2.5	-2.6	-1.6	-1.2	-1.1	-1.2	-0.9	-1.0	-0.9	-0.7	-1.2	-2.0	-1.4	-0.8	-0.5	-0.7
Missoula Int. Airport	Obs	-6.7	-4.4	-2.2	0.0	4.4	7.8	10.0	10.0	5.0	0.0	-3.3	-8.3	-6.7	0.6	9.4	0.0	0.6
	Est	-8.4	-6.4	-3.2	-0.1	3.8	7.3	9.7	9.5	4.3	-1.1	-4.8	-9.0	-7.9	0.2	8.9	-0.5	0.5
	Err	-1.7	-2.0	-1.0	-0.1	-0.6	-0.5	-0.3	-0.5	-0.7	-1.1	-1.5	-0.7	-1.2	-0.4	-0.5	-0.5	-0.1
Moss Peak	Obs	-6.7	-7.9	-5.7	-3.6	0.2	3.5	8.7	7.9	3.7	-0.8	-4.5	-7.5	-7.4	-3.1	7.1	-0.3	-1.4
	Est	-8.0	-9.7	-7.6	-4.4	-0.7	2.5	8.1	7.8	3.2	-1.9	-5.4	-8.5	-8.8	-4.0	6.3	-1.0	-2.2
	Err	-1.3	-1.8	-1.9	-0.8	-0.9	-1.0	-0.6	-0.1	-0.5	-1.1	-0.9	-1.0	-1.4	-0.9	-0.8	-0.7	-0.8
North Fork Jocko	Obs	-8.4	-11.0	-6.6	-4.3	-1.0	1.8	5.7	5.2	2.0	-1.4	-5.8	-8.7	-9.2	-3.7	4.4	-1.3	-1.9
	Est	-10.0	-11.8	-9.5	-5.0	-2.1	1.2	5.4	4.7	1.0	-2.8	-6.7	-10.3	-10.7	-4.9	3.8	-2.3	-3.1
	Err	-1.6	-0.8	-2.9	-0.7	-1.1	-0.6	-0.3	-0.5	-1.0	-1.4	-0.9	-1.6	-1.5	-1.2	-0.6	-1.0	-1.2
Polson Kerr Dam	Obs	-4.4	-3.3	-1.1	1.1	5.6	8.9	11.1	11.1	6.7	2.2	-1.1	-5.6	-4.4	1.7	10.6	2.2	2.2
	Est	-5.7	-4.3	-2.2	0.7	5.2	8.8	11.0	11.4	6.3	1.1	-2.5	-6.1	-5.4	1.2	10.5	1.5	1.9
	Err	-1.3	-1.0	-1.1	-0.4	-0.4	-0.1	-0.1	0.3	-0.4	-1.1	-1.4	-0.5	-1.0	-0.5	-0.1	-0.7	-0.3
Saint Ignatius	Obs	-4.4	-3.9	-1.7	1.1	4.4	7.8	10.0	9.4	5.6	1.1	-2.2	-6.1	-5.0	1.1	8.9	1.7	1.7
	Est	-7.3	-4.7	-2.6	0.1	4.2	7.9	9.7	9.6	5.0	0.1	-3.3	-7.4	-6.4	0.7	9.1	0.7	1.4
	Err	-2.9	-0.8	-0.9	-1.0	-0.2	0.1	-0.3	0.2	-0.6	-1.0	-1.1	-1.3	-1.4	-0.4	0.2	-1.0	-0.3
Seeley Lake RS	Obs	-10.0	-8.9	-5.0	-2.2	1.7	5.0	6.7	6.1	1.7	-1.7	-4.4	-11.1	-10.0	-2.2	5.6	-1.1	-1.1
	Est	-10.9	-9.5	-6.1	-2.9	1.6	5.3	6.4	5.9	2.1	-1.4	-5.2	-10.5	-10.4	-2.1	5.9	-1.3	-1.1
	Err	-0.9	-0.6	-1.1	-0.7	-0.1	0.3	-0.3	-0.2	0.4	0.3	-0.8	0.6	-0.4	0.1	0.3	-0.2	0.0
Superior	Obs	-5.0	-5.0	-2.2	0.0	3.9	7.8	9.4	9.4	5.0	0.6	-1.7	-6.1	-5.6	0.6	8.9	1.1	1.1
	Est	-6.1	-4.2	-2.4	0.1	4.2	7.9	9.7	9.6	5.1	0.6	-2.6	-6.4	-5.6	0.7	9.1	1.1	1.5
	Err	-1.1	0.8	-0.2	0.1	0.3	0.1	0.3	0.2	0.1	0.0	-0.9	-0.3	0.0	0.1	0.2	0.0	0.4
Mean Error		1.5	1.1	1.3	0.7	0.6	0.6	0.5	0.5	0.7	1.0	1.0	0.9	1.1	0.6	0.5	0.6	0.5

**Table B-9: Maximum of observed and estimated daily minimum SAT time series and related error over the validation period**

Station	Value	Jan	Feb	Mar	Apr	May	Jun	Jul	Aug	Sep	Oct	Nov	Dec	Win	Spr	Sum	Fal	Ann
Bigfork 13S	Obs	7.2	6.7	14.4	11.1	15.6	17.8	23.9	21.1	17.2	12.2	12.2	6.7	7.2	15.6	23.9	17.2	23.9
	Est	8.7	9.0	9.5	11.5	13.8	17.7	18.9	19.7	16.6	11.2	8.9	8.0	9.7	13.8	20.0	16.6	20.0
	Err	1.5	2.3	-4.9	0.4	-1.8	-0.1	-5.0	-1.4	-0.6	-1.0	-3.3	1.3	2.5	-1.8	-3.9	-0.6	-3.9
Hot Springs Montana	Obs	5.6	6.7	12.8	8.3	16.1	16.7	21.1	21.7	16.7	13.3	7.2	2.8	6.7	16.1	21.7	16.7	21.7
	Est	9.2	5.9	7.0	12.3	15.7	17.2	20.5	19.4	16.2	12.0	9.7	7.2	9.8	15.7	20.7	16.2	20.7
	Err	3.6	-0.8	-5.8	4.0	-0.4	0.5	-0.6	-2.3	-0.5	-1.3	2.5	4.4	3.1	-0.4	-1.0	-0.5	-1.0
Kraft Creek	Obs	6.2	3.7	4.8	6.3	9.6	13.0	17.7	17.7	13.3	10.5	4.4	2.9	6.2	9.6	17.7	13.3	17.7
	Est	9.4	3.6	4.7	5.7	9.3	12.3	15.8	14.6	11.7	8.2	8.0	8.2	10.3	9.3	15.9	11.8	16.0
	Err	3.2	-0.1	-0.1	-0.6	-0.3	-0.7	-1.9	-3.1	-1.6	-2.3	3.6	5.3	4.1	-0.3	-1.8	-1.5	-1.7
Missoula Int. Airport	Obs	3.9	4.4	6.1	10.6	13.3	17.2	19.4	19.4	15.6	10.6	10.0	2.8	4.4	13.3	19.4	15.6	19.4
	Est	12.1	9.4	9.2	10.1	13.9	17.7	20.2	20.0	16.5	10.4	9.2	9.0	12.5	13.9	20.8	16.5	20.8
	Err	8.2	5.0	3.1	-0.5	0.6	0.5	0.8	0.6	0.9	-0.2	-0.8	6.2	8.1	0.6	1.4	0.9	1.4
Moss Peak	Obs	2.0	1.2	3.6	4.5	9.1	10.9	16.6	16.3	13.6	9.3	3.0	1.6	2.0	9.1	16.6	13.6	16.6
	Est	4.3	2.5	3.6	5.0	9.2	10.8	16.8	15.7	11.7	8.7	5.4	2.6	4.9	9.2	17.0	11.7	17.0
	Err	2.3	1.3	0.0	0.5	0.1	-0.1	0.2	-0.6	-1.9	-0.6	2.4	1.0	2.9	0.1	0.4	-1.9	0.4
North Fork Jocko	Obs	4.3	0.7	1.3	1.6	3.9	9.8	12.7	11.2	8.3	6.2	1.5	1.9	4.3	3.9	12.7	8.3	12.7
	Est	5.5	2.7	4.1	4.8	5.5	8.3	12.1	11.6	8.9	6.8	5.5	4.7	6.5	6.2	12.3	9.1	12.3
	Err	1.2	2.0	2.8	3.2	1.6	-1.5	-0.6	0.4	0.6	0.6	4.0	2.8	2.2	2.3	-0.4	0.8	-0.4
Polson Kerr Dam	Obs	5.6	6.7	9.4	11.7	15.6	17.8	22.2	20.6	17.2	13.3	12.8	5.6	6.7	15.6	22.2	17.2	22.2
	Est	10.4	8.9	9.2	12.8	16.0	18.3	19.8	20.5	16.0	11.9	9.2	9.2	11.1	16.1	20.8	16.0	20.8
	Err	4.8	2.2	-0.2	1.1	0.4	0.5	-2.4	-0.1	-1.2	-1.4	-3.6	3.6	4.4	0.5	-1.4	-1.2	-1.4
Saint Ignatius	Obs	6.7	8.3	8.9	12.8	15.0	17.2	20.6	18.3	16.7	15.0	13.3	7.2	8.3	15.0	20.6	16.7	20.6
	Est	13.5	11.9	11.5	13.4	15.9	18.0	19.2	18.7	15.6	12.2	10.3	11.6	14.4	16.0	19.7	15.6	19.8
	Err	6.8	3.6	2.6	0.6	0.9	0.8	-1.4	0.4	-1.1	-2.8	-3.0	4.4	6.1	1.0	-0.9	-1.1	-0.8
Seeley Lake RS	Obs	2.2	2.8	2.2	8.9	15.6	14.4	15.6	16.7	13.3	11.1	8.3	1.1	2.8	15.6	16.7	13.3	16.7
	Est	12.0	12.6	10.8	9.7	14.1	15.9	18.3	18.7	13.5	9.7	8.6	9.7	13.7	14.2	19.3	13.6	19.3
	Err	9.8	9.8	8.6	0.8	-1.5	1.5	2.7	2.0	0.2	-1.4	0.3	8.6	10.9	-1.4	2.6	0.3	2.6
Superior	Obs	4.4	7.8	8.3	11.7	13.3	19.4	18.3	18.9	20.0	12.8	11.1	4.4	7.8	13.3	19.4	20.0	20.0
	Est	11.6	9.9	9.4	12.4	15.7	17.5	19.4	19.4	16.1	11.4	10.6	9.2	12.2	15.7	20.0	16.1	20.0
	Err	7.2	2.1	1.1	0.7	2.4	-1.9	1.1	0.5	-3.9	-1.4	-0.5	4.8	4.4	2.4	0.6	-3.9	0.0
Mean Error		4.9	2.9	2.9	1.2	1.0	0.8	1.7	1.2	1.3	1.3	2.4	4.2	4.9	1.1	1.4	1.3	1.4

**Table B-10: Minimum of observed and estimated daily minimum SAT time series and related error over the validation period**

Station	Value	Jan	Feb	Mar	Apr	May	Jun	Jul	Aug	Sep	Oct	Nov	Dec	Win	Spr	Sum	Fal	Ann
Bigfork 13S	Obs	-25.0	-29.4	-22.2	-5.6	-1.7	0.6	-1.1	2.8	-3.3	-10.6	-18.9	-25.6	-29.4	-22.2	-1.1	-18.9	-29.4
	Est	-25.1	-33.6	-18.4	-10.3	-5.3	-1.4	1.8	0.0	-8.3	-11.5	-17.8	-29.8	-33.9	-18.4	-1.7	-17.8	-33.9
	Err	-0.1	-4.2	3.8	-4.7	-3.6	-2.0	2.9	-2.8	-5.0	-0.9	1.1	-4.2	-4.5	3.8	-0.6	1.1	-4.5
Hot Springs Montana	Obs	-25.0	-19.4	-19.4	-7.8	-5.0	2.2	3.9	3.9	-1.7	-17.2	-19.4	-18.9	-25.0	-19.4	2.2	-19.4	-25.0
	Est	-24.1	-17.7	-12.7	-7.5	-5.4	1.4	5.9	3.6	-1.4	-12.8	-14.8	-17.0	-24.1	-12.7	1.3	-15.0	-24.1
	Err	0.9	1.7	6.7	0.3	-0.4	-0.8	2.0	-0.3	0.3	4.4	4.6	1.9	0.9	6.7	-0.9	4.4	0.9
Kraft Creek	Obs	-27.4	-24.6	-22.6	-17.1	-7.1	-0.1	3.0	1.1	-1.8	-18.4	-15.3	-27.6	-27.6	-22.6	-0.1	-18.4	-27.6
	Est	-29.8	-23.0	-17.8	-10.1	-6.7	-1.9	2.0	1.1	-3.7	-13.2	-17.9	-24.7	-30.0	-17.8	-1.9	-17.9	-30.0
	Err	-2.4	1.6	4.8	7.0	0.4	-1.8	-1.0	0.0	-1.9	5.2	-2.6	2.9	-2.4	4.8	-1.8	0.5	-2.4
Missoula Int. Airport	Obs	-31.1	-32.8	-22.8	-8.3	-6.1	-1.1	1.7	-1.1	-6.7	-15.6	-23.9	-34.4	-34.4	-22.8	-1.1	-23.9	-34.4
	Est	-32.4	-27.9	-17.5	-9.7	-6.5	-2.8	-0.3	-1.4	-8.6	-12.9	-21.6	-34.1	-34.8	-17.5	-3.1	-21.6	-34.8
	Err	-1.3	4.9	5.3	-1.4	-0.4	-1.7	-2.0	-0.3	-1.9	2.7	2.3	0.3	-0.4	5.3	-2.0	2.3	-0.4
Moss Peak	Obs	-27.8	-24.9	-19.7	-16.2	-9.0	-1.9	1.3	1.3	-2.5	-20.0	-18.2	-21.2	-27.8	-19.7	-1.9	-20.0	-27.8
	Est	-24.7	-23.5	-21.2	-13.4	-10.0	-4.7	-0.5	-1.6	-5.6	-17.5	-19.2	-22.3	-25.6	-21.2	-4.7	-19.5	-25.6
	Err	3.1	1.4	-1.5	2.8	-1.0	-2.8	-1.8	-2.9	-3.1	2.5	-1.0	-1.1	2.2	-1.5	-2.8	0.5	2.2
North Fork Jocko	Obs	-34.8	-29.7	-26.0	-18.8	-13.3	-2.9	-1.1	-0.4	-3.4	-22.4	-19.7	-27.2	-34.8	-26.0	-2.9	-22.4	-34.8
	Est	-29.8	-26.9	-24.7	-15.9	-9.5	-5.3	-1.6	-3.3	-6.5	-16.5	-21.1	-28.1	-31.1	-24.7	-5.3	-21.1	-31.1
	Err	5.0	2.8	1.3	2.9	3.8	-2.4	-0.5	-2.9	-3.1	5.9	-1.4	-0.9	3.7	1.3	-2.4	1.3	3.7
Polson Kerr Dam	Obs	-25.6	-28.9	-22.8	-7.8	-3.9	0.6	2.8	2.2	-5.6	-12.2	-23.3	-30.0	-30.0	-22.8	0.6	-23.3	-30.0
	Est	-26.1	-22.6	-16.6	-8.5	-4.8	-0.5	2.0	-0.4	-6.9	-11.3	-16.4	-29.0	-29.3	-16.6	-1.3	-16.5	-29.3
	Err	-0.5	6.3	6.2	-0.7	-0.9	-1.1	-0.8	-2.6	-1.3	0.9	6.9	1.0	0.7	6.2	-1.9	6.8	0.7
Saint Ignatius	Obs	-29.4	-33.9	-26.1	-8.3	-5.6	-1.1	2.2	1.1	-7.2	-16.1	-26.1	-33.3	-33.9	-26.1	-1.1	-26.1	-33.9
	Est	-31.5	-24.5	-18.6	-10.4	-6.9	-1.8	0.4	-1.6	-9.5	-13.0	-18.6	-33.3	-33.9	-18.6	-2.5	-18.6	-33.9
	Err	-2.1	9.4	7.5	-2.1	-1.3	-0.7	-1.8	-2.7	-2.3	3.1	7.5	0.0	0.0	7.5	-1.4	7.5	0.0
Seeley Lake RS	Obs	-37.2	-42.8	-31.1	-15.6	-8.3	-2.8	-2.2	-2.8	-9.4	-20.0	-28.9	-42.2	-42.8	-31.1	-2.8	-28.9	-42.8
	Est	-40.7	-46.1	-31.1	-14.2	-9.2	-4.5	-3.3	-4.8	-10.9	-13.1	-23.9	-46.4	-48.7	-31.1	-5.4	-23.9	-48.7
	Err	-3.5	-3.3	0.0	1.4	-0.9	-1.7	-1.1	-2.0	-1.5	6.9	5.0	-4.2	-5.9	0.0	-2.6	5.0	-5.9
Superior	Obs	-27.2	-30.0	-19.4	-10.0	-8.3	-6.7	0.6	0.6	-6.7	-16.1	-20.0	-31.1	-31.1	-19.4	-6.7	-20.0	-31.1
	Est	-27.7	-22.0	-15.8	-10.4	-6.0	-1.5	0.1	-2.2	-9.2	-11.3	-17.4	-26.0	-28.3	-15.8	-2.7	-17.4	-28.3
	Err	-0.5	8.0	3.6	-0.4	2.3	5.2	-0.5	-2.8	-2.5	4.8	2.6	5.1	2.8	3.6	4.0	2.6	2.8
Mean Error		1.9	4.4	4.1	2.4	1.5	2.0	1.4	1.9	2.3	3.7	3.5	2.2	2.4	4.1	2.0	3.2	2.4

**Table B-11: Variance of observed and estimated daily minimum SAT time series and related error over the validation period**

Station	Value	Jan	Feb	Mar	Apr	May	Jun	Jul	Aug	Sep	Oct	Nov	Dec	Win	Spr	Sum	Fal	Ann
Bigfork 13S	Obs	27.9	35.0	12.8	8.8	10.1	8.2	8.1	7.7	10.8	11.9	21.7	28.2	30.2	19.0	9.6	26.3	51.6
	Est	31.6	41.4	17.8	11.5	10.2	10.3	8.4	8.7	14.1	12.4	17.5	35.9	36.6	20.3	10.4	24.3	50.1
	Err	3.7	6.5	5.0	2.7	0.1	2.1	0.3	1.0	3.3	0.5	-4.2	7.7	6.3	1.3	0.8	-2.0	-1.4
Hot Springs Montana	Obs	33.2	24.9	26.3	8.7	16.3	10.5	12.2	10.3	13.4	21.5	23.9	18.2	25.8	25.3	14.1	37.4	59.0
	Est	45.4	21.8	14.2	13.0	17.6	9.3	8.3	9.6	11.4	18.0	24.1	21.8	30.5	24.4	11.6	32.7	59.8
	Err	12.3	-3.1	-12.2	4.3	1.4	-1.2	-3.9	-0.7	-2.0	-3.5	0.3	3.6	4.7	-1.0	-2.5	-4.8	0.9
Kraft Creek	Obs	38.7	25.3	24.7	12.2	11.8	8.9	9.9	11.3	10.1	22.9	20.1	25.5	30.0	23.3	13.0	31.6	53.3
	Est	56.4	27.4	20.0	9.7	10.4	8.0	7.6	7.4	9.9	14.3	26.8	40.9	42.5	21.5	10.8	28.6	56.6
	Err	17.7	2.1	-4.7	-2.5	-1.5	-0.9	-2.3	-3.9	-0.2	-8.7	6.7	15.5	12.5	-1.8	-2.2	-3.1	3.2
Missoula Int. Airport	Obs	42.1	43.2	11.9	12.6	13.2	11.2	9.8	10.4	14.8	13.7	25.1	40.3	42.9	20.2	11.4	31.3	62.9
	Est	53.5	36.9	18.6	10.7	12.3	12.1	11.7	11.5	16.0	14.0	24.9	43.9	46.4	22.4	12.9	32.1	65.3
	Err	11.5	-6.3	6.6	-1.9	-0.9	0.9	1.9	1.0	1.1	0.3	-0.2	3.7	3.5	2.2	1.6	0.8	2.4
Moss Peak	Obs	27.7	19.5	18.2	14.3	14.6	9.8	12.3	9.7	10.6	25.4	21.1	20.1	22.8	22.0	15.3	32.8	51.4
	Est	31.0	25.1	24.3	14.0	14.6	10.3	12.4	12.0	12.5	22.2	26.6	24.3	27.4	26.5	17.5	33.9	56.7
	Err	3.3	5.6	6.1	-0.3	0.1	0.6	0.1	2.3	1.9	-3.2	5.5	4.2	4.5	4.4	2.2	1.1	5.3
North Fork Jocko	Obs	41.9	33.6	26.3	15.0	10.2	7.2	7.7	6.5	6.9	20.6	25.8	33.3	37.3	22.9	9.5	30.7	50.8
	Est	47.5	32.9	28.5	15.6	8.8	7.2	7.7	9.2	9.5	17.5	27.3	39.2	40.8	27.4	11.2	29.1	54.6
	Err	5.6	-0.8	2.2	0.6	-1.4	-0.1	0.0	2.7	2.6	-3.2	1.5	5.9	3.4	4.5	1.6	-1.7	3.8
Polson Kerr Dam	Obs	29.4	39.1	13.6	12.7	11.7	9.9	8.4	9.3	13.8	15.0	23.7	32.0	33.5	21.8	10.5	30.7	57.1
	Est	38.5	28.1	17.8	10.8	12.3	10.6	8.9	10.5	13.2	13.8	17.0	36.0	35.0	23.5	11.2	27.3	57.3
	Err	9.1	-11.0	4.2	-1.9	0.6	0.7	0.5	1.2	-0.6	-1.2	-6.8	4.0	1.5	1.7	0.7	-3.4	0.2
Saint Ignatius	Obs	40.0	52.2	17.6	13.6	13.0	10.7	9.7	10.4	13.9	17.4	32.7	46.4	46.5	22.8	11.0	32.7	57.1
	Est	58.0	36.6	23.3	13.4	14.7	11.5	10.1	10.1	15.5	16.5	22.0	49.9	50.1	25.6	11.2	29.1	60.5
	Err	18.0	-15.6	5.7	-0.2	1.6	0.7	0.4	-0.3	1.6	-0.9	-10.7	3.5	3.6	2.9	0.2	-3.6	3.5
Seeley Lake RS	Obs	64.4	75.3	23.7	13.1	12.8	11.7	10.9	12.6	14.8	14.2	31.0	58.4	65.8	26.8	12.1	30.7	71.2
	Est	72.4	78.4	43.3	14.0	15.3	12.0	12.5	13.2	14.4	13.1	26.9	69.5	73.6	35.9	12.8	27.3	73.4
	Err	8.0	3.0	19.6	0.9	2.5	0.3	1.5	0.7	-0.4	-1.1	-4.1	11.1	7.8	9.2	0.8	-3.5	2.1
Superior	Obs	37.3	37.4	14.1	12.8	13.3	12.6	8.6	10.8	14.4	15.2	23.8	34.6	36.6	20.9	11.5	27.4	53.2
	Est	45.4	29.2	16.7	12.1	13.4	10.7	10.5	11.5	15.9	13.7	21.4	31.1	36.3	22.0	11.6	26.4	52.1
	Err	8.1	-8.2	2.6	-0.7	0.0	-2.0	1.8	0.7	1.5	-1.5	-2.4	-3.5	-0.3	1.0	0.0	-0.9	-1.1
Mean Error		9.7	6.2	6.9	1.6	1.0	0.9	1.3	1.5	1.5	2.4	4.2	6.3	4.8	3.0	1.3	2.5	2.4

**Table B-12: POT (0°C) of observed and estimated daily minimum SAT time series and related error over the validation period**

Station	Value	Jan	Feb	Mar	Apr	May	Jun	Jul	Aug	Sep	Oct	Nov	Dec	Win	Spr	Sum	Fal	Ann
Bigfork 13S	Obs	7.0	6.0	10.9	21.7	29.7	28.8	28.8	29.6	27.8	24.1	13.4	5.8	18.8	62.3	87.2	65.3	233
	Est	5.2	7.9	10.7	18.7	28.6	29.9	31.0	31.0	27.9	20.0	10.0	5.0	18.1	57.9	91.8	58.0	226
	Err	-1.8	1.9	-0.2	-3.0	-1.1	1.1	2.2	1.4	0.2	-4.1	-3.4	-0.8	-0.7	-4.3	4.7	-7.3	-7.6
Hot Springs Montana	Obs	5.0	3.6	13.2	22.2	29.0	30.0	31.0	30.6	29.8	22.8	9.8	4.4	13.0	64.4	91.6	62.4	231
	Est	6.4	3.1	8.9	20.9	27.6	30.0	31.0	31.0	29.5	22.8	10.7	5.6	15.1	57.4	92.0	63.0	228
	Err	1.4	-0.5	-4.3	-1.3	-1.4	0.0	0.0	0.4	-0.3	0.0	0.9	1.2	2.1	-7.0	0.4	0.6	-3.9
Kraft Creek	Obs	4.0	1.0	6.4	13.2	23.8	29.8	31.0	30.8	28.2	19.2	7.0	2.2	7.2	43.4	91.6	54.4	197
	Est	3.9	1.0	2.9	8.5	20.5	28.8	31.0	31.0	27.1	14.9	6.2	3.6	8.5	32.0	90.7	48.2	179
	Err	-0.1	0.0	-3.5	-4.7	-3.3	-1.1	0.0	0.2	-1.1	-4.3	-0.8	1.4	1.3	-11.4	-0.9	-6.2	-17.2
Missoula Int. Airport	Obs	3.0	3.3	8.0	17.0	27.4	29.9	31.0	31.0	27.1	16.3	5.9	1.7	7.9	52.4	91.8	49.2	201
	Est	3.5	3.6	6.8	14.5	26.4	29.5	31.0	30.9	25.7	11.8	4.7	2.1	9.2	47.7	91.4	42.3	191
	Err	0.6	0.3	-1.1	-2.5	-1.0	-0.3	0.0	-0.1	-1.4	-4.5	-1.1	0.4	1.3	-4.6	-0.4	-6.9	-10.7
Moss Peak	Obs	1.0	0.2	1.4	4.6	16.6	26.8	30.8	31.0	27.2	13.4	3.8	0.4	1.6	22.6	88.6	44.4	157
	Est	1.7	0.5	1.4	3.9	13.1	23.4	30.8	30.4	24.3	11.1	4.2	0.8	3.0	18.5	84.6	39.6	146
	Err	0.7	0.3	0.0	-0.7	-3.5	-3.4	0.0	-0.6	-2.9	-2.3	0.4	0.4	1.4	-4.1	-4.0	-4.8	-11.4
North Fork Jocko	Obs	1.0	0.2	1.6	3.4	13.0	23.0	30.4	30.2	22.8	10.4	1.6	1.2	2.4	18.0	83.6	34.8	139
	Est	1.8	0.5	0.9	3.1	7.4	20.1	30.2	28.4	18.8	7.7	2.5	1.2	3.5	11.5	78.7	28.9	123
	Err	0.8	0.3	-0.7	-0.3	-5.6	-2.9	-0.2	-1.8	-4.0	-2.7	0.9	0.0	1.1	-6.5	-4.9	-5.9	-16.2
Polson Kerr Dam	Obs	5.4	5.5	11.2	20.3	29.4	30.0	30.9	30.9	28.8	22.3	10.8	4.1	14.9	60.8	91.7	61.9	229
	Est	4.9	5.2	8.9	17.5	28.8	29.9	31.0	31.0	28.3	19.1	8.0	3.8	14.0	55.3	91.9	55.4	217
	Err	-0.5	-0.2	-2.2	-2.7	-0.6	0.0	0.1	0.1	-0.5	-3.2	-2.8	-0.2	-0.9	-5.5	0.3	-6.5	-12.7
Saint Ignatius	Obs	5.6	6.0	11.0	17.6	27.7	29.3	28.4	29.8	27.1	18.1	9.7	4.4	16.0	56.3	87.4	54.9	215
	Est	4.9	5.8	8.9	15.3	26.9	29.8	31.0	30.9	26.6	15.8	7.2	4.0	14.7	51.1	91.7	49.7	207
	Err	-0.7	-0.2	-2.1	-2.3	-0.7	0.5	2.6	1.1	-0.4	-2.3	-2.5	-0.4	-1.3	-5.1	4.3	-5.2	-7.3
Seeley Lake RS	Obs	0.8	0.8	2.5	7.8	21.0	28.8	30.5	30.2	21.8	10.3	2.7	0.7	2.2	31.3	89.4	34.7	158
	Est	2.5	3.0	4.6	6.5	20.4	28.2	30.2	29.6	21.3	10.8	4.1	1.9	7.5	31.5	88.1	36.2	163
	Err	1.7	2.3	2.1	-1.2	-0.6	-0.5	-0.2	-0.6	-0.5	0.6	1.4	1.3	5.3	0.3	-1.3	1.5	5.7
Superior	Obs	4.3	4.0	8.3	15.8	25.8	28.5	29.9	29.2	24.7	18.2	9.9	3.2	11.5	49.8	87.5	52.7	201
	Est	5.3	5.7	8.5	15.5	27.2	29.8	31.0	30.9	26.6	17.4	8.5	3.5	14.5	51.2	91.7	52.6	210
	Err	1.1	1.7	0.2	-0.2	1.4	1.3	1.1	1.7	2.0	-0.7	-1.4	0.3	3.1	1.4	4.2	-0.1	8.6
Mean Error		0.9	0.8	1.6	1.9	1.9	1.1	0.7	0.8	1.3	2.5	1.6	0.6	1.8	5.0	2.5	4.5	10.1

**Table B-13: PBT (-15°C) of observed and estimated daily minimum SAT time series and related error over the validation period**

Station	Value	Jan	Feb	Mar	Apr	May	Jun	Jul	Aug	Sep	Oct	Nov	Dec	Win	Spr	Sum	Fal	Ann
Bigfork 13S	Obs	1.5	2.2	0.1	0.0	0.0	0.0	0.0	0.0	0.0	0.0	0.7	1.4	5.0	0.1	0.0	0.7	5.8
	Est	1.8	2.0	0.3	0.0	0.0	0.0	0.0	0.0	0.0	0.0	0.2	2.3	6.1	0.3	0.0	0.2	6.6
	Err	0.4	-0.2	0.2	0.0	0.0	0.0	0.0	0.0	0.0	0.0	-0.4	1.0	1.1	0.2	0.0	-0.4	0.9
Hot Springs Montana	Obs	2.2	2.6	1.0	0.0	0.0	0.0	0.0	0.0	0.0	0.4	0.8	1.0	5.8	1.0	0.0	1.2	8.0
	Est	3.0	0.8	0.0	0.0	0.0	0.0	0.0	0.0	0.0	0.0	0.1	0.5	4.2	0.0	0.0	0.1	4.4
	Err	0.8	-1.8	-1.0	0.0	0.0	0.0	0.0	0.0	0.0	-0.4	-0.7	-0.5	-1.6	-1.0	0.0	-1.1	-3.6
Kraft Creek	Obs	3.2	1.8	1.2	0.2	0.0	0.0	0.0	0.0	0.0	0.8	0.2	2.4	7.4	1.4	0.0	1.0	9.8
	Est	5.9	3.8	0.9	0.0	0.0	0.0	0.0	0.0	0.0	0.0	0.7	3.9	13.6	0.9	0.0	0.7	15.2
	Err	2.7	2.0	-0.3	-0.2	0.0	0.0	0.0	0.0	0.0	-0.8	0.5	1.5	6.2	-0.5	0.0	-0.3	5.4
Missoula Int. Airport	Obs	5.0	2.9	0.2	0.0	0.0	0.0	0.0	0.0	0.0	0.1	1.1	5.2	13.0	0.2	0.0	1.1	14.3
	Est	5.9	2.6	0.2	0.0	0.0	0.0	0.0	0.0	0.0	0.0	0.9	5.7	14.3	0.2	0.0	0.9	15.3
	Err	1.0	-0.2	0.0	0.0	0.0	0.0	0.0	0.0	0.0	0.0	-0.2	0.5	1.3	0.0	0.0	-0.2	1.0
Moss Peak	Obs	2.2	2.8	1.2	0.2	0.0	0.0	0.0	0.0	0.0	1.0	1.0	1.8	6.8	1.4	0.0	2.0	10.2
	Est	3.9	4.6	2.7	0.0	0.0	0.0	0.0	0.0	0.0	0.4	1.3	3.7	12.1	2.7	0.0	1.7	16.6
	Err	1.7	1.8	1.5	-0.2	0.0	0.0	0.0	0.0	0.0	-0.6	0.3	1.9	5.3	1.3	0.0	-0.3	6.4
North Fork Jocko	Obs	4.2	7.0	2.0	0.6	0.0	0.0	0.0	0.0	0.0	1.0	2.8	5.8	17.0	2.6	0.0	3.8	23.4
	Est	7.5	8.1	4.8	0.2	0.0	0.0	0.0	0.0	0.0	0.3	2.2	7.1	22.8	5.1	0.0	2.5	30.3
	Err	3.3	1.1	2.8	-0.4	0.0	0.0	0.0	0.0	0.0	-0.7	-0.6	1.3	5.8	2.5	0.0	-1.3	6.9
Polson Kerr Dam	Obs	1.9	2.4	0.2	0.0	0.0	0.0	0.0	0.0	0.0	0.0	0.9	2.1	6.4	0.2	0.0	0.9	7.4
	Est	2.8	1.1	0.1	0.0	0.0	0.0	0.0	0.0	0.0	0.0	0.1	2.7	6.5	0.1	0.0	0.1	6.8
	Err	0.9	-1.3	0.0	0.0	0.0	0.0	0.0	0.0	0.0	0.0	-0.7	0.6	0.1	0.0	0.0	-0.7	-0.6
Saint Ignatius	Obs	2.4	3.1	0.5	0.0	0.0	0.0	0.0	0.0	0.0	0.1	1.2	3.5	9.0	0.5	0.0	1.3	10.7
	Est	5.3	1.7	0.3	0.0	0.0	0.0	0.0	0.0	0.0	0.0	0.3	4.4	11.4	0.3	0.0	0.3	11.9
	Err	2.9	-1.4	-0.2	0.0	0.0	0.0	0.0	0.0	0.0	0.0	-0.9	0.9	2.4	-0.2	0.0	-1.0	1.2
Seeley Lake RS	Obs	9.7	6.7	1.8	0.1	0.0	0.0	0.0	0.0	0.0	0.1	2.4	9.7	26.1	1.9	0.0	2.5	30.4
	Est	9.7	7.5	3.0	0.0	0.0	0.0	0.0	0.0	0.0	0.0	1.3	8.9	26.2	3.0	0.0	1.4	30.6
	Err	0.1	0.8	1.2	-0.1	0.0	0.0	0.0	0.0	0.0	0.0	-1.1	-0.8	0.1	1.1	0.0	-1.1	0.2
Superior	Obs	3.3	2.1	0.2	0.0	0.0	0.0	0.0	0.0	0.0	0.1	0.8	2.9	8.3	0.2	0.0	0.9	9.3
	Est	3.4	1.0	0.1	0.0	0.0	0.0	0.0	0.0	0.0	0.0	0.1	2.2	6.6	0.1	0.0	0.2	6.8
	Err	0.1	-1.1	-0.1	0.0	0.0	0.0	0.0	0.0	0.0	0.0	-0.7	-0.6	-1.6	-0.1	0.0	-0.7	-2.5
Mean Error		1.4	1.2	0.8	0.1	0.0	0.0	0.0	0.0	0.0	0.3	0.6	1.0	2.6	0.7	0.0	0.7	2.9

**Table B-14: 95<sup>th</sup> percentile of observed and estimated daily minimum SAT time series and related error over the validation period**

Station	Value	Jan	Feb	Mar	Apr	May	Jun	Jul	Aug	Sep	Oct	Nov	Dec	Win	Spr	Sum	Fal	Ann
Bigfork 13S	Obs	2.8	2.2	3.3	7.2	11.1	14.4	16.7	16.7	12.8	8.9	5.6	2.2	2.2	9.4	16.1	11.1	13.9
	Est	3.0	4.2	4.3	6.5	9.8	13.3	15.1	15.4	11.4	6.8	4.2	2.6	3.4	8.2	14.9	9.5	12.6
	Err	0.2	2.0	1.0	-0.7	-1.3	-1.1	-1.6	-1.3	-1.4	-2.1	-1.4	0.4	1.2	-1.2	-1.2	-1.6	-1.3
Hot Springs Montana	Obs	2.2	0.6	5.0	6.1	11.3	13.9	17.8	16.7	13.9	9.6	3.9	0.6	1.1	9.4	16.7	11.1	15.0
	Est	4.4	1.7	3.6	8.0	12.1	14.2	17.7	16.7	12.7	8.4	5.8	3.0	3.3	10.0	16.8	11.0	14.5
	Err	2.2	1.1	-1.4	1.9	0.8	0.3	-0.1	0.0	-1.2	-1.2	1.9	2.4	2.2	0.6	0.1	-0.1	-0.5
Kraft Creek	Obs	1.2	-0.6	2.0	3.8	7.9	10.7	14.4	14.4	10.2	7.2	1.5	0.3	0.6	6.5	14.1	8.3	11.9
	Est	3.1	-0.9	1.1	3.2	6.7	9.4	13.3	12.2	9.3	5.4	3.8	2.6	2.1	4.9	12.4	7.6	10.2
	Err	1.9	-0.3	-0.8	-0.6	-1.3	-1.2	-1.1	-2.2	-0.9	-1.9	2.4	2.3	1.5	-1.6	-1.7	-0.7	-1.7
Missoula Int. Airport	Obs	0.6	0.6	2.2	6.1	10.0	13.3	15.6	15.0	11.1	5.6	2.2	0.0	0.6	8.3	14.4	8.9	12.2
	Est	2.9	2.6	3.5	5.3	9.4	13.1	15.4	15.0	10.6	4.9	3.0	0.8	2.2	7.7	14.8	8.3	12.1
	Err	2.3	2.0	1.3	-0.8	-0.6	-0.2	-0.2	0.0	-0.5	-0.7	0.8	0.8	1.6	-0.6	0.3	-0.6	-0.1
Moss Peak	Obs	-0.8	-3.1	-0.2	2.7	6.6	9.2	14.7	13.2	9.7	6.4	1.8	-0.9	-1.4	4.4	13.3	7.8	10.7
	Est	0.1	-2.3	-0.2	1.7	5.7	8.0	14.0	12.8	8.8	5.3	2.1	-1.3	-0.9	3.7	12.9	7.2	10.0
	Err	0.9	0.8	-0.1	-0.9	-0.8	-1.1	-0.7	-0.3	-0.9	-1.0	0.3	-0.4	0.5	-0.7	-0.4	-0.6	-0.7
North Fork Jocko	Obs	-0.9	-3.5	-0.1	1.0	3.0	6.9	10.4	9.0	6.5	3.4	-0.2	-0.4	-1.1	2.0	9.4	5.2	7.2
	Est	0.2	-2.8	-1.4	1.5	2.7	5.7	9.9	9.2	6.2	3.5	1.0	-0.7	-0.7	1.8	9.1	4.9	6.9
	Err	1.1	0.7	-1.2	0.5	-0.3	-1.2	-0.5	0.1	-0.3	0.1	1.2	-0.3	0.4	-0.2	-0.3	-0.3	-0.3
Polson Kerr Dam	Obs	1.7	2.2	3.3	7.8	10.7	13.9	16.7	16.1	12.8	8.3	4.4	1.2	1.7	9.4	16.1	10.6	13.9
	Est	3.4	3.2	4.2	6.3	11.0	14.2	15.9	16.4	11.6	7.0	3.9	2.4	3.0	9.1	15.8	9.8	13.4
	Err	1.7	1.0	0.9	-1.5	0.3	0.3	-0.8	0.3	-1.2	-1.3	-0.5	1.2	1.3	-0.3	-0.3	-0.8	-0.5
Saint Ignatius	Obs	2.7	2.8	3.8	8.0	10.6	13.3	15.0	15.0	11.7	7.8	6.1	2.2	2.8	8.9	14.4	9.4	12.2
	Est	4.4	4.4	5.0	6.3	10.7	13.5	15.0	14.6	10.7	6.5	4.0	3.3	4.1	8.7	14.5	8.9	12.1
	Err	1.8	1.6	1.2	-1.7	0.1	0.2	0.0	-0.4	-1.0	-1.3	-2.1	1.1	1.3	-0.2	0.1	-0.5	-0.1
Seeley Lake RS	Obs	-1.1	-1.1	0.0	3.4	7.8	11.1	12.2	12.2	8.9	4.4	1.1	-1.1	-1.1	5.6	12.2	6.7	9.4
	Est	1.8	2.8	3.3	3.3	8.4	11.1	12.6	12.1	8.0	4.4	2.4	0.6	1.8	6.3	12.0	6.2	9.3
	Err	2.9	3.9	3.3	-0.1	0.6	0.0	0.4	-0.1	-0.9	0.0	1.3	1.7	2.9	0.7	-0.2	-0.5	-0.1
Superior	Obs	1.1	1.1	3.3	6.7	10.0	13.3	14.4	15.6	11.1	7.0	4.0	0.6	1.1	7.8	14.4	8.9	11.7
	Est	4.1	3.9	4.1	5.9	10.4	13.3	15.0	15.1	11.0	6.5	4.7	2.2	3.5	8.4	14.6	9.0	12.2
	Err	3.0	2.8	0.8	-0.8	0.4	0.0	0.6	-0.5	-0.1	-0.5	0.6	1.6	2.4	0.6	0.2	0.1	0.5
Mean Error		1.8	1.6	1.2	0.9	0.7	0.6	0.6	0.5	0.8	1.0	1.2	1.2	1.5	0.7	0.5	0.6	0.6

APPENDIX C: Analysis of SAT

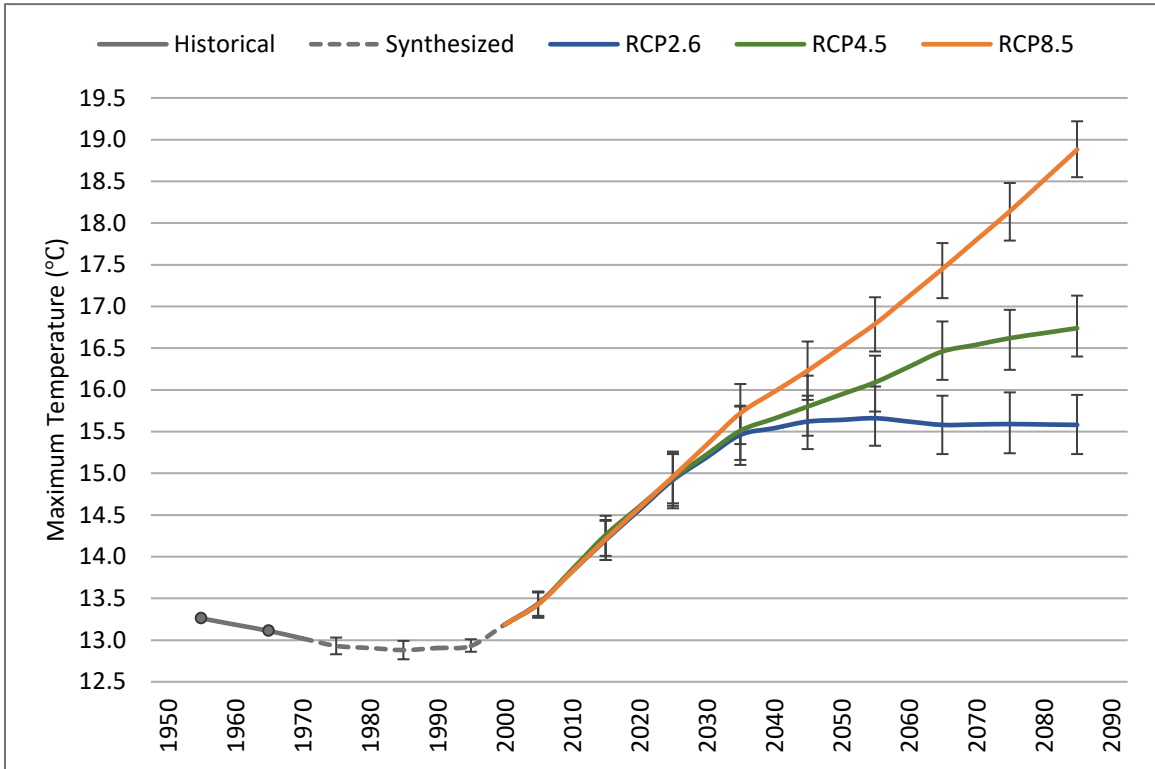


Figure C-1: Evolution and predicted accuracy of maximum SAT normals at Bigfork 13S

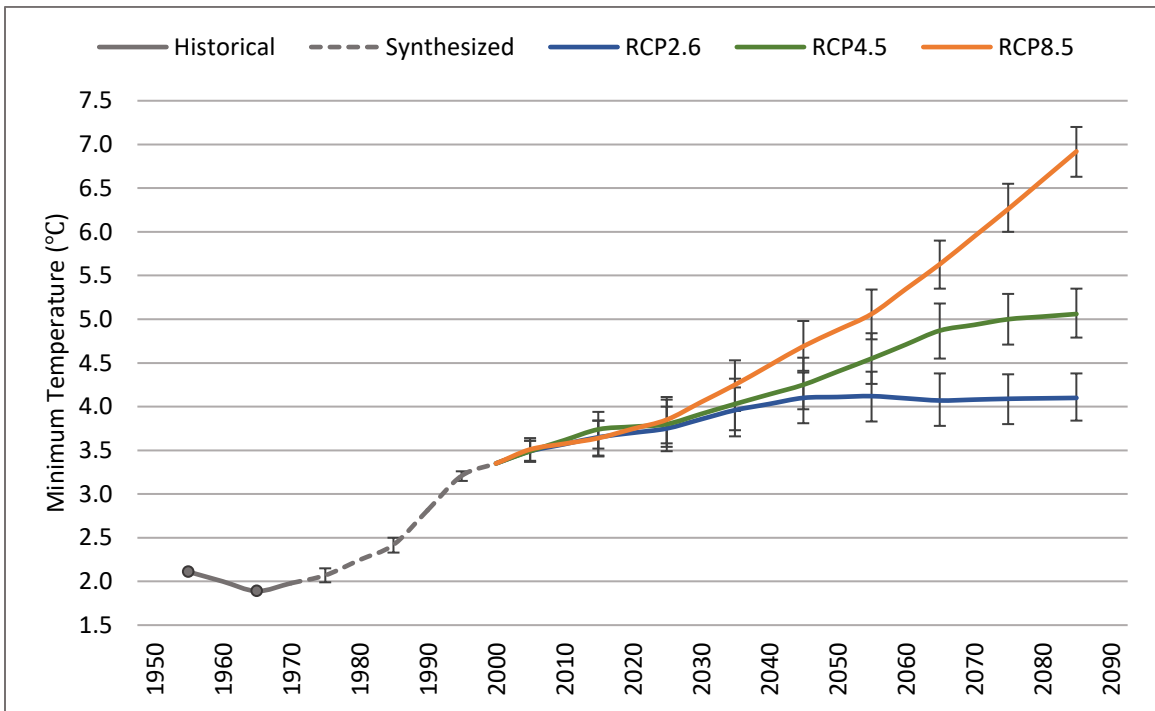


Figure C-2: Evolution and predicted accuracy of minimum SAT normals at Bigfork 13S

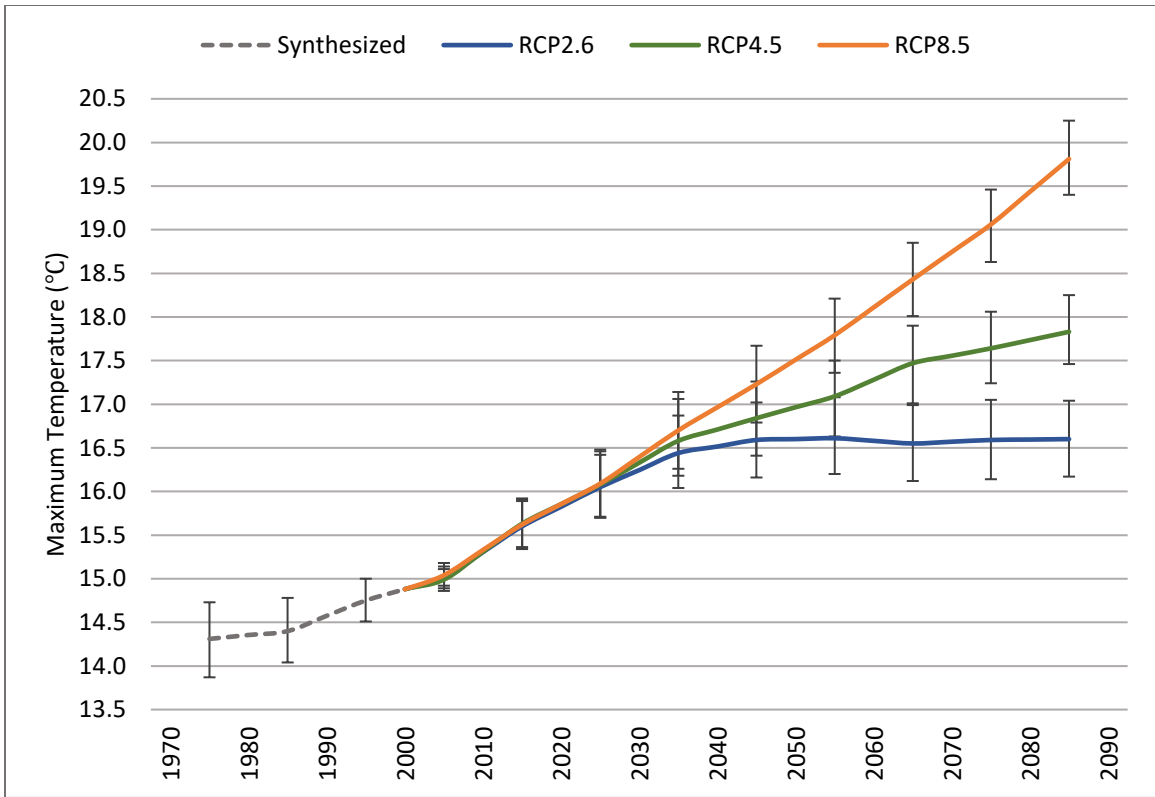


Figure C-3: Evolution and predicted accuracy of maximum SAT normals at Hot Springs Montana

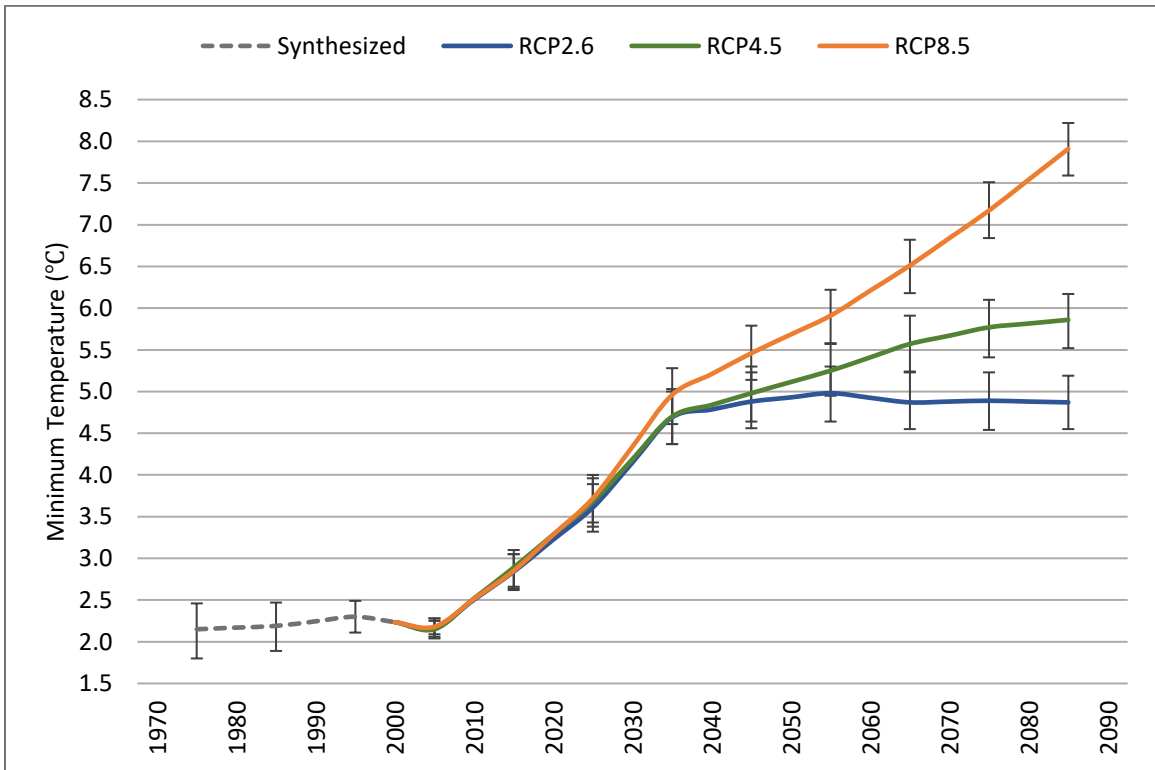


Figure C-4: Evolution and predicted accuracy of minimum SAT normals at Hot Springs Montana

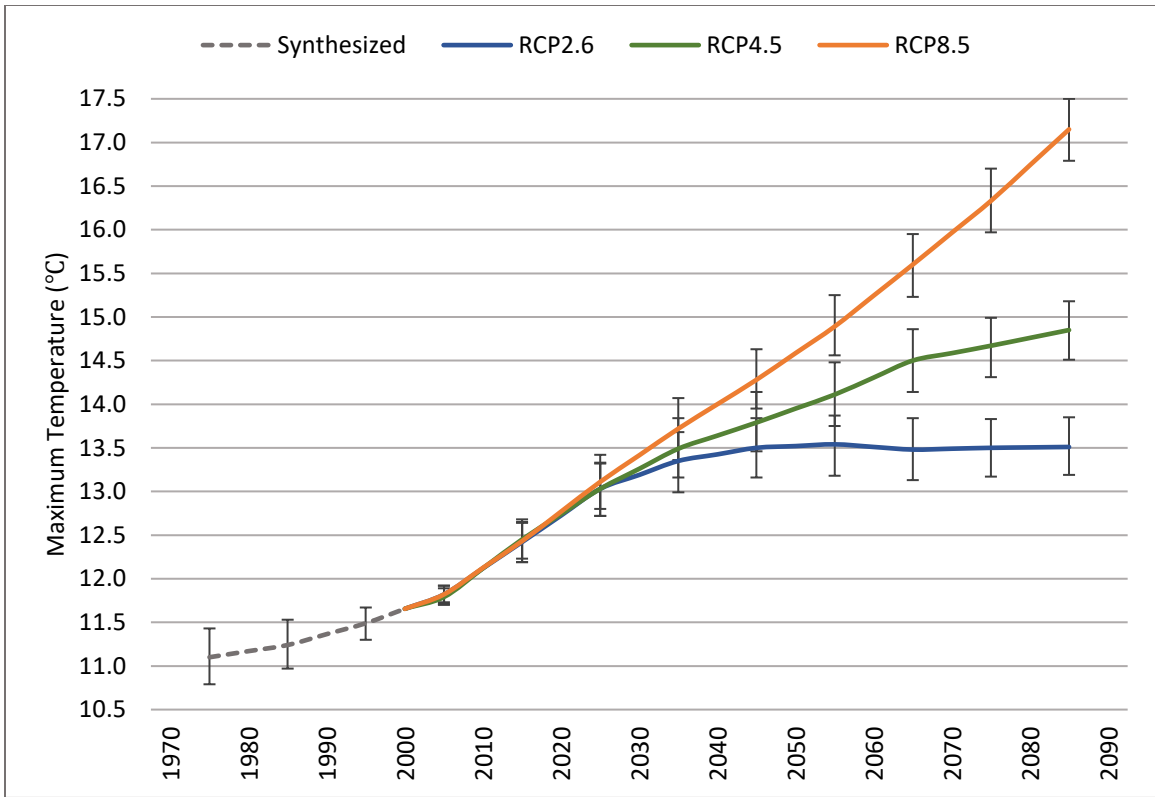


Figure C-5: Evolution and predicted accuracy of maximum SAT normals at Kraft Creek

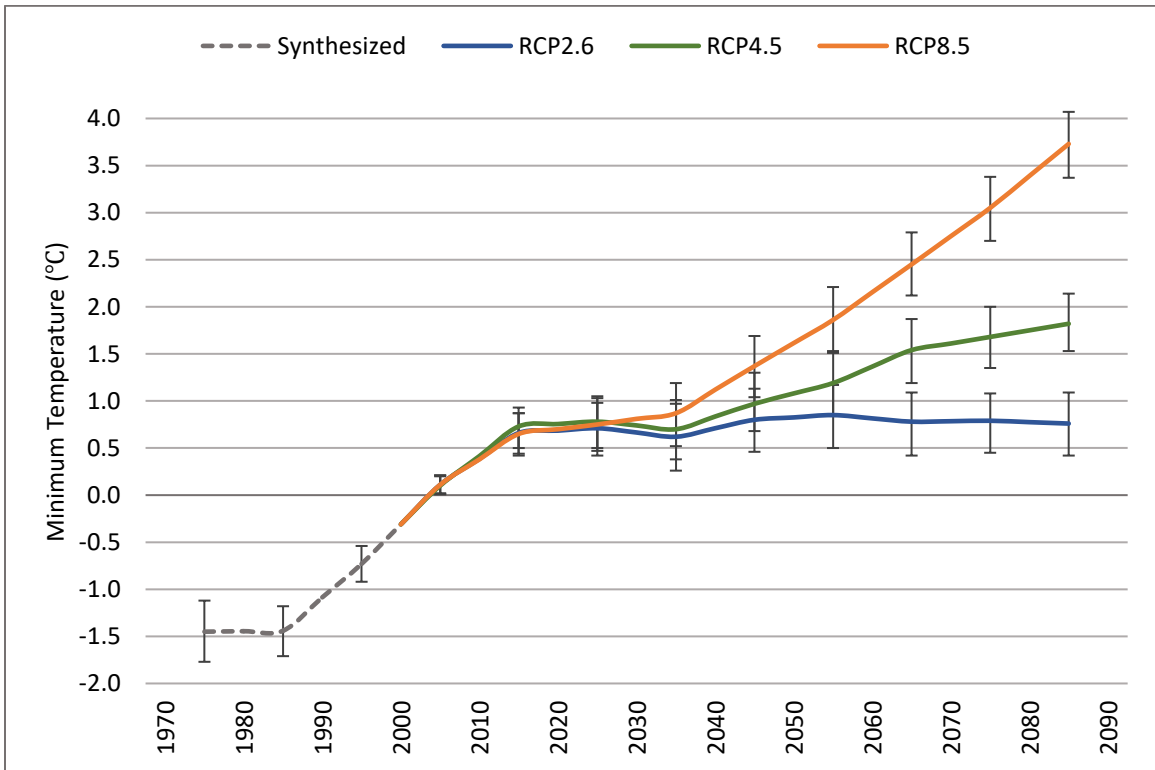


Figure C-6: Evolution and predicted accuracy of minimum SAT normals at Kraft Creek

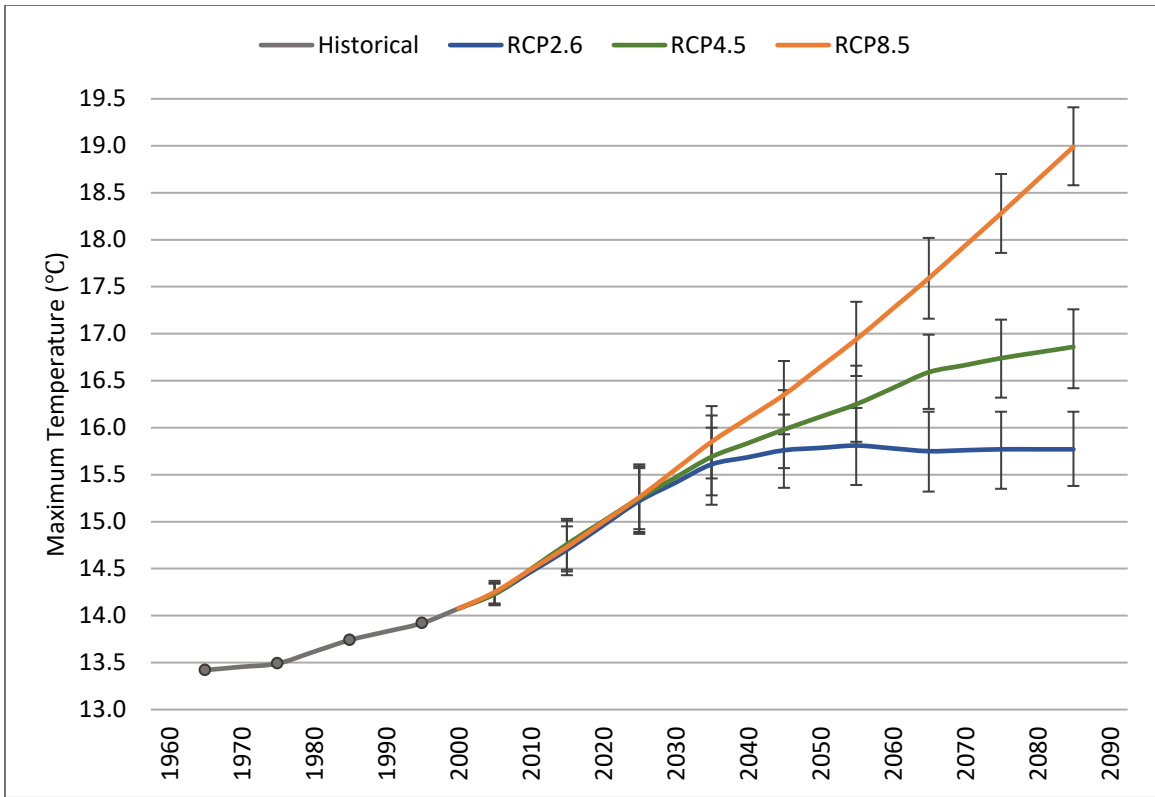


Figure C-7: Evolution and predicted accuracy of maximum SAT normals at Missoula Int. Airport

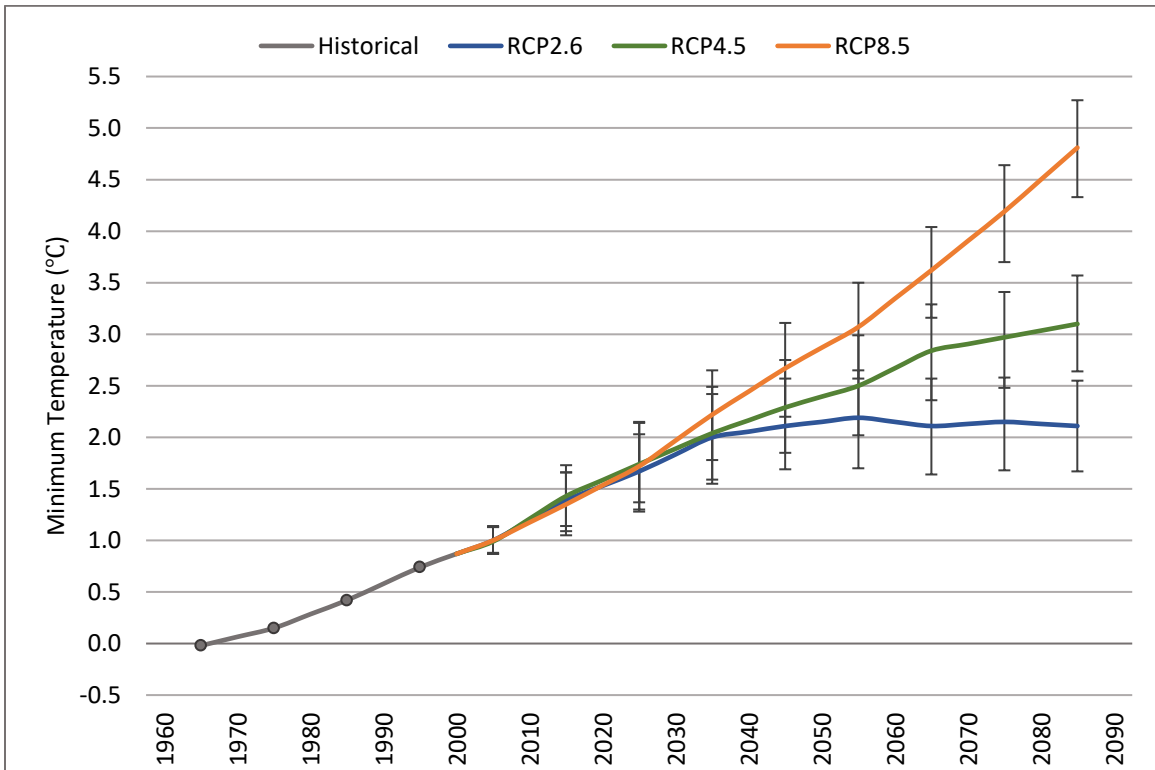


Figure C-8: Evolution and predicted accuracy of minimum SAT normals at Missoula Int. Airport

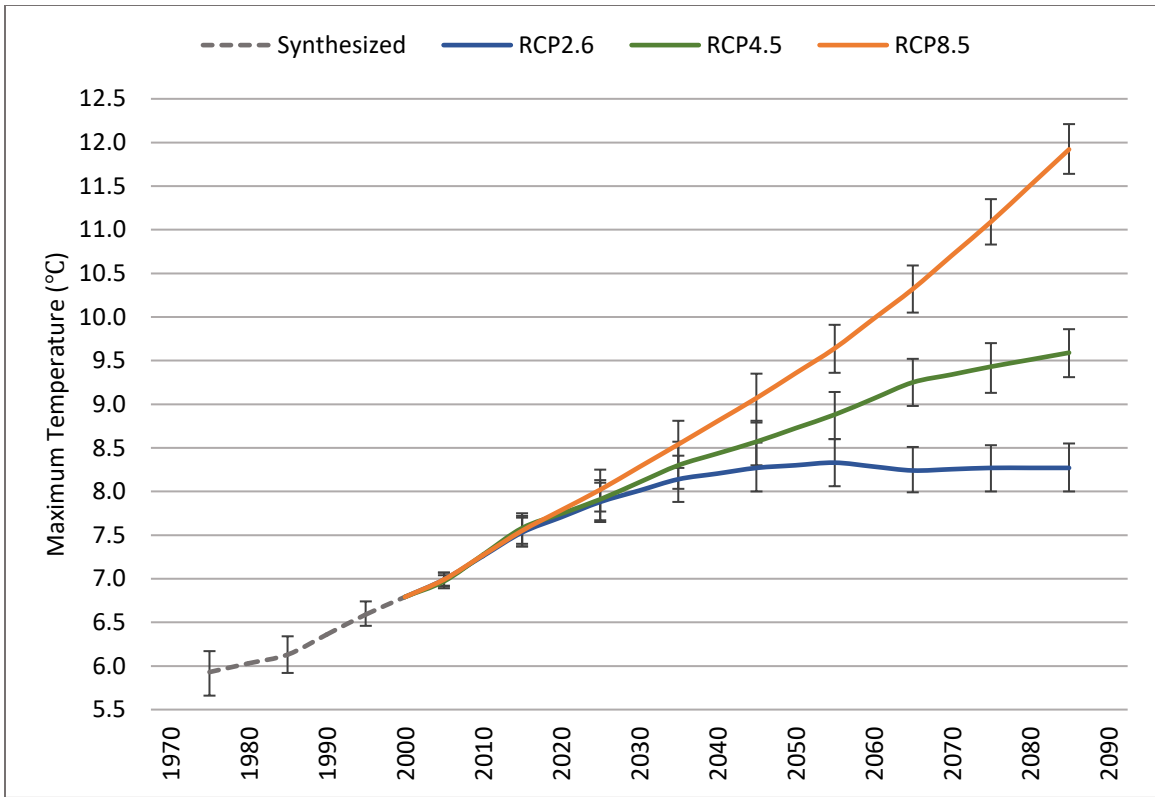


Figure C-9: Evolution and predicted accuracy of maximum SAT normals at Moss Peak

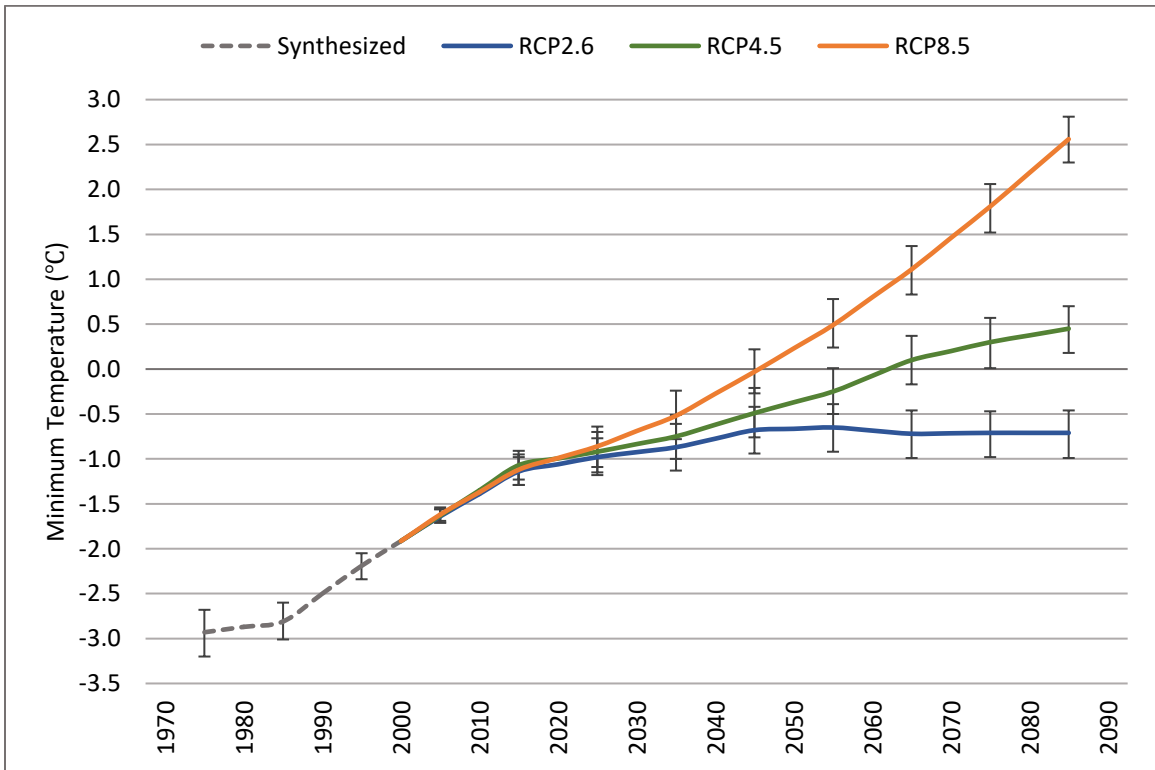


Figure C-10: Evolution and predicted accuracy of minimum SAT normals at Moss Peak

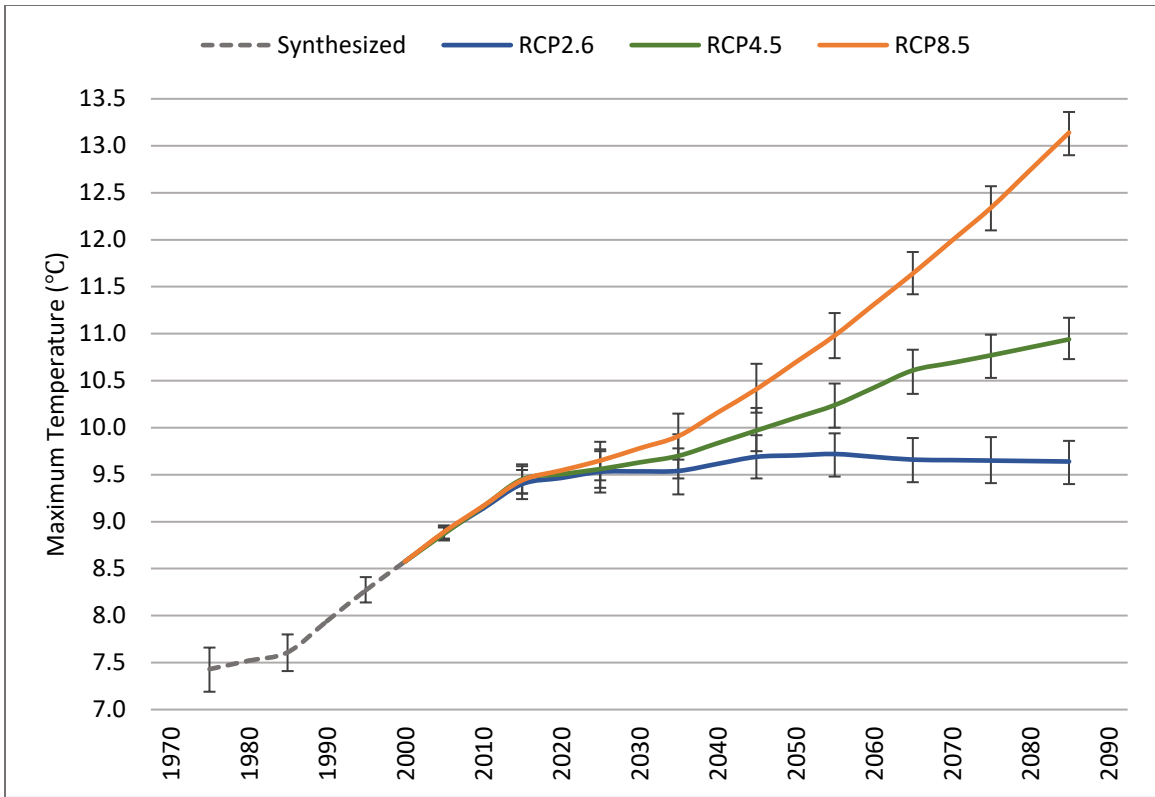


Figure C-11: Evolution and predicted accuracy of maximum SAT normals at North Fork Jocko

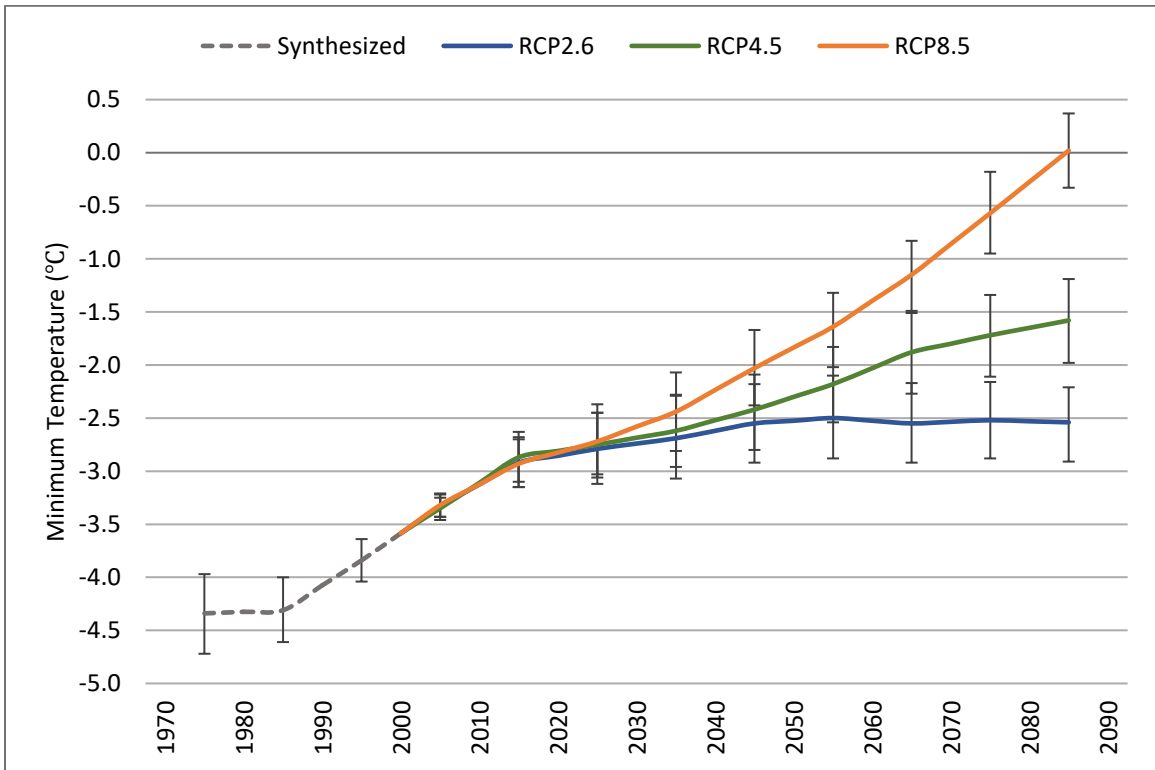


Figure C-12: Evolution and predicted accuracy of minimum SAT normals at North Fork Jocko

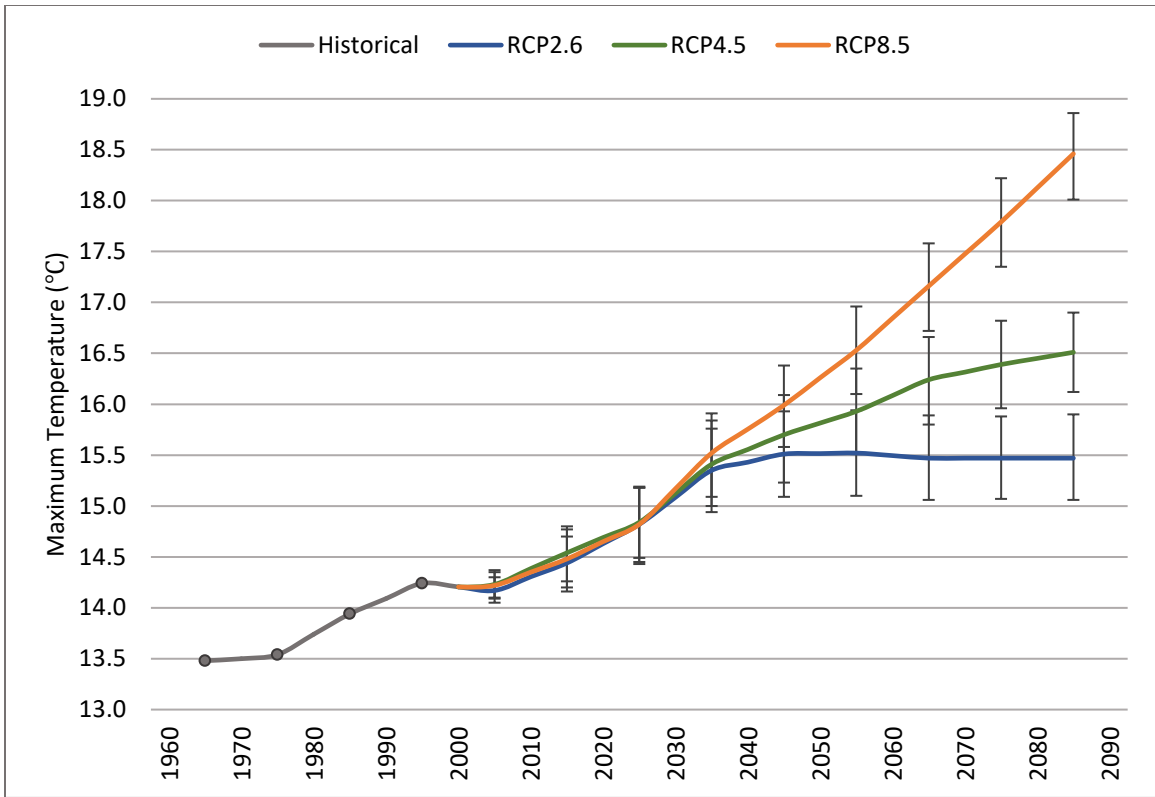


Figure C-13: Evolution and predicted accuracy of maximum SAT normals at Polson Kerr Dam

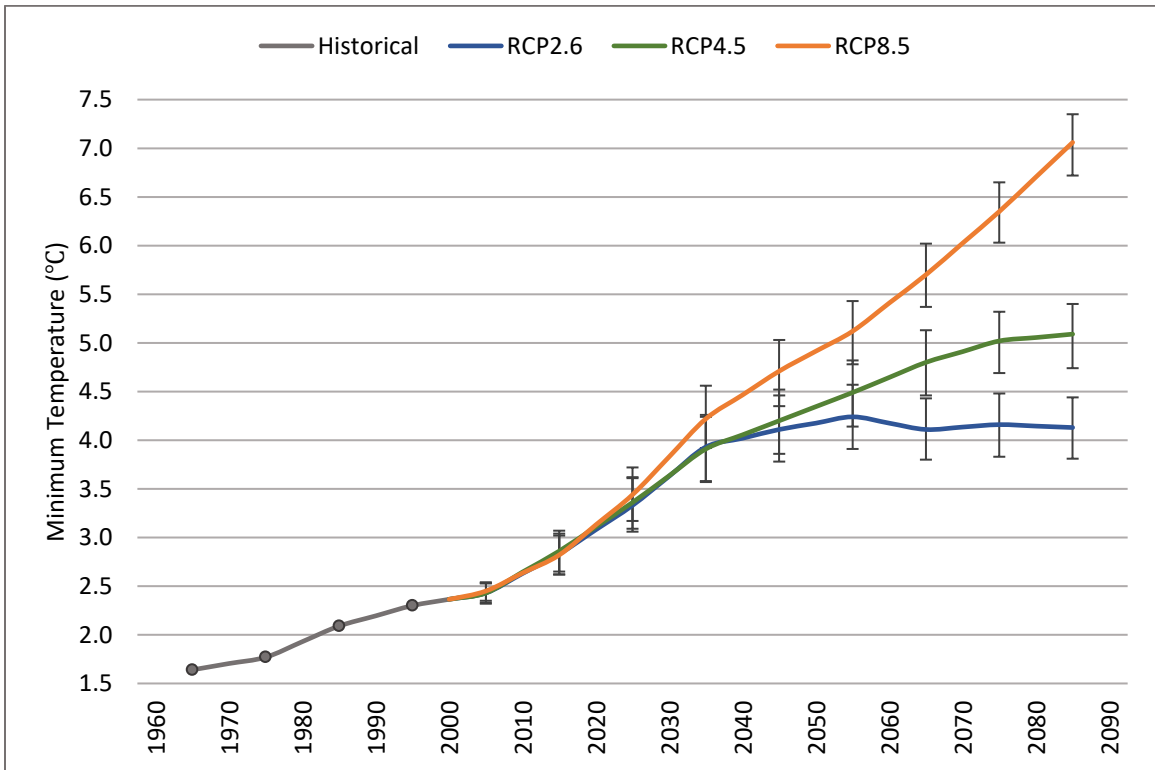


Figure C-14: Evolution and predicted accuracy of minimum SAT normals at Polson Kerr Dam

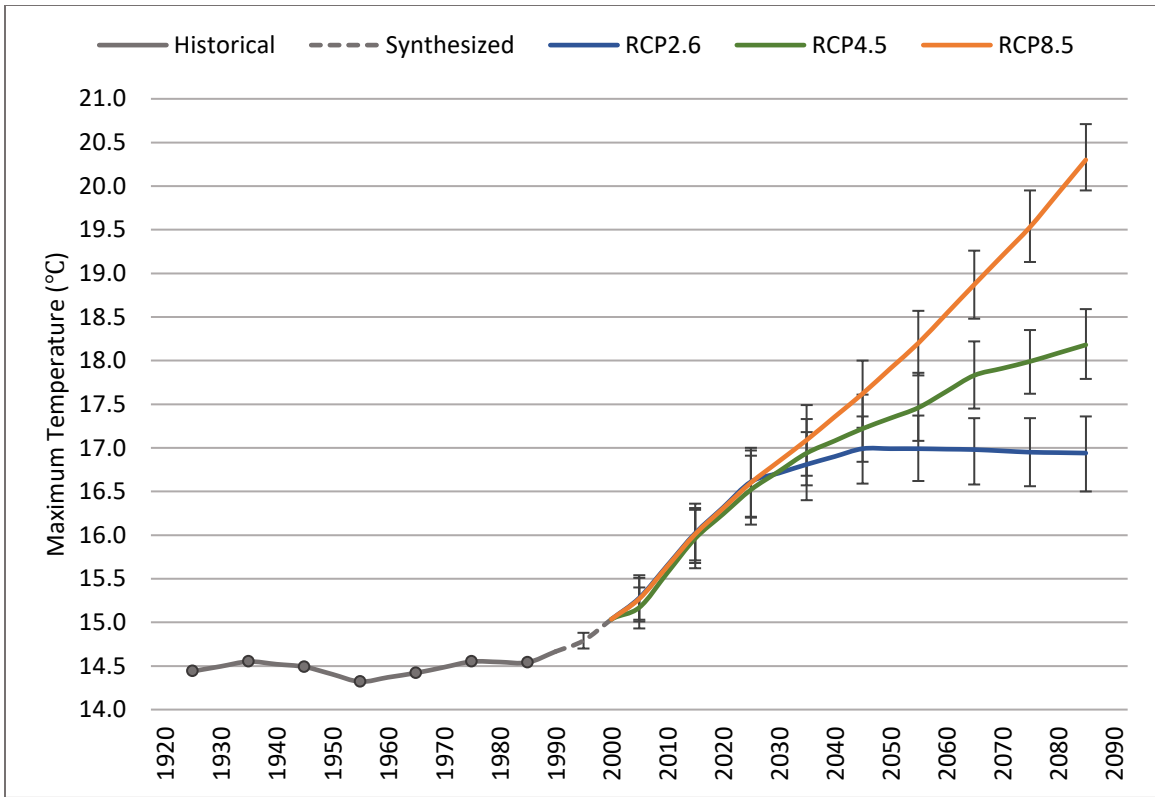


Figure C-15: Evolution and predicted accuracy of maximum SAT normals at Saint Ignatius

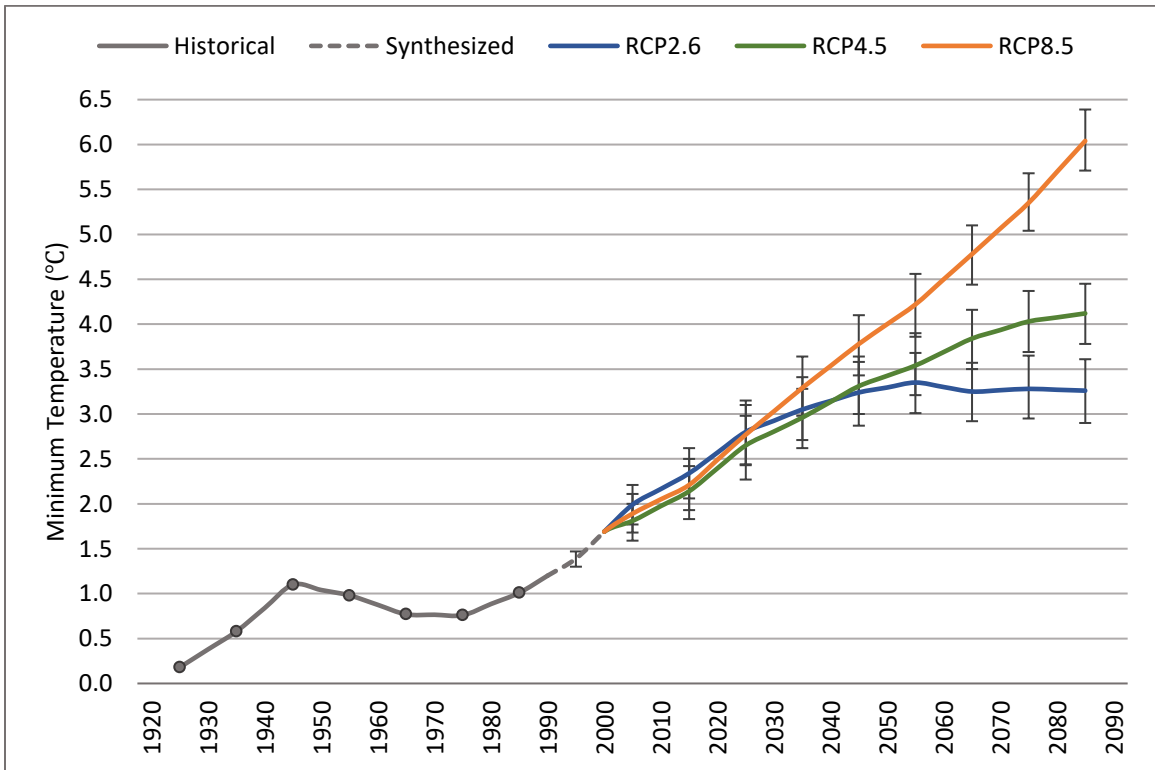


Figure C-16: Evolution and predicted accuracy of minimum SAT normals at Saint Ignatius

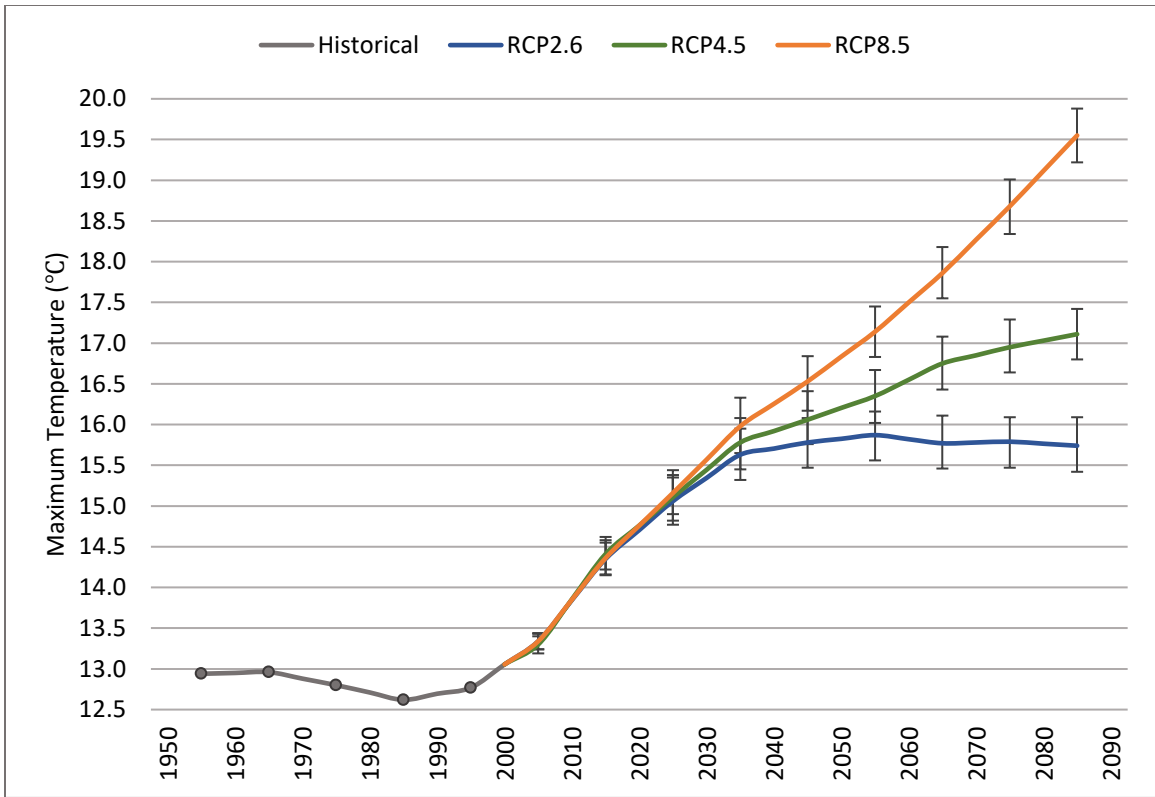


Figure C-17: Evolution and predicted accuracy of maximum SAT normals at Seeley Lake RS

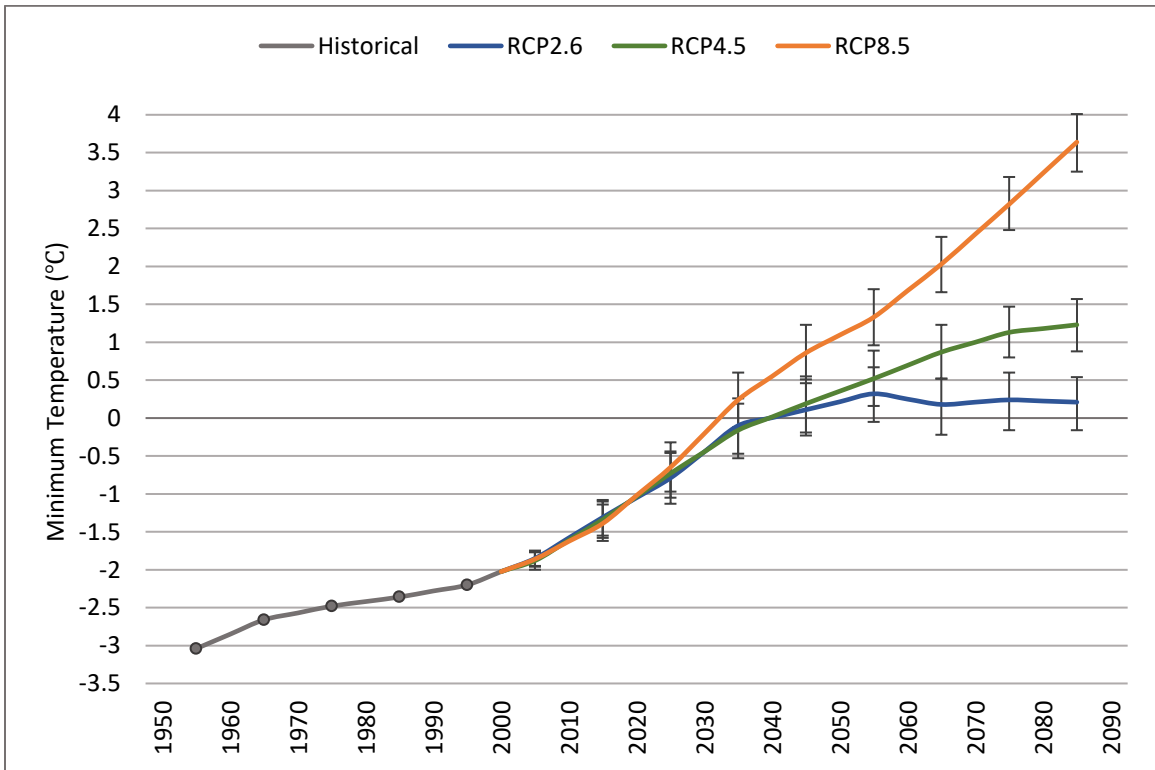


Figure C-18: Evolution and predicted accuracy of minimum SAT normals at Seeley Lake RS

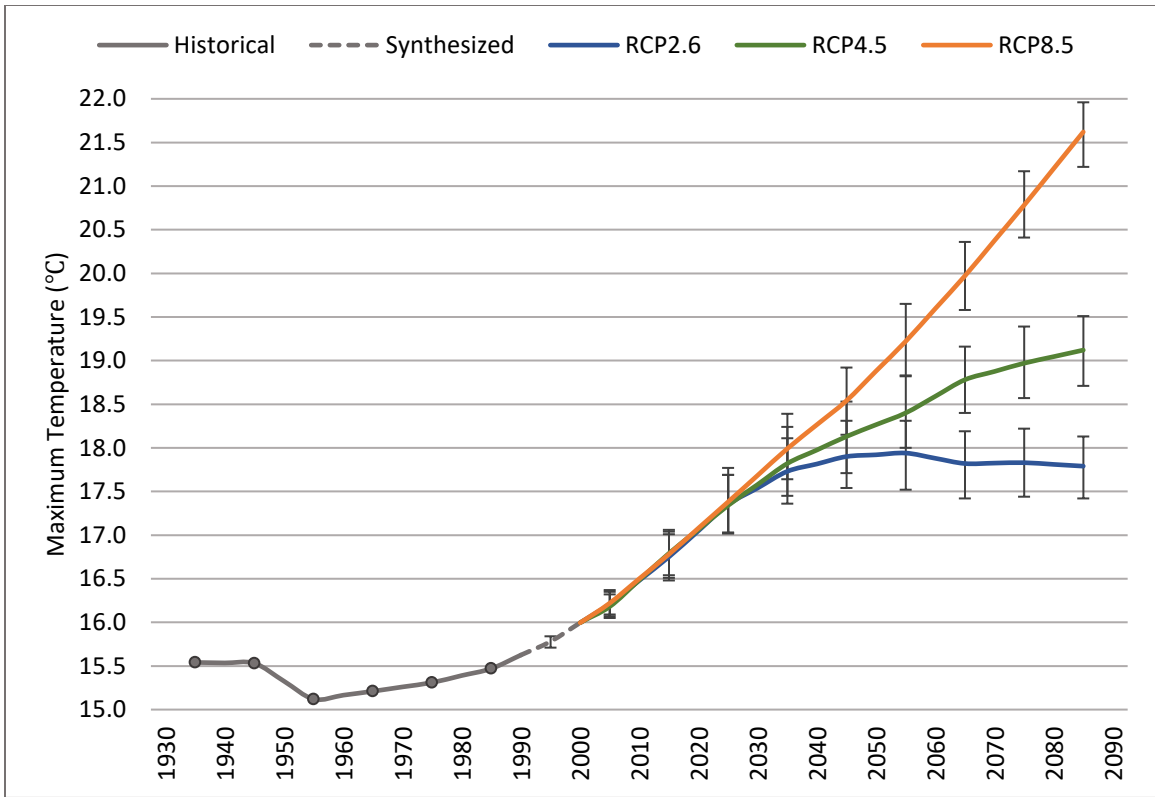


Figure C-19: Evolution and predicted accuracy of maximum SAT normals at Superior

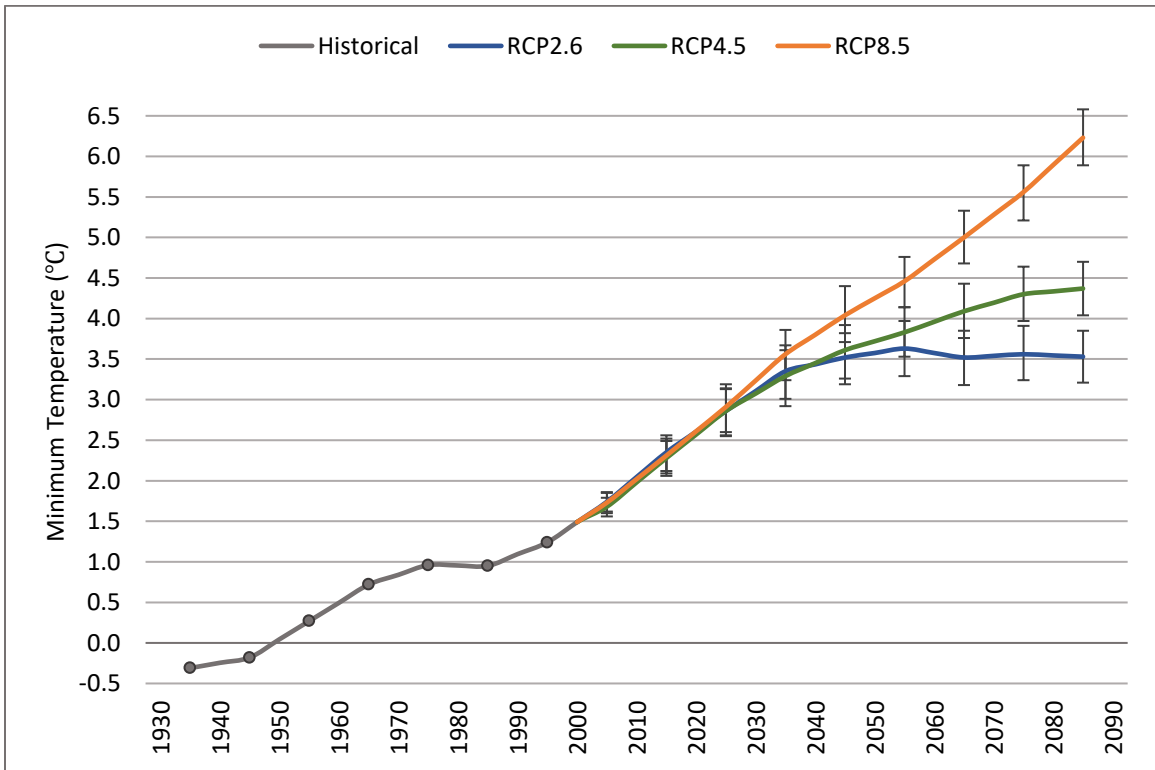
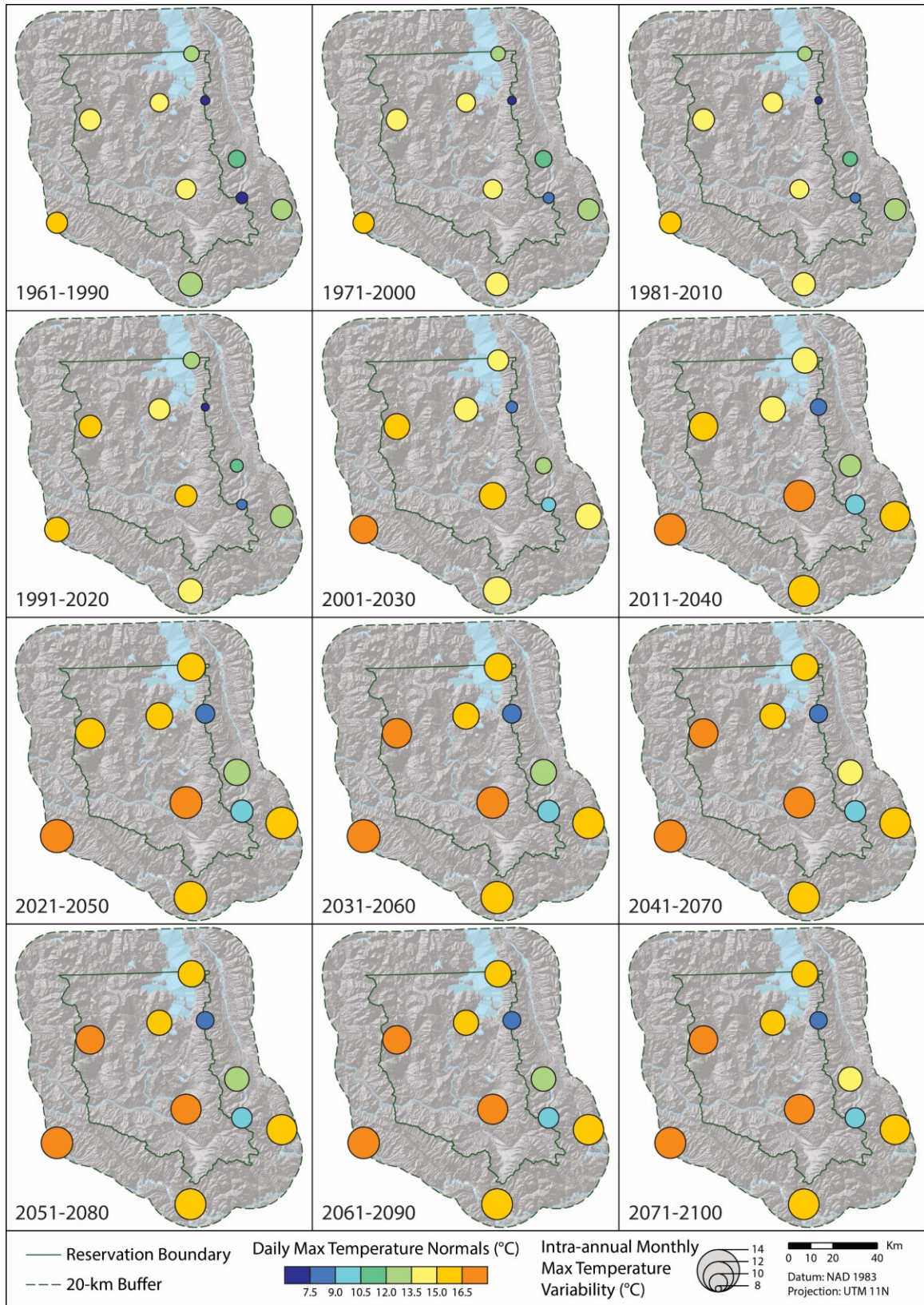
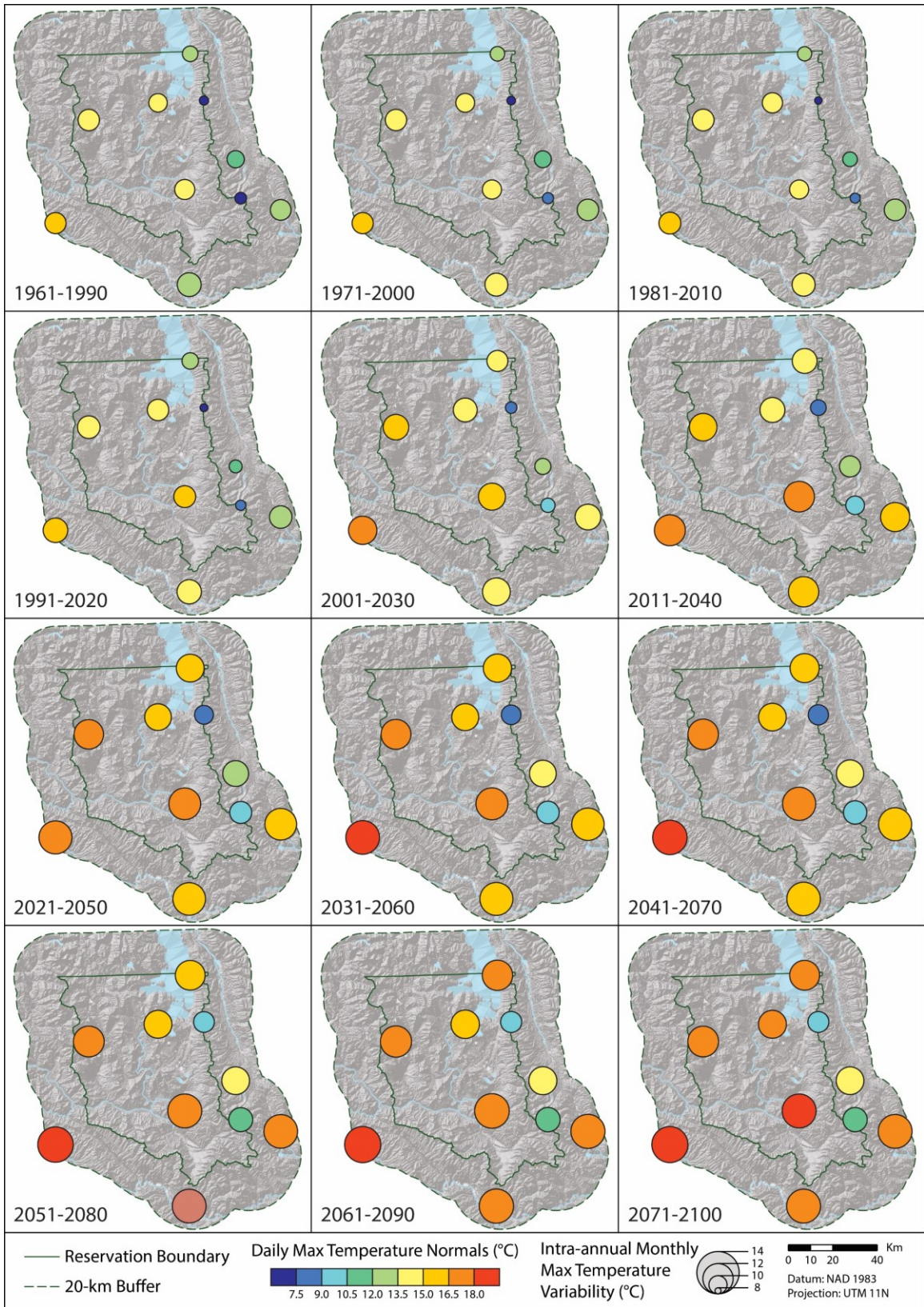


Figure C-20: Evolution and predicted accuracy of minimum SAT normals at Superior



**Figure C-21: Daily maximum temperature normals and intra-annual monthly maximum temperature variability according to historical data and the RCP2.6 scenario**



**Figure C-22: Daily maximum temperature normals and intra-annual monthly maximum temperature variability according to historical data and the RCP4.5 scenario**

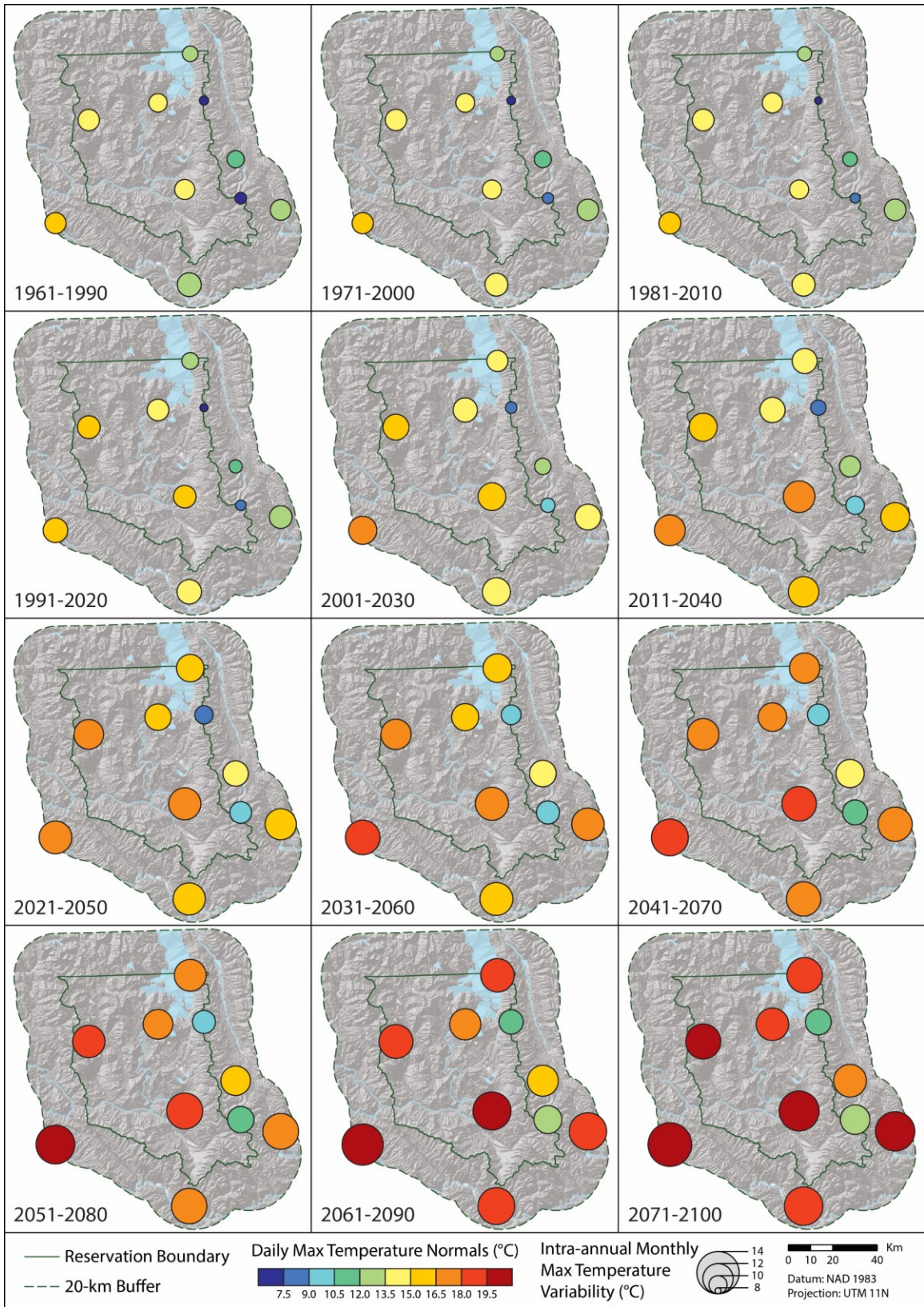


**Figure C-23: Daily maximum temperature normals and intra-annual monthly maximum temperature variability according to historical data and the RCP8.5 scenario**

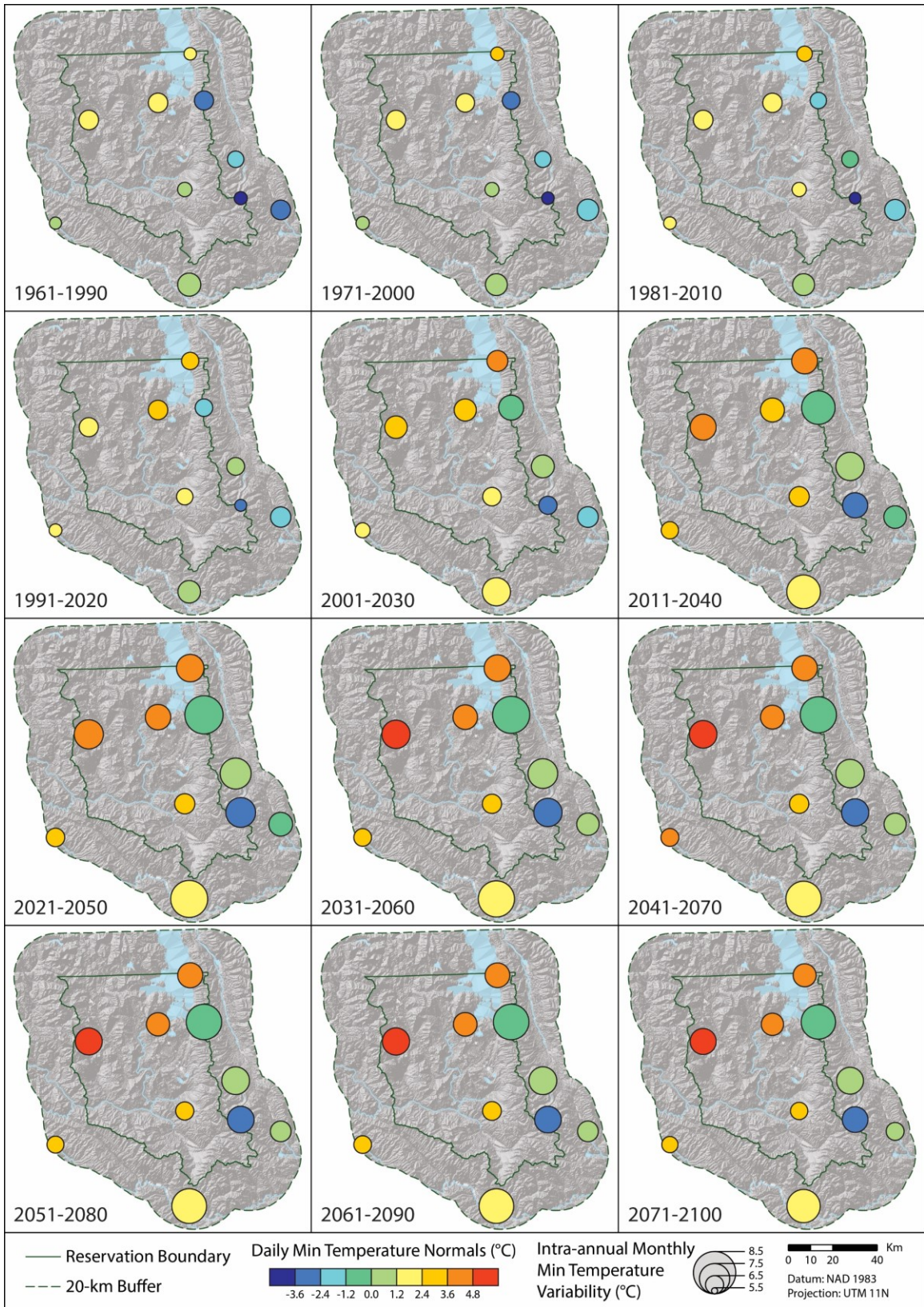


**Figure C-24: Daily minimum temperature normals and intra-annual monthly minimum temperature variability according to historical data and the RCP2.6 scenario**

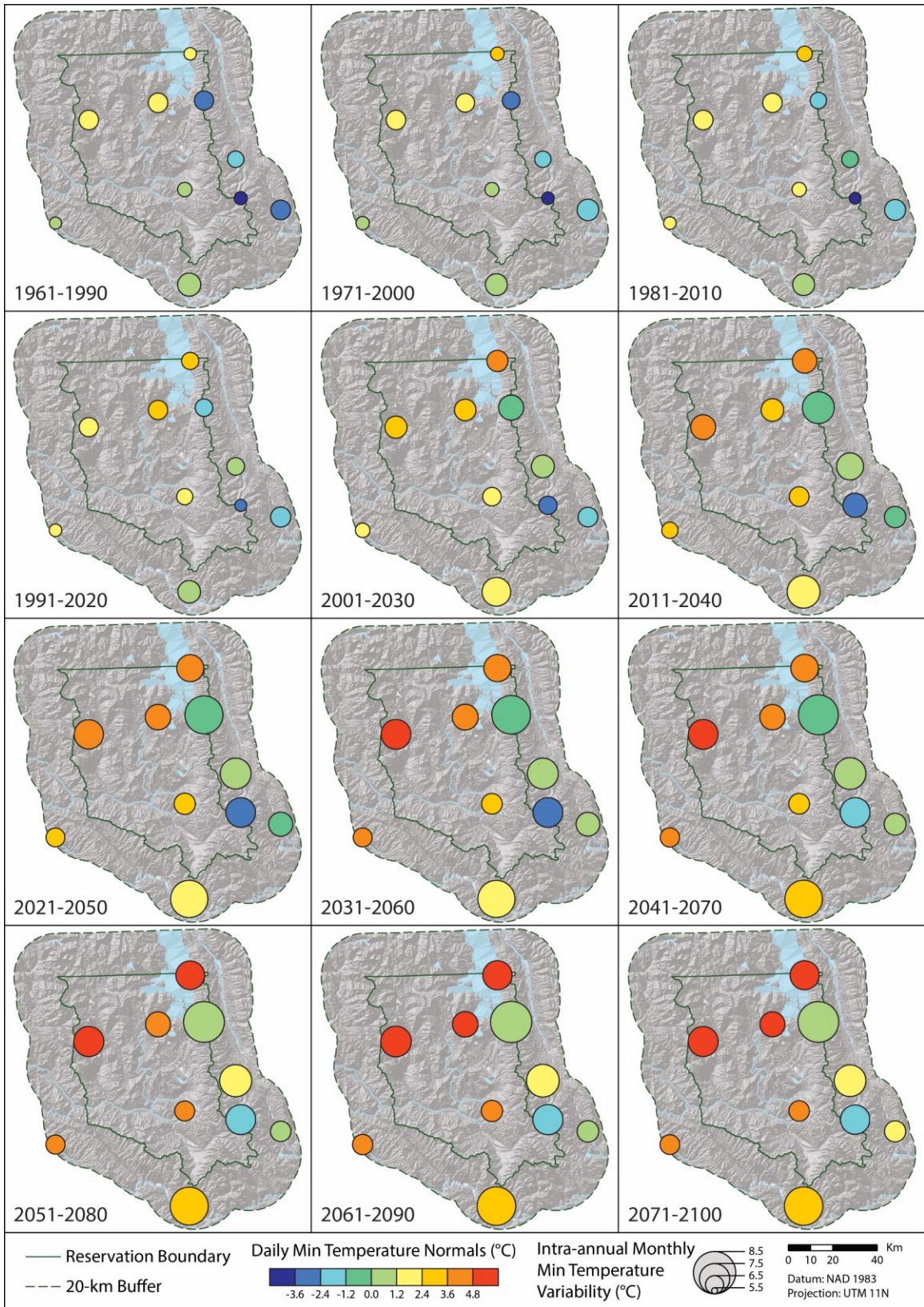


**Figure C-25: Daily minimum temperature normals and intra-annual monthly minimum temperature variability according to historical data and the RCP4.5 scenario**

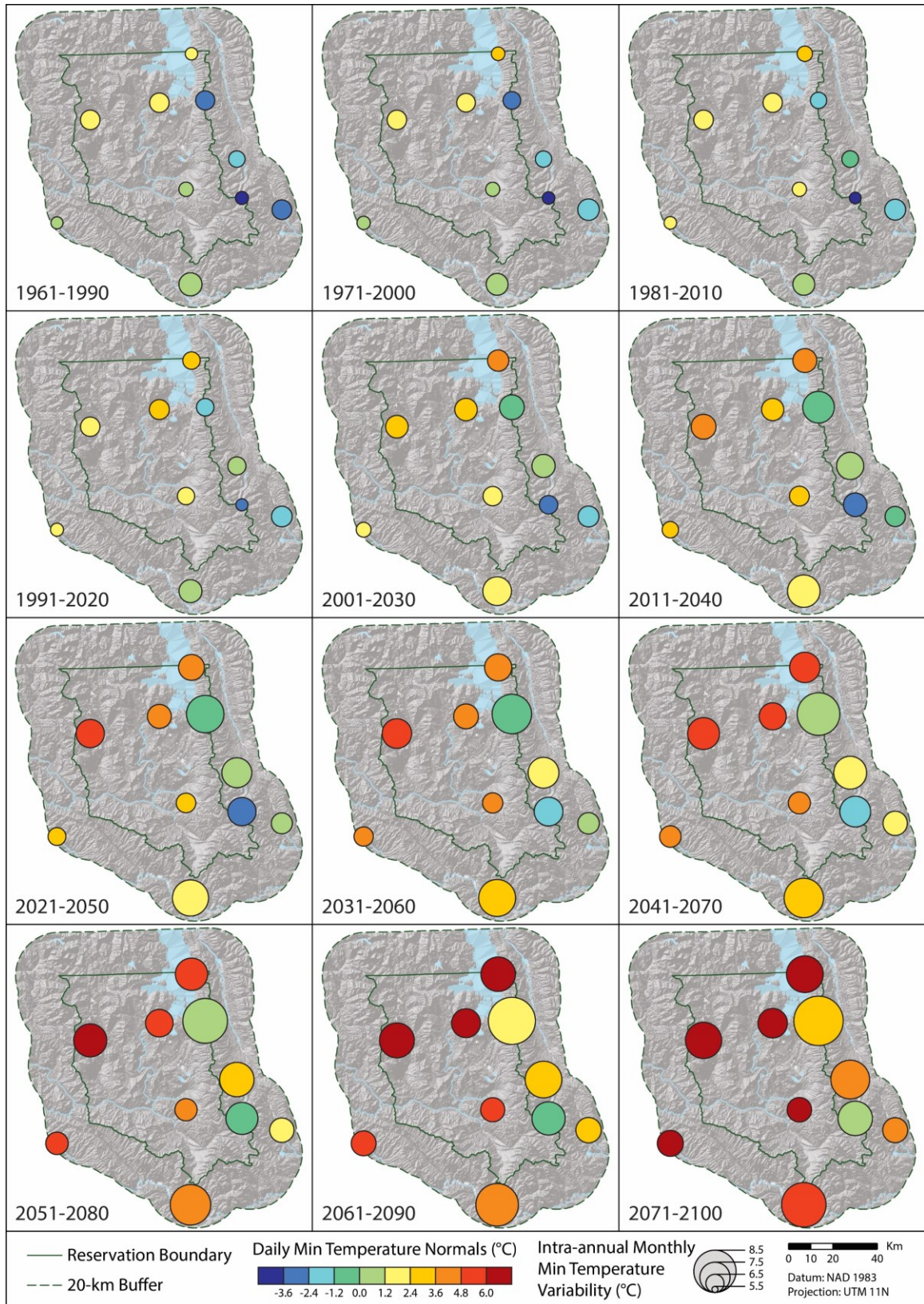


**Figure C-26: Daily minimum temperature normals and intra-annual monthly minimum temperature variability according to historical data and the RCP8.5 scenario**

**Table C-1: Main statistics – Theil-Sen’s slope (Sl.), Kendall’s statistic (S), p value (p), Kendall’s correlation coefficient ( $\tau$ ), and variance of the Kendall’s statistic (VarS) – related to the regional Kendall and Mann-Kendall tests applied to seasonal/annual means of maximum/minimum SAT within the 1961-2100 period across the Flathead Region according to the three RCP scenarios**

Variable	Scenario	Time	Regional					Big Fork 13S				
			Sl.	S	p	$\tau$	VarS	Sl.	S	p	$\tau$	VarS
Maximum SAT	RCP2.6	Win	0.02	40,002	0	0.33	4,334,133	0.02	3,596	0	0.37	308,093
		Spr	0.01	32,395	0	0.27	4,352,184	0.02	3,443	0	0.35	308,102
		Sum	0.05	67,041	0	0.55	4,385,949	0.06	5,138	0	0.53	308,105
		Fal	0.01	18,049	0	0.15	4,295,026	0.00	1,034	0.063	0.11	308,091
		Ann	0.02	64,110	0	0.55	4,117,003	0.03	5,507	0	0.57	308,102
	RCP4.5	Win	0.02	46,604	0	0.39	4,334,177	0.02	4,206	0	0.43	308,098
		Spr	0.02	45,471	0	0.38	4,352,197	0.02	4,658	0	0.48	308,097
		Sum	0.06	79,857	0	0.66	4,385,986	0.08	6,355	0	0.65	308,110
		Fal	0.02	45,514	0	0.38	4,295,032	0.02	3,462	0	0.36	308,092
		Ann	0.03	78,388	0	0.67	4,117,059	0.04	6,644	0	0.68	308,089
	RCP8.5	Win	0.03	59,356	0	0.49	4,334,203	0.03	5,233	0	0.54	308,109
		Spr	0.03	61,698	0	0.51	4,352,265	0.04	5,629	0	0.58	308,106
		Sum	0.09	90,225	0	0.74	4,385,994	0.11	7,389	0	0.76	308,110
		Fal	0.04	68,473	0	0.57	4,295,117	0.04	5,887	0	0.61	308,096
		Ann	0.05	87,500	0	0.75	4,117,131	0.06	7,530	0	0.77	308,102
Minimum SAT	RCP2.6	Win	0.03	49,386	0	0.41	4,355,081	0.02	3,264	0	0.34	308,101
		Spr	0.01	35,923	0	0.30	4,369,474	0.01	1,632	0.003	0.17	308,081
		Sum	0.04	71,607	0	0.59	4,370,212	0.04	5,537	0	0.57	308,095
		Fal	0.01	39,636	0	0.33	4,310,259	0.00	165	0.768	0.02	308,092
		Ann	0.02	68,564	0	0.58	4,151,687	0.02	5,071	0	0.52	308,075
	RCP4.5	Win	0.03	56,171	0	0.46	4,355,106	0.03	3,926	0	0.40	308,109
		Spr	0.01	49,027	0	0.40	4,369,508	0.01	3,326	0	0.34	308,074
		Sum	0.05	87,591	0	0.72	4,370,290	0.05	7,122	0	0.73	308,102
		Fal	0.02	60,091	0	0.50	4,310,296	0.01	2,674	0	0.27	308,077
		Ann	0.03	81,397	0	0.69	4,151,809	0.02	6,644	0	0.68	308,082
	RCP8.5	Win	0.04	66,657	0	0.55	4,355,121	0.04	5,030	0	0.52	308,099
		Spr	0.03	69,659	0	0.57	4,369,578	0.02	5,123	0	0.53	308,094
		Sum	0.07	96,969	0	0.80	4,370,318	0.08	8,206	0	0.84	308,107
		Fal	0.04	77,923	0	0.65	4,310,407	0.03	5,379	0	0.55	308,094
		Ann	0.04	91,335	0	0.78	4,151,904	0.04	7,585	0	0.78	308,101

Table C-1. Continued

Var.	Scen.	Time	Hot Springs Montana					Kraft Creek					Missoula International Airport				
			Sl.	S	p	$\tau$	VarS	Sl.	S	p	$\tau$	VarS	Sl.	S	p	$\tau$	VarS
Max SAT	RCP2.6	Win	0.02	3,569	0	0.37	301,562	0.02	3,426	0	0.36	301,559	0.02	3,141	0	0.32	308,098
		Spr	0.01	2,333	0	0.24	308,103	0.01	2,569	0	0.26	308,092	0.01	2,456	0	0.25	308,100
		Sum	0.05	5,515	0	0.57	308,103	0.05	4,984	0	0.51	308,107	0.05	5,310	0	0.55	308,109
		Fal	0.01	1,704	0.002	0.18	308,096	0.01	1,591	0.004	0.16	308,103	0.01	1,671	0.003	0.17	308,095
		Ann	0.02	5,378	0	0.55	308,093	0.02	5,459	0	0.56	308,100	0.02	5,353	0	0.55	308,090
	RCP4.5	Win	0.03	4,234	0	0.44	301,570	0.03	4,143	0	0.43	301,570	0.02	3,697	0	0.38	308,105
		Spr	0.02	3,391	0	0.35	308,108	0.02	3,645	0	0.37	308,096	0.02	3,506	0	0.36	308,097
		Sum	0.06	6,601	0	0.68	308,110	0.07	6,111	0	0.63	308,110	0.06	6,389	0	0.66	308,106
		Fal	0.02	4,339	0	0.45	308,100	0.02	3,938	0	0.40	308,083	0.02	4,098	0	0.42	308,096
		Ann	0.03	6,724	0	0.69	308,085	0.04	6,784	0	0.70	308,102	0.03	6,543	0	0.67	308,100
	RCP8.5	Win	0.04	5,405	0	0.56	301,574	0.04	5,443	0	0.57	301,568	0.03	4,745	0	0.49	308,108
		Spr	0.03	4,981	0	0.51	308,105	0.03	5,166	0	0.53	308,102	0.03	5,176	0	0.53	308,099
		Sum	0.09	7,577	0	0.78	308,110	0.10	7,094	0	0.73	308,111	0.09	7,470	0	0.77	308,107
		Fal	0.05	6,273	0	0.64	308,108	0.05	6,048	0	0.62	308,095	0.05	6,122	0	0.63	308,111
		Ann	0.05	7,587	0	0.78	308,105	0.06	7,644	0	0.79	308,105	0.05	7,532	0	0.77	308,106
Min SAT	RCP2.6	Win	0.03	4,322	0	0.45	301,563	0.02	3,116	0	0.32	301,559	0.02	3,249	0	0.33	308,096
		Spr	0.01	3,604	0	0.37	308,085	0.01	2,229	0	0.23	308,094	0.01	2,179	0	0.22	308,092
		Sum	0.04	4,737	0	0.49	308,101	0.04	5,386	0	0.55	308,094	0.04	5,218	0	0.54	308,085
		Fal	0.02	4,448	0	0.46	308,100	0.01	1,241	0.025	0.13	308,088	0.00	1,257	0.024	0.13	308,064
		Ann	0.03	5,216	0	0.54	308,090	0.02	4,292	0	0.44	308,080	0.02	5,825	0	0.60	308,072
	RCP4.5	Win	0.04	4,979	0	0.52	301,569	0.03	3,798	0	0.40	301,564	0.03	3,705	0	0.38	308,099
		Spr	0.02	4,802	0	0.49	308,095	0.02	3,611	0	0.37	308,096	0.01	3,914	0	0.40	308,085
		Sum	0.05	6,220	0	0.64	308,104	0.06	6,955	0	0.71	308,107	0.05	6,732	0	0.69	308,100
		Fal	0.03	5,617	0	0.58	308,100	0.02	3,635	0	0.37	308,104	0.01	4,050	0	0.42	308,081
		Ann	0.04	6,226	0	0.64	308,098	0.03	6,182	0	0.64	308,101	0.03	6,991	0	0.72	308,090
	RCP8.5	Win	0.05	5,592	0	0.58	301,565	0.04	4,926	0	0.51	301,570	0.04	4,995	0	0.51	308,108
		Spr	0.03	6,072	0	0.62	308,098	0.03	5,237	0	0.54	308,097	0.02	5,627	0	0.58	308,090
		Sum	0.08	7,241	0	0.74	308,108	0.08	8,064	0	0.83	308,108	0.08	7,752	0	0.80	308,109
		Fal	0.06	6,848	0	0.70	308,107	0.04	6,021	0	0.62	308,097	0.03	5,972	0	0.61	308,098
		Ann	0.05	7,104	0	0.73	308,107	0.05	7,382	0	0.76	308,104	0.04	7,960	0	0.82	308,096

Table C-1. Continued

Var.	Scen.	Time	Moss Peak					North Fork Jocko					Polson Kerr Dam				
			Sl.	S	p	$\tau$	VarS	Sl.	S	p	$\tau$	VarS	Sl.	S	p	$\tau$	VarS
Max SAT	RCP2.6	Win	0.02	3,358	0	0.35	301,573	0.01	2,621	0	0.27	301,568	0.02	2,836	0	0.29	308,087
		Spr	0.01	1,819	0.001	0.19	308,087	0.01	1,566	0.005	0.16	308,098	0.01	1,780	0.001	0.18	308,099
		Sum	0.05	5,379	0	0.55	308,094	0.05	5,400	0	0.55	308,104	0.04	5,265	0	0.54	308,101
		Fal	0.01	1,412	0.011	0.15	308,097	0.01	897	0.106	0.09	308,096	0.01	1,296	0.020	0.13	308,088
		Ann	0.02	5,466	0	0.56	308,101	0.02	4,788	0	0.49	308,093	0.02	4,752	0	0.49	308,077
	RCP4.5	Win	0.02	4,067	0	0.42	301,560	0.02	3,309	0	0.35	301,565	0.02	3,402	0	0.35	308,100
		Spr	0.02	3,039	0	0.31	308,097	0.02	2,877	0	0.30	308,090	0.02	2,983	0	0.31	308,101
		Sum	0.07	6,674	0	0.69	308,102	0.07	6,776	0	0.70	308,106	0.06	6,565	0	0.67	308,104
		Fal	0.02	3,681	0	0.38	308,092	0.02	3,319	0	0.34	308,098	0.02	3,780	0	0.39	308,099
		Ann	0.03	6,980	0	0.72	308,104	0.03	6,699	0	0.69	308,100	0.03	6,315	0	0.65	308,099
	RCP8.5	Win	0.04	5,413	0	0.56	301,569	0.03	4,694	0	0.49	301,566	0.03	4,373	0	0.45	308,108
		Spr	0.03	4,700	0	0.48	308,103	0.03	4,640	0	0.48	308,103	0.03	4,598	0	0.47	308,094
		Sum	0.10	7,669	0	0.79	308,101	0.10	7,776	0	0.80	308,108	0.08	7,622	0	0.78	308,111
		Fal	0.05	5,974	0	0.61	308,105	0.05	5,715	0	0.59	308,100	0.04	5,849	0	0.60	308,103
		Ann	0.05	7,821	0	0.80	308,101	0.05	7,697	0	0.79	308,106	0.05	7,305	0	0.75	308,103
Min SAT	RCP2.6	Win	0.02	2,737	0	0.29	301,563	0.01	2,152	0	0.22	301,563	0.03	4,295	0	0.44	308,101
		Spr	0.01	2,267	0	0.23	308,099	0.01	2,360	0	0.24	308,093	0.01	2,386	0	0.25	308,087
		Sum	0.05	5,543	0	0.57	308,104	0.04	5,291	0	0.54	308,078	0.04	5,418	0	0.56	308,095
		Fal	0.01	1,579	0.004	0.16	308,091	0.00	1,240	0.026	0.13	308,081	0.02	4,120	0	0.42	308,081
		Ann	0.02	5,151	0	0.53	308,077	0.02	4,737	0	0.49	308,092	0.02	5,812	0	0.60	308,091
	RCP4.5	Win	0.02	3,582	0	0.37	301,563	0.02	3,114	0	0.32	301,559	0.04	4,915	0	0.51	308,108
		Spr	0.02	3,716	0	0.38	308,086	0.02	3,651	0	0.38	308,106	0.01	3,455	0	0.36	308,077
		Sum	0.06	7,090	0	0.73	308,107	0.05	6,825	0	0.70	308,090	0.05	7,108	0	0.73	308,105
		Fal	0.02	4,151	0	0.43	308,102	0.01	3,749	0	0.39	308,076	0.02	5,743	0	0.59	308,085
		Ann	0.03	6,835	0	0.70	308,095	0.02	6,503	0	0.67	308,086	0.03	6,795	0	0.70	308,092
	RCP8.5	Win	0.03	4,835	0	0.50	301,567	0.03	4,206	0	0.44	301,565	0.05	5,850	0	0.60	308,111
		Spr	0.03	5,590	0	0.57	308,089	0.03	5,290	0	0.54	308,100	0.03	5,617	0	0.58	308,095
		Sum	0.09	8,083	0	0.83	308,112	0.07	7,797	0	0.80	308,098	0.07	7,876	0	0.81	308,107
		Fal	0.04	6,234	0	0.64	308,104	0.03	6,067	0	0.62	308,099	0.04	7,064	0	0.73	308,098
		Ann	0.05	7,910	0	0.81	308,105	0.04	7,406	0	0.76	308,097	0.05	7,761	0	0.80	308,105

Table C-1. Continued

Var.	Scen.	Time	Saint Ignatius					Seeley Lake Ranger Station					Superior				
			Sl.	S	p	$\tau$	VarS	Sl.	S	p	$\tau$	VarS	Sl.	S	p	$\tau$	VarS
Max SAT	RCP2.6	Win	0.01	2,328	0	0.24	308,107	0.03	4,105	0	0.42	308,090	0.01	3,166	0	0.33	308,094
		Spr	0.01	2,811	0	0.29	308,095	0.02	3,170	0	0.33	308,080	0.02	3,154	0	0.32	308,105
		Sum	0.05	4,963	0	0.51	308,096	0.06	5,330	0	0.55	308,103	0.06	5,423	0	0.56	308,106
		Fal	0.01	1,670	0.003	0.17	308,091	0.01	2,250	0	0.23	308,097	0.01	1,558	0.005	0.16	308,096
		Ann	0.02	5,369	0	0.55	308,094	0.03	5,512	0	0.57	308,087	0.02	5,478	0	0.56	308,091
	RCP4.5	Win	0.02	2,766	0	0.28	308,102	0.03	4,551	0	0.47	308,099	0.02	3,894	0	0.40	308,097
		Spr	0.02	4,246	0	0.44	308,093	0.03	4,394	0	0.45	308,095	0.02	4,319	0	0.44	308,101
		Sum	0.07	6,557	0	0.67	308,103	0.08	6,622	0	0.68	308,107	0.08	6,838	0	0.70	308,104
		Fal	0.02	4,353	0	0.45	308,094	0.03	4,439	0	0.46	308,102	0.02	3,993	0	0.41	308,094
		Ann	0.03	6,812	0	0.70	308,097	0.04	6,728	0	0.69	308,103	0.03	6,858	0	0.70	308,098
	RCP8.5	Win	0.02	3,716	0	0.38	308,097	0.04	5,598	0	0.58	308,095	0.03	4,944	0	0.51	308,093
		Spr	0.04	5,369	0	0.55	308,106	0.04	5,658	0	0.58	308,109	0.04	5,833	0	0.60	308,106
		Sum	0.10	7,636	0	0.78	308,100	0.11	7,659	0	0.79	308,106	0.11	7,949	0	0.82	308,110
		Fal	0.05	6,152	0	0.63	308,102	0.06	6,362	0	0.65	308,108	0.05	6,102	0	0.63	308,104
		Ann	0.05	7,664	0	0.79	308,104	0.06	7,586	0	0.78	308,107	0.06	7,775	0	0.80	308,103
Min SAT	RCP2.6	Win	0.03	3,791	0	0.39	308,106	0.04	4,507	0	0.46	308,101	0.03	4,384	0	0.45	308,106
		Spr	0.01	2,298	0	0.24	308,082	0.01	2,316	0	0.24	308,089	0.01	2,760	0	0.28	308,081
		Sum	0.03	5,210	0	0.54	308,100	0.03	5,081	0	0.52	308,106	0.04	5,585	0	0.57	308,087
		Fal	0.02	4,206	0	0.43	308,095	0.02	4,717	0	0.48	308,100	0.02	4,742	0	0.49	308,089
		Ann	0.02	5,589	0	0.57	308,068	0.03	5,815	0	0.60	308,098	0.02	5,859	0	0.60	308,073
	RCP4.5	Win	0.04	4,393	0	0.45	308,106	0.05	5,004	0	0.51	308,109	0.04	4,893	0	0.50	308,103
		Spr	0.01	3,319	0	0.34	308,090	0.02	3,183	0	0.33	308,105	0.01	3,558	0	0.37	308,094
		Sum	0.04	7,113	0	0.73	308,107	0.05	6,692	0	0.69	308,103	0.05	7,114	0	0.73	308,098
		Fal	0.03	5,645	0	0.58	308,100	0.03	5,666	0	0.58	308,091	0.03	5,829	0	0.60	308,103
		Ann	0.03	6,726	0	0.69	308,093	0.03	6,540	0	0.67	308,102	0.03	6,772	0	0.70	308,099
	RCP8.5	Win	0.05	5,130	0	0.53	308,105	0.07	5,972	0	0.61	308,102	0.05	5,558	0	0.57	308,111
		Spr	0.03	5,633	0	0.58	308,099	0.03	5,313	0	0.55	308,103	0.03	5,956	0	0.61	308,096
		Sum	0.06	7,919	0	0.81	308,106	0.07	7,468	0	0.77	308,105	0.07	7,926	0	0.81	308,098
		Fal	0.05	6,839	0	0.70	308,106	0.05	6,914	0	0.71	308,111	0.05	6,908	0	0.71	308,104
		Ann	0.05	7,706	0	0.79	308,107	0.06	7,551	0	0.78	308,108	0.05	7,732	0	0.79	308,104

APPENDIX D: Analysis of snowpack

**Table D-1: Main statistics – Kendall’s  $\tau$ , p value, Theil-Sen’s slope, Kendall’s statistic S and its variance, and rate of change ( $\phi$ ) – related to the Mann-Kendall and regional Kendall tests applied to thirteen snowpack indices over the 1994-2018 period (tests in which the null hypothesis is rejected are highlighted in gray and the corresponding p value in bold)**

Location	Statistic*	MSWE	DMSWE	SMO	SM50	1ASWE	PSO	PSE
Bisson Creek	$\tau$	0.09	-0.22	0.05	-0.06	0.01	0.16	-0.07
	p	0.53	0.14	0.73	0.71	0.98	0.27	0.64
	Slope	1.69	-0.74	0.18	-0.13	0.00	0.55	-0.18
	S	26	-61	15	-16	2	45	-20
	VarS	1,621	1,622	1,620	1,616	1,621	1,622	1,617
	$\phi$	40.6	-17.7	4.4	-3.1	0.0	13.3	-4.3
Kraft Creek	$\tau$	0.03	0.01	-0.03	-0.17	-0.03	0.24	-0.22
	p	0.86	0.96	0.86	0.26	0.88	0.11	0.14
	Slope	1.00	0.07	-0.02	-0.36	-1.19	0.60	-0.73
	S	8	3	-8	-46	-7	66	-60
	VarS	1,625	1,622	1,616	1,619	1,624	1,621	1,623
	$\phi$	24.0	1.7	-0.6	-8.7	-28.4	14.4	-17.6
Moss Peak	$\tau$	0.16	-0.17	-0.33	-0.07	0.17	0.05	-0.04
	p	0.29	0.26	<b>0.02</b>	0.64	0.26	0.77	0.82
	Slope	11.11	-0.28	-0.92	-0.14	7.08	0.13	-0.06
	S	44	-46	-92	-20	46	13	-10
	VarS	1,625	1,614	1,623	1,619	1,625	1,620	1,617
	$\phi$	266.7	-6.7	-22.1	-3.4	170.0	3.2	-1.5
North Fork Jocko	$\tau$	0.04	0.07	-0.02	0.02	0.01	0.35	-0.02
	p	0.80	0.65	0.92	0.92	0.98	<b>0.02</b>	0.90
	Slope	4.61	0.23	-0.13	0.00	1.61	0.78	-0.07
	S	11	19	-5	5	2	96	-6
	VarS	1,624	1,620	1,622	1,615	1,625	1,619	1,621
	$\phi$	110.6	5.4	-3.0	0.0	38.5	18.7	-1.6
Sleeping Woman	$\tau$	0.12	-0.12	0.06	-0.16	0.07	0.25	-0.19
	p	0.43	0.44	0.69	0.27	0.67	0.09	0.20
	Slope	2.04	-0.33	0.17	-0.33	2.04	0.60	-0.44
	S	33	-32	17	-45	18	70	-52
	VarS	1,622	1,621	1,618	1,612	1,623	1,621	1,613
	$\phi$	48.9	-8.0	4.0	-8.0	49.0	14.4	-10.7
Stuart Mountain	$\tau$	0.13	0.09	-0.09	0.03	0.11	-0.12	-0.01
	p	0.37	0.53	0.53	0.88	0.49	0.44	0.96
	Slope	6.27	0.39	-0.25	0.00	4.09	-0.40	0.00
	S	37	26	-26	7	29	-32	-3
	VarS	1,624	1,621	1,617	1,615	1,622	1,616	1,609
	$\phi$	150.4	9.3	-6.0	0.0	98.2	-9.6	0.0
Flathead Region	$\tau$	0.10	-0.05	-0.06	-0.07	0.05	0.16	-0.09
	p	0.11	0.36	0.32	0.25	0.37	<b>0.01</b>	0.13
	Slope	2.86	-0.13	-0.20	-0.15	2.13	0.44	-0.19
	S	159	-91	-99	-115	90	258	-151
	VarS	9,743	9,719	9,716	9,695	9,742	9,719	9,700
	$\phi$	68.6	-3.0	-4.8	-3.5	51.2	10.7	-4.5

Table D1. Continued

Location	Statistic*	PSD	SMD	SWE0	SAO	SME	SSD
Bisson Creek	$\tau$	-0.20	-0.14	0.26	0.02	-0.07	-0.06
	$\rho$	0.18	0.33	0.07	0.90	0.67	0.69
	Slope	-0.77	-0.38	1.00	0.05	-0.17	-0.27
	S	-55	-40	73	6	-18	-17
	VarS	1,622	1,619	1,622	1,619	1,619	1,622
	$\phi$	-18.5	-9.1	24.0	1.1	-4.0	-6.6
Kraft Creek	$\tau$	-0.25	-0.13	0.30	0.33	-0.30	-0.32
	$\rho$	0.09	0.38	<b>0.04</b>	<b>0.03</b>	<b>0.04</b>	<b>0.03</b>
	Slope	-1.35	-0.58	1.86	0.73	-1.39	-2.06
	S	-69	-36	84	90	-84	-87
	VarS	1,620	1,621	1,623	1,621	1,623	1,620
	$\phi$	-32.4	-14.0	44.6	17.5	-33.4	-49.4
Moss Peak	$\tau$	-0.10	0.26	0.11	0.05	-0.04	-0.06
	$\rho$	0.50	0.08	0.47	0.73	0.82	0.69
	Slope	-0.36	0.84	0.26	0.15	-0.06	-0.18
	S	-28	71	30	15	-10	-17
	VarS	1,621	1,620	1,619	1,620	1,617	1,620
	$\phi$	-8.7	20.1	6.2	3.7	-1.5	-4.3
North Fork Jocko	$\tau$	-0.20	0.04	0.20	0.15	-0.02	-0.11
	$\rho$	0.18	0.78	0.19	0.31	0.90	0.46
	Slope	-0.93	0.30	0.81	0.36	-0.07	-0.21
	S	-55	12	54	42	-6	-31
	VarS	1,620	1,623	1,621	1,619	1,621	1,618
	$\phi$	-22.4	7.2	19.5	8.5	-1.6	-5.1
Sleeping Woman	$\tau$	-0.30	-0.35	0.40	0.13	-0.20	-0.22
	$\rho$	<b>0.04</b>	<b>0.02</b>	<b>0.01</b>	0.38	0.17	0.14
	Slope	-0.89	-0.75	1.00	0.43	-0.50	-0.68
	S	-84	-97	111	36	-56	-60
	VarS	1,619	1,620	1,617	1,621	1,613	1,621
	$\phi$	-21.3	-18.0	24.0	10.3	-12.0	-16.4
Stuart Mountain	$\tau$	0.14	0.10	-0.03	-0.08	-0.01	0.13
	$\rho$	0.35	0.52	0.88	0.62	0.96	0.37
	Slope	0.50	0.31	-0.13	-0.20	0.00	0.48
	S	39	27	-7	-21	-3	37
	VarS	1,624	1,620	1,620	1,622	1,609	1,624
	$\phi$	12.0	7.3	-3.0	-4.8	0.0	11.6
Flathead Region	$\tau$	-0.15	-0.04	0.21	0.10	-0.11	-0.11
	$\rho$	<b>0.01</b>	0.53	<b>0.00</b>	0.09	0.07	0.08
	Slope	-0.60	-0.11	0.75	0.29	-0.25	-0.42
	S	-252	-63	345	168	-177	-175
	VarS	9,727	9,722	9,722	9,722	9,702	9,725
	$\phi$	-14.4	-2.6	18.0	7.1	-6.0	-10.1

\*  $\phi$  is measured either in mm (MSWE and 1ASWE) or days (all other indices) over the 24-year period

**Table D-2: Main statistics – Kendall’s  $\tau$ , p value, Theil-Sen’s slope, Kendall’s statistic S and its variance, and rate of change ( $\phi$ ) – related to the Mann-Kendall and regional Kendall tests applied to monthly averages of mean SAT and SPR over 1994-2018 (tests in which the null hypothesis is rejected are shown in gray and the related p value in bold)**

Location	Statistic*	Mean SAT (°C)							
		Oct	Nov	Dec	Jan	Feb	Mar	Apr	May
Bisson Creek	$\tau$	0.32	0.13	0.13	0.12	0.09	0.46	0.18	0.18
	p	<b>0.03</b>	0.39	0.39	0.44	0.57	<b>0.00</b>	0.22	0.22
	Slope	0.12	0.05	0.04	0.08	0.03	0.14	0.04	0.05
	S	88	36	36	32	24	128	50	50
	VarS	1,625	1,625	1,625	1,625	1,625	1,625	1,625	1,625
	$\phi$	2.9	1.1	0.9	1.9	0.8	3.4	1.0	1.2
Kraft Creek	$\tau$	0.51	0.36	0.07	0.36	0.28	0.43	0.22	0.39
	p	<b>0.00</b>	<b>0.02</b>	0.64	<b>0.02</b>	0.06	<b>0.00</b>	0.14	<b>0.01</b>
	Slope	0.19	0.14	0.03	0.15	0.15	0.17	0.08	0.10
	S	142	98	20	98	76	118	60	108
	VarS	1,625	1,625	1,625	1,625	1,625	1,625	1,625	1,625
	$\phi$	4.7	3.3	0.7	3.6	3.7	4.2	2.0	2.4
Moss Peak	$\tau$	0.27	0.25	0.04	0.28	0.17	0.46	0.26	0.25
	p	0.07	0.10	0.82	0.06	0.24	<b>0.00</b>	0.08	0.09
	Slope	0.10	0.10	0.02	0.10	0.09	0.16	0.09	0.06
	S	74	68	10	78	48	128	72	70
	VarS	1,625	1,625	1,625	1,625	1,625	1,625	1,625	1,625
	$\phi$	2.5	2.3	0.5	2.5	2.1	3.8	2.1	1.4
North Fork Jocko	$\tau$	0.34	0.25	0.04	0.32	0.22	0.42	0.25	0.36
	p	<b>0.02</b>	0.10	0.82	<b>0.03</b>	0.13	<b>0.00</b>	0.10	<b>0.02</b>
	Slope	0.11	0.08	0.02	0.09	0.09	0.15	0.04	0.07
	S	94	68	10	88	62	116	68	98
	VarS	1,625	1,625	1,625	1,625	1,625	1,625	1,625	1,625
	$\phi$	2.6	1.9	0.5	2.2	2.2	3.5	1.0	1.8
Sleeping Woman	$\tau$	0.31	0.25	0.20	0.29	0.13	0.48	0.22	0.22
	p	<b>0.03</b>	0.09	0.19	0.05	0.39	<b>0.00</b>	0.13	0.14
	Slope	0.12	0.08	0.06	0.10	0.06	0.15	0.06	0.07
	S	86	70	54	80	36	132	62	60
	VarS	1,625	1,625	1,625	1,625	1,625	1,625	1,625	1,625
	$\phi$	2.9	2.0	1.4	2.4	1.5	3.7	1.4	1.6
Stuart Mountain	$\tau$	0.27	0.21	0.04	0.18	0.32	0.42	0.31	0.21
	p	0.07	0.16	0.82	0.22	<b>0.03</b>	<b>0.00</b>	<b>0.03</b>	0.16
	Slope	0.14	0.07	0.01	0.08	0.10	0.14	0.09	0.06
	S	74	58	10	50	88	116	86	57
	VarS	1,625	1,625	1,625	1,625	1,625	1,625	1,625	1,624
	$\phi$	3.4	1.7	0.4	2.0	2.4	3.3	2.1	1.4
Flathead Region	$\tau$	0.34	0.24	0.08	0.26	0.20	0.45	0.24	0.27
	p	<b>0.01</b>	0.08	0.53	0.06	0.12	<b>0.00</b>	0.07	<b>0.04</b>
	Slope	0.13	0.09	0.03	0.10	0.09	0.15	0.07	0.07
	S	558	398	140	426	334	738	398	443
	VarS	49,079	51,689	49,397	51,023	46,193	51,273	49,609	46,149
	$\phi$	3.2	2.1	0.7	2.4	2.1	3.6	1.6	1.7

Table D-2. Continued

Location	Statistic*	Maximum Air Temperature (°C)							
		Oct	Nov	Dec	Jan	Feb	Mar	Apr	May
Bisson Creek	τ	0.31	0.18	0.09	0.20	0.13	0.52	0.14	0.09
	ρ	<b>0.03</b>	0.22	0.54	0.17	0.39	<b>0.00</b>	0.36	0.57
	Slope	0.09	0.08	0.02	0.08	0.05	0.17	0.05	0.07
	S	86	50	26	56	36	144	38	24
	VarS	1,625	1,625	1,625	1,625	1,625	1,625	1,625	1,625
	φ	2.1	1.8	0.6	1.9	1.3	4.1	1.1	1.6
Kraft Creek	τ	0.49	0.43	0.19	0.52	0.33	0.48	0.07	-0.01
	ρ	<b>0.00</b>	<b>0.00</b>	0.21	<b>0.00</b>	<b>0.02</b>	<b>0.00</b>	0.67	0.98
	Slope	0.17	0.19	0.11	0.19	0.11	0.15	0.02	-0.01
	S	134	118	52	144	92	132	18	-2
	VarS	1,625	1,625	1,625	1,625	1,625	1,625	1,625	1,625
	φ	4.0	4.5	2.6	4.7	2.7	3.5	0.4	-0.1
Moss Peak	τ	0.28	0.29	0.04	0.26	0.30	0.37	0.20	0.19
	ρ	0.06	<b>0.05</b>	0.82	0.08	<b>0.04</b>	<b>0.01</b>	0.17	0.21
	Slope	0.14	0.10	0.01	0.08	0.12	0.15	0.08	0.06
	S	76	80	10	72	82	102	56	52
	VarS	1,625	1,625	1,625	1,625	1,625	1,625	1,625	1,625
	φ	3.3	2.3	0.1	2.0	3.0	3.6	1.9	1.4
North Fork Jocko	τ	0.23	0.32	0.15	0.38	0.00	0.56	0.23	0.40
	ρ	0.12	<b>0.03</b>	0.31	<b>0.01</b>	1.00	<b>0.00</b>	0.12	<b>0.01</b>
	Slope	0.10	0.13	0.03	0.14	0.00	0.20	0.07	0.14
	S	64	88	42	106	0	154	64	110
	VarS	1,625	1,625	1,625	1,625	1,625	1,625	1,625	1,625
	φ	2.3	3.1	0.8	3.3	0.0	4.7	1.7	3.4
Sleeping Woman	τ	0.40	0.34	0.23	0.38	0.22	0.48	0.20	0.22
	ρ	<b>0.01</b>	<b>0.02</b>	0.12	<b>0.01</b>	0.14	<b>0.00</b>	0.19	0.14
	Slope	0.13	0.08	0.06	0.14	0.07	0.16	0.06	0.09
	S	110	94	64	104	60	132	54	60
	VarS	1,625	1,625	1,625	1,625	1,625	1,625	1,625	1,625
	φ	3.2	2.0	1.5	3.4	1.7	3.8	1.3	2.3
Stuart Mountain	τ	0.21	0.23	0.03	0.23	0.15	0.33	0.22	0.12
	ρ	0.16	0.12	0.84	0.12	0.31	<b>0.02</b>	0.14	0.41
	Slope	0.12	0.09	0.01	0.08	0.04	0.09	0.07	0.08
	S	58	64	9	64	42	92	60	34
	VarS	1,625	1,625	1,624	1,625	1,625	1,625	1,625	1,625
	φ	2.8	2.1	0.2	2.0	1.0	2.1	1.7	1.9
Flathead Region	τ	0.32	0.30	0.12	0.33	0.19	0.46	0.18	0.17
	ρ	<b>0.01</b>	<b>0.03</b>	0.36	<b>0.01</b>	0.14	<b>0.00</b>	0.17	0.18
	Slope	0.12	0.10	0.04	0.12	0.06	0.15	0.06	0.08
	S	528	494	203	546	312	756	290	278
	VarS	45,104	49,900	48,786	48,223	44,067	48,264	43,748	42,401
	φ	2.9	2.5	0.9	2.9	1.5	3.7	1.4	1.9

Table D-2. Continued

Location	Statistic*	Minimum Air Temperature (°C)							
		Oct	Nov	Dec	Jan	Feb	Mar	Apr	May
Bisson Creek	τ	0.33	0.07	0.05	0.12	0.06	0.41	0.13	0.32
	ρ	<b>0.02</b>	0.67	0.75	0.44	0.71	<b>0.01</b>	0.39	<b>0.03</b>
	Slope	0.14	0.03	0.02	0.07	0.02	0.14	0.04	0.08
	S	92	18	14	32	16	114	36	88
	VarS	1,625	1,625	1,625	1,625	1,625	1,625	1,625	1,625
	φ	3.3	0.7	0.4	1.7	0.4	3.3	0.9	2.0
Kraft Creek	τ	0.46	0.21	0.08	0.33	0.26	0.39	0.25	0.48
	ρ	<b>0.00</b>	0.16	0.60	<b>0.03</b>	0.08	<b>0.01</b>	0.09	<b>0.00</b>
	Slope	0.17	0.11	0.05	0.15	0.16	0.19	0.07	0.13
	S	128	58	22	90	72	108	70	132
	VarS	1,625	1,625	1,625	1,625	1,625	1,625	1,625	1,625
	φ	4.0	2.7	1.2	3.6	3.9	4.6	1.8	3.1
Moss Peak	τ	0.28	0.19	0.04	0.22	0.23	0.41	0.25	0.28
	ρ	0.06	0.21	0.82	0.13	0.12	<b>0.01</b>	0.10	0.06
	Slope	0.13	0.08	0.02	0.10	0.11	0.18	0.08	0.07
	S	78	52	10	62	64	114	68	76
	VarS	1,625	1,625	1,625	1,625	1,625	1,625	1,625	1,625
	φ	3.1	1.9	0.5	2.5	2.6	4.2	1.9	1.7
North Fork Jocko	τ	0.37	0.18	0.04	0.22	0.15	0.34	0.21	0.32
	ρ	<b>0.01</b>	0.22	0.82	0.14	0.31	<b>0.02</b>	0.16	<b>0.03</b>
	Slope	0.12	0.09	0.02	0.09	0.08	0.16	0.06	0.08
	S	102	50	10	60	42	94	58	88
	VarS	1,625	1,625	1,625	1,625	1,625	1,625	1,625	1,625
	φ	2.8	2.0	0.4	2.0	2.0	3.7	1.5	2.0
Sleeping Woman	τ	0.33	0.20	0.20	0.19	0.16	0.39	0.24	0.19
	ρ	<b>0.03</b>	0.19	0.19	0.21	0.29	<b>0.01</b>	0.11	0.21
	Slope	0.12	0.08	0.08	0.07	0.06	0.15	0.08	0.06
	S	90	54	54	52	44	108	66	52
	VarS	1,625	1,625	1,625	1,625	1,625	1,625	1,625	1,625
	φ	3.0	2.0	1.9	1.7	1.5	3.6	1.9	1.4
Stuart Mountain	τ	0.36	0.15	0.07	0.14	0.36	0.43	0.26	0.25
	ρ	<b>0.02</b>	0.31	0.67	0.33	<b>0.02</b>	<b>0.00</b>	0.08	0.09
	Slope	0.16	0.07	0.02	0.07	0.14	0.16	0.09	0.07
	S	98	42	18	40	98	120	72	70
	VarS	1,625	1,625	1,625	1,625	1,625	1,625	1,625	1,625
	φ	3.7	1.7	0.4	1.7	3.3	3.8	2.2	1.7
Flathead Region	τ	0.36	0.17	0.08	0.20	0.20	0.40	0.22	0.31
	ρ	<b>0.01</b>	0.23	0.56	0.14	0.13	<b>0.00</b>	0.09	<b>0.02</b>
	Slope	0.14	0.07	0.03	0.10	0.10	0.16	0.07	0.08
	S	588	274	128	336	336	658	370	506
	VarS	48,587	51,876	48,104	51,187	47,853	50,441	48,516	46,100
	φ	3.3	1.8	0.7	2.3	2.5	3.8	1.7	2.0

Table D-2. Continued

Location	Statistic*	SPR							
		Oct	Nov	Dec	Jan	Feb	Mar	Apr	May
Bisson Creek	$\tau$	-0.12	-0.13	0.09	0.16	0.15	-0.26	-0.01	-0.26
	$\rho$	0.44	0.37	0.55	0.29	0.32	0.08	0.98	0.06
	Slope	0.00	-0.01	0.00	0.00	0.01	-0.01	0.00	0.00
	S	-32	-37	25	44	39	-72	-2	-73
	VarS	1,609	1,622	1,624	1,623	1,432	1,625	1,625	1,500
	$\phi$	-0.07	-0.16	0.06	0.08	0.13	-0.21	0.00	-0.07
Kraft Creek	$\tau$	-0.23	-0.20	0.24	0.12	0.04	-0.13	0.25	-0.08
	$\rho$	0.12	0.19	0.11	0.41	0.82	0.39	0.09	0.53
	Slope	-0.01	-0.01	0.01	0.00	0.00	-0.01	0.01	0.00
	S	-64	-54	66	34	10	-36	70	-23
	VarS	1,609	1,625	1,625	1,625	1,625	1,625	1,617	1,217
	$\phi$	-0.23	-0.24	0.18	0.07	0.03	-0.28	0.32	0.00
Moss Peak	$\tau$	-0.17	-0.31	-0.08	-0.11	-0.30	0.10	0.07	0.03
	$\rho$	0.26	<b>0.04</b>	0.60	0.49	<b>0.04</b>	0.52	0.64	0.86
	Slope	-0.01	0.00	0.00	0.00	0.00	0.00	0.00	0.00
	S	-46	-85	-22	-29	-84	27	20	8
	VarS	1,625	1,624	1,625	1,624	1,625	1,624	1,625	1,625
	$\phi$	-0.18	-0.08	-0.03	-0.02	-0.06	0.02	0.05	0.02
North Fork Jocko	$\tau$	-0.21	-0.30	-0.16	0.00	0.08	-0.09	0.10	0.05
	$\rho$	0.16	<b>0.04</b>	0.29	1.00	0.60	0.54	0.50	0.75
	Slope	-0.01	-0.01	0.00	0.00	0.00	0.00	0.00	0.00
	S	-58	-84	-44	0	22	-26	28	14
	VarS	1,625	1,625	1,625	1,625	1,625	1,625	1,625	1,625
	$\phi$	-0.26	-0.19	-0.05	0.00	0.03	-0.06	0.09	0.06
Sleeping Woman	$\tau$	-0.16	-0.15	0.12	0.03	0.06	-0.27	-0.03	-0.12
	$\rho$	0.30	0.31	0.43	0.86	0.71	<b>0.04</b>	0.86	0.44
	Slope	-0.01	0.00	0.00	0.00	0.00	-0.01	0.00	0.00
	S	-43	-42	33	8	16	-74	-8	-32
	VarS	1,620	1,623	1,624	1,625	1,625	1,625	1,625	1,617
	$\phi$	-0.18	-0.09	0.06	0.01	0.02	-0.22	-0.04	-0.09
Stuart Mountain	$\tau$	-0.08	-0.14	0.04	0.06	0.16	0.04	0.21	0.16
	$\rho$	0.62	0.36	0.80	0.71	0.29	0.78	0.16	0.29
	Slope	0.00	0.00	0.00	0.00	0.00	0.00	0.01	0.01
	S	-21	-38	11	16	44	12	58	44
	VarS	1,624	1,625	1,624	1,625	1,625	1,625	1,625	1,625
	$\phi$	-0.04	-0.06	0.01	0.02	0.05	0.01	0.17	0.25
Flathead Region	$\tau$	-0.16	-0.21	0.04	0.04	0.03	-0.10	0.10	-0.04
	$\rho$	<b>0.01</b>	<b>0.00</b>	0.49	0.47	0.64	0.09	0.09	0.53
	Slope	-0.01	-0.01	0.00	0.00	0.00	0.00	0.00	0.00
	S	-264	-340	69	73	47	-169	166	-62
	VarS	35,137	33,895	24,447	21,212	13,944	14,092	22,354	27,129
	$\phi$	-0.15	-0.12	0.01	0.01	0.01	-0.08	0.10	0.00

\*  $\phi$  is either measured in °C (mean air temperature) or is dimensionless (SPR); in both cases,  $\phi$  refers to the entire 24-year period

**Table D-3: Main statistics – Kendall’s  $\tau$ ,  $p$  value, Theil-Sen’s slope, Kendall’s statistic  $S$  and its variance, and rate of change ( $\phi$ ) – related to the Mann-Kendall and regional Kendall tests applied to bimonthly averages of air temperature and SDN over 2003-2018 (tests in which the null hypothesis is rejected are highlighted in gray and the associated  $p$  value in bold)**

Station	Statistic	Mean SAT (°C)				Maximum SAT (°C)			
		Oct-Nov	Dec-Jan	Feb-Mar	Apr-May	Oct-Nov	Dec-Jan	Feb-Mar	Apr-May
Bisson Creek	$\tau$	0.02	0.07	-0.03	0.15	0.02	0.04	-0.04	0.18
	$p$	0.92	0.65	0.86	0.28	0.92	0.81	0.81	0.21
	Slope	0.02	0.03	-0.02	0.08	0.01	0.02	-0.01	0.12
	$S$	4	14	-6	32	4	8	-8	37
	VarS	817	817	817	817	817	817	817	816
	$\phi$	0.3	0.5	-0.3	1.2	0.1	0.4	-0.2	1.8
Kraft Creek	$\tau$	0.01	0.10	-0.03	0.12	0.00	0.09	0.06	0.21
	$p$	0.97	0.51	0.86	0.38	1.00	0.53	0.70	0.13
	Slope	0.01	0.09	-0.01	0.06	0.00	0.07	0.03	0.12
	$S$	2	20	-6	26	0	19	12	44
	VarS	817	817	817	817	817	816	817	817
	$\phi$	0.2	1.3	-0.1	0.9	0.0	1.1	0.5	1.8
Moss Peak	$\tau$	0.01	0.02	-0.04	0.16	-0.05	0.02	-0.05	0.13
	$p$	0.97	0.92	0.81	0.25	0.75	0.92	0.73	0.36
	Slope	0.01	0.02	-0.03	0.07	-0.04	0.01	-0.04	0.10
	$S$	2	4	-8	34	-10	4	-11	27
	VarS	817	817	817	817	817	817	816	816
	$\phi$	0.1	0.3	-0.4	1.1	-0.6	0.2	-0.6	1.5
North Fork Jocko	$\tau$	0.09	0.05	0.04	0.19	-0.03	0.00	-0.03	0.19
	$p$	0.55	0.73	0.81	0.17	0.86	1.00	0.86	0.18
	Slope	0.05	0.03	0.02	0.07	-0.02	0.00	-0.03	0.12
	$S$	18	11	8	40	-6	0	-6	39
	VarS	817	816	817	817	817	817	817	816
	$\phi$	0.7	0.5	0.3	1.1	-0.4	0.0	-0.5	1.8
Sleeping Woman	$\tau$	0.03	0.03	-0.03	0.22	0.00	0.04	0.00	0.21
	$p$	0.86	0.86	0.86	0.12	1.00	0.81	1.00	0.13
	Slope	0.02	0.01	-0.03	0.09	0.00	0.03	0.00	0.12
	$S$	6	6	-6	46	0	8	0	44
	VarS	817	817	817	817	817	817	817	817
	$\phi$	0.3	0.2	-0.5	1.3	0.0	0.4	0.0	1.7
Stuart Mountain	$\tau$	0.02	0.05	-0.01	0.16	-0.07	0.05	-0.05	0.17
	$p$	0.89	0.75	0.97	0.25	0.65	0.75	0.75	0.22
	Slope	0.02	0.03	-0.02	0.09	-0.03	0.03	-0.02	0.11
	$S$	5	10	-2	34	-14	10	-10	36
	VarS	816	817	817	817	817	817	817	817
	$\phi$	0.2	0.4	-0.3	1.4	-0.4	0.5	-0.3	1.7
Flathead Region	$\tau$	0.03	0.05	-0.02	0.17	-0.02	0.04	-0.02	0.18
	$p$	0.74	0.71	0.92	0.23	0.80	0.77	0.91	0.16
	Slope	0.02	0.03	-0.01	0.08	-0.02	0.03	-0.01	0.12
	$S$	37	65	-20	212	-26	49	-23	227
	VarS	11,945	28,742	40,307	31,165	9,903	27,786	39,680	25,967
	$\phi$	0.4	0.8	-0.2	1.8	-0.4	0.6	-0.3	2.8

\*  $\phi$  is measured either in °C (mean air temperature) or in kg/m<sup>3</sup> (SDN) over the 15-year period

Station	Statistic	Minimum Air Temperature (°C)				SDN (Kg/m <sup>3</sup> )			
		Oct-Nov	Dec-Jan	Feb-Mar	Apr-May	Oct-Nov	Dec-Jan	Feb-Mar	Apr-May
Bisson Creek	$\tau$	0.08	0.09	-0.04	0.08	-0.02	-0.07	-0.03	0.33
	$\rho$	0.60	0.55	0.81	0.60	0.93	0.65	0.86	<b>0.02</b>
	Slope	0.03	0.06	-0.03	0.03	-0.08	-0.53	-0.34	4.29
	S	16	18	-8	16	-3	-14	-6	57
	VarS	817	817	817	817	530	817	817	621
	$\phi$	0.4	0.8	-0.4	0.4	-1.1	-8.0	-5.1	64.3
Kraft Creek	$\tau$	0.16	0.14	0.08	0.15	-0.05	-0.26	0.29	0.45
	$\rho$	0.25	0.31	0.60	0.28	0.79	<b>0.04</b>	<b>0.04</b>	<b>0.01</b>
	Slope	0.08	0.11	0.03	0.06	-0.89	-2.01	2.44	10.31
	S	34	30	16	32	-7	-54	60	50
	VarS	817	817	817	817	532	817	817	378
	$\phi$	1.1	1.7	0.5	0.9	-13.3	-30.2	36.6	154.7
Moss Peak	$\tau$	0.07	0.11	-0.01	0.20	0.30	0.06	0.07	0.10
	$\rho$	0.65	0.42	0.97	0.15	<b>0.03</b>	0.70	0.65	0.46
	Slope	0.04	0.04	-0.01	0.05	4.69	0.51	0.57	1.19
	S	14	24	-2	42	62	12	14	22
	VarS	817	817	817	817	817	817	817	817
	$\phi$	0.6	0.5	-0.1	0.8	70.3	7.7	8.6	17.9
North Fork Jocko	$\tau$	0.16	0.09	0.05	0.14	0.15	-0.29	-0.24	0.03
	$\rho$	0.25	0.55	0.75	0.31	0.28	<b>0.04</b>	0.09	0.86
	Slope	0.10	0.08	0.05	0.04	2.15	-1.76	-1.45	0.32
	S	34	18	10	30	32	-60	-50	6
	VarS	817	817	817	817	817	817	817	817
	$\phi$	1.5	1.2	0.7	0.6	32.3	-26.4	-21.8	4.7
Sleeping Woman	$\tau$	0.10	0.10	-0.01	0.27	-0.08	-0.23	-0.02	0.13
	$\rho$	0.46	0.51	0.97	0.05	0.58	0.10	0.92	0.34
	Slope	0.06	0.04	-0.02	0.09	-0.89	-2.01	-0.12	1.91
	S	22	20	-2	56	-16	-48	-4	28
	VarS	817	817	817	817	742	817	817	817
	$\phi$	1.0	0.7	-0.3	1.3	-13.3	-30.1	-1.8	28.7
Stuart Mountain	$\tau$	0.20	0.06	0.05	0.22	0.13	-0.04	-0.05	0.11
	$\rho$	0.15	0.70	0.75	0.11	0.34	0.81	0.75	0.42
	Slope	0.10	0.03	0.02	0.10	1.95	-0.22	-0.26	1.03
	S	42	12	10	47	28	-8	-10	24
	VarS	817	817	817	816	817	817	817	817
	$\phi$	1.6	0.5	0.4	1.4	29.3	-3.3	-3.9	15.5
Flathead Region	$\tau$	0.13	0.10	0.02	0.18	0.09	-0.14	0.00	0.17
	$\rho$	0.15	0.49	0.90	0.22	0.15	<b>0.01</b>	0.97	<b>0.00</b>
	Slope	0.07	0.06	0.01	0.07	1.31	-0.92	0.05	1.96
	S	162	122	24	223	96	-172	4	187
	VarS	12,351	30,276	36,853	32,422	4,254	4,900	4,900	4,266
	$\phi$	1.7	1.5	0.3	1.6	31.4	-22.1	1.2	46.9

**Table D-4: Main statistics – Kendall’s  $\tau$ ,  $\rho$  value, Theil-Sen’s slope, Kendall’s statistic S and its variance, and rate of change per decade ( $\phi$ ) – related to the Mann-Kendall and regional Kendall tests applied to ten snowpack indices within the 1961-2100 period according to the three proposed RCP scenarios (tests in which the null hypothesis is accepted are highlighted in gray and the related p value in bold)**

Scenario	Location	Statistic*	MSWE	DMSWE	SMO	SM50	1ASWE	PSO	PSE	PSD	SMD	SWE0
RCP2.6	Kraft Creek	$\tau$	-0.63	-0.53	-0.53	-0.66	-0.65	0.39	-0.62	-0.55	0.21	0.54
		$\rho$	0	0	0	0	0	0.0038	0	0	<b>0.1228</b>	0.0001
		Slope	-7.24	-0.50	-1.22	-1.94	-11.13	0.91	-0.95	-1.87	0.46	1.80
		S	-240	-199	-201	-248	-246	147	-235	-208	79	203
		VarS	2,562	2,152	2,397	2,557	2,562	2,550	2,552	2,558	2,554	2,559
		$\phi$	-14.5	-1.0	-2.4	-3.9	-22.3	1.8	-1.9	-3.7	0.9	3.6
	Moss Peak	$\tau$	-0.49	-0.47	-0.43	-0.52	-0.52	0.24	-0.58	-0.51	-0.45	0.49
		$\rho$	0.0003	0.0005	0.0015	0.0001	0.0001	<b>0.0811</b>	0	0.0001	0.0008	0.0003
		Slope	-12.41	-0.80	-0.67	-1.10	-9.54	0.31	-1.50	-1.83	-0.76	1.90
		S	-186	-176	-161	-196	-196	89	-220	-193	-170	184
		VarS	2,562	2,551	2,546	2,547	2,562	2,545	2,549	2,557	2,549	2,551
		$\phi$	-24.8	-1.6	-1.3	-2.2	-19.1	0.6	-3.0	-3.7	-1.5	3.8
	North Fork Jocko	$\tau$	-0.46	-0.48	-0.40	-0.53	-0.46	0.01	-0.46	-0.46	-0.31	0.47
		$\rho$	0.0006	0.0004	0.0028	0.0001	0.0006	<b>0.9842</b>	0.0006	0.0007	0.0205	0.0005
		Slope	-14.29	-1.14	-0.73	-0.93	-13.66	0.00	-1.17	-1.38	-0.61	1.54
		S	-174	-181	-152	-202	-174	2	-175	-172	-118	177
		VarS	2,562	2,547	2,547	2,542	2,562	2,545	2,550	2,558	2,551	2,556
		$\phi$	-28.6	-2.3	-1.5	-1.9	-27.3	0.0	-2.3	-2.8	-1.2	3.1
	Flathead Region	$\tau$	-0.53	-0.49	-0.45	-0.57	-0.54	0.21	-0.56	-0.51	-0.18	0.50
		$\rho$	0	0	0	0	0	0.0067	0	0	0.0174	0
Slope		-9.95	-0.75	-0.83	-1.19	-11.67	0.38	-1.16	-1.67	-0.38	1.73	
S		-600	-556	-514	-646	-616	238	-630	-573	-209	564	
VarS		7,686	7,249	7,489	7,647	7,686	7,640	7,650	7,673	7,654	7,667	
$\phi$		-19.9	-1.5	-1.7	-2.4	-23.3	0.8	-2.3	-3.3	-0.8	3.5	

Table D-4. Continued

Scenario	Location	Statistic*	MSWE	DMSWE	SMO	SM50	1ASWE	PSO	PSE	PSD	SMD	SWE0
RCP4.5	Kraft Creek	$\tau$	-0.64	-0.55	-0.60	-0.75	-0.70	0.62	-0.68	-0.68	-0.05	0.67
		p	0	0	0	0	0	0	0	0	<b>0.7365</b>	0
		Slope	-9.04	-0.48	-1.23	-2.11	-13.29	1.33	-1.60	-3.00	-0.11	2.95
		S	-242	-207	-226	-282	-266	235	-257	-256	-18	254
		VarS	2,562	2,149	2,227	2,557	2,562	2,552	2,556	2,560	2,553	2,560
		$\phi$	-18.1	-1.0	-2.5	-4.2	-26.6	2.7	-3.2	-6.0	-0.2	5.9
	Moss Peak	$\tau$	-0.59	-0.52	-0.62	-0.58	-0.63	0.54	-0.56	-0.61	-0.17	0.58
		p	0	0.0001	0	0	0	0.0001	0	0	<b>0.2119</b>	0
		Slope	-15.91	-1.38	-1.26	-1.38	-13.42	0.89	-1.59	-2.37	-0.40	2.33
		S	-222	-195	-235	-220	-238	205	-211	-232	-64	221
		VarS	2,562	2,557	2,550	2,555	2,562	2,554	2,545	2,551	2,547	2,548
		$\phi$	-31.8	-2.8	-2.5	-2.8	-26.8	1.8	-3.2	-4.7	-0.8	4.7
	North Fork Jocko	$\tau$	-0.63	-0.56	-0.63	-0.64	-0.68	0.34	-0.48	-0.66	0.12	0.70
		p	0	0	0	0	0	0.0124	0.0003	0	<b>0.3628</b>	0
		Slope	-18.17	-1.57	-1.56	-1.13	-18.47	0.41	-1.24	-1.94	0.33	2.06
		S	-238	-213	-237	-242	-256	127	-182	-248	47	265
		VarS	2,562	2,550	2,546	2,551	2,562	2,540	2,543	2,558	2,555	2,557
		$\phi$	-36.3	-3.1	-3.1	-2.3	-36.9	0.8	-2.5	-3.9	0.7	4.1
	Flathead Region	$\tau$	-0.62	-0.54	-0.62	-0.66	-0.67	0.50	-0.57	-0.65	-0.03	0.65
		p	0	0	0	0	0	0	0	0	<b>0.6976</b>	0
Slope		-13.31	-1.00	-1.39	-1.50	-14.67	0.89	-1.50	-2.33	-0.05	2.38	
S		-702	-615	-698	-744	-760	567	-650	-736	-35	740	
VarS		7,686	7,256	7,324	7,663	7,686	7,647	7,644	7,669	7,655	7,665	
$\phi$		-26.6	-2.0	-2.8	-3.0	-29.3	1.8	-3.0	-4.7	-0.1	4.8	

Table D-4. Continued

Scenario	Location	Statistic*	MSWE	DMSWE	SMO	SM50	1ASWE	PSO	PSE	PSD	SMD	SWE0
RCP8.5	Kraft Creek	$\tau$	-0.71	-0.54	-0.64	-0.78	-0.75	0.70	-0.72	-0.73	-0.26	0.74
		$\rho$	0	0	0	0	0	0	0	0	<b>0.0578</b>	0
		Slope	-9.69	-0.50	-1.30	-2.51	-13.88	1.59	-2.38	-4.07	-0.86	4.11
		S	-270	-204	-241	-293	-285	264	-273	-275	-97	279
		VarS	2,562	2,223	2,348	2,559	2,558	2,553	2,556	2,559	2,561	2,559
		$\phi$	-19.4	-1.0	-2.6	-5.0	-27.8	3.2	-4.8	-8.1	-1.7	8.2
	Moss Peak	$\tau$	-0.70	-0.60	-0.67	-0.67	-0.74	0.69	-0.69	-0.74	-0.10	0.72
		$\rho$	0	0	0	0	0	0	0	0	<b>0.4765</b>	0
		Slope	-19.27	-1.89	-1.76	-1.92	-18.54	1.10	-2.11	-3.22	-0.27	3.33
		S	-264	-227	-254	-255	-278	260	-262	-278	-37	274
		VarS	2,562	2,559	2,555	2,554	2,562	2,551	2,557	2,560	2,557	2,553
		$\phi$	-38.5	-3.8	-3.5	-3.8	-37.1	2.2	-4.2	-6.4	-0.5	6.7
	North Fork Jocko	$\tau$	-0.58	-0.71	-0.69	-0.72	-0.72	0.57	-0.60	-0.75	0.23	0.78
		$\rho$	0	0	0	0	0	0	0	0	<b>0.0930</b>	0
		Slope	-18.95	-2.31	-2.21	-1.50	-21.79	0.85	-1.67	-2.64	0.56	2.78
		S	-220	-267	-259	-271	-274	214	-227	-285	86	295
		VarS	2,562	2,543	2,552	2,552	2,562	2,547	2,552	2,556	2,560	2,559
		$\phi$	-37.9	-4.6	-4.4	-3.0	-43.6	1.7	-3.3	-5.3	1.1	5.6
	Flathead Region	$\tau$	-0.66	-0.62	-0.66	-0.72	-0.74	0.65	-0.67	-0.74	-0.04	0.75
		$\rho$	0	0	0	0	0	0	0	0	<b>0.5917</b>	0
Slope		-14.97	-1.33	-1.68	-1.88	-18.07	1.20	-2.00	-3.18	-0.16	3.25	
S		-754	-698	-754	-819	-837	738	-762	-838	-48	848	
VarS		7,686	7,325	7,455	7,665	7,682	7,651	7,665	7,675	7,678	7,671	
$\phi$		-29.9	-2.7	-3.4	-3.8	-36.1	2.4	-4.0	-6.4	-0.3	6.5	

\*  $\phi$  is measured either in mm (MSWE and 1ASWE) or days (all other indices) per decade

APPENDIX E: Analysis of SWT

**Table E-1: Main statistics – Theil-Sen’s slope (Sl.), Kendall’s statistic (S), p value (p), Kendall’s correlation coefficient (τ), and variance of the Kendall’s statistic (VarS) – related to the MKTs applied to the seasonal and annual averages of daily maximum and minimum SWT time series that are observed and estimated at 28 SWT gaging stations across the Flathead Reservation for the period 1961-2100 according to the three proposed RCP scenarios**

Var.	Scen.	Time	BCR1				
			Sl.	S	p	τ	VarS
Max SAT	RCP2.6	Win	0.003	3,128	0	0.33	301,457
		Spr	0.011	3,181	0	0.33	308,088
		Sum	0.022	5,223	0	0.54	308,077
		Fal	0.002	728	0.190	0.07	308,077
		Ann	0.010	4,937	0	0.51	308,066
	RCP4.5	Win	0.005	3,956	0	0.41	301,507
		Spr	0.015	4,372	0	0.45	308,084
		Sum	0.025	5,934	0	0.61	308,076
		Fal	0.010	3,113	0	0.32	308,066
		Ann	0.014	6,271	0	0.64	308,075
	RCP8.5	Win	0.008	5,049	0	0.53	301,522
		Spr	0.025	5,478	0	0.56	308,094
		Sum	0.028	7,093	0	0.73	308,082
		Fal	0.024	5,615	0	0.58	308,088
		Ann	0.022	7,129	0	0.73	308,095
Min SAT	RCP2.6	Win	0.003	3,171	0	0.33	301,408
		Spr	0.003	1,616	0.004	0.17	308,043
		Sum	0.021	5,493	0	0.56	308,088
		Fal	0.000	-94	0.867	-0.01	308,071
		Ann	0.006	4,317	0	0.44	307,997
	RCP4.5	Win	0.004	3,868	0	0.40	301,445
		Spr	0.007	3,216	0	0.33	308,039
		Sum	0.026	6,707	0	0.69	308,098
		Fal	0.007	2,640	0	0.27	308,079
		Ann	0.011	6,651	0	0.68	308,064
	RCP8.5	Win	0.007	4,964	0	0.52	301,485
		Spr	0.015	5,054	0	0.52	308,068
		Sum	0.031	7,940	0	0.82	308,089
		Fal	0.020	5,304	0	0.55	308,082
		Ann	0.018	7,598	0	0.78	308,080

Table E-1. Continued

Var.	Scen.	Time	CCR1					CLC1					FCR1				
			SI.	S	p	$\tau$	VarS	SI.	S	p	$\tau$	VarS	SI.	S	p	$\tau$	VarS
Max SAT	RCP2.6	Win	0.005	2,379	0	0.25	301,526	0.008	3,189	0	0.33	301,542	0.004	2,802	0	0.29	301,498
		Spr	0.011	2,687	0	0.28	308,090	0.007	2,179	0	0.22	308,080	0.011	2,990	0	0.31	308,086
		Sum	0.029	4,945	0	0.51	308,091	0.019	5,441	0	0.56	308,080	0.021	5,078	0	0.52	308,057
		Fal	0.006	1,508	0.007	0.15	308,092	0.005	1,827	0.001	0.19	308,056	0.004	1,232	0.027	0.13	308,079
		Ann	0.013	4,861	0	0.50	308,071	0.010	5,107	0	0.52	308,061	0.010	4,770	0	0.49	308,082
	RCP4.5	Win	0.006	2,868	0	0.30	301,543	0.012	4,060	0	0.42	301,544	0.006	3,538	0	0.37	301,489
		Spr	0.016	4,044	0	0.42	308,093	0.011	3,272	0	0.34	308,089	0.015	4,087	0	0.42	308,086
		Sum	0.038	6,189	0	0.64	308,100	0.025	6,581	0	0.68	308,086	0.027	6,334	0	0.65	308,095
		Fal	0.017	4,326	0	0.44	308,085	0.011	4,407	0	0.45	308,070	0.011	3,662	0	0.38	308,088
		Ann	0.020	6,481	0	0.67	308,070	0.015	6,574	0	0.68	308,071	0.015	6,331	0	0.65	308,082
	RCP8.5	Win	0.010	3,994	0	0.42	301,545	0.018	5,399	0	0.56	301,557	0.009	4,636	0	0.48	301,524
		Spr	0.028	5,312	0	0.55	308,105	0.019	4,928	0	0.51	308,098	0.027	5,759	0	0.59	308,096
		Sum	0.046	7,291	0	0.75	308,099	0.033	7,683	0	0.79	308,104	0.034	7,620	0	0.78	308,095
		Fal	0.033	6,157	0	0.63	308,101	0.023	6,258	0	0.64	308,090	0.026	5,870	0	0.60	308,103
		Ann	0.030	7,357	0	0.76	308,095	0.024	7,564	0	0.78	308,094	0.024	7,294	0	0.75	308,102
Min SAT	RCP2.6	Win	0.007	3,362	0	0.35	301,533	0.007	3,280	0	0.34	301,528	0.010	4,192	0	0.44	301,549
		Spr	0.005	1,817	0.001	0.19	308,066	0.003	1,488	0.007	0.15	308,065	0.005	2,077	0	0.21	308,075
		Sum	0.022	5,357	0	0.55	308,077	0.025	5,475	0	0.56	308,082	0.015	4,650	0	0.48	308,077
		Fal	-0.001	-406	0.466	-0.04	308,080	0.000	-27	0.963	0.00	308,047	0.011	3,827	0	0.39	308,081
		Ann	0.008	4,195	0	0.43	308,027	0.008	4,945	0	0.51	308,038	0.010	5,481	0	0.56	308,060
	RCP4.5	Win	0.010	3,972	0	0.41	301,534	0.009	3,941	0	0.41	301,542	0.014	4,905	0	0.51	301,552
		Spr	0.010	3,470	0	0.36	308,083	0.007	3,258	0	0.33	308,055	0.007	3,066	0	0.32	308,075
		Sum	0.029	6,686	0	0.69	308,083	0.034	6,987	0	0.72	308,100	0.019	6,203	0	0.64	308,085
		Fal	0.007	2,254	0	0.23	308,081	0.006	2,709	0	0.28	308,050	0.019	5,741	0	0.59	308,096
		Ann	0.014	6,291	0	0.65	308,080	0.014	6,919	0	0.71	308,078	0.015	6,723	0	0.69	308,077
	RCP8.5	Win	0.017	5,030	0	0.52	301,559	0.015	5,029	0	0.52	301,554	0.021	5,707	0	0.60	301,563
		Spr	0.021	5,107	0	0.52	308,088	0.014	5,046	0	0.52	308,094	0.016	5,371	0	0.55	308,090
		Sum	0.035	7,930	0	0.82	308,099	0.046	8,145	0	0.84	308,106	0.024	7,012	0	0.72	308,089
		Fal	0.024	4,850	0	0.50	308,096	0.020	5,381	0	0.55	308,073	0.036	6,988	0	0.72	308,093
		Ann	0.024	7,279	0	0.75	308,095	0.024	7,774	0	0.80	308,085	0.025	7,642	0	0.79	308,097

Table E-1. Continued

Var.	Scen.	Time	FCR2					FHR1					FHR2				
			Sl.	S	p	$\tau$	VarS	Sl.	S	p	$\tau$	VarS	Sl.	S	p	$\tau$	VarS
Max SAT	RCP2.6	Win	0.004	2,852	0	0.30	301,479	0.003	1,709	0.002	0.18	301,520	0.007	2,789	0	0.29	301,526
		Spr	0.010	3,053	0	0.31	308,080	0.012	3,078	0	0.32	308,084	0.006	1,611	0.004	0.17	308,081
		Sum	0.022	5,245	0	0.54	308,080	0.030	5,393	0	0.55	308,095	0.021	4,841	0	0.50	308,092
		Fal	0.003	1,242	0.025	0.13	308,075	0.005	1,363	0.014	0.14	308,079	0.004	1,114	0.045	0.11	308,075
		Ann	0.010	4,975	0	0.51	308,039	0.013	5,005	0	0.51	308,078	0.010	4,449	0	0.46	308,070
	RCP4.5	Win	0.005	3,590	0	0.37	301,500	0.005	2,448	0	0.26	301,505	0.007	2,641	0	0.28	301,545
		Spr	0.013	4,187	0	0.43	308,089	0.017	4,190	0	0.43	308,087	0.009	2,766	0	0.28	308,090
		Sum	0.029	6,489	0	0.67	308,090	0.040	6,619	0	0.68	308,106	0.030	6,231	0	0.64	308,097
		Fal	0.010	3,817	0	0.39	308,074	0.013	3,805	0	0.39	308,084	0.012	3,650	0	0.38	308,081
		Ann	0.015	6,500	0	0.67	308,066	0.019	6,567	0	0.67	308,076	0.014	6,105	0	0.63	308,079
	RCP8.5	Win	0.008	4,666	0	0.49	301,529	0.008	3,310	0	0.35	301,507	0.010	3,536	0	0.37	301,555
		Spr	0.024	5,784	0	0.59	308,093	0.030	5,699	0	0.59	308,094	0.018	4,405	0	0.45	308,080
		Sum	0.037	7,718	0	0.79	308,093	0.051	7,773	0	0.80	308,100	0.039	7,368	0	0.76	308,101
		Fal	0.024	5,963	0	0.61	308,096	0.029	5,948	0	0.61	308,105	0.028	5,711	0	0.59	308,101
		Ann	0.023	7,443	0	0.76	308,078	0.030	7,515	0	0.77	308,096	0.024	7,183	0	0.74	308,103
Min SAT	RCP2.6	Win	0.010	4,428	0	0.46	301,539	0.018	4,320	0	0.45	301,566	0.018	4,256	0	0.44	301,562
		Spr	0.008	3,473	0	0.36	308,065	0.007	2,063	0	0.21	308,090	0.006	1,980	0	0.20	308,081
		Sum	0.013	4,532	0	0.47	308,048	0.025	5,037	0	0.52	308,082	0.026	5,035	0	0.52	308,097
		Fal	0.014	4,414	0	0.45	308,073	0.016	3,940	0	0.40	308,085	0.016	3,963	0	0.41	308,085
		Ann	0.011	5,026	0	0.52	308,061	0.017	5,671	0	0.58	308,090	0.017	5,715	0	0.59	308,087
	RCP4.5	Win	0.013	4,967	0	0.52	301,551	0.024	4,895	0	0.51	301,564	0.023	4,724	0	0.49	301,557
		Spr	0.011	4,679	0	0.48	308,076	0.010	3,049	0	0.31	308,090	0.010	2,943	0	0.30	308,089
		Sum	0.016	5,752	0	0.59	308,064	0.033	6,755	0	0.69	308,097	0.034	6,770	0	0.70	308,084
		Fal	0.020	5,834	0	0.60	308,085	0.026	5,797	0	0.60	308,101	0.025	5,685	0	0.58	308,092
		Ann	0.015	6,083	0	0.63	308,070	0.024	6,814	0	0.70	308,086	0.023	6,855	0	0.70	308,082
	RCP8.5	Win	0.019	5,772	0	0.60	301,552	0.035	5,696	0	0.59	301,573	0.034	5,543	0	0.58	301,567
		Spr	0.020	5,978	0	0.61	308,086	0.023	5,381	0	0.55	308,097	0.022	5,269	0	0.54	308,094
		Sum	0.019	6,781	0	0.70	308,083	0.042	7,558	0	0.78	308,100	0.045	7,567	0	0.78	308,099
		Fal	0.033	6,894	0	0.71	308,077	0.048	6,988	0	0.72	308,102	0.046	6,877	0	0.71	308,103
		Ann	0.023	6,944	0	0.71	308,089	0.037	7,679	0	0.79	308,101	0.037	7,733	0	0.79	308,096

Table E-1. Continued

Var.	Scen.	Time	FHR4					FHR5					FHR6				
			Sl.	S	p	$\tau$	VarS	Sl.	S	p	$\tau$	VarS	Sl.	S	p	$\tau$	VarS
Max SAT	RCP2.6	Win	0.006	3,329	0	0.35	301,508	0.003	1,276	0.020	0.13	301,533	0.006	2,929	0	0.31	301,530
		Spr	0.012	3,155	0	0.32	308,084	0.011	3,015	0	0.31	308,084	0.011	3,214	0	0.33	308,093
		Sum	0.035	5,078	0	0.52	308,100	0.032	5,288	0	0.54	308,101	0.037	5,072	0	0.52	308,091
		Fal	0.003	724	0.193	0.07	308,073	0.005	1,349	0.015	0.14	308,077	0.002	724	0.193	0.07	308,086
		Ann	0.014	5,102	0	0.52	308,076	0.012	4,950	0	0.51	308,064	0.014	5,153	0	0.53	308,070
	RCP4.5	Win	0.008	3,778	0	0.39	301,528	0.004	1,932	0	0.20	301,518	0.007	3,380	0	0.35	301,522
		Spr	0.015	4,352	0	0.45	308,088	0.015	4,092	0	0.42	308,084	0.014	4,361	0	0.45	308,083
		Sum	0.044	6,057	0	0.62	308,110	0.044	6,559	0	0.67	308,100	0.047	6,104	0	0.63	308,099
		Fal	0.011	3,115	0	0.32	308,080	0.012	3,768	0	0.39	308,075	0.011	3,108	0	0.32	308,077
		Ann	0.020	6,394	0	0.66	308,075	0.019	6,571	0	0.68	308,084	0.020	6,457	0	0.66	308,088
	RCP8.5	Win	0.013	4,849	0	0.51	301,547	0.007	2,718	0	0.28	301,533	0.012	4,463	0	0.47	301,552
		Spr	0.025	5,437	0	0.56	308,085	0.028	5,622	0	0.58	308,098	0.023	5,417	0	0.56	308,091
		Sum	0.054	7,058	0	0.73	308,099	0.057	7,676	0	0.79	308,109	0.058	7,072	0	0.73	308,104
		Fal	0.028	5,641	0	0.58	308,098	0.028	5,963	0	0.61	308,098	0.027	5,644	0	0.58	308,092
		Ann	0.031	7,247	0	0.74	308,089	0.030	7,516	0	0.77	308,104	0.031	7,308	0	0.75	308,095
Min SAT	RCP2.6	Win	0.018	4,229	0	0.44	301,549	0.017	4,311	0	0.45	301,568	0.017	4,178	0	0.44	301,571
		Spr	0.007	2,073	0	0.21	308,078	0.007	2,043	0	0.21	308,086	0.006	2,059	0	0.21	308,083
		Sum	0.026	4,972	0	0.51	308,086	0.027	4,987	0	0.51	308,070	0.029	4,972	0	0.51	308,091
		Fal	0.015	4,003	0	0.41	308,090	0.016	3,855	0	0.40	308,092	0.015	4,000	0	0.41	308,093
		Ann	0.017	5,605	0	0.58	308,072	0.017	5,642	0	0.58	308,087	0.018	5,666	0	0.58	308,076
	RCP4.5	Win	0.022	4,633	0	0.48	301,556	0.022	4,749	0	0.50	301,569	0.021	4,578	0	0.48	301,564
		Spr	0.010	3,041	0	0.31	308,088	0.010	2,996	0	0.31	308,076	0.009	3,005	0	0.31	308,086
		Sum	0.035	6,727	0	0.69	308,096	0.036	6,710	0	0.69	308,091	0.040	6,746	0	0.69	308,090
		Fal	0.025	5,791	0	0.60	308,094	0.026	5,733	0	0.59	308,096	0.025	5,796	0	0.60	308,093
		Ann	0.023	6,783	0	0.70	308,099	0.024	6,821	0	0.70	308,078	0.024	6,867	0	0.71	308,090
	RCP8.5	Win	0.033	5,476	0	0.57	301,562	0.032	5,560	0	0.58	301,569	0.031	5,447	0	0.57	301,557
		Spr	0.022	5,320	0	0.55	308,097	0.022	5,314	0	0.55	308,098	0.021	5,264	0	0.54	308,094
		Sum	0.046	7,528	0	0.77	308,111	0.048	7,517	0	0.77	308,099	0.055	7,503	0	0.77	308,095
		Fal	0.046	6,988	0	0.72	308,105	0.048	6,957	0	0.72	308,105	0.047	6,986	0	0.72	308,096
		Ann	0.037	7,646	0	0.79	308,101	0.038	7,690	0	0.79	308,097	0.039	7,678	0	0.79	308,094

Table E-1. Continued

Var.	Scen.	Time	JKR1					JKR2					JKR3				
			Sl.	S	p	$\tau$	VarS	Sl.	S	p	$\tau$	VarS	Sl.	S	p	$\tau$	VarS
Max SAT	RCP2.6	Win	0.007	3,527	0	0.37	301,516	0.004	3,100	0	0.32	301,482	0.003	3,000	0	0.31	301,458
		Spr	0.008	3,137	0	0.32	308,071	0.007	3,087	0	0.32	308,071	0.006	3,087	0	0.32	308,066
		Sum	0.027	4,941	0	0.51	308,072	0.022	5,189	0	0.53	308,088	0.020	5,154	0	0.53	308,086
		Fal	0.002	990	0.075	0.10	308,063	0.003	1,521	0.006	0.16	308,046	0.003	1,426	0.010	0.15	308,033
		Ann	0.011	5,179	0	0.53	308,034	0.009	5,190	0	0.53	308,054	0.008	5,143	0	0.53	308,046
	RCP4.5	Win	0.009	4,243	0	0.44	301,537	0.006	3,794	0	0.40	301,513	0.004	3,719	0	0.39	301,486
		Spr	0.011	4,338	0	0.45	308,073	0.010	4,250	0	0.44	308,072	0.008	4,219	0	0.43	308,054
		Sum	0.034	6,161	0	0.63	308,104	0.031	6,630	0	0.68	308,098	0.028	6,673	0	0.69	308,101
		Fal	0.008	3,456	0	0.36	308,038	0.009	3,988	0	0.41	308,071	0.007	3,876	0	0.40	308,063
		Ann	0.015	6,455	0	0.66	308,070	0.014	6,685	0	0.69	308,072	0.012	6,688	0	0.69	308,072
	RCP8.5	Win	0.013	5,184	0	0.54	301,547	0.008	4,860	0	0.51	301,533	0.007	4,794	0	0.50	301,506
		Spr	0.018	5,447	0	0.56	308,089	0.018	5,795	0	0.60	308,092	0.014	5,747	0	0.59	308,078
		Sum	0.044	7,232	0	0.74	308,107	0.043	7,767	0	0.80	308,104	0.041	7,770	0	0.80	308,104
		Fal	0.020	5,831	0	0.60	308,090	0.021	6,119	0	0.63	308,101	0.017	6,051	0	0.62	308,081
		Ann	0.024	7,350	0	0.76	308,087	0.023	7,610	0	0.78	308,089	0.020	7,634	0	0.78	308,081
Min SAT	RCP2.6	Win	0.013	4,226	0	0.44	301,564	0.012	4,359	0	0.45	301,546	0.010	4,190	0	0.44	301,541
		Spr	0.005	2,382	0	0.24	308,051	0.004	2,336	0	0.24	308,048	0.003	2,439	0	0.25	308,013
		Sum	0.017	5,146	0	0.53	308,065	0.014	5,280	0	0.54	308,065	0.013	5,338	0	0.55	308,061
		Fal	0.008	3,813	0	0.39	308,064	0.007	4,144	0	0.43	308,059	0.006	4,081	0	0.42	308,022
		Ann	0.011	5,522	0	0.57	308,064	0.009	5,692	0	0.58	308,053	0.008	5,702	0	0.59	308,023
	RCP4.5	Win	0.017	4,927	0	0.51	301,550	0.015	4,945	0	0.52	301,555	0.012	4,642	0	0.48	301,558
		Spr	0.007	3,409	0	0.35	308,042	0.006	3,327	0	0.34	308,042	0.004	3,377	0	0.35	308,004
		Sum	0.022	6,832	0	0.70	308,073	0.018	6,929	0	0.71	308,067	0.018	6,973	0	0.72	308,064
		Fal	0.013	5,645	0	0.58	308,074	0.011	5,812	0	0.60	308,067	0.009	5,666	0	0.58	308,064
		Ann	0.015	6,632	0	0.68	308,069	0.012	6,712	0	0.69	308,057	0.011	6,755	0	0.69	308,049
	RCP8.5	Win	0.024	5,776	0	0.60	301,552	0.021	5,727	0	0.60	301,556	0.017	5,528	0	0.58	301,550
		Spr	0.015	5,521	0	0.57	308,072	0.012	5,533	0	0.57	308,065	0.009	5,525	0	0.57	308,023
		Sum	0.029	7,698	0	0.79	308,082	0.024	7,653	0	0.79	308,081	0.025	7,618	0	0.78	308,093
		Fal	0.025	6,980	0	0.72	308,085	0.021	7,049	0	0.72	308,090	0.016	6,944	0	0.71	308,077
		Ann	0.023	7,603	0	0.78	308,094	0.019	7,612	0	0.78	308,087	0.017	7,641	0	0.79	308,080

Table E-1. Continued

Var.	Scen.	Time	JKR5					JMF1					JNF1				
			Sl.	S	p	$\tau$	VarS	Sl.	S	p	$\tau$	VarS	Sl.	S	p	$\tau$	VarS
Max SAT	RCP2.6	Win	0.003	2,813	0	0.29	301,420	0.004	2,931	0	0.31	301,498	0.003	2,816	0	0.29	301,435
		Spr	0.004	2,406	0	0.25	308,013	0.004	2,331	0	0.24	308,023	0.007	2,989	0	0.31	308,062
		Sum	0.017	5,225	0	0.54	308,080	0.009	4,227	0	0.43	308,063	0.023	5,140	0	0.53	308,087
		Fal	0.002	1,535	0.006	0.16	308,026	0.002	1,396	0.012	0.14	308,035	0.004	1,574	0.005	0.16	308,066
		Ann	0.006	5,298	0	0.54	308,005	0.005	4,458	0	0.46	307,986	0.009	5,088	0	0.52	308,041
	RCP4.5	Win	0.004	3,475	0	0.36	301,472	0.006	3,539	0	0.37	301,504	0.003	3,524	0	0.37	301,455
		Spr	0.005	3,460	0	0.36	307,992	0.005	3,312	0	0.34	308,059	0.009	4,110	0	0.42	308,063
		Sum	0.023	6,391	0	0.66	308,092	0.012	5,370	0	0.55	308,053	0.032	6,581	0	0.68	308,088
		Fal	0.006	4,077	0	0.42	308,043	0.007	3,813	0	0.39	308,058	0.009	4,048	0	0.42	308,053
		Ann	0.009	6,601	0	0.68	308,028	0.007	5,999	0	0.62	308,029	0.013	6,647	0	0.68	308,054
	RCP8.5	Win	0.006	4,573	0	0.48	301,498	0.008	4,613	0	0.48	301,514	0.005	4,531	0	0.47	301,490
		Spr	0.009	4,998	0	0.51	308,038	0.010	5,003	0	0.51	308,061	0.016	5,655	0	0.58	308,086
		Sum	0.032	7,437	0	0.76	308,108	0.015	6,228	0	0.64	308,076	0.045	7,646	0	0.79	308,098
		Fal	0.015	6,085	0	0.63	308,083	0.015	5,948	0	0.61	308,081	0.020	6,121	0	0.63	308,088
		Ann	0.015	7,568	0	0.78	308,059	0.012	6,943	0	0.71	308,064	0.022	7,585	0	0.78	308,090
Min SAT	RCP2.6	Win	0.007	4,525	0	0.47	301,492	0.010	4,379	0	0.46	301,520	0.003	3,271	0	0.34	301,444
		Spr	0.005	3,586	0	0.37	308,012	0.003	2,379	0	0.24	308,005	0.002	1,702	0.002	0.17	308,024
		Sum	0.015	4,732	0	0.49	308,019	0.009	4,486	0	0.46	308,042	0.017	5,248	0	0.54	308,054
		Fal	0.008	4,504	0	0.46	308,061	0.007	3,813	0	0.39	308,056	-0.001	-410	0.461	-0.04	308,052
		Ann	0.009	5,136	0	0.53	307,992	0.007	5,673	0	0.58	308,004	0.005	4,631	0	0.48	307,988
	RCP4.5	Win	0.009	4,847	0	0.51	301,524	0.012	4,808	0	0.50	301,532	0.005	3,852	0	0.40	301,485
		Spr	0.006	4,745	0	0.49	308,049	0.004	3,388	0	0.35	308,027	0.004	3,417	0	0.35	308,011
		Sum	0.020	6,178	0	0.63	308,084	0.013	6,346	0	0.65	308,058	0.024	6,827	0	0.70	308,078
		Fal	0.011	5,711	0	0.59	308,051	0.011	5,603	0	0.58	308,066	0.004	2,209	0	0.23	308,053
		Ann	0.011	6,267	0	0.64	308,005	0.010	6,740	0	0.69	308,039	0.009	6,723	0	0.69	308,026
	RCP8.5	Win	0.013	5,730	0	0.60	301,536	0.018	5,752	0	0.60	301,550	0.008	5,070	0	0.53	301,487
		Spr	0.010	5,993	0	0.62	308,070	0.009	5,547	0	0.57	308,049	0.009	5,096	0	0.52	308,063
		Sum	0.028	7,134	0	0.73	308,091	0.019	7,273	0	0.75	308,089	0.031	7,723	0	0.79	308,092
		Fal	0.019	6,935	0	0.71	308,080	0.019	6,870	0	0.71	308,085	0.013	4,890	0	0.50	308,072
		Ann	0.017	7,098	0	0.73	308,053	0.016	7,558	0	0.78	308,061	0.015	7,615	0	0.78	308,070

Table E-1. Continued

Var.	Scen.	Time	JNF2					JNF3					JSC1				
			Sl.	S	p	$\tau$	VarS	Sl.	S	p	$\tau$	VarS	Sl.	S	p	$\tau$	VarS
Max SAT	RCP2.6	Win	0.003	3,555	0	0.37	301,440	0.003	2,907	0	0.30	301,452	0.006	2,978	0	0.31	301,499
		Spr	0.006	3,244	0	0.33	308,068	0.003	1,539	0.006	0.16	308,032	0.005	2,378	0	0.24	308,066
		Sum	0.028	5,047	0	0.52	308,090	0.018	5,065	0	0.52	308,088	0.014	5,089	0	0.52	308,058
		Fal	0.002	1,105	0.047	0.11	308,050	0.002	1,141	0.040	0.12	308,032	0.003	1,772	0.001	0.18	308,051
		Ann	0.010	5,198	0	0.53	308,046	0.006	4,669	0	0.48	308,027	0.007	5,076	0	0.52	308,021
	RCP4.5	Win	0.004	4,153	0	0.43	301,456	0.003	2,888	0	0.30	301,458	0.008	3,599	0	0.38	301,528
		Spr	0.007	4,433	0	0.46	308,048	0.004	2,581	0	0.27	308,034	0.008	3,393	0	0.35	308,073
		Sum	0.036	6,141	0	0.63	308,103	0.025	6,404	0	0.66	308,098	0.018	6,046	0	0.62	308,087
		Fal	0.006	3,636	0	0.37	308,033	0.007	3,769	0	0.39	308,011	0.008	4,209	0	0.43	308,064
		Ann	0.013	6,474	0	0.67	308,065	0.010	6,302	0	0.65	308,024	0.010	6,282	0	0.65	308,063
	RCP8.5	Win	0.007	5,250	0	0.55	301,467	0.005	3,849	0	0.40	301,450	0.012	4,661	0	0.49	301,543
		Spr	0.012	5,440	0	0.56	308,067	0.008	4,258	0	0.44	308,068	0.014	5,093	0	0.52	308,090
		Sum	0.050	7,195	0	0.74	308,108	0.037	7,498	0	0.77	308,102	0.024	7,381	0	0.76	308,098
		Fal	0.015	5,906	0	0.61	308,071	0.016	5,879	0	0.60	308,082	0.017	6,181	0	0.64	308,074
		Ann	0.021	7,457	0	0.77	308,077	0.016	7,368	0	0.76	308,045	0.017	7,319	0	0.75	308,072
Min SAT	RCP2.6	Win	0.003	3,085	0	0.32	301,461	0.006	4,334	0	0.45	301,503	0.006	3,018	0	0.31	301,533
		Spr	0.002	1,728	0.002	0.18	307,981	0.003	2,122	0	0.22	308,035	0.003	2,378	0	0.24	308,029
		Sum	0.018	5,287	0	0.54	308,083	0.018	5,200	0	0.53	308,078	0.010	5,260	0	0.54	308,011
		Fal	0.000	-289	0.604	-0.03	308,037	0.007	3,876	0	0.40	308,069	0.001	955	0.086	0.10	307,964
		Ann	0.006	4,864	0	0.50	308,012	0.009	5,664	0	0.58	308,043	0.005	5,844	0	0.60	307,943
	RCP4.5	Win	0.005	3,607	0	0.38	301,480	0.008	4,739	0	0.49	301,496	0.007	3,480	0	0.36	301,521
		Spr	0.004	3,408	0	0.35	307,991	0.004	3,037	0	0.31	308,013	0.005	4,015	0	0.41	308,018
		Sum	0.025	6,862	0	0.71	308,094	0.024	6,617	0	0.68	308,097	0.013	6,678	0	0.69	308,034
		Fal	0.004	2,329	0	0.24	308,026	0.012	5,695	0	0.59	308,077	0.003	3,644	0	0.37	307,943
		Ann	0.009	6,897	0	0.71	308,060	0.012	6,894	0	0.71	308,065	0.007	6,870	0	0.71	308,029
	RCP8.5	Win	0.008	5,027	0	0.52	301,502	0.012	5,640	0	0.59	301,523	0.011	4,631	0	0.48	301,546
		Spr	0.008	5,108	0	0.52	308,053	0.009	5,254	0	0.54	308,052	0.008	5,642	0	0.58	308,025
		Sum	0.034	7,771	0	0.80	308,096	0.033	7,210	0	0.74	308,093	0.017	7,622	0	0.78	308,035
		Fal	0.012	5,027	0	0.52	308,062	0.022	6,932	0	0.71	308,087	0.008	5,715	0	0.59	308,034
		Ann	0.015	7,766	0	0.80	308,065	0.019	7,679	0	0.79	308,088	0.011	7,706	0	0.79	308,049

Table E-1. Continued

Var.	Scen.	Time	LBR1					MCR1					MCR2				
			Sl.	S	p	$\tau$	VarS	Sl.	S	p	$\tau$	VarS	Sl.	S	p	$\tau$	VarS
Max SAT	RCP2.6	Win	0.007	2,736	0	0.29	301,540	0.008	3,315	0	0.35	301,540	0.006	2,858	0	0.30	301,532
		Spr	0.019	3,016	0	0.31	308,093	0.011	3,286	0	0.34	308,088	0.006	2,235	0	0.23	308,071
		Sum	0.030	5,108	0	0.52	308,093	0.023	4,956	0	0.51	308,083	0.010	4,784	0	0.49	308,023
		Fal	0.005	978	0.078	0.10	308,091	0.003	1,015	0.068	0.10	308,074	0.003	1,380	0.013	0.14	308,064
		Ann	0.015	4,779	0	0.49	308,093	0.011	5,071	0	0.52	308,042	0.006	4,435	0	0.46	308,034
	RCP4.5	Win	0.010	3,552	0	0.37	301,539	0.011	4,101	0	0.43	301,554	0.008	3,556	0	0.37	301,511
		Spr	0.025	4,167	0	0.43	308,096	0.015	4,454	0	0.46	308,091	0.008	3,252	0	0.33	308,069
		Sum	0.034	5,943	0	0.61	308,088	0.029	6,085	0	0.63	308,097	0.012	5,709	0	0.59	308,068
		Fal	0.016	3,399	0	0.35	308,096	0.010	3,548	0	0.36	308,079	0.009	3,826	0	0.39	308,059
		Ann	0.022	6,142	0	0.63	308,096	0.016	6,349	0	0.65	308,063	0.009	5,906	0	0.61	308,041
	RCP8.5	Win	0.016	4,694	0	0.49	301,553	0.017	5,101	0	0.53	301,556	0.012	4,625	0	0.48	301,542
		Spr	0.042	5,398	0	0.55	308,106	0.024	5,604	0	0.58	308,098	0.016	4,986	0	0.51	308,075
		Sum	0.037	6,833	0	0.70	308,090	0.033	6,526	0	0.67	308,090	0.015	6,929	0	0.71	308,058
		Fal	0.040	5,729	0	0.59	308,104	0.025	5,832	0	0.60	308,093	0.019	5,919	0	0.61	308,088
		Ann	0.035	7,042	0	0.72	308,105	0.025	7,206	0	0.74	308,085	0.016	6,956	0	0.71	308,077
Min SAT	RCP2.6	Win	0.016	3,922	0	0.41	301,562	0.009	2,938	0	0.31	301,537	0.015	4,352	0	0.45	301,547
		Spr	0.008	1,993	0	0.20	308,090	0.005	1,545	0.005	0.16	308,079	0.005	2,239	0	0.23	308,047
		Sum	0.009	4,802	0	0.49	307,980	0.018	5,312	0	0.55	308,074	0.006	4,144	0	0.43	308,049
		Fal	0.012	3,909	0	0.40	308,087	-0.001	-277	0.619	-0.03	308,075	0.009	3,835	0	0.39	308,064
		Ann	0.012	5,290	0	0.54	308,067	0.007	4,044	0	0.42	308,057	0.009	5,524	0	0.57	308,050
	RCP4.5	Win	0.023	4,683	0	0.49	301,570	0.013	3,856	0	0.40	301,557	0.020	5,019	0	0.52	301,566
		Spr	0.014	3,201	0	0.33	308,092	0.010	3,269	0	0.34	308,074	0.008	3,323	0	0.34	308,071
		Sum	0.011	6,118	0	0.63	308,015	0.024	6,744	0	0.69	308,073	0.009	5,520	0	0.57	308,027
		Fal	0.020	5,853	0	0.60	308,092	0.007	2,452	0	0.25	308,057	0.014	5,677	0	0.58	308,086
		Ann	0.018	6,348	0	0.65	308,091	0.014	6,035	0	0.62	308,083	0.013	6,479	0	0.67	308,054
	RCP8.5	Win	0.033	5,543	0	0.58	301,566	0.019	4,573	0	0.48	301,560	0.028	5,759	0	0.60	301,570
		Spr	0.028	5,463	0	0.56	308,103	0.020	5,025	0	0.52	308,086	0.016	5,473	0	0.56	308,078
		Sum	0.013	6,900	0	0.71	308,005	0.030	7,898	0	0.81	308,089	0.011	6,137	0	0.63	308,032
		Fal	0.039	7,028	0	0.72	308,098	0.023	5,182	0	0.53	308,084	0.025	6,853	0	0.70	308,077
		Ann	0.029	7,551	0	0.78	308,090	0.023	7,164	0	0.74	308,091	0.020	7,413	0	0.76	308,076

Table E-1. Continued

Var.	Scen.	Time	PCR1					RSC2					RVC1				
			Sl.	S	p	$\tau$	VarS	Sl.	S	p	$\tau$	VarS	Sl.	S	p	$\tau$	VarS
Max SAT	RCP2.6	Win	0.008	3,416	0	0.36	301,547	0.009	3,573	0	0.37	301,537	0.004	3,439	0	0.36	301,406
		Spr	0.009	3,301	0	0.34	308,068	0.008	2,323	0	0.24	308,083	0.007	3,238	0	0.33	308,072
		Sum	0.021	5,078	0	0.52	308,090	0.017	4,779	0	0.49	308,084	0.027	5,003	0	0.51	308,088
		Fal	0.003	1,146	0.039	0.12	308,073	0.005	1,791	0.001	0.18	308,082	0.002	731	0.188	0.08	308,031
		Ann	0.010	5,269	0	0.54	308,057	0.010	4,849	0	0.50	308,053	0.010	5,048	0	0.52	308,023
	RCP4.5	Win	0.011	4,149	0	0.43	301,556	0.013	4,395	0	0.46	301,561	0.005	3,924	0	0.41	301,507
		Spr	0.012	4,471	0	0.46	308,079	0.012	3,442	0	0.35	308,094	0.009	4,408	0	0.45	308,058
		Sum	0.028	6,228	0	0.64	308,094	0.023	6,248	0	0.64	308,085	0.034	6,002	0	0.62	308,100
		Fal	0.008	3,660	0	0.38	308,061	0.012	4,168	0	0.43	308,082	0.008	3,186	0	0.33	308,028
		Ann	0.015	6,497	0	0.67	308,051	0.015	6,307	0	0.65	308,072	0.014	6,392	0	0.66	308,065
	RCP8.5	Win	0.015	5,120	0	0.53	301,553	0.019	5,316	0	0.55	301,563	0.008	5,028	0	0.52	301,523
		Spr	0.020	5,642	0	0.58	308,097	0.021	5,155	0	0.53	308,090	0.015	5,418	0	0.56	308,085
		Sum	0.033	6,734	0	0.69	308,099	0.031	6,988	0	0.72	308,099	0.042	6,985	0	0.72	308,092
		Fal	0.021	5,925	0	0.61	308,080	0.026	6,159	0	0.63	308,098	0.019	5,718	0	0.59	308,083
		Ann	0.023	7,301	0	0.75	308,078	0.024	7,326	0	0.75	308,082	0.022	7,271	0	0.75	308,086
Min SAT	RCP2.6	Win	0.007	2,875	0	0.30	301,536	0.005	2,883	0	0.30	301,509	0.004	3,087	0	0.32	301,474
		Spr	0.004	2,269	0	0.23	308,030	0.003	2,411	0	0.25	308,016	0.003	1,758	0.002	0.18	308,039
		Sum	0.020	5,164	0	0.53	308,062	0.021	5,201	0	0.53	308,084	0.022	5,281	0	0.54	308,077
		Fal	0.001	760	0.171	0.08	308,055	0.002	1,301	0.019	0.13	308,027	-0.001	-469	0.399	-0.05	308,060
		Ann	0.008	5,666	0	0.58	308,039	0.008	5,805	0	0.60	308,015	0.007	4,360	0	0.45	308,028
	RCP4.5	Win	0.009	3,429	0	0.36	301,543	0.008	3,435	0	0.36	301,533	0.005	3,629	0	0.38	301,490
		Spr	0.007	3,979	0	0.41	308,040	0.006	4,168	0	0.43	308,002	0.006	3,407	0	0.35	308,048
		Sum	0.026	6,677	0	0.69	308,072	0.028	6,746	0	0.69	308,086	0.029	6,644	0	0.68	308,089
		Fal	0.007	3,648	0	0.37	308,047	0.006	4,179	0	0.43	308,020	0.005	2,135	0	0.22	308,070
		Ann	0.012	6,998	0	0.72	308,065	0.012	7,182	0	0.74	308,047	0.011	6,610	0	0.68	308,065
	RCP8.5	Win	0.015	4,816	0	0.50	301,547	0.012	4,824	0	0.50	301,519	0.009	4,961	0	0.52	301,521
		Spr	0.014	5,660	0	0.58	308,062	0.011	5,755	0	0.59	308,070	0.012	5,089	0	0.52	308,082
		Sum	0.033	7,727	0	0.79	308,086	0.038	7,745	0	0.80	308,103	0.037	7,694	0	0.79	308,094
		Fal	0.017	5,837	0	0.60	308,078	0.014	6,060	0	0.62	308,074	0.019	4,856	0	0.50	308,088
		Ann	0.020	7,913	0	0.81	308,086	0.019	8,092	0	0.83	308,063	0.019	7,514	0	0.77	308,077

Table E-1. Continued

Var.	Scen.	Time	VCR1					VCR3					VCR4				
			Sl.	S	p	$\tau$	VarS	Sl.	S	p	$\tau$	VarS	Sl.	S	p	$\tau$	VarS
Max SAT	RCP2.6	Win	0.004	2,690	0	0.28	301,481	0.004	3,422	0	0.36	301,485	0.004	2,658	0	0.28	301,484
		Spr	0.004	1,353	0.015	0.14	308,063	0.008	3,264	0	0.34	308,059	0.012	3,051	0	0.31	308,092
		Sum	0.020	4,887	0	0.50	308,088	0.015	4,837	0	0.50	308,054	0.022	5,130	0	0.53	308,066
		Fal	0.003	899	0.106	0.09	308,088	0.001	346	0.534	0.04	308,031	0.004	1,235	0.026	0.13	308,086
		Ann	0.008	4,136	0	0.43	308,011	0.007	4,913	0	0.50	308,026	0.011	4,791	0	0.49	308,061
	RCP4.5	Win	0.006	3,408	0	0.36	301,513	0.005	4,201	0	0.44	301,500	0.005	3,386	0	0.35	301,492
		Spr	0.008	2,527	0	0.26	308,071	0.010	4,432	0	0.46	308,072	0.016	4,128	0	0.42	308,088
		Sum	0.027	6,138	0	0.63	308,100	0.018	5,819	0	0.60	308,079	0.028	6,282	0	0.65	308,085
		Fal	0.011	3,652	0	0.38	308,076	0.005	2,669	0	0.27	308,022	0.012	3,733	0	0.38	308,084
		Ann	0.013	6,021	0	0.62	308,072	0.010	6,243	0	0.64	308,066	0.016	6,313	0	0.65	308,074
	RCP8.5	Win	0.009	4,361	0	0.45	301,531	0.008	5,172	0	0.54	301,507	0.008	4,483	0	0.47	301,512
		Spr	0.016	4,233	0	0.44	308,094	0.016	5,497	0	0.56	308,078	0.029	5,775	0	0.59	308,097
		Sum	0.035	7,299	0	0.75	308,103	0.021	7,015	0	0.72	308,068	0.034	7,603	0	0.78	308,095
		Fal	0.026	5,750	0	0.59	308,091	0.015	5,480	0	0.56	308,073	0.027	5,938	0	0.61	308,097
		Ann	0.022	7,105	0	0.73	308,086	0.015	7,138	0	0.73	308,076	0.025	7,266	0	0.75	308,091
Min SAT	RCP2.6	Win	0.008	4,159	0	0.43	301,534	0.008	4,323	0	0.45	301,504	0.003	2,495	0	0.26	301,502
		Spr	0.005	2,146	0	0.22	308,064	0.004	2,139	0	0.22	308,009	0.005	2,375	0	0.24	308,052
		Sum	0.016	5,255	0	0.54	308,070	0.013	5,117	0	0.53	308,042	0.017	5,015	0	0.52	308,074
		Fal	0.008	3,629	0	0.37	308,076	0.008	3,991	0	0.41	308,045	0.002	697	0.210	0.07	308,056
		Ann	0.009	5,597	0	0.58	308,071	0.008	5,599	0	0.58	308,039	0.007	5,195	0	0.53	308,018
	RCP4.5	Win	0.011	4,940	0	0.52	301,526	0.010	4,932	0	0.51	301,527	0.004	2,971	0	0.31	301,514
		Spr	0.007	3,174	0	0.33	308,059	0.005	3,084	0	0.32	308,028	0.009	3,963	0	0.41	308,067
		Sum	0.020	6,691	0	0.69	308,054	0.017	6,643	0	0.68	308,054	0.021	6,351	0	0.65	308,078
		Fal	0.014	5,714	0	0.59	308,081	0.013	5,850	0	0.60	308,083	0.008	3,628	0	0.37	308,063
		Ann	0.013	6,719	0	0.69	308,067	0.012	6,749	0	0.69	308,034	0.011	6,923	0	0.71	308,058
	RCP8.5	Win	0.017	5,710	0	0.60	301,558	0.015	5,728	0	0.60	301,537	0.008	4,395	0	0.46	301,508
		Spr	0.016	5,359	0	0.55	308,082	0.012	5,333	0	0.55	308,061	0.016	5,554	0	0.57	308,079
		Sum	0.024	7,572	0	0.78	308,087	0.022	7,458	0	0.77	308,065	0.025	7,514	0	0.77	308,079
		Fal	0.028	7,057	0	0.73	308,083	0.024	7,082	0	0.73	308,089	0.020	5,839	0	0.60	308,090
		Ann	0.021	7,740	0	0.80	308,092	0.019	7,654	0	0.79	308,087	0.017	7,813	0	0.80	308,088

**Table E-2: Main statistics – Theil-Sen’s slope (Sl.), Kendall’s statistic (S), p value (p), Kendall’s correlation coefficient ( $\tau$ ), and variance of the Kendall’s statistic (VarS) – related to the RKTs applied to the seasonal and annual averages of maximum and minimum SWT calculated over the 1961-2100 period according to the three proposed RCP scenarios for five subregions and across the Flathead Reservation**

Var.	Scen.	Time	Flathead Reservation				Subregion 1				Subregion 2			
			Sl.	S	p	VarS	Sl.	S	p	VarS	Sl.	S	p	VarS
Max SAT	RCP2.6	Win	0.005	82,116	0	182,049,712	0.005	12,032	0	6,058,748	0.005	12,605	0	4,499,682
		Spr	0.008	77,428	0	215,298,528	0.010	14,073	0	7,127,834	0.007	11,689	0	4,614,798
		Sum	0.021	141,243	0	223,890,255	0.031	25,672	0	7,435,106	0.020	20,373	0	4,752,094
		Fal	0.003	33,792	0.023	221,182,349	0.004	5,274	0.050	7,243,231	0.003	5,709	0.008	4,673,689
		Ann	0.009	137,899	0	223,581,158	0.012	24,659	0	7,306,459	0.009	20,588	0	4,753,087
	RCP4.5	Win	0.006	99,797	0	190,228,356	0.006	14,179	0	6,565,856	0.006	15,355	0	4,552,811
		Spr	0.010	109,100	0	215,708,541	0.014	19,761	0	7,143,358	0.009	16,200	0	4,634,991
		Sum	0.027	173,948	0	228,908,526	0.040	31,570	0	7,519,313	0.027	25,510	0	4,805,433
		Fal	0.009	103,484	0	221,519,195	0.012	17,446	0	7,239,759	0.008	15,529	0	4,681,750
		Ann	0.014	178,554	0	230,423,089	0.018	32,094	0	7,463,173	0.013	26,110	0	4,817,810
	RCP8.5	Win	0.009	128,835	0	203,733,346	0.010	18,876	0	6,672,797	0.009	19,499	0	4,612,468
		Spr	0.019	148,985	0	224,924,768	0.025	26,580	0	7,308,034	0.016	22,082	0	4,734,681
		Sum	0.036	203,418	0	231,267,761	0.052	36,947	0	7,551,026	0.038	30,150	0	4,832,482
		Fal	0.022	165,341	0	231,995,959	0.028	28,907	0	7,453,386	0.019	24,182	0	4,823,525
		Ann	0.022	205,001	0	234,512,308	0.029	36,769	0	7,520,928	0.021	29,913	0	4,854,894
Min SAT	RCP2.6	Win	0.008	106,148	0	202,246,481	0.018	21,294	0	7,440,257	0.010	15,793	0	4,436,608
		Spr	0.004	60,616	0	197,416,966	0.007	10,218	0	7,646,027	0.003	9,535	0	4,534,825
		Sum	0.016	141,778	0	216,927,660	0.026	25,003	0	7,666,018	0.013	21,024	0	4,687,639
		Fal	0.006	69,338	0	172,230,607	0.015	19,761	0	7,618,220	0.005	12,993	0	4,157,496
		Ann	0.009	148,071	0	212,603,892	0.017	28,299	0	7,669,280	0.008	22,760	0	4,768,770
	RCP4.5	Win	0.011	121,973	0	209,388,161	0.022	23,579	0	7,444,354	0.012	17,994	0	4,487,759
		Spr	0.007	96,414	0	197,741,767	0.010	15,034	0	7,646,577	0.005	14,128	0	4,525,489
		Sum	0.022	184,419	0	223,604,096	0.035	33,708	0	7,671,455	0.017	27,412	0	4,774,419
		Fal	0.011	129,430	0	188,987,753	0.025	28,802	0	7,631,731	0.009	20,767	0	4,409,924
		Ann	0.013	187,340	0	225,917,251	0.024	34,140	0	7,673,408	0.011	26,969	0	4,815,342
	RCP8.5	Win	0.016	149,414	0	217,253,363	0.033	27,722	0	7,475,523	0.017	21,662	0	4,587,574
		Spr	0.014	151,034	0	217,297,161	0.022	26,548	0	7,667,383	0.010	22,221	0	4,721,538
		Sum	0.029	209,828	0	228,304,470	0.047	37,673	0	7,672,506	0.023	30,591	0	4,825,854
		Fal	0.023	177,349	0	215,817,526	0.047	34,796	0	7,640,771	0.017	26,688	0	4,665,765
		Ann	0.021	212,795	0	231,386,756	0.038	38,426	0	7,679,076	0.017	30,562	0	4,847,953

Table E-2. Continued

Var.	Scen.	Time	Subregion 3				Subregion 4				Subregion 5			
			Sl.	S	p	VarS	Sl.	S	p	VarS	Sl.	S	p	VarS
Max SAT	RCP2.6	Win	0.007	12,778	0	4,487,031	0.004	14,424	0	7,101,111	0.003	12,209	0	4,035,105
		Spr	0.008	11,001	0	4,540,844	0.009	13,711	0	7,089,712	0.005	10,103	0	4,471,324
		Sum	0.017	20,259	0	4,565,402	0.020	25,177	0	7,466,882	0.017	19,479	0	4,568,048
		Fal	0.003	5,368	0.012	4,594,089	0.003	4,954	0.065	7,197,877	0.002	5,216	0.015	4,589,854
		Ann	0.009	19,882	0	4,654,389	0.009	23,585	0	7,338,756	0.007	19,413	0	4,598,378
	RCP4.5	Win	0.010	15,866	0	4,554,461	0.005	18,123	0	7,196,049	0.004	14,104	0	4,175,021
		Spr	0.011	15,449	0	4,567,737	0.012	19,361	0	7,106,122	0.006	14,436	0	4,454,081
		Sum	0.022	24,603	0	4,647,905	0.025	31,062	0	7,535,400	0.024	24,496	0	4,648,215
		Fal	0.009	15,441	0	4,627,296	0.010	17,533	0	7,141,558	0.007	15,266	0	4,608,359
		Ann	0.014	25,326	0	4,753,613	0.013	31,408	0	7,496,629	0.011	25,422	0	4,724,333
	RCP8.5	Win	0.015	20,245	0	4,637,352	0.008	23,318	0	7,319,151	0.006	18,243	0	4,345,132
		Spr	0.020	21,160	0	4,668,705	0.022	27,048	0	7,287,688	0.011	20,356	0	4,624,232
		Sum	0.028	27,872	0	4,701,528	0.032	37,255	0	7,576,862	0.036	28,567	0	4,718,923
		Fal	0.022	23,934	0	4,782,037	0.023	29,001	0	7,454,696	0.016	23,854	0	4,776,933
		Ann	0.022	29,027	0	4,819,426	0.022	36,246	0	7,573,817	0.018	29,353	0	4,800,126
Min SAT	RCP2.6	Win	0.009	13,445	0	4,285,074	0.007	19,597	0	6,972,282	0.005	15,069	0	4,259,624
		Spr	0.004	7,541	0	4,180,188	0.005	12,210	0	6,898,837	0.002	7,931	0	4,194,791
		Sum	0.015	20,095	0	4,460,074	0.015	24,569	0	7,188,652	0.015	20,221	0	4,427,500
		Fal	0.003	4,291	0.027	3,742,556	0.008	16,558	0	6,234,341	0.004	6,990	0	3,512,483
		Ann	0.008	20,179	0	4,397,621	0.009	26,898	0	7,250,096	0.007	20,832	0	4,408,074
	RCP4.5	Win	0.012	16,245	0	4,409,617	0.010	22,715	0	7,065,727	0.007	17,006	0	4,413,339
		Spr	0.008	13,829	0	4,240,361	0.008	17,966	0	6,833,230	0.004	13,250	0	4,170,155
		Sum	0.022	25,928	0	4,554,996	0.019	31,640	0	7,298,879	0.021	26,652	0	4,635,119
		Fal	0.009	14,486	0	3,944,814	0.014	26,767	0	6,772,914	0.008	15,836	0	3,765,835
		Ann	0.013	26,431	0	4,639,549	0.013	33,197	0	7,417,011	0.010	27,254	0	4,682,071
	RCP8.5	Win	0.018	20,177	0	4,499,332	0.015	27,312	0	7,234,211	0.010	21,489	0	4,528,529
		Spr	0.016	21,204	0	4,491,403	0.016	27,595	0	7,272,228	0.009	21,005	0	4,531,000
		Sum	0.030	29,907	0	4,621,647	0.022	36,337	0	7,420,789	0.029	29,977	0	4,755,846
		Fal	0.021	23,253	0	4,531,571	0.027	33,860	0	7,211,710	0.017	23,719	0	4,356,307
		Ann	0.021	30,264	0	4,747,165	0.021	37,793	0	7,491,356	0.016	30,618	0	4,787,101

## REFERENCES

- Ahmadi-Nedushan, B., A. St-Hilaire, T. B. M. J. Ouarda, L. Bilodeau, É. Robichaud, N. Thiémonge, and B. Bobée. 2007. Predicting river water temperatures using stochastic models: case study of the Moisie River (Québec, Canada). *Hydrological Processes*, 21 (1): 21-34.
- Akaike, H. 1974. A new look at the statistical model identification. *IEEE Transactions on Automatic Control*, 19 (6): 716-723.
- Arora, V. K., J. F. Scinocca, G. J. Boer, J. R. Christian, K. L. Denman, G. M. Flato, V. V. Kharin, W. G. Lee, and W. J. Merryfield. 2011. Carbon emission limits required to satisfy future representative concentration pathways of greenhouse gasses. *Geophysical Research Letters*, 38 (5): 1-6.
- Basarin, B., T. Lukić, D. Pavić, and R. L. Wilby. 2016. Trends and multi-annual variability of water temperatures in the river Danube, Serbia. *Hydrological Processes*, 30 (18): 3315-3329.
- Beek, L. P. H., T. Eikelboom, M. T. H. Vliet, and M. F. P. Bierkens. 2012. A physically based model of global freshwater surface temperature. *Water Resources Research*, 48 (9): 1-17.
- Bigart, R. J., and C. Woodcock. 1996. In the name of the Salish and Kootenai Nation: The 1855 Hell Gate Treaty and the origin of the Flathead Indian Reservation. Pablo, MT: Salish Kootenai College Press.
- Bogan, T., O. Mohseni, and H. G. Stefan. 2003. Stream temperature-equilibrium temperature relationship. *Water Resources Research*, 39 (9): SWC71-SWC712.
- Bogan, T., J. Othmer, O. Mohseni, and H. G. Stefan. 2006. Estimating extreme stream temperatures by the standard deviate method. *Journal of Hydrology*, 317 (3): 173-189.
- Caissie, D. 2006. The thermal regime of rivers: a review. *Freshwater Biology*, 51 (8): 1389-1406.

- Caissie, D., N. El-Jabi, and A. St-Hilaire. 1998. Stochastic modelling of water temperatures in a small stream using air to water relations. *Canadian Journal of Civil Engineering*, 25 (2): 250-260.
- Caissie, D., N. El-Jabi, and M. G. Satish. 2001. Modelling of maximum daily water temperatures in a small stream using air temperatures. *Journal of Hydrology*, 251 (1-2): 14-28.
- Caissie, D., M. G. Satish, and N. El-Jabi. 2005. Predicting river water temperatures using the equilibrium temperature concept with application on Miramichi River catchments (New Brunswick, Canada). *Hydrological Processes*, 19 (11): 2137-2159.
- . 2007. Predicting water temperatures using a deterministic model: Application on Miramichi River catchments (New Brunswick, Canada). *Journal of Hydrology*, 336 (3): 303-315.
- CCSP (Climate Change Science Program). 2008. *Reanalysis of historical climate data for key atmospheric features: Implications for attribution of causes of observed change. A report by the U.S. CCSP and Subcommittee on Global Change Research*, ed. R. Dole, M. Hoerling, and S. Schubert. Ashville, NC: NOAA National Climatic Data Center.
- Chase, K., J., L. E., Hay, and S. L., Markstrom. 2012. Watershed scale response to climate change – South Fork Flathead River Basin, Montana. U.S. Geological Survey Fact Sheet 2011-3124. [https://pubs.usgs.gov/fs/2011/3124/FS11-3124\\_508.pdf](https://pubs.usgs.gov/fs/2011/3124/FS11-3124_508.pdf) [last accessed 1 June 2019].
- Chow, G. C. 1960. Tests of equality between sets of coefficients in two linear regressions. *Econometrica: Journal of the Econometric Society*, 28 (3): 591-605.
- Clow, D. W. 2010. Changes in the timing of snowmelt and streamflow in Colorado: A response to recent warming. *Journal of Climate*, 23 (9): 2293-2306.
- Cozzetto, K., K. Chief, K. Dittmer, M. Brubaker, R. Gough, K. Souza, F. Ettawageshik, S. Wotkyns, S. Opitz-Stapleton, S. Duren, and P. Chavan. 2013. Climate change impacts on the water resources of American Indians and Alaska Natives in the U.S. *Climatic Change*, 120 (3): 569-584.

- Cummins, C., J. Doyle, L. Kindness, M. J. Lefthand, U. J. Bear Don't Walk, A. L. Bends, S. C. Broadaway, A. K. Camper, R. Fitch, T. E. Ford, S. Hamner, A. R. Morrison, C. L. Richards, S. L. Young, and M. J. Eggers. 2010. Community-based participatory research in Indian Country: Improving health through water quality research and awareness. *Family and Community Health*, 33 (3): 166-174.
- Dittmer, K. 2013. Changing streamflow on Columbia basin tribal lands – climate change and salmon. *Climatic Change*, 120 (3): 627-641.
- Edinger, J. E., D. W. Duttweiler, and J. C. Geyer. 1968. The response of water temperatures to meteorological conditions. *Water Resources Research*, 4 (5): 1137-1143.
- Eggers, M. J., A. L. Moore-Nall, J. T. Doyle, M. J. Lefthand, S. L. Young, A. L. Bends, and A. K. Camper. 2015. Potential health risks from uranium in home well water: An investigation by the Apsaalooke (Crow) Tribal Research Group. *Geosciences*, 5 (1): 67-94.
- Elsner, M. M., L. Cuo, N. Voisin, J. S. Deems, A. F. Hamlet, J. A. Vano, K. E. B. Mickelson, S. Lee, and D. P. Lettenmaier. 2010. Implications of 21<sup>st</sup> century climate change for the hydrology of Washington State. *Climatic Change*, 102 (1-2): 225-260.
- Elwood, S. A. 2010. Mixed methods: Thinking, doing, and asking in multiple ways. In *The SAGE Handbook of Qualitative Geography*. London, UK: SAGE Publications.
- ECCC (Environment and Climate Change Canada). n.d.-a. CanESM2 predictors: CMIP5 experiments. <http://climate-scenarios.canada.ca/?page=pred-canesm2> [last accessed 1 June 2019].
- . n.d.-b. Note on predictors (large scale atmospheric variables). <http://climate-scenarios.canada.ca/?page=pred-help> [last accessed 1 June 2019].
- Evans, J., J. McGregor, and K. McGuffie. 2012. *Future Regional Climates. In Future of the World's Climate*. Waltham, USA: Elsevier.
- Fritze, H., I. T. Stewart, and E. Pebesma. 2011. Shifts in Western North American snowmelt runoff regimes for the recent warm decades. *Journal of Hydrometeorology*, 12 (5): 989-1006.

- Gauss, C. F. 1809. *Theoria motus corporum coelestium in sectionibus conicis solem ambientium*. Hamburg: Perthes and Besser.
- Gautam, M. R., K. Chief, and W. J. Smith Jr. 2013. Climate change in arid lands and Native American socioeconomic vulnerability: The case of the Pyramid Lake Paiute Tribe. *Climatic Change*, 120 (3): 585-599.
- Grah, O., and J. Beaulieu. 2013. The effect of climate change on glacier ablation and baseflow support in the Nooksack River basin and implications on Pacific salmonid species protection and recovery. *Climatic Change*, 120 (3): 657-670.
- Hand, J. P. 2007. Protecting the world's largest body of fresh water: The often overlooked role of Indian tribes' co-management of the Great Lakes. *Natural Resources Journal*, 47 (4): 815-847.
- Hébert, C., D. Caissie, M. G. Satish, and N. El-Jabi. 2011. Study of stream temperature dynamics and corresponding heat fluxes within Miramichi River catchments (New Brunswick, Canada). *Hydrological Processes*, 25 (15): 2439-2455.
- . 2015. Predicting hourly stream temperatures using the equilibrium temperature model. *Journal of Water Resource and Protection*, 7 (4): 322-338.
- Helsel, D. R. and R. M. Hirsch. 2002. *Statistical methods in water resources (Vol. 323)*. Reston, VA: US Geological Survey.
- Helsel, D. R. and L. M. Frans. 2006. Regional Kendall test for trend. *Environmental Science & Technology*, 40 (13): 4066-4073.
- Hilderbrand, R. H., M. T. Kashiwagi, and A. P. Prochaska. 2014. Regional and local scale modeling of stream temperatures and spatio-temporal variation in thermal sensitivities. *Environmental Management*, 54 (1): 14-22.
- Hirsch, R. M., J. R. Slack, and R. A. Smith. 1982. Techniques of trend analysis for monthly water quality data. *Water Resources Research*, 18 (1): 107-121.
- IPCC (Intergovernmental Panel on Climate Change). 2007. *Climate Change 2007: Impacts, Adaptation and Vulnerability – Contribution of Working Group II to the Fourth Assessment Report of the Intergovernmental Panel on Climate Change*. New York, NY: Cambridge University Press.

- . 2013. *Climate Change 2013: The Physical Science Basis – Contribution of Working Group I to the Fifth Assessment Report of the Intergovernmental Panel on Climate Change*. New York, NY: Cambridge University Press.
- . 2014. *Climate Change 2014: Synthesis Report – Contribution of Working Group I, II, and III to the Fifth Assessment Report of the Intergovernmental Panel on Climate Change*. New York, NY: Cambridge University Press.
- Isaak, D. J., S. Wollrab, D. Horan, and G. Chandler. 2012. Climate change effects on stream and river temperatures across the northwest US from 1980–2009 and implications for salmonid fishes. *Climatic Change*, 113 (2): 499-524.
- Jackson, F. L., D. M. Hannah, R. J. Fryer, C. P. Millar, and I. A. Malcolm. 2017. Development of spatial regression models for predicting summer river temperatures from landscape characteristics: Implications for land and fisheries management. *Hydrological Processes*, 31 (6): 1225-1238.
- Jeong, D. I., A. Daigle, and A. St-Hilaire. 2013. Development of a stochastic water temperature model and projection of future water temperature and extreme events in the Ouelle River basin in Québec, Canada. *River Research and Applications*, 29 (7): 805-821.
- Johnson, M. F., R. L. Wilby, and J. A. Toone. 2014. Inferring air-water temperature relationships from river and catchment properties. *Hydrological Processes*, 28 (6): 2912-2928.
- Jones, L. A., C. C. Muhlfeld, L. A. Marshall, B. L. McGlynn, and J. L. Kershner. 2014. Estimating thermal regimes of bull trout and assessing the potential effects of climate warming on critical habitats. *River Research and Applications*, 30 (2): 204-216.
- Kalnay, E., M. Kanamitsu, R. Kistler, W. Collins, D. Deaven, L. Gandin, M. Iredell, S. Saha, G. White, J. Woollen, Y. Zhu, M. Chelliah, W. Ebisuzaki, W. Higgins, J. Janowiak, K. C. Mo, C. Ropelewski, J. Wang, A. Leetmaa, R. Reynolds, R. Jenne, and D. Joseph. 1996. The NCEP/NCAR 40-year reanalysis project. *Bulletin of the American Meteorological Society*, 77 (3): 437-471.
- Kendall, M. G. 1975. *Rank Correlation Methods*. 4<sup>th</sup> Edition. London, UK: Charles Griffin.

- Krider, L. A., J. A. Magner, J. Perry, B. Vondracek, and L. C. Ferrington Jr. 2013. Air-water temperature relationships in the trout streams of Southeastern Minnesota's carbonate-sandstone landscape. *Journal of the American Water Resources Association*, 49 (4): 896-907.
- Lemke, C. E. 1954. The dual method of solving the linear programming problem. *Naval Research Logistics Quarterly*, 1 (1): 36-47.
- Letcher, B. H., D. J. Hocking, K. O'Neil, A. R. Whiteley, K. H. Nislow, and M. J. O'Donnell. 2016. A Hierarchical model of daily stream temperature using air-water temperature synchronization, autocorrelation, and time lags. *PeerJ*, 4 (e1727): 1-26.
- Li, H., X. Deng, D.-Y. Kim, and E. P. Smith. 2014. Modeling maximum daily temperature using a varying coefficient regression model, *Water Resources Research*, 50 (4): 3073-3087.
- Mann, H. B. 1945. Nonparametric tests against trend. *Econometrica: Journal of the Econometric Society*, 13:245-259.
- Marchetto, A. 2017. rkt: Mann-Kendal Test, Seasonal and Regional Kendall Tests (version 1.5). <https://CRAN.R-project.org/package=rkt> [last accessed 1 June 2019].
- Marsh, K. R., and M. D. Smith. 2015. The Native American voice in United States water rights. *Journal of Water, Sanitation and Hygiene for Development*, 5 (2): 173-182.
- McGinnis, S., and R. K. Davis. 2001. Domestic well water quality within tribal lands of eastern Nebraska. *Environmental Geology*, 41 (3-4): 321-329.
- Mearns, L. O., M. S. Bukovsky, S. C. Pryor, and V. Magaña. 2014. *Downscaling of climate information. In Climate Change in North America*. Cham, Switzerland: Springer International Publishing.
- Menne, M. J., I. Durre, B. Korzeniewski, S. McNeal, K. Thomas, X. Yin, S. Anthony, R. Ray, R. S. Vose, B. E. Gleason, and T. G. Houston. 2012. Global Historical Climatology Network - Daily (GHCN-Daily), Version 3.22. NOAA National Climatic Data Center. <http://doi.org/10.7289/V5D21VHZ> [last accessed 1 June 2019].

- Menne, M. J., I. Durre, R. S. Vose, B. E. Gleason, and T. G. Houston. 2012. An overview of the global historical climatology network-daily database. *Journal of Atmospheric and Oceanic Technology*, 29 (7): 897-910.
- Mizukami, N. and S. Perica. 2008. Spatiotemporal characteristics of snowpack density in the mountainous regions of the Western United States. *Journal of Hydrometeorology*, 9 (6): 1416-1426.
- Mohseni, O., and H. G. Stefan. 1999. Stream temperature/air temperature relationship: A physical interpretation. *Journal of Hydrology*, 218 (3): 128-141.
- Mohseni, O., H. G. Stefan, and T. R. Erickson. 1998. A nonlinear regression model for weekly stream temperatures. *Water Resources Research*, 34 (10): 2685-2692.
- Morrill, J. C., R. C. Bales, and M. H. Conklin. 2005. Estimating stream temperature from air temperature: Implications for future water quality. *Journal of Environmental Engineering*, 131 (1): 139-146.
- Mosteller, F., and J. W. Tukey. 1968. Data analysis, including statistics. In: *Handbook of social psychology*, ed. G. Lindzey and E. Aronson, 2: 80-203. Addison Wesley.
- O'Driscoll, M. A., and D. R. DeWalle. 2006. Stream–air temperature relations to classify stream–ground water interactions in a karst setting, central Pennsylvania, USA. *Journal of Hydrology*, 329 (1): 140-153.
- Pedersen, N. L., and K. Sand-Jensen. 2007. Temperature in lowland Danish streams: Contemporary patterns, empirical models and future scenarios. *Hydrological Processes*, 21 (3): 348-358.
- Pederson, G. T., L. J. Graumlich, D. B. Fagre, T. Kipfer, and C. C. Muhlfeld. 2010. A century of climate and ecosystem change in Western Montana: what do temperature trends portend? *Climatic Change*, 98 (1-2): 133-154.
- Pomeroy, J. W., and E. Brun. 2001. Physical properties of snow. In *Snow ecology: an interdisciplinary examination of snow-covered ecosystems*, Eds., Jones, H. G., Pomeroy, J. W., Walker, D. A., and Hoham, R. W., 45-126. Cambridge University Press.

- Rogers, P. D., and S. M. Edmiston. 2013. The Gila River Indian Community Water Rights Settlement and its impact on water resource management. *Water International*, 38 (3): 250-262.
- RStudio Team. 2015. RStudio: Integrated Development for R (version 1.0.153). Boston, MA: RStudio, Inc. <http://www.rstudio.com/> [last accessed 1 June 2019].
- Schwarz, G. 1978. Estimating the dimension of a model. *The annals of statistics*, 6 (2): 461-464.
- Sen, P. K. 1968. Estimates of the regression coefficient based on Kendall's tau. *Journal of the American Statistical Association*, 63 (324): 1379-1389.
- Serreze, M. C., M. P. Clark, R. L. Armstrong, D. A. McGinnis, and R. S. Pulwarty. 1999. Characteristics of the western United States snowpack from snowpack telemetry (SNOTEL) data. *Water Resources Research*, 35 (7): 2145-2160.
- Snyder, C. D., N. P. Hitt, and J. A. Young. 2015. Accounting for groundwater in stream fish thermal habitat responses to climate change. *Ecological Applications*, 25 (5): 1397-1419.
- Stewart, I. T., D. R. Cayan, and M. D. Dettinger. 2005. Changes toward earlier streamflow timing across Western North America. *Journal of Climate*, 18 (8): 1136-1155.
- Strasser, U., M. Bernhardt, M. Weber, G. E. Liston, and W. Mauser. 2008. Is snow sublimation important in the alpine water balance? *The Cryosphere*, 2 (1): 53-66.
- Theil, H. 1950. A rank-invariant method of linear and polynomial regression analysis, Part I, Part II, and Part III. In *Proceedings of the Royal Netherlands Academy of Sciences*, 53: 386-392, 521-525, and 1397-1412.
- Trzaska, S., and E. Schnarr. 2014. *A review of downscaling methods for climate change projections*. United States Agency for International Development by Tetra Tech ARD (2014): 1-42.
- Tryhorn, L., and A. DeGaetano. 2013. A methodology for statistically downscaling seasonal snow cover characteristics over the Northeastern United States. *International Journal of Climatology*, 33 (12): 2728-2743.

- U.S. Census Bureau. 2011. 2010 National Summary File of Redistricting Data – Technical Documentation. Washington, DC: United States Census Bureau.
- USGCRP (U.S. Global Change Research Program). 2009. *Global Climate Change Impacts in the United States*. New York, NY: Cambridge University Press.
- . 2014. *Climate Change Impacts in the United States: The Third National Climate Assessment*. Washington, DC: U.S. Government Printing Office.
- Webb, B. W., and F. Nobilis. 1997. Long-term perspective on the nature of the air-water temperature relationship: A case study. *Hydrological Processes*, 11 (2): 137-147.
- Webb, B. W., and Y. Zhang. 1999. Water temperatures and heat budgets in Dorset chalk water courses. *Hydrological Processes*, 13 (3): 309-321.
- Webb, B. W., P. D. Clack, and D. E. Walling. 2003. Water-air temperature relationships in a Devon river system and the role of flow. *Hydrological Processes*, 17 (15): 3069-3084.
- Webb, B. W., D. M. Hannah, R. D. Moore, L. E. Brown, and F. Nobilis. 2008. Recent advances in stream and river temperature research. *Hydrological Processes*, 22 (7): 902-918.
- Wehrly, K. E., L. Wang, and M. Mitro. 2007. Field-based estimates of thermal tolerance limits for trout: incorporating exposure time and temperature fluctuation. *Transactions of the American Fisheries Society*, 136 (2): 365-374.
- Wilby, R. L., and C. W. Dawson. 2007. SDSM 4.2: A decision support tool for the assessment of regional climate change impacts. User Manual. London, UK.
- . 2011. Statistical DownScaling Model (Version 4.2.9). Loughborough University, UK. <https://sdsd.org.uk/software.html> [last accessed 1 June 2019].
- . 2013. The Statistical DownScaling Model: Insights from one decade of application. *International Journal of Climatology*, 33 (7): 1707-1719.
- . 2015a. Statistical DownScaling Model – Decision Centric (SDSM-DC): Version 5.2 supplementary note. Loughborough University, UK. <https://sdsd.org.uk/software.html> [last accessed 1 June 2019].

- . 2015b. Statistical DownScaling Model (Version 5.2). Loughborough University, UK. <https://sdsdm.org.uk/software.html> [last accessed 1 June 2019].
- Wilby, R. L., C. W. Dawson, and E. M. Barrow. 2002. SDSM – A decision support tool for the assessment of regional climate change impacts. *Environmental Modelling & Software*, 17 (2): 145-157.
- Wilby, R. L., C. W. Dawson, C. Murphy, P. O'Connor, and E. Hawkins. 2014. The Statistical DownScaling Model-Decision Centric (SDSM-DC): Conceptual basis and applications. *Climate Research*, 61 (3): 251-268.
- WMO (World Meteorological Organization). 1989. Calculation of monthly and annual 30-year standard normals: Prepared by a meeting of experts, Washington, D.C., USA, March 1989. WCDP-No. 10, WMO-TD/No. 341. Geneva, Switzerland: World Meteorological Organization.
- Wu, H., J. S. Kimball, M. M. Elsner, N. Mantua, R. F. Adler, and J. Stanford. 2012. Projected climate change impacts on the hydrology and temperature of Pacific Northwest rivers. *Water Resources Research*, 48 (11): 1:23.
- WWAP (World Water Assessment Programme). 2009. *United Nations World Water Development Report 3: Water in a Changing World*. Paris/London, Fr/UK: UNESCO Publishing/Earthscan.